Thèse n° 9263

Nonperturbative Quantum Field Theory in Curved Spacetime

Présentée le 19 août 2022

Faculté des sciences de base
Laboratoire de théorie des champs et des cordes
Programme doctoral en physique

pour l’obtention du grade de Docteur ès Sciences

par

Kamran SALEHI VAZIRI

Acceptée sur proposition du jury

Prof. A. Pasquarello, président du jury
Prof. J. M. Augusto Penedones Fernandes, directeur de thèse
Prof. L. Senatore, rapporteur
Prof. B. Van Rees, rapporteur
Prof. V. Gorbenko, rapporteur

École
polytechnique
fédérale
de Lausanne

2022

Long you live and high you fly
And smiles you'll give and tears you'll cry
And all you touch and all you see
Is all your life will ever be.
— Roger Waters

To my mother…

Acknowledgements

My stay in Lausanne has been full of sweet and heartwarming memories with a long list of friends and colleagues. This long list, on the other hand, makes it impossible to do justice in acknowledgments. Nevertheless, let me do my best.

Joao was the best advisor I could imagine. It was a great pleasure to interact with someone with such a genius, extraordinary calculation skills and deep knowledge. Prioritizing a PhD student like me, with a smile whenever I knocked on his door to discuss a question was a boost in my motivation. Moreover, he is a kind, caring and open-minded human being. He was so patient with all the drama I made – from scientific politics to bursting into tears over a deadline! I will never stop bragging about him.

Cubotron is made of kind and friendly people. I was lucky to get the chance to take a course with Riccardo. His deep physical intuition is one of a kind and his love for physics is always inspiring. I will miss the jokes and discussions we had over lunch. I have to thank my collaborators for their amazing job. Marco with his impressive knowledge and precision in calculations was a great boost to our project. I cannot thank him enough for spending hours and hours explaining the basics to me. I have to thank Matthijs for his patience going through my chaotic notes and also for his great suggestions for how to live in Amsterdam. I have to acknowledge the great advices Denis gave me and thank him for being the only one who was fully on board with my edgy jokes – your energy is missed here!

Our PhD gang was phenomenal: The iconic Gabriel who had an answer to most of my physics questions while I was treating him back by telling him how we put ketchup on pasta in Iran. The legendary Andrea who taught me how to run SDPB on the cluster and accompanied me in once in a lifetime Vegas trip. Lorenzo, the Italian guy everyone wants in his group of friends that would be down for a short-notice road trip to Paris. Gil, that helped us with French and how to live in Switzerland all the time. Marten with the intense but fun discussions over lunch.

And most importantly, I have to thank my (ex-)officemates that are exceptional characters: Joao that pushed us to work hard. I will never forget the days that he used to put Rocky theme song to boost our motivation.

The Portuguese boi, Miguel. The one that brings out my inner 15 years old and jumped around with me in a samba bar in Rio. The one who I had the pleasure to solve the homework sets together and share many memes. Thanks for getting triggered easily and

creating the iconic FOB!

Aditya–the Bro! The one that shares the same music taste as me and agrees that Mikael Akerfeldt and Steven Wilson are legends, pioneers and geniuses. The guy from Bangalore that also experiences the pain of supporting Arsenal, believes that Antonio's cipollina pizza in Banane is the best and happily sings the Baker Street tune when it is the right time. The best friend that was always there for both deep conversations and partying late at night in Lapin Vert. Indeed, *517 = best office gg ez.*

I was blessed to have a great group of friends outside of our physics group. The road trip partners Laia and Fatemeh; Shayan with his intensive board game commitments; Khashayar, Omid and Navid that perfectly imported the Tarbiz culture to Lausanne. The Silo Blue gang: Melanie that like a younger sister was always dedicated to disagreeing with me even if she was fine with what I said deep down. Amirali with the late-night hang outs and laughters that lasted till morning, the one that gives the perfect *aaaakh* whenever I play King Crimson or Tool, and the one who truely understands the concept of *deperzer(n)* and deserves to be knighted as *Mohsen.* Debi who gives the best hugs, dances Persian better than any Iranian, and pumps energy into our gatherings. Last but not least, Ali Baran Ozaydin. The one that enjoys messing with us and celebrates it with his signature "I am awesome" move. The arkadas with whom I had many jams and music theory discussions that ended up debates about the history of Anatolia!

I was extremely lucky to be friends with the best couple on this planet: Mohammad Jafar and Shakiba. The warm and soothing evenings at their place with great food and music were always a blast; no need to mention all the amazing trips we had together. Thank you for adding me as Ted to your Marshall and Lily story. Special thanks to the cutest dog ever, Tileh, that walks around with me like a gentleman, knows me by name, and the only one that matches my energy.

Finally, let me thank my family: My father who introduced me from age of zero to the greatest band of all time, Pink Floyd. My mother who sacrificed her life to make my life way better. I owe every smile and joy I have in life to you mom. You never stopped trusting in me and never stopped supporting me. Hope I can return a small portion of the favor. And my brother, the kind boy with a pure heart. The one that always believed in me: from the time he got me an abacus when he was 6 years of age to when I drive fast now.

Abstract

This work is devoted to nonperturbative methods to study quantum field theories in curved maximally symmetric spacetimes like de Sitter and Anti-de Sitter.

In the first part, we cover some preliminary facts about conformal field theories in flat-space. Therein, the conformal algebra is derived and the unitarity bounds as well as the conformal bootstrap are discussed. Furthermore, we cover the basics of quantum field theories in a fixed de Sitter background. We develop the Hilbert space decomposition of quantum field theory in $d+1$-dimensional de Sitter into irreducible unitary representations of its isometry group $SO(d+1,1)$ as well as the notion of late-time boundary operators. We also review the massive free field theory, in-in formalism and de Sitter-Euclidean anti-de Sitter dictionary used in perturbative calculations.

The second part deals with the bulk two-point function and the boundary four-point function. Firstly, the Källén–Lehmann spectral decomposition of the bulk two-point functions is recovered and two inversion formulas for the spectral densities are presented – one through analytical continuation from the sphere and the other through analytical continuation from Anti-de Sitter. In the process, we exhibit a relation between poles in the corresponding spectral densities and boundary CFT data. Next, we study the conformal partial wave decomposition of the four-point functions of boundary operators. These correlation functions are very similar to the ones of standard conformal field theory but have different positivity properties that follow from unitarity in de Sitter. We conclude by proposing a nonperturbative conformal bootstrap approach to the study of these late-time four-point functions, and we illustrate our proposal with a concrete example for two-dimensional de Sitter.

The last part develops a nonperturbative method called Hamiltonian truncation to compute the energy spectrum of quantum field theories in two-dimensional anti-de Sitter. The infinite volume of constant timeslices of anti-de Sitter leads to divergences in the energy levels. We propose a simple prescription to obtain finite physical energies and test it with numerical diagonalization in several models: the free massive scalar field, $\lambda\phi^4$ theory, Lee-Yang and Ising field theory. Along the way, we discuss spontaneous symmetry breaking in AdS and derive a compact formula for perturbation theory in quantum mechanics at arbitrary order. Our results suggest that all conformal boundary conditions for a given theory are connected via bulk renormalization group flows in Anti-de Sitter.

Keywords:

Quantum field theory, Nonperturbative methods, de Sitter spacetime, Anti-de Sitter spacetime, Conformal bootstrap, Hamiltonian truncation

Résumé

Ce travail est consacré aux méthodes nonperturbatives pour étudier les théories quantiques des champs dans des espace-temps courbes à symétrie maximale comme de Sitter et Anti-de Sitter.

Dans la première partie, nous présentons quelques faits préliminaires sur les théories des champs conformes dans l'espace plat. L'algèbre conforme est dérivée et les limites d'unitarité ainsi que le bootstrap conforme sont discutés. De plus, nous abordons les bases des théories quantiques des champs dans un arrière-plan fixe de de Sitter. Nous développons la décomposition de l'espace de Hilbert de la théorie quantique des champs dans un espace de de Sitter de dimension $d+1$ en représentations unitaires irréductibles de son groupe d'isométrie $SO(d+1,1)$ ainsi que la notion d'opérateurs sur le bord au temps tardif. Nous passons également en revue la théorie des champs libres massifs, le formalisme in-in et le dictionnaire de Sitter-Anti-de Sitter Euclidéen utilisés dans les calculs perturbatifs.

La deuxième partie traite de la fonction à deux points massive et de la fonction à quatre points au bord. Tout d'abord, la décomposition spectrale de Källén–Lehmann des fonctions à deux points de l'intérieur est obtenue et deux formules d'inversion pour les densités spectrales sont présentées - l'une par continuation analytique à partir de la sphère et l'autre par continuation analytique à partir d'Anti-de Sitter. Au cours du processus, nous montrons une relation entre les pêles des densités spectrales correspondantes et les données de la CFT au bord. Ensuite, nous étudions la décomposition en ondes partielles conformes des fonctions à quatre points d'opérateurs au bord. Ces fonctions de corrélation sont très similaires à celles de la théorie des champs conforme standard mais ont des propriétés de positivité différentes qui découlent de l'unitarité en de Sitter. Nous concluons en proposant une approche non-perturbative par bootstrap conforme pour l'étude de ces fonctions à quatre points en temps tardif, et nous illustrons notre proposition par un exemple concret pour l'espace de de Sitter à deux dimensions.

La dernière partie développe une méthode non-perturbative appelée troncature Hamiltonienne pour calculer le spectre d'énergie des théories quantiques des champs en Anti-de Sitter à deux dimensions. Le volume infini des tranches de temps constant en Anti-de Sitter conduit à des divergences dans les niveaux d'énergie. Nous proposons une prescription simple pour obtenir des énergies physiques finies et la testons par diagonalisation numérique dans plusieurs modèles : le champ scalaire massif libre, la théorie $\lambda\phi^4$, les théories des champs de Lee-Yang et d'Ising. En cours de route, nous discutons de la brisure spontanée de symétrie en AdS et nous déduisons une formule compacte pour la théorie des perturbations en mécanique quantique à un ordre arbitraire. Nos résultats suggèrent que toutes les conditions au bord conformes pour une théorie donnée sont connectées via des flux du groupe de renormalisation à l'intérieur d'Anti-de Sitter.

Mots clés :

Théorie quantique des champs, Méthodes nonperturbatives, de Sitter espace-temps, Anti-de Sitter espace-temps, Bootstrap conforme, Troncature Hamiltonienne

Contents

Acknowledgements i

Abstract (English/Français) iii

Introduction 1

I Preliminaries 11

1 Conformal field theories 13

1.1 Conformal transformations 13
1.2 Conformal algebra 14
1.3 Ward identities and conformal charges 16
1.4 Conformal representation: Primary operators 17
1.5 Radial quantization 18
1.6 The state-operator correspondence and OPE 19
1.7 Unitarity bounds 21
1.8 Correlation functions 22
  1.8.1 Two-point functions 23
  1.8.2 Three-point functions 23
  1.8.3 Four-point function 24
1.9 Conformal blocks 25
1.10 The conformal bootstrap 26

2 Quantum field theory in de Sitter 29

2.1 Geometry of maximally symmetric spaces 29
  2.1.1 Sphere 30
  2.1.2 Euclidean Anti-de Sitter spacetime 31
  2.1.3 Anti-de Sitter spacetime 32
  2.1.4 de Sitter spacetime 33
2.2 Representation theory of $SO(d+1,1)$ 36
2.3 Correlation functions and boundary operators 39

2.4 Free scalar field in de Sitter 41
2.5 Perturbative QFT in de Sitter 44
2.5.1 In-in formalism 45
2.5.2 Two-point function in EAdS and dS 47
2.5.3 EAdS-dS dictionary 51
2.6 Non-perturbative QFT in de Sitter 53
2.6.1 Hilbert space 53
2.6.2 Representations in position space 55
2.6.3 Conformal Field Theory in de Sitter 57

II Nonperturbative cosmological bootstrap 59

3 Bulk two-point function 61
3.1 Källén–Lehmann decomposition 61
3.2 Late-time limit and boundary OPE 64
3.3 Analytic continuation from S^{d+1} 68
3.4 Analytic continuation from EAdS$_{d+1}$ 73
3.5 Examples 75
3.5.1 Massive free boson: $\langle\phi\phi\rangle$ 76
3.5.2 Massive free boson: $\langle\phi^2\phi^2\rangle$ 76
3.5.3 Bulk CFT correlator 78

4 Boundary four-point function 81
4.1 Partial wave expansion 81
4.2 Examples of partial wave coefficients 85
4.2.1 Mean Field Theory 86
4.2.2 Local terms in the Gaussian theory 87
4.2.3 Adding interactions; ϕ^4 theory at leading order 89

5 Setting up the QFT in dS Bootstrap 93
5.1 Review of CFT$_1$ 94
5.2 A toy example: almost MFT 97
5.3 Regularized crossing equation 100
5.4 An invitation to the numerical bootstrap 102

6 Conclusion 105

III Hamitonian truncation in
Anti-de Sitter spacetime 109

7 Set up of Hamiltonian truncation in AdS$_2$ 111
7.1 Geometry 111

7.2 The Hilbert space and the bulk-to-boundary OPE 112
7.3 The interacting Hamiltonian 114
7.4 The energy spectrum 116
7.5 Spontaneous symmetry breaking 117

8 How to tame divergences **121**
8.1 An example 122
8.2 The strategy 126
8.3 Divergence of the vacuum energy at second order 130
8.4 The argument at second order 131
8.5 Generalization at all orders 136
8.6 Degenerate spectra 138
8.7 Truncation errors 140

9 Deformations of a free massive scalar **143**
9.1 ϕ^2 deformation 145
9.2 ϕ^4 flow 151

10 Deformations of conformal field theories **159**
10.1 Virasoro minimal models and their deformations in AdS$_2$ 159
10.2 The Lee-Yang model 162
10.3 The Ising model 171
10.4 The Ising model with thermal deformation 173
10.5 The Ising model in a magnetic field 178

11 Conclusion **183**

IV Appendix **189**

A Special functions **191**
A.1 Common special functions 191
A.2 Estimates for $\tilde{F}$ at large Δ 193

B Action of $SO(d+1,1)$ generators **197**

C Spectral density inversion formula **203**
C.1 Froissart-Gribov trick 203
C.2 Example: a_J of the massive boson 205
C.3 Large J behavior 206

D From $SO(2,2)$ to $SO(2,1)$ **209**

E Semidefinite Programming for Conformal Bootstrap **215**

E.1 Expanding the blocks in polynomials of Δ 215
E.2 SDP set up 216
E.3 SDP for $\tilde{F}$ 217

F Symmetry constraints on matrix elements 221
F.1 Relations between matrix elements of descendants 221
F.2 Example: vacuum amplitudes 225
F.3 Universality of matrix elements if $\Delta_i - \Delta_j$ is an even integer 225

G Rayleigh-Schrödinger perturbation theory revisited 227
G.1 Rayleigh-Schrödinger coefficients and connected correlators 227
G.2 Feynman diagrams 235
G.3 Explicit calculations at second order in perturbation theory 236

H Short time singularities in the correlators of V 241
H.1 The vacuum two-point function 241
H.2 The two-point function in a generic state 245
H.3 Free scalar example 252

I Algorithms 255
I.1 Scalar field 255
I.2 Minimal models 257

J Spontaneous symmetry breaking in AdS 261
J.1 All or nothing 261
J.2 Inverted harmonic oscillator 264

Bibliography 269

Curriculum Vitae 281

Introduction

Why theoretical physics?[1]

Human beings have always been questioning. From the very early stages of history, we were amazed by the surrounding phenomena and tried to categorize, describe or explain them. Thanks to our arguably most important intellectual tool, *logic*, not only did we understand some of these phenomena, but also we were able to conquer nature with technology and *predict* other phenomena. At the top of these logical approaches to the world around us, sits a branch of science called *physics*. Some of the non-trivial byproducts of this approach to the world are its mysterious relation to abstract mathematics, its power to predict and its extreme objectiveness that unlike art does not vary in the spacetime of the cultures and subcultures. In the next few paragraphs, I will briefly use the historical facts I have in mind to describe my own motivation to study theoretical physics!

The modern scientific method went on a long journey after its birth by Galileo Galilei[2]. It went ahead of mathematics in the 17th and 18th centuries, enjoyed the powerful back and forth between abstraction and observation by the beautiful mind, Sir Isaac Newton and it got to relate the seemingly distinct subject of magnetism, electricity and light by James Maxwell. But in the early 20th century, it reached the most exciting time of its life when it got to the regime of Quantum Mechanics and Relativity. This stage has undeniable effects on every physicist's mind: First, the existence of phenomena well beyond our intuition. Second, the almost purely theoretical motivation for the development of general relativity by Albert Einstein, without the need to explain an already observed phenomenon. General relativity surpassed expectations and predicted the Big Bang, expansion of the universe, black holes, gravitational waves, etc that leads to Nobel prizes to this day. This theory was so beautiful and successful that every physicist dreams of coming up with a new theory like that!

---

[1] This subsection is a personal reply to a non-physicts and can be skipped.

[2] "All knowledge of reality starts from experience and ends in it. Propositions arrived at by purely logical means are completely empty as regards reality. Because Galileo saw this, and particularly because he drummed it into the scientific world, he is the father of modern physics – indeed, of modern science altogether"–Albert Einstein

Our universe is ruled by quantum mechanics and our macroscopic life is only a classical limit of it – whilst many of our daily experiences, like typing this thesis on a computer with billions of transistors, rely on quantum mechanical principles. The rapid and glorious development of quantum mechanics in the 1920s followed by Dirac's genius led to a relativistic wave equation with the *prediction* of the existence of a particle with the same mass and spin as the electron but the opposite electric charge – positron[3]. The field description of electromagnetism in classical physics motivated the development of a new quantum theory of fields that later on included other particles and gave birth to Quantum Electrodynamics (QED), "the most stringently tested and the most dramatically successful of all physical theories" [2]. These developments went on to make quantum field theory a framework that is now one of the pillars of modern physics. The fact that a person sits in a room and uses the mixture of his logic and some basic observations to build a consistent theory and then tells you to go out and find this particle in a lab or that pattern in the sky is like magic. The only difference is that that person, a theoretical physicist, quite willingly shares his tricks!

Nonperturbative quantum field theory

Quantum field theories (QFTs) have had incredible success in describing various phenomena in particle physics, condensed matter physics and cosmology. In spite of the extensive work on QFT in the last century, most of these studies are in a perturbative regime where a quantity such as interaction coupling or one over the rank of the gauge group is assumed to be very small ($\lambda \ll 1$, $\frac{1}{N} \ll 1$). These systems make up a very small region in theory space and cannot describe many of the most interesting physical phenomena.

The goal of this thesis is to nonperturbatively study QFT in a $(d+1)$ fixed curved background[4] and in particular maximally symmetric spacetimes. Maximally symmetric spacetimes are homogeneous and isotropic. Hence, they have the maximal number of isometries of $\frac{1}{2}(d+1)(d+2)$ with a constant Ricci scalar. A maximally symmetric spacetime with (negative)positive curvature is called (Anti-)de Sitter ((A)dS). There are multiple motivations to study (A)dS physics. First, let us mention the motivations for dS.

---

[3] As pointed out in [1], "there are serious reasons for being dissatisfied with the Dirac's original rationale" as (i) it would seem to rule out the existence of any particle of zero spin, (ii) the negative sea argument does not work for charged bosons and (iii) magnetic moment of the electron predicted by Dirac theory can be rescaled by adding another Lorentz invariant term called the Pauli term into wave equation. These issues all will be solved by quantum field theory.

[4] In contrast with dynamical background, where the gravity is quantized and we need a theory of quantum gravity.

Quantum field theory in dS: Motivation

It is widely believed that our universe has gone through an exponential expansion of spacetime called inflation [3–5]. Moreover, observations show that the universe is in an accelerating expanding state called the cosmological constant dominated phase. Both of these epochs are very well approximated by QFT in fixed background de Sitter [5].

It is difficult to put gravity and quantum mechanics together. String theory provides us with a perturbative description of quantum gravity in which it uses perturbative techniques to calculate the scattering amplitude of strings. Maldacena, in his revolutionary work of AdS/CFT correspondence [6], paved the way for a nonperturbative definition of quantum gravity in asymptotic AdS spacetime through the holographic principle. Now, the question is: *"can we propose a non-perturbation definition of quantum gravity in de Sitter and ultimately the universe we live in?"*. In this spirit, one finds the failed attempts to define a stable de Sitter vacuum in string theory that motivated several conjectures called Swampland–the low energy theories which are not compatible with string theory [7–12]. While QFT in rigid dS is fundamentally different from quantum gravity in a dynamical background, it shows us the (indirect) path to cosmology in quantum gravity. For instance, some large N QFTs on a rigid dS are the holographic dual of a gravitational spacetime that includes an FRW-like geometry [13–18].

In contrast with the extensive studies of theories in other maximally symmetric spaces, i.e. flat and AdS spacetimes, at both perturbative and nonperturbative levels, the QFT in dS stayed rather unexplored. Some of the more recent works include the study of non-gaussianities and perturbative calculations of boundary correlators such as cosmological collider [19], cosmological optical theorem [20], dS-AdS dictionary [21, 22] and cosmological bootstrap [23–25] as well as the resolution of IR instabilities [26]. The goal of this work is to approach dS physics from a nonperturbative perspective.

The dS late-time correlation functions transform as conformal correlation functions under the isometry group $SO(d+1,1)$ of dS_{d+1} [19]. This suggests that one can employ conformal bootstrap methods to study QFT in dS which is the key ingredient of our study section 4. Let us briefly recall the main ingredients of the conformal bootstrap approach [27, 28] applicable to Conformal Field Theories (CFTs) in $\mathbb{R}^d$.

Conformal bootstrap

An abstract picture of the space of QFTs is that they are Renormalization Groups (RG) flows between the scale-invariant theories called the UV and IR fixed points. For most of the known examples, the scale invariance enhances to conformal symmetry meaning that they are invariant under angle preserving transformations.[5] Conformal

---

[5] It is proven that scale invariance in two dimensional unitary theories get enhanced to conformal symmetry [29, 30] but for higher dimensions it is still an open problem [31–34]

Field Theories(CFTs) play a central role in different areas of physics such as critical phenomena in statistical mechanics and quantum gravity in AdS via holography, to name a few. They are highly constrained and the different microscopic systems can be described by the same CFT (universality classes). The surprising fact is that very different microscopic systems are described by the same CFT. The motivation to classify and solve the space of CFTs using basic properties such as symmetries and other consistency conditions led to a program called conformal bootstrap.

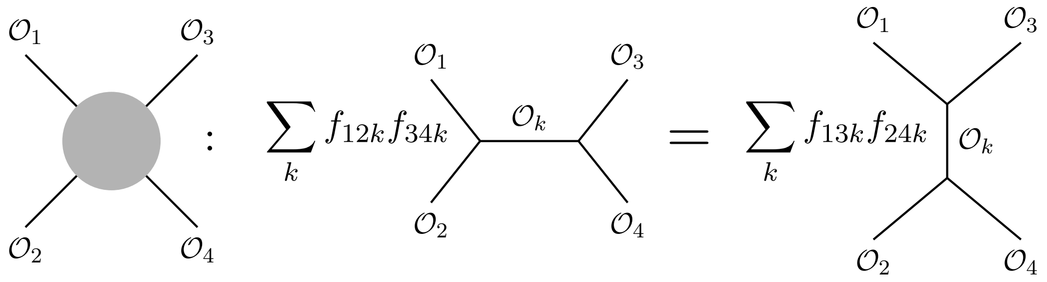

Figure 1: A schematic illustration of crossing equation: Correlators can be expanded in different channels using different operator product expansions with coefficients f_{ijk} that enjoy positivity conditions derived from unitarity.

In a CFT, the two and three-point functions are fixed up to a discrete set of numbers. Then, with the help of the Operator Product Expansion (OPE), which replaces a product of two local operators with a sum of operators (as represented by fusions of two legs in figure 1), higher-point functions can be reduced to infinite sums of three-point functions. Therefore, knowing this basic set of numbers, the so called CFT data, is the same as knowing all n-point functions. As illustrated in figure 1, depending on the order of performing OPE in correlators one obtains different expansions of the same correlator. The statement that all of these different expansions have to agree with each other is called crossing symmetry and it results in the consistency conditions called the bootstrap equations.

The idea of the conformal bootstrap, in fact, goes back to groundbreaking papers by Ferrara, Gatto, Grillo, and Polyakov [35, 36] which led to a partial classification of two-dimensional CFTs in the '80s and '90s while the study of higher dimensional theories procrastinated. The conformal bootstrap experienced a renaissance when the authors of [27] proposed a numerical method based on linear programming which extracts rigorous bounds on CFT data from conformal bootstrap equations.

Now let us sketch the key points of this method where the central observables are four-point functions of primary operators– see section 1.4. For simplicity, consider four identical scalar operators in Euclidean space,

$$G(x_1, x_2, x_3, x_4) = \langle \mathcal{O}(x_1)\mathcal{O}(x_2)\mathcal{O}(x_3)\mathcal{O}(x_4)\rangle \tag{1}$$

such that crossing symmetry is just invariance under permutations of the points $x_i \in \mathbb{R}^d$. Using the convergent Operator Product Expansion (OPE), one can derive the conformal block decomposition

$$G(x_1,x_2,x_3,x_4) = \sum_{\Delta,\ell} C^2_{\Delta,\ell}\, G^{12,34}_{\Delta,\ell}(x_1,x_2,x_3,x_4)\ , \qquad C^2_{\Delta,\ell} \geq 0\,, \tag{2}$$

where C_Δ are theory-dependent OPE coefficients corresponding to $f_{\mathcal{O}\mathcal{O}\mathcal{O}_k}$ in figure. 1. $G^{12,34}_{\Delta,\ell}$ are kinematic functions called conformal blocks. $SO(d,2)$ unitarity implies that $C^2_{\Delta,\ell} \geq 0$ and imposes lower bounds on the dimensions Δ that can appear in (2). Remarkably, the compatibility of crossing symmetry, unitarity and the conformal block expansion (2) leads to non-trivial bounds in the space of CFTs. For example, it leads to a very precise determination of critical exponents in the Ising and $O(N)$ models in three dimensions [37].

Nonperturbative cosmological bootstrap

QFT in dS contains observables like (1). These are obtained by studying four-point correlations functions in the late-time limit. In this context, crossing symmetry still holds. In fact, invariance under permutation of the points $x_i \in \mathbb{R}^d$ is an immediate consequence of operators commuting at spacelike separation. We can use the resolution of the identity decomposed into unitary irreducible representations of $SO(d+1,1)$ to obtain

$$G(x_1,x_2,x_3,x_4) = \sum_{\ell} \int d\nu\, I_\ell(\nu)\, \Psi^{12,34}_{\frac{d}{2}+i\nu,\ell}(x_1,x_2,x_3,x_4)\,, \qquad I_\ell(\nu) \geq 0\,, \tag{3}$$

where Ψ is a kinematic function often termed conformal partial wave[6]. $SO(d+1,1)$ unitarity implies positivity of the expansion coefficients $I_\ell(\nu) \geq 0$. Our main message in part I of this thesis is that the similarity between these two setups

Conformal Bootstrap : (1) + (2)
QFT in dS Bootstrap : (1) + (3)

suggests that one may be able to develop (numerical) conformal bootstrap methods to obtain non-perturbative constraints on the space of QFTs in dS. In this work, we give the first steps in this program.

Quantum field theory in AdS: Motivation

After a brief introduction on the Quantum field theory in dS spacetime, let us change the curvature sign and go to AdS. There are various motivations to study QFTs that live in

---

[6] For simplicity, here we assumed that only principal series representations contribute to this four-point function. We discuss the appearance of other representations in more details in section 2.2.

AdS. One is that it is the leading semi-classical approximation to quantum gravity where the gravitational fluctuations are suppressed and one can assume a rigid background. So, it carries some of the structures that appear in quantum gravity in AdS.

Second is that one can take the curvature of AdS to zero and recover the flat space limit in which instead of directly studying the flat space physics, we can look at the boundary correlation functions that define a conformal theory [7] and employ the power of the conformal bootstrap. The AdS zero curvature-limit corresponds to the large scaling dimension of the boundary operators. For instance, the authors of [38] find universal bounds on the cubic couplings in 2D flat space QFTs using 1D conformal bootstrap by obtaining flat space scattering amplitudes from the boundary correlators in this limit.

Lastly, AdS is like a box in both classical and quantum mechanical senses. At the classical level, massive (or massless) particles in AdS would propagate close to the boundary (in case of massless/light-like: all the way to the boundary) and bounce back. In the quantum mechanical sense, AdS introduces an IR cutoff where it forbids large wavelength. This leads to a discrete energy spectrum. Strictly speaking, the energies take the form of $\Delta + m$ where m is a set of non-positive integers. The discretized-spectrum nature of AdS makes it a great lab for numerical investigations such as Hamiltonian truncation.

Hamiltonian truncation

Hamiltonian truncation methods in QFT are the generalized versions of the variational method of Rayleigh-Ritz in quantum mechanics. They are numerical methods to find the energy spectrum and eigenstates of a theory. In these methods, one starts from a solvable theory with a known Hamiltonian H_0 deformed by potential $\mathfrak{V}$:

$$H = H_0 + \lambda \mathfrak{V} \tag{4}$$

where deformation parameter λ is not necessarily small meaning that this method is nonperturbative. Then, after introducing a UV cutoff Λ, the Hamiltonian matrix will be constructed in a truncated basis of the unperturbed theory, where the states have energy less than Λ. By diagonalizing this matrix, one expects to recover the spectrum of the theory as we increase Λ. Introducing a UV cutoff helps us to truncate the infinite-dimensional Hilbert space to a finite-dimensional basis and makes it possible to feed it to a computer.

In equal-time quantization of QFT in Minkowski or Euclidean space, one deals with the spectrum that is labeled with a continuous parameter like momentum. So, there are infinite number of states with energy less than a UV cutoff that makes it impossible to truncate the Hilbert space to a finite-dimensional basis. There are different approaches to this technical problem. One is to put the theory on a spacetime with a compact spatial section, for instance, on a cylinder $\mathbb{R}\times S^d$ [39–41] or sphere S^{d+1} [42] so that the spectrum becomes discretized with the natural IR regulator coming from the geometry. Then, one can recover the $\mathbb{R}^d$ or $\mathbb{M}^d$ by taking the limit of radius R to infinity. Another approach is to discretize the momentum directly [43, 44]. AdS spacetime, on the other hand, has a discretized spectrum to begin with. So it is a great candidate to implement Hamiltonian truncation.

---

[7] Here we avoid to call it a conformal "field" theory as this boundary theory does not possess stress tensor.

Hamiltonian truncation in AdS

In this thesis, we shall study deformations of exactly solvable theories. The action is given by

$$S = S_0 + \lambda \int_{\mathrm{AdS}_{d+1}} dx \sqrt{g}\, \mathcal{V}(x) \tag{5}$$

where g is the metric of AdS_{d+1} and $\mathcal{V}$ is a bulk local operator with mass dimension $\Delta_{\mathcal{V}} < d+1$. Let us emphasize that the metric is non-dynamical: this is a study of QFT in a fixed curved background. The unperturbed theory described by S_0 can either be a free theory or a solvable Boundary CFT (BCFT).[8]

In this setup, physical observables depend on the dimensionless parameter $\bar{\lambda} \equiv \lambda R^{d+1-\Delta_{\mathcal{V}}}$. This parameter allows us to continuously connect the perturbative regime of small $\bar{\lambda}$ with the strongly coupled regime of large $\bar{\lambda}$. This is similar to the case mentioned above of QFT on $\mathbb{R}\times S^d$. The choice of the AdS_{d+1} background has two main advantages. The first is that it preserves more symmetry. The isometry group of (Lorentzian) AdS_{d+1} is the conformal group $SO(2,d)$. This means that the Hilbert space of the theory organizes into representations of the conformal algebra. The second advantage is that AdS has a conformal boundary where we can place boundary operators and their correlation functions solve conformal bootstrap equations. This means that the well-established conformal bootstrap methods can be used to study non-conformal QFTs [38]. Notice that the extrapolation to $\bar{\lambda} \to \infty$ corresponds to the flat space limit where the mass spectrum and scattering amplitudes of the QFT in flat space can be recovered.

In the present thesis, we choose to study the above setup in the Hamiltonian framework. To be precise, we study the theory (5) in global coordinates, which endow AdS with the topology of a solid cylinder. The Hilbert space is that of the undeformed theory

---

[8] Notice that AdS_{d+1} is conformally equivalent to $\mathbb{R}^d \times \mathbb{R}^+$. This is obvious in Poincaré coordinates

$$ds^2_{\mathrm{AdS}} = \frac{R^2}{z^2}\left(dz^2 + dx^i dx_i\right)\,, \qquad x^i \in \mathbb{R}^d\,, \qquad z > 0\,.$$

corresponding to S_0. The time evolution is governed by a Hamiltonian of the form[9]

$$H = H_0 + \bar{\lambda}\, V \tag{6}$$

where H_0 is the Hamiltonian of the $\lambda = 0$ theory, and the interaction term V corresponds to $\mathcal{V}$ integrated over a timeslice (this is explained in detail in section 7.3).

The key problem we address in our work is the diagonalization of H for finite λ, which describes how the states and their energies change after turning on the bulk interaction $\mathcal{V}$. Since the strength of the dimensionless coupling $\bar{\lambda}$ grows with R, the small-radius limit can be attacked in Rayleigh-Schrödinger perturbation theory (see e.g. [45]), but when R is sufficiently large the theory is in a strong-coupling regime, and perturbation theory breaks down[10]. Nevertheless, we can attempt to study this diagonalization problem using the Hamiltonian truncation toolbox. In this work, as the first step in this direction, we focus on two-dimensional theories. We study several two-dimensional QFTs in AdS$_2$ including deformation of free massive scalar with ϕ^4 interaction and relevant deformations of minimal models such as the Lee-Yang model and the Ising model. It is worth stressing that the application of equal-time Hamiltonian truncation to infinite volume physics is new — although lightcone conformal truncation [43, 44] can be used to treat flat-space physics using Hamiltonian truncation technology.[11] In this respect, AdS is an ideal playground: due to the UV/IR connection familiar from AdS/CFT, the conformal theory on the boundary provides a handle on the infrared behavior of the observables.

Outline

This thesis is made of three main parts.

Part I is devoted to a brief summary of the basics of conformal field theories in $d \geq 3$ dimensions as well as QFT in dS. In section (1), we derive the conformal algebra and its representations, we discuss the state-operator correspondence, the unitarity bounds and operator product expansion, and we conclude with the conformal block expansion of the four-point functions and the conformal bootstrap. Although on the way we might spell out some details that have been skipped in standard sources, this section should be seen more as a review rather than a complete pedagogical reference. For a more detailed and self-contained discussion we refer to [48–51]. Section 2, provides some preliminaries for Part II. It includes a review of the basics of maximally symmetric geometries to highlight the similarities between (E)AdS, dS and Sphere, with a special emphasis on dS. Next, in section 2.2, we review the unitary representations of QFT in dS and and present a nonperturbative definition of dS correlation functions in section 2.3. Later, we solve free field theory in dS, canonically quantize it and construct its Hilbert space. In section 2.5, we review the in-in formalism that is used for perturbative calculations in dS, derive the massive free field two-point function in dS and EAdS and state why they are very similar. Then, we construct the dictionary between EAdS and dS Feynman diagrams. We conclude part I with a section that is less pronounced in the literature where we construct the Hilbert space representations and spell out the resolution of identity in (2.117).

---

[9] The Hamiltonian is dimensionless because we measure energies in units of $1/R$, with R the AdS radius.

[10] See the recent work [46] for a lattice Monte Carlo approach to address the finite-coupling regime in AdS$_2$.

[11] In lightcone conformal truncation, the need to work with a finite basis of states leads to an effective IR cutoff, see for instance the discussion in appendix F of [47].

Part ll aims to initiate a nonperturbative treatment of QFT in rigid dS background. In section 3, the focus is on the *bulk* two-point function, where we derive the Källén–Lehmann representation as well as an inversion formula for the spectral density with two different methods: analytical continuation from sphere in eq. (3.50a) and analytical continuation from EAdS in eq. (3.58). Next, we clarify the concept of boundary operators by relating them to spectral density poles and conclude with concrete examples of massive free field and CFT in bulk.

In section 4, we study the partial wave expansion of *boundary* four-point functions and derive the corresponding positivity conditions. We then calculate the partial wave coefficient of massive free theory in bulk as well as for the leading order of $\lambda\phi^4$ interaction in section 4.2. It turns out that unitarity requires appearance of local terms in free theory discussed in section 4.2.2. Lastly, in section 5, we focus on dS_2 to set up a de Sitter bootstrap program. After reviewing basics of the one-dimensional CFTs, we discuss the convergence issue of partial wave expansion in dS. This issue has been overcome by proposal of a regularization scheme in 5.3. In the end, a concrete example of non-trivial bound on partial wave coefficietns is presented in section 5.4

Part lll develops a Hamiltonian truncation method to compute the energy spectrum of QFTs in two-dimensional EAdS. In section 7, we review some basic features of the physics and symmetries of AdS_2. In section 8, we explain in detail the existence of UV divergences that arise in the Hamiltonian truncation scheme, and we explain how to obtain the correct continuum limit in a large class of theories. This section contains one of the main results of the this part, *i.e.* eq. (8.1), which allows to obtain the correct energy gaps. Finally, in sections 9 and 10, we present results for several theories. The massive free scalar deformed by ϕ^2 and ϕ^4 operators is discussed in detail in section 9. Next, in section 10, we study relevant deformations away from the Lee-Yang and Ising minimal models. The exactly solvable models – *e.g.* the massive free theories – allow to test the formula (8.1). On the contrary, figures 9.7, 10.5, 10.6, 10.17 and 10.18 contain genuinely nonperturbative results on the spectrum of strongly coupled theories in EAdS. Throughout this part and the corresponding appendices, we deal only with EAdS and not AdS. So for convenience, we drop "Euclidean" and simply use AdS for EAdS.

We also include several complementary **appendices**. Some of them are devoted to the list of identities: sections A and F, as well as detailed calculations and derivations of certain formulae: section B and C; while some of them are independent but conceptually important discussions that do not fit within the storyline of the main parts. This includes the derivation of a new simple formula for the order-λ^n correction to the eigenvalues of the Hamiltonian in perturbation theory in appendix G, discussion of spontaneous symmetry breaking in EAdS in appendix J and decomposition of unitary irreps of $SO(2,2)$ into $SO(2,1)$ in appendix D.

Notation and conventions

- In this thesis we use mostly positive metric signature. We also used the shorthand notation of $x.y$ for $x_\mu y^\mu$ and x^2 for $x_\mu x^\mu$. We discuss the dS_{d+1} and AdS_{d+1} with d-dimensional boundary theories.
- In the first and second part, when we are using the irreducible representations of $SO(d+1,1)$ or dimension of operators in QFT in dS, we frequently use $\Delta = \frac{d}{2} + i\nu$. Plus
- Any place we use $i\epsilon$ prescription as a regulator, we assume $\epsilon > 0$ with $\epsilon \to 0^+$.
- x_{ij} is a short notation for $x_i - x_j$.
- In the third part and its corresponding appendices, we consider Euclidean AdS but simply call it AdS for brevity.

Preliminaries Part I

1 Conformal field theories

1.1 Conformal transformations

The IR and UV fixed points of the Renormalization Groups (RGs) are scale invariant. The scale-invariance usually gets enhanced to the conformal invariance. This is proven in two-dimensional unitary theories [29] but there is no proof for higher dimensions [31–34]. For a pedological discussion see [49, sec. 1.3] or [30]. This makes the study of CFTs an important subject in theoretical physics.

Conformal invariance as transformations $x^\mu \to \tilde{x}^\mu$ that preserve the angles translate to diffeomorphisms in which the metric transforms as[1]

$$g_{\mu\nu}(x) \to \tilde{g}_{\mu\nu}(\tilde{x}) = \frac{\partial x^\alpha}{\partial \tilde{x}^\mu}\frac{\partial x^\beta}{\partial \tilde{x}^\nu} g_{\alpha\beta}(x) = \Omega^{-2}(x) g_{\mu\nu}(x) \ . \tag{1.1}$$

From now on, we work in Euclidean space with $g_{\mu\nu}(x) = \delta_{\mu\nu}$ except it is mentioned otherwise and $\mu = 1, 2, \cdots d$. The generators of these diffeomorphisms are labelled by the conformal Killing vector ϵ. For an infinitesimal transformation $x^\mu \to \tilde{x}^\mu = x^\mu + \epsilon^\mu(x)$, eq. (1.1) gives the conformal Killing equation:

$$\partial_\mu \epsilon_\nu + \partial_\nu \epsilon_\mu = \frac{2}{d} \partial . \epsilon \, \delta_{\mu\nu} \ . \tag{1.2}$$

This is similar to the Killing equation with the difference that right-hand side there is zero ($\partial.\epsilon = 0$). The solution to eq. (1.2) is

---

[1] This can be seen by considering the fact that the angle θ between two vectors $A^\mu(x)$ and $B^\mu(x)$ are $\cos(\theta) = \frac{A.B}{|A||B|} = \frac{\tilde{A}.\tilde{B}}{|\tilde{A}||\tilde{B}|}$, where $A.B = A^\mu B^\nu g_{\mu\nu}$ and $|A| = \sqrt{A.A}$.

$$\begin{aligned} &\epsilon^\mu(x) = a^\mu \ , && \text{(translation)} \\ &\epsilon^\mu(x) = m^\mu{}_\nu x^\nu \ , && \text{(rotation)} \\ &\epsilon^\mu(x) = c x^\mu \ , && \text{(dilatation)} \\ &\epsilon^\mu(x) = 2(x.b)x^\mu - x^2 b^\mu \ , && \text{(SCT)} \end{aligned} \tag{1.3}$$

where $a^\mu, m^\mu{}_\nu, c, b^\mu$ are constants and m^μ_ν is an antisymmetric tensor. Note that the first two are associated with the Poincare transformations ($\partial.\epsilon = 0$) only coming from homogeneity and isotropy of the space. One may exponentiate these and find the finite version of these transformations:

$$\begin{aligned} &\tilde{x}^\mu(x) = x^\mu + a^\mu \ , && \text{(translation)} \\ &\tilde{x}^\mu(x) = R^\mu{}_\nu x^\nu \ , && \text{(rotation)} \\ &\tilde{x}^\mu(x) = c x^\mu \ , && \text{(dilatation)} \\ &\tilde{x}^\mu(x) = \frac{x^\mu - b^\mu x^2}{1 - 2b.x + b^2 x^2} \ , && \text{(SCT)} \end{aligned} \tag{1.4}$$

where $R^\mu{}_\nu$ are rotation matrices in $\mathbb{R}^d$. The first three are easy to proof. To proof the last one, note that the infinitesimal version of SCT can be written as an inversion defined as

$$I : x^\mu \to \tilde{x}^\mu = \frac{x^\mu}{x^2} \ . \tag{1.5}$$

followed by a translation of $-b^\mu$ and another inversion:

$$\frac{\frac{x^\mu}{x^2} - b^\mu}{|\frac{x^\mu}{x^2} - b^\mu|^2} = x^\mu + 2(x.b)^\mu - x^2 b^\mu \tag{1.6}$$

where we dropped the higher order terms in b. Now since $I^2 = 1$, the finite version of SCT is also an inversion followed by a finite translation of $-b^\mu$ and another inversion which is given in (1.4).

1.2 Conformal algebra

The infinitesimal transformations of coordinates and the fields can in general be seen as

$$\tilde{x}^\mu = x^\mu + \epsilon^\mu = x^\mu + \omega_a \frac{\delta x^\mu}{\delta \omega_a} \ , \quad \tilde{\mathcal{O}}(\tilde{x}) = \mathcal{O}(x) + \omega_a \frac{\delta \mathcal{F}}{\delta \omega_a}(x) \tag{1.7}$$

where ω_a represent an infinitesimal parameter and index a is just a label, not a Lorentz index. The generator G_a is defined as[2]

$$\tilde{\mathcal{O}}(x) - \mathcal{O}(x) \equiv -\omega_a G_a \mathcal{O}(x) \tag{1.8}$$

– the variation of the field discarding the change of coordinates. Then by using the fact that

$$\tilde{\mathcal{O}}(\tilde{x}) = \mathcal{O}(\tilde{x}) - \omega_a \frac{\delta x^\mu}{\delta \omega_a} \partial_\mu \mathcal{O}(\tilde{x}) + \omega_a \frac{\delta \mathcal{F}}{\delta \omega_a}(\tilde{x}) \tag{1.9}$$

one finds

$$G_a \mathcal{O}(x) = -\frac{\delta x^\mu}{\delta \omega_a} \partial_\mu \mathcal{O}(x) + \frac{\delta \mathcal{F}}{\delta \omega_a}(x) \ . \tag{1.10}$$

Now, by asking that infinitesimal conformal transformations (1.3), leave our field invariant: $\delta\mathcal{F}/\delta\omega_a = 0$, we find the generators of the conformal group

$$\begin{aligned}
&\hat{P}_\mu = -\partial_\mu \ , && \text{(translation)} \\
&\hat{M}_{\mu\nu} = x_\mu \partial_\nu - x_\nu \partial_\mu \ , && \text{(rotation)} \\
&\hat{D} = -x.\partial \ , && \text{(dilatation)} \\
&\hat{K}_\mu = (x^2 \partial_\mu - 2x_\mu x.\partial) \ , && \text{(SCT)}
\end{aligned} \tag{1.11}$$

We name these differential generators with $\hat{Q}$ to contrast with the definition of corresponding charges that will be defined later in section 1.3, but for convenience we will drop the hat from now on. These generators satisfy commutation relation

$$\begin{gathered}
[D, P_\mu] = P_\mu \ , \qquad [D, K_\mu] = -K_\mu \ , \qquad [K_\mu, P_\nu] = 2\delta_{\mu\nu} D - 2M_{\mu\nu} \ , \\
[M_{\mu\nu}, P_\rho] = \delta_{\nu\rho} P_\mu - \delta_{\mu\rho} P_\nu \ , \qquad [M_{\mu\nu}, K_\rho] = \delta_{\nu\rho} K_\mu - \delta_{\mu\rho} K_\nu \ , \\
[M_{\mu\nu}, M_{\rho\sigma}] = \delta_{\nu\rho} M_{\mu\sigma} - \delta_{\mu\rho} M_{\nu\sigma} + \delta_{\nu\sigma} M_{\rho\mu} - \delta_{\mu\sigma} M_{\rho\nu}
\end{gathered} \tag{1.12}$$

as well as $[P_\mu, P_\nu] = 0$, $[K_\mu, K_\nu] = 0$ and $[D, M_{\mu\nu}] = 0$. This is called the Euclidean conformal algebra. Note that we found these commutation relations solely using group theory facts. Now let us define the following generators

$$\begin{gathered}
D = J_{-1,0} \ , \qquad M_{\mu\nu} = J_{\mu\nu} \ , \\
J_{-1,\mu} = \frac{1}{2}(P_\mu - K_\mu) \ , \qquad J_{0,\mu} = \frac{1}{2}(P_\mu + K_\mu)
\end{gathered} \tag{1.13}$$

where $J_{AB} = -J_{BA}$ and $A, B \in -1, 0, 1, \cdots, d$. These generators obey commutation relations:

$$[J_{AB}, J_{CD}] = -\eta_{AC} J_{BD} - \eta_{BD} J_{AC} + \eta_{BC} J_{AD} + \eta_{AD} J_{BC} \ , \tag{1.14}$$

where $\eta_{AB} = \text{diag}(-1, 1, \ldots, 1)$. This is the familiar $\mathfrak{so}(d+1, 1)$ algebra reminding us that the Euclidean conformal group is isomorphic to the Lorentz group $SO(d+1, 1)$. This means that the d-dimensional conformal group, unlike its rather non-trivial action on $\mathbb{R}^d$, acts much more naturally (linearly) on the $\mathbb{R}^{d+1,1}$. This is the basis of the embedding space formalism. One application of the embedding space formalism, for instance, is an easier way of finding the two and three-point functions. See e.g. [49, 50, 52].

---

[2] Some of the sources define G_a with a $-i$ in their definition: $\tilde{\mathcal{O}}(x) - \mathcal{O}(x) = -i\omega_a G_a \mathcal{O}(x)$. We picked the convention without i as it will put the commutation relation (1.12) in a more convenient form.

1.3 Ward identities and conformal charges

A local QFT possesses a stress tensor that satisfies the Ward identity[3]

$$\partial_\mu \langle T^{\mu\nu} \mathcal{O}_1(x_1) \cdots \mathcal{O}_n(x_n) \rangle = -\sum_i \delta^d(x-x_i) \partial^\nu \langle \mathcal{O}_1(x_1) \cdots \mathcal{O}_n(x_n) \rangle \ , \tag{1.15}$$

that in classical level reduces to the conversation of the stress tensor

$$\partial_\mu T^{\mu\nu} = 0 \ . \tag{1.16}$$

For each conformal Killing vector ϵ, there exists a conserved charge operator defined as

$$Q_\epsilon(\Sigma) = -\int_\Sigma dS_\mu \epsilon_\nu(x) T^{\mu\nu}(x) \ , \tag{1.17}$$

where Σ is a closed and oriented codimension-1 surface. Now, we will argue that the traceless-ness of the stress tensor implies (1.2)[4]. First, note that the $Q_\epsilon(\Sigma)$ being a conserved charge means that it is invariant under the deformations of surface Σ as long as it does not cross any operator. These type of operators are called topological surface operators. The integration in (1.17) can be rewritten using the divergence theorem as an integral over V, the interior of Σ:

$$Q_\epsilon(\Sigma) = -\int_V dV \partial_\mu(\epsilon_\nu(x) T^{\mu\nu}(x)) \ , \tag{1.18}$$

At the classical level, since the integration is valid for any deformation of Σ, one finds

$$\begin{aligned} 0 &= \partial_\mu(\epsilon_\mu T^{\mu\nu}) && (1.19)\\ &= \partial_\mu \epsilon_\nu T^{\mu\nu} + \epsilon_\nu \partial_\mu T^{\mu\nu} && (1.20)\\ &= \frac{1}{2}(\partial_\mu \epsilon_\nu + \partial_\nu \epsilon_\mu) T^{\mu\nu} \ , && (1.21) \end{aligned}$$

where we used the conservation of the stress tensor and the fact that it is a symmetric tensor. If we do not consider the traceless-ness of the stress tensor and take $T^{\mu\nu}$ as a generic tensor, we arrive at (1.2) with right-hand side equal to zero. The solution of ϵ is the translation and rotation that exist in any QFT with Poincare invariance. However, if traceless-ness is asked, the constraints are more powerful and we find (1.2) with the conformal Killing solution (1.3). At the quantum level, consider the correlation function

---

[3] For the definition of the stress tensor see e.g. section 2.3 of [50]

[4] Here we are neglecting Weyl anomoly as we focus on flat metric.

$$\langle Q_\epsilon(\Sigma)\mathcal{O}_1(x_1)\cdots\mathcal{O}_n(x_n)\rangle \ , \tag{1.22}$$

as long as we do not cross any operator by a deformation of Σ_1 to Σ_2, the charge Q would not change, then one finds (1.2) using the Ward identity (1.3). In summary, the assumption of traceless-ness of the stress tensor and the existence of the conserved charges imply the conformal Killing equation.

The inverse is also true: the conformal Killing equation and traceless-ness define conserved charges. The corresponding charges of the four types of the conformal transformation is defined by (1.17) as

$$\begin{aligned}
&a_\nu P^\nu = -\int_\Sigma dS_\mu a_\nu T^{\mu\nu} && \rightarrow \quad P^\nu = -\int_\Sigma dS_\mu T^{\mu\nu} \ , \\
&m_{\nu\sigma}M^{\nu\sigma} = -\int_\Sigma dS_\mu m_{\nu\sigma}x^\sigma T^{\mu\nu} && \rightarrow \quad M^{\nu\sigma} = -\frac{1}{2}\int_\Sigma dS_\mu \left(x^\sigma T^{\mu\nu} - x^\nu T^{\mu\sigma}\right) \ , \\
&cD = -\int_\Sigma dS_\mu c x_\nu T^{\mu\nu} && \rightarrow \quad D = -\int_\Sigma dS_\mu x_\nu T^{\mu\nu} \ , \\
&b_\nu K^\nu = -\int_\Sigma dS_\mu \left(2(x.b)x_\nu - x^2 b_\nu\right) T^{\mu\nu} && \rightarrow \quad K^\nu = -\int_\Sigma dS_\mu \left(2x^\nu x_\sigma T^{\mu\sigma} - x^2 T^{\mu\nu}\right) \ .
\end{aligned}$$

These charges satisfy the conformal algebra of (1.12). For a proof look at e.g [51, sec 3.2] where the commutation relations of charges with the stress tensor are established first.

1.4 Conformal representation: Primary operators

As usual in QFTs, we are interested in irreducible representations (irreps) of the symmetry group to describe the Hilbert space[5]. In what follows we will build this irreducible representation of the conformal group by organizing operators of the theory.

The dilatation and rotation in conformal algebra commute i.e. they belong to the Cartan subalgebra. That means we can diagonalize them simultaneously and label our representation with their eigenvalues. We choose to name the eigenvalue of rotation operator $M_{\mu\nu}$, the spin ℓ and the eigenvalue of dilatation operator D, the scaling dimension Δ. The reason for this particular naming will be apparent shortly. In summary, we have:

$$[D,\mathcal{O}(0)] = \Delta\mathcal{O}(0) \ , \qquad [M_{\mu\nu},\mathcal{O}^a(0)] = (\Sigma_{\mu\nu})^a{}_b\mathcal{O}^b(0) \tag{1.23}$$

where a, b are $SO(d)$ representation indices of $\mathcal{O}$ and $\Sigma_{\mu\nu}$ matrix satisfies the SO(d) algebra that is same algebra as $M_{\mu\nu}$s among themselves. According to (1.12), similar to quantum harmonic oscillator problem, P^μ and K^μ respectively raise and lower the scaling dimension. It is also a reasonable physical assumption to ask that the scaling dimension be bounded from below[6]. So we define the *conformal primary operators* as

---

[5] As a result of state-operator correspondence, we are able to do this for the operators as well. See section 1.6

$$[K_\mu, \mathcal{O}^a(0)] = 0 \; . \tag{1.24}$$

By this, we reach a lowest weight representation in which each multiplet is made of a primary operator and its tower of *descendants* with scaling dimensions integer-ly separated from Δ defined as:

$$\mathcal{O}(0) \to P_{\mu_1} \cdots P_{\mu_n} \mathcal{O}(0) \; , \qquad \Delta \to \Delta + n \; . \tag{1.25}$$

It turns out that in a unitary CFT, *all operators can be written as a linear combination of primaries and their descendants.* This makes the spectrum and operator content of CFTs pretty peculiar. As a side comment note that (1.23) commutation relations are not necessarily valid for a generic operator.

To find the commutation relations of a primary operator at location x, one can use the relation $\mathcal{O}(x) = e^{x.P}\mathcal{O}(0)e^{-x.P}$, the Baker-Campbell-Hausdorff formula and the conformal algebra to reach:

$$\begin{aligned}
[P_\mu, \mathcal{O}^a(x)] &= \partial_\mu \mathcal{O}^a(x) \\
[M_{\mu\nu}, \mathcal{O}^a(x)] &= (x_\nu \partial_\mu - x_\mu \partial_\nu)\mathcal{O}^a(x) \\
[D, \mathcal{O}^a(x)] &= (x.\partial + \Delta)\mathcal{O}^a(x) \\
[K_\mu, \mathcal{O}^a(x)] &= (2x_\mu x.\partial - x^2\partial_\mu + 2\Delta x_\mu - 2x^\nu (\Sigma_{\mu\nu})^a{}_b)\mathcal{O}^b(x)
\end{aligned} \tag{1.26}$$

1.5 Radial quantization

No matter how one quantizes the field theory – canonical quantization or path integral formalism – one needs a notion of the foliation of space-time. These foliations are the Cauchy surfaces on which one asks particular boundary conditions for the path integral quantization or particular commutation relations for canonical quantization. Then one can evolve to another foliation by a time-like vector field like hamiltonian. We usually quantize the theory with constant-time foliations (like most of the standard QFT textbooks). Even if the space is Euclidean, we chose one of the coordinates to be the time and foliate the space with constant-times. However, this is not the only way to quantize the theory. Consider the foliation of space with spheres of radius r centered at the origin. The time-evolution from one sphere with radius r_1 to sphere with radius r_2 is with the dilatation operator $\hat{\Delta} = x.\partial_x = r\partial_r$. It turns out that this quantization – so-called *radial quantization* – is a more convenient quatization in a CFT:

---

[6] For example, as we see in section 1.8.1, the scale invariance of a theory results in the two-point function of type: $\langle \mathcal{O}(x_1)\mathcal{O}(x_2)\rangle \propto |x_1 - x_2|^{-2\Delta}$. We expect that a physically sensible theory does not have growing two-point function when two operators are far from each other. This is similar to ask that the energy of the system be bounded from below.

Cylinder interpretation

The correlation functions of primary operators under Weyl transformations

$$g_{\mu\nu} \to \tilde{g}_{\mu\nu} = \Omega^2(x) g_{\mu\nu} \tag{1.27}$$

satisfy the relation:

$$\langle \mathcal{O}_1(x_1) \cdots \mathcal{O}_n(x_n) \rangle_{\Omega^2(x) g_{\mu\nu}} = \left(\prod_i \frac{1}{\Omega^{\Delta_i}(x_i)} \right) \langle \mathcal{O}_1(x_1) \cdots \mathcal{O}_n(x_n) \rangle_{g_{\mu\nu}} \ . \tag{1.28}$$

This is not a trivial statement and we do not provide a proof here. For the sketch of the proof see for example [51, section 6.4]. Equation (1.28) says that the correlation functions of a CFT in flat space are related to the correlation functions of a CFT with a metric equivalent to the flat space by Weyl transformation up to a product of some rescalling Weyl factors.

Now consider the cylinder $\mathbb{R} \times S^{d-1}$ that has the metric of the flat space $\mathbb{R}^d$ in radial coordinates:

$$\begin{aligned} ds^2_{\mathbb{R}^d} &= dr^2 + r^2 d\Omega^2_{d-1} \\ &= e^{2\tau} \left(d\tau^2 + d\Omega^2_{d-1} \right) \ , \qquad \text{with} \ \ r = e^{\tau} \ . \\ &= e^{2\tau} ds^2_{\mathbb{R} \times S^{d-1}} \end{aligned} \tag{1.29}$$

up to a Weyl factor of $\Omega = e^{\tau}$. So each sphere of radius r corresponds to a constant time slice τ on the cylinder. Therefore the radially quantized theory on flat space is equivalent to the theory with ordinary equal-time quantization on the cylinder up to the Weyl factors in (1.28). Moreover, the Dilatation in flat space is equal to the time translation on cylinder: $D = r\partial_r = \partial_\tau$. This says that the spectrum of the dilatation on $\mathbb{R}^d$ is the same as the energy spectrum for the theory on $\mathbb{R} \times S^{d-1}$. These are the basic ingredients of one of the proofs of the state-operator correspondence:

1.6 The state-operator correspondence and OPE

The state-operator correspondence states that there is a one-to-one map between states and local operators in a CFT. This can be seen by the cylinder picture we gave above. A local operator at origin in $\mathbb{R}^d$, prepares a state on $\tau = -\infty$ in the cylinder that can evolve and produce the state at time r or τ: *Operator* → *State*. On the other hand, a state at time defined in time τ can evolve back to $\tau = -\infty$ by the hamiltonian (and Dilatation operator at the same time) on the cylinder. This process translates to the shrinking of the spheres on $\mathbb{R}^d$ all the way to the origin and defining a local operator at the origin: *State* → *Operator*. In summary, we have:

$$\mathcal{O}(0) \longleftrightarrow \mathcal{O}(0) \left|0\right\rangle \equiv \left|\mathcal{O}(0)\right\rangle \tag{1.30}$$

One can also see that the operator at position x is a linear combination of descendants:

$$\mathcal{O}(x)\left|0\right\rangle = e^{x.P}O(0)e^{-x.P} = e^{x.P}\left|\mathcal{O}(0)\right\rangle = \sum_{n=0}^{\infty}(x.P)^n\left|\mathcal{O}(0)\right\rangle \ . \tag{1.31}$$

In the arguments above we used the flat space-cylinder map that takes advantage of the full conformal symmetry in equation (1.28) to prove the state-operator correspondence. However, only scale invariance is enough to derive the state-operator map. We refer to [51, sec 6] for the proof.

Operator product expansion

In a generic quantum field theory, one can expand a product of two operators in terms of a linear combination of local operators:

$$\mathcal{O}_1(x)\mathcal{O}_2(0) = \sum_n C_{12}^n(x)\mathcal{O}_n(0) \ . \tag{1.32}$$

This is called the Operator Product Expansion (OPE). In a radially quantized conformal field theory, such a product produces a state on a sphere with radius $r > |x|$. Since every state in a CFT is a linear combination of primaries and their descendants, we can decompose this state as

$$\mathcal{O}_1(x)\mathcal{O}_2(0)\left|0\right\rangle = \sum_k C_{12k}(x,P)\mathcal{O}_k(0)\left|0\right\rangle \ , \tag{1.33}$$

in which the sum is over primaries $\mathcal{O}_k$ and $C_{12k}(x,P)$ produces descendants with its dependency on translation generator P. As a result of the state-operator correspondence, one can write the equation above in the terms of operators

$$\mathcal{O}_1(x_1)\mathcal{O}_2(x_2) = \sum_k C_{12k}(x_{12},\partial_{x_2})\mathcal{O}_k(x_2) \ . \tag{1.34}$$

This is convergent inside any correlation function where one can find a sphere that involves only operator $\mathcal{O}_1$ and $\mathcal{O}_2$ ($|x_{12}| < |x_{1n}|$ and $|x_{12}| < |x_{2n}|$). The convergence can be easily shown by using the state operator-correspondence. Here we present a sketch of the proof based on [53]. Imagine the product $\mathcal{O}_1(x_1)\mathcal{O}_2(x_2)$ inside a correlation function (we may change the ordering as it is a Euclidean correlation function):

$$\left\langle \phi_1(y_1)\cdots\phi_n(y_n)\mathcal{O}(x_1)\mathcal{O}(x_2)\right\rangle \ . \tag{1.35}$$

Now we choose our quantization scheme to be a radial quantization of spheres with their center at x_2. The action of the operators $\mathcal{O}$ and ϕ on vacuum creates unique states in the Hilbert space according to the state-operator map:

$$|\Psi\rangle = \mathcal{O}_1(x_1)\mathcal{O}_2(x_2)\,|0\rangle \ , \qquad \langle\Phi| = \langle 0|\,\phi_1(y_1)\cdots\phi_n(y_n) \ , \tag{1.36}$$

and the correlation function (1.35) is the scalar product $\langle\Phi|\Psi\rangle$. Since the dilatation operator in radial quantization has a the hamiltonian interpretation on the cylinder, one can expand the state $|\Psi\rangle$ as energy eigenstates with some coefficients:

$$|\Psi\rangle = \alpha_n(x_{12})\,|E_n\rangle \ . \tag{1.37}$$

Note that the states $|E_n\rangle$ are made up of the action of operators with scaling dimension $\Delta_n = E_n$ according to the state-operator map and they can be written as primary operators acting on vacuum following (1.31):

$$|E_n\rangle \sim (x.P)^n\mathcal{O}(0)\,|0\rangle \ , \qquad \text{with } E_n = \Delta_{\mathcal{O}} + n \ . \tag{1.38}$$

which means that there is a one-to-one map between coefficients C_{12k} and $\alpha_n(x_{12})$. Now let us remind you that if one of the states in a scalar product of two states in a Hilbert is expanded in a basis, then the expansion is convergent. Here $|E_n\rangle$s make up such a basis as they are eigenvalues of the hamiltonian in the cylinder. Therefore, the expansion (1.34) is convergent.

This was another important application of the state-operator correspondence. The convergence of OPE has an important consequence in what comes next in this section. In particular, it makes the conformal block expansion in (1.59) exponentially convergent which is responsible for the power of the numerical bootstrap.

1.7 Unitarity bounds

The hermitian conjugation of real scalar operators in Euclidean signature translates to the reflection $\tau \to -\tau$:

$$\mathcal{O}^\dagger(\tau,\vec{x}) = e^{-\tau H}\mathcal{O}^\dagger(0,\vec{x})e^{\tau H} = \mathcal{O}(-\tau,\vec{x}) \tag{1.39}$$

where H is the hamiltonian–the time translation generator. A similar relation holds for spinning operators:

$$\mathcal{O}^\dagger_{\mu_1\cdots\mu_\ell}(\tau,\vec{x}) = \theta^{\nu_1}_{\mu_1}\cdots\theta^{\nu_\ell}_{\mu_\ell}\mathcal{O}^\dagger_{\nu_1\cdots\nu_\ell}(-\tau,\vec{x}) \ , \qquad \theta^\nu_\mu = \delta^\nu_\mu - 2\delta^1_\mu\delta^\nu_1 \tag{1.40}$$

where the euclidean time τ corresponds to the index $\mu,\nu = 1$. Now consider a state of the form

$$|\psi\rangle = \mathcal{O}_1(\tau_1,\vec{x}_1)\cdots\mathcal{O}_n(\tau_n,\vec{x}_n)\,|0\rangle \tag{1.41}$$

where the operators are time-ordered ($\tau_1 > \tau_2 > \cdots > \tau_n$). The norm of this state in a unitary theory has to be positive. This leads to the condition

$$\langle\psi|\psi\rangle = \langle\mathcal{O}_n(-\tau_n,\vec{x}_n)\cdots\mathcal{O}_n(-\tau_1,\vec{x}_1)\mathcal{O}_1(\tau_1,\vec{x}_1)\cdots\mathcal{O}_n(\tau_n,\vec{x}_n)\rangle \geq 0 \tag{1.42}$$

often called the *reflection positivity*.

The conjugation $\tau \to -\tau$ in a theory on the cylinder will be an inversion when we go back to flat space with radial quantization. More precisely we have:

$$\mathcal{O}_{\mu_1,\cdots,\mu_\ell}(x^\mu) = I^{\nu_1}_{\mu_1}\cdots I^{\nu_n}_{\mu_n} x^{-2\Delta}\mathcal{O}_{\nu_1,\cdots,\nu_\ell}(\frac{x^\mu}{x^2}) \ , \qquad I^\nu_\mu = \delta^\mu_\nu - \frac{2x^\mu x_\nu}{x^2} \ . \tag{1.43}$$

Using this, one can show how the stress tensor and consequently the conformal charges would transform under hermitian conjugation in radial quantization and find:

$$D^\dagger = D \ , \qquad {M^\dagger}_{\mu\nu} = -M_{\mu\nu} \ , \qquad P^\dagger_\mu = K_\mu \ . \tag{1.44}$$

Finally, let us consider the state

$$|\psi\rangle = P_\mu P^\mu \,|\mathcal{O}\rangle \tag{1.45}$$

where $\mathcal{O}$ is a scalar primary operator. By demanding positivity for $\langle\psi|\psi\rangle \geq 0$, and using $P^\dagger_\mu = K_\mu$ from (1.44) as well as conformal algebra in (1.12), one obtains bounds on dimensions of primary operators:

$$\Delta = 0 \text{ (identity operator)} \quad \text{or} \quad \Delta \geq \frac{d-2}{2} \ . \tag{1.46}$$

Similarly, there is a bound on the dimension of spinning primary operators given by:

$$\Delta \geq d - 2 + \ell \tag{1.47}$$

1.8 Correlation functions

The lack of existence of a scale in conformal theories, makes the notion of asymptotic states and consequently S-matrix hard to define (See [54] for a more recent discussion). However, we have the notion of correlation functions that are perfectly definable either through canonical quantization or path integral. This makes correlation functions of operators and in particular primary operators the central objects in CFTs. For simplicity, we focus on the scalar operators from now on except it is mentioned otherwise. Most of the found general properties are true for the spinning operators as well. For a systematic approach to the spinning correlators see [52].

1.8.1 Two-point functions

Due to translation and rotation invariance, the two-point functions is only a function of the distance between two points:

$$\langle \mathcal{O}_1(x_1)\mathcal{O}_2(x_2)\rangle = f(|x_1-x_2|)\ , \qquad \text{(translation and rotation invariance)}\ . \tag{1.48}$$

Using (1.26) and scale invariance (meaning that the simultaneous action of D on all operators in a correlator must vanish), we have

$$0 = (x_1.\partial_1 + \Delta_1 + x_2.\partial_2 + \Delta_2) f(|x_1-x_2|)\ , \qquad \text{(scale invariance)}\ . \tag{1.49}$$

which leads to

$$f(|x_1-x_2|) = \frac{C}{|x_1-x_2|^{\Delta_1+\Delta_2}} \tag{1.50}$$

where C is some normalization constant. Then after using the same procedure for the special conformal transformation, one finds

$$\begin{aligned}\langle \mathcal{O}_1(x_1)\mathcal{O}_2(x_2)\rangle &= \frac{\delta_{\Delta_1,\Delta_2}}{|x_{12}|^{2\Delta_1}} \\ &= \frac{\delta_{1,2}}{|x_{12}|^{2\Delta_1}}\end{aligned} \tag{1.51}$$

where in the second line we chose a basis in which the primaries are orthogonal. From now on we work in this basis.

1.8.2 Three-point functions

With a more involved but similar calculation, one can find the three-point function of primary operators as[7]

$$\langle \mathcal{O}_1(x_1)\mathcal{O}_2(x_2)\mathcal{O}_3(x_3)\rangle = \frac{\lambda_{123}}{|x_{12}|^{\Delta_1+\Delta_2-\Delta_3}|x_{23}|^{\Delta_2+\Delta_3-\Delta_1}|x_{13}|^{\Delta_1+\Delta_3-\Delta_2}} \tag{1.52}$$

where λ_{123} is the three-point function coefficient that cannot be set to 1 by rescaling. This coefficient is in fact same as the OPE coefficient this is easy to verify by simply writing OPE expansion of any two operators above and using (1.51)

$$\begin{aligned}\langle \mathcal{O}_1(x_1)\mathcal{O}_2(x_2)\mathcal{O}_3(x_3)\rangle &= \sum_i \frac{\lambda_{12i}}{|x_{12}|^{\Delta_1+\Delta_2-\Delta_i}} C_a(|x_{12},\partial_2|)\, \langle \mathcal{O}_i^a(x_2)\mathcal{O}_3(x_3)\rangle \\ &= \frac{\lambda_{123}}{|x_{12}|^{\Delta_1+\Delta_2-\Delta_3}} C(|x_{12}|,\partial_2)\frac{1}{|x_{23}|^{2\Delta_3}}\ .\end{aligned} \tag{1.53}$$

---

[7] see e.g. [55] that carries out the calculations directly or for example [49] that uses the embedding space formalism for a more staightforward derivation

Since $C(|x_{12}|, \partial_2)$, depends only on Δ_i's and x_i's and their derivatives and it should produce the three-point function structure of

$$\frac{1}{|x_{12}|^{\Delta_1+\Delta_2-\Delta_3}|x_{23}|^{\Delta_2+\Delta_3-\Delta_1}|x_{13}|^{\Delta_1+\Delta_3-\Delta_2}} \tag{1.54}$$

in (1.52), one can identify the three-point function coefficient f_{123} with the OPE coefficient λ_{123}:

$$f_{123} = \lambda_{123} \ . \tag{1.55}$$

1.8.3 Four-point function

CFT four-point function is the first non-trivial n-point function in the sense that it is not totally fixed (up to a coefficient) by conformal symmetry. Still, the conformal symmetry constraints the four-point function. In particular, it is a function two variables

$$u = z\bar{z} = \frac{|x_{12}|^2|x_{34}|^2}{|x_{13}|^2|x_{24}|^2} \ , \qquad v = (1-z)(1-\bar{z}) = \frac{|x_{14}|^2|x_{23}|^2}{|x_{13}|^2|x_{24}|^2} \ , \tag{1.56}$$

that are called conformal cross ratios (this is true for $d > 1$. for $d = 1$ look at section 5.1)[56]:

$$\langle \mathcal{O}_1(x_1)\mathcal{O}_2(x_2)\mathcal{O}_3(x_3)\mathcal{O}_4(x_4)\rangle = \left(\frac{|x_{14}|}{|x_{24}|}\right)^{\delta_{21}} \left(\frac{|x_{14}|}{|x_{13}|}\right)^{\delta_{34}} \frac{g(z,\bar{z})}{|x_{12}|^{\Delta_1+\Delta_2}|x_{34}|^{\Delta_3+\Delta_4}} \ , \tag{1.57}$$

where $\delta_{ij} = \Delta_i - \Delta_j$.

Let us give an intuitive way to see that the four-point function is indeed only a function of two cross ratios (up to the scaling factors behind $g(z, \bar{z}$ above)). Consider the following conformal transformation. First, perform an inversion around a random point that does not coincide with any of the points x_i. Then with a translation, move the origin to point x_4 and perform another inversion to send x_4 to ∞. So far this was only a special conformal transformation. Next, using translation place x_1 at the origin and afterward with a rotation put x_3 on the x-axis. Plus with a scaling, one can place x_3 at position $(1, 0, 0, \cdots)$. Finally, we can rotate to place all the operators in one plane and end up with two free parameters for the position of $\mathcal{O}_2$:

$$x_1 = (0,0,0,\cdots) \ , \quad x_2 = (x,y,0,\cdots) \ , \quad x_3 = (1,0,0,\cdots) \ , \quad x_4 = \infty \tag{1.58}$$

which plugging it back in (1.56), one finds $z = x + iy$ and $\bar{z} = x - iy$. This is showing the fact that in the Euclidean CFT that is the main focus of this thesis, all operators are spacelike separated. So, $z, \bar{z}$ are complex conjugates of each other since u, v are both real. However, in Lorentzian signature $z, \bar{z}$ are real but free parameters.

1.9 Conformal blocks

The CFT four-point function is the first non-trivial correlation function in CFTs that has dynamical content. For simplicity let us consider correlators with all identical operators from now on. The generalization to non-identical operators is straightforward. The four-point function can be expanded by taking the OPE of the first and the second operators plus the OPE of the third and the fourth operators:

$$\begin{aligned}\langle \overbracket{\phi(x_1)\phi(x_2)}\overbracket{\phi(x_3)\phi(x_4)}\rangle &= \sum_{\mathcal{O},\mathcal{O}'} f_{\phi\phi\mathcal{O}} f_{\phi\phi\mathcal{O}'} C_a(x_{12},\partial_{x_2}) C_b(x_{34},\partial_{x_4}) \left\langle \mathcal{O}^a(x_2)\mathcal{O}'^b(x_4)\right\rangle \\ &= \sum_{\mathcal{O}} f^2_{\phi\phi\mathcal{O}} C_a(x_{12},\partial_{x_2}) C_b(x_{34},\partial_{x_4}) \left\langle \mathcal{O}^a(x_2)\mathcal{O}^b(x_4)\right\rangle \\ &= \frac{1}{|x_{12}|^{2\Delta_\phi}|x_{34}|^{2\Delta_\phi}} \sum_{\mathcal{O}} f^2_{\phi\phi\mathcal{O}} G_{\Delta_{\mathcal{O}},\ell_{\mathcal{O}}}(z,\bar{z}) \ , \end{aligned} \tag{1.59}$$

in which a, b are short notations for the spin indices and $f_{\phi\phi\mathcal{O}}$ are the OPE coefficients that are real in a unitary theory. The function $G_{\Delta_{\mathcal{O}},\ell_{\mathcal{O}}}(z,\bar{z})$ is called the Conformal Block. This function is the solution of the Casimir equation meaning that if we act with a Casimir operator

$$C = D^2 - \frac{1}{2}\left(K_\mu P^\mu + P_\mu K^\mu + M_{\mu\nu}M^{\mu\nu}\right) = \Delta(\Delta-d) - \ell(\ell+d-2) \tag{1.60}$$

on both sides, we find

$$\hat{C}\ G_{\Delta_{\mathcal{O}},\ell_{\mathcal{O}}}(z,\bar{z}) = \left(\Delta(\Delta-d) - \ell(\ell+d-2)\right) G_{\Delta_{\mathcal{O}},\ell_{\mathcal{O}}}(z,\bar{z}) \ . \tag{1.61}$$

The solution to this equation has been found in $d = 1$, $d = 2$ and $d = 4$ [56, 57]:

$$\begin{aligned} G^{1d}_{\Delta,\ell}(z) &= k_{2\Delta}(z) \\ G^{2d}_{\Delta,\ell}(z,\bar{z}) &= k_{\Delta+\ell}(z)k_{\Delta-\ell}(\bar{z}) + k_{\Delta-\ell}(z)k_{\Delta+\ell}(\bar{z}) \\ G^{4d}_{\Delta,\ell}(z,\bar{z}) &= \frac{z\bar{z}}{z-\bar{z}}\left(k_{\Delta+\ell}(z)k_{\Delta-\ell-2}(\bar{z}) - k_{\Delta-\ell-2}(z)k_{\Delta+\ell}(\bar{z})\right) \end{aligned} \tag{1.62}$$

with

$$k_\beta(z) = z^{\beta/2}\,{}_2F_1(\beta/2,\beta/2,\beta,z) \ . \tag{1.63}$$

Note that in $d = 1$, there is only one cross ratio. This can be seen in (1.58) as there is only one coordinate (x and no y (no angle)). We have a specialized section about one-dimensional CFTs: section 5.1. For the odd dimension (except $d \neq 1$) there is no know closed formula for the conformal blocks; however, the solutions can be derived from series expansion or recursion relations [58]. For the case of spinning operators see for example [59].

The moral of this section is that four-point functions can be expanded in kinematical functions of conformal blocks with some theoretical-dependent positive coefficients.

1.10 The conformal bootstrap

In the previous section, we expand the four-point function by applying the OPE (1.59). There are multiple ways to apply the OPE. We fuse operators (1,2) and operators (3,4) in (1.59). Equivalently we could perform OPE between (1,3) operators and (2,4) operators or (1,4) and (2,3):

$$\wick{\langle \c1\phi(x_1)\c1\phi(x_2)\c2\phi(x_3)\c2\phi(x_4)\rangle} = \wick{\langle \c1\phi(x_1)\c2\phi(x_2)\c1\phi(x_3)\c2\phi(x_4)\rangle} = \wick{\langle \c1\phi(x_1)\c2\phi(x_2)\c2\phi(x_3)\c1\phi(x_4)\rangle} \tag{1.64}$$

which is visualized in figure 1. The important point is that no matter in what channel we expand the four-point function, they are still the expansion of the same four-point function and they have to be equal. This statement is called the *crossing symmetry* and (1.64) is called the crossing equation. The remaining question is: are the crossing equations trivial? The answer is no. Because of the positivity of the conformal block coefficients $f^2_{\phi\phi\mathcal{O}}$, the crossing equations put constraints on OPE data: $f^2_{\phi\phi\mathcal{O}}$ and $\Delta_{\mathcal{O}}, \ell_{\mathcal{O}}$. This is the philosophy behind the *conformal bootstrap*.

Let us illustrate the idea above with a concrete example. Take a four-point function of identical scalar operators and expand them in two channels: OPEs (1,2) and (3,4), and OPEs (1,4) and (2,3). The crossing equation reads

$$((1-z)(1-\bar{z}))^{\Delta_\phi}\, g(z,\bar{z}) = (z\bar{z})^{\Delta_\phi} g(1-z, 1-\bar{z}) \tag{1.65}$$

where we use the fact that channel (1,4)-(2,3) is related to channel (1,2)-(3,4) by exchanging points $x_1 \leftrightarrow x_3$ or $x_2 \leftrightarrow x_4$. The above equation can be rewritten in a more convenient form of

$$1 = \sum_{\Delta,\ell} f^2_{\Delta,\ell} F_{\Delta,\ell}(z,\bar{z}) \tag{1.66}$$

where we define

$$F_{\Delta,\ell}(z,\bar{z}) = \frac{v^{\Delta_\phi} G_{\Delta,\ell}(u,v) - u^{\Delta_\phi} G_{\Delta,\ell}(v,u)}{u^{\Delta_\phi} - v^{\Delta_\phi}} \tag{1.67}$$

and the sum is over all Δ, ℓ corresponding to the operators $\mathcal{O} \in \phi \times \phi$ except the identity that we isolated on the left side of the equation ($= 1$) and we used new subscripts for f. Before presenting a systematic treatment let us illustrate how the crossing equation (1.66) can lead to non-trivial bounds with a simple example. For simplicity, let us focus on $d = 1$ where the crossing equation is the same as (1.66) with $z = \bar{z}$ and there is no sum over spin (only parity even ($\ell = 0$) operators show up). There is a similar discussion for $d = 4$ in [27]. Let us look at the plot of functions F_Δ for a list of Δs taking $\Delta_\phi = 1.2$ for instance – figure 1.1. It turns out that function F_Δ has a similar shape for different Δs. In particular, pay attention to the symmetric point $z = \frac{1}{2}$. After a certain $\Delta^*(\sim 4.431)$, as we increase Δ, all the second derivatives of F_Δ are positive.

Now imagine a theory in which the first operator that shows up in $\phi \times \phi$ OPE has dimension higher than Δ^*. If we apply the second derivative of z to both sides of (1.66) for such theory, the left hand is trivially zero but the right-hand side will be a sum of positive terms $F^{''} > 0$ with positive coefficients f^2. This is a contradiction. The conclusion is that: there is no CFT in which the first non-trivial operator in $\phi \times \phi$ OPE has a dimension higher than Δ^* or equivalently any consistent CFT should have at least one non-trivial operator with a dimension less than Δ^* in its $\phi \times \phi$ OPE. Therefore we put a *bound* on dimension of the first operator in the OPE.

Let us conclude this section with a systematic method to put bounds on CFT data. The methodology is the same as above – finding an inconsistent theory. If one finds a linear functional such that

$$\begin{aligned} \alpha[1] &= 0 \ , \\ \alpha[F_{\Delta_i}] &> 0 \ , \quad \forall \Delta \geq \Delta^* \ , \end{aligned} \tag{1.68}$$

then a theory that does not have any operator in OPE with $\Delta < \Delta^*$ is ruled out. It was pointed out in [27] that this problem can become a simple linear programming question. Take α to be

$$\alpha \to \sum_{m,n}^{N_{\max}} a_{mn} \partial_z^{(2m)} \partial_{\bar{z}}^{(2n)} \ . \tag{1.69}$$

The set of $a_{m,n}$ that satisfies (1.68) is a linear programming problem that can be solved for example by *LinearProgramming* function of *Wolfram Mathematica*. As one increases $N_{\max}$, a better bound will be achieved. It is analytically shown in [60, 61] that for $d = 1$, the saturation of bounds is given by generalized free fermion with $\Delta^* = 2\Delta_\phi + 1$, meaning no theory has its first operator in $\phi \times \phi$ OPE with a dimension bigger than $2\Delta_\phi + 1$. Numerically this can be seen as the ruled out region in the space of inconsistent Δ^*s converges to $\Delta^* = 2\Delta_\phi + 1$ as one increases the cut-off $N_{\max}$.

The situation in higher dimensions is different. There is no analytical solution for such problems and the power of numerical methods is more appreciated. In particular, it turns out that sometimes there are kinks and islands in the space of allowed CFT data. Interestingly enough, these points happen to be known theories – the Ising model, see figure 1.2. The conformal bootstrap program has the record of the most precise determination of the 3d Ising critical exponents to this date [37].

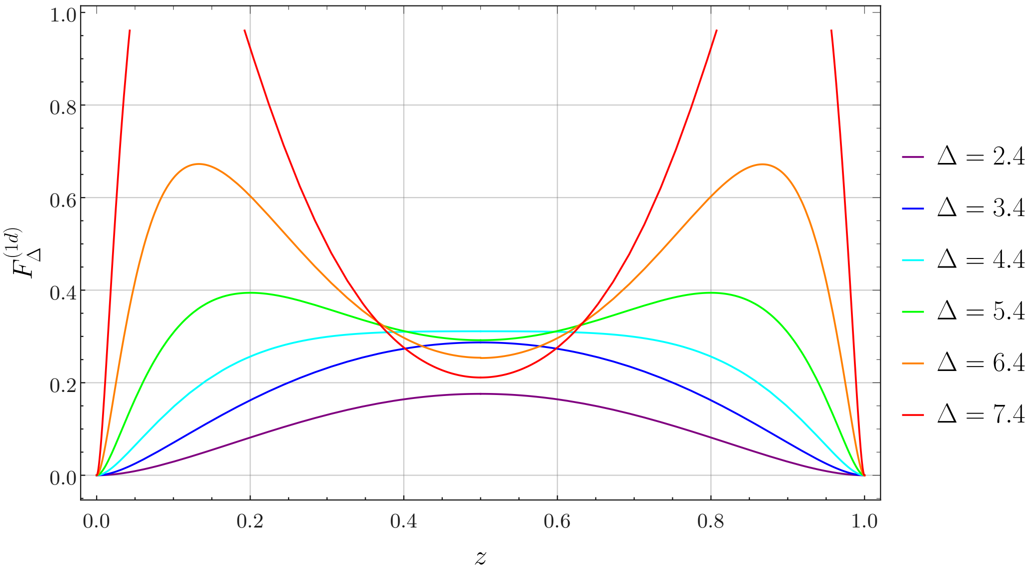

Figure 1.1: The plot of $F_\Delta(z)$ for CFT$_1$ with $\Delta_\phi = 1.2$. For all $\Delta \geq 4.4$, the second derivative at $z = \frac{1}{2}$ is positive.

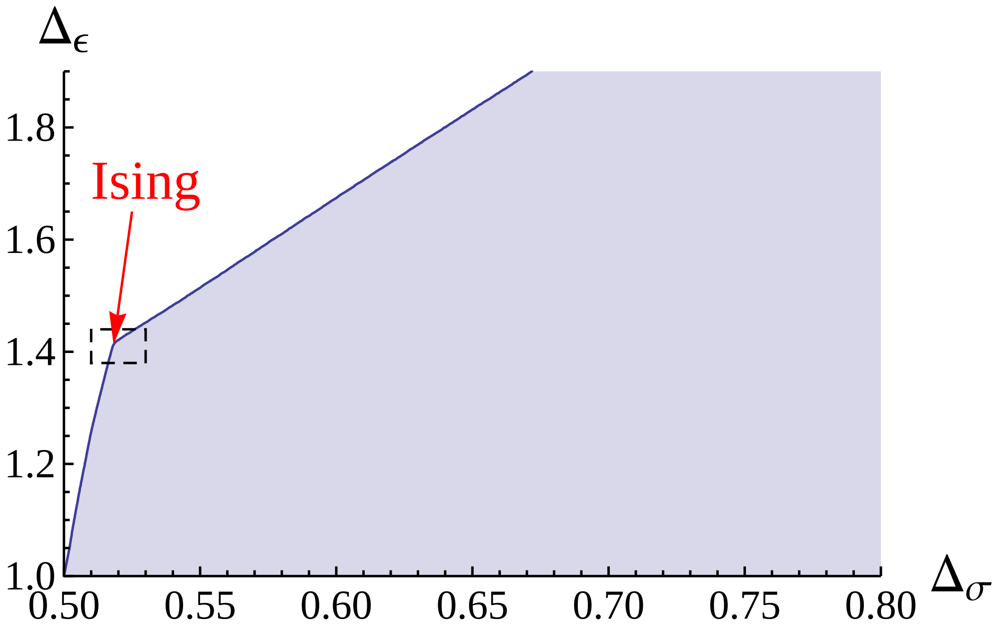

Figure 1.2: Constraints on CFT data of a theory with $\mathbb{Z}$ global symmetry that includes one $\mathbb{Z}_2$-even operator ϵ and $\mathbb{Z}_2$-odd operator σ. The white region is the ruled out region while the shaded region is allowed by the crossing symmetry constraint. The boundary of this region has a kink remarkably close to the known 3D Ising model operator dimensions. The plot is taken from [62].

2 Quantum field theory in de Sitter

This section reviews the basics of QFT in a fixed de Sitter background. After defining some maximally symmetric spaces including dS as hypersurfaces in the embedding space and introducing some commonly used coordinate systems, we discuss the isometry group of dS in detail. After that, we review the quantization of a massive free scalar field in de Sitter. In section 2.5 we restate the Feynman rules of dS correlators using the in-in formalism and derive the dS-EAdS dictionary. In 2.6, we state some non-perturbative properties of QFT in dS. Namely, we discuss the structure of the Hilbert space and correlation functions of bulk and boundary operators.

2.1 Geometry of maximally symmetric spaces

A $d+1$-dimensional maximally symmetric space is an isotropic and homogeneous manifold. Maximally symmetric spaces, therefore, have the maximum number of isometries of $(d+1)(d+2)/2$ with a constant curvature. For each signature of metric $(-,\cdots,-,+\cdots,+)$, they are categorized into three types: Zero curvature or flat, Positive curvature or de Sitter/sphere and negative curvature or anti-de Sitter/hyperbolic space[1].

In this section, we focus on two Euclidean space(time)s of Euclidean Anti-de Sitter (EAdS$_{d+1}$) and Sphere (S^{d+1}) as well as two Lorentzian[2] spacetimes of de Sitter (dS$_{d+1}$) and Anti-de Sitter (AdS$_{d+1}$). In what follows we discuss these geometries and some of their coordinate systems. Since we are mostly focusing on dS and EAdS, we cover them in more detail.

---

[1] Strictly speaking, the list of maximally symmetric spaces are longer and it includes the quotients/covers of the mentioned spaces. For example cylinder $\mathbb{R}^d/\mathbb{Z}$ and torus $\mathbb{R}^d/\mathbb{Z}^d$ are also maximally symmetric. See for example [63]

[2] By Lorentzian spacetime we mean the spacetimes that have only one time coordinate, meaning that their metric has the signature $(-,+.\cdots,+)$.

2.1.1 Sphere

$d+1$-dimensional sphere S^{d+1} is a compact Riemannian manifold which can be realized as the embedding of set of points that are a distance R from the origin in $\mathbb{R}^{d+2}$:

$$S^{d+1}: \qquad (X^0)^2 + (X^1)^2 + \ldots + (X^{d+1})^2 = R^2 \; . \tag{2.1}$$

Its symmetry group as seen from the definition (2.1) is $SO(d+2)$ with rotation generators that (2.1) is invariant under:

$$J_{AB} = X_A \frac{\partial}{\partial X^B} - X_B \frac{\partial}{\partial X^A} \tag{2.2}$$

with $A, B = 1, \ldots, d+2$. These generators obey commutation relations

$$[J_{AB}, J_{CD}] = -\delta_{AC} J_{BD} - \delta_{BD} J_{AC} + \delta_{BC} J_{AD} + \delta_{AD} J_{BC} \tag{2.3}$$

where δ_{AB} is the Kronecker delta or equivalently the metric on $\mathbb{R}^{d+2}$.

There are multiple coordinate systems for S^{d+1} but we present some of them that are closely related to the ones we introduce later on for dS and (E)AdS. First, let us introduce the global coordinates given by

$$X^0 = R \sin\theta \; , \qquad X^i = R \cos\theta \, y^i \tag{2.4}$$

where $i = 1, \ldots, d+1$, $\theta \in [-\pi/2, \pi/2)$[3], $y^i \in \mathbb{R}^{d+1}$ and themselves belong to a lower unit-dimensional sphere S^d meaning that $y^i y_i = 1$. The induced metric then reads

$$ds^2 = R^2 (d\theta^2 + \cos^2\theta \, d\Omega_d^2) \tag{2.5}$$

where $d\Omega_d^2$ is the metric of the unit S^d. Another coordinate system can be found by the change of variable $\tanh(\phi/2) = \tan(\theta/2)$ which leads to

$$X^0 = R \frac{\sinh\phi}{\cosh\phi} \; , \qquad X^i = R \frac{y^i}{\cosh\phi} \tag{2.6}$$

with $\phi \in \mathbb{R}$. This coordinate system has the conformally flat metric of

$$ds^2 = \frac{R^2}{\cosh^2\phi} \left(d\phi^2 + d\Omega_d^2 \right) \; . \tag{2.7}$$

---

[3] Except for S^1 that requires $\theta \in [-\pi, \pi)$

2.1.2 Euclidean Anti-de Sitter spacetime

Euclidean anti-de Sitter spacetime can be defined as a set of points embedded in Minkowski space $\mathbb{M}^{d+1,1}$:

$$\text{EAdS}_{d+1}: \qquad -(X^0)^2 + (X^1)^2 + \ldots + (X^{d+1})^2 = -R^2 \ , \tag{2.8}$$

which defines two disconnected hypersurfaces. In our convention, we pick EAdS to be the one with $X^0 > 0$. This definition makes it manifest that EAdS is invariant under $SO(d+1,1)$ rotation and boosts and hence its $(d+1)(d+2)/2$ generators satisfy the commutation relations of $SO(d+1,1)$ algebra in (2.33). Let us present three coordinate systems that are useful for us in this thesis. One is the *global coordinate* that is given by

$$X^0 = R\cosh\rho\cosh\tau \ , \quad X^{d+1} = R\cosh\rho\sinh\tau \ , \quad X^\mu = R\sinh\rho\, y^\mu \ . \tag{2.9}$$

where $\mu = 1, \ldots, d$, Euclidean time $\tau \in \mathbb{R}$, $\rho \in \mathbb{R}^+$(see footnote 4) and $y^\mu \in \mathbb{R}^d$ is a unit vector ($y^\mu y_\mu = 1$). This coordinate system leads to the induced metric of

$$ds^2 = R^2(\cosh^2\rho\, d\tau^2 + d\rho^2 + \sinh^2\rho\, d\Omega^2_{d-1}) \ . \tag{2.10}$$

with the change of variable of $\tanh\rho = \sin r$, we find *radial coordinates*:

$$X^0 = R\frac{\cosh\tau}{\cos r} \ , \quad X^{d+1} = R\frac{\sinh\tau}{\cos r} \ , \quad X^\mu = R\frac{\sin r}{\cos r} y^\mu \ , \tag{2.11}$$

where $r \in [0, \pi/2)$[4]. It is clear that these two coordinates satisfies $X^0 > 0$. Radial coordinate has the induced metric of

$$ds^2 = R^2\frac{d\tau^2 + dr^2 + \sin^2 r\, d\Omega^2_{d-1}}{\cos^2 r} \tag{2.12}$$

which shows that it is conformal to a solid cylinder with the boundary at $r = \pi/2$. An important feature of this coordinate system that is useful for the argument of bulk state-boundary operator map [38] is that the dilatation operator is the Hamiltonian conjugate to the global time τ: $D = \partial_\tau$.

Another extremely useful conformally flat coordinate system called *Poincare coordinates* is defined as

$$X^0 = R\frac{z^2 + x^2 + 1}{2z} \ , \quad X^{d+1} = R\frac{z^2 + x^2 - 1}{2z} \ , \quad X^\mu = R\frac{x^\mu}{z} \tag{2.13}$$

with metric

$$ds^2 = R^2\frac{dz^2 + d\vec{x}^2}{z^2} \tag{2.14}$$

where $x^\mu \in \mathbb{R}^d$ with $\mu = 1, \cdots, d$ makes a flat d-dimensional Euclidean spacial slice and

---

[4] This is true for $d \geq 2$. In $d = 1$ the range is instead $r \in (-\pi/2, \pi/2)$ or $\rho \in \mathbb{R}$.

$z > 0$ to satisfy $X^0 > 0$ condition. $z = 0$ plane is its conformal boundary meaning that all of the EAdS generators in these coordinates will boil down to generators of a d-dimensional conformal theory. We do not spell them out here but they are the same as the dS counterparts in (2.34) if $\eta \to z$.

2.1.3 Anti-de Sitter spacetime

Anti-de Sitter spacetime is a Lorentzian spacetime with a constant negative curvature defined as a universal cover of the set of points embedded in $\mathbb{R}^{d,2}$ with the signature $(-,+,\ldots,+,-)$:

$$\text{AdS}_{d+1}: \qquad -(X^0)^2 + (X^1)^2 + \ldots - (X^{d+1})^2 = -R^2 \tag{2.15}$$

which is related to EAdS by wick rotation of $X^n \to iX^n$ for one of the n's: $1 \leq n \leq d+1$. Eq. (2.15) shows that the symmetry group of AdS is $SO(d,2)$. We are not going to discuss about AdS spacetime in this thesis. Only for the sake of completeness let us introduce three coordinate systems. First is the global coordinates defined as

$$X^0 = R\cosh\rho\cos t\ , \qquad X^{d+1} = R\cosh\rho\sin t\ , \qquad X^\mu = R\sinh\rho\, y^\mu\ . \tag{2.16}$$

for $\mu = 1, \cdots, d$ with $\rho \in \mathbb{R}^+$ except for $d = 1$. $t \in [0, 2\pi)$ covers the whole hyperbola in (2.15) but to avoid closed timelike curves, we define AdS to be the universal cover with $t \in \mathbb{R}$. Global coordinates therefore have the metric

$$ds^2 = R^2(-\cosh^2\rho\, dt^2 + d\rho^2 + \sinh^2\rho\, d\Omega^2_{d-1})\ . \tag{2.17}$$

Radial coordinates are defined with the change of variable $\tanh\rho = \sin r$:

$$X^0 = R\frac{\cos t}{\cos r}\ , \quad X^{d+1} = R\frac{\sin t}{\cos r}\ , \quad X^\mu = R\frac{\sin r}{\cos r}y^\mu\ , \tag{2.18}$$

with $r \in [0, \pi/2)$ (except for $d = 1$ similar to EAdS case that is explained in footnote 4). In this coordinate system AdS is conformal to a solid cylinder with the conformal boundary at $r = \pi/2$. The metric in these coordinates reads:

$$ds^2 = R^2\frac{-dt^2 + dr^2 + \sin^2 r\, d\Omega^2_{d-1}}{\cos^2 r}\ . \tag{2.19}$$

The Poincare coordinates are defined as

$$X^0 = R\frac{z^2 + x^2 - \bar{t}^2 + 1}{2z}, \quad X^d = R\frac{z^2 + x^2 - \bar{t}^2 - 1}{2z}\ , \quad X^{d+1} = R\frac{\bar{t}}{z}\ , \quad X^j = R\frac{x^j}{z} \tag{2.20}$$

where $j = 1, \cdots, d-1$ and $z > 0$. z is a spatial coordinate as can be seen in the metric[5]:

$$ds^2 = \frac{-d\bar{t}^2 + dz^2 + d\vec{x}^2}{z^2} \ . \tag{2.21}$$

One important point is that unlike in Euclidean AdS, the Poincare coordinates do not cover all AdS(similar to dS conformal coordinates) and it only covers a sub-region bounded by a causal diamond wrapped around AdS. The $z = 0$ is the AdS conformal boundary and the $z \to \infty$ is the lightlike surface $X^0 - X^d = 0$ that is called the Poincare horizon.

As one can explicitly see from the coordinates or metrics, AdS and EAdS are related by the wick rotation in time coordinate $t \to i\tau$ or $\bar{t} \to ix^d$; hence, the "Euclidean" in EAdS.

2.1.4 de Sitter spacetime

De Sitter space in $d+1$ dimensions (or dS_{d+1}) can be realized as the embedding of the set of points that are a distance R from the origin[6] in Minkowski space $\mathbb{M}^{d+1,1}$ with the signature $(-, +, \ldots, +)$:

$$\mathrm{dS}_{d+1}: \qquad -(X^0)^2 + (X^1)^2 + \ldots + (X^{d+1})^2 = R^2 \ . \tag{2.22}$$

At this basic level, one can see the similarity between dS and sphere. They transform to each other by wick rotation in X^0. However, note that the embedding spaces are different. Indeed sphere is embedded in a Euclidean space while dS is embedded in a Minkowski space.

Let us present three different coordinate systems that cover all or part of dS. To start, we may introduce *global coordinates* as follows

$$X^0 = R \sinh t \ , \qquad X^i = R \cosh t \, y^i \tag{2.23}$$

in which $i = 1, \ldots, d+1$ and $y^i \in \mathbb{R}^{d+1}$ are unit vectors ($y^i y_i = 1$), so they span the d-sphere S^d . The induced metric in global coordinates is given by

$$ds^2 = R^2 \left(-dt^2 + \cosh^2 t \, d\Omega_d^2\right) \ , \tag{2.24}$$

where $d\Omega_d^2$ denotes the standard metric of the unit S^d. After the change of variable $\tan(\tau/2) = \tanh(t/2)$, we find

$$X^0 = R\frac{\sin\tau}{\cos\tau} \ , \qquad X^i = R\frac{y^i}{\cos\tau} \tag{2.25}$$

---

[5] This metric goes to EAdS metric in Poincare coordinates by $\bar{t} \to ix^d$ which is $X^d \to iX^d$

[6] Often the Hubble scale $H = 1/R$ is used instead of R.

from which the metric reads

$$ds^2 = R^2 \frac{-d\tau^2 + d\Omega_d^2}{\cos^2 \tau} \ , \tag{2.26}$$

with $\tau \in (-\pi/2, \pi/2)$. We conclude that in these coordinates dS is conformally equivalent to (part of) the Minkowski cylinder. This observation is important in the analysis of conformal field theories in dS (see section 2.6.3).

Finally, it will be useful to foliate dS using flat slices. This can be done by

$$X^0 = R\frac{\eta^2 - 1 - x^2}{2\eta} \ , \qquad X^{d+1} = R\frac{x^2 - 1 - \eta^2}{2\eta} \ , \qquad X^\mu = -R\frac{x^\mu}{\eta} \tag{2.27}$$

for $\mu = 1, \ldots, d$. For definiteness, we will pick the Poincaré patch covering $X^0 + X^{d+1} \geq 0$. So, strictly speaking, such foliations only cover half of de Sitter space. However, this region is causally complete, in the sense that it is impossible to send a message to the other patch with $X^0 + X^{d+1} < 0$. This parametrization is called *conformal* or *Poincaré coordinates* in which $\eta < 0$ and $x^\mu \in \mathbb{R}^d$.

The coordinate η plays the role of a conformal time, whereas the x^μ are spatial coordinates. Poincare coordinates have the conformally flat metric of

$$ds^2 = R^2 \, \frac{-d\eta^2 + d\vec{x}^2}{\eta^2} \ . \tag{2.28}$$

This will be the main coordinate system we use throughout this thesis, as it makes manifests the conformal symmetry of the late-time boundary $\eta = 0$. Global and conformal coordinates are related via the dictionary

$$\eta = -\frac{1}{\sinh(t) + \cosh(t) y^{d+1}} \ , \qquad x^\mu = \frac{y^\mu}{\tanh(t) + y^{d+1}} \ , \tag{2.29}$$

which maps the late-time Poincaré patch to the subset of global coordinates satisfying $y^{d+1} + \tanh(t) \geq 0$. Figure 2.1 shows a picture of dS_{d+1} in the global coordinates of Eq. (2.26), along with a Penrose diagram which shows timeslices with $\eta =$ constant.

Let us draw your attention to the connection between dS and sphere. At the level of embedding space, they are related by wick rotation $X^0 \to iX^0$. Moreover, the corresponding coordinates and metrics map to each other by a wick rotation in time $t \to i\theta$ or $\tau \to i\phi$[7]. In other words, Euclidean dS is indeed the sphere.

In summary, each of the mentioned $d+1$-maximally symmetric spaces can be realized as $d+1$-hypersurface of the set of points with distance R from the origin in a $d+2$-dimensional embedding space: AdS in $\mathbb{R}^{d,2}$, dS and EAdS in $\mathbb{R}^{d+1,1}$ and sphere in $\mathbb{R}^{d+2}$. The sphere

---

[7] This argument does not work for Poincare coordinates as we picked half of the space by condition $X^0 + X^{d+1} \geq 0$ and such a transformation does not match with this condition

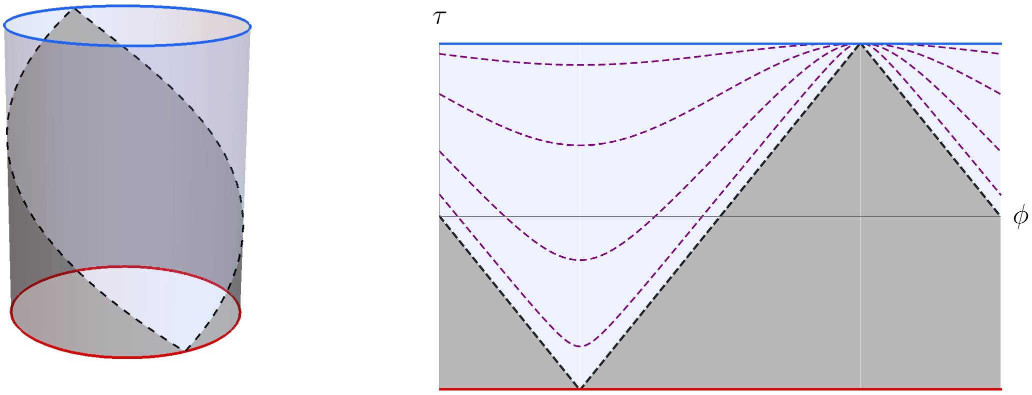

Figure 2.1: Left: de Sitter spacetime dS_{d+1} as a hollow Minkowski cylinder, cf. equation (2.26). Time τ runs upwards from $-\pi/2$ to $\pi/2$. Every horizonal timeslice corresponds to a copy of S^d. The infinite past (resp. future) is shown as a solid red (blue) line. The light blue area is the Poincaré patch $X^0 + X^{d+1} \geq 0$; the boundary between the two patches is shown as a dashed line. Right: Penrose diagram of the same spacetime, specializing to $d = 1$. Spatial slices S^1 are parametrized by an angle $\phi \sim \phi + 2\pi$. Several timeslices of fixed $\eta < 0$ in the conformal coordinates (2.28) are shown as thin purple lines. The left and right sides of the diagram are identified, owing to the periodicity of ϕ.

and EAdS are respectively the Euclidean version of dS and AdS with a Wick rotation of the time coordinate. dS and Sphere have positive Ricci curvature of $\mathcal{R} = d(d+1)/R^2$ while AdS and EAdS have the negative sign: $\mathcal{R} = -d(d+1)/R^2$.

Symmetries of dS

de Sitter space dS_{d+1} is manifestly invariant under $SO(d+1,1)$, as can be seen from its definition (2.22). As such, it has $\frac{1}{2}(d+2)(d+1)$ Killing vectors. The symmetry generators

$$J_{AB} = X_A \frac{\partial}{\partial X^B} - X_B \frac{\partial}{\partial X^A}, \qquad A, B = 1, \ldots, d+2 \tag{2.30}$$

are rotations and boosts that preserve the dS hypersurface in the embedding space, and they obey commutation relations

$$[J_{AB}, J_{CD}] = -\eta_{AC} J_{BD} - \eta_{BD} J_{AC} + \eta_{BC} J_{AD} + \eta_{AD} J_{BC} \tag{2.31}$$

where $\eta_{AB} = \mathrm{diag}(-1, 1, \ldots, 1)$. After relabeling the symmetry generators as follows

$$\begin{aligned} D &= J_{0,d+1}\ , \qquad & M_{\mu\nu} &= J_{\mu\nu}\ , \\ P_\mu &= J_{0,\mu} + J_{d+1,\mu}\ , \qquad & K_\mu &= J_{d+1,\mu} - J_{0,\mu} \end{aligned} \tag{2.32}$$

with $\mu, \nu = 1, \ldots, d$, we find that the new generators D, P_μ, K_μ, and $M_{\mu\nu}$ obey the familiar Euclidean conformal algebra:

$$\begin{gathered}
[D, P_\mu] = P_\mu \ , \qquad [D, K_\mu] = -K_\mu \ , \qquad [K_\mu, P_\nu] = 2\delta_{\mu\nu} D - 2M_{\mu\nu} \ , \\
[M_{\mu\nu}, P_\rho] = \delta_{\nu\rho} P_\mu - \delta_{\mu\rho} P_\nu \ , \qquad [M_{\mu\nu}, K_\rho] = \delta_{\nu\rho} K_\mu - \delta_{\mu\rho} K_\nu \ , \\
[M_{\mu\nu}, M_{\rho\sigma}] = \delta_{\nu\rho} M_{\mu\sigma} - \delta_{\mu\rho} M_{\nu\sigma} + \delta_{\nu\sigma} M_{\rho\mu} - \delta_{\mu\sigma} M_{\rho\nu}
\end{gathered} \tag{2.33}$$

as well as $[P_\mu, P_\nu] = 0$, $[K_\mu, K_\nu] = 0$ and $[D, M_{\mu\nu}] = 0$. In our conventions, all these generators are anti-hermitian.

Expressed in flat coordinates (η, x^μ), the corresponding Killing vectors of dS_{d+1} can be expressed as follows:[8]

$$\begin{aligned}
P_\mu &: \frac{\partial}{\partial x^\mu} \ , \\
M_{\mu\nu} &: x_\nu \frac{\partial}{\partial x^\mu} - x_\mu \frac{\partial}{\partial x^\nu} \ , \\
D &: \eta \frac{\partial}{\partial \eta} + x^\mu \frac{\partial}{\partial x^\mu} \ , \\
K_\mu &: (\eta^2 - x^2) \frac{\partial}{\partial x^\mu} + 2x_\mu \eta \frac{\partial}{\partial \eta} + 2x_\mu x^\nu \frac{\partial}{\partial x^\nu} \ .
\end{aligned} \tag{2.34}$$

Note that at the late-time boundary $\eta = 0$, the generators are the standard generators of the conformal algebra in flat space. We will exploit the conformal symmetry of late-time dS extensively throughout this thesis.

Finally, local operators in de Sitter transform under the $SO(d+1, 1)$ isometries according to (2.34). To be precise, a local scalar operator $\phi(\eta, x)$ transforms under the conformal generator Q as

$$[Q, \phi(\eta, x)] = \hat{Q} \cdot \phi(\eta, x) \tag{2.35}$$

where $\hat{Q}$ is the Killing vector differential operator from Eq. (2.34) — for instance

$$[P_\mu, \phi(\eta, x)] = \partial_\mu \phi(\eta, x) \ , \quad [D, \phi(\eta, x)] = (\eta \partial_\eta + x \cdot \partial) \phi(\eta, x) \tag{2.36}$$

and likewise for the other generators.

2.2 Representation theory of $SO(d+1, 1)$

Throughout this thesis, we will need to deal with Hilbert spaces of QFTs in de Sitter. Such Hilbert spaces are organized into unitary irreducible representations of the dS isometry group, $SO(d+1,1)$. The representation theory of this group is rather complicated, owing to its non-compactness, but for our purposes we will only need to recall some basic facts about the most common representations. In general, we refer to [64, 65] for an in-depth discussion of $SO(d+1,1)$ group theory relevant to high-energy physics, or more recently [66–68]. For a more pedological review also see [69, 70]. A technical and explicit discussion for general d with a focus on special functions is presented in Ref. [71]. Concerning the case of dS_2, the representation theory of $SO(2,1)$ or its double cover $SL(2,\mathbb{R})$ is discussed for example in [72–76].

---

[8] Strictly speaking, the Killing vectors from Eq. (2.34) need to be defined with an additional minus sign to be consistent with (2.33). The notation (2.34) will prove to be convenient later on. Here we avoid equality sign and instead used ":" to emphasis these are not the isometry generators or Killing vectors $\hat{Q}$. Instead we use the notation Q for the corresponding conserved charges.

As is well-known from d-dimensional CFT, one can construct infinite-dimensional representations of $SO(d+1,1)$ labeled by a dimension Δ and a representation ϱ of $SO(d)$. In the present thesis, only traceless symmetric tensor representations of $SO(d)$ will play a role, and these are labeled by an integer $\ell = 0,1,2,\ldots$, with $\ell = 0$ corresponding to the trivial representation. The dimension Δ can be any complex number, contrary to unitary CFTs where Δ is always real and positive. We define Δ so that the $SO(d+1,1)$ quadratic Casimir given by

$$C = D^2 - \tfrac{1}{2}(K_\mu P^\mu + P_\mu K^\mu + M_{\mu\nu}M^{\mu\nu}) \tag{2.37}$$

have the Casimir eigenvalue of the

$$C(\Delta,\ell) = \Delta(\Delta - d) + \ell(\ell + d - 2)\ . \tag{2.38}$$

So each multiplet of representation is defined by a pair of a dimension and a spin: $[\Delta,\ell]$. For generic values of Δ, the $[\Delta,\ell]$ representation is not unitary, and for special values of Δ it is reducible. In any dimension d, there are two continuous families of unitary irreps:

- The **principal series** $\mathcal{P}$ has $\Delta = \frac{d}{2} + i\nu$ with $\nu \in \mathbb{R}$, and it exists for any spin ℓ;
- The **complementary series** $\mathcal{C}$ has $\Delta = \frac{d}{2} + c$ with $c \in \mathbb{R}$, and the range of c depends on ℓ. To wit:

  for spin $\ell = 0$, $0 < |c| \leq \frac{d}{2}$;
  for spin $\ell \geq 1$, $0 < |c| \leq \frac{d}{2} - 1$.

  The endpoints of the complementary series are known as **exceptional series** of representations.
- In odd d, there are in addition **discrete series** representations $\mathcal{D}$ with integer or half-integer values of Δ.

Finally, we stress that the representation $[\Delta,\ell]$ and its so-called *shadow* $[d-\Delta,\ell]$ are unitarily equivalent. This means that principal series irreps with $\Delta = \frac{d}{2} \pm i\nu$ can be identified, as well as complementary series irreps with $\Delta = \frac{d}{2} \pm c$.

In $d = 1$, the group $SL(2,\mathbb{R}) \cong SU(1,1)$ has both "even" and "odd" principal series.[9] The odd series of irreps does not factor down to an irrep of $SO(2,1) \cong PSL(2,\mathbb{R}) \cong SL(2,\mathbb{R})/\{\pm\mathbb{1}\}$.

Tensor products

In this thesis, we expand correlation functions using the Hilbert space decomposition into unitary irreducible representations. More precisely, we inject the resolution of identity (2.117) into correlation functions of scalar operators. Therefore, to know which irreps have a non-zero contribution to our correlation function expansion, we have to know the decomposition of the tensor products of the mentioned irreps. We shall use the notation $\mathcal{R}_0$ to denote the scalar representation and $\mathcal{R}_s$ for the spinning one. In this work we start from states that belong to scalar principal series representations and then analytically continue to complimentary series. We will come back to the complimentary series shortly. Here we mention the list of tensor products of different representations that would shed lights on what we expect to appear in correlation functions. However, the two-point and four functions, we present a direct reasoning of what representations to expect.

For dimensions $d \geq 2$, it is known that the tensor product of two (scalar) principal series representations of the $SO(d+1,1)$ is decomposable into principal series representations [64, 77, 78] only. Schematically[10]:

$$\mathcal{P}_0 \otimes \mathcal{P}_0 = \mathcal{P}_0 \qquad \text{for } d \geq 2\ . \tag{2.40a}$$

In the case of $d = 1$ (that is to say dS_2); however, the tensor product of two (even or odd) principal series irreps generally contains both principal states irreps, as well as discrete series irreps [79]:

$$\mathcal{P}_0 \otimes \mathcal{P}_0 = \mathcal{P}_0 \oplus \mathcal{D}_0 \qquad \text{for } d = 1\ . \tag{2.40b}$$

For tensor products involving discrete series, we have schematically the tensor products

$$\mathcal{P}_0 \otimes \mathcal{D}_0 = \mathcal{P}_0 \oplus \mathcal{D}_0\,, \tag{2.40c}$$

$$\mathcal{D}_0 \otimes \mathcal{D}_0 = \mathcal{D}_0\ . \tag{2.40d}$$

In summary, in decomposition for $d \geq 2$ only principal series show up, while for $d = 1$ one has to add discrete series too. Note that this discussion is about the *bulk states*, not the

---

[9] For an explicit definition of these irreps, see [72, Ch. II §5], where they are labeled as $\mathscr{P}^{\pm,iv}$. The irreps $\mathscr{P}^{\pm}$ are indistinguishable at the level of the Lie algebra, but they differ for finite group transformations.

[10] In the case of spinning this is not the case and the discrete series show up:

$$\mathcal{P}_s \otimes \mathcal{P}_s = \mathcal{P}_s \oplus \mathcal{D}_s\ . \tag{2.39}$$

boundary operators. In fact, because of the lack of bulk state-boundary operator map in dS, the boundary operators follow (2.40) only in special cases like the free theory. In other words, in a generic interacting QFTs, late-time operators in dS do not necessarily fall into unitary irreps.

There are indirect ways to see the results above. For example in the case of boundary four-point function, the injection of resolution of identity (2.117) leads to conformal partial wave expansion (see 4). The completeness of partial waves that belong to principal series in $d \geq 2$ is another way to see the result above. For the case of $d = 1$, one indeed needs to add discrete series to the expansion. See [80, A.3] for a more detailed discussion[11]. Another indirect way to find the list above is to take a bulk CFT with symmetry group of $SO(d+1,2)$ and decompose its irreps to $SO(d+1,1)$ unitarity irreps. For the case of $d = 1$, we explicitly construct the states and recover the results above in appendix D.

Complementary series

The complementary series of representations can be thought of as the analytic continuation of the principal series. Moreover, it is shown in [81] that the complementary series would generally show up in tensor products as a discrete set of isolated points, not a continuous family:

$$\mathcal{C}_0 \otimes \mathcal{C}_0 = \mathcal{P}_0 \oplus \mathcal{C}_0 \text{ (isolated points)} . \tag{2.41}$$

This can also be seen in examples in [80, A.3] and section 3.5.3 for instance. As we shall see, the free massive scalar field with $m^2 \geq 0$ has single-particle states that fall into principal or complementary series representations depending on the value of m^2R^2. Since the Casimir eigenvalue is related to m via $\Delta(d-\Delta) = m^2R^2$, "light" fields with mass $mR < d/2$ give rise to states in the complementary series while "heavy" fields with mass $mR \geq d/2$ give rise to principal series states.

The full treatment of tensor products of unitary irreps of $SO(d+1,1)$ is quite technical and deserves a more detailed discussion. We postpone it to upcoming work of [81].

2.3 Correlation functions and boundary operators

Correlation functions of local operators are one of the most basic observables in QFT. In this thesis, we are interested in the expectation values of local operators in the Bunch-Davies vacuum of de Sitter spacetime. These can be conveniently defined by the analytic continuation of correlation functions of the same QFT on the Euclidean sphere S^{d+1}. As discussed in 2.1, in global coordinates this corresponds to writing $t = i\theta$, which transforms the metric (2.24) into the sphere metric

---

[11] The discussion there is about boundary operators with dimensions in the principal series or on the real line, but one can generalize the arguments to arbitrary dimensions by analytic continuation–taking the pole crossings into account

$$ds^2 = R^2 \left(d\theta^2 + \cos^2\theta \, d\Omega_d^2\right) = R^2 d\Omega_{d+1}^2 \,, \tag{2.42}$$

where $\theta \in \left[-\frac{\pi}{2}, \frac{\pi}{2}\right)$. We can then write[12]

$$\begin{aligned}&\langle \Omega | \phi_1(t_1, y_1) \dots \phi_n(t_n, y_n) | \Omega \rangle = \\ &\qquad \lim_{0<\epsilon_n<\dots<\epsilon_1 \to 0} \langle \phi_1(\theta_1 = \epsilon_1 - it_1, y_1) \dots \phi_n(\theta_n = \epsilon_n - it_n, y_n) \rangle_{S^{d+1}} \,,\end{aligned} \tag{2.43}$$

recalling that $y_j \in S^d$. We shall make heavy use of this approach in section 3.

The space of local operators of a QFT is independent of the background geometry where it is placed. Moreover, for a UV-complete QFT defined as a relevant deformation of a UV CFT, the space of local operators is the one of the UV CFT. In de Sitter, one can also define boundary operators by pushing bulk local operators to future (or past) infinity. This is more conveniently stated in conformal coordinates as an expansion around $\eta = 0$,

$$\begin{aligned}\phi(\eta, x) &= \sum_\alpha b_{\phi\alpha} (-\eta)^{\Delta_\alpha} \left[\mathcal{O}_\alpha(x) + c_1 \, \eta^2 \partial_x^2 \mathcal{O}_\alpha(x) + c_2 \, \eta^4 (\partial_x^2)^2 \mathcal{O}_\alpha(x) + \dots\right] \\ &= \sum_\alpha b_{\phi\alpha} \, (-\eta)^{\Delta_\alpha} {}_0F_1\left(\Delta_\alpha - \tfrac{d}{2} + 1, \, \tfrac{1}{4} \eta^2 \partial_x^2\right) \mathcal{O}_\alpha(x).\end{aligned} \tag{2.44}$$

The operators $\mathcal{O}_\alpha$ are primary boundary operators, obeying $[K_\mu, \mathcal{O}_\alpha(0)] = 0$, whereas operators of the form $\Box^n \mathcal{O}_\alpha$ are $SO(d+1,1)$ descendants. In passing to the second line in (2.44) we used the fact that the coefficients c_1, c_2, …are fixed by de Sitter isometries.[13] It is also easy to check that $\mathcal{O}_\alpha$ satisfy the other commutation relation of primary operators of a conformal theory– i.e. they define a conformal boundary theory. If the bulk operator ϕ is hermitian, then the boundary operators $\mathcal{O}_\alpha$ can either be hermitian with real Δ_α or appear in conjugate pairs $\mathcal{O}_\alpha$ and $\mathcal{O}_\alpha^\dagger$ with scaling dimensions Δ_α and Δ_α^*. The dimensions Δ_α of boundary operators should not be confused with the labels Δ of unitarity irreps in the Hilbert space. In particular, the values of Δ_α are not restricted to be real or of the form $\frac{d}{2} + i\nu$ with $\nu \in \mathbb{R}$.

For QFT in Anti-de Sitter spacetime (or Boundary CFT), there is a similar expansion

$$\phi(z, x) = \sum_\alpha a_{\phi\alpha} z^{\Delta_\alpha} \left[\mathcal{O}_\alpha(x) + \text{descendants}\right] \,. \tag{2.46}$$

---

[12] For simplicity we restricted to scalar local operators.

[13] In practice, this can be done by using the expansion above to compute the two-point function

$$\langle \Omega | \phi(\eta, x) \mathcal{O}_\alpha(y) | \Omega \rangle = b_{\phi\alpha} \frac{(-\eta)^{\Delta_\alpha}}{[(x-y)^2 - \eta^2]^{\Delta_\alpha}} \,, \tag{2.45}$$

which is fixed by symmetry. We normalize boundary operators to have unit two-point function. Also notice that the ${}_0F_1$ function in (2.44) can be recast as a Bessel function.

The convergence of this type of Operator Product Expansion (OPE) can be established using a state-operator map [82, 83, 38]. In dS, the convergence of the series (2.44) is more subtle. In particular, the OPE does not converge inside all matrix elements. For instance, using conformal symmetry we easily find that

$$\langle \Omega | \phi(\eta, x) | \tfrac{d}{2} + i\nu, y \rangle = c_\phi(i\nu) \left(\frac{-\eta}{|x-y|^2 - \eta^2} \right)^{\frac{d}{2}+i\nu}, \quad c_\phi(i\nu) \in \mathbb{C}. \tag{2.47}$$

At the same time,

$$\Delta_\alpha \neq \tfrac{d}{2} \pm i\nu \quad \Rightarrow \quad \langle \Omega | \mathcal{O}_\alpha(x) | \tfrac{d}{2} + i\nu, y \rangle = 0 \tag{2.48}$$

as also follows from a symmetry argument. If the OPE (2.44) converged, then (2.48) would imply that $c_\phi(i\nu)$ vanishes unless the late-time expansion (2.44) of ϕ contains an operator of dimension $\Delta_\alpha = \frac{d}{2} \pm i\nu$. Yet we will see later that $c_\phi(i\nu)$ is in general a smooth, non-zero distribution for any non-trivial bulk operator ϕ, even when its late-time expansion (2.44) does not contain any principal series operators.

2.4 Free scalar field in de Sitter

Let us start the discussion of QFT in dS by constructing an explicit example: the massive free scalar field. We will do so by canonically quantizing the theory in the flat slicing of Eq. (2.28). In the process, we will describe in detail the Hilbert space and its symmetry properties.

In order to construct the free scalar in dS_{d+1}, we start from the action

$$S = -\int d^{d+1}\mathbf{x}\, \sqrt{-g} \left[\frac{1}{2} g^{\mu\nu} \partial_\mu \phi \partial_\nu \phi + \frac{1}{2} m^2 \phi^2 \right] \tag{2.49a}$$

$$= R^{d-1} \int d^d x \int_{-\infty}^{0} \frac{d\eta}{(-\eta)^{d+1}} \left[\eta^2 \left(\frac{1}{2} \dot{\phi}^2 - \frac{1}{2} (\nabla \phi)^2 \right) - \frac{1}{2} R^2 m^2 \phi^2 \right] \tag{2.49b}$$

where we define $\dot{\phi} \equiv \partial\phi/\partial\eta$.[14] The Euler-Lagrange equation of motion for the field ϕ reads

$$\eta^2 \ddot{\phi}(\vec{x}, \eta) - \eta(d-1) \dot{\phi}(\vec{x}, \eta) + \left(m^2 R^2 - \eta^2 \partial_x^2 \right) \phi(\vec{x}, \eta) = 0 \,. \tag{2.50}$$

Introducing Fourier modes

$$\phi(x, \eta) = \frac{1}{R^{(d-1)/2}} \int \frac{d^d k}{(2\pi)^d}\, e^{ik\cdot x}\, \phi(k, \eta) \tag{2.51}$$

---

[14] Strictly speaking, in passing from the first to the second line in (2.49), we have discarded the early-time Poincaré patch covering $X^0 + X^{d+1} < 0$, but this will not influence the following discussion.

the equation of motion reads

$$\eta^2\ddot{\phi}(\vec{k},\eta) - \eta(d-1)\dot{\phi}(\vec{k},\eta) + \left(\Delta(d-\Delta) + k^2\eta^2\right)\phi(\vec{k},\eta) = 0 \tag{2.52}$$

using the notation

$$\Delta(d-\Delta) = m^2R^2 \tag{2.53}$$

for future convenience.

As we will see later, Δ can be interpreted as a scaling dimension once the limit $\eta \to 0$ is taken. Depending on the value of m^2R^2, the dimension Δ can either be real or complex. Let us discuss these cases separately. If $0 \leq m^2R^2 < d^2/4$, then Δ takes values in the range $(0,d)$, which is the $\ell = 0$ complementary series. On the other hand, if $m^2R^2 \geq d^2/4$ then Δ takes complex values: $\Delta = \frac{d}{2} + i\nu$ with $\nu \in \mathbb{R}$. This is exactly the $\ell = 0$ principal series. Remark that the label ν is only determined up to a sign. For a discussion of the $m^2 < 0$ case, we refer to [84].

To proceed, we note that the solutions to the equation of motion can be written as Hankel functions. The exact mode decomposition reads

$$\phi(\eta,k) = f_k(\eta)a_k^\dagger + \bar{f}_k(\eta)a_{-k} \tag{2.54}$$

where a_k and $a_k^\dagger$ obey canonical commutation relations

$$[a_{\vec{k}}, a_{\vec{k}'}^\dagger] = (2\pi)^d\delta^d(\vec{k}-\vec{k}') \tag{2.55}$$

and f_k, $\bar{f}_k$ are solutions to (2.52). As a second order differential equation, Eq. (2.52) has two solutions: Hankel functions of the first and second kind. It turns out that by looking at early times $\eta \to -\infty$ and requiring the absence of the states with negative energy, one of the solutions is not allowed. Look at our detailed discussion of the wave function of a generic QFT in section 3.1 or [85, section 7.2]. One then finds that the solutions are

$$f_k(\eta) = (-\eta)^{d/2}\, h_{i\nu}(|k|\eta)\ , \qquad \bar{f}_k(\eta) = (-\eta)^{d/2}\, \bar{h}_{i\nu}(|k|\eta) \tag{2.56a}$$

where

$$h_{i\nu}(z) := \frac{\sqrt{\pi}}{2}e^{\pi\nu/2}H_{i\nu}^{(2)}(-z)\ , \qquad \bar{h}_{i\nu}(z) := \frac{\sqrt{\pi}}{2}e^{-\pi\nu/2}H_{i\nu}^{(1)}(-z)\ . \tag{2.56b}$$

In particular, notice that $h_{i\nu}$ and $\bar{h}_{i\nu}$ are invariant under $\nu \mapsto -\nu$, which is to be expected since only the product $\Delta(d-\Delta) = d^2/4 + \nu^2$ is physical. Note that the normalization of the mode functions is chosen so that they obey

$$f_k(\eta)\frac{d}{d\eta}\bar{f}_k(\eta) - \bar{f}_k(\eta)\frac{d}{d\eta}f_k(\eta) = -i(-\eta)^{(d-1)} \tag{2.57a}$$

from which it follows that ϕ and its conjugate Π satisfy canonical commutation relations:

$$[\phi(\eta,x),\Pi(\eta,x')]=i\delta^{(d)}(x-x'),\quad \Pi(\eta,x)=\frac{\delta S}{\delta\dot{\phi}}=(-R/\eta)^{d-1}\,\dot{\phi}(\eta,x)\,. \tag{2.57b}$$

At early times $\eta\to-\infty$, the field $\phi(\eta,x)$ behaves similarly to a massless scalar field in $(d+1)$-dimensional flat space:

$$\phi(\eta,x)\underset{\eta\to-\infty}{\sim}(-\eta/R)^{(d-1)/2}\int\frac{d^dk}{(2\pi)^d\sqrt{2|k|}}\left[e^{ik\cdot x+i\eta|k|+i\pi/4}\,a_k^\dagger+\text{h.c.}\right], \tag{2.58}$$

The factor $-\eta/R$ is exactly the Weyl factor corresponding to the metric (2.28). This result can for instance be understood from the equation of motion (2.52), since at early times both the damping term $\dot{\phi}$ and the mass term proportional to $\Delta(d-\Delta)$ become irrelevant. Finally, we define the Bunch-Davies vacuum $|\Omega\rangle$ to be the state annihilated by all a_k, so that correlators at $\eta\to-\infty$ are similar to ordinary Minkowski correlators.

The Hilbert space of free theory

Analogously to the quantization of a scalar field in flat space, the Hilbert state of the scalar theory in dS is a Fock space consisting of a zero-particle vacuum state $|\Omega\rangle$, single-particle states $a_k^\dagger\,|\Omega\rangle$ and multi-particle states $a_{k_1}^\dagger\cdots a_{k_n}^\dagger\,|\Omega\rangle$. It will be instructive to study the properties of single-particle states, which we will denote by

$$|\Delta,k\rangle:=a_k^\dagger|\Omega\rangle\ . \tag{2.59}$$

These states inherit a normalization from (2.55), namely

$$\langle\Delta,k|\Delta,k'\rangle=(2\pi)^d\delta^d(k-k')\ . \tag{2.60}$$

We claim that the $|\Delta,k\rangle$ form an irreducible representation of the $SO(d+1,1)$ algebra. In order to obtain the transformation properties of the states in question, let us define wave functions

$$\Phi_k(\eta,x|\Delta):=R^{(d-1)/2}\langle\Omega|\phi(\eta,x)|\Delta,k\rangle=e^{-i\vec{k}\cdot\vec{x}}(-\eta)^{d/2}\,h_{i\nu}(|k|\eta) \tag{2.61}$$

where the explicit expression on the RHS was obtained using (2.54), and we set $\Delta=\frac{d}{2}+i\nu$. We will use the expression (2.61) to show how the states $|\Delta,k\rangle$ form a representation of $SO(d+1,1)$.

To start, notice that the vacuum state $|\Omega\rangle$ is annihilated by all generators. Moreover, since $\phi(\eta,x)$ is a local operator, it transforms under infinitesimal transformations as in (2.35). From the above facts, we deduce for example that

$$\begin{aligned} -ik_\mu \Phi_k(\eta, x|\Delta) &= \partial_\mu \Phi_k(\eta, x|\Delta) && (2.62a) \\ &= \langle \Omega | [P_\mu, \phi(\eta, x)] | \Delta, k\rangle && (2.62b) \\ &= 0 - \langle \Omega | \phi(\eta, x) P_\mu | \Delta, k\rangle && (2.62c) \end{aligned}$$

hence it follows that

$$P_\mu |\Delta, k\rangle = ik_\mu |\Delta, k\rangle \ . \tag{2.63a}$$

For the other generators, we find that similarly

$$D|\Delta, k\rangle = -\left[k\cdot\partial + \tfrac{d}{2}\right]|\Delta, k\rangle, \tag{2.63b}$$

$$K_\mu|\Delta, k\rangle = i\left[k_\mu \partial^2 - 2(k\cdot\partial)\partial_\mu - d\,\partial_\mu + (\Delta - \tfrac{d}{2})^2\frac{k_\mu}{|k|^2}\right]|\Delta, k\rangle \ , \tag{2.63c}$$

$$M_{\mu\nu}|\Delta, k\rangle = \left[k_\nu\partial_\mu - k_\mu\partial_\nu\right]|\Delta, k\rangle \tag{2.63d}$$

where all derivatives act in k-space, that is to say $\partial_\mu = \partial/\partial k^\mu$. The derivation of the identities (2.63) is tedious but straightforward. We perform these calculations in full detail in appendix B

It is easy to check that the commutators of (2.63) are consistent with the conformal algebra (2.33). Moreover, the Casimir (2.37) evaluates to

$$C|\Delta, k\rangle = \Delta(\Delta - d)|\Delta, k\rangle \ . \tag{2.64}$$

The action (2.63) is exactly the $\ell = 0$ representation of $SO(d+1, 1)$ from section 2.2. Multi-particle states can also be organized in representations of $SO(d+1, 1)$. If m^2 is sufficiently large, then the single-particle state $|\Delta, k\rangle$ is in the principal series, because $\Delta = \frac{d}{2} + i\nu$ for some $\nu \in \mathbb{R}$. In $d \geq 2$ dimensions, two-particle states are then a superposition of other principal series states $[\frac{d}{2} + i\nu', \ell]$ with $\nu' \in \mathbb{R}$ and $\ell = 0, 1, 2, \ldots$ [65]. For $d = 1$, we expect that the Hilbert space of the theory also contains states in the discrete series, having integer Δ. This observation will be important in section 5 when we set up the bootstrap for QFT in dS_2.

2.5 Perturbative QFT in de Sitter

In this section, we mention some of the tools that help us perform perturbative calculations in dS. We start with a quick review of in-in or Schwinger-Keldysh formalism that provides a recipe similar to Feynman rules in flat space to calculate correlators of dS. Moreover, we discuss the fruitful relation between de Sitter space dS_{d+1} and EAdS_{d+1}. This relation paves the wave of perturbative calculation in dS by introducing a simple map between dS late-time correlators and Witten diagrams in EAdS that have already developed to a great extent in the past few decades. We conclude this section by explicitly carrying out the relation between contact diagrams in dS and EAdS. Many of the results presented below have appeared before, in particular in [86–88, 21]. We reproduce them here for convenience but refer to the original works for more details.

2.5.1 In-in formalism

In the present section, we will briefly review the in-in formalism used in the computation of dS correlators. Recall that the flat-space S-matrix is related to correlation functions via LSZ reduction. There we assume cluster decomposition, meaning that in the far past (starting from a so-called "in" state) and the far future (evolving towards an "out" state), the states can be written as the product of non-interacting single-particle states. In particular, we assume that the vacuum is the free theory vacuum $|0\rangle$. In other words, we assume that we turn the interaction on and off adiabatically. In the case of dS, we still may ask to turn interactions on adiabatically, but correlation functions at late times (which are of interest to us) do not necessarily decompose into products of free single-particle states. As such, there is no well-defined notion of "out"-states.[15]

Consider correlator

$$\langle Q(\eta)\rangle = \langle \mathcal{O}(\eta, x_1)\mathcal{O}_2(\eta, x_2)\cdots\mathcal{O}_n(\eta, x_n)\rangle$$

at some time η. To calculate this correlation function, we use the *in-in formalism* in which we evolve with a unitary operator from time $\eta_0 = -\infty$ to η and evolve back in time again to $\eta_0 = -\infty$ as follows:

$$\langle Q(\eta)\rangle = \langle \bar{T}\{e^{i\int_{\eta_0(1-i\epsilon)}^{\eta(1-i\epsilon)} d\eta'' H_I(\eta'')}\} Q_I(\eta) T\{e^{-i\int_{\eta_0(1+i\epsilon)}^{\eta(1+i\epsilon)} d\eta' H_I(\eta')}\}\rangle \tag{2.65}$$

where the T (resp. $\bar{T}$) time-orders (anti-time-orders) operator products, cf. formula (1) from [86]. Note that the $i\epsilon$ on the right-hand side comes with a plus sign while the one on the left has a minus sign. This has a convenient representation in the so-called Schwinger-Keldysh picture, where we have a branch cut on the real axis of the η-plane. To calculate the above correlator $\langle Q(\eta)\rangle$, we first evolve from $\eta = -\infty$ and move below the cut to η (time ordered and $\eta(1 + i\epsilon)$ with $\eta < 0, \epsilon > 0$) and go back from above the cut (anti-time ordered and $\eta(1 - i\epsilon)$).

The prescription (2.65) results in a new set of Feynman rules, which are for instance explained in the appendix of [86]. We review them here for completeness:

---

[15] One way to derive perturbation theory in QFT textbooks makes use of the formula

$$\langle\Omega| T\{\phi(x)\phi(y)\} |\Omega\rangle = \lim_{T\to\infty(1-i\epsilon)} \frac{\langle 0| T\{\phi_I(x)\phi_I(y)e^{-i\int_{-\infty}^{\infty} dt H_I(t)}\} |0\rangle}{\langle 0| T\{e^{-i\int_{-\infty}^{\infty} dt H_I(t)}\} |0\rangle}$$

where the $|0\rangle$ and $|\Omega\rangle$ are respectively the vacuum of the free theory and interacting theory. However, to derive this formula, one needs to assume that it is possible to evolve back $|0\rangle$ with a unitary operator $U(t, t')$ from $T \to +\infty$ to some $t^* = \max(x, y, t_{\text{integral}})$. This is not possible in dS.

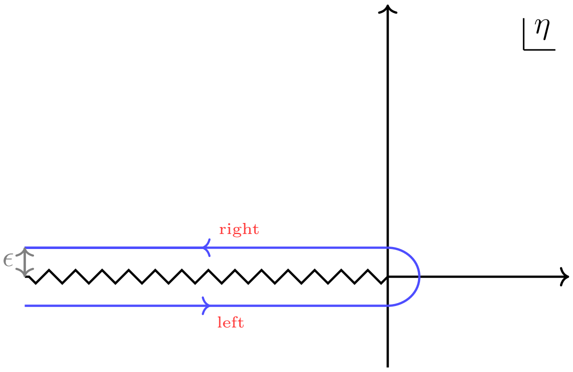

Figure 2.2: The contour integral of the in-in formalism.

- Two different sets of vertices correspond to time-ordered and anti-time-ordered terms. We call them right and left vertices, referring to their position in the operator product (2.65). The right vertex gets multiplied by $-i$, while the left vertex gets multiplied by $+i$.
- The external propagator emanating from a right vertex and the propagator between two right vertices refer to the time-ordered propagator $G^{rr} = \langle T\phi(\eta_1, x_1)\phi(\eta_2, x_2)\rangle$.
- Similarly, the external propagator leaving a left vertex and the propagator between two left vertices denotes the anti-time ordered propagator $G^{ll} = \langle \bar{T}\phi(\eta_1, x_1)\phi(\eta_2, x_2)\rangle$.
- The propagator between a right and a left vertex represents the Wightman function $G^{lr} = \langle \phi(\eta_1, x_1)\phi(\eta_2, x_2)\rangle$.

Another way to look at G^{rr}, G^{ll}, G^{lr} is indeed via their position on Schwinger-Keldysh contour. More precisely:

$$\begin{aligned} G^{rr} &= \langle \phi(\eta_1^r, x_1)\phi(\eta_2^r, x_2)\rangle \ , \\ G^{ll} &= \langle \phi(\eta_1^l, x_1)\phi(\eta_2^l, x_2)\rangle \ , \\ G^{lr} &= \langle \phi(\eta_1^l, x_1)\phi(\eta_2^r, x_2)\rangle \end{aligned} \tag{2.66}$$

where the left and right are respectively corresponding to time and anti-time ordered part of the contour with different $i\epsilon$ prescription:[16]

$$\eta^l = \eta(1 + i\epsilon) \ , \qquad \eta^r = \eta(1 - i\epsilon) \ . \tag{2.67}$$

Consequently, to perform perturbation theory computations in dS, one requires the two-point function of free theory. In the next section we restate the connection between EAdS and dS, find the explicit expressions of their propagators and establish the relation between the perturbative calculation of QFT in dS$_{d+1}$ and EAdS$_{d+1}$ via analytical continuation.

---

[16] Note that one could equivalently define the integral paths in (2.65) to be $\eta \mp i\epsilon$ instead of $\eta(1 \pm i\epsilon)$, and consequently $\eta^l = \eta - i\epsilon$, $\eta^r = \eta + i\epsilon$ considering $\eta < 0$. However, this will modify the sign of $i\epsilon$ prescription in (2.81) to $-i\epsilon$.

2.5.2 Two-point function in EAdS and dS

EAdS and dS are both maximally symmetric spacetimes that can be seen as hypersurfaces living in the Minkowski space of $\mathcal{M}^{d+2}$. In what follows we will show that this simple fact implies that the Wightman two-point function of one of these spacetimes can be written as a linear combination of the other one. For simplicity, we focus on scalar fields but a similar result holds for spinning two-point functions as well [89, 22]. This section is heavily inspired by the beautiful paper of [89].

Let us, again, spell out the definition of dS and EAdS as hypersurfaces living in the Minkowski space of $\mathcal{M}^{d+2}$:

$$X.X = X_A X^A = -(X^0)^2 + (X^1)^2 + \ldots + (X^{d+1})^2 = R^2 \qquad \mathrm{dS}_{d+1} \tag{2.68a}$$

$$Y.Y = Y_A Y^A = -(Y^0)^2 + (Y^1)^2 + \ldots + (Y^{d+1})^2 = -R^2 \qquad \mathrm{EAdS}_{d+1}\ . \tag{2.68b}$$

Notice that with the Wick rotation $R \to iR$ one goes from dS to EAdS and vice versa. Let us also define the two-point invariants σ as

$$\sigma^{\mathrm{dS}} = \frac{X_1.X_2}{R^2}\ , \qquad \sigma^{\mathrm{EAdS}} = \frac{Y_1.Y_2}{R^2}\ . \tag{2.69}$$

which for instance in Poincare coordinates are given by

$$\sigma^{\mathrm{dS}} = \frac{\eta_1^2 + \eta_2^2 - |x_{12}|^2}{2\eta_1\eta_2}\ , \qquad \sigma^{\mathrm{EAdS}} = -\frac{z_1^2 + z_2^2 + |x_{12}|^2}{2z_1 z_2} \tag{2.70}$$

and are related to chordal distances via

$$\zeta^{\mathrm{dS}} \equiv \frac{(X_1 - X_2)^2}{R^2} = 2(1 - \sigma^{\mathrm{dS}})\ , \qquad \zeta^{\mathrm{EAdS}} \equiv \frac{(Y_1 - Y_2)^2}{R^2} = -2(1 + \sigma^{\mathrm{EAdS}})\ . \tag{2.71}$$

Note that $\sigma^{\mathrm{EAdS}} \in (-\infty, -1]$ and saturates the bound at -1 when the points are on top of each other $X_1 \to X_2$ while $\sigma^{\mathrm{dS}} \in \mathbb{R}$. Moreover $\sigma^{\mathrm{dS}} > 1$ corresponds to timelike separated point, $\sigma^{\mathrm{dS}} < 1$ corresponds to spacelike separated points and $\sigma^{\mathrm{dS}} = 1$ is when the two points are on each other's lightcone.

The Wightman two-point function of a massive free scalar theory in dS and EAdS

$$\langle \phi(Z_1)\phi(Z_2)\rangle_{\mathrm{f}} = \frac{1}{R^{d-1}}\, G_{\mathrm{f}}(Z_1, Z_2), \tag{2.72}$$

is defined as the solution of the Klein-Gordon equation[17] [89, 19, 90]

$$\left(\nabla^2 - m^2\right) G_{\mathrm{f}}(Z_1, Z_2) = 0\ . \tag{2.73}$$

---

[17] Strictly speaking, Wightman two-point function is the solution of Green's equation with the right hand side proportional to a $\delta^{d+1}(Z_1 - Z_2)$. We eventually find the solution of this equation by requiring the short distance limit to match with the flat space solution.

where ∇^2 is the Laplacian in corresponding space that can be calculated from Laplacian in embedding space

$$\mp R^2\nabla^2 = \frac{1}{2}J_{AB}J^{AB} = -Z^2\partial_Z^2 + Z.\partial_Z(d + Z.\partial_Z) \tag{2.74}$$

followed by a projection to dS or EAdS [50, 3.1]. The minus in $\mp$ corresponds to dS and the plus sign represents EAdS. The subscript "f" stands for the fact that we are calculating the two-point function of the *free* theory. The solution to this equation is a function of the two-point invariant $\sigma = Z_1.Z_2/R^2$ and reads

$$\left[(1-\sigma^2)\partial_\sigma^2 - (d+1)\sigma\partial_\sigma \mp m^2R^2\right] G_{\mathrm{f}} = 0 \ , \tag{2.75}$$

which after a change of variable of $\rho = (1 \mp \sigma)/2$ becomes a hypergeometric equation [90]

$$\left[\rho(1-\rho)\partial_\rho^2 + \left(\frac{d+1}{2} - (d+1)\rho\right)\partial_\rho \mp m^2R^2\right] G_{\mathrm{f}} = 0 \ . \tag{2.76}$$

The solutions to this equation can be expressed in terms of two independent solutions of 24 Kummer's solutions. For later convenience, we chose the particular linear combination of

$$G_{\mathrm{f}}(\rho) = \mathcal{C}_\Delta \psi_\Delta(1/\rho) + \mathcal{D}_\Delta \psi_{d-\Delta}(1/\rho) \tag{2.77a}$$

with

$$\psi_\Delta(\xi) = \xi^\Delta \, {}_2F_1\left[\begin{matrix}\Delta, \Delta - \frac{d}{2} + \frac{1}{2} \\ 2\Delta - d + 1\end{matrix}\middle|\, \xi\right] \ , \qquad \Delta = \frac{d}{2} + \frac{1}{2}\sqrt{d^2 \mp 4m^2R^2} \tag{2.77b}$$

where Δ is the scaling dimension of dS in (2.53) and EAdS satisfying $\Delta(\Delta - d) = \mp m^2R^2$. So far the result of the calculations of dS and EAdS are the same up to the Wick rotation of $R \to iR$. Moreover, it is now apparent that Wightman two-point functions of dS_{d+1} and EAdS_{d+1} are related with a linear map. We may now specify the boundary conditions to fix $\mathcal{C}_\Delta$ and $\mathcal{D}_\Delta$ that appear in the eq. (2.77a):

- Regularity of the solution for
  - EAdS: the long-distance limit corresponding to $\rho \to \infty$. Considering that for a unitary theory in EAdS we have $m^2 \geq 0$ or equivalently $\Delta \geq d$, this condition leads to $\mathcal{D}_\Delta^{\mathrm{EAdS}} = 0$.
  - dS: antipodal points i.e. $\sigma^{\mathrm{dS}} \to -1$ or $\rho^{\mathrm{dS}} \to 1$. This condition leads to $\mathcal{C}_\Delta^{\mathrm{dS}} = \mathcal{D}_{d-\Delta}^{\mathrm{dS}}$.
- Recovering the flat space limit in short-distance limit. According to (2.74) this corresponds to $\sigma^{\mathrm{dS}} \to 1$ and $\sigma^{\mathrm{EAdS}} \to -1$ or equivalently $\rho^{\mathrm{dS}} \to 0$ and $\rho^{\mathrm{EAdS}} \to 1$.

In the end by recalling that $\sigma^{\mathrm{EAdS}} = 2\rho - 1$ and $\sigma^{\mathrm{dS}} = 1 - 2\rho$, one finds the EAdS propagator to be

$$G_{\rm f}^{\rm EAdS}(\sigma^{\rm EAdS}) = \frac{\mathcal{C}_\Delta}{(-2-2\sigma^{\rm EAdS}))^\Delta}\,{}_2F_1\left[\begin{matrix}\Delta, \Delta-\frac{d}{2}+\frac{1}{2}\\ 2\Delta-d+1\end{matrix}\,\middle|\,\frac{2}{1+\sigma^{\rm EAdS}}\right] \tag{2.78}$$

where

$$\mathcal{C}_\Delta = \frac{\Gamma(\Delta)}{2\pi^{\frac{d}{2}}\Gamma(\Delta-\frac{d}{2}+1)}\ , \tag{2.79}$$

and the dS propagator to be

$$\begin{aligned} G_{\rm f}^{\rm dS}(\sigma^{\rm dS}) &= \frac{\Gamma(\frac{d}{2}-\Delta)\Gamma(\Delta)}{2^{\Delta+2}\pi^{d/2+1}}\frac{1}{(1-\sigma^{\rm dS})^\Delta}\,{}_2F_1\left[\begin{matrix}\Delta, \Delta-\frac{d}{2}+\frac{1}{2}\\ 2\Delta-d+1\end{matrix}\,\middle|\,\frac{2}{1-\sigma^{\rm dS}}\right] \;+\; \Delta\leftrightarrow d-\Delta \\ &= \frac{\Gamma(\Delta)\Gamma(d-\Delta)}{(4\pi)^{\frac{d+1}{2}}\Gamma(\frac{d+1}{2})}\,{}_2F_1\left(\Delta, d-\Delta;\, \frac{d+1}{2};\, \frac{1+\sigma^{\rm dS}}{2}\right) \end{aligned} \tag{2.80}$$

where we used the identity (A.10) to go from the first line to the second.

Remark that $\sigma^{\rm EAdS} \leq -1$, therefore two-point function found in (2.78) is indeed regular at any separation as expected for a Euclidean free two-point function. On the other hand, $\sigma^{\rm dS} \in \mathbb{R}$ and when two points are timelike separated ($\sigma^{\rm dS} > 1$), then one needs an $i\epsilon$ prescription to deal with the branch cut in (2.80). In practice, when we are calculating the in-in diagrams, we have a definite $i\epsilon$ prescription given by (2.66):

$$G^{rr} = G_{\rm f}^{\rm dS}(\sigma^{\rm dS}-i\epsilon)\ , \quad G^{ll} = G_{\rm f}^{\rm dS}(\sigma^{\rm dS}+i\epsilon)\ , \quad G^{lr} = G_{\rm f}^{\rm dS}(\sigma^{\rm dS}-i\epsilon\,{\rm sgn}(\eta^l-\eta^r))\ . \tag{2.81}$$

One may also derive this by Fourier transforming the two-point function to momentum space using (2.54). For future reference, we note the Fourier decomposition in question:

$$G_{\rm f}^{\rm dS}(\sigma^{\rm dS}) = (\eta\eta')^{d/2}\int \frac{d^dk}{(2\pi)^d}\, e^{-ik\cdot(x-x')}\,\overline{h}_{i\nu}(|k|\eta)h_{i\nu}(|k|\eta')\ . \tag{2.82}$$

Let us comment on the meaning of regularity for antipodal separation in dS. This is connected to the definition of the vacuum state. Indeed, dS does not possess a unique solution for the vacuum state. There are a family of vacua that are invariant under dS isometries. This family of vacua is labeled by a continuous complex parameter α and they are called α-vacua. For more details look at e.g. [91–94]. Indeed the two-point function in (2.80) is in the Bunch-Davies vacuum. We discussed a perturbative way of defining the Bunch-Davies vacuum in section 2.4. Another way of defining the Bunch-Davies vacuum is through analytical continuation from the sphere discussed in (2.3); hence, some call the Bunch-Davies vacuum, the Euclidean vacuum. The vacuum state on the sphere is well-defined and unique and it is natural to ask regularity of two-point functions when the points are at antipodal positions. Therefore, after analytically continuing back to dS, we require the two-point functions to be regular when $\sigma^{\rm dS} \to -1$. On the other hand, the two-point function in alpha vacuum admits solutions that are singular at antipodal points [91]:

$$\begin{aligned}\langle\alpha|\,\phi(X_1)\phi(X_2)\,|\alpha\rangle = \cosh^2\alpha\, G_{\text{BD}}(X_1,X_2) + \sinh^2\alpha\, G_{\text{BD}}(\tilde{X}_1,\tilde{X}_2)\\ + \frac{1}{2}\sinh 2\alpha\,\Big(G_{\text{BD}}(\tilde{X}_1,X_2) + G_{\text{BD}}(X_1,\tilde{X}_2)\Big)\end{aligned} \tag{2.83}$$

where $|\alpha\rangle$ is the α-vacuum, and we pick $\alpha\in\mathbb{R}$ ($\alpha=0$ corresponds to the Bunch-Davies), G_{BD} is the Wightman two-point function in the Bunch-Davies vacuum found in eq. (2.80) and $\tilde{X}=-X$ is the antipodal transformation.

Late-time limit and boundary operators

Let us briefly discuss the late-time boundary operators in a massive free theory. Take the bulk-to-boundary expansion in (2.46) and (2.44). The action of the symmetry group on these fields will fix the dimension of the first (primary) operator that shows up in the expansion:

$$\begin{aligned}\text{EAdS:}\qquad &\phi(z,x) \underset{z\to0^+}{\sim} a_\Delta\, z^\Delta\mathcal{O}(x)\\ \text{dS:}\qquad &\phi(x,\eta) \underset{\eta\to0^-}{\sim} b_\Delta\,(-\eta)^\Delta\mathcal{O}(x) + b^*_\Delta\,(-\eta)^{\Delta^*}\mathcal{O}^\dagger(x)\ .\end{aligned} \tag{2.84}$$

Note that since the scaling dimension Δ in EAdS in real and positive, only one term shows up in the expansion but in dS if the free field is heavy enough ($m^2R^2 > d^2/4$) then there appears a pair of hermitian conjugate operators with an equal real part for scaling dimension. In the case of light fields ($m^2R^2 < d^2/4$), the boundary operators are hermitian $\mathcal{O}=\mathcal{O}^\dagger$ and $b_\Delta = b^*_\Delta$. Now let us look at the late-time of two-point functions (2.78) (for $z_1=z_2=z$) and (2.80)(for $\eta_1=\eta_2=\eta$):

$$\begin{aligned}G_{\text{f}}^{\text{EAdS}} &\underset{z\to0^+}{\sim} \frac{\Gamma(\Delta)}{2\pi^{\frac{d}{2}}\Gamma(\Delta-\frac{d}{2}+1)} z^{2\Delta}\frac{1}{|x_{12}|^{2\Delta}}\ ,\\ G_{\text{f}}^{\text{dS}} &\underset{\eta\to0^-}{\sim} \frac{\Gamma(\Delta)\Gamma(\frac{d}{2}-\Delta)}{4\pi^{\frac{d}{2}+1}}(-\eta)^{2\Delta}\frac{1}{|x_{12}|^{2\Delta}}\ +\ \Delta\leftrightarrow d-\Delta\ +\ (\text{local terms})\ .\end{aligned} \tag{2.85}$$

Note that both of them have the CFT two-point function structures on the right side ($|x_{12}|^{-2\Delta}$). This is expected from (2.84) since, as mentioned in 2.3, the late-time boundary is conformal meaning that the action of EAdS and dS isometries on the boundary operators are the same as the ones of primary operators of a CFT. In this thesis, we pick the convention that the two-point function is unit normalized: $\langle\mathcal{O}(x_1)\mathcal{O}(x_2)\rangle = |x_{12}|^{-2\Delta}$, this fixes the bulk-boundary coefficients of (2.84):

$$a_\Delta = \sqrt{\mathcal{C}_\Delta} = \left[\frac{\Gamma(\Delta)}{2\pi^{\frac{d}{2}}\Gamma(\Delta-\frac{d}{2}+1)}\right]^{\frac{1}{2}}\ ,\qquad b_\Delta = \left[\frac{\Gamma(\Delta)\Gamma(\frac{d}{2}-\Delta)}{4\pi^{\frac{d}{2}+1}}\right]^{\frac{1}{2}}\ . \tag{2.86}$$

Here, we neglect the local terms in eq. (2.85), but it turns out that their existence is essential for maintaining unitarity. We will discuss this matter in detail in section 4.2.2.

2.5.3 EAdS-dS dictionary

In this section, we will reproduce the simple recipe to transform the Feynman diagrams in dS to their EAdS counterparts with a Wick rotation. For definiteness, let us pick the Poincare coordinates for both spacetimes. As discussed in section (2.5.1), the calculation of Feynman diagrams in dS involves three types of propagators: G^{ll}, G^{rr}, G^{lr}. These propagators can be found by tracking their position on Schwinger-Keldysh contour (2.66) and the notion of η^l and η^r defined in (2.67).

Consider the transformation that Wick rotate the left and right Euclidean times differently:

$$\eta^l \to -e^{i\frac{\pi}{2}} z \ , \qquad \eta^r \to -e^{-i\frac{\pi}{2}} z \ . \tag{2.87}$$

This transformation implies

$$\sigma^{\mathrm{dS}}_{lr} \to \sigma^{\mathrm{EAdS}} \ , \qquad \sigma^{\mathrm{dS}}_{rr(ll)} \to -\sigma^{\mathrm{EAdS}} \tag{2.88}$$

where $\sigma^{\mathrm{dS}}_{ab}$ corresponds to the two-point function invariant σ^{dS} in (2.70) with $\eta_1 = \eta^a$ and $\eta_2 = \eta^b$. Using the hypergeometric identity (A.8), one can easily show that under the map of (2.87), G^{lr} transforms as

$$G^{lr} \to \mathfrak{g}(\Delta) G^{\mathrm{EAdS}}_{\Delta}(\sigma^{\mathrm{EAdS}}) + \mathfrak{g}(d-\Delta) G^{\mathrm{EAdS}}_{d-\Delta}(\sigma^{\mathrm{EAdS}}) \tag{2.89}$$

with

$$\mathfrak{g}(\Delta) = \frac{b_{\Delta}^2}{a_{\Delta}^2} = \frac{\Gamma(\Delta - \frac{d}{2})\Gamma(\frac{d}{2} - \Delta)}{2\pi} \left(\Delta - \frac{d}{2}\right) \tag{2.90}$$

where we used the notation $G^{\mathrm{EAdS}}_{\Delta}$ for $G^{\mathrm{EAdS}}_{\mathrm{f}}$ with scaling dimension Δ. Moreover, by plugging transformation (2.88) in the first equation of (2.80) and using the (2.81) $i\epsilon$ prescription, one finds transformation rules

$$\begin{aligned} G^{rr} &\to e^{-i\pi\Delta} \mathfrak{g}(\Delta) G^{\mathrm{EAdS}}_{\Delta}(\sigma^{\mathrm{EAdS}}) + e^{-i\pi(d-\Delta)} \mathfrak{g}(d-\Delta) G^{\mathrm{EAdS}}_{d-\Delta}(\sigma^{\mathrm{EAdS}}) \ , \\ G^{ll} &\to e^{i\pi\Delta} \mathfrak{g}(\Delta) G^{\mathrm{EAdS}}_{\Delta}(\sigma^{\mathrm{EAdS}}) + e^{i\pi(d-\Delta)} \mathfrak{g}(d-\Delta) G^{\mathrm{EAdS}}_{d-\Delta}(\sigma^{\mathrm{EAdS}}) \ . \end{aligned} \tag{2.91}$$

Equations (2.89) and (2.91) have a very important consequence: *all dS in-in Feynman diagrams map to a linear combination of EAdS diagrams.* Notice that this statement is true for any order in perturbation theory.

The only remaining required ingredient to complete the dS-EAdS dictionary is the measure of in-in left and right vertices that are given by

$$\begin{aligned} \text{right vertex :} \qquad & -i\int \frac{d\eta^r}{(-\eta^r)^{d+1}} \to e^{i\frac{\pi}{2}(d-1)} \int \frac{dz}{z^{d+1}} \\ \text{left vertex :} \qquad & i\int \frac{d\eta^l}{(-\eta^l)^{d+1}} \to e^{-i\frac{\pi}{2}(d-1)} \int \frac{dz}{z^{d+1}} \ . \end{aligned} \tag{2.92}$$

There is a beautiful way to organize these rules presented by [21]. In this paper, the authors propose an effective action of a theory with potential V^{EAdS} that naturally produces the the correlator of a theory with potential V^{dS}.

Example: dS contact diagram

As the simplest example of the mentioned dictionary, let us consider the first order correction to the dS scalar boundary n-point function–generated by the n-point contact diagram of a $\lambda\phi_1\cdots\phi_n$ interaction:

$$\langle\phi_1(\eta_0,x_1)\cdots\phi_n(\eta_0,x_n)\rangle_\lambda = \langle\phi_1(\eta_0,x_1)\cdots\phi_n(\eta_0,x_n)\rangle_{\text{free}} \ + \ \lambda\mathfrak{D}(\eta_0) \tag{2.93}$$

where we set $R=1$. According to the in-in formalism, this contact diagram is the sum of two diagrams of n-external propagators that meet at left and right vertices:

$$\mathfrak{D}(\eta_0) = -i\mathfrak{D}^r(\eta_0) + i\mathfrak{D}^l(\eta_0) \ , \tag{2.94}$$

$$\mathfrak{D}^\alpha(\eta_0) = \int_{-\infty}^{\eta_0} \frac{d\eta^\alpha}{(-\eta^\alpha)^{d+1}} \int d^dx \prod_{i=1}^{n} G^{\alpha\alpha}(\eta_0,x_i,\eta^\alpha,x) \ . \tag{2.95}$$

As seen in (2.91), each $G^{\alpha\alpha}$ produces two bulk-boundary propagators related by a shadow transformation corresponding to the two boundary operators $\mathcal{O}$ and $\mathcal{O}^\dagger$. Therefore, to calculate the perturbative contribution to the correlator

$$\langle\mathcal{O}(x_1)\cdots\mathcal{O}(x_n)\rangle_{\text{dS}} \ ,$$

we assign the first terms in (2.91), and define bulk to boundary propagators as

$$\begin{aligned} K^{rr} &:= \lim_{\eta_0\to 0^-} \mathfrak{g}(\Delta)e^{-i\pi\Delta}G^{\text{EAdS}}_\Delta \ , \\ K^{ll} &:= \lim_{\eta_0\to 0^-} \mathfrak{g}(\Delta)e^{i\pi\Delta}G^{\text{EAdS}}_\Delta \ . \end{aligned} \tag{2.96}$$

We shall show that the dS contact diagram is simply proportional to the EAdS counterpart. Let the dimension of each operator ϕ_i be Δ_i. The two boundary correlators are generated by the corresponding bulk correlators as

$$\begin{aligned} \langle \phi_1 \cdots \phi_n \rangle_{\text{EAdS}} : \quad & \prod_{i=1}^{n} a_{\Delta_i}\, z_0^{\Delta_t}\, \langle \mathcal{O}(x_1) \cdots \mathcal{O}(x_n) \rangle_{\text{EAdS}} \ , \\ \langle \phi_1 \cdots \phi_n \rangle_{\text{dS}} : \quad & \prod_{i=1}^{n} b_{\Delta_i}\, (-\eta)_0^{\Delta_t}\, \langle \mathcal{O}(x_1) \cdots \mathcal{O}(x_n) \rangle_{\text{dS}} \ . \end{aligned} \tag{2.97}$$

where $\Delta_t = \sum_{i=1}^{n} \Delta_i$ and $a_{\Delta_i}, b_{\Delta_i}$ are field ϕ_i bulk-to-boundary coefficient in (2.84)– explicitly given by (2.86). Using (2.91) and (2.92) we then find:

$$\langle \mathcal{O}_1 \cdots \mathcal{O}_n \rangle_{\text{dS}}^{\text{contact}} \to 2 \sin\left(\frac{\pi}{2}(d - \Delta_t)\right) \frac{\prod_{i=1}^{n} a_{\Delta_i}\, \mathfrak{g}(\Delta_i)}{\prod_{i=1}^{n} b_{\Delta_i}} \langle \mathcal{O}_1 \cdots \mathcal{O}_n \rangle_{\text{EAdS}}^{\text{contact}} \tag{2.98}$$

where $\langle \mathcal{O}_1 \cdots \mathcal{O}_n \rangle^{\text{contact}}$ is the contribution of a bulk contact interaction (i.e. order λ contribution) to the boundary n-point function.

It is customary to write the EAdS contact diagram as

$$\langle \mathcal{O}_1 \cdots \mathcal{O}_n \rangle_{\text{EAdS}}^{\text{contact}} = \left(\prod_{i=1}^{n} a_{\Delta_i} \right) D_n(x_i) \tag{2.99}$$

with

$$D_n(x_i) = \int_0^\infty \frac{dz}{z^{d+1}} \int_{\mathbb{R}^d} d^d y \prod_{i=1}^{n} \left(\frac{z}{z^2 + |y - x_i|^2} \right)^{\Delta_i} \tag{2.100}$$

which is know as the *D-function* in the literature. Consequently, we have

$$\langle \mathcal{O}_1 \cdots \mathcal{O}_n \rangle_{\text{dS}}^{\text{contact}} = 2 \sin\left(\frac{\pi}{2}(d - \Delta_t)\right) \left(\prod_{i=1}^{n} b_{\Delta_i} \right) D_n(x_i) \ . \tag{2.101}$$

2.6 Non-perturbative QFT in de Sitter

2.6.1 Hilbert space

In a general QFT, we expect that the Hilbert space falls into irreducible representations of the isometry group of its spacetime, plus any additional global symmetries of the theory in question. For a QFT on dS_{d+1}, we therefore expect that all states form representations of $SO(d+1,1)$, like the single-particle states $|\Delta, k\rangle$ from section 2.4. In this section, will argue that after taking spin into account, the representation (2.63) is essentially unique up to a choice of Δ. For generic Δ such representations are non-unitary, but for special values of Δ these states form principal, complementary or discrete series irreps, as described in section 2.2. To prove this, let us write a generic state as $|\Delta, k\rangle_A$, where A is an abstract $SO(d)$ index. Since the anti-hermitian momentum generators P_μ commute, we can diagonalize them

$$P_\mu|\Delta,k\rangle_A = ik_\mu|\Delta,k\rangle_A \tag{2.102}$$

as in (2.63). Next, let us briefly introduce some notation to describe spinning states $|\Delta,k\rangle_A$ where A is an abstract $SO(d)$ index. Rotations act on such a state as

$$M_{\mu\nu}|\Delta,k\rangle_A = (k_\nu\partial_\mu - k_\mu\partial_\nu + \Sigma_{\mu\nu})|\Delta,k\rangle_A \tag{2.103}$$

where $\Sigma_{\mu\nu} = -\Sigma_{\nu\mu}$ acts on the A indices and obeys the same commutation relations as $M_{\mu\nu}$. In the present thesis, we will only deal with states that transform as traceless symmetric tensors of spin ℓ. It will be convenient to use an index-free notation as follows:

$$|\Delta,k,z\rangle := |\Delta,k\rangle_{\mu_1\cdots\mu_\ell}\, z^{\mu_1}\cdots z^{\mu_\ell} \tag{2.104}$$

where the indices $\mu_1,\ldots,\mu_\ell$ run over $1,\ldots,d$. The tensor properties of the above state imply that

$$z^\mu\frac{\partial}{\partial z^\mu}|\Delta,k,z\rangle = \ell\,|\Delta,k,z\rangle \quad \text{and} \quad \frac{\partial}{\partial z^\mu}\frac{\partial}{\partial z_\mu}|\Delta,k,z\rangle = 0\ . \tag{2.105}$$

The spin operator $\Sigma_{\mu\nu}$ now acts as

$$\Sigma_{\mu\nu}|\Delta,k,z\rangle = \left(z_\nu\frac{\partial}{\partial z^\mu} - z_\mu\frac{\partial}{\partial z^\nu}\right)|\Delta,k,z\rangle \tag{2.106}$$

such that

$$-\tfrac{1}{2}\Sigma_{\mu\nu}\Sigma^{\mu\nu}|\Delta,k,z\rangle = \ell(\ell+d-2)\,|\Delta,k,z\rangle \tag{2.107}$$

which recovers the usual $SO(d)$ Casimir eigenvalue of a spin-ℓ representation. From Eqs. (2.102) and (2.103), the action of the other generators is fixed up to a single parameter. For instance, the generator D should act as a scalar that assigns appropriate weights to k^μ and $\partial/\partial k^\mu$ because $[D,P_\mu]=P_\mu$. Hence D should be of the form

$$D|\Delta,k\rangle_A = -\left(k\cdot\partial+\beta\right)|\Delta,k\rangle_A \tag{2.108}$$

with some constant β to be determined. Likewise, we can write down a completely general ansatz for K_μ which transforms as a vector and is built out of k^μ, $\partial/\partial k^\mu$ and $\Sigma_{\mu\nu}$. By imposing that $[D,K_\mu]$ and $[K_\mu,P_\nu]$ close as in (2.33), and that $[K_\mu,K_\nu]=0$, we find that K_μ is fixed to

$$\begin{aligned}&K_\mu|\Delta,k\rangle_A = \\ &i\Big[k_\mu\partial^2 - 2(k\cdot\partial)\partial_\mu - d\,\partial_\mu + (\Delta-\tfrac{d}{2})^2\frac{k_\mu}{|k|^2} - 2\Sigma_{\mu\nu}\left(\partial^\nu \pm (\Delta-\tfrac{d}{2})\frac{k^\nu}{|k|^2}\right)\Big]|\Delta,k\rangle_A\end{aligned} \tag{2.109}$$

where Δ is now an arbitrary parameter. The requirement that $[K_\mu,P_\nu]$ reproduces the commutation relation (2.33) fixes $\beta=d/2$ in (2.108). The equations (2.103), (2.102), (2.108) and (2.109) thus form the most general consistent representation of $SO(d+1,1)$

that diagonalize P_μ. In addition, it is easy to see that the state $|\Delta, k\rangle_A$ will have conformal Casimir eigenvalue $\Delta(\Delta-d) - \frac{1}{2}\Sigma^2_{\mu\nu}$, which for a spin-$\ell$ representation becomes $\Delta(\Delta-d) + \ell(\ell+d-2)$.

Notice that in (2.109) the action of K_μ is only determined up to a choice of sign, at least for spinning states where $\Sigma_{\mu\nu} \neq 0$: both sign choices respect the conformal algebra and lead to the same Casimir eigenvalue. Changing the sign is equivalent to redefining $\Delta \mapsto d - \Delta$. In what follows, we will choose the + sign for definiteness.

Finally, the ground state $|\Omega\rangle$ of any QFT in dS must be annihilated by all of the symmetry generators, and as such it transforms as a trivial representation of dimension $\Delta = 0$, $\ell = 0$ and $k_\mu = 0$.

2.6.2 Representations in position space

Although the above representations look complicated, we can show that they take a more familiar form after introducing a specific Fourier-like transformation. To wit, define a new family of states as[18]

$$|\Delta, x\rangle_A := \int \frac{d^d k}{(2\pi)^d}\, e^{ik\cdot x}\, |k|^{\Delta - d/2}\, |\Delta, k\rangle_A \tag{2.110}$$

where a factor of $|k|^{\Delta-d/2}$ has been introduced for future convenience. We will argue that the state $|\Delta, x\rangle_A$ transforms just like a primary operator of dimension Δ in flat-space CFT. As a first hint, one readily computes that for a scalar state

$$\langle \Delta, x | \Delta, x'\rangle = \int \frac{d^d k}{(2\pi)^d}\, e^{ik\cdot(x-x')}\, |k|^{\Delta+\bar{\Delta}-d} \tag{2.111}$$

provided that the k-space state $|\Delta, k\rangle$ is normalized such that

$$\langle \Delta, k | \Delta, k'\rangle = (2\pi)^d \delta^d(k-k') \ . \tag{2.112}$$

There are now two possibilities: if Δ is real (i.e. when Δ is in the complementary series), then $\bar{\Delta} = \Delta$. On the other hand, if Δ is in the principal series then $\bar{\Delta} = d - \Delta$. We conclude that

$$\langle \Delta, x | \Delta, x'\rangle = \begin{cases} \delta^d(x-x') & \Delta \in d/2 + i\mathbb{R} \\ c_\Delta / |x-x'|^{2\Delta} & \Delta \in \mathbb{R} \end{cases} \tag{2.113}$$

for some computable coefficient c_Δ.[19] For real Δ this is the form of a two-point function in flat-space CFT, but when Δ is in the principal series the states $|\Delta, x\rangle_A$ have a delta function normalization.

---

[18] These states can be found in the literature with different but equivalent definitions. see e.g. [64, 69, 70]

[19] The integral (2.111) diverges for $\Delta \in \mathbb{R}$, so (2.113) is only true in the sense of distributions.

Let us make the above statement precise by computing the action of the $SO(d+1,1)$ generators. On a state of the form (2.110), P_μ acts as

$$P_\mu|\Delta,x\rangle_A = \int d^dk\; e^{ik\cdot x}\,|k|^{\Delta-d/2}(ik_\mu)|\Delta,k\rangle_A = \frac{\partial}{\partial x^\mu}\,|\Delta,x\rangle_A \tag{2.114a}$$

and likewise

$$D|\Delta,x\rangle_A = (x\cdot\partial+\Delta)\,|\Delta,x\rangle_A \tag{2.114b}$$
$$M_{\mu\nu}|\Delta,x\rangle_A = (x_\nu\partial_\mu - x_\mu\partial_\nu + \Sigma_{\mu\nu})|\Delta,x\rangle_A \tag{2.114c}$$
$$K_\mu|\Delta,x\rangle_A = \big(2x_\mu(x\cdot\partial) - x^2\partial_\mu + 2\Delta x_\mu - 2\Sigma_{\mu\nu}\,x^\nu\big)|\Delta,x\rangle_A \tag{2.114d}$$

where all derivatives act on x. We spell out the derivation for the case of the scalar states in appendix B. These formulas are exactly identical to those obtained by applying a fictitious CFT operator $\mathcal{O}^{(\Delta)}_A(x)$ of dimension Δ to the Bunch-Davies vacuum. From a practical point of view, this implies that any n-point amplitude

$$\langle\Omega|\phi(\eta_1,x_1)\cdots\phi(\eta_n,x_n)|\Delta,x\rangle_A \tag{2.115a}$$

has the exact same $SO(d+1,1)$ transformation properties as an $(n+1)$-point vacuum expectation value with an insertion of an operator $\mathcal{O}^{(\Delta)}_A(x)$:

$$\langle\Omega|\phi(\eta_1,x_1)\cdots\phi(\eta_n,x_n)\mathcal{O}^{(\Delta)}_A(x)|\Omega\rangle\ . \tag{2.115b}$$

However, unlike in flat-space CFT there is no state-operator correspondence: in general there is no relation between the states $|\Delta,x\rangle_A$ and the algebra of local operators on the timeslice $\eta=0$.

For future reference, we remark that from (2.113) it follows that the resolution of the identity operator inside an irrep can then be written as

$$\Delta\in\frac{d}{2}+i\mathbb{R}:\qquad \int d^dx\;|\Delta,x\rangle_A\;{}^A\langle\Delta,x| \tag{2.116}$$

that after summing over all the irreps leads to:

$$\boxed{\mathbb{1} = |\Omega\rangle\langle\Omega| + \sum_A\int_{\frac{d}{2}-i\infty}^{\frac{d}{2}+i\infty}\frac{d\Delta}{2\pi i N_x(\Delta,\ell)}\int d^dx\;|\Delta,x\rangle_A\;{}^A\langle\Delta,x|\ +\ \text{other irreps}} \tag{2.117}$$

where the sum over A formally stands for the sum over $SO(d)$ representations, which for our case of traceless symmetric representation will be simply a sum over spin ℓ. Here we did not explicitly spell out contributions from the irreps other than principal series as it will not be apparent in our discussion for scalar operators in the next sections. $N_x(\Delta,\ell)$ is a positive normalization coming from the Plancherel measure that we do not need its explicit expression and the subscript x stands for normalization in position space. There is a similar formula in momentum space that we mention here for completeness and future convenience:

$$\mathbb{1} = |\Omega\rangle\langle\Omega| + \sum_A \int \frac{d\Delta}{2\pi i} \frac{1}{N_k(\Delta,\ell)} \int \frac{d^d k}{(2\pi)^d} \, |\Delta, k\rangle_A \, {}^A\langle\Delta, k| \; + \; \text{other irreps} \, . \tag{2.118}$$

2.6.3 Conformal Field Theory in de Sitter

It is instructive to consider the case of a CFT on a de Sitter background. Given that the de Sitter metric (2.28) is conformally flat, we can immediately write

$$\phi(\eta, x) = (-\eta/R)^{\Delta_\phi} \phi_{\text{flat}}(\eta, x) \, , \tag{2.119}$$

where we assumed that ϕ is a primary scalar operator of the bulk CFT and we denoted by $\phi_{\text{flat}}(\eta, x)$ the same operator in flat Minkowski space with metric $ds^2 = -d\eta^2 + dx^2$. The OPE (2.44) then follows from expanding $\phi_{\text{flat}}(\eta, x)$ around the constant timeslice $\eta = 0$. Clearly, in this case, the primary boundary operators $\mathcal{O}_\alpha$ are nothing but time derivatives of ϕ_{flat}. Thus a conformal primary of dimension Δ_ϕ gives rise to a family of boundary operators with dimensions $\Delta_\alpha = \Delta_\phi + p$ with $p = 0, 1, 2, \ldots$.

This construction is useful because it gives us an infinite set of data to test any bootstrap approach to QFT in de Sitter. In particular, any CFT correlation function with all operators inserted on a constant timeslice in Minkowski (or Euclidean) space can be interpreted as a correlation function of operators on the future boundary of de Sitter spacetime.

As mentioned above, the metric of de Sitter space (2.26) is a Weyl transformation of a part of the Minkowski cylinder. It is instructive to understand how a unitary conformal highest-weight representation on the Minkowski cylinder decomposes into irreps of the dS isometry group. For this purpose it is useful to think of the CFT living on the lightcone

$$-(X^{-1})^2 - (X^0)^2 + (X^1)^2 + \ldots (X^{d+1})^2 = 0 \tag{2.120}$$

of the embedding space $\mathbb{R}^{d,2}$. Then dS_{d+1} is the section defined by $X^{-1} = R$ — compare with (2.22) — and the Minkowski cylinder is the universal cover of the section defined by $(X^{-1})^2 + (X^0)^2 = R^2$. The de Sitter isometry group $SO(d+1, 1)$ can immediately be identified as the subgroup of $SO(d+1, 2)$ that leaves the coordinate X^{-1} invariant.

In appendix D, we focus on the $d = 1$ case and build unitary irreps of $SO(2, 1)$ inside the usual conformal family of $SO(2, 2)$ labeled by the primary state $|\tilde{\Delta}, \ell\rangle$ of dimension $\tilde{\Delta}$ and spin ℓ. We show that there are principal series irreps with $\Delta = \frac{1}{2} + i\nu$ for all $\nu \in \mathbb{R}$ and one discrete series irrep as long as $\ell \geq 1$. We also found a complementary series irrep if $\tilde{\Delta} < \frac{1}{2}$. We leave for the future the instructive exercise of extending this analysis to general spacetime dimension.

Part II

Nonperturbative cosmological bootstrap

3 Bulk two-point function

In this chapter, we compute the two-point function (3.1) using the Hilbert space framework from section 2.6 and in particular the resolution of identity in (2.118). This will lead to an expression for $G_{12}(\xi)$ in terms of a spectral integral with definite positivity properties, also known as the Källén–Lehmann decomposition. After that, we relate the correlator (3.1) to its counterpart on sphere S^{d+1} and its decomposition in terms of spherical harmonics. After employing a Watson-Sommerfeld transformation, this leads to an explicit formula, the so-called *inversion formula*, expressing the Källén–Lehmann spectral density in terms of an integral over the discontinuity of $G_{12}(\xi)$. Moreover, we find another inversion formula from the analytical continuation and harmonic analysis in EAdS and prove their equivalence. Finally, we analyze the Källén–Lehmann decomposition in several examples.

3.1 Källén–Lehmann decomposition

Consider the two-point function of two scalar operators. Due to the translation and rotation invariance of dS, this correlation function should be of the form

$$\langle\Omega|\phi_1(\eta,x)\phi_2(\eta',x')|\Omega\rangle = G_{12}(\xi) \tag{3.1}$$

where we define

$$\xi = \frac{4R^2}{(X-X')^2} = \frac{2}{1-\sigma^{\mathrm{dS}}} = \frac{4\eta\eta'}{-(\eta-\eta')^2+|\vec{x}-\vec{x}'|^2} \tag{3.2}$$

as another representation of the only $SO(d+1,1)$ invariant that can be built out of two bulk points. We used the conformal coordinates defined in (2.27) for definiteness. Using ξ instead of σ is for later convenience. The invariant ξ is positive ($\xi > 0$) when X, X' are spacelike separated, negative ($\xi < 0$) when they are timelike separated and ξ diverges when X, X' are lightlike separated. As such an $i\epsilon$ prescription is required to define (3.1) properly when $\xi < 0$. As discussed in full detail in section 2.5.2, the free propagator reads

$$\langle\phi(\eta,x)\phi(\eta',x')\rangle_{\mathrm{f}} = \frac{1}{R^{d-1}}\, G_{\mathrm{f}}(\xi;\nu)\ , \tag{3.3}$$

where

$$G_{\mathrm{f}}(\xi;\nu) := \frac{\Gamma(\frac{d}{2}+i\nu)\Gamma(\frac{d}{2}-i\nu)}{(4\pi)^{\frac{d+1}{2}}\Gamma(\frac{d+1}{2})}\ {}_2F_1\!\left(\frac{d}{2}+i\nu, \frac{d}{2}-i\nu; \frac{d+1}{2}; 1-\frac{1}{\xi}\right) \tag{3.4}$$

writing $m^2R^2 = (d/2)^2 + \nu^2$ as before. From now on we will set $R = 1$ unless otherwise noted.

Let us now turn to the analysis of a generic two-point function of identical operators, $\langle\Omega|\phi(\eta,x)\phi(\eta',x')|\Omega\rangle$. We will assume that $\phi(\eta,x)$ is a Hermitian operator, although much of the argument holds as well for a generic two-point function $\langle\phi_i(\eta,x)\phi_j(\eta',x')\rangle$ of different scalar operators. We can analyze the $\langle\Omega|\phi(\eta,x)\phi(\eta',x')|\Omega\rangle$ correlator by inserting a resolution of the identity (2.118):

$$\mathbb{1} = |\Omega\rangle\langle\Omega| + \sum_{\ell}\int\frac{d\Delta}{2\pi i}\frac{1}{N(\Delta,\ell)}\int\frac{d^dk}{(2\pi)^d}\,|\Delta,k\rangle_{\mu_1\ldots\mu_\ell}\ {}^{\mu_1\ldots\mu_\ell}\langle\Delta,k| + \ldots \tag{3.5}$$

writing … for states with $SO(d)$ representations other than traceless symmetric tensors. In the above formula, we allow for an arbitrary normalization factor $N(\Delta,\ell) > 0$, depending on the normalization of the states $|\Delta,k\rangle_{\mu_1\ldots\mu_\ell}$ (which cannot depend on k_μ). We also dropped the subscript k compare to (2.118) to avoid clutter. Of course, there might be several irreps with the same quantum numbers $\{\Delta,\ell\}$, in which case an additional label α is needed to distinguish such states. We will not explicitly write such a label, but it is straightforward to adapt our analysis to this degenerate situation. In (3.5) we assume that only states in the principal series contribute, so the Δ-integral runs from $d/2 - i\infty$ to $d/2 + i\infty$. This assumption seems to be correct in general; in specific examples we will briefly revisit this assumption. For a more complete discussion, we refer to section 2.2. Moreover, when we find an inversion formula, based on completeness of Gegenbauer functions in the sphere or harmonic functions in EAdS, we basically prove the completeness of principal series as far as the inversion formula is convergent.

After inserting the resolution of the identity (3.5) in the two-point function, one finds

$$\begin{aligned}\langle\Omega|\phi(\eta,x)\phi(\eta',x')|\Omega\rangle &= \langle\Omega|\phi(\eta,x)|\Omega\rangle\langle\Omega|\phi(\eta',x')|\Omega\rangle\\ &+\sum_{\ell}\int\frac{d\Delta}{2\pi i}\frac{1}{N(\Delta,\ell)}\int\frac{d^dk}{(2\pi)^d}\,\langle\Omega|\phi(\eta,x)|\Delta,k\rangle_{\mu_1\ldots\mu_\ell}\ {}^{\mu_1\ldots\mu_\ell}\langle\Delta,k|\phi(\eta',x')|\Omega\rangle\ .\end{aligned} \tag{3.6}$$

First of all, remark that the one-point functions $\langle\Omega|\phi(\eta',x')|\Omega\rangle$ do not depend on the coordinates η and x^μ because $|\Omega\rangle$ is $SO(d+1,1)$ invariant. Hence we can replace the second term with the constant $\langle\phi\rangle^2 := \langle\Omega|\phi|\Omega\rangle^2$.

Moving to the second term of (3.6), one can show that matrix elements of the form $\langle\Omega|\phi(\eta,x)|\Delta,\ell\rangle$ with $\ell\geq 1$ vanish. This can be proven either by using an explicit computation or by working in embedding space. Therefore, only states with $\ell=0$ contribute, and the contribution of such a state is fixed by $SO(d+1,1)$ symmetry up to two constants. Using an $SO(d+1,1)$ symmetry argument, one can show that the most general form of the amplitude with the $\ell=0$ state is given by

$$\langle\Omega|\phi(\eta,x)|\Delta,k\rangle = e^{-ik\cdot x}\,(-\eta)^{d/2}\left[c_\phi(i\nu)\,\bar{h}_{i\nu}(\eta|k|)+c^\sharp_\phi(i\nu)\,h_{i\nu}(\eta|k|)\right]\ , \tag{3.7}$$

for two undetermined coefficients $c_\phi(i\nu)$, $c^\sharp_\phi(i\nu)\in\mathbb{C}$ and $\Delta=\frac{d}{2}+i\nu$. We will now argue that $c^\sharp_\phi(i\nu)$ has to vanish in any unitary QFT. For this argument, consider the early-time limit $\eta\to-\infty$, where dS can be compared to flat space. Using the asymptotics of the Hankel functions, the matrix element behaves in this limit as

$$\langle\Omega|\phi(\eta,x)|\Delta,k\rangle \underset{\eta\to-\infty}{\sim} \frac{e^{-ik\cdot x}(-\eta)^{(d-1)/2}}{\sqrt{2\omega(k)}}\left[c_\phi(i\nu)e^{-i\eta\omega(k)-i\pi/4}+c^\sharp_\phi(i\nu)e^{i\eta\omega(k)+i\pi/4}\right] \tag{3.8}$$

with $\omega(k):=|k|$ and two important phases $\pm i\eta\omega(k)$. The formula (3.8) is reminiscent of flat-space QFT, where operators evolve in time as

$$\phi(t,x)=e^{iHt}\phi(0,x)e^{-iHt}\ . \tag{3.9}$$

Moreover, according to the Wightman axioms, the state $\phi(0,x)|\Omega\rangle$ can only have support inside the positive future lightcone. Consequently, if $|E,k\rangle$ is a state that diagonalizes H and P_μ, we must have

$$\text{flat space}:\quad \langle\Omega|\phi(t,x)|E,k\rangle \ \propto\ \Theta(E)e^{-ik\cdot x}e^{-iEt} \tag{3.10}$$

up to some constant that depends on the local operator ϕ. We thus interpret the second term in (3.8) as originating from a state of negative energy, which would violate the Wightman axioms. Consequently, we have to require that $c^\sharp_\phi(i\nu)=0$ for all ν.

We are now ready to compute the k-integral in (3.6). Since ϕ is a hermitian operator, it follows that

$$\langle\Delta,k|\phi(\eta',x')|\Omega\rangle=\langle\Omega|\phi(\eta',x')|\Delta,k\rangle^*=c_\phi(i\nu)^*\,e^{ik\cdot x'}(-\eta')^{d/2}\,h_{i\nu}(\eta'|k|) \tag{3.11}$$

using the properties of the Hankel functions under complex conjugation. By performing the k-integral in (3.6) and using Eq. (2.82), we conclude that

$$\boxed{\langle\Omega|\phi(\eta,x)\phi(\eta',x')|\Omega\rangle=\langle\phi\rangle^2+\int_{\mathbb{R}}\frac{d\nu}{2\pi}\,\rho_\phi(\tfrac{d}{2}+i\nu)\,G_{\mathrm{f}}(\xi;\nu)} \tag{3.12}$$

with

$$\rho_\phi(\tfrac{d}{2}+i\nu):=\frac{|c_\phi(i\nu)|^2}{N(\frac{d}{2}+i\nu,0)}\geq 0\ . \tag{3.13}$$

This is the desired Källén–Lehmann decomposition which applies to any two-point function of bulk scalar operators. It is clear that similar Källén–Lehmann decompositions exist for all possible time-orderings.

In passing, let us comment on the apparent absence of states in the complementary series of $SO(d+1,1)$, having $0 \leq \Delta \leq d$, or even discrete series states. We did not explicitly include such states in the resolution of the identity (3.6). One can nevertheless accommodate for complementary series states in (3.12), by modifying the contour and integrating over small imaginary values of ν. This is equivalent to looking for a pole crossing after analytical continuation off of the principal series.

Finally, we want to mention that (3.12) is not a novel result. Versions of the Källén–Lehmann decomposition have already appeared in the literature, using different derivations and levels of mathematical rigor. An early reference to the Källén–Lehmann decomposition in dS appeared in [95], and later works using such a representation can be found in [96–104, 84].

3.2 Late-time limit and boundary OPE

Starting from the Källén–Lehmann representation (3.12), let us consider the late-time behavior of the correlator $\langle\phi(\eta,x)\phi(\eta',x')\rangle$ in the limit $\eta,\,\eta' \to 0^-$ at fixed x, x'. At the level of the invariant ξ from (3.2), this corresponds to the limit $\xi \to 0^+$. Also notice that for sufficiently small η and η' the two insertions are spacelike separated, so there are no subtleties regarding $i\epsilon$ prescriptions.

Let us rewrite $G_{\mathrm{f}}(\xi;\nu)$ in (3.4) in terms of a function $\psi_\nu(\xi)$ and its shadow ($\nu \mapsto -\nu$ or $\Delta \mapsto d-\Delta$) given by (2.80):

$$G_{\mathrm{f}}(\xi;\nu) = \frac{\mathsf{g}(\frac{d}{2}+i\nu)\psi_{\frac{d}{2}+i\nu}(\xi) + (\nu \mapsto -\nu)}{2} \tag{3.14a}$$

with

$$\mathsf{g}(\Delta) = \frac{\Gamma(\frac{d}{2}-\Delta)\Gamma(\Delta)}{2^{2\Delta+1}\pi^{d/2+1}} \quad \text{and} \quad \psi_\Delta(\xi) = \xi^\Delta \, {}_2F_1\left(\begin{matrix}\Delta,\, \Delta-\frac{1}{2}(d-1)\\ 2\Delta-d+1\end{matrix}\,\middle|\,\xi\right). \tag{3.14b}$$

The representation (3.14) is convenient to study the $\xi \to 0$ limit of the correlator because when ξ is small the hypergeometric function simplifies and we can replace it with the leading term $\psi_\Delta(\xi) \approx \xi^\Delta$.

We would now like to perform the Källén–Lehmann integral (3.12) by deforming the contour. As it stands, we can interpret the contour in (3.12) as running upwards in the complex Δ plane, along the vertical line $\Re(\Delta) = d/2$. We would like to close the contour to the right by adding an arc at infinity and picking up any possible poles. As a first step, we therefore write

$$\langle\Omega|\phi(\eta,x)\phi(\eta',x')|\Omega\rangle = \langle\phi\rangle^2 + \int_{\frac{d}{2}-i\infty}^{\frac{d}{2}+i\infty} \frac{d\Delta}{2\pi i}\,\rho_\phi(\Delta)\mathsf{g}(\Delta)\psi_\Delta(\xi) \tag{3.15}$$

exploiting the shadow symmetry of the representation (3.14) to drop one of the terms. We claim that for sufficiently small ξ, the integration contour in (3.15) can be deformed by closing the contour to the right. To prove this, we first notice that for sufficiently small $\xi > 0$, the function $\psi_\Delta(\xi)$ falls off for large real Δ:

$$0 < \xi \ll 1: \quad \psi_\Delta(\xi) \underset{\Delta\to\infty}{\sim} \mathsf{w}(\xi)^\Delta, \quad \mathsf{w}(\xi) = \frac{4\xi}{(1+\sqrt{1-\xi})^2} \tag{3.16}$$

and for the limit in question $0 \leq \mathsf{w}(\xi) \approx \xi \ll 1$, so the special function $\psi_\Delta(\xi)$ indeed decays exponentially fast on the right half-plane. This statement does *not* hold for the shadow function $\psi_{d-\Delta}(\xi)$. Next, let us investigate the function $\mathsf{g}(\Delta)$. On the real line, we have

$$\mathsf{g}(\Delta) \underset{\Delta\to\infty}{\sim} \frac{1}{2\pi^{d/2}} \cdot \frac{\Delta^{d/2-1}}{4^\Delta \sin\bigl(\pi(\frac{d}{2}-\Delta)\bigr)} \tag{3.17}$$

up to a Δ-independent coefficient. It follows that $\mathsf{g}(\Delta)$ has single poles at $\Delta = \frac{d}{2} + \mathbb{N}$. Away from the real axis, the function $\mathsf{g}(\Delta)$ decays rapidly.

Finally, we need to make some assumptions about the behavior of the distribution $\rho_\phi(\Delta)$: (i) Originally $\rho_\phi(\Delta)$ is only defined on the axis $\Re(\Delta) = d/2$, but we assume that it can be analytically continued away from this axis. (ii) $\rho_\phi(\Delta)$ does not grow too fast at infinity. This is not a strong condition as

$$\mathsf{g}(\Delta)w(\Delta) \underset{\Delta\to\infty}{\sim} \frac{1}{2\pi^{d/2}} \cdot \frac{\Delta^{d/2-1}\xi^\Delta}{4^\Delta \sin\bigl(\pi(\frac{d}{2}-\Delta)\bigr)} \tag{3.18}$$

for small ξ. (iii)we assume that

$$\rho_\phi(d/2) = 0 \tag{3.19}$$

in order to avoid picking up the pole at $\Delta = d/2$ coming from $\mathsf{g}(\Delta)$. The assumption (3.19) seems to be satisfied in all known examples, cf. later in this section. However, this assumption can be relaxed by explicitly adding the residue of the possible pole at $\Delta = d/2$. (iv) we assume that ρ_ϕ is meromorphic, with single poles Δ_* on the right half-plane:

$$\rho_\phi(\Delta) \underset{\Delta\to\Delta_*}{\sim} \frac{\operatorname{Res}\rho_\phi(\Delta_*)}{\Delta-\Delta_*}\ , \quad \Re(\Delta_*) > d/2\ . \tag{3.20}$$

Considering these assumptions now, we may deform the contour. By Cauchy's theorem, the $\langle\phi\phi\rangle$ correlator will pick up two series of poles: one family coming from the function $\mathsf{g}(\Delta)$ at $\Delta = \frac{d}{2} + \{1,2,3,\ldots\}$, and a second family of poles coming from the spectral density ρ_ϕ. Bringing everything together, we have[1]

$$\begin{aligned}\langle\Omega|\phi(\eta,x)\phi(\eta',x')|\Omega\rangle = \langle\phi\rangle^2 - \sum_{\Delta_*} \operatorname{Res}\rho_\phi(\Delta_*)\,\mathsf{g}(\Delta_*)\,\psi_{\Delta_*}(\xi) \\ + \sum_{n=1}^{\infty}\frac{(-1)^n\Gamma(\frac{d}{2}+n)}{2^{d+1+2n}\pi^{d/2}n!}\,\rho_\phi(\tfrac{d}{2}+n)\,\psi_{\frac{d}{2}+n}(\xi)\ .\end{aligned} \tag{3.21}$$

In particular in the late-time limit, setting $\eta=\eta'$ for convenience:

$$\langle\Omega|\phi(\eta,x)\phi(\eta,x')|\Omega\rangle \underset{\eta\to0^-}{\sim} \langle\phi^2\rangle - \sum_{\Delta_*}\operatorname{Res}\rho_\phi(\Delta_*)\,\mathsf{g}(\Delta_*)\left(\frac{-2\eta}{|x-x'|}\right)^{2\Delta_*} \tag{3.22}$$

omitting terms that are subleading as $\eta\to0$.[2] Here we did not write the contributions from residues of $\mathsf{g}(\Delta_*)$. We will come back to that shortly at the end of this section. From (3.22) it is clear that the leading late-time behavior of the $\langle\phi\phi\rangle$ correlator comes from poles in $\rho_\phi(\Delta)$ with the smallest real part, or to be precise the smallest $\Re(\Delta_*-\frac{d}{2})>0$. In addition, if $\rho_\phi(\frac{d}{2}+n)\neq0$ then there are terms that scale as $(-\eta)^{d+2n}$ with $n\geq1$.

Boundary OPE

We may now derive the result above from the OPE (2.44). This bulk-boundary OPE is not necessarily convergent, but we can still try to reproduce the late-time behavior of the $\langle\phi(\eta,x)\phi(\eta,x')\rangle$ correlator. The two-point function of conformal operators can only be non-vanishing if they have the same scaling dimension[3]:

$$\langle\mathcal{O}_\alpha(x)\mathcal{O}_{\alpha'}(y)\rangle = \frac{\delta_{\alpha\alpha'}}{|x-y|^{2\Delta_\alpha}} \tag{3.23}$$

which still holds when Δ_α is a complex number. The double sum over boundary operators; therefore, collapses to a single sum, hence

$$\langle\Omega|\phi(\eta,x)\phi(\eta',x')|\Omega\rangle \ \sim\ \langle\phi^2\rangle + \sum_\alpha (b_{\phi\alpha})^2(\eta\eta')^{\Delta_\alpha}\ \mathcal{D}_\alpha(\eta\partial_x)\mathcal{D}_\alpha(\eta'\partial_{x'})\,\frac{1}{|x-x'|^{2\Delta_\alpha}} \tag{3.24a}$$

where

$$\mathcal{D}_\alpha(\eta\partial_x) = {}_0F_1\big(\Delta_\alpha-d/2+1,\,\tfrac14\eta^2\partial_x^2\big) = 1+\mathrm{O}(\eta^2\partial_x^2)\ . \tag{3.24b}$$

---

[1] The minus sign in the second term of (3.21) arises from the fact that the contour is taken in the clockwise direction.

[2] There are two types of subleading terms. First, we have only kept the leading term in ξ in the hypergeometric function $\psi_{i\nu}(\xi)$. Second, we have approximated the invariant ξ by its leading piece in the limit $\eta\to0$.

[3] Here we are assuming that x and y are separate points. So we do not deal with contact terms discussed in 4.2.2

As before, we are interested in the limit $\eta, \eta' \to 0^-$. Hence we can approximate the differential operator $\mathcal{D}_\alpha$ by its leading term, which leads to the asymptotic behavior

$$\langle \Omega | \phi(\eta, x) \phi(\eta, x') | \Omega \rangle \underset{\eta \to 0^-}{\sim} \langle \phi^2 \rangle + \sum_\alpha (b_{\phi\alpha})^2 \left(\frac{-\eta}{|x - x'|} \right)^{2\Delta_\alpha} \tag{3.25}$$

For this expansion to match (3.22), we require first of all that the poles Δ_* equal the boundary operator spectrum $\{\Delta_\alpha\}$ exactly. Moreover, the residues of ρ_ϕ are related to the $b_{\phi\alpha}$ according to the dictionary

$$\boxed{(b_{\phi\alpha})^2 = -4^{\Delta_\alpha} \mathtt{g}(\Delta_\alpha) \operatorname{Res} \rho_\phi(\Delta_\alpha)} \,. \tag{3.26}$$

This result should not be surprising. After all, the special functions $\psi_\Delta(\xi)$ appearing in (3.21) are nothing but boundary conformal blocks [82] in $d+1$ dimensions. To wit, the spectral integral and its counterpart (3.21) appeared before in the BCFT context in a slightly different form [105].

Notice that neither $b_{\phi\alpha}$ nor $\operatorname{Res} \rho_\phi(\Delta_\alpha)$ is required to be real-valued: in a generic QFT in dS they are complex-valued. Nevertheless, the hermiticity of ϕ implies that

$$\rho_\phi(\Delta)^* = \rho_\phi(\Delta^*) \tag{3.27}$$

hence the residue of a pole at Δ_α and its complex conjugate Δ_α^* are necessarily related via complex conjugation.

Finally, the terms scaling as $\xi^{d/2+n}$ with $n = 1, 2, 3, \ldots$ in (3.21) and (3.22) cannot be reproduced from the bulk-boundary OPE (2.44). It is therefore natural to assume that

$$\rho_\phi(\tfrac{d}{2} + n) = 0 \quad \text{for all} \quad n = 0, 1, 2, \ldots. \tag{3.28a}$$

We do not have a proof of this fact, beyond the fact that in all known examples

$$\rho_\phi(\tfrac{d}{2} + i\nu) \;\propto\; \nu \sinh(\pi\nu) = \frac{\pi}{\Gamma(\Delta - \frac{d}{2})\Gamma(\frac{d}{2} - \Delta)} \tag{3.28b}$$

which indeed vanishes at $\Delta = d/2 + \mathbb{N}$. Likely this phenomenon has a group-theoretical explanation. In the literature, it is common to write spectral integrals with a Plancherel measure, schematically $1/(2\pi i) \sum_\ell \int d\Delta\, \mathfrak{P}(\Delta, \ell)$ — see for instance [65, Eq. (8.7)] or [106, Eq. (74)] and [67]. This measure is not physical: from our point of view, it amounts to a simple redefinition of $\rho_\phi(\Delta) \mapsto \rho_\phi(\Delta)/\mathfrak{P}(\Delta, 0)$ which does not affect observables. Nevertheless, the analytic structure of $\rho_\phi(\Delta)$ is affected by this rescaling, and indeed the $\ell = 0$ Plancherel measure $\mathfrak{P}(\Delta, 0)$ contains a factor $\nu \sinh(\pi\nu)$ which furnishes the desires zeroes (3.28a).

3.3 Analytic continuation from S^{d+1}

As discussed in section 2.3, the dS correlation functions, and in particular two-point functions, can be defined by the analytic continuation of correlation functions on the sphere S^{d+1}. In what follows, we use this fact to find a formula for the spectral density of a generic scalar field theory in dS as an integral over the discontinuity of the two-point function.

Let us therefore consider the two-point function $\langle\phi(X)\phi(X')\rangle_{S^{d+1}}$ of a hermitian operator $\phi(X)$ on the sphere, where we parametrize S^{d+1} by embedding space coordinates $X^A \in \mathbb{R}^{d+2}$ obeying $X \cdot X = R^2$. Such a two-point function can only depend on the invariant

$$x := \frac{X \cdot X'}{R^2} \ , \quad -1 \leq x \leq 1 \tag{3.29}$$

where $x = 1$ (resp. $x = -1$) corresponds to identical (resp. antipodal) insertions. Consequently we write

$$\langle\phi(X)\phi(X')\rangle_{S^{d+1}} = \widehat{G}(x) \tag{3.30}$$

for some function $\widehat{G}(x)$ which is not determined by symmetries. This correlator maps to the dS two-point function from Eq. (3.1) via

$$\xi = \frac{2}{1-x} \ , \quad \text{or} \quad \widehat{G}(x) = G\left(\xi = \frac{2}{1-x}\right) . \tag{3.31}$$

From now on we will use this formula to identify both correlators, and write $G(x)$ instead of $\widehat{G}(x)$ to avoid clutter.

It is well-known that any function of the invariant x can be decomposed in terms of $SO(d+2)$ Gegenbauer polynomials:

$$G(x) = \sum_{J=0}^{\infty} a_J \, C_J^{\frac{d}{2}}(x) \tag{3.32}$$

for some coefficients a_J that depend on the $\langle\phi\phi\rangle$ correlator in question. The Gegenbauers form an orthogonal basis with respect to the norm

$$\|f\|^2 := \int_{-1}^{1} dx \, (1-x^2)^{(d-1)/2} \, |f(x)|^2 \ . \tag{3.33}$$

Most physical correlators are not square-integrable with respect to the measure (3.33) due to singularities near $x = 1$. To be precise, for a correlator G to be square integrable, we need that[4]

$$G(\xi) \underset{\xi\to\infty}{\sim} \xi^\gamma \quad \text{and} \quad G(\xi) \underset{\xi\to 1^+}{\sim} 1/(\xi-1)^\gamma \quad \text{with} \quad \gamma < (d+1)/4\ . \tag{3.34}$$

The Gegenbauer polynomials obey

$$\|C_J^{\frac{d}{2}}\|^2 = 1/\kappa_J\ , \quad \kappa_J := \frac{2^{d-1}J!(J+\frac{d}{2})\Gamma(\frac{d}{2})^2}{\pi\Gamma(d+J)} \tag{3.35}$$

and in particular it follows that the coefficients a_J can be recovered using orthogonality of Gegenbauer polynomials (A.5) as

$$a_J = \kappa_J \int_{-1}^{1} dx\, (1-x^2)^{(d-1)/2}\, C_J^{\frac{d}{2}}(x) G(x)\ . \tag{3.36}$$

for $J = 0, 1, 2, \ldots$.

Let us print a formula for the a_J in a specific case, taking ϕ to be a free massive scalar, so $G(x)$ is the function $G_{\mathrm{f}}(\xi;\nu)$ from Eq. (3.3). The correlator in question is not square-integrable in $d \geq 3$ dimensions: indeed the correlator grows as $G_{\mathrm{f}}(\xi;\nu) \sim \xi^{(d-1)/2}$, so in $d \geq 3$ dimensions it does not represent a square-integrable function on S^{d+1}. Nevertheless one can compute the cofficients a_J using the inversion formula (3.36), for instance by analytically continuing in d. This computation was carried out in [100], yielding

$$a_J = \frac{1}{R^{d-1}} \frac{\Gamma(\frac{d}{2})}{4\pi^{\frac{d}{2}+1}} \frac{2J+d}{J(J+d)+m^2R^2}\ . \tag{3.37}$$

We will shortly revisit the formula (3.37) from a different point of view in (3.60).

In Eq. (3.36), we presented a formula to invert the expansion (3.32), expressing a_J as an integral over the correlator $G(x)$. The inversion formula (3.36) applies to integer J. In appendix C, we obtain an alternative inversion formula that applies to *complex* values of J. This inversion formula reads

$$a_J = \frac{1}{2\pi i} \frac{\Gamma(\frac{d}{2})\Gamma(J+1)}{\Gamma(J+\frac{d}{2})2^J} \int_1^\infty dx\, \frac{(x+1)^{\frac{d}{2}-\frac{1}{2}}}{(x-1)^{J+\frac{d}{2}+\frac{1}{2}}}\, {}_2F_1\left[\begin{matrix} J+d, J+\frac{d}{2}+\frac{1}{2} \\ 2J+d+1 \end{matrix} \middle| \frac{2}{1-x}\right] \mathrm{Disc}[G(x)] \tag{3.38}$$

where the discontinuity $\mathrm{Disc}[G(x)]$ is defined as

$$\mathrm{Disc}[f(x)] := f(x+i\epsilon) - f(x-i\epsilon)\ . \tag{3.39}$$

Since the RHS of (3.38) is an analytic function of J, the above identity extends a_J to an analytic function of J on the complex plane.

---

[4] An equivalent condition for square integrability is that the coefficients a_J decrease faster than $|a_J| \underset{J\to\infty}{\sim} 1/J^{(d-1)/2}$, as follows from Parseval's theorem.

Let us briefly discuss the convergence of the integral in (3.38). Suppose that near $x = 1$ and $x = \infty$ the discontinuity of $G(x)$ behaves as

$$\operatorname{Disc} G(x) \underset{x\to 1}{\sim} \frac{1}{(x-1)^{\delta}} \quad \text{and} \quad \operatorname{Disc} G(x) \underset{x\to\infty}{\sim} x^{\varepsilon} \tag{3.40}$$

for some exponents δ, ε. Then convergence requires that $\delta < 1$ and $\Re(J) > \varepsilon$, as follows from analyzing the $x \to 1, \infty$ asymptotics of the ${}_2F_1$ hypergeometric appearing in (3.38). Whenever $\Re(J) \leq \varepsilon$, the function a_J can have singularities in the complex J-plane. Also notice that the integrand involves the correlator $G(x)$ analytically continued beyond the Euclidean region $-1 \leq x \leq 1$. In fact, $x \geq 1$ maps to $\xi < 0$, which describes timelike separated points in de Sitter. In practice; however, one can calculate a_J for a two-point functions with $\delta \geq 1$ by means of analytical continuation from the convergent region, see e.g. (3.5). In what follows, we will rederive the Källén–Lehmann decomposition using the above inversion formula.

Recovering the spectral density

In order to derive the desired decomposition (3.12), let us turn our attention to the original expansion (3.32). The two-point function is a sum over non-negative integers:

$$G(x) = \sum_{J=0}^{\infty} g_J(x)\,, \qquad g_J(x) \coloneqq a_J\, C_J^{\frac{d}{2}}(x)\ . \tag{3.41}$$

Suppose that we can extend $g_J(x)$ to a function $\tilde{g}_J(x)$ which is analytic in J and coincides with $g_J(x)$ at integers: $\tilde{g}_J(x) = g_J(x)$ at $J = 0, 1, 2, \ldots$. Moreover, we imagine that we are given a kernel $K(J)$ that is meromorphic, having poles at the non-negative integers with unit residue. We can then replace the sum (3.41) by the following integral:

$$G(x) = \oint_{c_0} \frac{dJ}{2\pi i}\, K(J)\, \tilde{g}_J(x) \tag{3.42}$$

where the contour c_0 consists of small circles around the non-negative integers, passed in the counterclockwise sense. Such a contour is illustrated in figure 3.1. If we in addition assume that the product $K(J)\,\tilde{g}_J(x)$ decays sufficiently fast at large $|J|$, one can deform the contour to an integral over a line with fixed real part, e.g. c_2 in figure 3.1. The act of expressing a discrete sum as contour integral in the complex plane is known as a *Watson-Sommerfeld transformation*, see for instance [100].

The discussion so far was general and did not involve details about the decomposition (3.32) of the $\langle\phi\phi\rangle$ correlator. At this point, we will use some properties of the Gegenbauer polynomials, and we will propose an explicit kernel $K(J)$ as well as an analytic extension

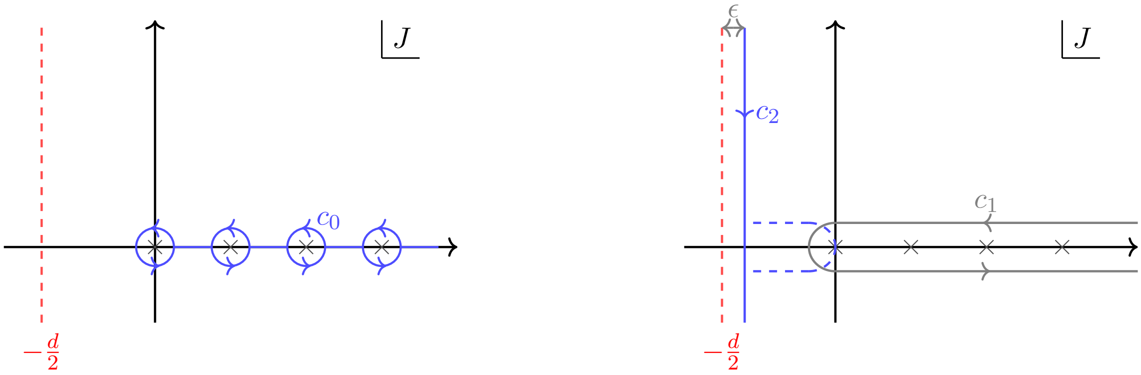

Figure 3.1: Illustration of contour integrals of Watson-Sommerfeld transformation. Left: sum over non-negative integers as a set of contour integrals around the integers (3.42). Right: Deforming the contour to a line integral with constant real part.

$\tilde{g}_J(x)$ of $g_J(x)$, to wit

$$K(J) := \frac{\pi e^{i\pi J}}{\sin(\pi J)} \quad \text{and} \quad \tilde{g}_J(x) := e^{-i\pi J} a_J\, C_J^{\frac{d}{2}}(-x) \tag{3.43}$$

cf. [100, Eqs. (20) and (21)]. For $J \notin \mathbb{N}$, the functions $C_J^{\frac{d}{2}}(-x)$ are so-called Gegenbauer functions, which can be expressed as hypergeometric functions, cf. equation (A.4). The choice of writing the function in terms of $-x$ will be apparent soon in (3.47). For integer J, the Gegenbauer functions reduce to the Gegenbauer polynomials that we have encountered so far, up to a sign:

$$J \in \mathbb{N}: \quad C_J^{\frac{d}{2}}(-x) = (-1)^J C_J^{\frac{d}{2}}(x) \quad \Rightarrow \quad \tilde{g}_J(x) = g_J(x) \tag{3.44}$$

as required. Moreover, it is easy to check that $K(J)$ from (3.43) has poles at integer J with unit residue.

To see that we are able to deform the contour, let us comment on the large-J behavior of the integrand in (3.42). In appendix C.3, we show that the leading contribution at large J of (3.38) is dominated by the $x \to 1$ part of the integral. For a two-point function with a power-law singularity at $x = 1$

$$G(x) \underset{x\to 1}{\sim} \frac{1}{(1-x)^{\delta}}\ , \tag{3.45a}$$

the large-J behaviour of a_J is given by[5]

$$\lim_{J\to\infty} a_J \sim \frac{1}{|J|^{d-2\delta}} \tag{3.45b}$$

---

[5] The proof in question assumes that $\delta < 1$. We expect (3.45) to hold for larger values of δ as well. This can be seen, for example, if one calculates a_J for a CFT in the bulk.

up to a J-independent constant. We are now ready to analyze the product $K(J)\tilde{g}_J(x)$ at large J:

$$K(J)\tilde{g}_J(x) \approx \frac{e^{-\arccos(x)|\operatorname{Im}(J)|}}{|J|^{d/2-2\delta+1}} \tag{3.46}$$

so away from the real axis, the function decreases exponentially, provided that x is in the Euclidean region $(-1,1)$. For sufficiently small δ the function decays as a power law along the real axis as well. It is therefore possible to deform the contour c_0 to c_2, as in Figure 3.1.

At this point, let us go back to the expression of the free theory two-point function in eq. (3.3). The formula in question is valid both for S^{d+1} and dS_{d+1}–as long as the insertions are spacelike separated, otherwise an $i\epsilon$ prescription is required. Given the definition of the Gegenbauer functions (A.4) and (3.29), one can rewrite the propagator as

$$G_{\mathrm{f}}(\xi;\nu) = \frac{\Gamma(\frac{d}{2})}{4\pi^{\frac{d}{2}}\sin(\pi\Delta)}\, C^{\frac{d}{2}}_{-\Delta}(-x)\ , \quad \Delta = \frac{d}{2} + i\nu\ . \tag{3.47}$$

using the invariant ξ instead of x for convenience from (3.31). Identifying $-J$ with Δ, we can therefore recast Eq. (3.42) as an integral of $a_{-\Delta}$ running over the principal series spectrum $\Re(\Delta) = d/2$, to wit

$$G(\xi) = \int_{\frac{d}{2}-i\infty}^{\frac{d}{2}+i\infty} \frac{d\Delta}{2\pi i}\, \frac{4\pi^{\frac{d}{2}+1}}{\Gamma(\frac{d}{2})}\, a_{-\Delta}\, G_{\mathrm{f}}(\xi;\nu)\ , \tag{3.48}$$

Note that the minus sign $a_J \mapsto a_{-\Delta}$ has changed the orientation of the c_2 contour. Of course, we recognize the above equation (3.48) as the Källén–Lehmann decomposition (3.12), after identifying

$$\rho_\phi(\tfrac{d}{2} + i\nu) = \frac{2\pi^{\frac{d}{2}+1}}{\Gamma(\frac{d}{2})} \lim_{\epsilon\to 0^+} \left(a_{i\nu-\frac{d}{2}+\epsilon} + a_{-i\nu-\frac{d}{2}+\epsilon}\right) \tag{3.49}$$

where we used the symmetry of the free propagator $G_{\mathrm{f}}(\xi;\nu) = G_{\mathrm{f}}(\xi;-\nu)$ to replace $a_{-\Delta} = a_{-i\nu-\frac{d}{2}}$ in (3.48) by the shadow symmetric combination. We also kept the ϵ regulator that is important if a_J has singularities on the line $\Re(J) = -\frac{d}{2}$ as depicted in figure 3.1. The only difference between (3.48) and (3.12) is the missing $\langle\phi\rangle^2$ term, which should correspond to a pole at $\Delta = 0$ (or equivalently $J = 0$).

In case of no singularity on $\Re(\Delta) = d/2$, one can use the hypergeometric identities (A.8) and (A.9) to rewrite (3.49) as

$$\boxed{\rho_\phi(\Delta) = \beta(\Delta) \int_1^\infty dx\ {}_2F_1\left[\begin{matrix}1-\Delta, 1-d+\Delta\\ \frac{3-d}{2}\end{matrix}\,\middle|\,\frac{1-x}{2}\right] \mathrm{Disc}[G(x)]} \tag{3.50a}$$

where

$$\beta(\Delta) = \frac{-i(4\pi)^{(d+1)/2}}{\Gamma(\frac{3-d}{2})} \frac{\Gamma(1-\Delta)\Gamma(1-d+\Delta)}{\Gamma(\Delta-\frac{d}{2})\Gamma(\frac{d}{2}-\Delta)} \tag{3.50b}$$

writing $\Delta = d/2 + i\nu$. This is the promised inversion formula for spectral density. Let us remind you that the integration is over timelike separation $x = X.X' > 1$ which corresponds to the timelike separated points in dS. So we expected a discontinuity in the two-point function in this region. We will use this formula in section 3.5 to find for instance the spectral density for a two-point function of a scalar operator of a bulk CFT.

The derivation in Sec. 3.1 was based on symmetry properties of the dS Hilbert space alone which the positivity of $\rho_\phi(\frac{d}{2}+i\nu)$ at real values of ν is manifest there. The present derivation was based on the analytic continuation of correlators from S^{d+1} to dS$_{d+1}$ which leads to an explicit formula for $\rho_\phi(\Delta)$ at complex values Δ but does not show a positivity manifestly.

Note that we assumed that the complimentary series are not apparent here; however, contour c_2 in figure 3.1 can be extended (to the dashed line) to take the complimentary series into account. As is discussed in section 2.2, the complimentary series can be seen as an analytic continuation of the principal series that will appear as pole crossings over the solid line c_2 in figure 3.1. In section (3.5) we will see that this precisely happens for a range of dimensions of operators in a bulk CFT.

3.4 Analytic continuation from EAdS$_{d+1}$

In this section, we derive an inversion formula for spectral density similar to the one in (3.50a); instead, by analytic continuation of correlators from EAdS$_{d+1}$ to dS$_{d+1}$. In the end, we show that these two inversion formulae are equivalent.

There is a simple dictionary between EAdS correlaros and dS correlators. We reviewed it in section 2.5.3. In particular, the free scalar two-point function in dS can be written as

$$G_{\mathrm{f}}(\xi) = \Gamma(i\nu)\Gamma(-i\nu)\Omega_\nu(\xi) \tag{3.51}$$

where ξ is the dS two-point function invariant defined in (3.2), again $\Delta = \frac{d}{2} + i\nu$ and $\Omega_\nu(\xi)$ is the EAdS harmonic function [107]:

$$\Omega_\nu = \frac{i\nu}{2\pi}(G_\nu^{\mathrm{EAdS}} - G_{-\nu}^{\mathrm{EAdS}}) \tag{3.52}$$

This can be easily derived by using identity (A.8) in the definitions (2.78) and (2.80), or directly from (2.89).

The harmonic functions are orthonormal basis in AdS [107]:

$$\int_{\mathrm{AdS}} dY\, \Omega_\nu(X_1,Y)\Omega_{\bar{\nu}}(Y,X_2) = \frac{1}{2}\left[\delta(\nu+\bar{\nu})+\delta(\nu-\bar{\nu})\right]\Omega_\nu(X_1,X_2) \tag{3.53}$$

Here we explicitly use the coordinates on EAdS with uppercase letterd instead of the EAdS two-point function invariant ξ^{AdS}. Now, imagine that one analytically continues the formula (3.12) to EAdS. Then the above orthogonality relation can be easily used to invert (3.12) to find

$$\rho(\frac{d}{2}+i\nu) = \frac{2\pi}{\Gamma(i\nu)\Gamma(-i\nu)\Omega_\nu(X_1,X_2)}\int_{\mathrm{AdS}} dY\, \Omega_\nu(X_1,Y)G(Y,X_2) \tag{3.54}$$

using that spectral density is shadow symmetric: $\rho(\nu)=\rho(-\nu)$. Here $G(X_1,X_2)$ is the dS two-point function in (3.12) analytically continued to EAdS for two separate points X_1 and X_2.

An important feature of this equation is that after the integration over EAdS, the integral should produce something proportional to $\Omega_\nu(X_1,X_2)$. In other words, the equality above is true for any X_1 and X_2, so we are free to pick any two points on EAdS. A convenient choice is to take them equal and place them at the origin:

$$X = X_1 = X_2 = \text{Origin}\ , \quad \text{EAdS origin in global coordinates:} \quad \rho = 0$$

Note that unlike the AdS propagator, $\Omega_\nu(X,X)$ is regular. Since we put X on the origin, the angular part of the integral (3.54) is trivial. In global coordinates (2.16), we have

$$s \equiv X.Y = -\cosh(\rho)\ , \quad dY = d\rho \sinh^d(\rho) d\Omega_d\ . \tag{3.55}$$

where $d\Omega_d$ is the angular volume element that after integration produces the vol(S^d) spelled out in (4.14). Here, again we set AdS radius $R=1$. Note that $s=\sigma^{\mathrm{EAdS}}$ is equal to x after analytical continuation. We keep two separate letters for them to emphasize which analytical continuation we are doing. Now we analytically continue back to dS by requiring that

$$\xi = \frac{2}{1-s}\ . \tag{3.56}$$

Substituting the ratio

$$\frac{\Omega_\nu(X,Y)}{\Omega_\nu(X,X)} = {}_2F_1\left[\begin{matrix}\frac{d}{2}+i\nu, \frac{d}{2}-i\nu \\ \frac{d+1}{2}\end{matrix}\,\middle|\,\frac{1+s}{2}\right] \tag{3.57}$$

and (3.55) in (3.54), we find an inversion formula for the spectral density:

$$\boxed{\rho_\phi(\Delta) = \frac{4\pi^{\frac{d+3}{2}}}{\Gamma(\Delta-\frac{d}{2})\Gamma(\frac{d}{2}-\Delta)\Gamma(\frac{d+1}{2})}\int_{-\infty}^{-1} ds\ (s^2-1)^{\frac{d-1}{2}}\,{}_2F_1\left[\begin{matrix}\Delta, d-\Delta\\ \frac{d+1}{2}\end{matrix}\middle|\frac{1+s}{2}\right]G(s)} \tag{3.58}$$

where $G(s)$ is the dS Wightman two-point function $\langle\Omega|\phi(\eta,x)\phi(\eta',x')|\Omega\rangle$ with the two-point invariant ξ related to s by (3.56).

This is another version of the inversion formula (3.50a) that was found by analytical continuation from the sphere. The integration in (3.58) is over the spacelike separated region where the Wightman two-point function is assumed to be well-defined and single-valued, while the integral in 3.50a is over the timelike separated region ($x \in [1,\infty)$) where the two-point function has a branch cut and the integration is over its discontinuity.

We now argue that these two formulae are simply equivalent assuming that the Wightman two-point function G is analytic in s (or x) except for the cut on timelike separated region corresponding to $x > 1$.

Consider the integral (3.50a). The integral can be written as a contour integral going around the branch cut $x \in [1,\infty)$ using the definition of discontinuity in (3.39). One can deform the contour to the branch cut of ${}_2F_1$ in the integral that is $x \in (-\infty,-1]$. In this contour deforming process we assumed $G(x)$ is analytic everywhere but the mentioned branch cut and it decays sufficiently fast so that the contribution from the arc at infinity vanishes[6]. Discontinuity of the hypergeometric functions is given by (A.15). So discontinuity of the hypergeometric function in (3.50a) reads

$$\begin{aligned}\mathrm{Disc}[{}_2F_1&\left[\begin{matrix}1-\Delta, 1-d+\Delta\\ \frac{3-d}{2}\end{matrix}\middle|\frac{1-x}{2}\right]] = \\ &\frac{2^{2-d}\pi i\Gamma(\frac{3-d}{2})}{\Gamma(1-\Delta)\Gamma(1-d+\Delta)\Gamma(\frac{d+1}{2})}(x^2-1)^{\frac{d-1}{2}}\,{}_2F_1\left[\begin{matrix}\Delta, d-\Delta\\ \frac{d+1}{2}\end{matrix}\middle|\frac{1+x}{2}\right].\end{aligned} \tag{3.59}$$

Using this, one finds that (3.58) and (3.50a) are equivalent.

3.5 Examples

In the final part of this chapter, we will consider the Källén–Lehmann decomposition in two different settings. First, we will consider the $\langle\phi\phi\rangle$ and $\langle\phi^2\phi^2\rangle$ correlator in the theory of a free massive scalar ϕ, followed by the analysis of a generic conformally invariant two-point function in dS.

---

[6] The hypergeometric in (3.50a) falls like $x^{-1+\frac{d}{2}}$, so the G(x) has to fall faster that $x^{-\frac{d}{2}}$ for this contribution to vanish.

3.5.1 Massive free boson: $\langle\phi\phi\rangle$

As a first example, consider the correlator $\langle\phi\phi\rangle = G_{\rm f}$ where ϕ is a free massive field in the bulk with mass m. Let us write $\Delta_\phi(d-\Delta_\phi) = m^2R^2$ and set $\Delta_\phi = \frac{d}{2} + i\mu$ in order to avoid overloading the labels Δ and ν. There are two possible ways to obtain the distribution $a_{-\Delta}$ for complex values of Δ. On the one hand, in Eq. (3.37), a formula for a_J at integer J was presented, and the formula at hand can be analytically continued simply by replacing $J \mapsto -\Delta$. Alternatively, one can explicitly perform the integral (3.38), as is done in appendix C.2. Regardless of the chosen method, the result reads

$$\frac{4\pi^{\frac{d}{2}+1}}{\Gamma(\frac{d}{2})}a_{-\Delta} = \frac{2\Delta-d}{\Delta(d-\Delta)-m^2R^2} = -\frac{1}{\Delta-\Delta_\phi} - \frac{1}{\Delta-d+\Delta_\phi}\,. \tag{3.60}$$

This has poles at $\Delta = \Delta_\phi$ and $\Delta = d-\Delta_\phi$, which fall exactly on the axis of integration $\Re(\Delta) = \frac{d}{2}$. Using the prescription (3.49), we find

$$\frac{1}{2\pi}\rho_{\rm f}(\tfrac{d}{2}+i\nu) = \frac{\delta(\mu+\nu)+\delta(\mu-\nu)}{2} \tag{3.61}$$

which reproduces the correct answer. In the case where $m^2 < d^2/4$ such that Δ_ϕ is on the complementary series, it is straightforward to adapt the above argument to obtain a similar result. This can be done by two different means, one is take the contour c_2 to include dashed line around complimentary series in figure 3.1 or simply take the results from principal series and analytically continue Δ_ϕ away from principal series to complimentary series.

3.5.2 Massive free boson: $\langle\phi^2\phi^2\rangle$

Next, we can consider the two-point function of the (normal-ordered) operator ϕ^2 in the Gaussian theory. By Wick's theorem

$$\langle\phi^2(\eta,x)\phi^2(\eta',x')\rangle = 2\,G_{\rm f}(\xi;\mu)^2 \tag{3.62}$$

and as a matter of principle, the spectral density $\rho_{\phi^2}(\Delta)$ can be obtained by applying the inversion formula to the RHS of (3.62). For the moment let us assume that Δ_ϕ belongs to principal series. We will comment on the case of complementary series shortly. It turns out that $\rho_{\phi^2}(\Delta)$ has already been computed through other means in Ref. [84, Eq. (3.25)][7].

---

[7] In that work, the Källén–Lehmann decomposition of the more general correlator $G_{\rm f}(\xi;\mu_1)G_{\rm f}(\xi;\mu_2)$ is presented, which reduces to (3.63) for $\mu_1 = \mu_2$.

The resulting formula is given by

$$\begin{aligned}\rho_{\phi^2}(\Delta) = &\frac{\nu\sinh(\pi\nu)}{2^3\pi^{\frac{d}{2}+2}\Gamma(\frac{d}{2})}\frac{\Gamma^2(\frac{\Delta}{2})\Gamma^2(\frac{d-\Delta}{2})}{\Gamma(\Delta)\Gamma(d-\Delta)}\\ &\times\Gamma\Big(\frac{2\Delta_\phi+\Delta-d}{2}\Big)\Gamma\Big(\frac{2\Delta_\phi-\Delta}{2}\Big)\Gamma\Big(\frac{d-2\Delta_\phi+\Delta}{2}\Big)\Gamma\Big(\frac{2d-2\Delta_\phi-\Delta}{2}\Big)\end{aligned} \tag{3.63}$$

writing $\Delta = d/2 + i\nu$ as usual. It is easy to check that ρ_{ϕ^2} is invariant under $\Delta \mapsto d - \Delta$. Moreover, the correlator is apparently completely representated by the principal series: the contour in (3.12) does not need to be deformed to account for complementary series states.

At this point, we can analyze the spectrum of late-time operators appearing on the bulk-boundary OPE of $\phi^2 \sim \sum_\alpha \mathcal{O}_\alpha$. On the right half plane, the density has three families of single poles:

$$\Delta = 2\Delta_\phi + 2\mathbb{N}\ , \quad \Delta = 2(d-\Delta_\phi) + 2\mathbb{N} \quad \text{and} \quad \Delta = d + 2\mathbb{N}\ . \tag{3.64a}$$

Because of their dimensions, the corresponding operators $\mathcal{O}_\alpha(x)$ can be interpreted as scalar "double-trace" operators of the late-time CFT, schematically

$$\mathcal{O}\Box^n\mathcal{O}\ , \quad \mathcal{O}^\dagger\Box^n\mathcal{O}^\dagger \quad \text{and} \quad \mathcal{O}^\dagger\Box^n\mathcal{O} + \mathcal{O}\Box^n\mathcal{O}^\dagger \tag{3.64b}$$

where $\mathcal{O}$ and $\mathcal{O}^\dagger$ have dimension $\Delta_\phi = d/2 + i\mu$ resp. $d - \Delta_\phi = d/2 - i\mu$. Since the late-time CFT is a mean-field theory built out of the operators $\mathcal{O}$, $\mathcal{O}^\dagger$, this is exactly the expected result: there are no other $SO(d)$ scalar operators built out of two operators in the CFT in question that one can write down. Of course, the bulk-to-boundary OPE coefficients $b_{\phi^2 k}$ can be obtained from (3.63) by computing residues.

In the case where Δ_ϕ is real and belongs to the complementary series, one can repeat the above analysis by analytic continuation. Notice that (3.63) has poles at

$$\Delta = 2\Delta_\phi - d - 2n$$

for non-negative integers n. When one analytically continues Δ_ϕ to the real line a pole crossing in integral of (3.12) can happen. More precisely, for $\frac{3d}{4} < \Delta_\phi < d$ one has to deform the contour to go around these poles. Similar to what was discussed above and in 2.2, one might interpret these poles as the complementary series contribution to (3.12).

3.5.3 Bulk CFT correlator

As the second applicatoon of the Källén–Lehmann representation, we consider the correlation function of the following form:

$$G_\delta(x) = \frac{1}{(1-x)^\delta} \quad \text{i.e.} \quad G_\delta(\xi) = \frac{1}{2^\delta}\,\xi^\delta \ . \tag{3.65}$$

Such a correlator arises for instance when one constructs a bulk CFT in de Sitter: the correlator (3.65) corresponds to a scalar two-point function of an operator φ of dimension $[\varphi] = \delta$. Unitarity requires that

$$\delta \geq \frac{d-1}{2} \ , \quad \text{(unitarity)}. \tag{3.66}$$

Note that $\delta = (d-1)/2$ corresponds to a conformally coupled free boson. One can easily check that (3.4) boils down to (3.65) after requiring $\Delta_\phi = \delta = (d-1)/2$ up to some normalization.

The spectral density $\rho_\delta(\Delta)$ for (3.65) can be computed in several ways, for instance using alpha space techniques [105]. Alternatively, it can be computed starting from the inversion formula (3.58) or (3.50a), making use of the fact that

$$\operatorname{Disc} G_\delta(x) = \frac{2i\sin(\pi\delta)}{(x-1)^\delta} \ .$$

The integral appearing in the inversion formula can be computed exactly using (A.7) yielding to

$$\rho_\delta(\Delta) = \frac{2^{d+2-\delta}\pi^{(d+1)/2}}{\Gamma(\delta)\Gamma(\delta-\frac{d}{2}+\frac{1}{2})}\,\nu\sinh(\pi\nu)\,\Gamma(\delta-\Delta)\Gamma(\delta-d+\Delta) \ . \tag{3.67}$$

As before, the spectral density has support on the axis $\Re(\Delta) = d/2$ and *does not* require separate contributions from states in the complementary series – except for $\delta < d/2$ that we will come back to it shortly. This appears to be specific to *scalar* two-point functions. For the two-point functions of spinning bulk operators in dS_2, it seems possible to have contributions of discrete series states, as is discussed in appendix D. In an upcoming work, we calculate the spectral density of bulk CFT for spinning operators and show that indeed for $d \geq 2$ only principal series appear while for $d = 1$ there are contributions from discrete series.

The bulk-boundary OPE of the CFT operator $\varphi \sim \sum_\alpha \mathcal{O}_\alpha$ can be analyzed by closing the contour in (3.12) and picking up poles on the right half-plane. For the density in question (3.67), there is a single family of poles at

$$\Delta = \delta + \mathbb{N} \ . \tag{3.68}$$

An exception is given by the massless case $\delta = (d-1)/2$, where only the term with $\Delta = \delta$ arises. This set of boundary operators is precisely what we expect from the discussion in 2.6.3.

Finally, some care must be taken when $(d-1)/2 < \delta < d/2$. In that case, the first pole in (3.68) has $\Re(\Delta_1) = \Re(\delta) < d/2$, so it is located left of the axis $\Re(\Delta) = d/2$. To reproduce the full correlator $G(\xi)$, the contour in (3.12) must be deformed to include this pole (and to exclude its shadow). This pole again can be interpreted as the contribution from complementary series states. This is consistent with our analysis of the decomposition of an $SO(2,2)$ conformal family into irreps of $SO(2,1)$, in appendix D.

4 Boundary four-point function

The late-time expansion (2.44) defines boundary operators $\mathcal{O}_\alpha$. The action of the conformal generators on these boundary operators is like that of Euclidean conformal generators on primary operators. In particular, (2.34) shows that the late-time boundary operator $\mathcal{O}_\alpha(x)$ transforms as a primary operator with dimension Δ_α. The (infinite) set of correlation functions of the $\{\mathcal{O}_\alpha\}$ therefore defines a d-dimensional CFT on the $\eta = 0$ timeslice. This CFT lacks some useful features of flat-space CFT, e.g. the state-operator correspondence and OPE convergence. Moreover, the late-time CFT does not have a stress-energy tensor $T_{\mu\nu}$. Nevertheless, one still can use the conformal symmetry on the boundary to find non-trivial constraints.

In this section, by writing the complete set of states introduced previously, we expand the four-point function of boundary operators in conformal partial waves and using unitarity, we find positivity properties of their coefficients. We analyze the corresponding partial wave expansion extensively in the case of the free massive field, and furthermore we explore the $\lambda\phi^4$ theory in dS_{d+1} to leading order in λ. Along the way, we show that unitarity suggests the existence of local terms in two-point functions.

4.1 Partial wave expansion

A four-point function of boundary operators can be expressed in terms of conformal partial waves by adding a complete set of states (2.116)

$$\begin{aligned}\langle\mathcal{O}_1\mathcal{O}_2\mathcal{O}_3\mathcal{O}_4\rangle &= \langle\Omega|\mathcal{O}_1\mathcal{O}_2|\Omega\rangle\langle\Omega|\mathcal{O}_3\mathcal{O}_4|\Omega\rangle \\ &\quad + \sum_\ell \int_{\frac{d}{2}}^{\frac{d}{2}+i\infty} \frac{d\Delta}{2\pi i}\frac{1}{N(\Delta,\ell)}\int d^dx\, \langle\mathcal{O}_1\mathcal{O}_2|\Delta,x\rangle_{\mu_1\dots\mu_\ell}{}^{\mu_1\dots\mu_\ell}\langle\Delta,x|\mathcal{O}_3\mathcal{O}_4\rangle\end{aligned} \tag{4.1}$$

omitting the explicit x_i-dependence of the operators $\mathcal{O}_i(x_i)$ and dropping x subscript of $N(\Delta,\ell)$ to avoid clutter. Once again we are assuming that the operators $\mathcal{O}_i$ are scalars, so only traceless symmetric tensor states are exchanged. We take only principal series states contribution to the decomposition of this four-point function; however, the complimentary series contribution can be recast by analytic continuation as discussed in 2.2. In the next chapter, we revisit this decomposition by reintroducing the discrete series that appear only in $d=1$ for scalar four-point functions. We shall often omit the vacuum symbol $|\Omega\rangle$ to avoid cluttering.

We now establish explicitly the crucial fact that the matrix elements $\langle\mathcal{O}_1\mathcal{O}_2|\Delta,x,z\rangle$ and $\langle\Delta,x,z|\mathcal{O}_3\mathcal{O}_4\rangle$ have the same structure as the three-point function $\langle\mathcal{O}_1\mathcal{O}_2\mathcal{O}(x)\rangle$ and $\langle\tilde{\mathcal{O}}(x)\mathcal{O}_3\mathcal{O}_4\rangle$, where $\mathcal{O}$ is a fictional operator of dimension Δ and $\tilde{\mathcal{O}}$ its shadow [108] of dimension $d-\Delta$.[1] Here we used the index-free notation mentioned in 2.104. We stress that $\mathcal{O}$ and $\tilde{\mathcal{O}}$ are not physical operators: they are only used to label certain conformally covariant objects. This follows from the fact that the action of isometries on $|\Delta,x,z\rangle$ and $\mathcal{O}(x)|\Omega\rangle$ are the same. The action of a general conformal charge on a correlator is

$$\begin{aligned}(\hat{Q}_1+\hat{Q}_2+\ldots+\hat{Q}_n)\langle\mathcal{O}_1\cdots\mathcal{O}_n\rangle &= \sum_i\langle\mathcal{O}_1\cdots[Q,\mathcal{O}_i]\cdots\mathcal{O}_n\rangle \\ &= \langle Q\,\mathcal{O}_1\cdots\mathcal{O}_n\rangle-\langle\mathcal{O}_1\cdots\mathcal{O}_nQ\rangle=0\end{aligned} \tag{4.2}$$

in which $\hat{Q}_i$ is a differential operator acting on x_i, that is to say

$$[Q,\mathcal{O}_i(x_i)]=\hat{Q}_i\,\mathcal{O}_i(x_i)\ . \tag{4.3}$$

Similarly, we have

$$\begin{aligned}&(\hat{Q}_1+\hat{Q}_2+\hat{Q}_\Delta)\langle\mathcal{O}_1\mathcal{O}_2|\Delta,x,z\rangle\\ &\quad=\langle[Q,\mathcal{O}_1]\mathcal{O}_2|\Delta,x,z\rangle+\langle\mathcal{O}_1[Q,\mathcal{O}_2]|\Delta,x,z\rangle+\langle\mathcal{O}_1\mathcal{O}_2Q|\Delta,x,z\rangle\\ &\quad=\langle Q\,\mathcal{O}_1\mathcal{O}_2|\Delta,x,z\rangle=0\end{aligned} \tag{4.4}$$

in which we used the result of the previous section to substitute the action of differential operator with the Hilbert space operator Q on state $|\Delta,x,z\rangle$. This is exactly the same differential equation one finds for a three-point function. Therefore, $\langle\mathcal{O}_1\mathcal{O}_2|\Delta,x,z\rangle$ is proportional to the conformal three-point structure (4.6b) which is fixed by the conformal symmetry:

$$\langle\mathcal{O}_1\mathcal{O}_2|\Delta,x,z\rangle=\mathcal{F}_{12}(\Delta,\ell)\ \langle\mathcal{O}_1\mathcal{O}_2\mathcal{O}(x,z)\rangle\ , \tag{4.5}$$

where $\mathcal{F}$ is independent of position. Using the shorthand notation $|x_{ij}|=|x_i-x_j|$, the three-point structure is given by

$$\langle\mathcal{O}_1(x_1)\mathcal{O}_2(x_2)\mathcal{O}_3(x_3,z)\rangle=\langle\mathcal{O}_1(x_1)\mathcal{O}_2(x_2)\mathcal{O}_3^{\mu_1\cdots\mu_\ell}(x_3)\rangle z_{\mu_1}\ldots z_{\mu_\ell} \tag{4.6a}$$

---

[1] Here we used that the three-point structure of $\langle\mathcal{O}^\dagger(x)\mathcal{O}_3\mathcal{O}_4\rangle$ is proportional to $\langle\tilde{\mathcal{O}}(x)\mathcal{O}_3\mathcal{O}_4\rangle$ when $\mathcal{O}$ is living on principal series, having $\Delta\in\frac{d}{2}+i\mathbb{R}$.

with

$$\langle \mathcal{O}_1(x_1)\mathcal{O}_2(x_2)\mathcal{O}_3^{\mu_1\ldots\mu_\ell}(x_3)\rangle = \frac{Z^{\mu_1}\ldots Z^{\mu_\ell} - \text{traces}}{|x_{12}|^{\Delta_1+\Delta_2-\Delta_3}|x_{13}|^{\Delta_1+\Delta_3-\Delta_2}|x_{23}|^{\Delta_2+\Delta_3-\Delta_1}} \ , \tag{4.6b}$$

$$Z^\mu \equiv \frac{|x_{13}||x_{23}|}{|x_{12}|}\left(\frac{x_{13}^\mu}{x_{13}^2} - \frac{x_{23}^\mu}{x_{23}^2}\right) \ . \tag{4.6c}$$

Let us stress that the notation $\langle\langle \mathcal{O}_1\mathcal{O}_2\mathcal{O}(x,z)\rangle\rangle$ in (4.5) does not refer to a physical correlation function: it is just a shorthand notation for the object (4.6b). Similarly, we can write

$$\begin{aligned}\langle \mathcal{O}_1^\dagger\mathcal{O}_2^\dagger|\Delta,x,z\rangle &= \mathcal{F}_{1^\dagger 2^\dagger}(\Delta,\ell)\langle\langle \mathcal{O}_1^\dagger\mathcal{O}_2^\dagger\mathcal{O}(x,z)\rangle\rangle \ ,\\ \langle \Delta,x,z|\mathcal{O}_1\mathcal{O}_2\rangle &= \mathcal{F}^*_{1^\dagger 2^\dagger}(\Delta,\ell)\langle\langle \tilde{\mathcal{O}}(x,z)\mathcal{O}_1\mathcal{O}_2\rangle\rangle \ ,\end{aligned}$$

where the second line is obtained from the first by complex conjugation. We also used $\langle\langle \mathcal{O}_1^\dagger\mathcal{O}_2^\dagger\mathcal{O}(x)\rangle\rangle^* = \langle\langle\tilde{\mathcal{O}}(x)\mathcal{O}_1\mathcal{O}_2\rangle\rangle$ which can be explicitly checked from eq. (4.6b) when $\mathcal{O}$ is in the principal series.

Using the above facts, Eq. (4.1) can be recast as

$$\boxed{\langle \mathcal{O}_1\mathcal{O}_2\mathcal{O}_3\mathcal{O}_4\rangle = \sum_\ell \int_{\frac{d}{2}}^{\frac{d}{2}+i\infty}\frac{d\Delta}{2\pi i}\, I_{\Delta,\ell}\ \Psi^{\Delta_i}_{\Delta,\ell}(x_i) + \langle \mathcal{O}_1\mathcal{O}_2\rangle\langle \mathcal{O}_3\mathcal{O}_4\rangle} \tag{4.7}$$

where we defined

$$I_{\Delta,\ell} := \frac{\mathcal{F}_{12}(\Delta,\ell)\mathcal{F}^*_{3^\dagger 4^\dagger}(\Delta,\ell)}{N(\Delta,\ell)} \ , \tag{4.8}$$

$$\Psi^{\Delta_i}_{\Delta,\ell}(x_i) := \int d^dx\ \langle\langle \mathcal{O}_1(x_1)\mathcal{O}_2(x_2)\mathcal{O}_{\mu_1\ldots\mu_\ell}(x)\rangle\rangle\langle\langle\tilde{\mathcal{O}}^{\mu_1\ldots\mu_\ell}(x)\mathcal{O}_3(x_3)\mathcal{O}_4(x_4)\rangle\rangle \ . \tag{4.9}$$

We emphasize that unitarity leads to positivity properties of the partial wave coefficients $I_{\Delta,\ell}$. In particular, we have

$$I_{\Delta,\ell} \geq 0 \qquad \textbf{if}: \qquad \mathcal{O}_1 = \mathcal{O}_3^\dagger \quad \text{and} \quad \mathcal{O}_2 = \mathcal{O}_4^\dagger \ . \tag{4.10}$$

Note that $\langle \mathcal{O}_1\mathcal{O}_2|\Delta,x,z\rangle$ is symmetric under exchange of $\mathcal{O}_1$ and $\mathcal{O}_2$ because boundary operators commute, while the three-point structure (4.6b) changes by the factor $(-1)^\ell$. This means $\mathcal{F}_{12}$ changes by the same factor under exchange of $\mathcal{O}_1$ and $\mathcal{O}_2$. This leads to

$$\bar{I}_{\Delta,\ell} \equiv I_{\Delta,\ell}(-1)^\ell \geq 0 \qquad \textbf{if}: \qquad \mathcal{O}_1 = \mathcal{O}_4^\dagger \quad \text{and} \quad \mathcal{O}_2 = \mathcal{O}_3^\dagger \ . \tag{4.11}$$

This positivity property is at the core of the bootstrap approach to dS late-time correlators that will be presented in the next section. The function $\Psi^{\Delta_i}_{\Delta,\ell}$ defined in (4.9) is a solution of the conformal Casimir equation, and is known as the Conformal Partial Wave.

The set of conformal partial waves with Δ running over the principal series forms a complete basis of four-point correlation functions, in a way that can be made precise [80].[2][3] In the case of $d=1$, we need to add discrete series states with $\Delta \in \mathbb{N}^+$ to have a complete set of states. Strictly speaking, eq .(4.7) will have an extra sum over positive integers. We will see this explicitly in section 5.

We would like to briefly mention some properties of the conformal partial waves. The partial waves satisfy the orthogonality relation

$$\int \frac{d^dx_1 \dots d^dx_4}{\mathrm{vol}(\mathrm{SO}(d+1,1))} \Psi^{\Delta_i}_{\Delta,\ell}(x_i) \Psi^{\tilde{\Delta}_i}_{\tilde{\Delta}',\ell'}(x_i) = 2\pi n_{\Delta,\ell}\, \delta_{\ell,\ell'} \delta(\nu-\nu') \ , \tag{4.12}$$

where $\Delta = \frac{d}{2} + i\nu$, $\Delta' = \frac{d}{2} + i\nu'$ and the normalization factor reads

$$n_{\Delta,\ell} = \frac{\pi^{d+1}\mathrm{vol}(S^{d-2})}{\mathrm{vol}(\mathrm{SO}(d-1))} \frac{(2\ell+d-2)\Gamma(\ell+d-2)\Gamma(\ell+1)}{2^{2\ell+d-2}\Gamma(\ell+\frac{d}{2})^2(\Delta+\ell-1)(\tilde{\Delta}+\ell-1)} \frac{\Gamma(\Delta-\frac{d}{2})\Gamma(\tilde{\Delta}-\frac{d}{2})}{\Gamma(\Delta-1)\Gamma(\tilde{\Delta}-1)} \ . \tag{4.13}$$

Here we use the shorthand notation $\tilde{\Delta} = d - \Delta$ and [109]

$$\mathrm{vol}(S^{d-1}) = \frac{2\pi^{d/2}}{\Gamma(\frac{d}{2})}, \quad \mathrm{vol}(SO(d-1)) = \frac{2^{d-2}\pi^{(d-2)(d+1)/4}}{\prod_{j=2}^{d-1}\Gamma(\frac{j}{2})}. \tag{4.14}$$

The partial waves can also be written in terms of conformal blocks,

$$\Psi^{\Delta_i}_{\Delta,\ell}(x_i) = K^{\Delta_3\Delta_4}_{\tilde{\Delta},\ell} G^{\Delta_i}_{\Delta,\ell}(x_i) + K^{\Delta_1,\Delta_2}_{\Delta,\ell} G^{\Delta_i}_{\tilde{\Delta},\ell}(x_i) \ , \tag{4.15}$$

$$K^{\Delta_1,\Delta_2}_{\Delta,\ell} = \frac{\pi^{\frac{d}{2}}\Gamma(\Delta-\frac{d}{2})\Gamma(\Delta+\ell-1)\Gamma(\frac{\tilde{\Delta}+\Delta_1-\Delta_2+\ell}{2})\Gamma(\frac{\tilde{\Delta}+\Delta_2-\Delta_1+\ell}{2})}{\Gamma(\Delta-1)\Gamma(d-\Delta+\ell)\Gamma(\frac{\Delta+\Delta_1-\Delta_2+\ell}{2})\Gamma(\frac{\Delta+\Delta_2-\Delta_1+\ell}{2})} \tag{4.16}$$

where $G^{\Delta_i}_{\Delta,\ell}(x_i)$ is proportional to the usual conformal block $G^{\Delta_i}_{\Delta,\ell}(z,\bar{z})$, to be precise:

$$G^{\Delta_i}_{\Delta,\ell}(x_i) = \frac{1}{|x_{12}|^{\Delta_1+\Delta_2}|x_{34}|^{\Delta_3+\Delta_4}} \left(\frac{|x_{14}|}{|x_{24}|}\right)^{\Delta_2-\Delta_1} \left(\frac{|x_{14}|}{|x_{13}|}\right)^{\Delta_3-\Delta_4} G^{\Delta_i}_{\Delta,\ell}(z,\bar{z}) \ , \tag{4.17}$$

and we have introduced cross ratios $z, \bar{z}$ as

$$\frac{|x_{12}|^2|x_{34}|^2}{|x_{13}|^2|x_{24}|^2} = z\bar{z}, \quad \frac{|x_{14}|^2|x_{23}|^2}{|x_{13}|^2|x_{24}|^2} = (1-z)(1-\bar{z}) \ . \tag{4.18}$$

For small $z, \bar{z}$, the above definition of the conformal blocks fixes their short-distance behavior to be

---

[2] Whenever $\Re(\Delta_1-\Delta_2)$ or $\Re(\Delta_3-\Delta_4)$ are large, the question of completeness of the principal series of partial waves is subtle, see for instance [80, appendix A.3].

[3] When the external operators $\mathcal{O}_i$ all belong to the principal series, e.g. when the $\mathcal{O}_i$ appear in the boundary OPE of a massive free field ϕ, this follows also from the tensor products (2.40).

$$G^{\Delta_i}_{\Delta,\ell}(z,\bar{z}) \to (-1)^\ell \,\frac{\Gamma(\ell+1)\Gamma(\frac{d-2}{2})}{2^\ell\Gamma(\ell+\frac{d-2}{2})}\,(z\bar{z})^{\frac{\Delta}{2}}\, C_\ell^{\frac{d-2}{2}}\left(\frac{z+\bar{z}}{2\sqrt{z\bar{z}}}\right) \qquad z\sim\bar{z}\ll 1\ , \tag{4.19a}$$

$$G^{\Delta_i}_{\Delta,\ell}(z,\bar{z}) \to \left(-\frac{1}{2}\right)^\ell z^{\frac{\Delta-\ell}{2}}\bar{z}^{\frac{\Delta+\ell}{2}} \qquad z\ll\bar{z}\ll 1\ . \tag{4.19b}$$

OPE for boundary operators

Combining (4.7) with (4.15), one can write

$$\langle\mathcal{O}_1\mathcal{O}_2\mathcal{O}_3\mathcal{O}_4\rangle = \sum_\ell \int_{\frac{d}{2}-i\infty}^{\frac{d}{2}+i\infty} \frac{d\Delta}{2\pi i}\, I_{\Delta,\ell}\, K^{\Delta_3\Delta_4}_{\tilde{\Delta},\ell} G^{\Delta_i}_{\Delta,\ell}(x_i) + \langle\mathcal{O}_1\mathcal{O}_2\rangle\langle\mathcal{O}_3\mathcal{O}_4\rangle\ . \tag{4.20}$$

Since the conformal block $G^{\Delta_i}_{\Delta,\ell}(x_i)$ decays exponentially when $\mathrm{Re}\,\Delta\to\infty$ (whilst keeping the x_i fixed) we can deform the contour to the right and pick up poles along the way. This gives

$$\langle\mathcal{O}_1\mathcal{O}_2\mathcal{O}_3\mathcal{O}_4\rangle = -\sum_\ell\sum_{\Delta_\alpha} \mathrm{Res}_{\Delta=\Delta_\alpha} I_{\Delta,\ell}\, K^{\Delta_3\Delta_4}_{\tilde{\Delta}_\alpha,\ell} G^{\Delta_i}_{\Delta_\alpha,\ell}(x_i) + \langle\mathcal{O}_1\mathcal{O}_2\rangle\langle\mathcal{O}_3\mathcal{O}_4\rangle\ . \tag{4.21}$$

As discussed in [110, 65, 80] there are non-trivial cancellations among poles of the conformal blocks and poles of the partial wave coefficients. When the dust settles, what is left is the contribution from the dynamical (not spurious) poles of $I_{\Delta,\ell}$; these therefore control the expansion in powers of $|x_1-x_2|^2$.

This gives rise to an OPE between boundary operators, and we can read off the dimension of the exchanged boundary operators from the position of the poles in the partial wave coefficients $I_{\Delta,\ell}$. This is similar to what we saw in section 3.2 for the late time expansion of the bulk two-point function from the Källén-Lehnmann spectral decomposition.

4.2 Examples of partial wave coefficients

Before using the partial wave expansion in crossing equations to find non-trivial bounds, we would like to present some simple examples to gain more intuition about the partial wave coefficients $I_{\Delta,\ell}$. In what follows, we first consider a free massive field in dS which leads to Mean Field Theory (MFT) type conformal correlators for late-time boundary operators. We shall see that the positivity condition (4.10) requires a careful treatment of contact terms in late-time correlators. Then, we consider a $\lambda\phi^4$ bulk interaction and calculate the partial wave coefficients to the leading order in λ.

4.2.1 Mean Field Theory

Consider the following four-point function of late-time boundary operators of a free massive scalar field in dS,

$$\langle \mathcal{O}_1 \mathcal{O}_2^\dagger \mathcal{O}_3^\dagger \mathcal{O}_4 \rangle \tag{4.22}$$

where we used $\mathcal{O}_i$ as a short notation for $\mathcal{O}(x_i)$. Since the bulk field is free, the four-point function is given by three Wick contractions. Of course, this has the same structure as MFT,

$$\langle \mathcal{O}_1 \mathcal{O}_2^\dagger \mathcal{O}_3^\dagger \mathcal{O}_4 \rangle_{\text{MFT}} = \langle \mathcal{O}_1 \mathcal{O}_2^\dagger \rangle \langle \mathcal{O}_3^\dagger \mathcal{O}_4 \rangle + \langle \mathcal{O}_1 \mathcal{O}_4 \rangle \langle \mathcal{O}_2^\dagger \mathcal{O}_3^\dagger \rangle + \langle \mathcal{O}_1 \mathcal{O}_3^\dagger \rangle \langle \mathcal{O}_2^\dagger \mathcal{O}_4 \rangle \tag{4.23}$$

which can also be expanded as

$$\begin{aligned} \langle \mathcal{O}_1 \mathcal{O}_2^\dagger \mathcal{O}_3^\dagger \mathcal{O}_4 \rangle_{\text{MFT}} =& \langle \mathcal{O}_1 \mathcal{O}_2^\dagger \rangle \langle \mathcal{O}_3^\dagger \mathcal{O}_4 \rangle \\ &+ \sum_\ell \int_{\frac{d}{2}}^{\frac{d}{2}+i\infty} \frac{d\Delta}{2\pi i} I^{\text{MFT}}_{\Delta,\ell} \Psi^{\Delta_i}_{\Delta,\ell}(x_i) + \sum_\ell \int_{\frac{d}{2}}^{\frac{d}{2}+i\infty} \frac{d\Delta}{2\pi i} I^{\delta}_{\Delta,\ell} \Psi^{\Delta_i}_{\Delta,\ell}(x_i) \end{aligned} \tag{4.24}$$

Here we wrote the partial wave decomposition in the (12)(34) channel, identifying the expansion of each of the 3 terms in (4.23). Namely, the first corresponds to the vacuum contribution, the second we call $I^{\text{MFT}}_{\Delta,\ell}$ and the third we denote as $I^{\delta}_{\Delta,\ell}$ because it is a pure contact term. Moreover, as we will see in (4.34), the operators $\mathcal{O}$ and $\mathcal{O}^\dagger$ do not commute. For the four-point function (4.22) we implictly use the radial ordering and therefore MFT expansion of it has the unique form of (4.23).

Let us first calculate $I^{\text{MFT}}_{\Delta,\ell}$. We have

$$\langle \mathcal{O}_1 \mathcal{O}_4 \rangle \langle \mathcal{O}_2^\dagger \mathcal{O}_3^\dagger \rangle = \frac{1}{|x_1 - x_4|^{d+2i\mu}} \frac{1}{|x_2 - x_3|^{d-2i\mu}} = \sum_\ell \int_{\frac{d}{2}}^{\frac{d}{2}+i\infty} \frac{d\Delta}{2\pi i} I^{\text{MFT}}_{\Delta,\ell} \Psi^{\Delta_i}_{\Delta,\ell}(x_i) \,.$$

Using the orthogonality relation (4.12), one finds

$$\begin{aligned} I^{\text{MFT}}_{\Delta,\ell} &= \frac{1}{n_{\Delta,\ell}} \int \frac{d^d x_1 \dots d^d x_5}{\text{vol(SO}(d{+}1,1))} \langle \mathcal{O}_1 \mathcal{O}_4 \rangle \langle \tilde{\mathcal{O}}_2 \tilde{\mathcal{O}}_3 \rangle \langle \tilde{\mathcal{O}}_1 \mathcal{O}_2 \tilde{O}_{\mu_1 \dots \mu_\ell}(x_5) \rangle \langle O^{\mu_1 \dots \mu_\ell}(x_5) \mathcal{O}_3 \tilde{\mathcal{O}}_4 \rangle \\ &= \frac{S([\tilde{\mathcal{O}}]\mathcal{O}O) S([\mathcal{O}]\mathcal{O}O)}{n_{\Delta,\ell}} \int \frac{d^d x_1 d^d x_2 d^d x_5}{\text{vol(SO}(d{+}1,1))} \langle \tilde{\mathcal{O}}_1 \mathcal{O}_2 \tilde{O}_{\mu_1 \dots \mu_\ell}(x_5) \rangle \langle O^{\mu_1 \dots \mu_\ell}(x_5) \tilde{\mathcal{O}}_2 \mathcal{O}_1 \rangle \\ &= (-1)^\ell \frac{2^{\ell-1} \Gamma(\ell + \frac{d}{2})}{\pi^{\frac{d}{2}} \Gamma(\ell+1)} \frac{\Gamma(i\mu) \Gamma(-i\mu)}{\Gamma(\frac{d}{2} + i\mu) \Gamma(\frac{d}{2} - i\mu)} \frac{(\Delta + \ell - 1)(\tilde{\Delta} + \ell - 1) \Gamma(\Delta - 1) \Gamma(\tilde{\Delta} - 1)}{\Gamma(\Delta - \frac{d}{2}) \Gamma(\frac{d}{2} - \Delta)} \end{aligned} \tag{4.25}$$

where we used shorthand notation $\tilde{\Delta} = d - \Delta$ as well as O to denote the exchanged operator with spin ℓ in the integral representation of the conformal partial wave to contrast with external operator $\mathcal{O}$. In addition, we used the identity [67]

$$\begin{aligned}\zeta_{d,\ell} \equiv& \int \frac{d^dx_1d^dx_2d^dx_5}{\text{vol(SO(d+1,1))}}\langle\mathcal{O}_1(x_1)\mathcal{O}_2(x_2)O_{5,\ell}(x_5)\rangle\langle\tilde{O}_{5,\ell}(x_5)\tilde{\mathcal{O}}_1(x_1)\tilde{\mathcal{O}}_2(x_2)\rangle\\ =&\frac{\text{vol}(S^{d-2})}{\pi^{\frac{d}{2}-1}\text{vol}(SO(d-1))}\frac{\Gamma(\ell+d-2)}{2^{\ell+d-2}\Gamma(\ell+\frac{d}{2}-1)}\ ,\end{aligned} \tag{4.26}$$

and the notion of shadow transform $\mathbf{S}[\mathcal{O}(x)]$ that creates a linear map on the space of three-point functions as [67][4]

$$\langle\mathbf{S}[\mathcal{O}_1](x_1)\mathcal{O}_2(x_2)\mathcal{O}_3(x_3)\rangle = S([\mathcal{O}_1]\mathcal{O}_2\mathcal{O}_3)\langle\tilde{\mathcal{O}}_1(x_1)\mathcal{O}_2(x_2)\mathcal{O}_3(x_3)\rangle\ . \tag{4.27}$$

In particular, for scalar operators $\mathcal{O}_1$ and $\mathcal{O}_2$ we have the explicit formula

$$S([\mathcal{O}_1]\mathcal{O}_2\mathcal{O}_{3,\ell}) = \frac{\pi^{\frac{d}{2}}\Gamma(\Delta_1-\frac{d}{2})\Gamma(\frac{d-\Delta_1+\Delta_2-\Delta_3+\ell}{2})\Gamma(\frac{d-\Delta_1+\Delta_3-\Delta_2+\ell}{2})}{\Gamma(d-\Delta_1)\Gamma(\frac{\Delta_1+\Delta_2-\Delta_3+\ell}{2})\Gamma(\frac{\Delta_1+\Delta_3-\Delta_2+\ell}{2})}\ . \tag{4.28}$$

Note that in (4.25), we used the fact that by swapping $\mathcal{O}_1$ and $\mathcal{O}_2$ in the three-point structure defined in (4.6b), one picks a factor of $(-1)^\ell$.

$I^{\text{MFT}}_{\Delta,\ell}$ is negative for odd spins. On the other hand, according to (4.10) the partial wave coefficients of the correlator (4.22) have to be non-negative for all spins and values of $\Delta = \frac{d}{2}+i\nu$ with $\nu \geq 0$. We shall now see that the third term in (4.24) solves this problem.

4.2.2 Local terms in the Gaussian theory

At late times, the propagator of a massive field in dS_{d+1} contains a delta function term [19]. In this section, we calculate this local term explicitly, starting from the momentum-space expression (2.82) of the propagator. We will also make contact with the boundary OPE (2.44).

As before, we encode the mass m^2 of the scalar by the dimension $\Delta = d/2+i\mu$. Expanding the Hankel functions in (2.82) around $\eta = 0$, we obtain

$$\langle\phi(\eta,x)\phi(\eta,y)\rangle \underset{\eta\to 0}{\sim} (-\eta)^d\int\frac{d^dk}{(2\pi)^d}\,e^{-ik\cdot(x-y)}\left[\frac{\Gamma(-i\mu)^2}{4\pi}\left(\frac{-|k|\eta}{2}\right)^{2i\mu}+\text{c.c}+\frac{\coth(\pi\mu)}{2\mu}\right]. \tag{4.29}$$

---

[4] The shadow transformation is defined as

$$\mathbf{S}[\mathcal{O}(x)] = \int d^dy\langle\tilde{\mathcal{O}}(x)\tilde{\mathcal{O}}(y)\rangle\mathcal{O}(y)$$

where $\langle\tilde{\mathcal{O}}(x)\tilde{\mathcal{O}}(y)\rangle = \frac{1}{|x-y|^{2d-2\Delta}}$ is two-point structure of operators $\tilde{\mathcal{O}}$ with dimension $\tilde{\Delta} = d-\Delta$.

Performing the k-integral using

$$\int d^dx\ e^{ik\cdot k}|x|^{-2a} = \pi^{\frac{d}{2}}\frac{\Gamma(\frac{d}{2}-a)}{\Gamma(a)}\left(\frac{|k|}{2}\right)^{2a-d}$$

we find that

$$\begin{aligned}\langle\phi(\eta,x,)\phi(\eta,y)\rangle \underset{\eta\to 0^-}{\sim} & (-\eta)^{d+2i\mu}\,\frac{\Gamma(-i\mu)\Gamma(\frac{d}{2}+i\mu)}{4\pi^{\frac{d}{2}+1}}\frac{1}{|x-y|^{d+2i\mu}} \ + \ \text{c.c.} \\ & +(-\eta)^d\,\frac{\coth(\pi\mu)}{2\mu}\delta^{(d)}(x-y)\ .\end{aligned} \tag{4.30}$$

In what follows, we will refer to the third term as a *local* term.[5]

This expression should be compared with the expectation from the late-time OPE (2.44), which in the case of a free massive bulk field simplifies to

$$\phi(x,\eta) \underset{\eta\to 0^-}{\sim} b(-\eta)^{\Delta}\mathcal{O}(x) + b^*(-\eta)^{\Delta^*}\mathcal{O}^\dagger(x)\ , \qquad \Delta = \frac{d}{2}+i\mu\ . \tag{4.31}$$

The late time limit of the bulk two-point function is then given by

$$\begin{aligned}\langle\phi(x,\eta)\phi(y,\eta)\rangle \underset{\eta\to 0^-}{\sim} & (-\eta)^{2\Delta}b^2\langle\mathcal{O}(x)\mathcal{O}(y)\rangle \ + \ (-\eta)^{2\Delta^*}b^{*2}\langle\mathcal{O}^\dagger(x)\mathcal{O}^\dagger(y)\rangle \\ & + \, (-\eta)^d|b|^2\left(\langle\mathcal{O}(x)\mathcal{O}^\dagger(y)\rangle + \langle\mathcal{O}^\dagger(y)\mathcal{O}(x)\rangle\right)\ .\end{aligned} \tag{4.32}$$

Comparing with (4.30), one finds the anti-commutator to be

$$\left\{\mathcal{O}(x),\mathcal{O}^\dagger(y)\right\} = \frac{\coth(\pi\mu)}{2\mu|b|^2}\delta^{(d)}(x-y)\ , \qquad b = \sqrt{\frac{\Gamma(-i\mu)\Gamma(\frac{d}{2}+i\mu)}{4\pi^{\frac{d}{2}+1}}} \tag{4.33}$$

Let us draw your attention to the fact that $\mathcal{O}(x)$ and $\mathcal{O}(y)^\dagger$ do not commute at coinciding points $x \to y$[6]. One way to see this is the canonical commutation relations of ϕ and its conjugate Π in (2.57b) which gives

$$\left[\mathcal{O}(x),\mathcal{O}^\dagger(y)\right] = \frac{1}{2\mu|b|^2}\delta^{(d)}(x-y)\ . \tag{4.34}$$

---

[5] The local term in (4.30) can be derived in an alternative way. Recall that the two-point function can be written as $\langle\phi(x,\eta)\phi(y,\eta)\rangle = F(\xi)$ with $\xi = 4\eta^2/|x-y|^2$. In the limit $\eta\to 0$, we can then write $\langle\phi(x,\eta)\phi(y,\eta)\rangle \sim (-\eta)^d\delta^{(d)}(x-y)\int d^dwF(4/|w|^2) + \ldots$ where the remaining terms vanish when integrated over $\int d^dx$. Using the explicit expression $F = G_{\mathrm{f}}(\xi;\mu)$ given in (3.4) one recovers the coefficient of the local term in (4.30).

[6] We thank Victor Gorbenko and Matteo Delladio for pointing out this fact[111].

This together with (4.33) leads to

$$\langle \mathcal{O}(x)\mathcal{O}^\dagger(y)\rangle = \frac{\coth(\pi\mu)+1}{4\mu|b|^2}\delta^{(d)}(x-y) \equiv C_\delta \delta^{(d)}(x-y)\ , \tag{4.35a}$$

$$\langle \mathcal{O}^\dagger(x)\mathcal{O}(y)\rangle = \frac{\coth(\pi\mu)-1}{4\mu|b|^2}\delta^{(d)}(x-y) \equiv \bar{C}_\delta \delta^{(d)}(x-y) \tag{4.35b}$$

where b here is same as b_Δ in (2.86) with $\Delta = \frac{d}{2}+i\mu$.

Now, let us go back to (4.24) and find $I^\delta_{\Delta,\ell}$. The calculation is very similar to the one of $I^{\text{MFT}}_{\Delta,\ell}$ in (4.25) except that we have the delta function of (4.35b) instead of the conformal two-point functions that can easily be calculated by (4.26):

$$\begin{aligned} I^\delta_{\Delta,\ell} &= \frac{C_\delta \bar{C}_\delta}{n_{\Delta,\ell}} \int \frac{d^dx_1 \dots d^dx_5}{\text{vol}(\text{SO}(d{+}1{,}1))} \delta^{(d)}(x_1-x_3)\delta^{(d)}(x_2-x_4)\langle \tilde{\mathcal{O}}_1\mathcal{O}_2\tilde{\mathcal{O}}_5\rangle\langle O_5\mathcal{O}_3\tilde{\mathcal{O}}_4\rangle \\ &= \zeta_{d,\ell}\frac{C_\delta \bar{C}_\delta}{n_{\Delta,\ell}} = (-1)^\ell I^{\text{MFT}}_{\Delta,\ell} > 0\ . \end{aligned} \tag{4.36}$$

This leads to the total partial wave coefficient

$$I_{\Delta,\ell} = I^{\text{MFT}}_{\Delta,\ell} + I^\delta_{\Delta,\ell} = \left(1+(-1)^\ell\right) I^\delta_{\Delta,\ell}\ . \tag{4.37}$$

This means that the total partial wave expansion vanishes for the odd spin and is positive for even spins which agrees with the positivity condition (4.10). In summary, the existence of the local terms is essential in unitary Mean Field Theories in dS.

Let us remark that one could consider the correlator $\langle \mathcal{O}_1(x_1)\mathcal{O}_2(x_2)\mathcal{O}_2(x_3)\mathcal{O}_1(x_4)\rangle$ with two different bulk fields. In this case, we would find a similar expression for $I^{\text{MFT}}_{\Delta,\ell}$ as in (4.25) but there would be no local contribution. This is not in contradiction with unitarity as this correlator no longer fulfills the positivity condition (4.10).

4.2.3 Adding interactions; ϕ^4 theory at leading order

So far, we have considered the spectral decomposition of the correlator $\langle \mathcal{O}\mathcal{O}^\dagger\mathcal{O}^\dagger\mathcal{O}\rangle$, where $\mathcal{O}$ and $\mathcal{O}^\dagger$ were boundary operators with scaling dimensions $d/2 \pm i\mu$. This led to the spectral density $I^{\text{MFT}}_{\Delta,\ell}$ from Eq. (4.25). Closing the contour and picking up poles in the Δ-plane, we find that the $x_{12}\to 0$ OPE limit of $\langle \mathcal{O}\mathcal{O}^\dagger\mathcal{O}^\dagger\mathcal{O}\rangle$ is governed by boundary operators with dimension

$$\Delta = d+\ell+2\mathbb{N}, \quad \ell = 0,1,2,\dots . \tag{4.38a}$$

Had we instead considered the correlators $\langle\mathcal{O}\mathcal{O}\mathcal{O}\mathcal{O}\rangle$ or $\langle\mathcal{O}^\dagger\mathcal{O}^\dagger\mathcal{O}^\dagger\mathcal{O}^\dagger\rangle$, then we would have instead found double-trace operators with dimensions

$$d + 2i\mu + \ell + 2\mathbb{N} \quad \text{resp.} \quad d - 2i\mu + \ell + 2\mathbb{N}\ . \tag{4.38b}$$

The locations of these three families of poles are depicted in figure 4.1.

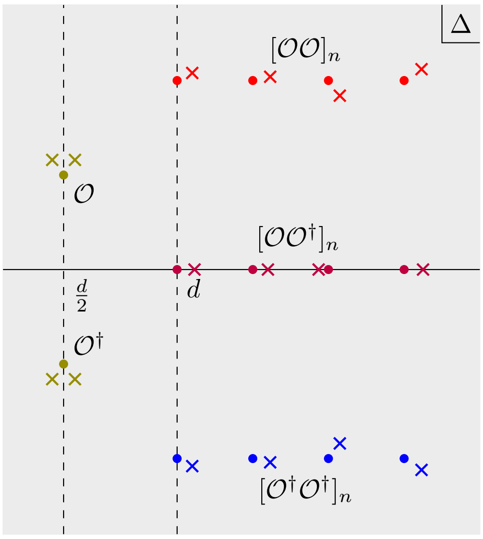
Δ
$[\mathcal{O}\mathcal{O}]_n$
$\mathcal{O}$
$[\mathcal{O}\mathcal{O}^\dagger]_n$
$\frac{d}{2}$
d
$\mathcal{O}^\dagger$
$[\mathcal{O}^\dagger\mathcal{O}^\dagger]_n$

Figure 4.1: Analytic structure of the spectral density $I_{\Delta,\ell=0}$ in the case of a free and a weakly-coupled theory in dS. The solid circles are the locations of the poles for "single-trace" and "double-trace" operators of the dS mean field theory. The single-trace poles appear for instance in the two-point function of the bulk field. The three families of double-trace poles are visible in different correlators, namely $\langle\mathcal{O}\mathcal{O}\mathcal{O}\mathcal{O}\rangle$, $\langle\mathcal{O}\mathcal{O}^\dagger\mathcal{O}\mathcal{O}^\dagger\rangle$ and $\langle\mathcal{O}^\dagger\mathcal{O}^\dagger\mathcal{O}^\dagger\mathcal{O}^\dagger\rangle$. After turning on interactions, the locations of the poles shifts, indicating that boundary operators pick up anomalous dimensions. These shifted poles are shown as crosses in the figure. Of course, new poles may appear too.

The above picture must be modified in interacting theories. If one can construct a QFT in dS_{d+1} that is controlled by a small coupling $\lambda \ll 1$, we expect that its spectrum is close to (4.38), up to corrections of order λ (or λ^2, depending on the operator and interaction in question). Let us denote the dimensions of some boundary operator $\mathcal{O}_\alpha$ as $\Delta_\alpha(\lambda)$, such that $\Delta_\alpha(0) = \Delta_\alpha^{\mathrm{MFT}}$. The shifting of poles is shown in figure 4.1. We can ask how this behavior can be reproduced from perturbation theory. Including interactions, a general four-point function is modified according to

$$\langle\mathcal{O}_1\mathcal{O}_2\mathcal{O}_3\mathcal{O}_4\rangle_\lambda = \langle\mathcal{O}_1\cdots\mathcal{O}_4\rangle_{\mathrm{MFT}} + \lambda\mathcal{A}(x_1,\ldots,x_4) + \mathrm{O}(\lambda^2) \tag{4.39a}$$

for some diagram $\mathcal{A}(x_1,\ldots,x_4)$, or by passing to the spectral representation

$$I_{\Delta,\ell}(\lambda) = I^{\mathrm{MFT}}_{\Delta,\ell} + \lambda I^{\mathcal{A}}_{\Delta,\ell} + \mathrm{O}(\lambda^2). \tag{4.39b}$$

Now suppose that the full spectral density $I_{\Delta,\ell}(\lambda)$ has a simple pole at $\Delta = \Delta_\alpha(\lambda)$ with residue $s(\lambda)$. Expanding around $\lambda = 0$, we then must have

$$\frac{s(\lambda)}{\Delta - \Delta_\alpha(\lambda)} = \frac{s(0)}{\Delta - \Delta_\alpha^{\mathrm{MFT}}} + \lambda \left[\frac{s'(0)}{\Delta - \Delta_\alpha^{\mathrm{MFT}}} + \frac{s(0)\Delta_\alpha'(0)}{(\Delta - \Delta_\alpha^{\mathrm{MFT}})^2} \right] + \mathrm{O}(\lambda)^2. \tag{4.40}$$

In particular, a double pole in the spectral density $I^{\mathcal{A}}_{\Delta,\ell}$ signifies the fact that $\mathcal{O}_\alpha$ has an anomalous dimension already at order λ.

To give an example of this phenomenon, let us consider ϕ^4 theory in dS_{d+1}. Despite the extensive literature calculating Witten diagrams in AdS (starting with [112, 113]), the knowledge of late-time correlators in dS has been primitive until recent years. A recent series of papers [87, 114, 115] has shed light on the relation between tree-level diagrams in AdS and dS. We reviewed their result in section 2.5.2. For the case at hand, let us rewrite (2.101), which states that for a general dS contact diagram

$$\langle \mathcal{O}_1(x_1)\mathcal{O}_2(x_2)\mathcal{O}_3(x_3)\mathcal{O}_4(x_4)\rangle_{\text{contact}} = -2\sin(\frac{\pi}{2}\zeta)\prod_{i=1}^{4} b_{\Delta_i}\, D_{\Delta_1\Delta_2\Delta_3\Delta_4}(x_i) \tag{4.41a}$$

where

$$\Delta_i = \frac{d}{2} + i\mu_i \quad \text{and} \quad \zeta = d + i(\mu_1 + \ldots + \mu_4)\ . \tag{4.41b}$$

and b_Δ is given by (2.86). The special function that appears here,

$$D_{\Delta_1\Delta_2\Delta_3\Delta_4}(x_1,\ldots,x_4) = \int_0^\infty \frac{dz}{z^{d+1}} \int_{\mathbb{R}^d} d^dy \prod_{i=1}^{4} \left(\frac{z}{z^2 + |y - x_i|^2} \right)^{\Delta_i}\ , \tag{4.41c}$$

represents a contact diagram in Euclidean AdS. For definiteness, let us compute the leading correction to the four-point function

$$\langle \mathcal{O}(x_1)\mathcal{O}(x_2)\mathcal{O}^\dagger(x_3)\mathcal{O}^\dagger(x_4)\rangle \tag{4.42}$$

which according to (4.10) has a positive spectral density. This is an example of a correlator of the above type, with $\mu_1 = \mu_2 = \mu$ and $\mu_3 = \mu_4 = -\mu$, such that $\zeta = d$ in the phase factor $\sin(\frac{\pi}{2}\zeta)$. Moreover, the D-function has a known spectral representation [116]. Using these facts, we conclude that

$$\begin{aligned} I_{\Delta,\ell}^{\text{contact}} = &- \sin(\pi\tfrac{d}{2}) \frac{\Gamma(\frac{d}{2} \pm i\mu)\Gamma(\pm i\mu)}{8\pi^{d+2}} \times \\ &\Gamma\left(\frac{\Delta}{2} \pm i\mu\right)\Gamma\left(\frac{d-\Delta}{2} \pm i\mu\right) \frac{\Gamma\left(\frac{\Delta}{2}\right)^2 \Gamma\left(\frac{d-\Delta}{2}\right)^2}{\Gamma(\frac{d}{2} - \Delta)\Gamma(\Delta - \frac{d}{2})}\, \delta_{\ell,0}\ . \end{aligned} \tag{4.43}$$

Here we use the shorthand notation of $\Gamma(a \pm b) := \Gamma(a+b)\Gamma(a-b)$. Interestingly, the above analysis seems to indicate that the diagram in question vanishes identically when d

is even.

In order to read off the physical content of the partial wave coefficient $I^{\text{contact}}_{\Delta,0}$, one has to multiply $I^{\text{contact}}_{\Delta,\ell}$ by the coefficient $K^{\Delta_3,\Delta_4}_{\tilde{\Delta},0}$, see for instance Eq. (4.20). In the s-channel, corresponding to $\mathcal{O}\times\mathcal{O}\to\mathcal{O}^\dagger\times\mathcal{O}^\dagger$, we find that the physical poles are at $\Delta = d\pm 2i\mu+2\mathbb{N}$:

$$K^{\frac{d}{2}-i\mu,\frac{d}{2}-i\mu}_{\tilde{\Delta},0}\, I^{\text{contact}}_{\Delta,0} \underset{\Delta\to d\pm 2i\mu+2n}{\sim} \frac{\rho^{\pm}_n}{\Delta-d\mp 2i\mu-2n}. \tag{4.44}$$

Since these are single poles, they do not have an interpretation of giving rise to anomalous dimensions: instead, they mean that the boundary OPE coefficients $c_{\mathcal{O}\mathcal{O}[\mathcal{O}^\dagger\mathcal{O}^\dagger]_{n,0}}$ and their counterparts with $\mathcal{O}\leftrightarrow\mathcal{O}^\dagger$ are generated at order λ. In the cross-channel, corresponding to the exchange $\mathcal{O}\times\mathcal{O}^\dagger\to\mathcal{O}\times\mathcal{O}^\dagger$, we find both double and single poles at $\Delta = d+2\mathbb{N}$:

$$K^{\frac{d}{2}+i\mu,\frac{d}{2}-i\mu}_{\tilde{\Delta},0}\, I^{\text{contact}}_{\Delta,0} \underset{\Delta\to d+2n}{\sim} \frac{\sigma_n}{\Delta-d-2n}+\frac{\tau_n}{(\Delta-d-2n)^2}, \quad n=0,1,2,\dots \tag{4.45}$$

but there are no other physical poles present. This indicates that the double-trace operators $[\mathcal{O}\mathcal{O}^\dagger]_{n,0}$ with spin $\ell=0$ and dimension $\Delta = d+2\mathbb{N}$ have their scaling dimension corrected at tree level. The presence of a single pole in (4.45) indicates that their residues, i.e. the OPE coefficients $c^2_{\mathcal{O}\mathcal{O}^\dagger[\mathcal{O}\mathcal{O}^\dagger]}$, also get renormalized.

5 Setting up the QFT in dS Bootstrap

The Euclidean conformal boundary four-point functions enjoy crossing symmetry. In other words, the four-point function is invariant under permutations of the external operators. The partial wave expansions in each channel do not transform trivially under these permutations. This results in a non-trivial set of equations called crossing equations. This is the basic idea behind the conformal bootstrap program [27, 117]. Let us see how the same philosophy works for QFTs in de Sitter.

Consider the four-point function of late-time boundary operators

$$\langle \mathcal{O}_1(x_1)\mathcal{O}_2(x_2)\mathcal{O}_3(x_3)\mathcal{O}_4(x_4)\rangle \,. \tag{5.1}$$

Out of 24 permutations of partial wave expansions for scalar operators, there are 3 equivalence classes. This can be checked from explicit expression of partial waves in (4.15). We choose the channels s, t and u as representatives of these equivalence classes. Hence, we end up with two sets of non-trivial crossing equations

$$\begin{aligned}\sum_\ell \int_{\frac{d}{2}}^{\frac{d}{2}+i\infty} \frac{d\Delta}{2\pi i}\, I^s_{\Delta,\ell}\; \Psi^s_{\Delta,\ell}(x_i) + D^s(x_i) &= \sum_\ell \int_{\frac{d}{2}}^{\frac{d}{2}+i\infty} \frac{d\Delta}{2\pi i}\, I^t_{\Delta,\ell}\; \Psi^t_{\Delta,\ell}(x_i) + D^t(x_i) \;,\\ \sum_\ell \int_{\frac{d}{2}}^{\frac{d}{2}+i\infty} \frac{d\Delta}{2\pi i}\, I^s_{\Delta,\ell}\; \Psi^s_{\Delta,\ell}(x_i) + D^s(x_i) &= \sum_\ell \int_{\frac{d}{2}}^{\frac{d}{2}+i\infty} \frac{d\Delta}{2\pi i}\, I^u_{\Delta,\ell}\; \Psi^u_{\Delta,\ell}(x_i) + D^u(x_i) \;,\end{aligned} \tag{5.2}$$

where $D^j(x_i)$ is the contribution from the vacuum state in channel j:

$$D^s(x_i) = \frac{\delta_{\mathcal{O}_1\mathcal{O}_2}\delta_{\mathcal{O}_3\mathcal{O}_4}}{x_{12}^{2\Delta_1}x_{34}^{2\Delta_3}} \;, \qquad D^t(x_i) = \frac{\delta_{\mathcal{O}_2\mathcal{O}_3}\delta_{\mathcal{O}_1\mathcal{O}_4}}{x_{23}^{2\Delta_3}x_{14}^{2\Delta_1}} \;, \qquad D^u(x_i) = \frac{\delta_{\mathcal{O}_1\mathcal{O}_3}\delta_{\mathcal{O}_2\mathcal{O}_4}}{x_{13}^{2\Delta_1}x_{24}^{2\Delta_2}} \;, \tag{5.3}$$

and we defined the s, t and u channel partial waves as follows

$$\begin{aligned}\Psi^{s}_{\Delta,\ell}(x_i) &= \Psi^{\Delta_1,\Delta_2,\Delta_3,\Delta_4}_{\Delta,\ell}(x_1,x_2,x_3,x_4)\\ \Psi^{t}_{\Delta,\ell}(x_i) &= \Psi^{\Delta_3,\Delta_2,\Delta_1,\Delta_4}_{\Delta,\ell}(x_3,x_2,x_1,x_4)\\ \Psi^{u}_{\Delta,\ell}(x_i) &= \Psi^{\Delta_1,\Delta_3,\Delta_2,\Delta_4}_{\Delta,\ell}(x_1,x_3,x_2,x_4)\ .\end{aligned} \tag{5.4}$$

As discussed in section 4.1, the partial wave expansion is derived by inserting a complete set of states in the four-point function and the unitarity of the bulk theory puts positivity constraints on partial wave coefficients.[1] As a simple first step to extend the conformal bootstrap approach to cosmological correlators, we will focus on correlators of the form

$$\langle \mathcal{O}(x_1)\mathcal{O}^\dagger(x_2)\mathcal{O}(x_3)\mathcal{O}^\dagger(x_4)\rangle \tag{5.5}$$

where $\mathcal{O}$ may have complex dimension $\Delta_{\mathcal{O}} = \Delta_{re} + i\Delta_{im}$ with real part $\Delta_{re} \geq \frac{d}{2}$. In this case, the t and s channels are equivalent, therefore $I^{t}_{\Delta,\ell} = I^{s}_{\Delta,\ell}$. In addition, the positivity conditions (4.10) or (4.11) are satisfied in all channels. More precisely, we have

$$\bar{I}^{s}_{\Delta,\ell} \equiv I^{s}_{\Delta,\ell}(-1)^{\ell} \geq 0\ , \qquad\qquad I^{u}_{\Delta,\ell} \geq 0\ .$$

For simplicity, from now on we focus on QFT on dS_2, *i.e.* we take $d = 1$. This has the important advantage of removing the infinite sums over spin ℓ. However, it forces us to take into account discrete series irreps of $SO(2,1) \cong SL(2,\mathbb{R})$ [80, 119, 120, 79]. This is what we explain next. We plan to extend the analysis to higher dimensions in the future.

5.1 Review of CFT_1

We shall proceed with reviewing some basics of $d = 1$ conformal partial waves similar to what we did in section 4.1. The four-point function, after stripping out the appropriate scaling factors, is a function of a single cross ratio,

$$\langle \mathcal{O}_1(x_1)\mathcal{O}_2(x_2)\mathcal{O}_3(x_3)\mathcal{O}_4(x_4)\rangle = \frac{1}{|x_{12}|^{\Delta_{12}}|x_{34}|^{\Delta_{34}}}\left|\frac{x_{14}}{x_{24}}\right|^{\delta_{21}}\left|\frac{x_{14}}{x_{13}}\right|^{\delta_{34}}\mathcal{G}(z) \tag{5.6}$$

with a single cross ratio of

$$z = \frac{x_{12}x_{34}}{x_{13}x_{24}} \in \mathbb{R}\,, \tag{5.7}$$

where we used $x_{ij} = x_i - x_j$, $\Delta_{ij} = \Delta_i + \Delta_j$ and $\delta_{ij} = \Delta_i - \Delta_j$. $\mathcal{G}(z)$ is singular at $z = 0, 1, \infty$ corresponding to coincident points. We will fix the external dimensions accordingly with the correlator (5.5), *i.e.* $\Delta_1 = \Delta_3 = \Delta_{re} + i\Delta_{im}$ and $\Delta_2 = \Delta_4 = \Delta_{re} - i\Delta_{im}$.

---

[1] The constraints are more general for mixed correlators. The conformal bootstrap approach to mixed correlators has been studied in great detail. A similar approach can be taken here by considering the analogy between $\mathcal{F}_{12}(\Delta,\ell)$ in (4.5) and the OPE coefficients $\lambda_{12\mathcal{O}}$ in the usual conformal bootstrap. Then, we reach a more general bootstrap problem. e.g. look at eq. (2.10) of [118].

Let us expand the correlator $\mathcal{G}(z)$ in a complete set of eigenfunctions of the Casimir operator, orthogonal with respect to inner product [120, 119]

$$(f, g) = \int_{-\infty}^{\infty} dz z^{-2} f(z) g(z) \ . \tag{5.8}$$

These are the conformal partial waves introduced in the previous chapter. However, for $d = 1$ the complete basis includes both principal and discrete series ($\Delta \in \mathbb{N}$) with both parities, which we denote by spin $\ell \in \{0, 1\}$ [80]. These obey the orthogonality relations

$$(\Psi_{\frac{1}{2}+i\alpha,\ell}, \Psi_{\frac{1}{2}+i\beta,\ell'}) = 2\pi n_{\Delta,\ell}\ \delta_{\ell\ell'}\delta(\alpha-\beta) \qquad \alpha, \beta \in \mathbb{R}_+ \ , \tag{5.9}$$

$$(\Psi_{m,\ell}, \Psi_{n,\ell'}) = \frac{4\pi^2}{2m-1}\delta_{\ell\ell'}\delta_{mn} \qquad m, n \in \mathbb{N} \ , \tag{5.10}$$

with vanishing inner product between partial waves in the discrete and principal series. Notice that in this equation δ is the Kronecker delta. The normalization factor $n_{\Delta,\ell}$ will be given below. Using this basis, we can write the s-channel decomposition

$$\mathcal{G}(z) = \sum_{\ell=0,1} \int_0^\infty \frac{d\nu}{2\pi} I^s_{\frac{1}{2}+i\nu,\ell} \Psi_{\frac{1}{2}+i\nu,\ell}(z) + \sum_{\substack{n\in\mathbb{N} \\ \ell=0,1}} \tilde{I}^s_{n,\ell} \Psi_{n,\ell}(z) \,, \tag{5.11}$$

that replaces (4.7) in $d = 1$.

The partial waves are given by integrals of the product of three-point structures as in (4.9). More precisely, for $\ell = 0$ we have

$$\begin{aligned}\Psi_{\Delta,0}(z) &= \left|\frac{x_{14}}{x_{24}}\right|^{\delta_{12}} \left|\frac{x_{14}}{x_{13}}\right|^{\delta_{43}} \int_{-\infty}^{\infty} dx_5 \frac{|x_{12}|^\Delta}{|x_{15}|^{\Delta+\delta_{12}}|x_{25}|^{\Delta-\delta_{12}}} \frac{|x_{34}|^{1-\Delta}}{|x_{35}|^{1-\Delta+\delta_{34}}|x_{45}|^{1-\Delta-\delta_{34}}} \\ &= |z|^\Delta \int_{-\infty}^{\infty} dx\ \frac{|x-1|^{\Delta-1-2i\Delta_{im}}}{|x-z|^{\Delta-2i\Delta_{im}}|x|^{\Delta+2i\Delta_{im}}} \ ,\end{aligned} \tag{5.12}$$

where in the second line, we fixed the conformal gauge by setting $x_1 = 0$, $x_2 = z$, $x_3 = 1$, $x_4 = \infty$ and $x_5 = x$. In the case $\ell = 1$, the three-point structure has an extra numerator Z that can be derived from the higher dimensional scalar-scalar-spin-ℓ correlator in (4.6b)

$$\langle \mathcal{O}_1(x_1)\mathcal{O}_2(x_2)\mathcal{O}_3(x_3)\rangle = \frac{Z}{x_{12}^{\Delta_1+\Delta_2-\Delta_3} x_{23}^{\Delta_2+\Delta_3-\Delta_1} x_{13}^{\Delta_1+\Delta_3-\Delta_2}} \ , \tag{5.13}$$

with $Z = \frac{|x_{13}||x_{23}|}{|x_{12}|}(\frac{1}{x_{13}} - \frac{1}{x_{23}}) = -\operatorname{sgn}(x_{13})\operatorname{sgn}(x_{23})\operatorname{sgn}(x_{12})$. Let us define $\Theta \equiv$

$\text{sgn}(x_{12}x_{15}x_{25}x_{34}x_{35}x_{45})$, then one finds

$$\begin{aligned}\Psi_{\Delta,1}(z) &= \left(\frac{x_{14}}{x_{24}}\right)^{\delta_{12}}\left(\frac{x_{14}}{x_{13}}\right)^{\delta_{43}}\int_{-\infty}^{\infty} dx_5 \frac{|x_{12}|^{\Delta}}{|x_{15}|^{\Delta+\delta_{12}}|x_{25}|^{\Delta-\delta_{12}}}\frac{|x_{34}|^{1-\Delta}}{|x_{35}|^{1-\Delta+\delta_{34}}|x_{45}|^{1-\Delta-\delta_{34}}}\Theta \\ &= |z|^{\Delta}\int_{-\infty}^{\infty} dx\ \frac{|x-1|^{\Delta-1-2i\Delta_{im}}}{|x-z|^{\Delta-2i\Delta_{im}}|x|^{\Delta+2i\Delta_{im}}}\ \text{sgn}(xz(x-1)(z-x))\ . \end{aligned} \tag{5.14}$$

For $z \in (0,1)$, the partial waves with Δ on the principal series can be written as a linear combination of a conformal block and its shadow

$$\Psi_{\Delta,\ell}(z) = K_{1-\Delta,\ell}\, G_{\Delta,\ell}(z) + K_{\Delta,\ell}\, G_{1-\Delta,\ell}(z)\ , \tag{5.15}$$

where

$$G_{\Delta,\ell}(z) = (-1)^{\ell} z^{\Delta}\, {}_2F_1(\Delta+2i\Delta_{im}, \Delta-2i\Delta_{im}; 2\Delta; z)\ , \tag{5.16}$$

$$K_{\Delta,\ell} = \frac{\sqrt{\pi}\Gamma(\Delta-\frac{1}{2})\Gamma(\Delta+\ell-1)}{\Gamma(\Delta-1)\Gamma(1-\Delta+\ell)}\frac{\Gamma(\frac{1-\Delta+2i\Delta_{im}+\ell}{2})\Gamma(\frac{1-\Delta-2i\Delta_{im}+\ell}{2})}{\Gamma(\frac{\Delta+2i\Delta_{im}+\ell}{2})\Gamma(\frac{\Delta-2i\Delta_{im}+\ell}{2})}\ . \tag{5.17}$$

One way to find these expressions is to perform integrals (5.12) and (5.14) explicitly. Alternatively, one can set $d = 1$ in the general formula (4.15). For integer Δ, corresponding to the discrete series, we have instead

$$n \in \mathbb{N}: \quad \Psi_{n,\ell}(z) = K_{1-n,\ell}\, G_{n,\ell}(z)\ . \tag{5.18}$$

Finally, we would like to show that

$$n_{\Delta,\ell} = \frac{4\pi\tan(\pi\Delta)}{2\Delta-1}\ . \tag{5.19}$$

As it is stated in [80][2], $n_{\Delta,\ell}$ in general dimension d can be written as

$$n_{\Delta,\ell} = \frac{\text{vol}(S^{d-2})(2\ell+d-2)\Gamma(\ell+d-2)}{\text{vol}(SO(d-1))}\frac{\pi\Gamma(\ell+1)}{2^{2\ell+d-2}\Gamma(\ell+\frac{d}{2})^2}K_{\tilde{\Delta},\ell}K_{\Delta,\ell}\ . \tag{5.20}$$

In order to take the limit $d \to 1$ of this expression, we shall analytically continue in d using the recursion relation

$$\text{vol}(SO(d)) = \text{vol}(S^{d-1})\,\text{vol}(SO(d-1))\ , \tag{5.21}$$

and the fact that $\text{vol}(SO(2)) = \text{vol}(S^1) = 2\pi$. This leads to the formal results $\text{vol}(SO(1)) = 1$ and $\text{vol}(SO(0)) = \frac{1}{2}$. Therefore, we find $\lim_{d\to 1} n_{\Delta,\ell} = 0$ for all $\ell \geq 2$.

---

[2] There is a slight difference in notations: $I^{\text{here}} = I^{\text{there}}n^{\text{there}}$, $K^{\text{here}} = S^{\text{there}} = (-2)^J K^{\text{there}}$ but $n^{\text{here}} = n^{\text{there}}$.

On the other hand, we find

$$\lim_{d\to 1} n_{\Delta,0} = \lim_{d\to 1} n_{\Delta,1} = \frac{4\pi\tan(\pi\Delta)}{2\Delta-1}\ . \tag{5.22}$$

5.2 A toy example: almost MFT

We would like to understand the convergence properties of the partial wave decomposition (5.11). This is very important for the goal of developing a numerical bootstrap approach to QFT in dS. With this in mind, let us consider the example of a weakly coupled massive scalar field in dS_2. In this case, we expect boundary operators almost on the principal series, *i.e.* $\Delta_{re}-\frac{1}{2}\ll 1$. On the other hand, the imaginary part Δ_{im} can be large because it is related to the mass of the bulk field via $m^2R^2=\frac{1}{4}+\Delta_{im}^2$, if we turn off interactions.

The disconnected part of four-point function $\langle \mathcal{O}_1\mathcal{O}_2^\dagger\mathcal{O}_3\mathcal{O}_4^\dagger\rangle_{\text{disc}} = \langle\mathcal{O}_1\mathcal{O}_3\rangle\langle\mathcal{O}_2^\dagger\mathcal{O}_4^\dagger\rangle$ gives:[3]

$$\mathcal{G}_{\text{disc}}(z) = |z|^{\Delta_\mathcal{O}+\Delta_\mathcal{O}^*} = |z|^{2\Delta_{re}}\ . \tag{5.23}$$

Notice that if $\Delta_{re}\neq\frac{d}{2}$ the local terms discussed in section 4.2.2 are not allowed in the two-point function $\langle\mathcal{O}\mathcal{O}^\dagger\rangle$. Using orthogonality relation of Ψ_Δ, one is able to calculate the partial wave coefficients. The basic integral to compute is the following

$$W_{\Delta,\ell} = \int_{-\infty}^{\infty}\frac{dz}{z^2}\,\mathcal{G}_{\text{disc}}(z)\Psi_{\Delta,\ell}(z) \tag{5.24a}$$

$$= \int_{-\infty}^{\infty}dx\,\frac{|x-1|^{\Delta-1-2i\Delta_{im}}}{|x|^{\Delta+2i\Delta_{im}}}\int_{-\infty}^{\infty}\frac{dz}{z^2}\,\frac{|z|^{\Delta+2\Delta_{re}}}{|x-z|^{\Delta-2i\Delta_{im}}}(\delta_{\ell,0}+\delta_{\ell,1}\,\mathrm{sgn}(xz(x-1)(z-x))). \tag{5.24b}$$

This integral can be done explicitly:[4]

$$W_{\Delta,\ell} = \frac{2^\ell\sqrt{\pi}\Gamma(\ell+\frac{1}{2})}{\Gamma(\ell+1)}\frac{\Gamma(\frac{1}{2}+i\Delta_{im}-\Delta_{re})\Gamma(\frac{1}{2}-i\Delta_{im}-\Delta_{re})}{\Gamma(\Delta_{re}+i\Delta_{im})\Gamma(\Delta_{re}-i\Delta_{im})} \times\frac{\Gamma(\frac{\ell-\Delta+2\Delta_{re}}{2})\Gamma(\frac{\ell-1+\Delta+2\Delta_{re}}{2})}{\Gamma(\frac{1+\ell+\Delta-2\Delta_{re}}{2})\Gamma(\frac{2+\ell-\Delta-2\Delta_{re}}{2})}\ . \tag{5.25}$$

---

[3] In the case of a single real operator $\mathcal{O}=\mathcal{O}^\dagger$, there are two more contributions from other channels. The (stripped) four-point function for identical external operators reads

$$\mathcal{G}_{\text{disc}}(z) = 1+|z|^{2\Delta_\mathcal{O}}+\left|\frac{z}{z-1}\right|^{2\Delta_\mathcal{O}}\ .$$

The first term (= 1, from the s-channel) is non-normalizable with respect to the inner product (5.8). The spectral density $I^{(3)}_{\Delta,\ell}$ corresponding to the third term is equal to the density $I^{(2)}_{\Delta,\ell}$ up to a factor $(-1)^\ell$. This is a consequence of the behavior of the partial waves under $z\mapsto z/(z-1)$.

[4] In practice, we divide the integration domain in 9 regions according to the position of x with respect to 0 and 1 and the position of z with respect to 0 and x.

Then, the principal series partial wave coefficients are given by

$$I^{\text{disc}}_{\Delta,\ell} = \frac{1}{n_{\Delta,\ell}} W_{\Delta,\ell} = \frac{2^{\ell-2}\Gamma(\ell+\frac{1}{2})}{\sqrt{\pi}\Gamma(\ell+1)} \frac{\Gamma(\frac{1}{2}+i\Delta_{im}-\Delta_{re})\Gamma(\frac{1}{2}-i\Delta_{im}-\Delta_{re})}{\Gamma(\Delta_{re}+i\Delta_{im})\Gamma(\Delta_{re}-i\Delta_{im})} \frac{(2\Delta-1)}{\tan(\pi\Delta)}$$
$$\times \frac{\Gamma(\frac{\ell-\Delta+2\Delta_{re}}{2})\Gamma(\frac{\ell-1+\Delta+2\Delta_{re}}{2})}{\Gamma(\frac{1+\ell+\Delta-2\Delta_{re}}{2})\Gamma(\frac{2+\ell-\Delta-2\Delta_{re}}{2})} \, , \tag{5.26}$$

for $\Delta = \frac{1}{2} + i\nu$ and $\nu > 0$, and the discrete series by

$$\tilde{I}^{\text{disc}}_{n,\ell} = \frac{2n-1}{4\pi^2} W_{n,\ell} = \frac{2^{\ell-2}\Gamma(\ell+\frac{1}{2})}{\pi^{\frac{3}{2}}\Gamma(\ell+1)} \frac{\Gamma(\frac{1}{2}+i\Delta_{im}-\Delta_{re})\Gamma(\frac{1}{2}-i\Delta_{im}-\Delta_{re})}{\Gamma(\Delta_{re}+i\Delta_{im})\Gamma(\Delta_{re}-i\Delta_{im})}$$
$$\times \frac{(2n-1)\Gamma(\frac{\ell-n+2\Delta_{re}}{2})\Gamma(\frac{\ell-1+n+2\Delta_{re}}{2})}{\Gamma(\frac{1+\ell+n-2\Delta_{re}}{2})\Gamma(\frac{2+\ell-n-2\Delta_{re}}{2})} \, . \tag{5.27}$$

Notice that $I^{\text{disc}}_{\Delta,\ell}$ is shadow symmetric (*i.e* invariant under $\Delta \to 1-\Delta$) and has poles on the real line at $\Delta \in \mathbb{Z}$ and $\Delta = 2\Delta_{re} + 2k + \ell$ for $k \in \mathbb{N}$ and their shadow. The attentive reader may worry that these partial wave coefficients do not satisfy the unitarity condition $I_{\frac{1}{2}+i\nu,\ell}(-1)^{\ell} \geq 0$ for $\nu \in \mathbb{R}$. The obvious solution is that $I^{\text{disc}}_{\frac{1}{2}+i\nu,\ell}$ is different from the full $I_{\frac{1}{2}+i\nu,\ell}$. Nevertheless, it would be useful to better understand the emergence of the free theory in dS, described in section 4.2, as the limit of an interacting QFT in dS.

Let us go back to (5.11) and use (5.15) to write,

$$\mathcal{G}_{\text{disc}}(z) = \sum_{\ell=0,1} \int_{\frac{1}{2}}^{\frac{1}{2}+i\infty} \frac{d\Delta}{2\pi i} I^{\text{disc}}_{\Delta,\ell} \Psi_{\Delta,\ell}(z) + \sum_{\substack{n\in\mathbb{N} \\ \ell=0,1}} \tilde{I}^{\text{disc}}_{n,\ell} \Psi_{n,\ell}(z) \tag{5.28}$$
$$= \sum_{\ell=0,1} \int_{\frac{1}{2}-i\infty}^{\frac{1}{2}+i\infty} \frac{d\Delta}{2\pi i} I^{\text{disc}}_{\Delta,\ell} K_{1-\Delta,\ell} G_{\Delta,\ell}(z) + \sum_{\substack{n\in\mathbb{N} \\ \ell=0,1}} \tilde{I}^{\text{disc}}_{n,\ell} \Psi_{n,\ell}(z) \, .$$

Now, we can deform the Δ-contour to the right and pick up residues of the poles on the positive real line. The poles at integer Δ precisely cancel the contribution from the discrete series because $\tilde{I}^{\text{disc}}_{n,\ell} = \text{Res}_{\Delta=n} I^{\text{disc}}_{\Delta,\ell}$. We are left with the contribution of the poles at $\Delta = 2\Delta_{re} + 2k + \ell$ for $k \in \mathbb{N}$,

$$\mathcal{G}^{\text{disc}}(z) = |z|^{2\Delta_{re}} = -\sum_{\ell=0,1}\sum_{k=1}^{\infty} \text{Res}_{\Delta=2\Delta_{re}+\ell+2k}(I^{\text{disc}}_{\Delta,\ell}) K_{1-(2\Delta_{re}+\ell+2k),\ell} G_{2\Delta_{re}+\ell+2k,\ell}(z)$$
$$=: \sum_{\ell=0,1}\sum_{k=1}^{\infty} c^2_{\mathcal{O}\mathcal{O}^\dagger[\mathcal{O}^\dagger\mathcal{O}]_{k,\ell}} G_{2\Delta_{re}+\ell+2k,\ell}(z). \tag{5.29}$$

The second line defines OPE coefficients $c^2_{\mathcal{O}\mathcal{O}^\dagger\mathcal{O}^\dagger[\mathcal{O}^\dagger\mathcal{O}]_{k,\ell}}$. The latter must be positive because the double-trace exchanged operators $[\mathcal{O}^\dagger\mathcal{O}]_{k,\ell}$ are hermitian.

(Non)-Convergence

Although the sum (5.29) converges for any external dimension $\Delta_{\mathcal{O}} = \Delta_{re} + i\Delta_{im}$, the integral (5.28) is not always convergent. Let us take a closer look at this issue. We need to study the asymptotic behavior of partial waves Ψ and the associated coefficients I. Using Stirling's approximation,

$$I^{\text{disc}}_{\frac{1}{2}+i\nu,\ell} \underset{\nu\to\infty}{\sim} Q\nu^{4\Delta_{re}-1} , \qquad \tilde{I}^{\text{disc}}_{n,\ell} \underset{n\to\infty}{\sim} \frac{Q}{\pi}(-1)^{\ell+n} n^{4\Delta_{re}-1} , \tag{5.30}$$

where we defined

$$Q \equiv \frac{\Gamma(\frac{1}{2}-\Delta_{re}-i\Delta_{im})\Gamma(\frac{1}{2}-\Delta_{re}+i\Delta_{im})}{2^{4\Delta_{re}-1}\Gamma(\Delta_{re}+i\Delta_{im})\Gamma(\Delta_{re}-i\Delta_{im})} . \tag{5.31}$$

Using (5.15) and the known large Δ behavior of conformal blocks [27, 121],

$$G_{\Delta,\ell}(z) \underset{\Delta\to\infty}{\sim} (-1)^{\ell} \frac{(4\rho)^{\Delta}}{\sqrt{1-\rho^2}} , \tag{5.32}$$

one can find the asymptotic behavior of the partial waves:

$$\Psi_{\frac{1}{2}+i\nu,\ell}(z) \underset{\nu\to\infty}{\sim} 2(-1)^{\ell}\sqrt{\frac{\pi}{\nu}}\frac{(4\rho)^{\frac{1}{2}}}{\sqrt{1-\rho^2}}\cos(x\,\nu-\frac{\pi}{4}) , \tag{5.33}$$

$$\Psi_{n,\ell}(z) \underset{n\to\infty}{\sim} 2\sqrt{\frac{\pi}{n}}\frac{(-1)^{\ell}+(-1)^{n}\cosh(2\pi\Delta_{im})}{\sqrt{1-\rho^2}}\rho^{n} , \tag{5.34}$$

where we used the ρ-coordinate defined as

$$\rho(z) = \frac{z}{\left(\sqrt{1-z}+1\right)^2} , \qquad x = \log(\rho(z)) . \tag{5.35}$$

Finally, the large ν behavior of the integrand in (5.28) is

$$\sim \nu^{4\Delta_{re}-\frac{3}{2}}\cos(x\,\nu-\frac{\pi}{4}) , \tag{5.36}$$

which means the integral is not convergent for $\Delta_{re} > \frac{1}{8}$.[5] On the other hand, the structure is somewhat familiar. This is like the Fourier transform of a monomial and it corresponds to the behaviour $\sim |x|^{\frac{1}{2}-4\Delta_{re}}$ as $x \to 0$. Notice that $x \to 0$ corresponds to $z \to 1$ or equivalently $x_2 \to x_3$, which is the t channel OPE limit. In fact, it is instructive to compute the behavior as $z \to 1$ of each term in (5.28). Using [122, 123]

$$G_{\Delta,\ell}(z) \underset{\Delta\to\infty}{\sim} (-1)^{\ell}4^{\Delta}\sqrt{\frac{\Delta}{\pi}}K_0(2\Delta\sqrt{1-z}) \qquad \text{when} \quad (1-z)^{-\frac{1}{2}} \sim \Delta , \tag{5.37}$$

---

[5] One way to make this integral convergent is to introduce a Gaussian regulator $e^{-\epsilon\nu^2}$ with $\epsilon \to 0$.

we find

$$\int_{\frac{1}{2}}^{\frac{1}{2}+i\infty} \frac{d\Delta}{2\pi i} I^{\text{disc}}_{\Delta,\ell}\Psi_{\Delta,\ell}(z) \underset{z\to1}{\sim} \frac{Q\cos(2\pi\Delta_{re})\Gamma^2(2\Delta_{re})}{2\pi}\frac{(-1)^\ell}{(1-z)^{2\Delta_{re}}} \tag{5.38a}$$

$$\sum_{n\in\mathbb{N}} \tilde{I}^{\text{disc}}_{n,\ell}\Psi_{n,\ell}(z) \underset{z\to1}{\sim} \frac{Q\cosh(2\pi\Delta_{im})\Gamma^2(2\Delta_{re})}{2\pi}\frac{(-1)^\ell}{(1-z)^{2\Delta_{re}}}\,. \tag{5.38b}$$

Although every term diverges as $z \to 1$, the leading singular behavior cancels between the spin 0 and spin 1 contributions. This had to happen because the correlator $\mathcal{G}^{\text{disc}}(z) = |z|^{2\Delta_{re}}$ is regular.

Consider now the u channel OPE limit $z \to \infty$. For the case $\Delta_{im} = 0$, one can easily obtain the the partial waves for negative z using the symmetry:

$$\Psi_{\Delta,\ell}(z) = (-1)^\ell \Psi_{\Delta,\ell}\left(\frac{z}{z-1}\right)\,, \qquad z<0\,. \tag{5.39}$$

This gives

$$\int_{\frac{1}{2}}^{\frac{1}{2}+i\infty} \frac{d\Delta}{2\pi i} I^{\text{disc}}_{\Delta,\ell}\Psi_{\Delta,\ell}(z) \underset{z\to-\infty}{\sim} \frac{Q\cos(2\pi\Delta_{re})\Gamma^2(2\Delta_{re})}{2\pi}(-z)^{2\Delta_{re}} \tag{5.40a}$$

$$\sum_{n\in\mathbb{N}} \tilde{I}^{\text{disc}}_{n,\ell}\Psi_{n,\ell}(z) \underset{z\to-\infty}{\sim} \frac{Q\Gamma^2(2\Delta_{re})}{2\pi}(-z)^{2\Delta_{re}} \tag{5.40b}$$

which means that every term in (5.28) contributes to the leading divergence of $\mathcal{G}^{\text{disc}}(z) = |z|^{2\Delta_{re}}$ as $z \to \infty$. In general, we expect $\mathcal{G}(z) \approx \mathcal{G}^{\text{disc}}(z)$ as $z \to \infty$ because the identity dominates the u channel OPE. Therefore, we expect the full partial wave coefficients $I_{\frac{1}{2}+i\nu,\ell}$ and $\tilde{I}_{n,\ell}$ to scale as in (5.30) for large ν or n.[6]

This argument shows that the integral over the principal series in the partial wave decomposition (5.11) does not converge absolutely. This issue poses an important obstacle to any numerical bootstrap approach. In what follows, we will overcome this obstacle by integrating the crossing equation over z against functions that vanish sufficiently fast at $z = 0$ and $z = 1$.

5.3 Regularized crossing equation

In this section, we want to explore the consequences of the crossing equation (5.2) for the case of a general correlator $\langle \mathcal{O}(x_1)\mathcal{O}^\dagger(x_2)\mathcal{O}(x_3)\mathcal{O}^\dagger(x_4)\rangle$, which is invariant under $x_1 \leftrightarrow x_3$ or $x_2 \leftrightarrow x_4$, which corresponds to the $s-t$ channel. We start with a method to regularized the convergence issue mentioned in the previous section. To do so, we shall use the following linear functional,

---

[6] Note that the precise asymptotic behavior must be different to be compatible with unitarity. Nevertheless, we expect the same asymptotic power law behavior.

$$\omega[f] := \int_0^1 dz\ z^{\gamma}(1-z)^{\sigma} f(z)\ , \tag{5.41}$$

where γ and σ should be large enough.

Since the partial wave coefficient of s-channel and t-channel of the correlator

$$\langle \mathcal{O}(x_1)\mathcal{O}^{\dagger}(x_2)\mathcal{O}(x_3)\mathcal{O}^{\dagger}(x_4)\rangle$$

are the same, the crossing equation will look like[7]

$$\int_0^{\infty} \frac{d\nu}{2\pi} \sum_{\ell=0,1} I^s_{\frac{1}{2}+i\nu,\ell} F^{s-t}_{\frac{1}{2}+i\nu,\ell}(z) + \sum_{\ell=0,1}\sum_{n\in\mathbb{N}} \tilde{I}^s_{n,\ell} F^{s-t}_{n,\ell}(z) = 0\ , \tag{5.43}$$

where we define

$$F^{s-t}_{\Delta,\ell}(z) \equiv (1-z)^{2\Delta_{re}}\Psi_{\Delta,\ell}(z) - z^{2\Delta_{re}}\Psi_{\Delta,\ell}(1-z)\ , \tag{5.44}$$

and used $\Psi^t_{\Delta,\ell}(z) = \Psi^s_{\Delta,\ell}(1-z) = \Psi_{\Delta,\ell}(1-z)$. Acting with the functional ω introduced in (5.41) on this equation and using the identity (A.16), one finds a new form of the crossing equation

$$\int_0^{\infty} \frac{d\nu}{2\pi} \sum_{\ell=0,1} I^s_{\frac{1}{2}+i\nu,\ell} \tilde{F}^{s-t}_{\frac{1}{2}+i\nu,\ell} + \sum_{\ell=0,1}\sum_{n\in\mathbb{N}} \tilde{I}^s_{n,\ell} \tilde{F}^{s-t}_{n,\ell} = 0\ , \tag{5.45}$$

where

$$\begin{aligned} \tilde{F}^{s-t}_{\Delta,\ell} &= (-1)^{\ell} \frac{K^{\Delta_{re}+i\Delta_{im},\Delta_{re}-i\Delta_{im}}_{1-\Delta,\ell}}{\Gamma(\Delta+2\Delta_{re}+\gamma+\sigma+2)} \\ &\quad \times \left[\Gamma(\Delta+\gamma+1)\Gamma(2\Delta_{re}+\sigma+1)\, {}_3F_2\left[\begin{matrix}\Delta+2i\Delta_{im},\Delta-2i\Delta_{im},\Delta+\gamma+1\\ 2\Delta,\Delta+2\Delta_{re}+\gamma+\sigma+2\end{matrix}\ \middle|\ 1\right] - \gamma\leftrightarrow\sigma\right] \\ &\quad +\ \ \Delta\leftrightarrow 1-\Delta\ . \end{aligned} \tag{5.46}$$

---

[7] In case of identical operators, there would be contributions from disconnected parts on the right side:

$$\int_0^{\infty} \frac{d\nu}{2\pi} I_{\frac{1}{2}+i\nu} F_{\frac{1}{2}+i\nu}(z) + \sum_{n\in 2\mathbb{N}} \tilde{I}_n F_n(z) = z^{2\Delta_{\mathcal{O}}} - (1-z)^{2\Delta_{\mathcal{O}}}\ . \tag{5.42}$$

The formula for $\tilde{F}^{s-t}_{n,\ell}$ instead reads

$$\begin{aligned}\tilde{F}^{s-t}_{n,\ell} &= (-1)^\ell \frac{K^{\Delta_{re}+i\Delta_{im},\Delta_{re}-i\Delta_{im}}_{1-n,\ell}}{\Gamma(n+2\Delta_{re}+\gamma+\sigma+2)} \\ &\times \left[\Gamma(n+\gamma+1)\Gamma(2\Delta_{re}+\sigma+1)\,{}_3F_2\left[{n+2i\Delta_{im},n-2i\Delta_{im},n+\gamma+1 \atop 2n,n+2\Delta_{re}+\gamma+\sigma+2}\middle|1\right] - \gamma\leftrightarrow\sigma\right] .\end{aligned} \tag{5.47}$$

The advantage of the functional (5.41) is that we could compute its action on partial waves in terms of the hypergeometric function ${}_3F_2(1)$. In principle another linear function might not lead to an analytical expressions like what we found above.

In appendix A.2, we show that

$$\tilde{F}^{s-t}_{\frac{1}{2}+i\nu,\ell} \underset{\nu\to\infty}{\sim} \nu^{-2-4\Delta_{re}-2\min(\sigma,\gamma)} , \tag{5.48}$$

which together with (5.30) implies that the ν integral in the regularized crossing equation (5.45) is convergent as long as

$$\min(\sigma,\gamma) > -1 . \tag{5.49}$$

Similar crossing equations can be written down for decompositions in the other channels.

5.4 An invitation to the numerical bootstrap

The crossing symmetry plus positivity (from unitarity) lead to bounds on the space on conformal field theories. In this section, following the strategy of the conformal bootstrap, we will show that the same is true for QFT in dS.

Consider for definiteness the $s-t$ crossing equation in (5.43) that is anti-symmetric under exchange of $\gamma \leftrightarrow \sigma$. Therefore, it is sufficient to concentrate on the case $\gamma > \sigma$. In addition, we take external operators to be identical and hermitian with dimension $\Delta_\phi > \frac{1}{2}$. This means we have to reintroduce disconnected terms in (5.43), which amounts to adding a term

$$D(\gamma,\sigma) = \frac{\Gamma(\gamma+1)\Gamma(2\Delta_\phi+\sigma+1) - \Gamma(\sigma+1)\Gamma(2\Delta_\phi+\gamma+1)}{\Gamma(2\Delta_\phi+\gamma+\sigma+2)} \tag{5.50}$$

to (5.45). For identical operators, the parity odd sector ($\ell = 1$) contribution vanishes and we can rewrite a regularized crossing equation (5.45) as follows:

$$\int_0^\infty \frac{d\nu}{2\pi}\, I_{\frac{1}{2}+i\nu,0}\tilde{F}^{s-t}_{\frac{1}{2}+i\nu,0}(\gamma,\sigma) + \sum_{n\in\mathbb{N}} \tilde{I}_{n,0}\tilde{F}^{s-t}_{n,0}(\gamma,\sigma) + D(\gamma,\sigma) = 0 , \tag{5.51}$$

At this point, we can rule out putative theories by applying linear functionals to this equation (5.51). As an example of a putative theory, assume that the spectral density obeys $I_{\frac{d}{2}+i\nu,0}=0$ for $|\nu|<\nu^*$. Now, if one finds a linear functional α satisfying

$$\begin{aligned} \alpha\left[\tilde{F}^{s-t}_{\frac{1}{2}+i\nu,0}(\gamma,\sigma)\right] &> 0\ , &\qquad \text{for all } |\nu|>\nu^*,\\ \alpha\left[\tilde{F}^{s-t}_{n,0}(\gamma,\sigma)\right] &> 0\ , &\qquad \text{for all } n\in\mathbb{N},\\ \alpha\left[D(\gamma,\sigma)\right] &= 1\ , \end{aligned} \tag{5.52}$$

then (5.51) cannot be satisfied by a unitary QFT in dS (since in a unitary QFT we must have $I_{\frac{d}{2}+i\nu,0}\geq 0$ and $\tilde{I}_{n,0}\geq 0$).

One may also find bounds on partial wave coefficients. For example, imagine that one can find a linear functional α obeying the first two positivity conditions of (5.52), but now $\alpha\left[D(\gamma,\sigma)\right]=-1$. Then one obtains an upper bound on every discrete series partial wave coefficient,

$$\tilde{I}_{n,0}\leq\frac{1}{\alpha\left[\tilde{F}^{s-t}_{n,0}(\gamma,\sigma)\right]}\ , \tag{5.53}$$

and this bound can be optimized by maximizing $\alpha\left[\tilde{F}^{s-t}_{n,0}(\gamma,\sigma)\right]$. We leave for the future a systematic implementation using linear programming methods or the semidefinite solver SDPB [124] that we expand a bit for the case of $d=1$ in appendix E.

We conclude this section with a *proof-of-concept* example of a ruled-out theory. Consider equation (5.51) for an external operator of dimension $\Delta_\phi=\frac{1}{2}+\frac{1}{8}$ and let $\gamma=2.1$ and $\sigma=2$. It turns out that $\tilde{F}^{s-t}_{\frac{1}{2}+i\nu,0}(\gamma,\sigma)$ is positive for all $\nu\geq 8.53$ and $\tilde{F}^{s-t}_{n,0}(\gamma,\sigma)$ is also positive for all even $n\in\mathbb{N}$.[8] Imagine a theory with vanishing $I_{\frac{d}{2}+i\nu,0}$ for $\nu<8.53$. Then there is an upper bound on $\tilde{I}_{2,0}$:

$$\tilde{I}_{2,0}<\frac{-D(\gamma=2.1,\sigma=2)}{\tilde{F}^{s-t}_{2,0}(\gamma=2.1,\sigma=2)}\approx 6.43174\ . \tag{5.54}$$

One can improve this bound using linear programming methods. For example, taking linear combinations with a specific set of eight different values of $\{\gamma,\sigma\}$, we found a stronger bound

$$\tilde{I}_{2,0}<\frac{-\alpha\left[D(\gamma,\sigma)\right]}{\alpha\left[\tilde{F}^{s-t}_{2,0}(\gamma,\sigma)\right]}\approx 5.67049\ . \tag{5.55}$$

We hope this simple example convinces the reader that these equations have the potential to put non-trivial bounds on the space of QFTs in dS. Optimistically, with a proper systematic treatment, they are sufficient to identify interesting theories at kinks or islands of the allowed theory space.

---

[8] Note that odd values of n do not contribute for a four point function of identical hermitian operators because $\tilde{F}^{s-t}_{n,0}$ vanishes identically.

6 Conclusion

Albeit its direct connection to the real world, Quantum Field Theory (QFT) in de Sitter (dS) spacetime has remained largely unexplored. $d+1$-dimensional de Sitter (dS$_{d+1}$) is a maximally symmetric spacetime with the conformal group symmetry $SO(d+1,1)$. The correlation functions of local operators, as the main observables of QFT in dS$_{d+1}$ are constraint subject to the mentioned dS isometry group. In particular, the late-time boundary of de Sitter defines a conformal theory in which one can define correlation functions of primary boundary operators that satisfy the same Ward identities as the correlation functions of primary operators in a CFT. Furthermore, the unitarity of the theory in the bulk is highly constraining. All together, these properties of QFT in dS suggest employing the conformal bootstrap methods [28, 27].

In this work, we took the first steps towards a nonperturbative treatment of QFT in rigid dS$_{d+1}$ utilizing the conformal bootstrap ideology. The main toolbox is the Hilbert space decomposition derived from the first principles in 2. The identity operator can be decomposed into the unitary irreducible representations of dS isometry group $SO(d+1,1)$. In chapter 3, we make use of the resolution of identity in (2.118) to recover the Källén–Lehmann decomposition of the *bulk two-point function* with a positive spectral density. The spectral density carries information about the bulk-boundary expansion spelled out in 3.2. In sections 3.3 and 3.4, we find two equivalent *inversion formulas* for spectral density by analytic continuation from the sphere and Euclidean Anti-de Sitter spaces. Through these inversion formulas, one can find the spectral density of theory such as free field and bulk CFT and explore their boundary operator content – section 3.5.

The dS boundary four-point functions admit a partial wave expansion. The coefficients of this expansion I satisfy positivity conditions due to the unitarity of the bulk theory. This has been shown in section 4.1. We illustrate the concept of Is by explicitly calculating them in Generalized Free Field theory and to the first order of perturbation theory for $\lambda\phi^4$ interaction. Along the way, it turns out that the local terms are unavoidable for a unitary

Mean Field Theory. Finally, we focus on two-dimensional de Sitter spacetime and find non-trivial bounds for partial wave coefficients in a particular setting as a *proof-of-concept*.

Our work, as a new approach, leaves many open questions for the future. Let us list some of them:

- The **Hilbert space** of a QFT in dS_{d+1} must decompose in unitary irreducible representations of $SO(d+1,1)$. Although these are studied and classified in a formal way in the past, a more straightforward and more intuition-friendly group theoretical treatment is lacking. There are two concrete cases where this question can certainly be answered using group theory. The first is CFT in dS where one should be able to decompose conformal multiplets of $SO(d+1,2)$ into irreps of $SO(d+1,1)$, as we illustrated in appendix D for the case of dS_2. The second is free QFT in dS where one should be able to decompose the Fock space into irreps of $SO(d+1,1)$. In this case, it would also be interesting to study the effect of perturbative interactions on the structure of the Hilbert space. We investigate these in a simple group theoretical approach using Harish-Chandra characters that we hope to report on soon [81].
- What is the set of **boundary operators** present in a generic interacting QFT in dS? For CFT in dS, we saw that all boundary operators are hermitian with real scaling dimension Δ. On the other hand, a (sufficiently) massive free scalar in dS gives rise to a pair of hermitian conjugate boundary operators of dimension $\Delta = \frac{d}{2} \pm i\mu$ with $\mu \in \mathbb{R}$. How do these two special cases change under continuous deformations of the QFT? In practice, we can study deformations of the CFT by relevant bulk operators and of the free theory by turning on interactions.[1]
- The generalization of the **Källén-Lehmann** decomposition of the bulk two-point functions for local operators with spin would be very helpful to shed light on the two previous questions. We are planning to report on this soon.
- We introduced **regularised crossing equations** to ameliorate the convergence properties of the integral over the continuous label ν of principal series irreps. It is important to develop a more systematic approach to this issue. In particular, we did not address the case of higher dimensions $d > 1$.
- Pragmatically, the main open task is to set up a **numerical conformal bootstrap** approach to the crossing equations for boundary four-point functions of QFT in dS. We gave a proof of principle by deriving a bound in a toy example but it is important to develop a systematic algorithm. To use SDPB [124] we will need

---

[1] One intriguing feature of the free limit of an interacting QFT is the appearance of local terms in the two-point function of boundary operators $\langle \mathcal{O}\mathcal{O}^\dagger \rangle$ when $\Delta_{\mathcal{O}} = \frac{d}{2} + i\mu$. This seems to be a discontinuous effect because conformal symmetry forces $\langle \mathcal{O}\mathcal{O}^\dagger \rangle = 0$ as long as real part of the scaling dimension $\Re\Delta_{\mathcal{O}} \neq \frac{d}{2}$ and we expect $0 < \Re\Delta_{\mathcal{O}} - \frac{d}{2} \ll 1$ for a weakly coupled massive scalar field in dS.

to devise a polynomial approximation to the partial waves (or their regularized version). We initiated this for the case of $d = 1$ in appendix E.

- There is an alternative approach based on **6j symbols** that does not use conformal partial waves. For simplicity let us focus on the first equation in (5.2). Integrating both sides over all points x_i against $\Psi^t_{\Delta,\ell}(x_i)$ and using orthogonality of partial waves, we find

$$I^t_{\Delta,\ell} = \frac{1}{n_{\Delta,\ell}} \sum_{\ell'} \int \frac{d\Delta'}{2\pi i} \, I^s_{\Delta',\ell'} \, \mathcal{J}_d(\tilde{\Delta}', \ell', \tilde{\Delta}, \ell | \tilde{\Delta}_1, \tilde{\Delta}_2, \tilde{\Delta}_3, \tilde{\Delta}_4) + \mathcal{D}^{st}_{\Delta,\ell} \, , \tag{6.1a}$$

$$\mathcal{D}^{st}_{\Delta,\ell} \equiv \frac{1}{n_{\Delta,\ell}} \int \frac{d^d x_1 \cdots d^d x_4}{\text{vol}(SO(d+1,1))} \left(D^s_{\Delta_i}(x_i) - D^t_{\Delta_i}(x_i) \right) \Psi^{t,\tilde{\Delta}_i}_{\Delta,\ell}(x_i) \, , \tag{6.1b}$$

  where we used the notation of [125] for the $6j$ symbol $\mathcal{J}_d$. The disconnected contribution $\mathcal{D}^{st}_{\Delta,\ell}$ can be computed in a similar fashion to the MFT partial wave coefficients in (4.25) [67]. For the simple case $\langle \mathcal{O}\mathcal{O}^\dagger \mathcal{O}\mathcal{O}^\dagger \rangle$ discussed in (5.5), there is no s or t channel disconnect contribution and $I^s = I^t$. Therefore, equation (6.1a) says that I^s is invariant under convolution with the $6j$ symbol. It would be interesting to explore this constraint together with positivity of I^s.

- What are the **interesting questions** about QFT in dS? In standard CFT, the basic CFT data are scaling dimensions and OPE coefficients and most bootstrap studies derive bounds on these quantities. For QFT in dS, partial wave coefficients $I_{\Delta,\ell}$ play a similar role to OPE coefficients in CFT. However, the former include a set of non-negative functions of the continuous label ν of principal series irreps. What type of bounds should we aim for such functions? It would be useful to develop more intuition from perturbative computations. Ideally, we would like to find questions that can isolate some physical theory inside an island of the allowed space of QFTs.

- It would be interesting to understand the **flat space limit** of dS correlators [126, 23]. Perhaps there is a limiting procedure that takes dS partial wave coefficients $I_{\Delta,\ell}$ into flat space partial amplitudes $f_\ell(s)$, where the square of the center of mass energy $s \sim \nu^2/R^2$. This is similar to known formulas for AdS [127–131, 38, 132, 133].

- The consequences of **perturbative unitarity** are currently being investigated in a program known as the *cosmological bootstrap* [23, 25, 134, 20]. Is it possible to make contact between our work and the perturbative cosmological bootstrap? Perhaps recent advances concerning cutting rules in (A)dS [135–137] can play a role here.

- **Massless fields** in dS are known to give rise to infrared divergences in perturbation theory [138–141]. Recently, the authors of [26] claimed to have resolved this issue. It would be interesting to analyse this problem within our non-perturbative approach.

- Can **quantum gravity** in dS be studied with our conformal bootstrap approach? In the case of AdS, there is a rather systematic way to go from QFT to quantum gravity. In fact, the conformal bootstrap equations for the boundary correlators are unchanged. The sole effect of quantum gravity in the bulk is the appearance of new boundary operator: the stress tensor. The stress tensor is a special operator because its correlation functions are constrained by Ward identities. It is tempting to imitate this strategy in dS. As a first step, one should study a bulk massless spin 2 field and analyse the correlators of its associated boundary operators. It would also be very interesting to compare this approach to previous proposals for a dS/CFT correspondence [142–144].

Part III

Hamitonian truncation in Anti-de Sitter spacetime

7 Set up of Hamiltonian truncation in AdS$_2$

As promised, we will study QFTs defined in the bulk of $(d+1)$-dimensional Euclidean AdS spacetime, specializing to $d = 1$. We will drop the word "Euclidean" from now on for convenience and simply use AdS. The generalization to higher d is relatively straightforward, but will not be necessary in the rest of this work. For other studies of QFT in AdS see *e.g.* [145–152]. In this section, we review some basic facts about the correspondence between bulk (non-gravitational) AdS physics and the conformal theory that lives on the boundary of AdS. For a more extensive pedagogical treatment, we refer for instance to [153] and [50].

7.1 Geometry

Euclidean AdS$_2$ with radius R can be defined as a hyperboloid

$$-(X^0)^2 + (X^1)^2 + (X^2)^2 = -R^2 \ , \qquad X^0 > 0 \tag{7.1}$$

inside $\mathbb{R}^{1,2}$, which we will endow with global coordinates $\tau \in \mathbb{R}$ and $r \in [-\tfrac{1}{2}\pi, \tfrac{1}{2}\pi]$ via

$$X^\mu(\tau, r) = \frac{R}{\cos r}\,(\cosh\tau, \sinh\tau, \sin r)\,. \tag{7.2}$$

The coordinate τ (resp. r) plays the role of a Euclidean time (resp. a space) coordinate. In the above coordinates, the AdS metric is given by

$$ds^2 = \left(\frac{R}{\cos r}\right)^2 \left[d\tau^2 + dr^2\right]. \tag{7.3}$$

The conformal boundary of AdS$_2$ is the union of the two lines $r = \pm\tfrac{1}{2}\pi$.

It follows from the definition (7.1) that AdS$_2$ is manifestly invariant under a group

$SO(1,2) \sim SL(2,\mathbb{R})$ of continuous isometries. The corresponding Lie algebra is described by three generators $\{H, P, K\}$ with commutators

$$[H,P] = P, \quad [H,K] = -K, \quad [P,K] = -2H. \tag{7.4}$$

The generators act on local scalar bulk operators as

$$[G, \mathcal{O}(\tau,r)] = \mathcal{D}_G \cdot \mathcal{O}(\tau,r) \tag{7.5}$$

where

$$\mathcal{D}_H = \partial_\tau, \tag{7.6a}$$

$$\mathcal{D}_P = e^{-\tau}(\sin r\,\partial_\tau + \cos r\,\partial_r), \tag{7.6b}$$

$$\mathcal{D}_K = e^{\tau}(\sin r\,\partial_\tau - \cos r\,\partial_r). \tag{7.6c}$$

In addition, there is a parity symmetry $\mathtt{P}$ (with $\mathtt{P}^2 = 1$) that maps $r \mapsto -r$. Under parity, the generators transform as

$$\mathtt{P}\begin{pmatrix} H \\ P \\ K \end{pmatrix}\mathtt{P}^{-1} = \begin{pmatrix} +H \\ -P \\ -K \end{pmatrix}. \tag{7.7}$$

The symmetries of AdS put strong constraints on correlation functions of bulk operators. For instance, any one-point correlation function $\langle \mathcal{O}_i(\tau,r)\rangle = \langle\Omega\rangle\, \mathcal{O}_i(\tau,r)\Omega$ in the vacuum state $|\Omega\rangle$ must be constant.[1] Vacuum two point correlation functions of scalar bulk operators — at say (τ,r) and (τ',r') — only depend on a single $SO(1,2)$ invariant

$$\xi = \frac{(X^\mu(\tau,r) - X^\mu(\tau',r'))^2}{4R^2} = \frac{\cosh(\tau-\tau') - \cos(r-r')}{2\cos r\cos r'} \geq 0. \tag{7.8}$$

Vacuum higher-point correlators or correlators inside excited states depend on a larger number of $SL(2,\mathbb{R})$ invariants.

7.2 The Hilbert space and the bulk-to-boundary OPE

The Hilbert space of a QFT in AdS$_2$ decomposes into multiplets of the isometry group $SL(2,\mathbb{R})$. Such a multiplet is defined by a primary state $|\psi_i\rangle$, satisfying $H|\psi_i\rangle = \Delta_i|\psi_i\rangle$ and $K|\psi_i\rangle = 0$. In a unitary QFT, all primary states must have $\Delta_i \geq 0$. Associated to any primary state with $\Delta_i > 0$ are infinitely many descendant states of the form

$$|\psi_i, n\rangle := \frac{1}{\sqrt{n!(2\Delta_i)_n}} P^n|\psi_i\rangle, \quad n = 0,1,2,\ldots \tag{7.9}$$

---

[1] By assumption, the vacuum state $|\Omega\rangle$ is annihilated by all $SL(2,\mathbb{R})$ generators.

identifying $|\psi_i, 0\rangle = |\psi_i\rangle$, and writing $(x)_n = \Gamma(x+n)/\Gamma(x)$ for the Pochhammer symbol. The normalization in (7.9) is chosen such that the descendant states are unit-normalized, as long as the primary state $|\psi_i\rangle$ is unit-normalized as well. The state $|\psi_i, n\rangle$ has energy $\Delta_i + n$, and the generators K and P act as

$$K\,|\psi_i, n\rangle = \gamma(\Delta_i, n)\,|\psi_i, n-1\rangle \quad \text{and} \quad P\,|\psi_i, n\rangle = \gamma(\Delta_i, n+1)\,|\psi_i, n+1\rangle \tag{7.10}$$

using the shorthand notation $\gamma(\Delta, n) := \sqrt{n(2\Delta + n - 1)}$. In addition, there is a unique vacuum state $|\Omega\rangle$ without descendants that is annihilated by all $SL(2,\mathbb{R})$ generators, so in particular it has $\Delta_\Omega = 0$. Moreover, if the theory is invariant under parity, all primary states have a definite parity, meaning that $\mathtt{P}\,|\psi_i\rangle = \pi_i\,|\psi_i\rangle$ with $\pi_i = \pm 1$. Then from (7.7) it follows that descendant states transform as

$$\mathtt{P}\,|\psi_i, n\rangle = (-1)^n \pi_i\,|\psi_i, n\rangle\,. \tag{7.11}$$

In a QFT in AdS, one can define boundary operators as (rescaled) limits of local bulk operators pushed to the conformal boundary of AdS. According to the bulk state – boundary operator map [38], any primary state $|\psi_i\rangle$ corresponds to a boundary primary operator $\mathcal{O}_i$ with dimension Δ_i, according to the rule

$$|\psi_i\rangle = \lim_{\tau \to -\infty} e^{-\Delta_i \tau} \mathcal{O}_i(\tau)\,|\Omega\rangle\,. \tag{7.12}$$

Often, we will therefore use the notation $|\mathcal{O}_i\rangle$ for boundary states instead of $|\psi_i\rangle$. Likewise, descendant states $|\psi_i, n\rangle$ can be obtained from boundary descendants $[P, \cdots [P, \mathcal{O}_i(\tau)] \cdots]$. Sometimes the operator picture will be useful, but we will not always explicitly identify the local operators that generate specific states. For instance, a simple-looking state in the Fock space of a massive boson could originate from a complicated-looking boundary operator, and vice versa.

In turn, the state-operator map implies that any bulk operator can be expanded in a basis of boundary scaling operators, placed at an arbitrary point in AdS. For instance, one can replace a bulk operator $\mathcal{V}(\tau, r)$ with its bulk-to-boundary operator product expansion (OPE) at the $r = \pi/2$ boundary:

$$\mathcal{V}(\tau, r) = \sum_i b_i \left(\frac{\pi}{2} - r\right)^{\Delta_i} [\mathcal{O}_i(\tau) + \text{descendants}] \tag{7.13}$$

where the sum runs over all primary operators $\mathcal{O}_i$ and the b_i are so-called bulk-to-boundary OPE coefficients. As we will see shortly, the low-lying operators in the bulk-to-boundary OPE of the deforming operator in eq. (5) are important in establishing the UV completeness of the resulting interacting QFT.

In particular, all the examples treated in sections 9 and 10 belong to a special class of

QFTs in AdS: the Hilbert space of the undeformed theory has a gap larger than one above the vacuum. In equations:

$$\Delta_i > 1 \ , \quad \forall \ |\psi_i\rangle \neq |\Omega\rangle \ . \tag{7.14}$$

The absence of relevant deformations on the boundary removes the necessity of fine tuning. Together with the absence of bulk UV divergences, which are the same as in flat space, this condition ensures that the action (5) is well-defined without the addition of counterterms, in a neighborhood of $\lambda = 0$.[2] Concretely, we shall point out at various points in the next subsection and in section 8 where this condition is important.

7.3 The interacting Hamiltonian

Suppose that we're given an exactly solvable QFT in AdS$_2$; denote its Euclidean action by S_0. This can for instance be a two-dimensional rational BCFT, or a theory of free massive bosons and/or fermions.[3] We can then turn on a relevant interaction, by shifting

$$S_0 \mapsto S = S_0 + \lambda \int_{\text{AdS}_2} \sqrt{g} d^2x \, \mathcal{V}(x) \tag{7.15}$$

where $\mathcal{V}(x)$ is a bulk operator to which we can assign a scaling dimension $\Delta_{\mathcal{V}} < 2$.[4] The generalization to multiple relevant operators $\mathcal{V}_i$ is straightforward, but won't be discussed explicitly here. In the Hamiltonian picture, this translates to

$$H_0 \mapsto H = H_0 + \bar{\lambda} V, \qquad V := R^{\Delta_{\mathcal{V}}} \int_{-\pi/2}^{\pi/2} \frac{dr}{(\cos r)^2} \, \mathcal{V}(\tau = 0, r) \tag{7.16}$$

writing $\bar{\lambda} := \lambda R^{2-\Delta_{\mathcal{V}}}$. The factor of $R^{\Delta_{\mathcal{V}}}$ is absorbed into V in order to make the matrix elements of V dimensionless.

We would like to study the spectrum and eigenstates of H by diagonalizing it inside the Hilbert space from section 7.2. Before we do so, let us first remark that the Hamiltonian H from eq. (7.16) is not necessarily well-defined, since V may not exist. A sufficient condition for V to be well-defined is that $\mathcal{V}(\tau, r)$ vanishes sufficiently fast near the boundary. In particular, we require that

$$\lim_{r \to \pm\pi/2} \frac{1}{\cos r} \, \mathcal{V}(\tau = 0, r) = 0 \tag{7.17}$$

---

[2] Non-perturbatively, the scaling dimension may be pushed down to $\Delta = 1$ at some value $\bar{\lambda}^*$. In this case the boundary condition becomes unstable and generically the theory cannot be defined beyond this value. In chapters 9 and 10 we shall see that this phenomenon is generic. Further discussion can be found in section 7.5 and section 11.

[3] See for example appendix A of [149] for a discussion of general free fields in AdS$_{d+1}$.

[4] In the $2d$ Landau-Ginzburg theory of a scalar ϕ, all polynomial operators $\mathcal{V} = \phi^p$ have $\Delta_{\mathcal{V}} = 0$.

inside any normalizable state. This means that the bulk-to-boundary OPE (7.13) of $\mathcal{V}$ should not contain operators with $\Delta_i \leq 1$. If this condition is *not* satisfied, an IR regulator needs to be introduced and boundary counterterms corresponding to the offending operators must be added to H. In particular, we require that the bulk one-point function $\langle\mathcal{V}\rangle$, which corresponds to the identity on the r.h.s. of eq. (7.13), vanishes.[5] From the point of view of the boundary, the condition (7.14) corresponds to the fine tuning of relevant operators at leading order in $\bar{\lambda}$. Therefore, it is not surprising that it may not be sufficient for the theory to be well defined at finite $\bar{\lambda}$. Nevertheless, (7.17) is special from the point of view of Hamiltonian truncation, since it ensures that the matrix elements of V are finite. Notice also that it is special to AdS: for instance, it does not appear when one attempts to study renormalization group (RG) flows on the strip $\mathbb{R} \times [0, \pi]$ using the Truncated Conformal Space Approach (TCSA) [154]. Although we will focus on theories which do not require an IR cutoff owing to the condition (7.14), we will nevertheless introduce an IR cutoff ϵ in certain arguments in chapter 8.

Even after ensuring that all the individual matrix elements of V are well-defined, the operator H may not be diagonalizable due to the presence of high-energy states in the UV theory. This is a familiar problem in Hamiltonian truncation: for instance, it is well-known in TCSA on $\mathbb{R} \times S^d$ that any perturbation with $\Delta_{\mathcal{V}} \geq \frac{1}{2}(d+1)$ leads to a divergent cosmological constant [40]. As we mentioned, this is not surprising, since UV-completeness in perturbation theory may require fine tuning at all orders in the coupling. However, it turns out that *any* AdS$_2$ theory suffers from this problem, regardless of the unperturbed theory S_0 or the pertubation $\mathcal{V}$. We shall address this issue in detail in chapter 8.

In actual Hamiltonian truncation computations, one diagonalizes the Hamiltonian (7.16) inside a subspace of the full Hilbert space. Typically, one fixes a UV cutoff Λ and keeps all states with energy smaller than Λ in the $\lambda = 0$ theory. Let us make this procedure explicit by introducing some notation. In the Hilbert space, the action of the operator V can be represented by a matrix $\mathbf{V}$, namely:

$$V\,|\psi_i, n\rangle = \sum_j \sum_{m=0}^{\infty} \mathbf{V}^{j;m}{}_{i;n}\,|\psi_j, m\rangle\,. \tag{7.18}$$

In turn, the matrix elements of $\mathbf{V}$ can be computed by integrating wavefunctions over timeslices:

$$\mathbf{V}^{j;m}{}_{i;n} = R^{\Delta_{\mathcal{V}}} \int_{-\pi/2}^{\pi/2} \frac{dr}{(\cos r)^2}\,\langle\psi_j, m|\mathcal{V}(0,r)|\psi_i, n\rangle. \tag{7.19}$$

Such integrals always exist, owing to the condition (7.17). Consequently, the operator H

---

[5] In fact, removing the identity operator does not require the introduction of an explicit IR cutoff. Since $\langle\mathcal{V}(0,r)\rangle$ does not depend on r, one can simply replace $\mathcal{V} \to \mathcal{V} - \langle\mathcal{V}\rangle$, which is equivalent to adding a cosmological constant counterterm to S.

acts as

$$H\,|\psi_i, n\rangle = (\Delta_i + n)\,|\psi_i, n\rangle + \bar{\lambda}\sum_j \sum_{m=0}^{\infty} \mathbf{V}^{j;m}{}_{i;n}\,|\psi_j, m\rangle\,. \tag{7.20}$$

In Hamiltonian truncation, one defines a truncated Hamiltonian $H(\Lambda)$ simply starting from (7.20) by discarding all states with energy strictly larger than Λ.

Due to the $SL(2,\mathbb{R})$ symmetry of the theory, matrix elements with different m, n are linearly related — see *e.g.* Ref. [45] for a discussion of this phenomenon in AdS$_3$. The resulting constraints on the matrix elements are discussed in appendix F.

Finally, let us comment on the choice of basis of the Hilbert space. In a unitary QFT, it is always possible to organize the states such that the primaries are orthonormal, that is to say $\langle\psi_i|\psi_j\rangle = \delta_{ij}$ for all i, j. This convention is assumed above in (7.18) and (7.19). In practice, it is not necessary to organize the Hilbert space in terms of primaries and descendants, let alone to impose an orthonormality condition between different primaries of the same dimension Δ. Working in a completely general basis of states $|\varphi_i\rangle$, the eigenvalue equation $H\,|\Psi\rangle = \mathcal{E}\,|\Psi\rangle$ can be recast as

$$H_{ij}\,\beta^j = \mathcal{E}\,G_{ij}\,\beta^j, \quad |\Psi\rangle = \beta^i\,|\varphi_i\rangle \tag{7.21}$$

where $H_{ij} = \langle\varphi_i\rangle\,H\varphi_j$ and $G_{ij} = \langle\varphi_i|\varphi_j\rangle$ are Hermitian; the matrix G is known as the Gram matrix corresponding to the basis $|\varphi_i\rangle$. The energies $\mathcal{E}$ and eigenstates $|\Psi\rangle$ of H are physical (up to a choice of normalization of $|\Psi\rangle$), although the coefficients β^i are basis-dependent. This is particularly important when the unperturbed theory is non-unitary, in which case the Gram matrix is not positive definite, and there exists no orthonormal basis of states. We will encounter a non-unitary QFT in the form of the Lee-Yang model, discussed in section 10.2.

7.4 The energy spectrum

Let $\Delta_i(\bar{\lambda})$ be the eigenvalues of the AdS Hamiltonian. The dimensionless coupling appearing in the Hamiltonian is $\bar{\lambda} = \lambda R^{2-\Delta_\mathcal{V}}$ so in the limit $R \to 0$ the interaction vanishes and $\Delta_i(0)$ is the dimension of the i-th state in the non-interacting theory. At small radius we can write

$$\Delta_i(\bar{\lambda}) = \Delta_i(0) + \omega_{i,1}\bar{\lambda} + \omega_{i,2}\bar{\lambda}^2 + \ldots \tag{7.22}$$

for some coefficients $\omega_{i,n}$ that can be determined through Rayleigh-Schrödinger perturbation theory (or alternatively, using Witten diagrams). In the presence of multiple relevant interactions, Eq. (7.22) is modified in a straightforward way. Depending on the UV theory and the perturbation in question, the perturbative expansion (7.22) can be asymptotic, or it can have a finite radius of convergence. Crucially, every level $\Delta_i(\bar{\lambda})$ corresponding to an $SL(2,\mathbb{R})$ primary is accompanied by an infinite tower of descendants with energies $\Delta_i(\bar{\lambda})+\mathbb{N}$.

When AdS has a large radius, it is expected to approximate flat-space physics. In this work, we are interested in *massive* flows, where at low energies the Hamiltonian H describes a theory of particles with masses $m_i > 0$. We then have

$$\Delta_i(\bar{\lambda}) \underset{\bar{\lambda}\to\infty}{\sim} m_i R = \kappa_i \bar{R}\ , \tag{7.23}$$

for the lightest primary states, corresponding to single-particle states in the flat space limit. In eq. (7.23), we defined the radius of AdS in units of the coupling:[6]

$$\bar{R} := |\lambda|^{1/(d+1-\Delta_{\mathcal{V}})} R = |\bar{\lambda}|^{1/(d+1-\Delta_{\mathcal{V}})}. \tag{7.24}$$

A simple way to derive the linear growth in eq. (7.23) is by noticing that a rescaling $(\tau, r) \to (\tau, r)/R$ is needed to obtain the flat space metric from eq. (7.3) in the $R \to \infty$ limit. The dimensionless coefficients $\kappa_i > 0$ can in general only be determined non-perturbatively. More generally, the eigenvalues Δ_i will grow like $E_i R$ when $R \to \infty$, with E_i the center of mass energy of the corresponding state in the flat space limit.

In figure 7.1 we have drawn a schematic plot of the first few energies of an AdS Hamiltonian as a function of R. Notice that the structure of $SL(2,\mathbb{R})$ multiplets implies the existence of many level crossings. These must occur whenever two primary states asymptote to states of different (center of mass) energy in the flat space limit $R \to \infty$. This is surprising because the interaction V has non-zero matrix elements between different (undeformed) $SL(2,\mathbb{R})$ multiplets and generic Hamiltonians show level repulsion. In fact, this is what we see at finite truncation Λ, since the cutoff breaks the $SL(2,\mathbb{R})$ symmetry. As we shall see, exact level crossing only happens in the limit $\Lambda \to \infty$.

Alternatively, it is possible to flow to a massless theory at large radius. In that case, the levels Δ_i will have a finite limit as $R \to \infty$, coinciding with the spectrum of a specific boundary CFT. Such RG flows will not be encountered in the present work, hence we will not discuss this case in more detail.

7.5 Spontaneous symmetry breaking

In flat space and infinite volume, QFTs may spontaneously break symmetries. It is natural to ask if the same can happen in AdS. The answer is not obvious because AdS spatial slices of constant τ have infinite volume but behave like a box of finite volume, in the sense that they give rise to a discrete energy spectrum. In addition, one may entertain the possibility that a symmetry may be spontaneously broken inside a finite region of

---

[6] The notation $\bar{R}$ becomes ambiguous when there is more than one coupling, but this will not play a role in the present work.

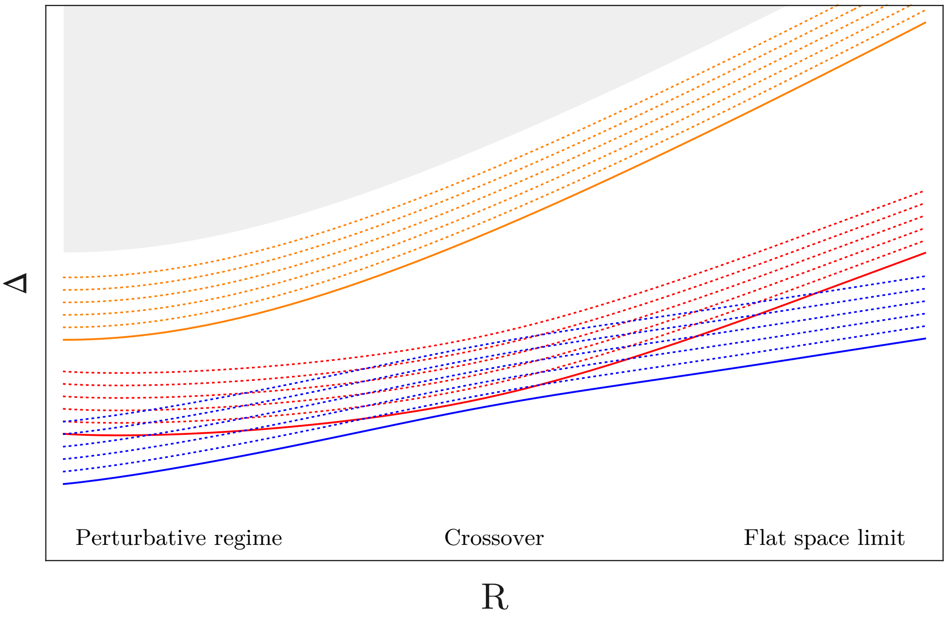

Figure 7.1: Sketch of the spectrum of the AdS Hamiltonian as a function of the AdS radius R. The solid lines describe different primary states, and for every primary we have drawn its five lowest descendants (dotted). Additional states at higher energies are not shown (shaded region). The slope of the lines on the right side of the plot measures the masses of different particles in flat space.

AdS and restored near the boundary due to the effect of symmetry-preserving boundary conditions.

In [147], the phases of the $O(N)$ model in AdS where studied at large N. The effective potential was found to allow for symmetry preserving and symmetry breaking vacua, both stable under small fluctuations of the fields. Expanding the fields around the two vacua, the properties of the two phases where studied, but the existence of a phase transition and the possibility of phase coexistence were not clarified.

In order to address these questions, in appendix J.1, we consider the following simple model of a scalar field in AdS with Euclidean action

$$S = \int d^{d+1}x\sqrt{g}\left[\frac{1}{2}(\partial\phi)^2 + V(\phi)\right] , \tag{7.25}$$

where $V(0) = 0$ and $V(-\phi) = V(\phi)$ is $\mathbb{Z}_2$ symmetric. Furthermore, we impose symmetry-preserving boundary conditions $\phi \to 0$ at the AdS boundary. The global minimum of $V(\phi)$ is attained at $\phi = \phi_t \neq 0$ in order to favour spontaneous symmetry breaking.

We claim that there are only two possibilities:

1. The global minimum of the action is zero and it is attained by the constant solution

$\phi = 0$.

2. The action is not bounded from below and its value can always be decreased further by setting $\phi = \phi_t$ in a bigger region of AdS.

The main consequence of this claim is that there is no choice of potential $V(\phi)$ for which the Euclidean path integral is dominated by a finite size bubble of the true vacuum surrounded by a region of false vacuum close to the boundary of AdS. Notice that this scenario would conflict with the homogeneous property of AdS. Indeed, if we could decrease the action with a finite size bubble then we would decrease the action further with several of them placed far apart. But merging bubbles of true vacuum decreases the action further and we fall into case **2.**.

In flat Euclidean space only **2.** is possible, except if $\phi = 0$ is the global minimum of $V(\phi)$. This is obvious because a large bubble of true vacuum gives a negative contribution to the action (from the potential term) proportional to the volume of the bubble and a positive contribution (from the kinetic term) proportional to the surface area of the bubble. However, in AdS, area and volume both grow exponentially with the geodesic radius and it is not obvious which term dominates. In appendix J.1 we will use the thin wall approximation to get some intuition for the claim above. We present a more general argument in appendix J.1. A quantitative conclusion of the argument presented there is that, at least at the classical level, the symmetry preserving vacuum is unstable if $V''(0) < -d^2/4$. We recognize this as the Breitenlohner-Freedman bound [155].

The analysis of this simple model suggest that spontaneous symmetry breaking can happen for QFT in AdS. Moreover, when it happens, it is very similar to infinite volume flat space time. The main novelty is that symmetry preserving AdS boundary conditions can make some stationary points of the potential fully stable even if they are not its global minimum. However, if these vacua become unstable, then the true vacua correspond to field configurations that break the symmetry all the way to the AdS boundary. Moreover, as in flat space, they give rise to superselection sectors.

In this thesis, we shall study the theory of a scalar field with a quartic potential in section 9.2. The considerations presented above suggest that the theory in AdS has two phases, where the $\mathbb{Z}_2$ symmetry is respectively preserved or broken. While in the flat space limit the phase transition is continuous, we do not expect this to be the case at finite R, since, as discussed, the $\mathbb{Z}_2$ preserving boundary conditions may stabilize the theory for a negative value of the mass square mass. Although studying the symmetry breaking line will prove difficult in Hamiltonian truncation, we shall offer some more comments in section 9.2.

8 How to tame divergences

The computation of the spectrum of the interacting theory via Hamiltonian truncation is straightforward in principle. The Hamiltonian of the exactly solvable theory induces a grading of the Hilbert space, which is labeled by the discrete set of energies e_i. We can truncate the Hilbert space to the finite-dimensional space of states with energies $e_i \leq \Lambda$, and diagonalize the interacting Hamiltonian (6) in this subspace. As the cutoff is raised, one expects to approximate the exact spectrum of the interacting energies with increasing accuracy.

However, a naive implementation of this procedure for any theory in AdS_2 runs into trouble: the vacuum energy $\mathcal{E}_{\text{vac}}(\Lambda)$, as well as the rest of the spectrum $\mathcal{E}_i(\Lambda)$, diverge in the $\Lambda \to \infty$ limit. Let us remark that these divergences do not arise from short-distance singularities in the bulk. Rather, they are related to the non-compact nature of space. Due to the UV-IR connection familiar from the AdS/CFT correspondence, in Hamiltonian truncation the same divergences originate from the high-energy tail of the unperturbed spectrum.

As a matter of principle, it is possible to subtract $\mathcal{E}_{\text{vac}}(\Lambda)$ from the Hamiltonian (adding a cutoff-dependent counterterm proportional to the identity operator), which amounts to measuring energy gaps $\mathcal{E}_i(\Lambda) - \mathcal{E}_{\text{vac}}(\Lambda)$. Surprisingly, these gaps display a systematic shift away from their physical values: they oscillate and fail to converge to a definite value in the $\Lambda \to \infty$ limit — see figure 8.3. Instead, we claim that the exact physical energy spectrum is recovered by means of the following prescription:

$$\boxed{\mathcal{E}_i - \mathcal{E}_{\text{vac}} = \lim_{\Lambda \to \infty} \mathcal{E}_i(\Lambda + e_i) - \mathcal{E}_{\text{vac}}(\Lambda)\ .} \tag{8.1}$$

The aim of this chapter is to illustrate the origin of the divergences, describe their nature in Rayleigh-Schrödinger perturbation theory, and give an argument for the validity of the simple prescription (8.1) to all orders. The examples in chapters 9 and 10 provide further evidence to our claim.

8.1 An example

To get some intuition for the prescription (8.1), let us start with an example where we know the exact spectrum of the Hamiltonian. Consider the case where H_0 describes a free scalar ϕ of mass m in AdS$_2$. The field ϕ admits the following mode expansion

$$\phi(\tau=0,r)=\sum_{n=0}^{\infty} f_n(r)\left(a_n^\dagger + a_n\right) \ . \tag{8.2}$$

The functions $f_n(r)$ are given explicitly in eq. (9.4), but their form will not be important here. The creation and annihilation operators satisfy the usual commutation relations $\left[a_n, a_m^\dagger\right] = \delta_{nm}$. The Hilbert space of the theory is the Fock space generated by acting with creation operators on the vacuum $|\Omega\rangle$. In this basis, the non-interacting normal-ordered Hamiltonian reads

$$H_0=\sum_{n=0}^{\infty}(\Delta+n)a_n^\dagger a_n \,, \tag{8.3}$$

where Δ is related to the mass m of the scalar field via $\Delta(\Delta-1)=m^2R^2$.

We will study the following Hamiltonian:

$$H = H_0 + \bar{\lambda}\, V \tag{8.4}$$

where $\bar{\lambda}=\lambda R^2$ and

$$V=\int_{-\pi/2}^{\pi/2}\frac{dr}{(\cos r)^2} :\phi^2(\tau=0,r): \ . \tag{8.5}$$

The new Hamiltonian H describes a free massive scalar with mass squared $m^2+2\lambda$. Therefore, its spectrum is the same as H_0 if we replace Δ by

$$\Delta(\bar{\lambda})=\frac{1}{2}+\sqrt{\left(\Delta-\frac{1}{2}\right)^2+2\bar{\lambda}}=\Delta+\frac{\bar{\lambda}}{\Delta-\frac{1}{2}}-\frac{\bar{\lambda}^2}{2(\Delta-\frac{1}{2})^3}+O(\bar{\lambda}^3) \ . \tag{8.6}$$

Let us now see how this result emerges in the Hamiltonian truncation approach. Firstly, we write V in terms of the ladder operators

$$V=\sum_{m,n=0}^{\infty} A_{mn}(\Delta)(a_m^\dagger a_n^\dagger + 2a_m^\dagger a_n + a_m a_n) \ , \tag{8.7}$$

where the coefficients $A_{mn}(\Delta)$ are given explicitly in eq. (9.15), but their form will not be important here. Secondly, we truncate the Hilbert space to the states with unperturbed energy less than Λ. We will finally diagonalize H inside this truncated Hilbert space.

It is instructive to study this problem perturbatively in λ, using Rayleigh–Schrödinger perturbation theory. We focus on the vacuum $|\Omega\rangle$ and on the first excited state $|\chi\rangle := |0\rangle = a_0^\dagger |\Omega\rangle$. Explicitly, we obtain

$$\mathcal{E}_{\text{vac}}(\Lambda) = -\bar{\lambda}^2 \sum_{m\geq n\geq 0}^{m+n+2\Delta<\Lambda} \frac{|\langle\Omega|V|m,n\rangle|^2}{2\Delta+m+n} , \tag{8.8a}$$

$$\mathcal{E}_{\chi}(\Lambda) = \Delta + \bar{\lambda}\langle\chi|V|\chi\rangle - \bar{\lambda}^2 \sum_{m\geq 1}^{m+\Delta<\Lambda} \frac{|\langle\chi|V|m\rangle|^2}{m} - \bar{\lambda}^2 \sum_{m\geq n\geq 0}^{m+n+3\Delta<\Lambda} \frac{|\langle\chi|V|m,n,0\rangle|^2}{2\Delta+m+n} , \tag{8.8b}$$

where we omit $O(\bar{\lambda}^3)$ terms with the sums running over normalized single-particle states $|m\rangle = a_m^\dagger|\Omega\rangle$, two particle states $|m,n\rangle \propto a_m^\dagger a_n^\dagger|\Omega\rangle$ and three-particle states $|m,n,0\rangle \propto a_m^\dagger a_n^\dagger a_0^\dagger|\Omega\rangle$ with unperturbed energy less than Λ. It is possible to use a diagrammatic language to depict the terms in these expressions, as shown in figure 8.1. In these diagrams, time runs upwards and the horizontal axis corresponds to different mode numbers, *e.g.* the state $|1,2,2,4\rangle \propto a_1^\dagger (a_2^\dagger)^2 a_4^\dagger |\Omega\rangle$ would be represented by single lines at $n=1$ and $n=4$ and a double line at $n=2$. The vertex V is represented by crosses on the same dashed horizontal line and it can either lower or raise occupation numbers according to (8.7). The original state appears both at the bottom and at the top of the diagram. At order $\bar{\lambda}^2$, the operator V is applied twice and, in principle, all possible intermediate states need to be taken into account. However, working at finite cutoff Λ means that only a finite number of intermediate states are allowed, namely those with unperturbed energy smaller than Λ. This diagramatics is explained in more detail in appendix G.2.

As shown in appendix G.3, both energies (at order $\bar{\lambda}^2$) diverge linearly with Λ,

$$\mathcal{E}_{\text{vac}}(\Lambda) \approx \mathcal{E}_{\chi}(\Lambda) \approx -\sigma_\infty(\Delta)\bar{\lambda}^2\Lambda . \tag{8.9}$$

This divergence emerges from the double sums in (8.8), or equivalently from the diagrams on the left most column of figure 8.1. Naively, one could think that the energy gap could be obtained from the difference

$$\lim_{\Lambda\to\infty} \mathcal{E}_{\chi}(\Lambda) - \mathcal{E}_{\text{vac}}(\Lambda) . \tag{8.10}$$

However this does not reproduce the exact result (8.6) at $\mathcal{O}(\bar{\lambda}^2)$. To find the solution of this puzzle, let us look more carefully at the structure of the perturbative formulas (8.8).

We can write

$$\begin{aligned}\mathcal{E}_\chi(\Lambda_1)-\mathcal{E}_{\text{vac}}(\Lambda_2) =& \Delta+\bar{\lambda}\langle\chi|V|\chi\rangle-\bar{\lambda}^2\sum_{m\geq 1}^{m+\Delta<\Lambda_1}\frac{|\langle\chi|V|m\rangle|^2}{m}-\bar{\lambda}^2\sum_{m\geq 0}^{m+3\Delta<\Lambda_1}\frac{|\langle\chi|V|m,0,0\rangle|^2}{2\Delta+m} \qquad (8.11)\\ &+\bar{\lambda}^2\sum_{m\geq 0}^{m+2\Delta<\Lambda_2}\frac{|\langle\Omega|V|m,0\rangle|^2}{2\Delta+m}-\bar{\lambda}^2\sum_{m\geq n\geq 1}^{\substack{m+n+3\Delta<\Lambda_1\\ m+n+2\Delta>\Lambda_2}}\frac{|\langle\Omega|V|m,n\rangle|^2}{2\Delta+m+n}+\mathcal{O}(\bar{\lambda}^3)\ ,\end{aligned}$$

where we used that $\langle\chi|V|m,n,0\rangle=\langle\Omega|V|m,n\rangle$ for both m and n different from 0. Notice that the last sum is suspicious because it only involves two-particle states with energy between Λ_2 and $\Lambda_1-\Delta$.[1] Indeed, the exact result is obtained in the limit $\Lambda_1,\Lambda_2\to\infty$ simply by dropping the contribution of the last term. This is what happens if we apply the prescription (8.1). Diagrammatically, this corresponds to the cancellation of the diagrams on the first two columns in figure 8.1. Although the diagrams in the first column give rise to a linear divergence, the prescription (8.1) ensures that they cancel exactly. Notice that, if we keep $\Lambda_1-\Lambda_2$ fixed in the limit $\Lambda_1,\Lambda_2\to\infty$, then the last sum in (8.11) gives a finite contribution, due to the growth of the overlaps $|\langle\Omega|V|m,n\rangle|$. This is the same growth responsible for the linear divergence (8.9). Furthermore, the discreteness of the unperturbed spectrum, labeled by integers m, n, generates the order one oscillation visible in the left panel of figure 8.3. We shall comment further on these oscillations in section 8.4.

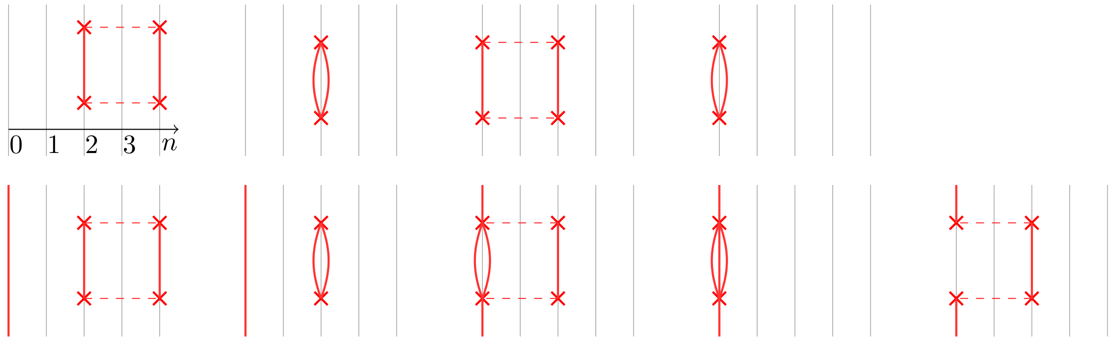

Figure 8.1: Diagrams contributing at second order in perturbation theory to the vacuum energy (top row) and to the energy of the first excited state $|\chi\rangle=a_0^\dagger|\Omega\rangle$ (bottom row). In the top row, we have intermediate two-particle states, while in the bottom row, we have intermediate one and three particle states.

The divergence of the ground state energy as the cutoff is removed is a consequence of the infinite volume of space. In fact, it is instructive to regulate the interaction term in the free boson example so that it affects only a finite volume:

---

[1] For simplicity, we assumed $\Lambda_2<\Lambda_1-\Delta$.

$$V_\epsilon = \int_{-\pi/2+\epsilon}^{\pi/2-\epsilon} \frac{dr}{(\cos r)^2} :\phi^2(\tau = 0, r): . \tag{8.12}$$

For $\epsilon > 0$ the eigenvalues of the Hamiltonian are finite as $\Lambda \to \infty$. In particular, in figure 8.2 we compare the order $\bar{\lambda}^2$ contribution to the vacuum energy, as given by (8.8), for the theory with $\epsilon = 0$ (in blue) with the same quantity for $\epsilon = 1/10$ (in green) and $\epsilon = 1/5$ (in orange). The Casimir energy of the $\epsilon = 0$ theory grows linearly with Λ, whereas the regulated theories have a finite limit as $\Lambda \to \infty$.

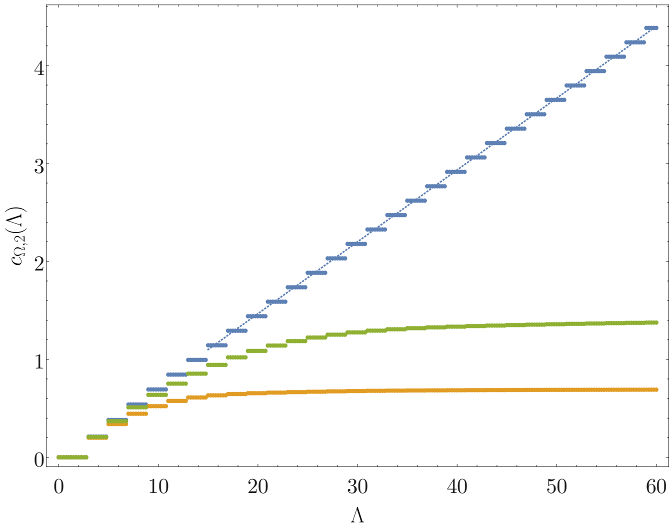

Figure 8.2: Order λ^2 contribution to the Casimir energy of the ϕ^2 flow, where the UV theory is a massive free boson with $\Delta = \sqrt{2}$. The notation $c_{i,n}$ is defined in (8.19). Blue dots: the theory without a spatial cutoff as given by (8.8a); green resp. orange dots: the same theory cut off at $\epsilon = 1/10$ resp. $\epsilon = 1/5$. Notice that the Casimir energy of the full theory diverges linearly with Λ, whereas the same interaction with $\epsilon > 0$ asymptotes to a finite value. The asymptotic value appears to be reached when $\Lambda \sim 1/\epsilon$. The dotted blue line shows the large-Λ behavior predicted using (8.9).

We can also study the energy gap between the state $|\chi\rangle = a_0^\dagger|\Omega\rangle$ and the vacuum. In the theory regulated with $\epsilon > 0$, we can compute the energy gap as in (8.10) because the energy levels remain finite as $\Lambda \to \infty$. However, convergence only emerges for $\Lambda \gtrsim 1/\epsilon$. This explains why we cannot use the naive prescription (8.10) in the unregulated theory. These issues are depicted in figure 8.3.

Let us summarize the general lesson. If we fix the vacuum energy to vanish for the unperturbed Hamiltonian, then the energy of each state receives an infinite contribution in the perturbed theory. The divergence of the vacuum energy is a general feature of any QFT in infinite volume, and is not an issue in the continuum limit, since in a

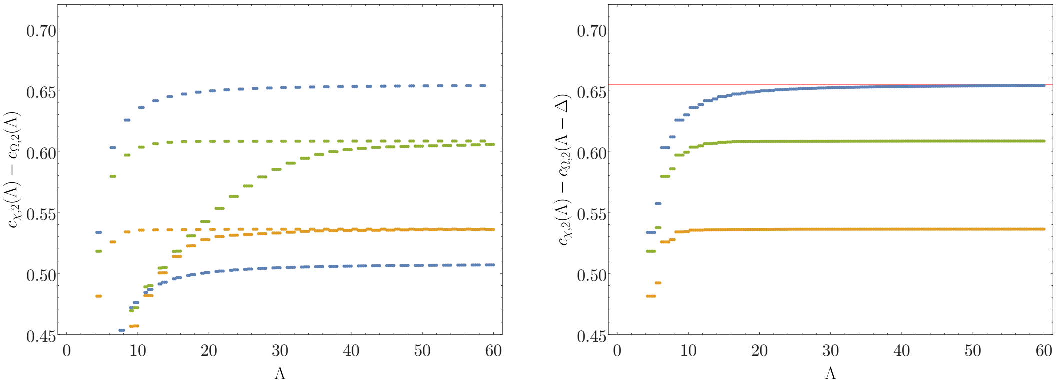

Figure 8.3: Order λ^2 contribution to the energy gap of the massive boson with $\Delta = \sqrt{2}$, comparing the naive prescription (8.10) (left) and the prescription (8.1) (right). The unregulated theory is shown in blue; the same theory regulated with $\epsilon = 1/10$ (resp. $\epsilon = 1/5$) are shown in green (orange). For $\epsilon > 0$ the two prescriptions agree as $\Lambda \to \infty$. However, there are significant deviations (oscillations) for $\Lambda \lesssim (\text{few})/\epsilon$. In particular, for $\epsilon = 0$, only the prescription (8.1) converges to the exact result shown as a solid red line; there are O(1) oscillations that persist up to arbitrarily large cutoff if the naive prescription is used.

fixed background the vacuum energy is not observable. On the other hand, this means that the spectrum of the Hamiltonian does not have a limit as the truncation level is increased, which is the source of the ambiguity in the determination of the energy gaps. We saw in a specific example that the divergence of the vacuum energy is linear with the truncation cut-off Λ. In section 8.3, we show that this is a general feature of second order perturbation theory. More generally, we expect this to be true at all orders, as we will explain in section 8.5. In the same example, we also saw that the prescription (8.1) solves the ambiguity and leads to the correct energy gaps.

It is worth noticing that, due to the mentioned UV/IR connection, the manifestation of the problem in perturbation theory, *i.e.* the state-dependence of the contributions of intermediate states close to the cutoff, is analogous to the situation in flat space when authentic UV divergences are present [156, 47]. Contrary to the latter, though, the infinite volume divergences we are concerned with all come from disconnected contributions. This makes it plausible that the simple prescription (8.1) has a chance of working at all orders. Indeed, let us now justify eq. (8.1) for a generic QFT in AdS$_2$.

8.2 The strategy

As remarked in section 7.3, the theory associated to the action (5) may require a regulator to cutoff divergences close to the boundary of AdS. If the QFT is UV complete, as we shall assume in this thesis, a set of counterterms exist such that all correlation functions are finite and invariant under the AdS isometries when the cutoff is removed [157]. This ensures that the energy gaps above the vacuum are well defined in the continuum limit, as it can be seen for instance via the state operator map. In the following, we assume the spectral condition (7.14), together with $\langle \mathcal{V} \rangle = 0$, so that such a procedure is not necessary. Furthermore, we also assume that local UV divergences in the bulk are absent.

Nevertheless, our strategy will precisely consist in introducing a local cutoff at the AdS boundary, such that, in the regulated theory, the individual energy levels are finite as well. We shall find the regulated spectrum via Hamiltonian truncation, and analyze the convergence properties as the truncation cutoff Λ is removed. Concretely, let us regulate the theory by cutting off all integrals over AdS at a coordinate distance ϵ from the boundary, *i.e.* $r \in [-\pi/2+\epsilon, \pi/2-\epsilon]$. This means modifying the operator V from (7.16) as follows:

$$V_\epsilon := R^{\Delta_\mathcal{V}} \int_{-\pi/2+\epsilon}^{\pi/2-\epsilon} \frac{dr}{(\cos r)^2}\, \mathcal{V}(\tau=0,r). \tag{8.13}$$

We shall keep ϵ finite for the moment, and take the limit $\epsilon \to 0$ only when computing physical observables. Quantities computed in the regulated theory will contain ϵ as a subscript or a superscript.

Our argument in favor of the validity of eq. (8.1) at all orders requires recasting the usual Rayleigh-Schrödinger perturbation theory in a convenient if unusual form. A reminder of perturbation theory in Quantum Mechanics can be found in appendix G, together with the proof of the formulas which we use below. The interacting energies admit an expansion of the form[2]

$$\mathcal{E}_i^\epsilon = e_i + \sum_{n=1}^{\infty} (-1)^{n+1} c_{i,n}^\epsilon\, \bar{\lambda}^n \ , \tag{8.14}$$

including the vacuum to which we associate the index $i = \Omega$. Notice that the bare energies e_i do not need to be regulated. The coefficients $c_{i,n}^\epsilon$ admit a compact expression in terms of the spectral densities defined as follows:

$$\begin{aligned}\langle i | V_\epsilon(\tau_1 + \dots \tau_{n-1}) \cdots V_\epsilon(\tau_1+\tau_2) V_\epsilon(\tau_1) V_\epsilon(0) | i \rangle_{\text{conn}} \\ = \prod_{\ell=1}^{n-1} \int_0^\infty d\alpha_\ell\, e^{-(\alpha_\ell - e_i)\tau_\ell}\, \rho_{i,n}^\epsilon(\alpha_1,\dots,\alpha_{n-1}) \ .\end{aligned} \tag{8.15}$$

The correlator on the left hand side is depicted in figure 8.4. Crucially, it is connected with respect to the state $|i\rangle$, meaning that all the subtractions are evaluated in the same state. Explicit examples for the first few values of n are given in appendix G, along with the expression of the spectral densities in terms of the matrix elements of V. Now, the

---

[2] We assume that the ith state is non degenerate. We will comment on the degenerate case in section 8.6.

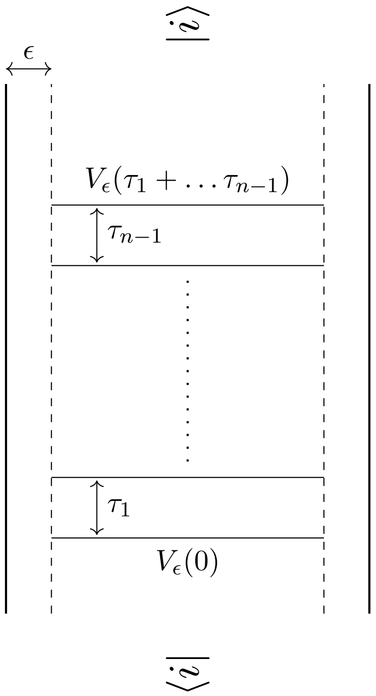

Figure 8.4: A depiction of the correlation function on the l.h.s. of eq. (8.15). The vertical thick lines denote the boundary of AdS$_2$. The horizontal lines denote insertions of the regulated potential V_ϵ, as defined in eq. (8.13). The subtractions of disconnected pieces, which define the connected correlator in eq. (8.15), are not shown.

general term in the perturbative expansion (8.14) reads

$$c^\epsilon_{i,n} = \int_0^\infty \prod_{\ell=1}^{n-1} \frac{d\alpha_\ell}{\alpha_\ell - e_i}\, \rho^\epsilon_{i,n}(\alpha_1, \dots, \alpha_{n-1}) \,. \tag{8.16}$$

This remarkably compact expression, compared to the increasingly convoluted textbook formulas, does not seem to be well-known in the QFT literature. The fact that the Casimir energy can be expressed in terms of connected Feynman diagrams appears (without proof) already in refs. [158, 159] by Bender and Wu. A proof of the formula for the Casimir energy is given in ref. [160] by Klassen and Melzer, specializing to the case of a perturbed $2d$ QFT. Finally, in [161, eq. (2.25)] by the same authors a formula is given (without proof) for the Rayleigh-Schrödinger coefficients of the i-th state in the case of a perturbed $2d$ CFT on the cylinder. The formula appearing in [161] is generically divergent and needs to be regulated — in the time domain, its integrands generically blow up as $\tau_i \to \infty$. We prove (8.16) in appendix G. Notice that, as long as ϵ is finite, the integrals in eq. (8.16) converge.

The coefficients of the perturbative expansion of the physical energy gaps can be written as follows:

$$c_{i,n} - c_{0,n} = \lim_{\epsilon\to 0} \int_0^\infty \frac{d\vec{\alpha}}{\vec{\alpha} - e_i} \left[\rho^\epsilon_{i,n}(\vec{\alpha}) - \rho^\epsilon_{0,n}(\vec{\alpha} - e_i)\right] \ , \tag{8.17}$$

where the vector notation abbreviates the product in eq. (8.16). This formula is crucial and deserves an important comment: the $\epsilon \to 0$ limit is not guaranteed to commute with the integral. The fact that it does is equivalent to the validity of eq. (8.1). Indeed, *if* the limit can be taken inside the integration, we obtain the following simple chain of equalities:

$$\begin{aligned} c_{i,n} - c_{0,n} &= \lim_{\epsilon\to 0} \lim_{\Lambda\to\infty} \int_0^\Lambda \frac{d\vec{\alpha}}{\vec{\alpha} - e_i} \left[\rho^\epsilon_{i,n}(\vec{\alpha}) - \rho^\epsilon_{0,n}(\vec{\alpha} - e_i)\right] \\ &= \lim_{\Lambda\to\infty} \int_0^\Lambda \frac{d\vec{\alpha}}{\vec{\alpha} - e_i} \left[\rho_{i,n}(\vec{\alpha}) - \rho_{0,n}(\vec{\alpha} - e_i)\right] \\ &= \lim_{\Lambda\to\infty} \left(c_{i,n}(\Lambda) - c_{0,n}(\Lambda - e_i)\right) \ , \end{aligned} \tag{8.18}$$

where we defined the expansion of the truncated energies:

$$\mathcal{E}_i(\Lambda) = e_i + \sum_{n=1}^\infty (-1)^{n+1} c_{i,n}(\Lambda)\, \bar{\lambda}^n \ . \tag{8.19}$$

Hence, we are left with the task of proving that the $\epsilon \to 0$ and the $\Lambda \to \infty$ limits do commute. Of course, for this to be true it is not sufficient that the integral in the second line of eq. (8.18) converges. Indeed, intuitively we should rule out the existence of bumps which give a finite contribution to the integral, and run away to infinity as $\epsilon \to 0$. Formally, the dominated convergence theorem states that the limits commute if, for all $\epsilon < \epsilon_0$, the integrand is bounded by a *fixed* function whose integral from 0 to ∞ converges.

Before engaging in the details of the argument, let us describe the main ingredients, which are few and simple. Clearly, establishing the validity of the manipulations in eq. (8.18) requires to bound the large $\vec{\alpha}$ limit of the spectral densities $\rho^\epsilon_{i,n}$. It is intuitive, albeit hard to prove, that this limit is controlled by the small $\vec{\tau}$ limit of the correlator on the l.h.s. of eq. (8.15). As it can be seen in figure 8.4, when one, or more, of the τ_m go to zero, the insertions of the potential collide. Non-analyticities in these limits may arise because a subset of the perturbing operators $\mathcal{V}$ collide in the bulk, or, if $\epsilon = 0$, on the boundary. Both contributions are important in establishing the rate of convergence of the energy gaps as we lift the cutoff Λ, which we will analyze in section 8.7. On the contrary, by assumption, the individual energy levels themselves are finite as long as $\epsilon > 0$. Hence, in order to establish the prescription (8.1) we are only interested in the fusion of the insertions $\mathcal{V}$ with the boundary of AdS. As explained above, our assumptions also imply that the OPE (7.13) is sufficiently soft to make the matrix elements of V finite. We conclude that the relevant small $\vec{\tau}$ singularities are due to the simultaneous collision of *multiple* local operators $\mathcal{V}$ on a *unique* point on the AdS boundary. This prompts us to study the OPE depicted in figure 8.5: the lightest operator appearing in the OPE, whose

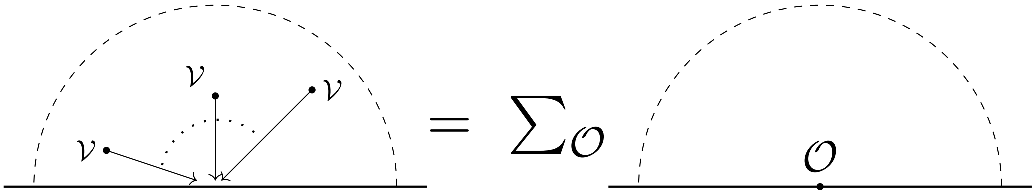

Figure 8.5: Sketch of the OPE channel relevant to establishing the singular behavior of the correlator in eq. (8.15) as some of the $\tau_m \to 0$. The OPE is obtained, as usual, by projecting the insertions of the $\mathcal{V}$ operators on the l.h.s. onto a complete set of states on the dashed semicircle. The coefficients of the OPE are higher-point functions involving the insertions of $\mathcal{V}$ and the boundary operator $\mathcal{O}$. An explicit example is considered in appendix H.2, see eq. (H.31) and figure H.3.

expectation value in the external state $|i\rangle$ does not vanish, is responsible for the small $\vec{\tau}$ singularity, and eventually for the growth of the spectral density at infinity.

In the following, we shall detail the above steps in the first non-trivial order in perturbation theory. Then, we will discuss the generalization of the procedure to all orders in perturbation theory. Finally, we will discuss the rate of convergence of Hamiltonian truncation in AdS.

8.3 Divergence of the vacuum energy at second order

Let us begin by showing that the linear divergence of the vacuum energy with the truncation level, which we observed in the example 8.1, is a general feature at second order in perturbation theory. Since $\langle\Omega|\mathcal{V}|\Omega\rangle = 0$, eq. (8.15) reduces in this case to

$$\langle\Omega|V(\tau)V(0)|\Omega\rangle = \int_0^\infty d\alpha\, e^{-\alpha\tau}\, \rho_{0,2}(\alpha)\ . \tag{8.20}$$

Since we are interested in characterizing the behavior of the first energy level as a function of the cutoff Λ, we set $\epsilon = 0$ in this section. More general results can be found in appendix H.1. As explained in section 8.2, we need to extract the large α behavior of $\rho_{0,2}(\alpha)$. Reflection positivity ensures that $\rho_{0,2}(\alpha) > 0$. This allows us to invoke a Tauberian theorem [53] to rigorously tie the large α limit of the spectral density to the small τ limit of the correlator on the l.h.s. of eq. (8.20).

The latter limit is computed in appendix H.1, and reads as follows:[3]

$$\langle\Omega|V(\tau)V(0)|\Omega\rangle \overset{\tau\to 0}{\sim} \frac{c}{\tau^2}\ . \tag{8.21}$$

---

[3] As explained in appendix H.1, this result is valid if $\Delta_{\mathcal{V}} < 3/2$, otherwise it must be replaced by eq. (H.8). In particular, if $\Delta_{\mathcal{V}} > 3/2$, the leading contribution to the divergence of the vacuum energy comes from a bulk UV singularity, which we assumed to avoid in this work.

The coefficient of the singularity is theory dependent, and, as explained in the same appendix, it can be computed as follows:

$$R^{2\Delta_\mathcal{V}}\langle\Omega|\mathcal{V}(\tau,r)\mathcal{V}(0,r')|\Omega\rangle \equiv f_\Omega(\xi)\ , \tag{8.22}$$

$$c = 8\int_0^\infty d\xi\, \mathrm{arcsinh}\left(2\sqrt{\xi(\xi+1)}\right) f_\Omega(\xi)\ , \tag{8.23}$$

where we recall that ξ is defined in eq. (7.8). In the language of the OPE described in figure 8.5, the small τ limit corresponds to the contribution of the identity operator, the only one surviving when the r.h.s. of the OPE is evaluated in the vacuum.

As advertised, the Tauberian theorem reviewed in [53] implies the following asymptotics for the integrated spectral density:

$$\int_0^\Lambda d\alpha\, \rho_{0,2}(\alpha) \overset{\Lambda\to\infty}{\sim} \frac{c}{2}\Lambda^2\ . \tag{8.24}$$

The contribution to the vacuum energy at second order can then be extracted from eq. (8.14), by truncating the integral in eq. (8.16) to the region $[0,\Lambda]$ and integrating by parts:

$$\mathcal{E}_\Omega(\Lambda) \overset{\Lambda\to\infty}{\sim} -c\,\Lambda\,\bar\lambda^2 + O(\bar\lambda^3)\ . \tag{8.25}$$

We will have opportunities to check this formula in the examples of chapters 9 and 10.

8.4 The argument at second order

Let us now turn to our goal of establishing the prescription (8.1). At second order in perturbation theory, the object of interest is the two-point function of the potential:

$$\langle i|V_\epsilon(\tau)V_\epsilon(0)|i\rangle_{\text{conn}} = \langle i|V_\epsilon(\tau)V_\epsilon(0)|i\rangle - \langle i|V_\epsilon|i\rangle^2\ . \tag{8.26}$$

Let us first point out the following simple but crucial fact. The difference of the spectral densities appearing in eq. (8.18), *with* the shift in their arguments, is the spectral density of the difference of the correlators in state $|i\rangle$ and in the vacuum:

$$\begin{aligned} g_\epsilon(\tau) = \langle i|V_\epsilon(\tau)V_\epsilon(0)|i\rangle_{\text{conn}} - \langle\Omega|V_\epsilon(\tau)V_\epsilon(0)|\Omega\rangle_{\text{conn}} \\ = \int_{-e_i}^\infty d\alpha\, e^{-\alpha\tau}\left(\rho^\epsilon_{i,2}(\alpha+e_i) - \rho^\epsilon_{0,2}(\alpha)\right)\ . \end{aligned} \tag{8.27}$$

We shall denote the new spectral density as

$$\boldsymbol{\Delta}\rho^\epsilon_{i,2}(\alpha) = \rho^\epsilon_{i,2}(\alpha+e_i) - \rho^\epsilon_{0,2}(\alpha)\ . \tag{8.28}$$

We are interested in the large α behavior of the spectral density, and we would like to leverage our knowledge of the correlation functions in position space. While it is clear that singularities at small τ in $g_\epsilon(\tau)$ are related to the large α behavior of the spectral density, it is non-trivial to obtain a precise correspondence. Indeed, $\boldsymbol{\Delta}\rho^\epsilon_{i,2}(\alpha)$ is a non-positive distribution, and the Tauberian theorems which usually provide those estimates cannot be applied.[4] Instead, we shall tackle the question directly, and point out the additional assumptions necessary to obtain the needed asymptotics. Let us first recall the naive answer. *If* the correlator has a singular power-like small τ limit, *i.e.*

$$if \qquad g_\epsilon(\tau) \overset{\tau\to 0}{\sim} \tau^{-\beta} \ , \quad \beta > 0 \ , \tag{8.29}$$

and *if* the spectral density had a power-like behavior at large α as well, then we would conclude that

$$\boldsymbol{\Delta}\rho^\epsilon_{i,2}(\alpha) \overset{\alpha\to\infty}{\sim} \alpha^{\beta-1} \ . \tag{8.30}$$

Since the spectral densities are in general infinite sums of delta functions, we have to interpret the last equation in an averaged sense. Let us describe how this works in more detail.

We focus our attention on the following averaged spectral density:

$$R_\epsilon(\Lambda) = \int_{-\infty}^{\Lambda} d\alpha\, \boldsymbol{\Delta}\rho^\epsilon_{i,2}(\alpha) = \int_{\gamma-\mathrm{i}\infty}^{\gamma+\mathrm{i}\infty} \frac{d\tau}{2\pi\mathrm{i}\tau} e^{\Lambda\tau} g_\epsilon(\tau) \ , \qquad \gamma > 0 \ . \tag{8.31}$$

$R_\epsilon(\Lambda)$ is a finite sum which can be easily inferred from eq. (G.8b). The right hand side is obtained by commuting the α-integral with the inverse Laplace transform of $g_\epsilon(\tau)$, and one can explicitly check that eq. (8.31) gives the correct result.[5] While the correlation functions in eq. (8.27) are analytic when $\Re\tau > 0$, singularities may arise in the left half plane. In particular, as we show in appendix H.2, $g_\epsilon(\tau)$ generically has a branch point at $\tau = 0$,

$$g_\epsilon(\tau) \overset{\tau\to 0}{\sim} \tau^{\Delta_*-2} \ , \tag{8.32}$$

where Δ_* is the dimension of the leading boundary operator above the identity in the OPE illustrated in figure 8.5 - see also figure H.3 and the detailed explanation in appendix H.2. If the exactly solvable Hamiltonian corresponds to a CFT, then $\Delta_* \leq 2$, due to the universal presence of the displacement operator, see e.g. [163]. If $\Delta_* = 2$, the singularity is logarithmic. More precisely, in appendix H.2, we show that, if $\Delta_* \leq 2$, $g_\epsilon(\tau)$ is bounded as follows:[6]

---

[4] See however [162], where a lower bound on the average of a non-positive spectral density was obtained, subject to a condition on the amount of negativity allowed.

[5] This is how it goes: $g_\epsilon(\tau) = \sum_{n=0}^\infty a_n e^{-\alpha_n\tau}$. This sum converges absolutely for $\Re\tau > 0$. Hence, we can commute the sum and the integral to get $R_\epsilon(\Lambda) = \sum_{n=0}^\infty a_n \int_{\gamma-\mathrm{i}\infty}^{\gamma+\mathrm{i}\infty} \frac{d\tau}{2\pi\mathrm{i}\tau} e^{(\Lambda-\alpha_n)\tau}$. The last integral converges and the result is the expected $R_\epsilon(\Lambda) = \sum_{\alpha_n<\Lambda} a_n$.

$$|g_\epsilon(\tau)| < C(\tau_0) \begin{cases} |\tau|^{\Delta_*-2} \,, & \Delta_* < 2 \\ \log|\tau| \,, & \Delta_* = 2 \,, \end{cases} \qquad |\tau| < \tau_0 \,. \tag{8.33}$$

Here, $\tau_0 > 0$ is an arbitrary fixed number. The crucial step in the derivation of this result is that, when replacing the OPE of figure 8.5 in the left hand side of eq. (8.27), the identity operator cancels out, and with it the strongest singularity (8.21) at small τ. As a consequence, the spectral density (8.28) has a softer large α behavior than what would happen without the shift. It is important that the bound (8.33) is uniform in ϵ.

In chapter 9, we will consider deformations of free massive QFTs, for which $\Delta_* > 2$ is possible. Although we have not analyzed this case in detail, we are confident that the bound (8.33) still holds, up to analytic terms at $\tau = 0$. In other words, a strict bound can be obtained when $\Delta_* > 2$ by taking enough derivatives of $g_\epsilon(\tau)$. We offer some comments in this direction in appendix H.2. This turns into a bound for a higher moment of $\boldsymbol{\Delta}\rho$, which still allows to proceed with the argument. The examples in chapter 9 lend support to this conclusion.

On the other hand, further singularities may appear on the imaginary τ axis. A generic example of the analytic structure in the τ plane is depicted in figure 8.6. Let us now shift the integration contour in (8.31) to the left, as shown in figure 8.6. It is clear from

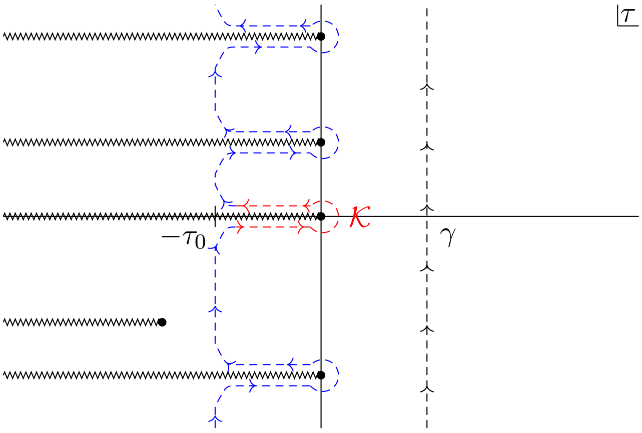

Figure 8.6: A sketch of the generic singularity structure of $g_\epsilon(\tau)$ The singularities are generically branch points, and the cuts are oriented away from the region $\Re\tau > 0$, where the correlator is analytic. The black dashed contour is the original one in eq. (8.31), while the blue dashed one is shifted to the left in order to leverage the exponential suppression at large Λ. Finally, the red contour is $\mathcal{K}$ in eq. (8.34).

---

[6] More precisely, this result assumes that the bulk OPE is non-singular. In appendix H.2 we also discuss what happens if this is not the case, in a restricted scenario – see the paragraph around eq. (H.42). See also the discussion in section 8.7. In general, as long as the small τ limit is less singular than τ^{-1} and it is uniform in ϵ, the rest of the argument goes through. The first condition is equivalent to $\Delta_{\tilde{\mathcal{V}}} > 2\Delta_{\mathcal{V}} - 2$, $\Delta_{\tilde{\mathcal{V}}}$ being the first operator above the identity in the $\mathcal{V} \times \mathcal{V}$ OPE. This is the same as requiring that bulk UV divergences are absent, which we assume in this work.

eq. (8.31) that the part of the contour which runs in the left half plane is exponentially suppressed at large Λ. As for the $\Re\tau = 0$ axis, if $\boldsymbol{\Delta}\rho^{\epsilon}_{i,2}(\alpha)$ was positive, the stronger singularity would be at $\tau = 0$, as it is easy to deduce from eq. (8.27). The large Λ limit of $R_\epsilon(\Lambda)$ would then be controlled by the strength of this singularity, a result familiar from the Hardy-Littlewood Tauberian theorem. Since the spectral density is not necessarily positive, we will *assume* that the large Λ behaviour of $R_\epsilon(\Lambda)$ is still dominated by the singularity at $\tau = 0$. This assumption is not harmless, and we shall offer some comments about it at the end of this chapter. Keeping in mind figure (8.6), we then obtain

$$|R_\epsilon(\Lambda)| \sim \left| \int_{\mathcal{K}} \frac{d\tau}{2\pi\mathrm{i}} \frac{e^{\Lambda\tau} - 1}{\tau} g_\epsilon(\tau) + \int_{\mathcal{K}} \frac{d\tau}{2\pi\mathrm{i}\tau} g_\epsilon(\tau) \right| . \tag{8.34}$$

Here, $\mathcal{K}$ is a keyhole contour around the origin which extends up to $\Re\tau = -\tau_0$. With the benefit of hindsight, we added and subtracted 1. Indeed, we can now shrink to the real axis the first $\mathcal{K}$ contour, and we can use the inequality (8.33) to write

$$|R_\epsilon(\Lambda)| \leq 2C(\tau_0) \int_{-\tau_0}^{0} \frac{d\tau}{2\pi} |e^{\Lambda\tau} - 1||\tau^{\Delta_* - 3}| + \left| \int_{\mathcal{K}} \frac{d\tau}{2\pi\tau} g_\epsilon(\tau) \right| . \tag{8.35}$$

Notice that the first integral converges if $\Delta_* > 1$, which is guaranteed by the condition (7.14). The second integral is finite and Λ independent. Therefore, under the assumptions we have made, we conclude that[7]

$$|R_\epsilon(\Lambda)| \leq F(\Lambda) \overset{\Lambda\to\infty}{\sim} \Lambda^{2-\Delta_*} , \tag{8.36}$$

with $F(\Lambda)$ independent of ϵ. We shall now assume (8.36) to prove (8.18). It is sufficient to integrate by parts once, to express the energy shift (8.17) in terms of $R_\epsilon(\Lambda)$:

$$c_{i,2} - c_{0,2} = \lim_{\epsilon\to 0} \lim_{\Lambda\to\infty} \left(\frac{R_\epsilon(\Lambda - e_i)}{\Lambda - e_i} + \frac{R_\epsilon(-e_i)}{e_i} + \int_0^\Lambda \frac{d\alpha}{(\alpha - e_i)^2} R_\epsilon(\alpha - e_i) \right) . \tag{8.37}$$

Thanks to eq. (8.36), we clearly can swap the small ϵ and the large Λ limits in the first two addends. As for the last integral, we can fix a constant Λ_* and write the following inequality:

---

[7] It should be noted that, when $\Delta_* = 2$, one obtains $F(\Lambda) \sim \log^2 \Lambda$ in eq. (8.36). This is sufficient to prove the prescription (8.1), but is a weak bound. Indeed, the integrated spectral density $R(\Lambda)$ is expected to only grow like $\log \Lambda$. The weak point is the inequality (8.35): when we shrink the contour $\mathcal{K}$ onto the real axis, the integral of the left hand side reduces to the discontinuity, which replaces $\log \tau$ with a constant and does lead to the expected asymptotics.

$$\begin{aligned}
&\int_0^{\Lambda_*}\frac{d\alpha}{(\alpha-e_i)^2}R_0(\alpha-e_i)-\int_{\Lambda_*}^{\infty}\frac{d\alpha}{(\alpha-e_i)^2}F(\alpha-e_i)\\
\leq&\lim_{\epsilon\to 0}\int_0^{\infty}\frac{d\alpha}{(\alpha-e_i)^2}R_\epsilon(\alpha-e_i)\\
\leq&\int_0^{\Lambda_*}\frac{d\alpha}{(\alpha-e_i)^2}R_0(\alpha-e_i)+\int_{\Lambda_*}^{\infty}\frac{d\alpha}{(\alpha-e_i)^2}F(\alpha-e_i)\ .
\end{aligned}\tag{8.38}$$

Here, we took the $\epsilon\to 0$ limit inside the integral over the finite domain $[0,\Lambda_*]$, and used the inequality (8.36) to express the remaining integrand in terms of the positive and ϵ independent function $F(\Lambda)$. Taking $\Lambda_*\to\infty$, we finally obtain the sought result (8.18). The prescription (8.1) at order λ^2 in perturbation theory immediately follows.

Let us now come back to the additional singularities on the $\mathrm{Im}\,\tau$ axis in figure 8.6. Contrary to the singularity at $\tau=0$, the contribution of each of them is not enhanced by the $1/\tau$ pole in (8.31). Hence, if they are not enhanced with respect to eq. (8.33), they are subleading at large Λ. This assumption hides a remarkable series of cancellations, analogous to the cancellation of the identity block at $\tau=0$, which, as discussed, leads to the bound (8.33). Indeed, each of the correlators in eq. (8.27) is expected to have an infinite series of double poles along the imaginary axis. The reason for this is that such double poles lead to order one oscillations in the $c_{i,2}(\Lambda)$, the second order energy shifts in eq. (8.19). The oscillations, visible for instance in figure 8.2, are a generic consequence of the discreteness of the spectrum. Without an exact cancellation, the oscillations affect the energy gaps as well, as in figure 8.3. The absence of order one oscillations in the examples treated in chapters 9 and 10, then, gives evidence for the correctness of the prescription (8.1) beyond the arguments presented so far. Analyzing these cancellations in detail requires studying the correlators of the deformation V_ϵ in Lorentzian kinematics: an interesting task for the future. For the moment, let us make a couple of simple remarks. If the unperturbed spectrum has integer scaling dimensions, then all correlators are periodic for $\tau\to\tau+2\pi\mathrm{i}$. This is the case for the minimal models with the boundary condition we choose in chapter 10. Then, barring additional singularities within the first period, the cancellation of all the double poles simply follows from the result we proved for $\tau=0$. On the other hand, the periodicity is broken in the general case, including the perturbation of massive free theories which we will treat in chapter 9. An example of this non periodic behavior can be seen in appendix H.3. Nevertheless, we can still envision a mechanism for the cancellation of the double poles. As we discussed in section 8.3 and in appendix H, the double pole at $\tau=0$ in each correlator in eq. (8.27) is due to a disconnected contribution. If the unperturbed theory is free, such contribution corresponds to a disconnected Witten diagram, where the boundary operators which create and annihilate the states $|i\rangle$ are spectators. Such diagrams exchange a fixed number of particles, and so they are periodic in $\mathrm{Im}(\tau)$ with period 2π up to a phase, which is crucially independent of the boundary state $|i\rangle$. Therefore, again, each correlator in eq. (8.27) has an infinite series of double poles, which all cancel in $g_\epsilon(\tau)$. The absence of the double poles can be exhibited in the example of a massive free scalar, and we do so in appendix H.3. More specifically, there we also check that the remaining non-analyticities on the imaginary τ axis are not enhanced with respect to the $\tau = 0$ singularity.

A last comment is in order. Even if the leftover singularities in figure 8.6 are softer than the one at $\tau = 0$, one could still worry that there is an infinite sum over all of them at $\tau = it_n$ for real t_n. However, this sum is suppressed by the presence of the rapidly oscillating phases $e^{i\Lambda t_n}$. The convergence of the sum then depends on the density of the singularities along the imaginary axis, as $\operatorname{Im}\tau \to \infty$. One might expect this density to be approximately constant. If the boundary spectrum of the unperturbed theory is integer, this is obvious. In the general case, the exact periodicity may be replaced by some recurrence time, fixed by the scaling dimensions Δ, which nevertheless should not change this picture. Notice, however, that it is conceivable that non-analyticities appear with a periodicity of some multiple of π even in the general case, in keeping with the periodic structure of AdS in real time: this happens in the scalar example analyzed in appendix H.3. All in all, if the density is at most constant, the sum converges at least conditionally.

8.5 Generalization at all orders

The aim of this section is to sketch the generalization of the previous argument to all orders in perturbation theory. We shall not attempt to be detailed in this case, rather we will stress the ingredients that should make the argument follow through.

At n-th order in perturbation theory, we need to bound the (average of the) spectral density

$$\boldsymbol{\Delta}\rho^\epsilon_{i,n}(\vec{\alpha}) = \rho^\epsilon_{i,n}(\vec{\alpha}+e_i) - \rho^\epsilon_{0,n}(\vec{\alpha}) \ , \tag{8.39}$$

as the vector $\vec{\alpha}$ becomes large in a generic direction of its $(n-1)$ dimensional space. The bound should be uniform in ϵ and allow the integration of

$$\int_0^\Lambda \frac{d\vec{\alpha}}{\vec{\alpha}-e_i}\boldsymbol{\Delta}\rho^\epsilon_{i,n}(\vec{\alpha}-e_i) \tag{8.40}$$

over a hypercube of size Λ, as $\Lambda \to \infty$: see eq. (8.18). It is easy to see that, also in the general case, $\boldsymbol{\Delta}\rho^\epsilon_{i,n}(\vec{\alpha})$ is the Laplace transform of the following difference of connected correlators:

$$\begin{aligned} g^n_\epsilon(\vec{\tau}) = \langle i|V_\epsilon(\tau_1+\dots\tau_{n-1})\cdots V_\epsilon(\tau_1+\tau_2)V_\epsilon(\tau_1)V_\epsilon(0)|i\rangle_{\text{conn}} \\ - \langle \Omega|V_\epsilon(\tau_1+\dots\tau_{n-1})\cdots V_\epsilon(\tau_1+\tau_2)V_\epsilon(\tau_1)V_\epsilon(0)|\Omega\rangle_{\text{conn}} \ . \end{aligned} \tag{8.41}$$

Recall that all the subtractions of disconnected pieces are computed in the state $|i\rangle$ for the first correlator and $|\Omega\rangle$ for the second. We maintain the assumption that the large $\vec{\alpha}$ limit of the spectral density is controlled by the limit of $g^n_\epsilon(\vec{\tau})$ when a subset of components of the vector $\vec{\tau}$ vanish. In turn, this limit is controlled by the OPE channel of figure 8.5, at the level of the correlation function of the local operators $\mathcal{V}$.

Then, let us first consider the case where a proper subset of components of $\vec{\tau}$ vanish together. In this case, the contribution from the identity in the OPE in figure 8.5 vanishes separately in each connected correlator on the right hand side of eq. (8.41). This is a general property of cumulants, valid in any state: they vanish whenever a subset of random variables is statistically independent from the others.[8]

On the other hand, if all the components of $\vec{\tau}$ vanish together, then the contribution of the identity does not cancel out at the level of the single connected correlator. Rather, it cancels out in the difference (8.41), as it can be checked again by inserting a complete set of states in the generating function.

The cancellation of the identity should be sufficient for the integral in eq. (8.40) to converge uniformly in ϵ and allow the chain of equalities (8.18) to hold. Let us sketch the argument at the level of power counting, and let us focus on the radial behavior, where all components of $\vec{\alpha}$ diverge with fixed ratios. In this case, the asymptotics of $\boldsymbol{\Delta}\rho^\epsilon_{i,n}$ is controlled by the small $|\vec{\tau}|$ limit, for which we expect

$$|g^n_\epsilon(\vec{\tau})| < C(\tau_0)|\vec{\tau}|^{\Delta_*-n} \ , \qquad |\vec{\tau}| < \tau_0 \ . \tag{8.43}$$

Here, Δ_* is the lowest state above the identity which couples to the n insertions of $\mathcal{V}$, and in the absence of selection rule it is the same as in eq. (8.32). The spectral density would then be bounded by a function with the following asymptotics:

$$|\boldsymbol{\Delta}\rho^\epsilon_{i,n}(\vec{\alpha})| \lesssim |\vec{\alpha}|^{1-\Delta_*} \ . \tag{8.44}$$

Of course, this equation is understood in an averaged sense, and a detailed computation would make use of the integrated density analogous to eq. (8.31). Convergence of eq. (8.40) is then guaranteed in the limit under scrutiny as long as $\Delta_* > 1$, which is enforced by the spectral condition (7.14).

Let us finally point out that, running the previous argument for each connected correlator in eq. (8.41), the presence of the identity in the OPE implies that each individual energy level diverges linearly with Λ at all orders in perturbation theory.

---

[8] In practice, it can be easily verified by noticing that the OPE can be applied at the level of the generating function. Schematically, for the case where one subset Π of the insertions coalesce:

$$\mathcal{Z}_{|i\rangle} = \langle i|e^{\sum_m J(x_m)\mathcal{V}(x_m)}|i\rangle \to \langle\Omega|e^{\sum_{p\in\Pi} J(x_p)\mathcal{V}(x_p)}|\Omega\rangle\langle i|e^{\sum_{m\notin\Pi} J(x_m)\mathcal{V}(x_m)}|i\rangle \equiv \mathcal{Z}_\Pi\mathcal{Z}_{\bar{\Pi}} \ . \tag{8.42}$$

Since the generating function factorizes, its log splits into a sum, and the connected correlator immediately vanishes.

8.6 Degenerate spectra

The main formula presented in (8.1) applies to *any* AdS Hamiltonian regulated by a hard cutoff. However, the argument presented in chapter 8.4 and 8.5 is based on the fact that in perturbation theory, energies $\mathcal{E}_i$ are closely related to integrated correlation functions. To be precise, the n-th order contribution of the energy $\mathcal{E}_i$ is related to the n-point connected correlator of $V(\tau)$ in the state $|i\rangle$, as is shown in appendix G. This relation does not hold in degenerate perturbation theory, as we will briefly discuss here. Physically, theories with degenerate spectra are particularly important for Hamiltonian truncation in AdS$_2$, hence they deserve special attention. In 2d BCFTs degeneracies arise because of the very nature of Virasoro modules, and in theories of free bosons or fermions, degeneracies naturally arise from multi-particle states in Fock space.

For concreteness, we have in mind a unitary quantum theory where $g \geq 2$ states have the same unperturbed energy e_*. There are three different scenarios for the spectrum at non-zero coupling λ:

(i) the g-fold degeneracy is completely lifted at first order in perturbation theory;

(ii) the degeneracy is only fully lifted at some order $n \geq 2$ in perturbation theory;

(iii) the degeneracy is exact and present for any value of λ.

Let us focus on the first scenario, since it applies generically.[9] It is well-known that the appropriate eigenstates are eigenvectors $|\alpha\rangle$ of V restricted to the degenerate subspace $\mathscr{D}$, that is to say states satisfying

$$H_0\,|\alpha\rangle = e_*\,|\alpha\rangle \quad \text{and} \quad \langle\alpha|V|\beta\rangle = v_\alpha \delta_{\alpha\beta} \tag{8.45}$$

and the requirement that the degeneracy is lifted at first order means that all $v_\alpha \in \mathbb{R}$ must be different. The energies $\mathcal{E}_\alpha$ are then determined unambiguously, taking the form

$$\mathcal{E}_\alpha = e_* + \bar{\lambda} v_\alpha - \bar{\lambda}^2 e_\alpha^{(2)} + \bar{\lambda}^3 e_\alpha^{(3)} + \dots \tag{8.46}$$

for some coefficients $e_\alpha^{(n)}$ that can be determined using Rayleigh-Schrödinger perturbation theory. Using the shorthand notation $V_{\phi\psi} = \langle\phi|V|\psi\rangle$, the first two coefficients can be expressed as

$$e_\alpha^{(2)} = V_{\alpha\psi}\,\frac{1}{e_\psi - e_*}\,V_{\psi\alpha} \tag{8.47a}$$

---

[9] Case (ii) can happen when V explicitly breaks a symmetry of the unperturbed Hamiltonian, and (iii) is the hallmark of an unbroken symmetry/integrability, e.g. a boson or fermion perturbed by a mass term ϕ^2 or $\bar{\psi}\psi$.

and

$$e_\alpha^{(3)} = V_{\alpha\psi}\,\frac{1}{e_\psi - e_*}\,V_{\psi\phi}\,\frac{1}{e_\phi - e_*}\,V_{\phi\alpha} - v_\alpha \cdot V_{\alpha\psi}\,\frac{1}{(e_\psi - e_*)^2}\,V_{\psi\alpha} \\ - V_{\alpha\psi}\,\frac{1}{e_\psi - e_*}\,V_{\psi\beta}\,\frac{1}{v_\beta - v_\alpha}\,V_{\beta\phi}\,\frac{1}{e_\phi - e_*}\,V_{\phi\alpha}\,. \quad (8.47b)$$

In both (8.47a) and (8.47b) sums over intermediate states are implicit: sums over ψ, ϕ run over all states outside of $\mathscr{D}$, whereas the sum over β runs over all states in $\mathscr{D}$ except the state $|\alpha\rangle$ itself. As a matter of fact, the second-order energy $e_\alpha^{(2)}$ can be extracted from the connected correlation function

$$g_{\alpha,2}(\tau) = \langle\alpha|V(\tau)V(0)|\alpha\rangle - \langle\alpha|V|\alpha\rangle^2 \qquad (8.48)$$

exactly like in the case of non-degenerate quantum mechanics. However, the term in the second line of (8.47b) appearing in the second line of the third-order energy (8.47b) is qualitatively different. For one, it features four insertions of the matrix V, hence $e_\alpha^{(3)}$ is at best related to a four-point function of $V(\tau)$ inside the state $|\alpha\rangle$. More importantly, one of the factors appearing on the second line of (8.47b) has $1/(v_\beta - v_\alpha)$ as a denominator. Such a denominator cannot arise from a correlation function of $V(\tau)$ in the interaction picture, obeying $\partial_\tau V(\tau) = [H_0, V(\tau)]$. We conclude that in general, the $e_\alpha^{(n)}$ cannot be expressed in terms of connected correlators of $V(\tau)$.

Nevertheless, it appears that the prescription (8.1) correctly predicts the spectra of AdS theories with degenerate unperturbed spectra. It is not difficult to check the prescription up to low orders in perturbation theory (for example in the case of a massive scalar with integer Δ).[10] In section 10.4, the ϵ deformation of the $2d$ Ising model is studied; it is again degenerate at zero coupling, but its degeneracies are partially resolved at finite coupling. This RG flow is studied using Hamiltonian truncation, and the results agree well with analytic predictions (up to truncation errors), see figure 10.10. The other Virasoro theories featured in this work also have denegeracies, but since they aren't exactly solvable, one cannot explicitly check the prescription (8.1) *a posteriori*.

In summary, there is no reason to doubt that the prescription (8.1) predicts correct spectra for the case of degenerate AdS spectra, but we have not found a simple modification of the proof from the non-degenerate case. We leave this problem open for future work.[11]

---

[10] For generic Δ, the degeneracies present in the spectrum spectrum of the free massive scalar theory persist when a ϕ^2 interaction is turned on. When Δ is an integer there are additional degeneracies that are lifted by a ϕ^2 deformation.

[11] In the presence of degeneracies, it is tantalizing to split the Hamiltonian $H = H_0 + \lambda V$ into two pieces as $H = \tilde{H}_0 + \lambda\tilde{V}$, where $\tilde{H}_0 = H_0 + \lambda \mathrm{P}V\mathrm{P}$ and $\tilde{V} = V - \mathrm{P}V\mathrm{P}$, where P projects onto a degenerate subspace. The new unperturbed Hamiltonian $\tilde{H}_0$ is now non-degenerate when $\lambda \neq 0$. One can try to rederive the prescription by treating $\tilde{V}$ as a perturbation instead of V.

8.7 Truncation errors

In the previous sections, we have discussed in detail a procedure that is needed to study AdS Hamiltonians using a hard energy cutoff. In particular, we showed that the standard TCSA prescription — fixing a cutoff Λ and subtracting the Casimir energy — predicts wrong energy spectra. Given the correct prescription (8.1), Hamiltonian truncation in AdS is still an approximation, since one necessarily works at some finite cutoff Λ. In this section, we estimate the error on the energy levels due to this truncation, comparing the situation in AdS to the better-understood problem of Hamiltonian truncation on finite volume spaces.

The basic result we will work towards is closely related to the discussion from section 8.4 and its generalization to higher orders in perturbation theory from section 8.5. Concretely, let's consider the second-order contribution of some interaction $\bar{\lambda} V$ to the i-th energy level, working at cutoff Λ:

$$\begin{aligned} \boldsymbol{\Delta}\mathcal{E}_i(\Lambda) &:= \mathcal{E}_i(\Lambda) - \mathcal{E}_{\text{vac}}(\Lambda - e_i) \\ &= e_i + \bar{\lambda}\langle i|V|i\rangle + \sum_{n=2}^{\infty}(-1)^{n+1}\bar{\lambda}^n \boldsymbol{\Delta} c_{i,n}(\Lambda) \ , \end{aligned} \tag{8.49a}$$

where the first cutoff-dependent term is given by

$$\boldsymbol{\Delta} c_{i,2}(\Lambda) = \int^{\Lambda} \frac{d\alpha}{\alpha - e_i}\, \boldsymbol{\Delta}\rho_{i,2}(\alpha - e_i) \ . \tag{8.49b}$$

Here, we use the definition (8.28) for the shifted spectral density $\boldsymbol{\Delta}\rho_{i,2}(\alpha)$. Likewise, the higher-order coefficients $\boldsymbol{\Delta} c_{i,n}(\Lambda)$ can be expressed in terms of spectral densities $\boldsymbol{\Delta}\rho_{i,n}(\vec{\alpha})$. In contrast to the previous sections, here we no longer consider a spatial cutoff ϵ, working in full AdS$_2$ with $\epsilon = 0$ throughout. In an otherwise UV-finite theory, the energy gap $\boldsymbol{\Delta}\mathcal{E}_i(\Lambda)$ has a finite limit as $\Lambda \to \infty$, so the cutoff error is given by tails of spectral integrals:

$$\text{cutoff error} = \boldsymbol{\Delta}\mathcal{E}_i(\infty) - \boldsymbol{\Delta}\mathcal{E}_i(\Lambda) = -\bar{\lambda}^2 \int_{\Lambda}^{\infty} \frac{d\alpha}{\alpha - e_i}\, \boldsymbol{\Delta}\rho_{i,2}(\alpha - e_i) + \mathrm{O}(\bar{\lambda}^3). \tag{8.50}$$

If we can bound integrals like (8.50), we immediately obtain the desired error estimates for energy gaps in AdS$_2$. But this is precisely what we did in section 8.4, using the crucial eq. (8.36). Recall that this equation follows from considering the leading non-trivial contribution to the OPE of figure 8.5, coming from a boundary operator $\Psi(\tau)$ of dimension Δ_*. We should expect the bound to be saturated, generically, and therefore we obtain an error of the order

$$\boldsymbol{\Delta}\mathcal{E}_i(\infty) - \boldsymbol{\Delta}\mathcal{E}_i(\Lambda) \underset{\Lambda\to\infty}{\sim} \frac{c_i}{\Lambda^{\Delta_* - 1}} \ . \tag{8.51}$$

In light of the discussion in section 8.5, we expect eq. (8.51) to be true at all orders in

$\bar{\lambda}$. The state-dependent coefficient $c_i(\bar{\lambda})$ encodes the large-α asymptotics of the densities $\boldsymbol{\Delta}\rho_{i,n}(\alpha)$. For instance, eq. (9.21) gives c_1, the coefficient of the first excited state for a free massive boson, at second order in perturbation theory. More generally, c_i can be determined in perturbation theory following the computations of appendix H.2 – see in particular formula (H.31). For later reference, we mention that c_i is proportional to the boundary OPE coefficient $C_{\mathcal{O}_i\mathcal{O}_i\Psi}$ (up to a number that depends on $\mathcal{V}$ and Ψ but not on the state $|i\rangle$), where $\mathcal{O}_i(\tau)$ is the boundary operator corresponding to the state $|i\rangle$.

Now, by assumption there are no boundary states of dimension ≤ 1 — otherwise, the Hamiltonian is IR-divergent to begin with — hence error terms of the form (8.51) always vanish as the cutoff is removed, but when the exponent $\Delta_* - 1$ is small, they can be important. In particular, the identity module in Virasoro minimal models in AdS$_2$ contains a state with $\Delta_* = 2$ that describes the displacement operator, leading to a $1/\Lambda$ error. For theories of massive particles in the bulk of AdS, the dimension Δ_* of the leading boundary state depends on the particle's mass (in units of the AdS radius): the heavier the bulk particle is taken to be, the smaller the error (8.51) will be.

We stress that eq. (8.51) is true asymptotically, that is to say for Λ bigger than some cutoff scale Λ_0 which is *a priori* unknown. In particular, if Hamiltonian truncation computations only probe cutoffs below Λ_0, the formula in question does not necessarily predict the order of magnitude of actual cutoff errors. Nonetheless, the formula (8.51) is consistent with all of the computations performed in the present work.

It is natural to ask whether the error (8.51) can be removed by adding so-called *improvement terms* to the Hamiltonian. These would be proportional to either boundary or (integrated) bulk operators, with cutoff-dependent coefficients that vanish as $\Lambda \to \infty$, and their role would be precisely to cancel large truncation errors in observables. Indeed, since c_i only depends on the state $|i\rangle$ through the OPE coefficient $C_{\mathcal{O}_i\mathcal{O}_i\Psi}$, it should be possible to remove the error (8.51) by adding a term to the Hamiltonian of the form

$$H \mapsto H + \frac{\xi_\Psi \bar{\lambda}^2}{\Lambda^{\Delta_*-1}} \Psi(\tau = 0) + \dots \tag{8.52}$$

for some computable coefficient ξ_Ψ. As follows from eq. (H.31), the coefficient ξ_Ψ is theory-dependent: it's related to the integrated bulk-bulk-boundary correlator $\langle \mathcal{V}\mathcal{V}\Psi\rangle$, which is not fixed by conformal symmetry alone. We have not undertaken this exercise in the present work, but it looks like an important step to take with the goal of performing high-precision Hamiltonian truncation computations in the future, especially in the case of Virasoro minimal models.

As we emphasized, eq. (8.51) captures the contribution of the bundary of AdS to the truncation error. However, the large α behavior of the spectral density is also influenced by bulk contributions. Equivalently, the bulk OPE contributes non-analytic terms in τ to the correlation functions (8.15). Let us focus again on the second order in perturbation theory. The singularities in question are in one-to-one correspondence with operators appearing in the $\mathcal{V}\times\mathcal{V}$ OPE (taking the UV theory to be conformal for concreteness). Indeed, suppose that $\mathcal{V}\times\mathcal{V}$ contains an operator $\tilde{\mathcal{V}}$ of dimension $\Delta_{\tilde{\mathcal{V}}}$. Then, as discussed in appendix H.2 – see in particular eq. (H.42) – the subtracted two-point function of the potential is expected to receive at small τ a contribution of the following kind:

$$\langle i|V(\tau)V(0)|i\rangle_{\text{conn}} - \langle\Omega|V(\tau)V(0)|\Omega\rangle_{\text{conn}} \underset{\tau\to 0}{\sim} \tau^{1-2\Delta_{\mathcal{V}}+\Delta_{\tilde{\mathcal{V}}}}\,. \tag{8.53}$$

Such terms have nothing to do with the geometry of AdS: they are also present if one quantizes the same theory on the cylinder $\mathbb{R}\times S^1$, see for example [40]. When eq. (8.53) gives the leading small τ behavior, the energy gaps have errors that go as

$$\boldsymbol{\Delta}\mathcal{E}_i(\infty) - \boldsymbol{\Delta}\mathcal{E}_i(\Lambda) \underset{\Lambda\to\infty}{\sim} \frac{d_i}{\Lambda^h}, \qquad h = \Delta_{\tilde{\mathcal{V}}} - 2\Delta_{\mathcal{V}} + 2 \tag{8.54}$$

for some coefficient d_i which is proportional to the matrix element $\langle i|\tilde{\mathcal{V}}(\tau = 0, r)|i\rangle$, integrated over a timeslice. Here the exponent h only depends on the UV properties of the theory: it does not depend on the choice of boundary conditions, for instance. By definition, $h > 0$ in a UV-finite theory, as is the case for all theories discussed in the present work, so errors of the above type vanish as the cutoff is removed. Nevertheless, a word of caution is in order about eq. (8.53): boundary effects might modify it when the integral of $\langle i|\tilde{\mathcal{V}}|i\rangle$ over a time slice diverges. In appendix H.2, the precise conditions are discussed. In the rest of the work, the bulk OPE will cause the leading truncation error only for the ϕ^4 deformation of a free massive scalar, see section 9.2. In that case, this boundary enhancement does not take place.[12]

Truncation errors coming from bulk singularities can also be removed by adding local counterterms to the Hamiltonian, i.e. by modifying H as follows:

$$H \mapsto H + \frac{c_{\tilde{\mathcal{V}}}\bar{\lambda}^2}{\Lambda^h}\int_{-\pi/2}^{\pi/2}\frac{dr}{(\cos r)^2}\,\tilde{\mathcal{V}}(\tau = 0, r) + \dots \tag{8.55}$$

for some computable coefficient $c_{\tilde{\mathcal{V}}}$. For CFTs quantized on $\mathbb{R}\times S^{d-1}$, these counterterms were discussed in detail in [40] (and in the $d = 2$ case before in [164] and [165]). A detailed discussion for the massive scalar on $\mathbb{R}\times S^1$ is presented in [41] and related works [166–168]. In this thesis, we will not actually add improvement terms of the form (8.55), so we will not discuss Hamiltonians of the above form in detail. The computation of the coefficient $c_{\tilde{\mathcal{V}}}$ would go along the same lines as computations from the literature, apart from an integration over an (infinite-volume) timeslice of AdS$_2$, contrasting with the computation on S^1 from [166].[13]

---

[12] However, when h is integer, $h = 2$ in this case, the scaling (8.54) is typically enhanced by logarithms, and in fact we will find the error to go as $\ln(\Lambda)/\Lambda^2$.

[13] The computation on S^1 is simpler for an additional reason, namely the $U(1)$ global symmetry that acts by translations on the spatial circle, which is absent in AdS.

9 Deformations of a free massive scalar

After the general discussion of Hamiltonian truncation in the previous chapters, we will now turn to a concrete quantum field theory: a massive scalar ϕ, described by the action:

$$S = \int d^2x\sqrt{g}\left(\frac{1}{2}(\partial_\mu\phi)^2 + \frac{1}{2}m^2\phi^2 + \frac{\kappa}{2}\mathbf{R}\phi^2 + \text{local interactions}\right) , \tag{9.1}$$

where $\mathbf{R} = -2/R^2$ is the scalar curvature of AdS$_2$. The curvature coupling κ is arbitrary, but since the curvature is constant, any shift in κ can be reabsorbed into the definition of m^2, and henceforth we will set $\kappa = 0$. The free theory was briefly treated in section 8.1; here we will discuss the quantization in slightly more detail. We recall that $\phi(\tau, r)$ has a mode decomposition

$$\phi(\tau = 0, r) = \sum_{n=0}^{\infty} f_n(r)(a_n + a_n^\dagger) \tag{9.2}$$

with creation and annihilation operators that obey canonical commutation relations

$$[a_m, a_n^\dagger] = \delta_{mn} \ . \tag{9.3}$$

The mode functions $f_n(r)$ are given by

$$f_n(r) = \sqrt{\frac{4^\Delta}{4\pi}\frac{\Gamma^2(\Delta)}{\Gamma(2\Delta)}}\sqrt{\frac{n!}{(2\Delta)_n}}\,(\cos r)^\Delta\, C_n^\Delta(\sin r) \ . \tag{9.4}$$

Here Δ is a positive root of $\Delta(\Delta-1) = m^2R^2$ and $C_n^\nu(\cdot)$ denotes a Gegenbauer polynomial. The free Hamiltonian H_0 is given in (8.3), and from it we can deduce that the n-th mode $a_n^\dagger$ has energy $\Delta + n$.

As a consistency check of the above, we find that the Green's function of the field ϕ is given by

$$\langle\Omega|\mathrm{T}\phi(\tau,r)\phi(\tau',r')|\Omega\rangle = \frac{1}{4\pi}\frac{\Gamma^2(\Delta)}{\Gamma(2\Delta)}\,\xi^{-\Delta}\,{}_2F_1\left[\begin{matrix}\Delta,\Delta\\ 2\Delta\end{matrix}\,\middle|\,-\frac{1}{\xi}\right] =: G(\xi) \tag{9.5}$$

where ξ is the cross ratio from Eq. (7.8). This result could also have been derived directly, by looking for $SL(2,\mathbb{R})$-invariant solutions of the equation of motion with the correct boundary conditions.

In what follows, we will analyze the scalar theory in AdS$_2$ with the following interaction terms turned on:

$$S = S_0 + \int_{\mathrm{AdS}_2}(\lambda_2\phi^2 + \lambda_4\phi^4 + \ldots) \tag{9.6}$$

where the ... can denote any local bulk interaction (not necessarily $\mathbb{Z}_2$-even, and possibly containing derivatives). In the Hamiltonian language, these interactions read

$$H = H_0 + \bar{\lambda}_2 V_2 + \bar{\lambda}_4 V_4 + \ldots \tag{9.7}$$

where[1]

$$\bar{\lambda}_n := \lambda_n R^2 \quad \text{and} \quad V_n := \int \frac{dr}{(\cos r)^2} :\phi^n(\tau=0,r):. \tag{9.8}$$

The operators H, V_n etc. act on the Hilbert space of the free theory, which is the Fock space generated by the modes $\{a_n^\dagger\}_{n=0}^\infty$. Its states can be labeled as follows

$$|\psi\rangle = \frac{1}{\mathcal{N}_{|\psi\rangle}}\prod_{k\geq 0}(a_k^\dagger)^{n_k}|\Omega\rangle\,, \qquad \mathcal{N}_{|\psi\rangle} = \sqrt{\textstyle\prod_{k\geq 0} n_k!}\,. \tag{9.9}$$

The factor $\mathcal{N}_{|\psi\rangle}$ has been chosen to make such a state unit-normalized. A state of the form (9.9) has energy

$$H_0|\psi\rangle = e_{|\psi\rangle}|\psi\rangle\,, \quad e_{|\psi\rangle} = \sum_{k\geq 0} n_k(\Delta + k)\ . \tag{9.10}$$

In Hamiltonian truncation, we keep only states with energy $e \leq \Lambda$ below a cutoff Λ. Since the spectrum of H_0 is discrete, this means that H becomes a finite matrix, denoted by $H(\Lambda)$. If we let $\{|\psi_i\rangle\}$ be a basis of low-energy states, then the matrix elements of $H(\Lambda)$ have the following form:

$$H(\Lambda)_{ij} = \langle\psi_i|H_0|\psi_j\rangle + \bar{\lambda}_2\langle\psi_i|V_2|\psi_j\rangle + \ldots = e_{|\psi_i\rangle}\delta_{ij} + \bar{\lambda}_2\langle\psi_i|V_2|\psi_j\rangle + \ldots \tag{9.11}$$

Finally, the spectrum of H can be approximated by explicitly diagonalizing $H(\Lambda)$ for sufficiently large values of Λ. We will explore this for both a ϕ^2 and a ϕ^4 deformation in the next sections.

---

[1] Here normal ordering simply means moving annihilation operators to the right, e.g. $:a_1^\dagger a_1 a_2^\dagger: = a_2^\dagger a_1^\dagger a_1$.

9.1 ϕ^2 deformation

In this section, we study the ϕ^2 deformation, meaning that in (9.6) we allow for an arbitrary value of $\lambda = \lambda_2$, but all other couplings are set to zero. Since this theory is exactly solvable, it provides a way to test the proposed diagonalization procedure in a controlled setting. To be precise, the spectrum of the theory with $\lambda \neq 0$ is that of a free theory with redefined mass $m^2 \to m^2 + 2\lambda$, or equivalently

$$\Delta \to \Delta(\bar{\lambda}) = \frac{1}{2} + \sqrt{(\Delta - \tfrac{1}{2})^2 + 2\bar{\lambda}}\ . \tag{9.12}$$

The spectrum of the theory with coupling $\lambda \neq 0$ consists of single-particle states with energy $\Delta(\bar{\lambda}) + \mathbb{N}_0$ – $\mathbb{N}_0$ being the set of non-negative integers – two-particle states with energies $2\Delta(\bar{\lambda}) + \mathbb{N}_0$ (most of which are degenerate), and likewise there are n-particle states of energy $n\Delta_{\bar{\lambda}} + \mathbb{N}_0$ for any integer n. The energy $\Delta(\bar{\lambda})$ can be computed in perturbation theory; expanding (9.12) in a Taylor series around $\lambda = 0$, we find that Rayleigh-Schrödinger perturbation theory converges if and only if

$$|\bar{\lambda}| < \lambda_\star(\Delta) = \frac{1}{2}\left(\Delta - \frac{1}{2}\right)^2 . \tag{9.13}$$

For couplings larger than $\lambda_\star(\Delta)$, the correct spectrum can only be computed nonperturbatively.

In order to set up the Hamiltonian truncation, it will be convenient to express V_2 in terms of creation and annihilation operators

$$V_2 = \sum_{m,n=0}^{\infty} A_{mn}(\Delta)(a_m^\dagger a_n^\dagger + 2a_m^\dagger a_n + a_m a_n)\ , \tag{9.14}$$

with coefficients

$$A_{mn}(\Delta) = \int_{-\pi/2}^{\pi/2} \frac{dr}{\cos^2 r}\, f_m(r) f_n(r) = \frac{\mathscr{V}_{mn}(\Delta)}{2\Delta - 1}\ , \tag{9.15}$$

where the matrix $\mathscr{V}_{mn}$ is computed in appendix F.3, and we report here the result for convenience:

$$\mathscr{V}_{mn}(\Delta) = \begin{cases} 0 & \text{if } m+n \text{ is odd;} \\ \sqrt{(m+1)_{n-m}/(2\Delta+m)_{n-m}} & m \leq n,\ m+n \text{ even;} \\ \mathscr{V}_{nm}(\Delta) & m > n. \end{cases} \tag{9.16}$$

An algorithm that can be used to compute and diagonalize $H(\Lambda)$ is described in great detail in appenidx I. In what follows, we will simply discuss the results of various numerical computations. In particular, we will check whether the spectrum of $H(\Lambda)$ reproduces the exact spectrum predicted by Eq. (9.12).

Before turning to the numerical results, let us comment on the role of discrete symmetries. Both the ϕ^2 and ϕ^4 interactions are invariant under parity $\mathtt{P}$ and the $\mathbb{Z}_2$ symmetry $\mathscr{Z} : \phi \to -\phi$. The individual creation operators $a_k^\dagger$ have quantum numbers $(-1)^k$ under parity and -1 under $\mathscr{Z}$.[2] Therefore, a Fock space state $|\psi\rangle = |n_0, n_1, n_2, \ldots\rangle$ has quantum numbers

$$\mathtt{P}\,|\psi\rangle = (-1)^{\pi_\psi}\,|\psi\rangle\,, \quad \mathscr{Z}\,|\psi\rangle = (-1)^{z_\psi}\,|\psi\rangle\,, \quad \text{for} \quad \pi_\psi = \sum_{k\geq 0} k n_k, \quad z_\psi = \sum_{k\geq 0} n_k\,. \tag{9.17}$$

Given these symmetries, the diagonalization of $H(\Lambda)$ can be performed independently in the four different sectors of Hilbert space that contain states with quantum numbers $\mathtt{P} = \pm 1$ and $\mathscr{Z} = \pm 1$. Notice that the Casimir energy is determined by the vacuum state which has quantum numbers $\mathtt{P} = \mathscr{Z} = +1$, so this sector plays a special role. For fixed Λ and fixed couplings $\lambda_2, \ldots$, eigenvalues of $H(\Lambda)$ corresponding to *different* symmetry sectors are expected to cross. However, we stress that the physical energies are not quite the eigenvalues of $H(\Lambda)$: the Casimir energy needs to be subtracted from the individual levels, in accordance to the discussion in chapter 8.

Cutoff effects

As mentioned in section 8.1, one expects that the vacuum energy $\mathcal{E}_\Omega(\Lambda)$ grows linearly with the cutoff Λ. We can check this both perturbatively (by means of a Rayleigh-Schrödinger computation at second order in λ^2) and non-perturbatively, using Hamiltonian truncation. Details for the perturbative computation are given in appendix G.3. The result of both computations is shown in Figure 9.1. For concreteness, we take the single-particle energy in the free theory to be $\Delta = 1.62$.[3] For the nonperturbative plot on the right hand side we have set $\bar\lambda = 2$, beyond the radius of convergence of perturbation theory (9.13). By eye, the linear growth of $\mathcal{E}(\Lambda) \underset{\Lambda\to\infty}{\sim} \Lambda$ can easily be seen in both cases.

Next, we can study the energy shift of the first excited state $|\chi\rangle = a_0^\dagger\,|\Omega\rangle$. From (9.12), we see that

$$\Delta_\chi(\lambda) = \Delta + \frac{\bar\lambda}{\Delta - \frac{1}{2}} - c_\chi \bar\lambda^2 + \mathrm{O}(\bar\lambda^3), \qquad c_\chi = \frac{4}{(2\Delta-1)^3}\,. \tag{9.18}$$

We can first of all reproduce this result analytically, using Rayleigh-Schrödinger perturbation theory. This involves computing the difference $g_\chi(\tau)$ of the connected two-point correlators of V_2 inside the state $|\chi\rangle$ and the vacuum. For details, we refer to Appendix G; the exact function $g_\chi(\tau)$ is spelled out in eq. (G.68). Integrating this correlator over τ

---

[2] For the V_2 interaction, parity invariance follows from the fact that the coefficients $A_{mn}(\Delta)$ from (9.15) vanish if $m+n$ is odd.

[3] This corresponds to a mass $m^2R^2 = \Delta(\Delta-1) \approx 1$, so a mass ≈ 1 in units of the AdS radius.

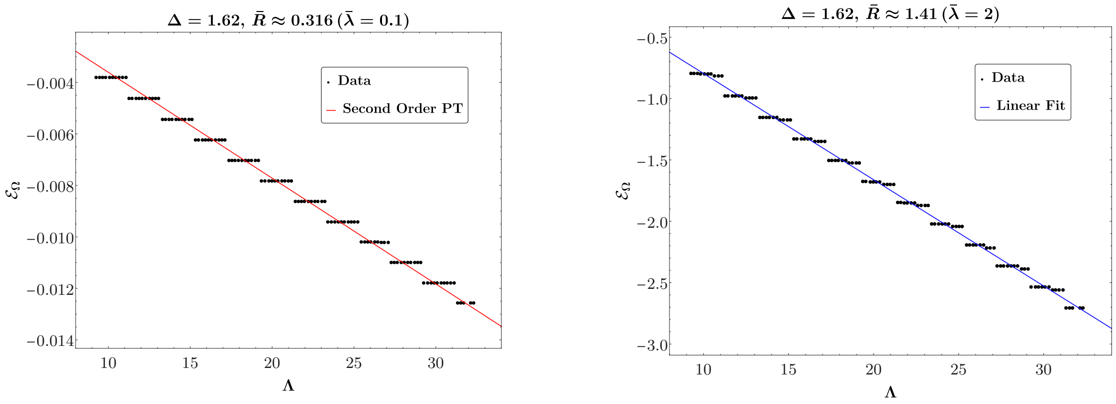

Figure 9.1: The vacuum energy linear growth in cutoff. The left plot shows the agreement of the data with second order perturbation theory. The right plot shows the linear growth beyond perturbation theory ($\bar{\lambda} = 2$). $\bar{R}$ is the radius of AdS in units of the coupling, as defined in eq. (7.24).

reproduces the exact result, as it should. At small τ, the function $g_\chi(\tau)$ behaves as

$$g_\chi(\tau) \underset{\tau\to 0}{\sim} -\frac{2\pi}{(\Delta - \frac{1}{2})\sin(2\pi\Delta)}\,\tau^{2\Delta-2} + \text{analytic} + \mathrm{O}(\tau^{2\Delta-1}). \tag{9.19}$$

While a logarithmic singularity appears for integer Δ, here we will assume for simplicity that Δ is generic (and $\Delta > 1$). The expression (9.19) can be used to deduce the large-Λ behavior of Hamiltonian truncation. Indeed, the Laplace transform of $g_\chi(\tau)$ must behave as

$$\boldsymbol{\Delta}\rho_\chi(\alpha) \underset{\alpha\to\infty}{\sim} \frac{\Gamma(2\Delta)}{(\Delta - \frac{1}{2})^2}\,\alpha^{1-2\Delta}, \quad g_\chi(\tau) = \int_0^\infty d\alpha\, e^{-(\alpha-\Delta)\tau}\,\boldsymbol{\Delta}\rho_\chi(\alpha) \tag{9.20}$$

so the cutoff error can be estimated to be

$$\bar{\lambda}^2 \int_\Lambda^\infty \frac{d\alpha}{\alpha - \Delta}\,\boldsymbol{\Delta}\rho_\chi(\alpha) \underset{\Lambda\to\infty}{\sim} \frac{\Gamma(2\Delta-1)}{(\Delta-\frac{1}{2})^2}\,\frac{\bar{\lambda}^2}{\Lambda^{2\Delta-1}}. \tag{9.21}$$

This convergence rate is in complete agreement with the discussion from section 8.7, since the lowest-dimension boundary state that can be generated is the two-particle state with dimension 2Δ. We therefore predict that at finite cutoff Λ, we measure an energy gap

$$\begin{aligned}\boldsymbol{\Delta}\mathcal{E}_\chi &= e_\chi + \frac{\bar{\lambda}}{\Delta - \frac{1}{2}} - \bar{\lambda}^2\left(c_\chi - \frac{\Gamma(2\Delta-1)}{(\Delta-\frac{1}{2})^2}\,\frac{1}{\Lambda^{2\Delta-1}} + \dots\right) + \mathrm{O}(\bar{\lambda}^3)\\ &\approx 1.62 + 0.893\bar{\lambda} - \bar{\lambda}^2\left(0.356 - \frac{0.898}{\Lambda^{2.24}} + \dots\right) + \mathrm{O}(\bar{\lambda}^3)\end{aligned} \tag{9.22}$$

plugging in $\Delta = 1.62$ when passing from the first to the second line.

In the left plot of figure 9.2, we compare Eq. (9.22) to Hamiltonian truncation data, setting $\bar{\lambda} = 0.1$ such that terms of order $\bar{\lambda}^3$ and higher are subleading. We find excellent agreement between the numerical results and the analytical prediction (9.22). This agreement relies crucially on the prescription (8.1): without the correct subtraction of the Casimir energy, there would be a mismatch of order $\mathrm{O}(1) \times \bar{\lambda}^2$. The second excited state is the first $SL(2,\mathbb{R})$ descendent of $|\chi\rangle$, namely $|\chi'\rangle = a_1^\dagger\,|\Omega\rangle$, which in the full theory has energy $\boldsymbol{\Delta}\mathcal{E}_{\chi'} = \boldsymbol{\Delta}\mathcal{E}_{\chi} + 1$: we will come back to this state in the next paragraph. After that, the third excitated state is $(a_0^\dagger)^2\,|\Omega\rangle$, which describes two particles at rest. In the right plot of figure 9.2, we compare Hamiltonian truncation data for this state to the exact result $\boldsymbol{\Delta}\mathcal{E} = 2\Delta(\bar{\lambda})$.

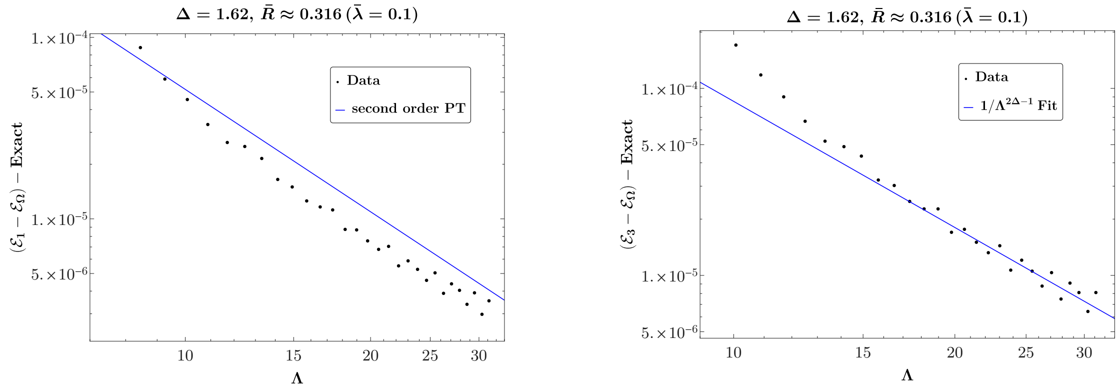

Figure 9.2: Log–log plot of Hamiltonian truncation deviation from the exact value as a function of the cutoff Λ for coupling $\bar{\lambda} = 0.1$. The left plot shows the convergence for the first excited state with the blue line equal to $-\bar{\lambda}^2 \frac{0.898}{\Lambda^{2.24}}$ extracted from eq. (9.22). The right plot shows the convergence for the third excited state corresponding to a state with two particles at rest. The blue line is a single parameter fit $\frac{a}{\Lambda^{2.24}}$.

An additional test of the truncation procedure involves computing differences of energies between a primary state and its descendants. As a consequence of $SL(2,\mathbb{R})$ invariance, such differences must be exactly integer. However, the truncation breaks the $SL(2,\mathbb{R})$ symmetry, which can only be recovered in the continuum $\Lambda \to \infty$. We expect that the energy of the second state in the spectrum $|\chi'\rangle = a_1^\dagger\,|\Omega\rangle$ scales as

$$\boldsymbol{\Delta}\mathcal{E}_{\chi'}(\Lambda) - \boldsymbol{\Delta}\mathcal{E}_{\chi}(\Lambda) \underset{\Lambda\to\infty}{\sim} 1 + \frac{a}{\Lambda^b} + \dots \tag{9.23}$$

for some power $b > 0$ and some coefficient a. In figure 9.3, we check this prediction numerically for different values of the coupling $\bar{\lambda}$. Both for small ($\bar{\lambda} = 0.1$) and large ($\bar{\lambda} = 2$) values of the coupling, we observe that $SL(2,\mathbb{R})$ is restored in the continuum; however, the plots show that this phenomenon is slower for the larger values of the coupling. In passing, let us mention that it would be interesting to predict the coefficients a, b appearing in (9.23), by analyzing the $SL(2,\mathbb{R})$ breaking directly. We have not studied this problem in more detail in the present work.

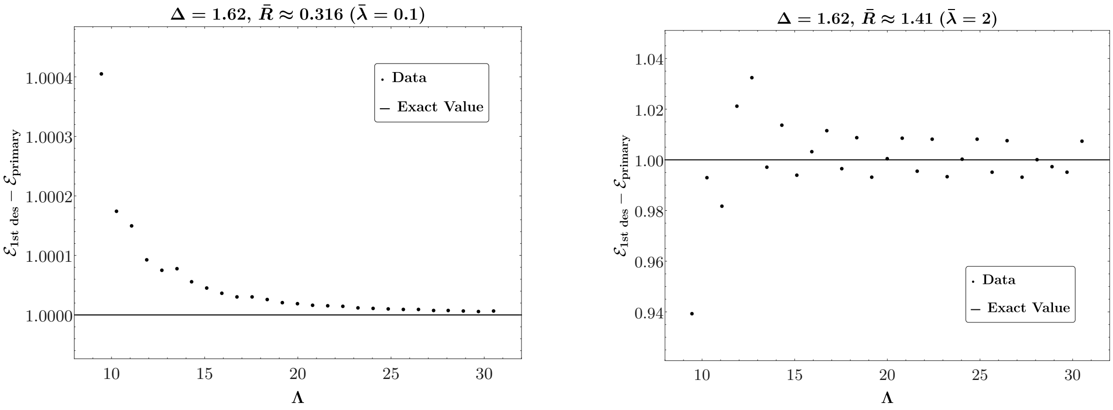

Figure 9.3: Difference of energies between the first primary state $|\chi\rangle$ and its first descendant, verifying that the $SL(2,\mathbb{R})$ spacetime symmetry of AdS is restored in the continuum limit $\Lambda \to \infty$.

Spectrum

So far, we have checked in some examples that with the prescription (8.1), Hamiltonian truncation in AdS agrees with exact results in the limit where the cutoff Λ is sent to infinity. At this point, we can be more systematic and compute the first six energy levels of the ϕ^2 theory for a range of couplings, once more comparing the numerical data to exact results. The results are shown in figure 9.4. Dots correspond to Hamiltonian truncation data; the solid curves are the exact values. This plot probes couplings beyond the perturbation theory radius of convergence $\lambda_\star(\Delta)$, which for $\Delta = 1.62$ equals $\lambda_*(1.62) \approx 0.63$. To show the breakdown of perturbation theory, we have in addition plotted the energy of the state $|\chi\rangle$ computed up to order $\bar{\lambda}^2$ (shown in red) resp. $\bar{\lambda}^3$ (green) in perturbation theory; it is clear that these perturbative curves deviate from the exact levels when $\bar{\lambda} \gtrsim \lambda_\star(\Delta)$. In contrast, the Hamiltonian truncation data agrees with the exact data within error bars also for larger values of $\bar{\lambda}$. Finally, we want to mention that differences between energies are indeed approximately integer, in accordance with $SL(2,\mathbb{R})$ symmetry.

In figure 9.4, we notice crossings between one- and two-particle states, shown in black resp. blue. These states have different quantum numbers: one-particle states have $\mathcal{Z} = -1$, whereas the blue curves have $\mathcal{Z} = 1$. Therefore, there is no level repulsion even at finite cutoff.

The data points in the above plot are extracted from "raw" Hamiltonian truncation data, computed at some finite cutoff Λ, by extrapolating to $\Lambda = \infty$. Let us explain in some detail the procedure that is used to go from unprocessed eigenvalues to these extrapolated data with error bars. For the n-th excited state $\boldsymbol{\Delta}\mathcal{E}_n$, we gather a sequence of energies $\{\boldsymbol{\Delta}\mathcal{E}_n(\Lambda) \mid \Lambda \leq \Lambda_{\max}\}$ by varying the cutoff Λ, going up to some maximal cutoff $\Lambda_{\max}$.

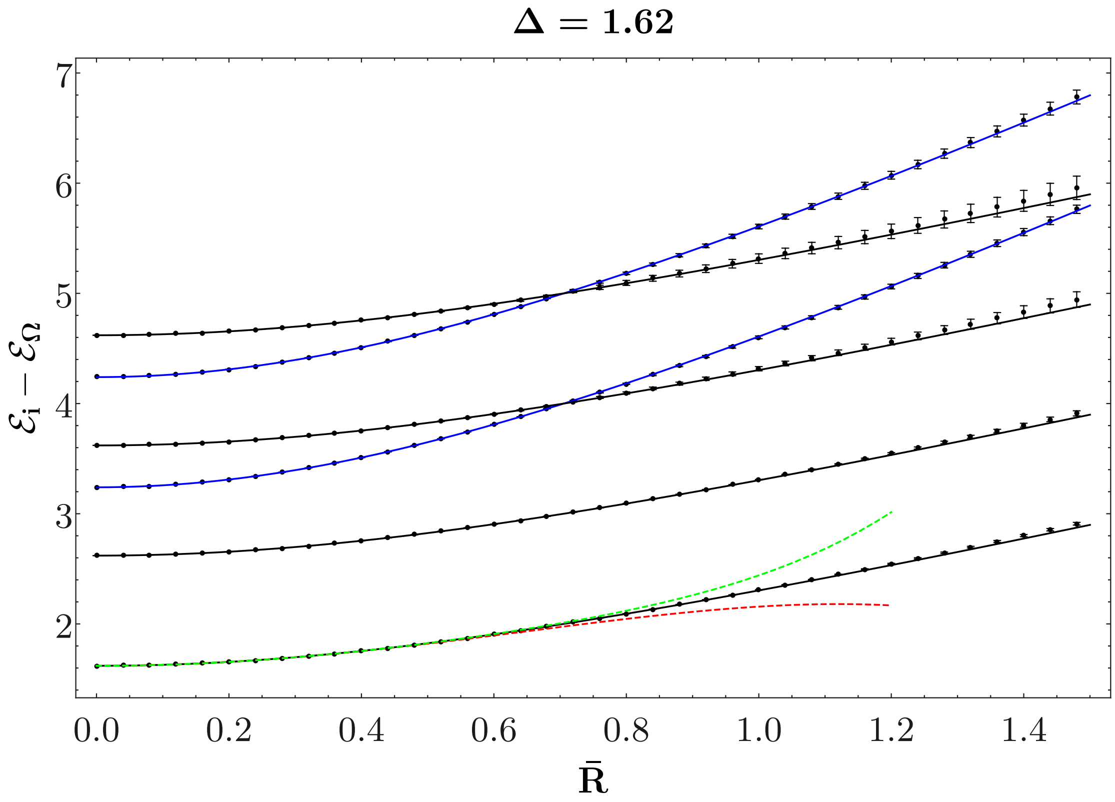

Figure 9.4: Spectrum of the first six excited energies in the ϕ^2 theory with $\Delta = 1.62$. Dots with error bars: Hamiltonian truncation data. Black and blue solid curves represent the exact spectrum; the red and green dashed lines are exact results for the first level, truncated to second resp. third order in perturbation theory. The black curves are the one-particle state $|\chi\rangle$ and its first three descendants; the blue curves are the two-particle state $(a_0^\dagger)^2 |\Omega\rangle$ and its first descendant.

We then fit this sequence to the function

$$\boldsymbol{\Delta}\mathcal{E}_n(\Lambda|\Lambda_{\max}) \approx a_n(\Lambda_{\max}) + \frac{b_n(\Lambda_{\max})}{\Lambda^{2\Delta-1}} \tag{9.24}$$

which gives an optimal value of $a_n(\Lambda_{\max})$, the energy in the limit $\Lambda \to \infty$. There are two sources of error associated to this procedure:

- For a given cutoff $\Lambda_{\max}$, the truncation data don't exactly match the fit (9.24). This is the usual χ^2 or goodness-of-fit error, caused by the fact that we are only taking the leading cutoff error $1/\Lambda^{2\Delta-1}$ into account. The size of this error can be extracted from the `ParameterTable` option of `NonLinearModelFit` in `Mathematica`.
- The restriction to cutoffs up to $\Lambda_{\max}$ is arbitrary: if we changed $\Lambda_{\max}$ by one or several units, the fit procedure would lead to a different extrapolated energy a_n. By computing a_n for a range of maximal cutoffs $\Lambda_{\max}$, we can obtain an estimate

for the uncertainty associated to this phenomenon.

The total error bar we assign to an energy $\mathcal{E}_n$ is the sum of these uncertainties.

9.2 ϕ^4 flow

So far, we have discussed in detail Hamiltonian truncation result for the ϕ^2 flow in AdS$_2$. This flow is exactly solvable, so it provided a good laboratory to test the prescription (8.1). It is of course more interesting to study flows that are *not* exactly solvable, like the ϕ^4 interaction. To be precise, we will consider Hamiltonians of the form (9.7) with $\bar{\lambda}_4 \neq 0$. The two-dimensional ϕ^4 flow has already been studied in detail using Hamiltonian truncation, but on $\mathbb{R} \times S^1$ (see [41, 166, 169, 168]): here we will explore the same QFT, but defined in AdS$_2$ instead of the cylinder.

Let us briefly discuss the physics to be expected as a function of the bare quartic coupling λ_4 and the bare mass m^2. On $\mathbb{R}^2$, the theory displays spontaneous symmetry breaking (SSB): if the dimensionless ratio m^2/λ_4 is sufficiently large, the vacuum is $\mathbb{Z}_2$-invariant, but below some critical value the field ϕ obtains a VEV and the $\phi \to -\phi$ symmetry is broken.[4] The transition between both phases is continuous and describes the $2d$ Ising universality class. All of these effects have previously been observed in Hamiltonian truncation on $\mathbb{R} \times S^1$, which is Weyl-equivalent to $\mathbb{R}^2$. Away from this critical value, the mass gap is finite.

What is the fate of the phase transition in AdS? At finite radius, the physics depends now on the two dimensionless couplings m^2R^2 and $\bar{\lambda}_4$.[5] As discussed in section 7.5, SSB happens in AdS in a way analogous to flat space, up to boundary effects which might make the false vacuum stable. Therefore, in the limit where m^2R^2, $\bar{\lambda}_4 \to +\infty$ with fixed ratio, the physics ought to be the same as in flat space. In this thesis, we mainly focus on testing this hypothesis. However, it is worth asking about the general features of the phase diagram in the $(m^2R^2, \bar{\lambda}_4)$ plane. In particular, does the line of phase separation extend all the way to $\bar{\lambda}_4 = 0$? Is the phase transition continuous? Is it described by the $2d$ Ising CFT in AdS? As we shall see below, it is not easy to tackle these questions with Hamiltonian truncation, so we will leave most of them open to future work. Nevertheless, we can at least gather some information from the weak coupling side, $\bar{\lambda}_4 \ll 1$. In this limit, we can trust the semi-classical analysis of appendix J.1. In particular, let us recall that the line $\bar{\lambda}_4 = 0$, $m^2R^2 > -1/4$, with $\mathbb{Z}_2$ preserving boundary conditions, belongs to the symmetric phase. We expect therefore the line of phase transition to obey the equation $m^2R^2 = -1/4 + O(\bar{\lambda}_4)$. This answers in the negative two of the above questions.

---

[4] The critical value of m^2/λ_4 is of course scheme-dependent.

[5] In this initial discussion, we absorb $\bar{\lambda}_2$ in m^2R^2. The distinction will become relevant in the next paragraph, where $\bar{\lambda}_2$ will be chosen as a specific finite counterterm, to make the comparison to flat space easier.

At the phase transition, the expectation value of ϕ jumps from zero to a finite value: *i.e.* the phase transition is discontinuous. Furthermore, as $\bar{\lambda}_4 \to 0$, the spectrum is continuously connected to the one of a free *boson* with $\Delta = 1/2$, while, as we shall recall in section 10.3, the Ising CFT is described by a free *fermion*.

Fixing the ϕ^2 counterterm

We are most of all interested in the flat-space limit $R \to \infty$, keeping the bare couplings λ_2 and λ_4 fixed. Any "RG trajectory" (i.e. a sequence of spectra for a range of radii R) therefore depends on the ratio λ_2/λ_4 and in addition on the UV scaling dimension Δ of the single-particle state (or equivalently on its mass $m^2 = \Delta(\Delta-1)/R^2$). Note that the Hamiltonian is normal-ordered at fixed radius R. Therefore a trajectory of the form

$$H = H_0 + \sum_{k=2,4} \bar{\lambda}_k V_k, \qquad \lambda_2,\, \lambda_4 \;\; \text{fixed} \tag{9.25}$$

does *not* describe a good RG trajectory: the normal-ordering counterterms implicit in (9.25) are not the same as those in flat space, as has been explained in [41]. Instead, we should use a Hamiltonian of the form

$$H = H_0 + \bar{\lambda} V_4 + 6 z(\Delta) \bar{\lambda} V_2 \tag{9.26}$$

omitting terms proportional to the identity operator, since the Casimir energy is not observable in AdS. We can compute the coefficient $z(\Delta)$ by adapting the derivation from reference [41]. First, we notice that in flat space, the local operators ϕ^2 and ϕ^4 are normal-ordered as follows

$$:\!\phi^2\!:_\Delta = \phi^2 - Z_\Delta, \qquad :\!\phi^4\!:_\Delta = \phi^4 - 6 Z_\Delta \phi^2 + 3 Z_\Delta^2 \tag{9.27}$$

where Z_Δ formally denotes the contraction

$$Z_\Delta = \lim_{Y \to X} \left[\phi(X)\phi(Y) - :\!\phi(X)\phi(Y)\!:\right] = \lim_{Y \to X} \langle \phi(X)\phi(Y) \rangle_R \tag{9.28}$$

keeping the dependence of the correlator on the AdS radius explicit. This expression is formal, since the limit $Y \to X$ diverges. However, the difference of Z measured at two different radii is physical. For instance, we can compare the theory at a given R to the same QFT quantized in the flat-space limit $R = \infty$. This leads to

$$z(\Delta) \equiv Z_\Delta - Z_\infty = \frac{1}{2\pi}\left(-\frac{1}{2}\log \Delta(\Delta-1) + \psi(\Delta)\right) \tag{9.29}$$

where $\psi(\cdot)$ is the digamma function. This completely fixes the Hamiltonian (9.26).

Convergence estimates

Before we turn to numerical computations, let us first of all discuss the convergence rate, that is to say the error due to working at finite cutoff Λ. Although in the previous section we fixed a specific ϕ^2 counterterm, let us for now consider the general Hamiltonian (9.25)

$$H = H_0 + \bar{\lambda}_2 \, V_2 + \bar{\lambda}_4 \, V_4. \tag{9.30}$$

For definiteness, let us focus on the leading energy shift of the first excited state $|\chi\rangle = a_0^\dagger \, |0\rangle$, although much of the discussion does not depend sensitively on the choice of state. In Rayleigh-Schrödinger perturbation theory, we have

$$\boldsymbol{\Delta}\mathcal{E}_\chi(\bar{\lambda}_2, \bar{\lambda}_4) = \Delta + \frac{2}{2\Delta - 1} \, \bar{\lambda}_2 - W \cdot \bar{\lambda}_2^2 - 2A \cdot \bar{\lambda}_2 \bar{\lambda}_4 - B \cdot \bar{\lambda}_4^2 + \ldots \tag{9.31}$$

subtracting the Casimir energy and omitting terms of cubic and higher order in perturbation theory. The coefficients W, A and B depend on Δ, and importantly they are sensitive to the cutoff Λ, although they should have a finite limit as $\Lambda \to \infty$. We have already encountered the W-term in section 9.1, and found that it evaluates to

$$W(\Lambda) = \frac{4}{(2\Delta - 1)^3} + \mathrm{O}\bigg(\frac{1}{\Lambda^{2\Delta - 1}}\bigg). \tag{9.32}$$

The coefficients A and B cannot be calculated in closed form, but they can be obtained as integrals over AdS:

$$A = \int_0^\infty d\tau \, \mathcal{A}(\tau) \quad \text{and} \quad B = \int_0^\infty d\tau \, \mathcal{B}(\tau) \tag{9.33}$$

where

$$\mathcal{A}(\tau) = 24 \int_{-\pi/2}^{\pi/2} \frac{dr dr'}{(\cos r \cos r')^2} \, f_0(r')^2 \, G(\xi(\tau, r, r'))^2, \tag{9.34a}$$

$$\mathcal{B}(\tau) = 192 \cosh(\Delta \tau) \int_{-\pi/2}^{\pi/2} \frac{dr dr'}{(\cos r \cos r')^2} \, f_0(r) f_0(r') \, G(\xi(\tau, r, r'))^3. \tag{9.34b}$$

The expressions were obtained by evaluating connected two-point correlation functions of V_2 and V_4 inside the state $|\chi\rangle$, and subtracting the same correlator inside the vacuum state. In particular, $G(\xi)$ was defined in eq. (9.5), and the cross ratio ξ of eq. (7.8) is evaluated at $\tau' = 0$. Let $\rho_A(\alpha)$ and $\rho_B(\alpha)$ be the spectral densities associated to $\mathcal{A}(\tau)$ resp. $\mathcal{B}(\tau)$, that is to say

$$\mathcal{A}(\tau) = \int_0^\infty d\alpha \, \rho_A(\alpha) e^{-(\alpha - \Delta)\tau} \tag{9.35}$$

and likewise for $\mathcal{B}(\tau)$. We can likewise associate a spectral density $\rho_W(\alpha)$ to the diagram W — in fact, $\rho_W(\alpha)$ is exactly identical to $\boldsymbol{\Delta}\rho_\chi(\alpha)$ from (9.20). The total cutoff error is then

$$-\int_{\Lambda}^{\infty}\frac{d\alpha}{\alpha-\Delta}\left[\rho_W(\alpha)\cdot\bar{\lambda}_2^2+2\rho_A(\alpha)\cdot\bar{\lambda}_2\bar{\lambda}_4+\rho_B(\alpha)\cdot\bar{\lambda}_4^2\right]+\text{subleading in pert. theory.} \tag{9.36}$$

If Λ is large, this error term is controlled by the asymptotic behavior of the densities $\rho_W(\alpha)$, $\rho_A(\alpha)$ and $\rho_B(\alpha)$. We have already seen that $\rho_W(\alpha) \underset{\alpha\to\infty}{\sim} 1/\alpha^{2\Delta-1}$. We will see that for $\Delta > 3/2$, the error will be dominated by the other two terms. Indeed, we claim that

$$\rho_A(\alpha) \underset{\alpha\to\infty}{\sim} 1/\alpha^2 \quad\text{and}\quad \rho_B(\alpha) \underset{\alpha\to\infty}{\sim} \ln(\alpha)/\alpha^2. \tag{9.37}$$

Numerical evidence for this claim is presented in figure 9.5. If this claim holds, then the total error term is of the order of

$$\text{error term} = \left(2\varepsilon_A\cdot\bar{\lambda}_2\bar{\lambda}_4+\varepsilon_B\cdot\bar{\lambda}_4^2+\varepsilon_B'\cdot\bar{\lambda}_4^2\ln\Lambda\right)\frac{1}{\Lambda^2}+\ldots \tag{9.38}$$

for some coefficients ε_A, ε_B and ε_B', omitting terms subleading in Λ and in perturbation theory. The leading large-α behavior of the diagrams A and B is due to *bulk* effects, contrary to the diagram W which was due to a contribution close to the boundary. Indeed, the same scaling has been observed on the cylinder $\mathbb{R}\times S^1$ [41].

To make (9.38) precise, it makes sense to estimate the large-α asymptotics of ρ_A and ρ_B directly — or equivalently, the small-τ asymptotics of $\mathcal{A}(\tau)$ and $\mathcal{B}(\tau)$. We can do so following the example of reference [41]. In particular, we choose to study $d\mathcal{A}(\tau)/d\tau$ and $d\mathcal{B}(\tau)/d\tau$ instead of $\mathcal{A}(\tau)$ and $\mathcal{B}(\tau)$, and we replace the bulk-bulk propagator $G(\xi)$ by its Taylor series in the short-distance limit, to wit

$$G(\xi)\approx-\frac{\ln\xi+2\gamma_E+2\psi(\Delta)}{4\pi} \tag{9.39}$$

dropping analytic terms that vanish as $\xi\to 0$. This yields

$$\rho_A(\alpha) \underset{\alpha\to\infty}{\sim} \frac{24(\Delta-1)}{\alpha^2\pi(2\Delta-3)(2\Delta-1)}, \tag{9.40a}$$

$$\rho_B(\alpha) \underset{\alpha\to\infty}{\sim} \frac{144(\Delta-1)}{\alpha^2\pi^2(2\Delta-3)(2\Delta-1)}\left[2\ln\alpha-\frac{2}{\Delta-1}+\psi(\Delta-\tfrac{3}{2})-3\psi(\Delta-1)\right]. \tag{9.40b}$$

These formulas make precise the scaling predicted by (9.37). At the same time, we can compute the densities $\rho_{A,B}(\alpha)$ directly for finite values of α, by expanding the integrals (9.34) around large τ. In figure 9.5, the asymptotic formulas are compared to these exact results for $\Delta = 2, 2.5$ and 4, finding good agreement.

Let us make two comments about eqs. (9.40). For one, both densities have a pole at $\Delta = 3/2$. This is due to the truncation (9.39), which leads to additional divergences close to the boundary of AdS — yet the *full* correlators $\mathcal{A}(\tau)$ and $\mathcal{B}(\tau)$ are integrable

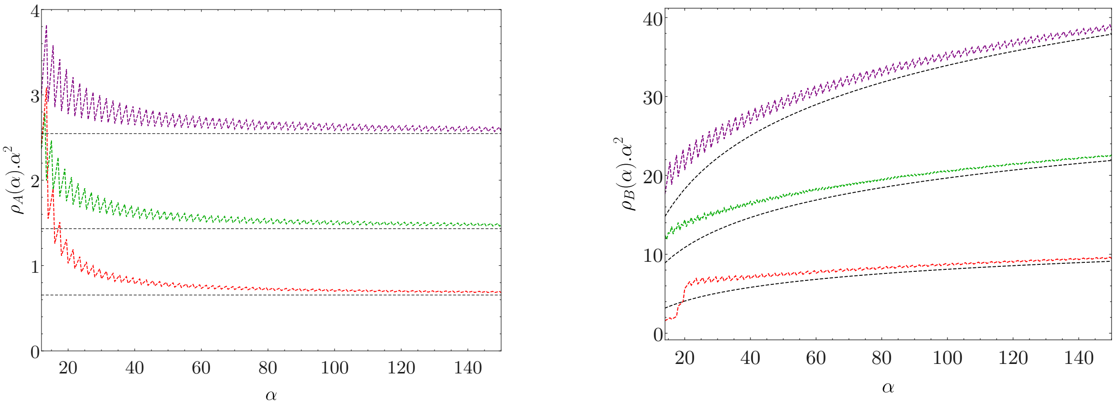

Figure 9.5: Left: the spectral density $\rho_A(\alpha)$ multiplied by α^2, for $\Delta = 2$ (purple), $\Delta = 2.5$ (green) and $\Delta = 4$ (red), averaged over intervals $[\alpha - 2, \alpha + 2]$ (since the densities have delta function support). The horizontal dashed lines are the large-α predictions from formula (9.40). Right: the same plot for the spectral density $\rho_B(\alpha)$, plus comparison to the asymptotic formula (9.40) (dashed).

for dimensions $\Delta > 1$, where eq. (7.14) holds. Second, the asymptotic density shown for $\rho_B(\alpha)$ can become negative for small values of α; for instance for $\Delta = 1.62$, the terms shown are only positive for $\alpha \gtrsim 43$. However, it can be shown that the full density $\rho_B(\alpha)$ is manifestly positive. This means that the asymptotic formula (9.40) is not necessarily a good approximation to the actual density $\rho_B(\alpha)$ for values of α that can be realized in Hamiltonian truncation (say $\alpha \leq 25 - 40$), at least for small values of Δ. Nevertheless, figure 9.5 shows that for sufficiently large α, the scaling behavior (9.37) is observed.

Let us finally compare this asymptotic prediction from second-order perturbation theory to Hamiltonian truncation data. It follows from the above discussion that the truncation error of the ϕ^4 Hamiltonian should be of the order of $\ln(\Lambda)/\Lambda^2$, at least at second order in the coupling[6]. We can thus fix the V_2 counterterm according to section 9.2 and diagonalize the Hamiltonian H for finite values of the cutoff Λ, computing the first excitated energy level non-perturbatively using the presription (8.1). The results of this procedure are shown in figure 9.6. As expected, we observe that the truncation data converge to a constant in the limit $\Lambda \to \infty$, and we see that the truncation error goes to zero as $\ln(\Lambda)/\Lambda^2$.

Evidence for a phase transition

As we already discussed, we expect that the ϕ^4 theory in AdS$_2$ exhibits sponteanous symmetry breaking, just as in flat space. Already in finite volume, working on $\mathbb{R} \times S^1$ where the S^1 has length L, truncation methods were used to study this transition [41]. In that work, the bare mass m^2 was fixed, and for fixed but large $mL \gtrsim$ O(few) the authors

---

[6] We don't expect higher-order diagrams to be *more* UV-sensitive.

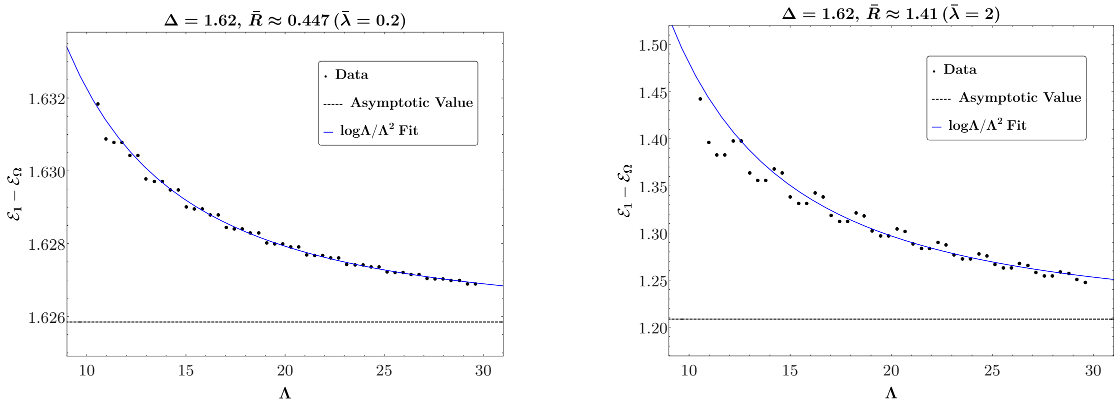

(a) $\bar{\lambda} = 0.2$

(b) $\bar{\lambda} = 2$

Figure 9.6: Hamiltonian truncation data for the energy shift of the state $|\chi\rangle$ due to the ϕ^4 Hamiltonian (9.26) with $\Delta = 1.62$, for a range of cutoffs up to $\Lambda = 30$. The left (right) plot corresponds to quartic coupling $\bar{\lambda} = 0.2$ ($\bar{\lambda} = 2$). Blue curve: fit of the form $u - v\ln(\Lambda)/\Lambda^2$, with the asymptotic value u shown as a horizontal dotted line.

scanned over the quartic coupling λ_4. For λ_4 sufficiently small and positive bare mass, the system is in the unbroken phase. In this phase, the energy gap of the theory, closes continuously as λ_4 is increased to its critical value. For λ_4 larger than its critical value the system is in the broken phase.

Here we can attempt to do the same thing: we can fix the bare mass m^2 and scan over the dimensionless coupling λ/m^2. Since we want to be close to the flat-space limit, we need to make sure that R is large compared to m^2, or in other words that the UV scaling dimension Δ is sufficiently large. To connect the notation used so far, this means that we fix $\Delta \gtrsim \mathrm{O}(\text{few})$ and scan over the dimensionless coupling $\bar{\lambda}/(m^2R^2) = \bar{\lambda}/[\Delta(\Delta-1)] =: \mathsf{x}$. For any value of Δ and x, we can measure the mass gap. The resulting curves $\boldsymbol{\Delta}\mathcal{E}(\mathsf{x}, \Delta)$ will depend on Δ, but if there is any universal flat-space physics, they should have a well-defined limit as $\Delta \to \infty$. The limiting curve $\boldsymbol{\Delta}\mathcal{E}(\mathsf{x}, \infty)$ should exhibit a gap that closes in accordance with the critical exponents of the Ising universality class, and as a matter of principle one should be able to read off the Ising BCFT spectrum. In fact, we expect that the gap $\boldsymbol{\Delta}\mathcal{E}$ closes at the same critical coupling as in flat space.

In figure 9.7, we plot precisely these curves $\boldsymbol{\Delta}\mathcal{E}(\mathsf{x}, \Delta)$. As always, we subtract the Casimir energy according to (8.1), and we divide the mass gap by Δ such that we can compare curves of different UV dimensions Δ. On the x-axis, we vary the dimensionless quartic coupling $\mathsf{x} = \bar{\lambda}/[\Delta(\Delta-1)]$. The plot provides evidence that the curves $\boldsymbol{\Delta}\mathcal{E}(\mathsf{x}, \Delta)$ indeed have a finite limit as $\Delta \to \infty$, although we cannot increase Δ further than $\Delta \approx 10$ for computational reasons. Semi-quantitatively, the plot is consistent with a critical coupling of the order of $\lambda/m^2 \approx 3$. Numerically, the convergence rate decreases rapidly for large couplings: this can be seen for example by the large error bars appearing in figure 9.7. Therefore, analyzing the phase transion in more detail is not feasible in the current set-up, even by going to rather large cutoffs with $\sim 5 \cdot 10^4$ states.

The prescription (8.1) does not always lead to positive energies, contrary to differences of energies of a Hamiltonian, which are positive by construction. The value of e.g. the first excited state $\mathcal{E}_1(\Lambda) - \mathcal{E}_\Omega(\Lambda - \Delta)$ can indeed be negative, as seems to happen to points with large couplings in figure 9.7. This would indicate that the vacuum exchanges roles with an excited state (which has different quantum numbers!). However, we stress that for the data points in question, the error bars are very significant, and it is not excluded that the true energy in the limit $\Lambda \to \infty$ is in fact slightly positive. For this reason, and to avoid clutter, we have not shown any points with a seemingly negative energy. In appendix J.2, we study an inverted harmonic oscillator with Hamiltonian truncation to illustrate how the states in the broken phase are expected to have a large overlap with unperturbed states close to the cutoff.

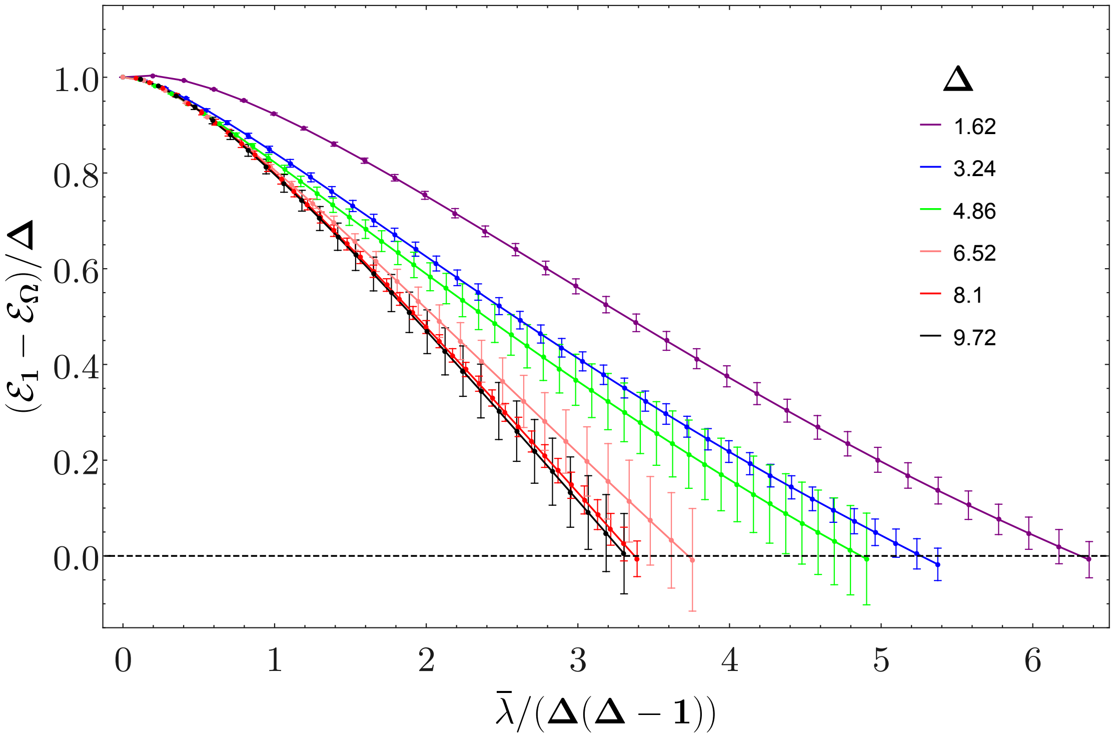

Figure 9.7: Mass gap of the ϕ^4 Hamiltonian (9.26) for a range of quartic couplings $\bar{\lambda}$ (x-axis), for a different set of UV scaling dimensions Δ (different curves, see legend).

10 Deformations of conformal field theories

In this chapter, the unperturbed Hamiltonian corresponds to a conformal field theory in AdS. The deformation is triggered by a relevant operator. We shall focus, in particular, on the simplest two dimensional CFTs, *i.e.* the Lee-Yang and the Ising models. Since AdS is conformally flat, a CFT placed in AdS is equivalent to a CFT in the presence of a flat boundary. More precisely, the equivalence is true if the boundary conditions preserve the Weyl invariance of the bulk. This setup is usually referred to as a boundary conformal field theory (BCFT) [170]. Since the subgroup of the conformal group preserved by a flat boundary coincides with the isometries of AdS, any CFT placed in AdS with isometry preserving boundary conditions will be related to a BCFT by a Weyl transformation.[1]

In this chapter, we adopt the usual $2d$ CFT convention, reserving the name primaries for the Virasoro primaries. On the other hand, the $SL(2,\mathbb{R})$ primaries will be sometimes denoted as quasiprimaries.

10.1 Virasoro minimal models and their deformations in AdS$_2$

We begin with a reminder of the basics of minimal models [171] in the presence of a boundary, before moving on to AdS. A detailed exposition can be found in the original references [170, 172–175], in chapter 11 of [48], or in the dedicated book [176]. A flat boundary preserves a single copy of the Virasoro algebra, whose generators L_n, $n \in \mathbb{Z}$ obey the usual commutation relation

$$[L_m, L_n] = (m-n)L_{m+n} + \frac{c}{12}m(m^2-1)\delta_{m+n,0} \ , \tag{10.1}$$

---

[1] We are assuming that conformal symmetry automatically promotes to Weyl invariance.

where c is the central charge of the $2d$ CFT.[2] The $SL(2,\mathbb{R})$ generators can be identified with Virasoro generators as follows:

$$H = L_0, \quad P = L_{-1}, \quad K = L_1. \tag{10.2}$$

The spectrum of boundary scaling operators, corresponding to the constant time slice Hilbert space in AdS, is organized in representations of the Virasoro algebra. In the minimal models, there are a finite number of so called Verma modules, which have a Virasoro primary $|\chi_i\rangle$ as a lowest-weight state. The primary satisfies $L_n |\chi_i\rangle = 0$ for all $n \geq 1$. The full Hilbert space is spanned by states of the form

$$L_{-n_1} \cdots L_{-n_p} |\chi_i\rangle \tag{10.3}$$

running over all Virasoro primaries $|\chi_i\rangle$ and all integers $n_1, \ldots, n_p \geq 1$. The $SL(2,\mathbb{R})$ primaries are those states $|\Psi\rangle$ satisying $L_1 |\Psi\rangle = 0$. Under the parity transformation $\mathtt{P} : r \mapsto -r$, the Virasoro generators transform as

$$\mathtt{P} L_n \mathtt{P}^{-1} = (-1)^n L_n \tag{10.4}$$

which generalizes eq. (7.7).

Given a minimal model, the set of consistent boundary conditions is known [173, 175]. They are in one to one correspondence with the scalar Virasoro primary operators of the CFT. In the following, we will only consider diagonal minimal models, where all primaries are spinless. For instance, the Ising model has three Virasoro primaries: the identity, the spin field σ, the energy field ϵ. Correspondingly, there are three conformal boundary conditions. The boundary spectrum supported by each boundary condition is determined as follows. Consider the fusion coefficients in the OPE

$$V_\phi \times V_\phi \sim {n_{\phi\phi}}^i V_i \ , \tag{10.5}$$

where V_ϕ and V_i denote representations of the Virasoro algebra. Then, the boundary condition labeled by ϕ supports boundary operators falling in the representations such that ${n_{\phi\phi}}^i \neq 0$. For instance, the boundary spectrum of the σ boundary condition in the Ising model comprises the identity and the ϵ module, whose Virasoro primaries have dimension $\Delta_0 = 0$ and $\Delta_\epsilon = 1/2$ respectively.

It is sometimes useful to map the theory to the exterior of the unit circle. In this setup, the boundary condition generates a state in radial quantization, the so called Cardy state, which allows for a decomposition in terms of local operators of the bulk CFT [174]. Only the operators appearing in this decomposition acquire a one-point function in the presence of the boundary. For instance, the boundary state generated by the σ boundary condition in the Ising model is

---

[2] A $2d$ CFT admits a conformal boundary only if the left and right central charges coincide, $c = \bar{c}$ [163].

$$|\sigma\rangle_{\text{Cardy}} = |1\rangle\!\rangle - |\epsilon\rangle\!\rangle \ , \tag{10.6}$$

where the Ishibashi states on the right hand side are a sum of left-right symmetric descendants of the Virasoro primary, whose specific form we will not need [177]:

$$|\phi\rangle\!\rangle = |\phi\rangle + \frac{L_{-1}\bar{L}_{-1}}{\Delta_\phi}\,|\phi\rangle + \dots \tag{10.7}$$

A special boundary condition exists in all the minimal models. It is the one labeled by the identity operator. It only supports the identity module, hence it does not allow for relevant deformations. In the generic minimal model, denoted by $\mathcal{M}(p,q)$ in [48], the identity module has two null vectors, at level 1 and $(p-1)(q-1)$. In particular, the non trivial null states are found at level 4 in the Lee-Yang model and at level 6 in the Ising model. The leading boundary operator supported by the identity Cardy state is the displacement operator [163], *i.e.* $L_{-2}\,|\Omega\rangle$,[3] which has $\Delta = 2$. This means that the rate of convergence of TCSA in AdS cannot be faster than $\sim 1/\Lambda$, as explained in subsection 8.7. The identity boundary condition corresponds to the so called extraordinary transition in the corresponding statistical models, *i.e.* it breaks all the global symmetries of the CFT. Indeed, the boundary OPE (7.13) of any bulk operator cannot be empty, and therefore it must contain the identity module. Hence, all the bulk scalar operators acquire a one-point function in the presence of the boundary. Although we will comment about other boundary conditions in what follows, we shall be mainly interested in the one labeled by the identity.

When mapping the CFT with a flat boundary to AdS$_2$, it is important to notice that the anomalous contribution to the stress tensor vanishes. Hence, the ground state energy vanishes.[4] This is most easily checked in Poincaré coordinates. Using a pair of complex coordinates z, $\bar{z}$, the metric reads

$$ds^2_{\text{AdS}} = \frac{R^2}{(\text{Im}\, z)^2}\, dz d\bar{z} \ . \tag{10.8}$$

Under the Weyl map from flat space, the stress tensor is in fact unchanged:

$$ds^2_{\text{AdS}} = e^{2\sigma} ds^2_{\text{flat}} \ , \quad \sigma = \log\frac{R}{\text{Im}\, z} \ , \qquad T^{\text{AdS}}_{zz} = T^{\text{flat}}_{zz} + \frac{c}{12\pi}\left(\partial_z^2\sigma - (\partial_z\sigma)^2\right) = T^{\text{flat}}_{zz} \ . \tag{10.9}$$

It is then easy to check that the generators (10.1), obtained as modes of the stress tensor, provide conserved quantities in AdS as well.

---

[3] Recall that $|\Omega\rangle$ is the vacuum in radial quantization around a point on the defect. This quantization scheme, which is the one relevant to the Hamiltonian truncation, should not be confused with the scheme that gives rise to the Cardy states, as explained above.

[4] This should be contrasted with the BCFT on a strip, which is a finite volume system and as such has a Casimir energy proportional to the central charge.

In what follows, we will trigger an RG flow in AdS by turning on a relevant Virasoro scalar primary $\mathcal{V}$. The relation between such operator in AdS and in flat space is

$$\mathcal{V}_{\text{AdS}} = \left(\frac{\operatorname{Im} z}{R}\right)^{\Delta_{\mathcal{V}}} \mathcal{V}_{\text{flat}} \ . \tag{10.10}$$

One can then work out the action of the Virasoro generators on the AdS operator:

$$[L_n, \mathcal{V}_{\text{AdS}}] = \left[z^{n+1}\partial_z + \bar{z}^{n+1}\partial_{\bar{z}} + \frac{\Delta_{\mathcal{V}}}{2}\left((n+1)(z^n+\bar{z}^n) - 2\,\frac{z^{n+1}-\bar{z}^{n+1}}{z-\bar{z}}\right)\right]\mathcal{V}_{\text{AdS}} \ . \tag{10.11}$$

As expected, the term proportional to $\Delta_{\mathcal{V}}$ vanishes for the $SL(2,\mathbb{R})$ generators (10.2), which simply act as diffeomorphisms. Henceforth, we drop the subscript from $\mathcal{V}_{\text{AdS}}$, and resume the convention set up in eq. (5). Eq. (10.11) allows to compute all the matrix elements of the perturbing operator $\mathcal{V}$ between states of the kind (10.3), and hence the matrix elements of the potential V, once the three-point functions $\langle \chi_i|\mathcal{V}|\chi_i\rangle$ are known.[5] Since the potential preserves the isometries of AdS, not all the matrix elements between states belonging to the same $SL(2,\mathbb{R})$ families are in fact independent. Rather, there are recurrence relations between them, as is described in appendix F. Nevertheless these relations do not speed up the computation of the matrix elements significantly, as we discuss at the end of appendix I; instead, we compute all matrix elements individually in our algorithm.

10.2 The Lee-Yang model

The Lee-Yang CFT is the diagonal modular invariant of the simplest minimal model, denoted $\mathcal{M}(5,2)$ in [48]. This model was the theater where TCSA was first applied [39], and was studied with the same technique on a strip in [154, 178]. It has central charge

$$c = -\frac{22}{5} \ , \tag{10.12}$$

and it is therefore non unitary. It contains two scalar Virasoro primaries, the identity $\mathbb{1}$ and the field $\mathcal{V}$, with scaling dimensions

$$\Delta_{\mathbb{1}} = 0 \ , \qquad \Delta_{\mathcal{V}} = -\frac{2}{5} \ . \tag{10.13}$$

---

[5] Of course, to obtain the potential one can alternatively compute the matrix elements of $\mathcal{V}_{\text{flat}}$ in flat space, and multiply them by the Weyl factor in eq. (10.10) before integrating on a constant time slice.

Consequently, it allows for two conformal boundary conditions[6]:

$$|\mathbb{1}\rangle_{\text{Cardy}} = \left(\frac{\sqrt{5}+1}{2\sqrt{5}}\right)^{1/4} |\mathbb{1}\rangle\rangle + \left(\frac{\sqrt{5}-1}{2\sqrt{5}}\right)^{1/4} |\mathcal{V}\rangle\rangle \,, \tag{10.14a}$$

$$|\mathcal{V}\rangle_{\text{Cardy}} = -\left(\frac{\sqrt{5}-2}{\sqrt{5}}\right)^{1/4} |\mathbb{1}\rangle\rangle + \left(\frac{\sqrt{5}+2}{\sqrt{5}}\right)^{1/4} |\mathcal{V}\rangle\rangle \,. \tag{10.14b}$$

As mentioned, we shall be primarily interested in the identity Cardy state. Eq. (10.14a) implies that the operator $\mathcal{V}$ acquires a one-point function in the presence of the boundary:

$$\langle \mathcal{V}|\mathbb{1}\rangle_{\text{Cardy}} = \left(\frac{\sqrt{5}-1}{2\sqrt{5}}\right)^{1/4} \,. \tag{10.15}$$

With the boundary state (10.14a), the partition function on the disk is not normalized to one, rather

$$\langle \mathbb{1}|\mathbb{1}\rangle_{\text{Cardy}} = \langle \Omega|\Omega\rangle = -\left(\frac{\sqrt{5}+1}{2\sqrt{5}}\right)^{1/4} \,, \tag{10.16}$$

where we emphasized that the same quantity gives the normalization of the vacuum in AdS. This normalization is irrelevant to the problem of finding the spectrum of the Hamiltonian, and we shall find it convenient to remove this factor from our basis of states, multiplying each one by $\langle \Omega|\Omega\rangle^{-1/2}$.[7] Then, the expectation value of $\mathcal{V}$ in AdS, with unit normalized vacuum, is

$$\langle \mathcal{V}\rangle = (2R)^{-\Delta_{\mathcal{V}}} \frac{\langle \mathcal{V}|\mathbb{1}\rangle_{\text{Cardy}}}{\langle \Omega|\Omega\rangle} = -(2R)^{-\Delta_{\mathcal{V}}} \left(\frac{2}{1+\sqrt{5}}\right)^{1/2} \equiv -R^{-\Delta_{\mathcal{V}}} a_{\mathcal{V}} \,. \tag{10.17}$$

For the matrix elements of the potential to be finite, the one-point function of $\mathcal{V}$ must be fine tuned in the Hamiltonian. We therefore perturb the conformal fixed point with the following coupling:

$$\bar{\lambda} V = \bar{\lambda} \int_{-\pi/2}^{\pi/2} \frac{dr}{(\cos r)^2} \left(\frac{R^{\Delta_{\mathcal{V}}}}{a_{\mathcal{V}}} \mathcal{V}(\tau=0,r) + 1\right) \,. \tag{10.18}$$

The theory can be studied for both signs of the coupling. The expectation from the flow in flat space [39] is that $\bar{\lambda} > 0$ leads to a well defined flat space limit. This will be confirmed by the numerics.

The Hilbert space of the model at the conformal fixed point consists of the states (10.3), where the primary $|\chi\rangle = |\Omega\rangle$ is created by the identity operator on the boundary. The first few states and their degeneracies can be found in the following table:

---

[6] In order for the coefficients of the boundary state to be real, it is necessary to normalize the vacuum in radial quantization around a point *in the bulk* as $\langle \mathbb{1}|\mathbb{1}\rangle = -1$, see *e.g.* [178].

[7] The fact that this normalization is purely imaginary is not an issue. We simply define the scalar product to be linear rather than sesquilinear, so that the vacuum is now unit normalized.

Δ	0	1	2	3	4	5	6	7	8	9	10
states	1	0	1	1	1	1	2	2	3	3	4
$sl(2)$ primaries	1		1				1		1		1

In the flat space limit, the Lee-Yang model flows to a massive theory, whose spectrum includes a single stable particle. Since the flat space flow is integrable, the mass is computable as a function of the scale set in the UV [179, 180]. Recalling that $\bar{\lambda} = \lambda R^{2-\Delta_{\mathcal{V}}}$, we approach the flat space limit by taking $R \to \infty$ after the rescaling $(\tau, r) \to (\tau, r)/R$. The flat space coupling is then found to be $\lambda/a_{\mathcal{V}}$. The mass of the stable particle is expressed in term of the coupling as follows [180]:

$$m = \kappa \left(\frac{\lambda}{a_{\mathcal{V}}} \right)^{\frac{1}{2-\Delta_{\mathcal{V}}}} , \qquad \kappa = 2^{19/12} \sqrt{\pi} \frac{\left(\Gamma(3/5)\Gamma(4/5)\right)^{5/12}}{5^{5/16}\Gamma(2/3)\Gamma(5/6)} = 2.643 \ldots \tag{10.19}$$

Plugging this relation in eq. (7.23), we obtain a prediction for the slope of the energy levels of single particle states in the flat space limit:

$$\frac{\Delta_{\text{single particle}}}{\bar{R}} \xrightarrow[\bar{R}\to\infty]{} \frac{\kappa}{a_{\mathcal{V}}^{\frac{1}{2-\Delta_{\mathcal{V}}}}} = 2.603 \ldots \tag{10.20}$$

Here we used the definition of the AdS radius in units of the coupling, which in this case reads

$$\bar{R} = R \lambda^{\frac{1}{2-\Delta_{\mathcal{V}}}} = R \lambda^{5/12} . \tag{10.21}$$

Eq. (10.20) is useful because it allows to estimate the finite size corrections in AdS. As we shall see, the non unitary nature of this model hinders our ability to reach large values of the radius within our computational limits.

Cutoff effects

As with every QFT in AdS, the vacuum energy is not observable in the continuum limit: it diverges linearly with the cutoff Λ, as showcased in figure 10.1. However, we explained in section 8.3 that the vacuum energy is computable in the Hamiltonian truncation framework. In particular, we can compare the function $\mathcal{E}_\Omega(\Lambda)$ at small $\bar{\lambda}$ with its value at second order in perturbation theory. We recall from section 8.3 that the linear divergence is given by

$$\mathcal{E}_\Omega(\Lambda) \xrightarrow[\Lambda\to\infty]{} c \left(\frac{\bar{\lambda}}{a_{\mathcal{V}}} \right)^2 \Lambda + O(\bar{\lambda}^3) , \quad c = -8 \int_0^\infty d\xi \, \text{arcsinh} \left(2\sqrt{\xi(\xi+1)} \right) F(\xi) , \tag{10.22}$$

where $F(\xi)$ is the connected two-point function of the perturbation:

$$F(\xi) = R^{2\Delta_{\mathcal{V}}} \langle \mathcal{V}(\tau, r)\mathcal{V}(0,0)\rangle - a_{\mathcal{V}}^2 \ , \tag{10.23}$$

with the cross ratio ξ defined in eq. (7.8). The correlation function is easily written as a sum of two Virasoro blocks, corresponding to the fusion rule $\mathcal{V} \times \mathcal{V} = \mathbb{1} + \mathcal{V}$, see *e.g.* [178]:

$$F(\xi) = -f_{\mathbb{1}}(\xi) + \frac{2}{1+\sqrt{5}} \frac{\Gamma(1/5)\Gamma(6/5)}{\Gamma(3/5)\Gamma(4/5)} f_{\mathcal{V}}(\xi) - a_{\mathcal{V}}^2 \ , \tag{10.24}$$

with

$$f_{\mathbb{1}}(\xi) = \left(\frac{4\xi}{1+\xi}\right)^{2/5} {}_2F_1\left(\frac{3}{5}, \frac{4}{5}, \frac{6}{5}, \frac{\xi}{1+\xi}\right) \ , \quad f_{\mathcal{V}}(\xi) = \left(\frac{16\xi}{1+\xi}\right)^{1/5} {}_2F_1\left(\frac{2}{5}, \frac{3}{5}, \frac{4}{5}, \frac{\xi}{1+\xi}\right) \ . \tag{10.25}$$

Performing the integration in eq. (10.22) numerically, we obtain

$$c = 0.5786\ldots \ , \qquad \mathcal{E}_\Omega(\Lambda) \underset{\Lambda\to\infty}{\longrightarrow} 0.5377\,\bar{\lambda}^2\Lambda + O(\bar{\lambda}^3) \ . \tag{10.26}$$

The left panel of figure 10.1 shows that eq. (10.26) does indeed fit the data accurately at weak coupling. In the right panel, we see that the behavior is still linear when the coupling is order one, as expected.

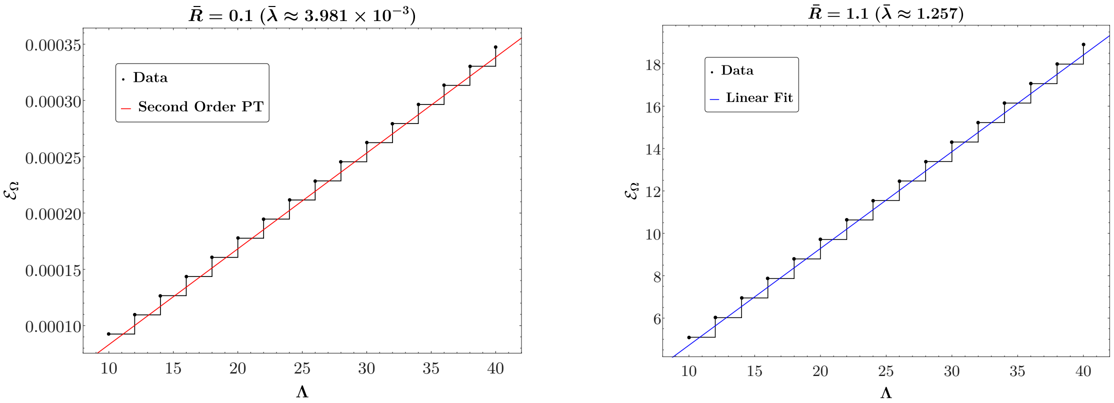

Figure 10.1: Vacuum energy as a function of the cutoff in the Lee-Yang model. The black dots are the Hamiltonian truncation data: since the vacuum is parity even, the Hamiltonian needs to be diagonalized anew only when Λ jumps by an even integer. In the left plot, the solid red line is eq. (10.26). In the right plot, the solid blue line is a fit to the data.

Since the lightest operator in the spectrum is the displacement operator, with $\Delta = 2$, the rate of convergence of the truncated spectrum to the exact values is Λ^{-1} – see section 8.7. This can be checked up to couplings of order one, as shown in figure 10.2.

On the other hand, the Lee-Yang model presents a specific obstruction to the computation

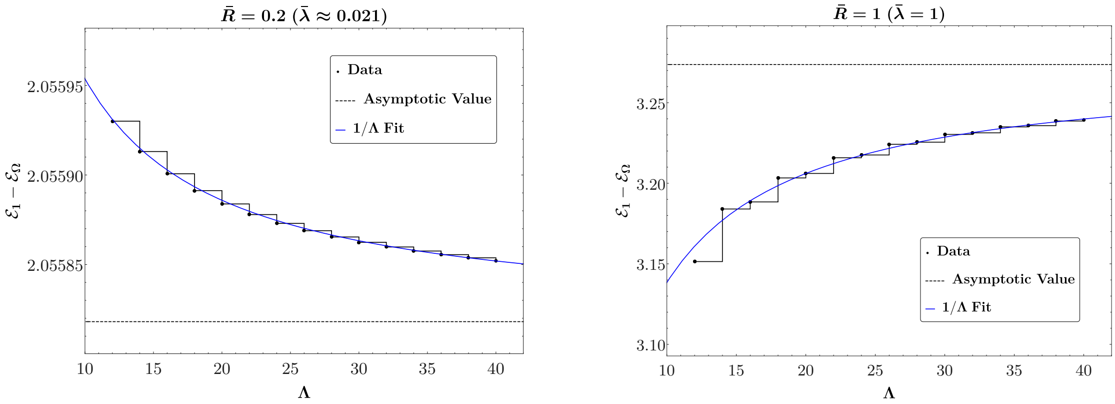

Figure 10.2: Energy of the first excited state in the Lee-Yang model, as a function of the cutoff at weak and strong coupling. Notice that the first excited state is parity even, hence again only points were Λ is even need to be computed. The asymptotic value is obtained from the fit.

of the spectrum for large values of the coupling. Since the Hamiltonian is not Hermitian, its eigenvalues are not guaranteed to be real at any finite value of the cutoff. In the continuum limit, the spectrum is real in the flat space limit, and it is real at the conformal fixed point. Our working hypothesis is that the Lee-Yang model is well defined in the continuum in AdS for any value of the radius. However, for finite Λ the eigenvalues do pick up an imaginary part when the radius is larger than a certain value $\bar{R}^*$. For the vacuum energy, this can be seen in figure 10.3.

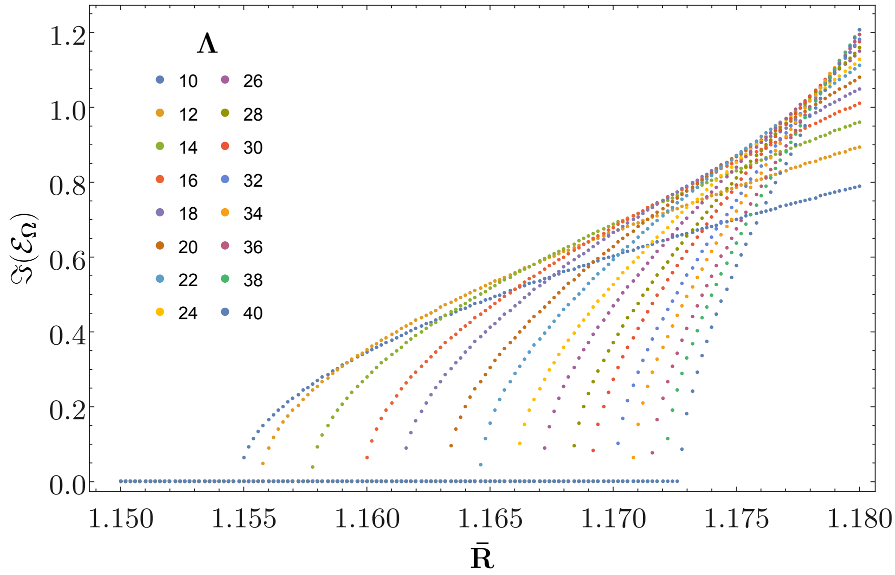

Figure 10.3: Imaginary part of the vacuum energy in the Lee-Yang model as a function of the radius of AdS, for different cutoffs.

In order to provide evidence for the reality of the spectrum in AdS, we explored the dependence of $\bar{R}^*$ on the cutoff. Figure 10.4 shows that a logarithmic fit describes reasonably well the data in our possession. If this behavior is valid at asymptotically large values of Λ, the Lee-Yang model does indeed possess real energy levels in the continuum limit. However, the computational effort to reach this regime is severe: since the number of states grows exponentially with the cutoff, the spectrum cannot be real for a given value $\bar{R}$ unless we include a number of states of the order $\sim \exp(\alpha \exp(\beta \bar{R}))$, for some positive constants α and β.

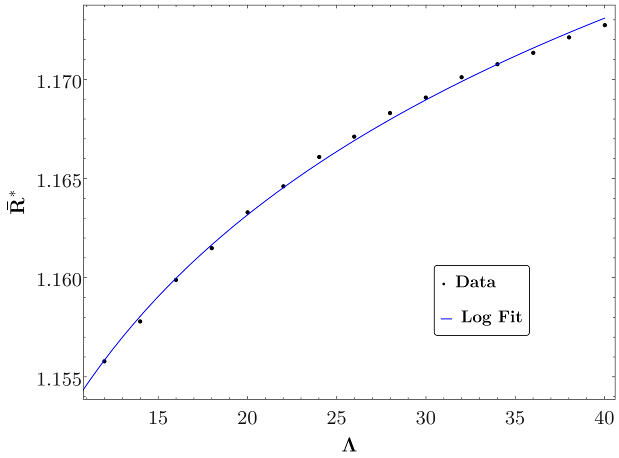

Figure 10.4: $\bar{R}^*$ is the value of the coupling beyond which the vacuum energy in the Lee-Yang model becomes complex. The logarithmic fit is phenomenological, and the best fitting function is $\bar{R}^* = 1.12 + 0.01 \log(\Lambda)$. Notice that with the available range of values for Λ it is hard to distinguish, for instance, between a logarithm and a power law with a sufficiently small exponent.

The spectrum

Figure 10.5 shows the energy of the first excited state as a function of the radius of AdS. At small radius, the slope of the curve is fixed by perturbation theory. The first excited state starts its life as the displacement operator, with dimension $\Delta = 2$, and deviates from that value as $\sim R^{2-\Delta_{\mathcal{V}}} = R^{12/5}$. On the other hand, at radii of order 1 in units of the coupling, the truncation effects become big, and our extrapolation to the continuum limit correspondingly poor. This is related to the appearance of complex energies described in the previous subsection. Since the Hamiltonian is real, complex eigenvalues can only arise in pairs, and the vacuum energy in particular can only become complex after colliding with the first excited state. This is clearly visible in figure 10.5. Finally, the bulk of the plot contains genuine non perturbative data. The extrapolation to infinite cutoff is reliable, and the curve can be trusted. Although the energy of the first excited state is order one, we may be tempted to recognize a region where the dependence on the radius

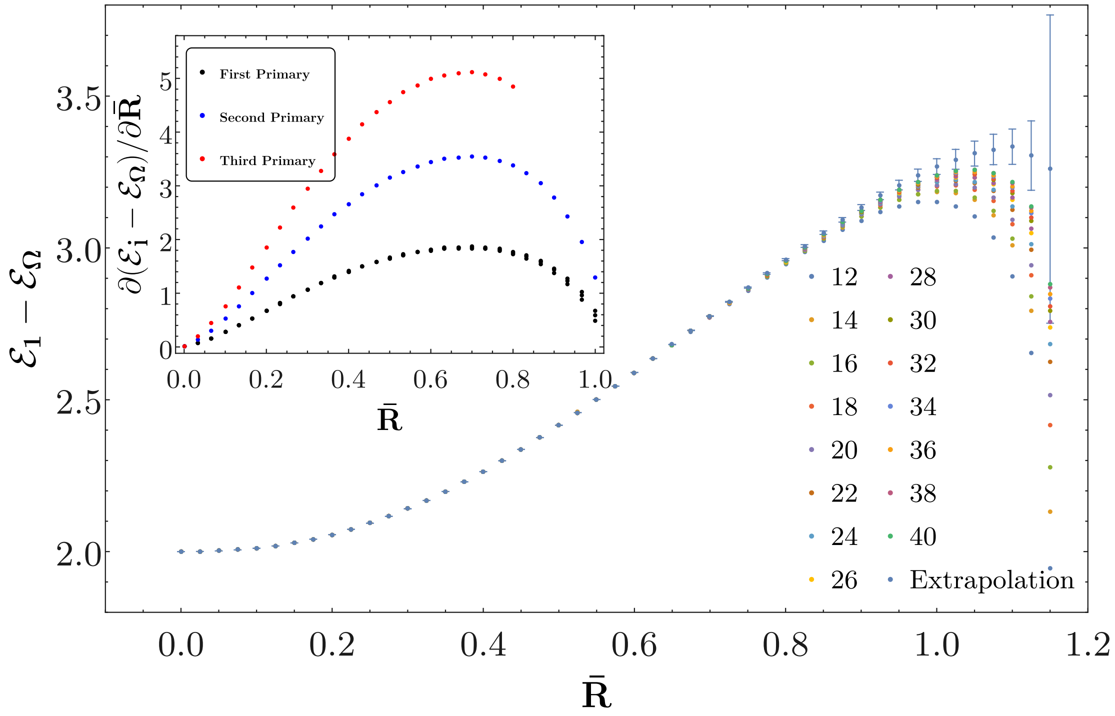

Figure 10.5: Main plot: energy of the first excited state in the Lee Yang model, as a function of the radius of AdS, for various choices of cutoff. The error bars are computed according to the procedure explained in subsection 9.1. In the inset, the derivative of the gap is computed discretely, by measuring the gap at two nearby values of $\bar{R}$.

is approximately linear, see eq. (7.23). To test whether this is the case, in the inset of figure 10.5 we plot the derivative of the energy of a few states with respect to the radius of AdS. The curves do not show a pronounced plateau, which casts doubts on the fact that flat space physics is already visible in the plot. A quantitative check in this direction is provided by comparing the maximal slope of the first excited state, about ~ 1.85, with the flat space prediction ~ 2.60 in eq. (10.20). The inset also reports the slope of the energy levels which in the flat space limit we can tentatively associate to two and three particle states, with all particles at rest. The peaks in this case lie at about ~ 3.5 and ~ 5.1 respectively. The ratios of these slopes to the slope of the first excited state are 1.9 and 2.8 respectively, which are not too far from the value 2 and 3 expected in the flat space limit.[8]

Figure 10.6 shows the dependence of the energy of the first few excited states on the AdS

---

[8] Notice that the deviation of the energies of the multiparticle states from the sum of their constituents is a measure of the strength of the (non gravitational) interactions, and they do not need to be of the same order as the deviation of the energy of the single particle state from its value in the flat space limit. For instance, in the case of a free scalar the binding energies are exactly zero for any value of the radius.

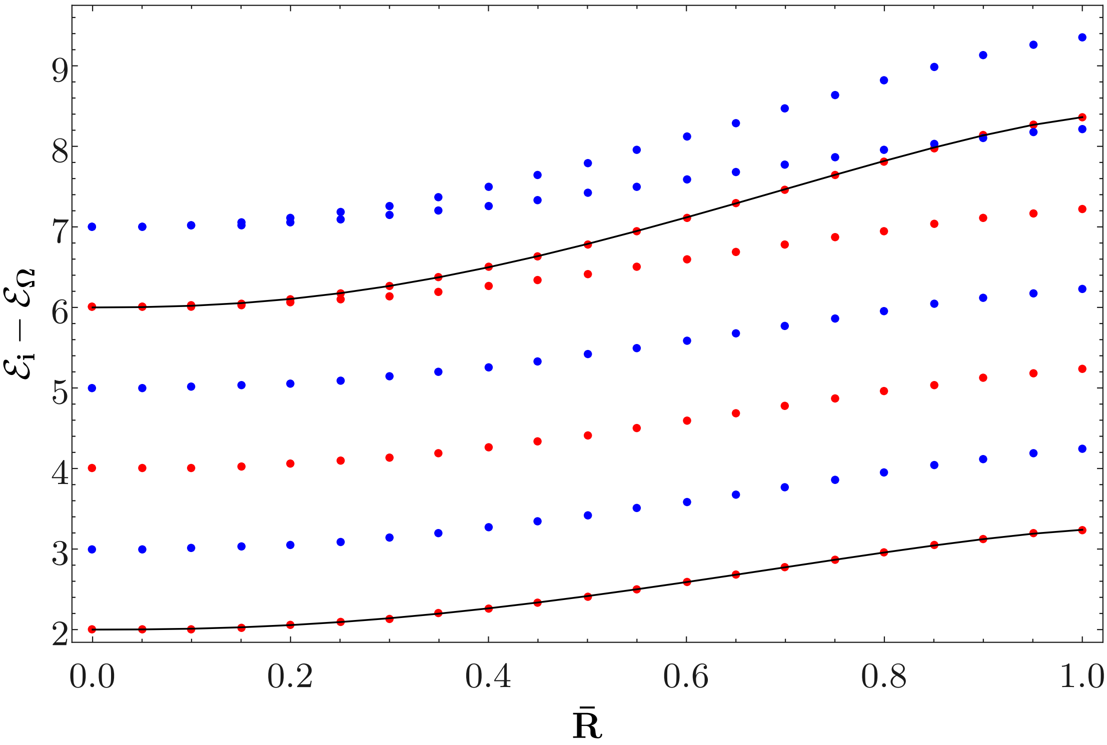

Figure 10.6: Spectrum of the Lee-Yang model. All the data points are computed with cutoff $\Lambda = 40$. To avoid clutter, we did not plot the extrapolated data with their error bars, although the latter would be pretty small up to $\bar{R} \sim 0.8$ as in figure 10.5. As discussed in text, we cannot trust the data beyond $\bar{R} \sim 1$, due to large truncation effects.

radius. We highlighted in red the parity even and in blue the parity odd eigenstates of the Hamiltonian, recognizable from their CFT ancestors according to eq. (10.4). As it can be checked via the character of the vacuum module, there are two quasi-primaries in the Lee-Yang CFT in the range of scaling dimensions shown in figure 10.6: the displacement operator at $\Delta = 2$ and a new quasi-primary at $\Delta = 6$. These are marked with a solid line in the figure. Correspondingly, all states up to level 5 are non-degenerate, while the states at level 6 and 7 are two-fold degenerate. The quasiprimary state starting at level 6 is on its way to become a two-particle state in the flat space limit. The connection between quasiprimaries in the BCFT and multiparticle states in the flat space limit has been explained in section 7.4: since in the continuum the $SL(2,\mathbb{R})$ structure forces smooth level crossing between a quasiprimary and the descendants of a different conformal family, we can track the quasiprimary state all the way from its origin in the BCFT to the flat space limit.

Finally, figure 10.7 shows the gap as a function of $\bar{\lambda}$, for an interval extending to negative values. The energy of the first excited state is monotonic with $\bar{\lambda}$, and we expect that for a certain value $\bar{\lambda}_{\text{min}}$ of the coupling a new boundary operator with dimension $\Delta = 1$ emerges.

We cannot reliably compute the spectrum for $\bar{\lambda}$ close to $\bar{\lambda}_{\text{min}}$, since the truncation errors become large, as it is visible towards the left of figure 10.7. Nevertheless, we can speculate that $\bar{\lambda}_{\text{min}}$ is the minimal value of the coupling for which the spectrum in the continuum limit is real. Indeed, when the bulk perturbation turns on a marginal coupling, the latter cannot be fine tuned, and generically a fixed point exists only on one side of $\bar{\lambda}_{\text{min}}$. In fact, a natural scenario is that when $\bar{\lambda} = \bar{\lambda}_{\text{min}}$ two fixed points collide and annihilate. In this case, the only other available fixed point is obtained by deforming the Lee-Yang CFT with the coupling (10.18), but this time starting from the boundary condition captured by the Cardy state $|\mathcal{V}\rangle_{\text{Cardy}}$ (10.14b). This suggests a scenario analogous to the structure of boundary conditions of a free scalar with negative mass squared in AdS. We shall further discuss this hypothesis in section 11. For the moment, let us conclude by pointing out an obvious consequence of these considerations: the theory defined by deforming the Lee-Yang CFT with a coefficient $\lambda < 0$ does not admit a flat space limit. On the contrary, it features a maximum radius $R_{\text{max}} = (\bar{\lambda}_{\text{min}}/\lambda)^{5/12}$.

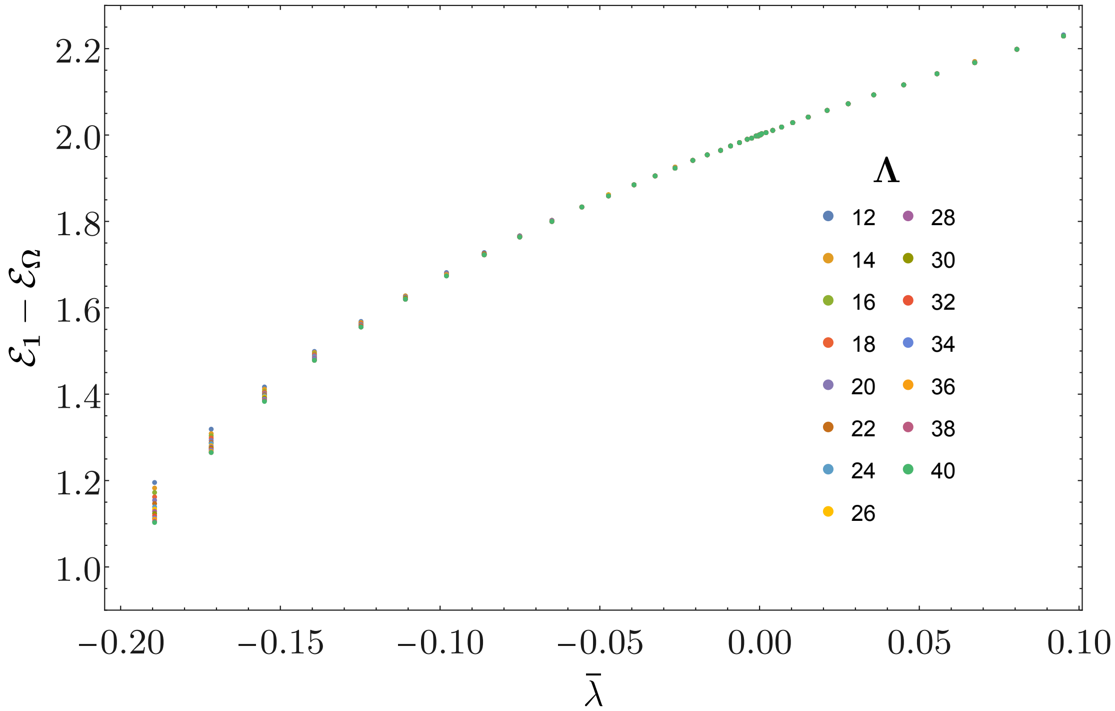

Figure 10.7: First excited state energy in the Lee-Yang model in a range of couplings around $\bar{\lambda} = 0$. For the values of $\bar{\lambda}$ towards the left of the plot, the convergence with the cutoff Λ is very slow, and does not allow to extrapolate the value $\bar{\lambda}_{\text{min}}$ defined in the main text.

10.3 The Ising model

The Ising model is the diagonal minimal model $\mathcal{M}(4,3)$ with central charge

$$c = \frac{1}{2} \ . \tag{10.27}$$

Its field content consists of three Virasoro families:

$$\Delta_{\mathbb{1}} = 0 \ , \qquad \Delta_\sigma = \frac{1}{8} \ , \qquad \Delta_\epsilon = 1 \ . \tag{10.28}$$

The spin operator σ is odd under the $\mathbb{Z}_2$ symmetry of the model, while the energy operator ϵ is even. The Ising model enjoys a Kramers-Wannier duality [181] which flips the sign of the ϵ operator and replaces the σ operator with its disorder counterpart μ. The most general bulk RG emanating from the 2d Ising model which preserves the AdS isometries is given by the action

$$S = S_{\text{Ising CFT}} - \lambda_\epsilon \int_{\text{AdS}} \sqrt{g}\, d^2x\ \epsilon(x) - \lambda_\sigma \int_{\text{AdS}} \sqrt{g}\, d^2x\ \sigma(x) + \lambda_{\mathbb{1}} \int_{\text{AdS}} \sqrt{g}\, d^2x \ , \tag{10.29}$$

where λ_ϵ (resp. λ_σ) has mass dimension 1 (resp. 15/8) – there are no other relevant scalar operators in the theory. The signs in front of λ_ϵ and λ_σ are chosen for later convenience. As before, the cosmological constant $\lambda_{\mathbb{1}}$ must be tuned to make the theory finite. Physically, λ_ϵ and λ_σ can be interpreted as a temperature $T - T_c$ resp. a magnetic field. The action (10.29) is sometimes referred to as the *Ising field theory*.

In the following sections, we will study the action (10.29) in AdS$_2$, picking a definite boundary state. Let us first discuss the phenomenology of (10.29) in flat space, where it has been studied in detail. Notice that the long-distance physics of (10.29) is controlled by the dimensionless coupling $\eta = \lambda_\epsilon / |\lambda_\sigma|^{8/15}$, where the absolute value is a consequence of the $\mathbb{Z}_2$ symmetry. Due to Kramers-Wannier duality, η parametrizes the projective line: the points $\eta = \pm\infty$ are identified. There are two integrable points in the phase diagram: $\eta = 0$ ($\lambda_\epsilon = 0$), called the *magnetic* deformation, and $\eta = \infty$ ($\lambda_\sigma = 0$), the *thermal* deformation. The thermal deformation is identical to the theory of a Majorana fermion with mass $m = 2\pi\lambda_\epsilon$, provided that ϵ has the canonical CFT normalization $\langle \epsilon(x)\epsilon(0)\rangle = 1/|x|^2$. Surprisingly, the magnetic deformation can be exactly solved as well [182, 183], and its particle content is known. For generic η, the theory in flat space or on the cylinder cannot be solved exactly, but a quantitative understanding of the spectrum has been obtained in the series of papers [184–188], some of which use variants of Hamiltonian truncation on the cylinder $\mathbb{R} \times S^1$. Finally, the thermal deformation of the Ising model in AdS$_2$ was studied in Ref. [150].

Let us now turn to the definition of the model (10.29) in AdS. At the conformal fixed point, as explained above, the relevant boundary conditions are labeled by the three primaries of the model:

$$|\mathbb{1}\rangle_{\text{Cardy}} = \frac{1}{2^{1/2}}|\mathbb{1}\rangle\!\rangle + \frac{1}{2^{1/2}}|\epsilon\rangle\!\rangle + \frac{1}{2^{1/4}}|\sigma\rangle\!\rangle \ , \tag{10.30a}$$

$$|\epsilon\rangle_{\text{Cardy}} = \frac{1}{2^{1/2}}|\mathbb{1}\rangle\!\rangle + \frac{1}{2^{1/2}}|\epsilon\rangle\!\rangle - \frac{1}{2^{1/4}}|\sigma\rangle\!\rangle \ , \tag{10.30b}$$

$$|\sigma\rangle_{\text{Cardy}} = |\mathbb{1}\rangle\!\rangle - |\epsilon\rangle\!\rangle \ . \tag{10.30c}$$

The boundary conditions labeled by $\mathbb{1}$ and ϵ are mapped to each other by a spin flip: they are fixed boundary conditions for the microscopic degrees of freedom. The spectrum supported on both boundary conditions only includes the identity module. The σ Cardy state, which is invariant under $\mathbb{Z}_2$, corresponds to free boundary conditions. Its spectrum contains the identity module and the $\mathbb{Z}_2$ odd module labeled by $\Delta = 1/2$, which can be identified with the family of states with an odd number of particles in the free fermion description.

In the critical model, Kramers-Wannier duality can be implemented by a topological defect D_σ [189], whose action on the boundary states teaches us how the boundary conditions are mapped to each other:

$$D_\sigma\,|\mathbb{1}\rangle_{\text{Cardy}} = D_\sigma\,|\epsilon\rangle_{\text{Cardy}} = |\sigma\rangle_{\text{Cardy}} \ , \qquad D_\sigma\,|\sigma\rangle_{\text{Cardy}} = |\mathbb{1}\rangle_{\text{Cardy}} + |\epsilon\rangle_{\text{Cardy}} \ . \tag{10.31}$$

As we shall discuss in a moment, the action of the duality is useful in understanding the RG flow triggered by deforming the theory in AdS by the ϵ operator.

We shall perform a Hamiltonian truncation study of the RG flows emanating from the critical Ising model with $\mathbb{1}$ boundary condition. Here are the first few states and their degeneracies:

Δ	0	1	2	3	4	5	6	7	8	9	10
states	1	0	1	1	2	2	3	3	5	5	7
$sl(2)$ primaries	1		1		1		1		2		2

We shall comment along the way about the other boundary conditions. Once we normalize the vacuum state to one, the expectation values of the deforming operators are

$$\langle\epsilon\rangle = (2R)^{-\Delta_\epsilon}\frac{\langle\epsilon|\mathbb{1}\rangle_{\text{Cardy}}}{\langle\Omega|\Omega\rangle} = \frac{1}{2R} \ , \tag{10.32}$$

$$\langle\sigma\rangle = (2R)^{-\Delta_\sigma}\frac{\langle\sigma|\mathbb{1}\rangle_{\text{Cardy}}}{\langle\Omega|\Omega\rangle} = \frac{2^{1/4}}{(2R)^{1/8}} \ . \tag{10.33}$$

These values determine $\lambda_{\mathbb{1}}$ in eq. (10.29), as a function of λ_σ and λ_ϵ.

10.4 The Ising model with thermal deformation

In this section, we will consider the purely thermal deformation, setting $\lambda_\sigma = 0$ in eq. (10.29). Keeping into account eq. (10.32), the potential reads

$$\bar{\lambda} V = -\bar{\lambda} \int_{-\pi/2}^{\pi/2} \frac{dr}{(\cos r)^2} \left(R\, \epsilon(\tau = 0, r) - \frac{1}{2} \right) , \tag{10.34}$$

with $\bar{\lambda} = R\lambda_\epsilon$. This flow is exactly solvable, since, as advertised, it is described by a free Majorana fermion in AdS, with mass $m = 2\pi\lambda_\epsilon$. In fact, there is hardly the need to perform any computation in order to describe the spectrum. Let us start from the critical theory. A free Majorana fermion on the upper half plane admits two boundary conditions, $\psi = \nu\bar{\psi}$, with $\nu = \pm 1$. The chiral flip $(\psi, \bar{\psi}) \to (-\psi, \bar{\psi})$, which corresponds to the Kramers-Wannier duality of the Ising model, flips the sign of the mass and swaps the boundary conditions. Hence, the theory in AdS is only allowed to depend on the product $m\nu$. Furthermore, leading order perturbation theory is exact, so the trajectories $\mathcal{E}(mR)$ must be linear. Finally, looking at the sign of m which admits a flat space limit, we conclude that the slope of the first excited state is precisely the fermion mass:

$$\mathcal{E} = m\nu R + \frac{1}{2} , \qquad \nu = \pm 1 . \tag{10.35}$$

The constant term is just the scaling dimension of a free massless fermion. The rest of the spectrum is easily obtained by the usual Fock space construction. At the critical point, a fermion in mode n has energy

$$e_f = \frac{1}{2} + n , \tag{10.36}$$

and following the Pauli exclusion principle, no pair of fermions share the same mode. Therefore, the energy of a state with N fermions is

$$\mathcal{E}_N = N m\nu R + \frac{N}{2} + \sum_{i=1}^{i=N} n_i , \qquad n_i \neq n_j \tag{10.37}$$

where n_i is a non negative integer: $n_i \in \mathbb{N}_0$.

In fact, the argument above fixes eq. (10.35) only up to a sign, but we can define the sign in front of m in the Hamiltonian so as to obtain eq. (10.35) as written. Of course, the sign might be fixed by computing the leading (and only) order in Rayleigh-Schrödinger (RS) perturbation theory. Further details about the quantization of the free Majorana fermion in AdS$_2$ can be found in [150]. Eq. (10.35) determines the spectrum of the Ising model with any of the boundary states (10.30). Before comparing this prediction with the result of Hamiltonian truncation, let us briefly discuss the cutoff effects.

Cutoff effects

As for any minimal model with the boundary condition labeled by the identity, the leading operator at the conformal fixed point has $\Delta = 2$. Hence, we expect the convergence rate to approach Λ^{-1} for a large enough cutoff. This is indeed the case, as it can be seen in figure 10.8. The right panel, in particular, shows that in this case we can follow the first excited state up to a larger coupling than in our previous examples: $\bar{\lambda} = 2$ corresponds to $Rm = 4\pi \simeq 12.6$, so the radius of AdS is more than ten times larger than the Compton wavelength of the fermion. On the other hand, it is worth mentioning a feature of the convergence rate at weak coupling. Following appendix H.2, one can compute the coefficient of the Λ^{-1} term – *i.e.* c_i in eq. (8.51) – at second order in perturbation theory. It turns out that $c_1 = O(\bar{\lambda}^3)$, c_1 being the coefficient associated to the convergence of the first excited state. By reproducing the left plot of figure 10.8 at different values of $\bar{\lambda}$, it is possible to confirm this fact.

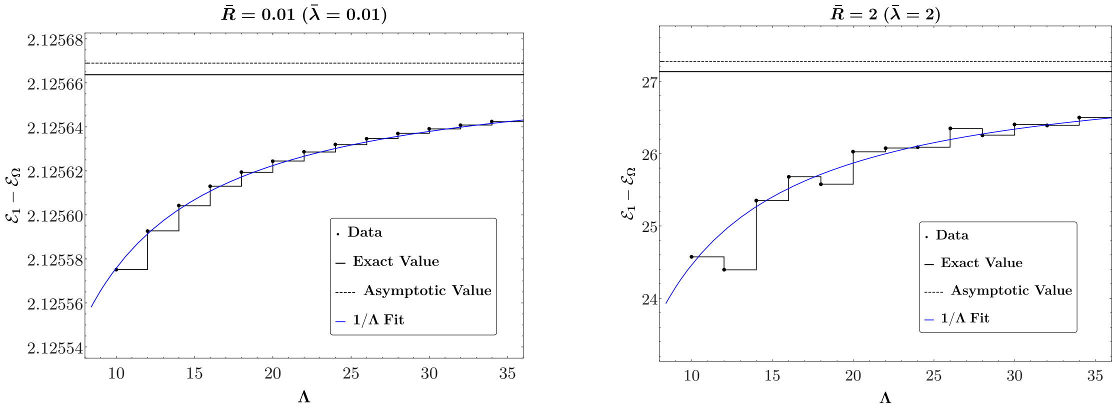

Figure 10.8: Energy of the first excited state in the Ising model deformed by ϵ versus the cutoff, for weak and strong couplings. The dashed lines are the asymptotic values extracted from the fit. The error bar can be found in figure 10.9.

Spectrum

Let us now associate the spectrum (10.35) to the boundary states (10.30) of the Ising model. Again, let us start from the UV fixed point. The $\mathbb{1}$ and ϵ boundary conditions only support the vacuum Virasoro character. Hence, their spectrum at the fixed point is integer spaced, and can be obtained from the Majorana fermion by projecting onto the states with even fermion number.[9] The projection is obviously maintained by the deformation (10.34). Therefore, the spectrum in AdS is obtained from eq. (10.37) with the same projection. In particular, at $\bar{\lambda} = 0$ the first excited state is made of two fermions

---

[9] This projection is obtained by orbifolding the $\mathbb{Z}_2$ symmetry, the twisted sector being implemented by Ramond boundary conditions. In fact, the Ramond Ishibashi state for the Majorana fermion equals $|\sigma\rangle\rangle$ in eq. (10.30) [190]. Correspondingly, the two available boundary conditions for periodic (Neveu-Schwarz) fermions equal $|\mathbb{1}\rangle_{\text{Cardy}} + |\epsilon\rangle_{\text{Cardy}}$ and $|\sigma\rangle_{\text{Cardy}}$ respectively.

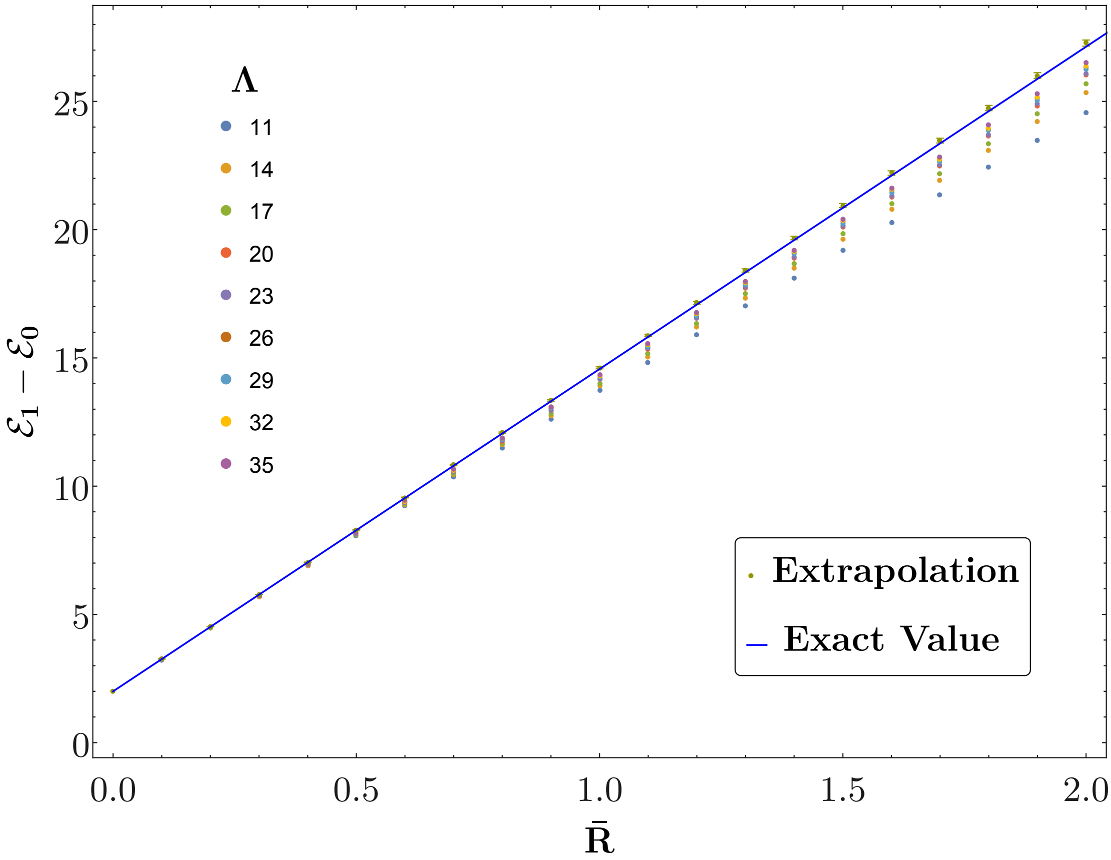

Figure 10.9: Energy of the first excited state in the Ising model with thermal deformation as a function of $\bar{R}$.

in modes $n = 0$ and $n = 1$, with energy $\mathcal{E} = 2$. Similarly, the lowest energy state with four fermions appears at $\mathcal{E} = 8$. In order to identify the spectrum, we still need to fix the sign of ν in eq. (10.35). The simplest way to do it is to perform a leading order computation in RS perturbation theory. The result shows that, with the identification $m = 2\pi\lambda_\epsilon$, $\nu = +1$ for the $\mathbb{1}$ boundary condition.

We are ready to compare with the results of Hamiltonian truncation. The gap is shown in figure 10.9, where the good convergence up to large values of the coupling is evident. Figure 10.10 gathers several low lying states, up to the first couple of four-particle states. Comparing with the table of quasiprimaries presented above, we see that, contrary to the other examples considered in this work, the second quasiprimary above the vacuum ($\Delta = 4$ at $\bar{\lambda} = 0$) has the same slope as the first excited state. This agrees with the usual expectation: while all the excited single particle states are $SL(2, \mathbb{R})$ descendants, the spectrum of two-particle states includes infinitely many quasiprimaries. Truncation errors are small, but visible: they begin to lift the degeneracies in the upper right corner of the plot.

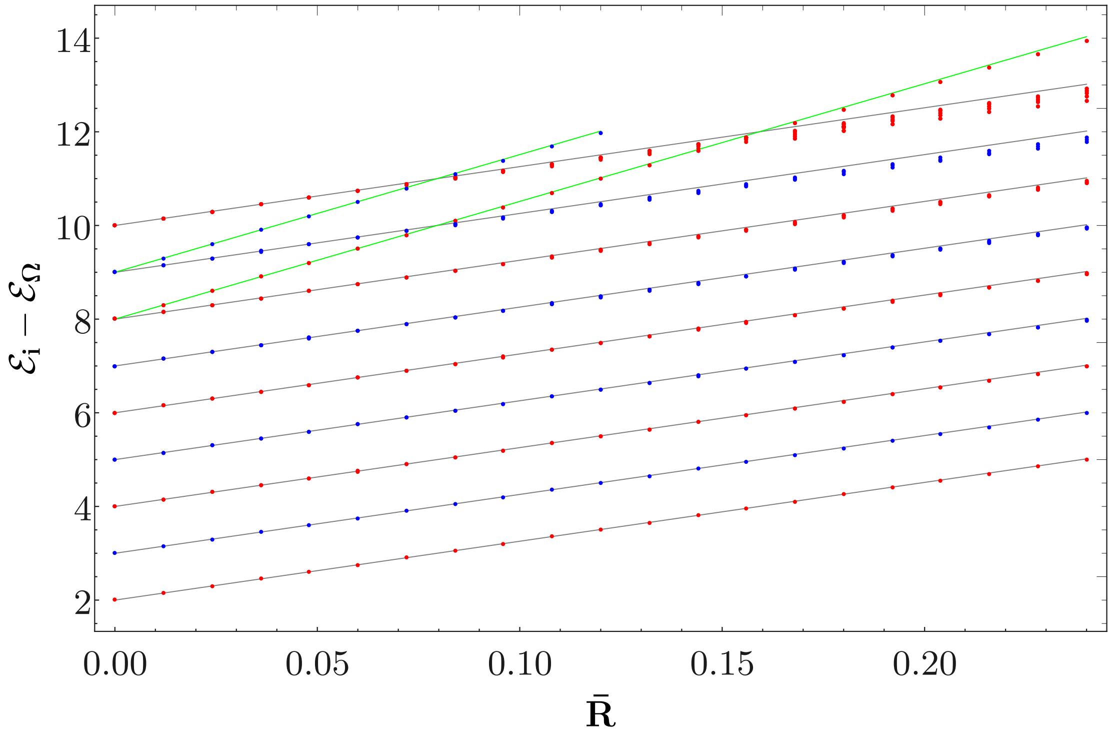

Figure 10.10: Spectrum of the Ising model with thermal deformation. The color distinguishes parity even (red) from parity odd (blue) eigenstates. The data is computed at $\Lambda = 28$. Black and green lines mark the exact spectrum for the states with two and four fermions respectively.

The level crossing among the first four-particle state and the two-particle states leaving from $\Delta = 10$ deserves a special discussion. This is the first example where level crossing happens among states in the same parity sector. As we pointed out in subsection 7.4, in the continuum limit the $SL(2,\mathbb{R})$ symmetry implies exact level crossing. On the other hand, at every finite truncation one expects level repulsion to take place. This creates a puzzle for the prescription (8.1). What is the correct bare energy e_i to be used in the formula? The question is non trivial since our argument for the validity of eq. (8.1) relies on studying the theory with a spatial cutoff, which again breaks $SL(2,\mathbb{R})$. We find experimentally that the correct procedure is to assign the bare energy e_i following the exact ($\Lambda = \infty$) lines. In other words, the red data points on the green line on the right of the crossing points are obtained from eq. (8.1) with $e_i = 8$. Since level repulsion is forbidden in the continuum, the prescription is in principle well defined. However, for a finite cutoff Λ the levels do not exactly cross, so the procedure becomes ambiguous in a region around the crossing point, whose size shrinks as the cutoff is increased.

Let us now briefly discuss the σ boundary condition, eq. (10.30c). Since Kramers-Wannier duality maps $\mathbb{1}$ to σ – see eq. (10.31) – the spectrum originating from the

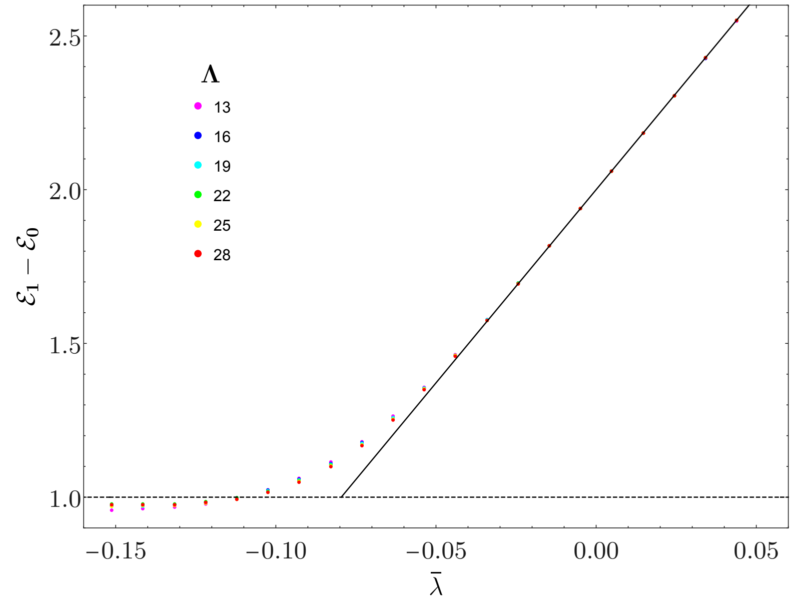

Figure 10.11: Energy of the first excited state in the Ising model with thermal deformation, in a range of couplings including $\bar{\lambda} < 0$. The solid line is the exact solution. Notice that in this model $\bar{\lambda} = \bar{R}$, hence this plot is the continuation of the plot in figure 10.9. We use the label $\bar{\lambda}$ for consistency with the other examples.

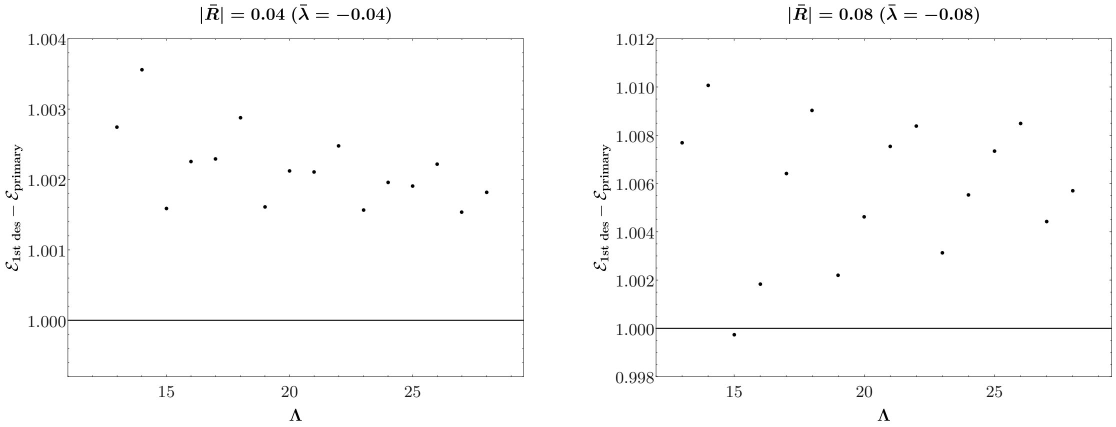

Figure 10.12: Gap between the first excited state and its leading descendant, in the Ising model with thermal deformation, for $\bar{\lambda} < 0$. When the coupling is sufficiently negative, the restoration of conformal invariance is extremely slow, if at all present.

thermal deformation of the latter is obtained by choosing $\nu = -1$ in eq. (10.37). Since the σ boundary condition admits a state with $\Delta = 1/2$, the gap is given by the single particle state in eq. (10.35), with slope -2π as a function of $\bar{R}$. In general, the spectrum is composed of both even and odd fermion states. The gap as a function of the radius of AdS, for all the boundary conditions, is presented together in fig 11.2.

Finally, let us again discuss what happens if we turn on the coupling with the *wrong* sign, *i.e.* the sign which does not allow to reach the flat space limit. We expored this question with Hamiltonian truncation, the result being shown in figure 10.11. Like with the Lee-Yang model, our data become unreliable as the gap approaches $\Delta = 1$. This is showcased not only by the discrepancy between the data and the exact solution, but also by the lack of $SL(2,\mathbb{R})$ invariance of the spectrum – see figure 10.12. In the exact theory, the gap $\Delta = 1$ corresponds to $\bar{\lambda} = -1/4\pi$. There, the free fermion Hamiltonian, with the boundary conditions we are considering, stops being well defined. Indeed, the integral of the Hamiltonian density diverges due to the behavior of the Fermi fields close to the boundary [150]. On the other hand, the theory emanating from the σ boundary condition has rising trajectories in the direction of negative $\bar{\lambda}$, and is well defined beyond the $\Delta = 1$ point. Precisely at $\bar{\lambda} = -1/4\pi$, the spectra of the two theories, remarkably, match, including all the multiplicities, as one can check by plugging $mR = -1/2$ in eq. (10.37), and recalling that when $\nu = 1$ the Ising model is obtained by restricting to even N. This situation is coherent with both the free boson spectrum at the BF bound and the picture we sketched while discussing the Lee-Yang model. Again, we delay until section 11 a unified discussion.

10.5 The Ising model in a magnetic field

We now move on to discuss the deformation triggered by λ_σ in eq. (10.29). More precisely, we perturb the fixed point Hamiltonian with

$$\bar{\lambda} V = -\bar{\lambda} \int_{-\pi/2}^{\pi/2} \frac{dr}{(\cos r)^2} \left(\frac{R^{\Delta_\sigma}}{a_\sigma} \sigma(\tau = 0, r) - 1 \right) , \qquad a_\sigma = 2^{1/8} . \tag{10.38}$$

Again, we consider the flow originating from the boundary condition labeled by the identity. The sign is chosen so that, deforming the fixed point Hamiltonian with $\bar{\lambda} > 0$, the energies monotonically increase with R. Notice that, since the $\mathbb{Z}_2$ symmetry maps the $\mathbb{1}$ boundary condition into ϵ, the sign of the magnetic field is meaningful. In particular, comparing with eq. (10.33), we see that $\bar{\lambda} > 0$ corresponds to a magnetic field in the same direction in the bulk as on the boundary. We shall analyze both positive and negative values of $\bar{\lambda}$ below.

In the $R \to \infty$ limit, the particle content is known thanks to the integrability of the flow in flat space. The integrable flat space theory contains 8 particles, 3 of which have mass below the two-particle continuum [182]. The mass ratio of the two lightest particles is given by

$$\frac{m_2}{m_1} = 2 \cos \frac{\pi}{5} \approx 1.618 . \tag{10.39}$$

The Ising model with a magnetic field is not exactly solvable in AdS, and the results for the spectrum presented below are new.

Cutoff effects

The analysis of the cutoff effects proceeds in parallel with the previous examples. In figure 10.13 the expected $1/\Lambda$ convergence rate is tested, for $\bar{\lambda} > 0$, both at weak and at strong coupling. While the left plot gives confidence that the asymptotic region has been reached, the fit in the right plot is poorer. A similar situation emerges from the study of the gap between the first excited state and its first descendant. In the left panel of figure 10.14, we observe a steady convergence to the unit gap expected in the continuum. In the right panel, the size of the violation of the $SL(2,\mathbb{R})$ symmetry rapidly drops, but then the convergence becomes slow. These are signs that around $\bar{\lambda} = 1$ it may be worth pushing the numerics further in the future, or improving the convergence rate along the lines of subsection 8.7. However, it is not easy to draw an indication of the size of the error. For instance, primaries and descendants may be affected by cutoff effects in a similar way, thus reducing the violation of conformal symmetry visible in figure 10.14. On the other hand, the procedure explained in subsection 9.1, which extracts error bars from the quality of the fits in figure 10.13, yields a small error: the error bars are smaller than the size of the points in figure 10.17.

Finally, in figures 10.15 and 10.16, we repeated the analysis with a choice of two negative values for $\bar{\lambda}$. As in the previous examples, if the sign of the coupling does not allow for a flat space limit, the convergence rapidly deteriorates. As shown in the right panel of both figures, at a coupling $\bar{\lambda} \simeq -0.1$ the spectrum is hardly converged in the range of cutoffs available to us.

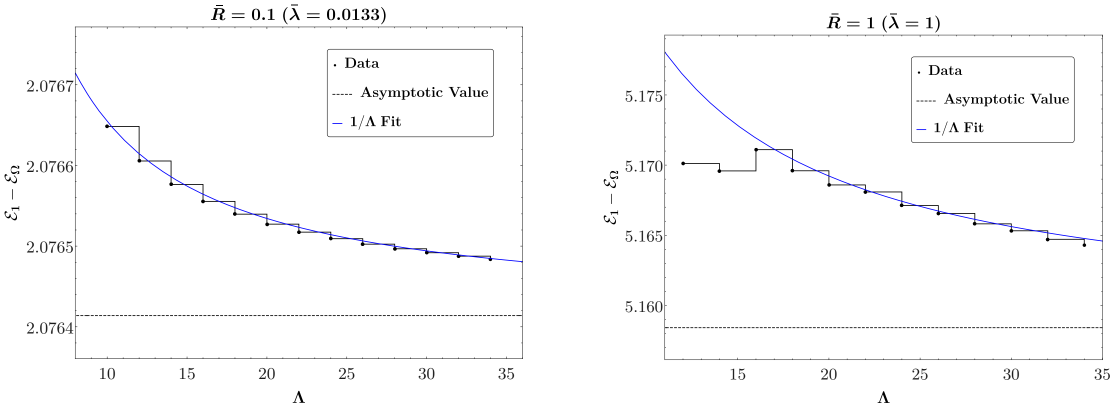

Figure 10.13: Energy of the first excited state in the Ising model deformed by σ, as a function of the cutoff, at weak and strong coupling.

Spectrum

We are ready to present the results of the TCSA applied to this model. Figure 10.17 shows the growth of the energy gaps with R, when the magnetic field in the bulk and on the boundary are aligned ($\bar{\lambda} > 0$). Two conformal families are visible, the quasiprimaries

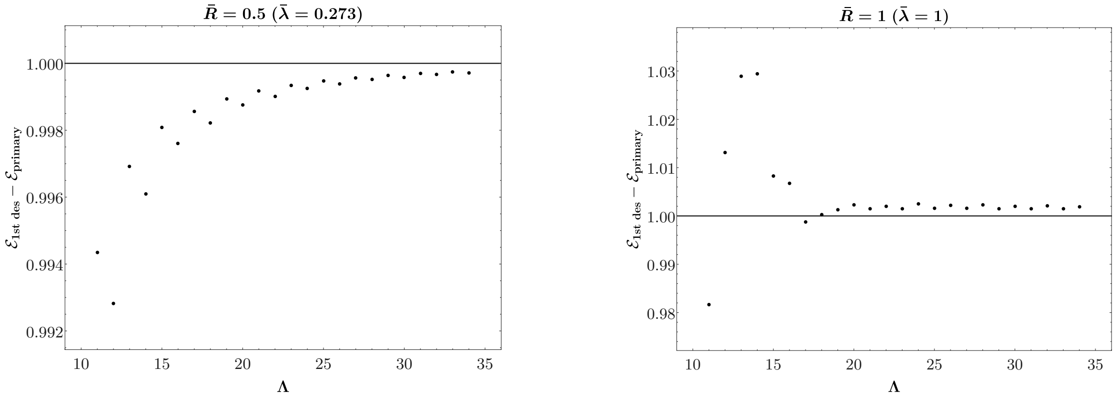

Figure 10.14: Energy gap between the first primary and its first descendant for two different couplings, in the Ising model with a magnetic field.

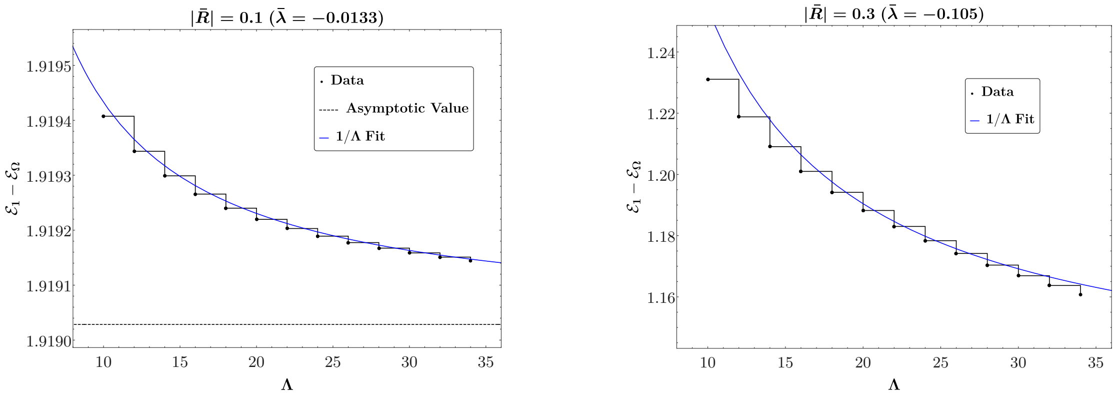

Figure 10.15: Energy of the first excited state in the Ising model, as a function of the cutoff, for two choices of negative magnetic field, $\bar{\lambda} < 0$.

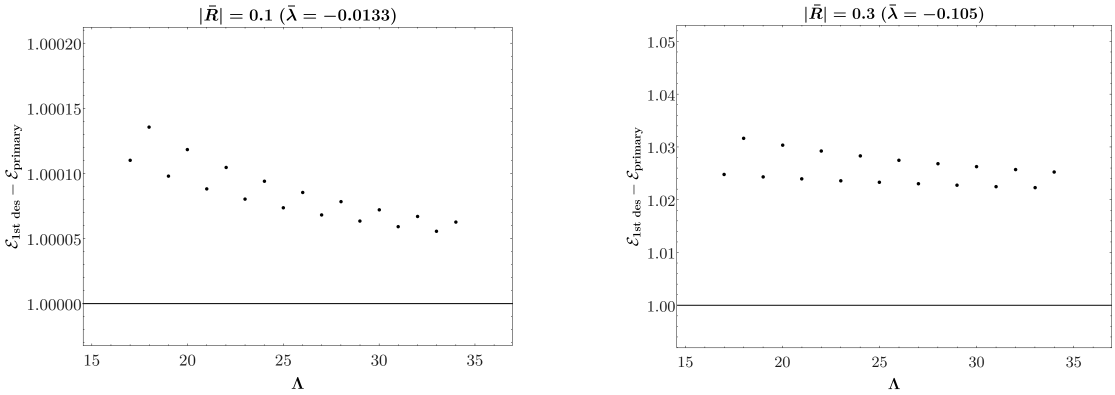

Figure 10.16: Energy gap between the first primary and its first descendant, as a function of the cutoff, for two choices of negative magnetic field, $\bar{\lambda} < 0$.

being highlighted by black lines. They are on their way to become the first two particles in the flat space spectrum with masses satisfying (10.39). However, the effects of the curvature are still sizable at these values of $\bar{R}$: the ratio of the two slopes is at most ~ 1.5, to be compared with the exact value 1.618.

Figure 10.18 again shows the low lying spectrum, this time as a function of the intensity of the magnetic field $\bar{\lambda}$. For negative values of $\bar{\lambda}$, the first excited state approaches the threshold $\Delta = 1$. As we pointed out in the previous examples, we expect the theory to become unstable when this happens. Correspondingly, the convergence of the truncation is poor for the leftmost points in the plot, and we cannot reliably draw conclusions about the value of $\bar{\lambda}$ where a new marginal operator arises, nor about the dependence $\Delta(\bar{\lambda})$ close to that point.

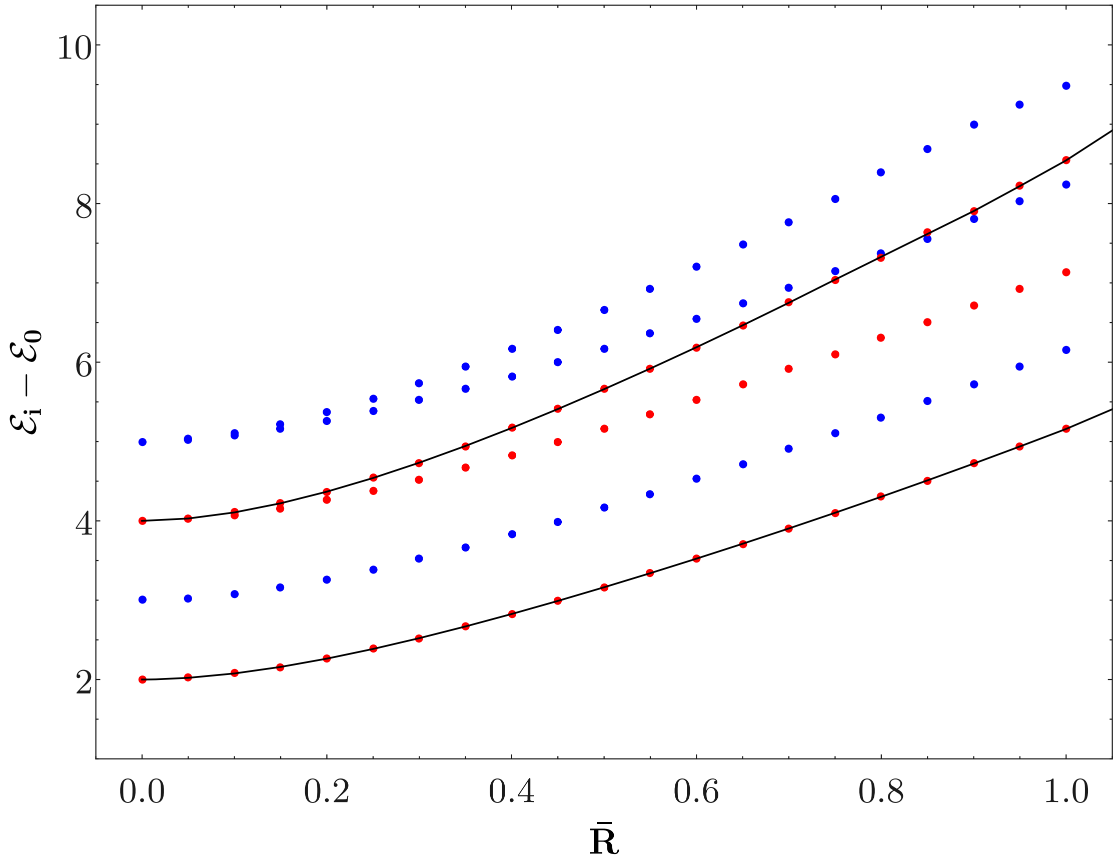

Figure 10.17: Spectrum of the Ising model in a positive magnetic field, $\bar{\lambda} > 0$, as a function of the radius of AdS. The red and blue points are the extrapolated data, even and odd respectively under parity. The black lines highlight the first two quasiprimaries, and are only meant to guide the eye.

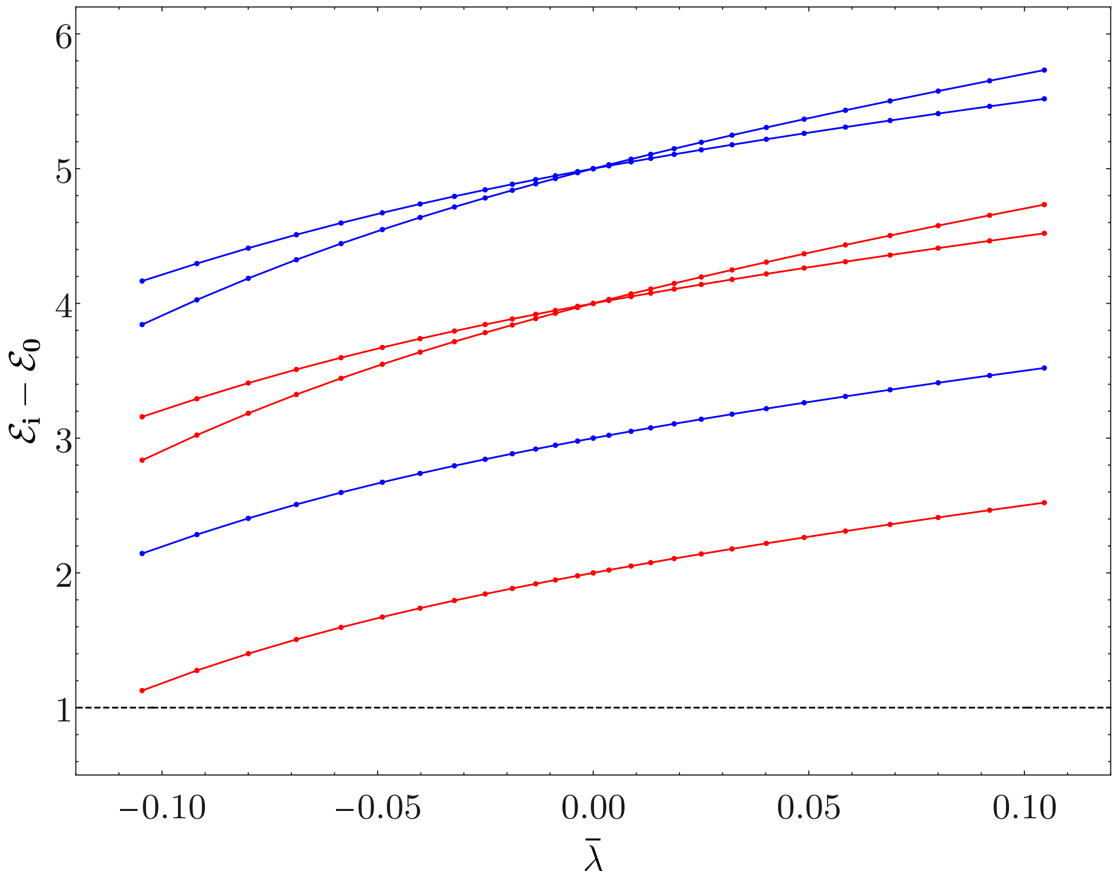

Figure 10.18: Spectrum of the Ising model in a magnetic field, as a function of the magnitude of the field. Error bars as measured from the uncertainty in the extrapolation are not shown: they would be small, throughout the plot, but as discussed in the text they probably underestimate the deviation from the continuum limit.

11 Conclusion

AdS spacetime provides a maximally symmetric IR regulator for QFT. Furthermore, one can place operators at the conformal boundary of AdS and their correlations functions obey all the conformal bootstrap axioms (except for the existence of a stress tensor). This opens the possibility to study massive QFT with the non-perturbative conformal bootstrap methods [38]. There are two main difficulties to realize this idea in practice. The first is technical: the standard numerical conformal bootstrap methods converge poorly for large scaling dimension of the external operators, which corresponds to the regime of large AdS radius. The second is conceptual: how to specify the particular solutions of the bootstrap equations that corresponds to a particular QFT in AdS? One of our motivations to develop the present work was the need for more data to help address the second question.

In this work, we showed that QFT in AdS$_2$ can be studied non-perturbatively using Hamiltonian truncation. Our main target was the computation of the low-lying spectrum of the Hamiltonian conjugate to global time (or equivalently the scaling dimensions of boundary operators). We presented a concrete method to renormalize divergences in Hamiltonian truncation and obtain finite physical results for the energy spectrum. In this way, this work opens a new non-perturbative window into QFT on AdS spacetime.

Along the way, we gathered data about the spectrum at finite radius of a variety of two dimensional QFTs. A striking feature of all the models we studied is the existence of a minimal value of the coupling, λ_{min}, beyond which the convergence of Hamiltonian truncation becomes poor. When the model is exactly solvable, *i.e.* for the free boson and the Ising model with zero magnetic field, the minimal coupling can be precisely identified: it is the point where the spectra of the theories defined in the UV with different boundary conditions become identical. This leads us to the following speculation:

All conformally invariant boundary conditions for a given CFT are connected by relevant *deformations of this CFT in AdS.*

In figures 11.1 and 11.2 we depict how this may work for the spectrum of boundary operators in the Lee-Yang and the Ising field theories. This speculation is supported by the numerical results in figures 10.7 and 10.18. In figure 11.3, we show the analogous figure for the exactly solvable model of a free massive scalar in AdS_{d+1}. It is interesting to notice that the free massive fermion provides an additional, somewhat degenerate, instance of this phenomenon. Indeed, the spectra obtained by quantizing the theory with the two possible boundary conditions are reported in eq. (10.37): rather than being connected by a flow in AdS, they precisely coincide at the conformal fixed point $\bar{\lambda} = 0$.[1]

Leaving aside the case of the free fermion, let us comment on the expected behavior close to the merging point of two curves. For concreteness, consider figure 11.1. The theory emanating from the $\mathcal{V}$ boundary condition has a relevant operator, which generically has to be fine tuned on the boundary, in order to preserve the AdS isometries. Let us call g the coupling of this operator. The fine tuning is possible as long as the operator is not marginal, so this leads us to identify $\bar{\lambda}_{\text{min}}$ with the coupling where $\Delta = d = 1$. If we perturb $\bar{\lambda}$ away from this value, the beta function has the form

$$\beta(g) = (\bar{\lambda} - \bar{\lambda}_{\text{min}}) - g^2 + \dots \tag{11.1}$$

where we neglect higher order terms in the boundary coupling g and in the bulk coupling $(\bar{\lambda} - \bar{\lambda}_{\text{min}})$.[2] We are also careless about the magnitude of the coefficients in eq. (11.1): they can be related to the appropriate bulk-to-boundary two-point function and boundary three-point function. On the other hand, the signs have been chosen to match the phenomenology in figure 11.1. Indeed, for $\bar{\lambda} > \bar{\lambda}_{\text{min}}$ there are two fixed points with $g = g_\pm = \pm\sqrt{\bar{\lambda} - \bar{\lambda}_{\text{min}}}$. These fixed points correspond to the two curves merging at $\bar{\lambda} = \bar{\lambda}_{\text{min}}$. In fact, the corresponding scaling dimension of the lightest boundary operator is given by

$$\Delta_\pm = d + \frac{d\beta}{dg}(g_\pm) = d \pm 2\sqrt{\bar{\lambda} - \bar{\lambda}_{\text{min}}}\,, \tag{11.2}$$

in agreement with our sketch. The theory at $\bar{\lambda} < \bar{\lambda}_{\text{min}}$ should instead be described by a complex CFT [191, 192]. The same features present themselves in all of the figures in this chapter, except for the left panel in figure 11.2. In this case, the two curves cross rather than merging smoothly, and the lower curve is allowed to proceed to the left towards the flat space limit. The reason for this exception is simple: the relevant operator σ_b is $\mathbb{Z}_2$ odd, while the bulk perturbation is $\mathbb{Z}_2$ even. No fine tuning is necessary in this case, hence no dangerous marginal operator is turned on at $\bar{\lambda} = \bar{\lambda}_{\text{min}}$. Finally, this discussion suggests that turning on the relevant boundary operator allows to flow between the theories which merge at $\bar{\lambda}_{\text{min}}$.

---

[1] Notice instead that they do not coincide at λ_{min} as defined in figure 11.2. As explained in section 10.4, the spectrum of the Ising model with the $|\mathbb{1}\rangle_{\text{Cardy}}$ boundary condition equals the free fermion spectrum, projected onto the even fermion number. It is this projected spectrum which merges with the full fermionic theory flowing from the $|\sigma\rangle_{\text{Cardy}}$ boundary condition. Without the projection, the two spectra have different multiplicities at $\lambda = \lambda_{\text{min}}$. Moreover, the $|\mathbb{1}\rangle_{\text{Cardy}}$ boundary condition has an additional single fermion state with vanishing energy.

[2] A term proportional to $g(\bar{\lambda} - \bar{\lambda}_{\text{min}})$ can be eliminated by shifting g.

We look forward to learn about other studies that confirm or disprove the speculation above.

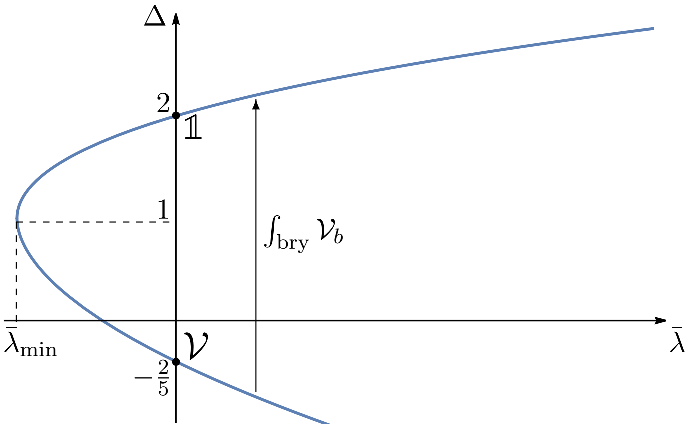

Figure 11.1: Sketch of the scaling dimension of the first boundary operator (above the identity) for the scaling Lee-Yang model in AdS$_2$. At $\lambda = 0$, the bulk theory is conformal and the two black dots correspond to the two possible BCFTs (labeled by $\mathbb{1}$ and $\mathcal{V}$) for the Lee-Yang minimal model. We conjecture that the two curves merge (smoothly) at $\bar{\lambda} = \bar{\lambda}_{\text{min}} \approx -0.5$ and $\Delta = 1$ (see figure 10.7). We expect that Δ becomes complex for $\bar{\lambda} < \bar{\lambda}_{\text{min}}$ similarly to what happens for complex CFTs [192]. There is also a boundary RG flow generated by the relevant boundary operator with $\Delta < 1$ that goes from the lower to the upper curve.

In this work, we also explored other aspects of QFT in curved space. In particular, we discussed spontaneous symmetry breaking in AdS, both in the classical theory, in section 7.5, and via Hamiltonian truncation for ϕ^4 in section 9.2. Our considerations leave open a few interesting questions, related to the nature of symmetry breaking at finite AdS radius. Probably the most pressing one is: what is the signal on the boundary of the phase transition in the bulk? When analyzing the ϕ^4 theory, we provided evidence for the fact that the bulk theory is not described by a CFT at the phase transition. This evidence was based at weak coupling on connecting the phase transition line to a free massive boson at the BF bound, whose stress tensor is not traceless. Hence, we should not be looking for Virasoro symmetry in the boundary spectrum. On the other hand, the appearance of the BF bound raises the tantalizing hypothesis that the (in)stability of the false vacuum shares some similarities with the previously discussed (in)stability of a theory under bulk deformations beyond a coupling $\bar{\lambda}_{\text{min}}$, due to the flow generated by a marginal operator. It would be interesting to scrutinize this hypothesis further, perhaps via a higher order computation at weak coupling.

Moving on to the more technical aspects, a lot of effort was devoted in this work to overcome the challenges presented by Hamiltonian truncation in infinite volume, leading

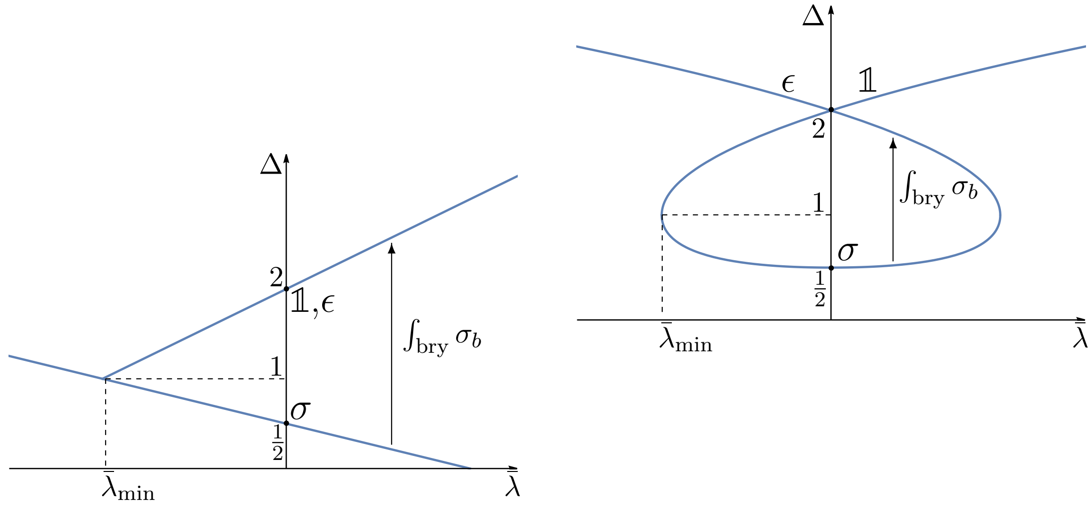

Figure 11.2: Sketch of the scaling dimension of the first boundary operator (above the identity) for the Ising field theory in AdS_2. The black dots mark the three possible BCFTs (labeled by $\mathbb{1}$, ϵ and σ) for the Ising minimal model. On the left, we show the thermal deformation that is exactly solvable in terms of a massive free fermion [150]. On the right, we show (our best guess for) the magnetic deformation. The curve marked $\mathbb{1}$ was studied with Hamiltonian truncation (see figure 10.18). The curve marked ϵ is obtained from this one by the $\mathbb{Z}_2$ (spin flip) symmetry of the Ising model. This $\mathbb{Z}_2$ symmetry implies that the right picture should be symmetric under the reflection $\bar{\lambda} \to -\bar{\lambda}$. We conjecture that the curves merge (smoothly) at $\bar{\lambda} = \pm\bar{\lambda}_{\text{min}} \approx \pm 0.1$ and $\Delta = 1$. There is also a boundary RG flow generated by the relevant boundary operator with $\Delta < 1$ that goes from the lower to the upper curves. In the right plot, the flow is expected to land on the first stable fixed point. This is clearly visible from the perturbative beta function (11.1) close to $\bar{\lambda}_{\text{min}}$, which describes a one-parameter flow.

up to the prescription (8.1). We hope that the lessons learned here will be useful in studying other UV sensitive flows with the same framework. While the prescription has been tested in a variety of situations, we came short of rigorously proving its validity. The main obstacle is the lack of positivity of the spectral densities involved in the computation, whose large energy limit is therefore not easily tied to the short distance limit of the Laplace transform. Famously [53], this problem would not be present if we wanted to estimate the large energy limit of the spectral density averaged over a smooth measure. This suggests that it may be worth applying to this problem the ideas of [193], where a smooth cutoff was used instead of the usual sharp truncation of the Hilbert space to a finite subspace. Another direction worth exploring is the possibility for eq. (8.1) to emerge from a renormalization procedure, where the high energy tail of the spectrum is integrated out systematically [40]. The difficulty is of course that the Hamiltonian in AdS does not possess a continuum limit to start from. One possible starting point is the theory with a spatial cutoff ϵ, as in eq. (8.13), which is well defined. An RG derivation of the prescription might be useful in elucidating the UV sensitivity of eq. (8.1), which depends explicitly on the bare energies. For instance, this feature gives rise to an ambiguity along

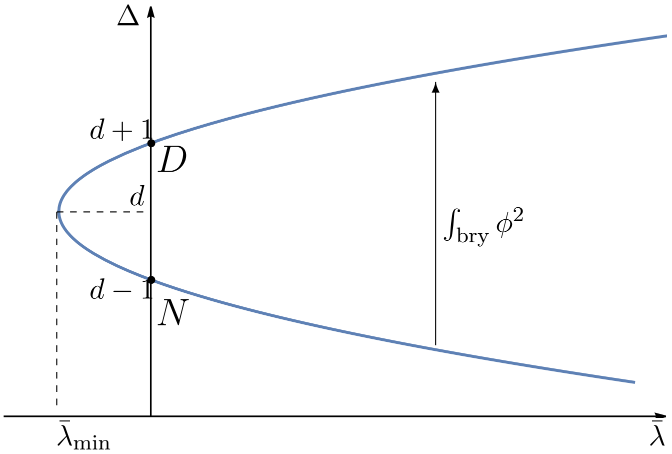

Figure 11.3: Scaling dimension of the first $\mathbb{Z}_2$-even boundary operator (above the identity) for a free massive scalar field in AdS_{d+1}, namely $\Delta = d \pm \sqrt{1+4\bar{\lambda}}$. The value $\bar{\lambda} = 0$ corresponds to a conformally coupled scalar. The black dots mark the two possible BCFTs (Dirichlet or Neunmann boundary conditions). We see that the 2 curves merge smoothly at $\bar{\lambda} = -\frac{1}{4}$ and $\Delta = d$. There is also a ($\mathbb{Z}_2$ preserving) boundary RG flow generated by the relevant boundary operator (ϕ^2) with $\Delta < d$ that goes from the lower to the upper curve.

the flow, namely the identification of the correct shift in the neighborhood of a level crossing, as discussed in section 10.4.

With the aim of obtaining high precision results in Hamiltonian truncation at larger values of the the AdS radius, it will be necessary to systematically improve the action along the lines explained in section 8.7. This was important in previous works [41, 166, 168], and it would be especially worth trying it when the UV boundary spectrum contains operators with low scaling dimension, like the in the case of the minimal models.

A more ambitious way of improving the procedure is related to the fact that, in this work, we did not take full advantage of the symmetries of AdS spacetime. The isometry group of AdS_2 is $SL(2,\mathbb{R})$ and states must fall into irreducible representations of this group. We used this fact to test numerical convergence, but it would be interesting to exploit it to accelerate the algorithm. Perhaps, we could start by finding the subspace of the Hilbert space generated by primary operators by looking at the kernel of the symmetry generator K, and then diagonalize H in this subspace. We leave the exploration of this idea for the future.

One can also wonder if Hamiltonian truncation can be used to compute observables other than the spectrum. One motivation is the following. It is well known that one can extract scattering amplitudes from the finite size behaviour of the energy levels on a compact space [194]. However, in its standard form, this method only gives access to the elastic region of the 2 to 2 scattering amplitude. One advantage of AdS is that one can extract scattering amplitudes at arbitrarily high energy from the flat space limit of the boundary correlation functions [128, 130, 38, 195, 132, 133]. It would be interesting to adapt Hamiltonian truncation to compute boundary correlation functions and test this idea in practice.

Finally, a rewarding byproduct of our efforts was the formula (G.9), which summarizes the cumbersome sums characterizing Rayleigh-Schrödinger perturbation theory in a compact and useful expression. We proved eq. (G.9) for non-degenerate perturbation theory. It would be nice to generalize the formula to the degenerate case.

Appendix Part IV

A Special functions

In this appendix, we list a number of identities that are used throughout this thesis.

A.1 Common special functions

Gamma function

The large limit of the gamma function is given by Stirling's approximation as

$$\lim_{|z|\to\infty} \Gamma(z) = \sqrt{\frac{2\pi}{z}} e^{-z} z^{z}. \tag{A.1}$$

This is true for any x on the complex plane but the negative real line. The convergence is weaker as x approaches the negative real line and to get to the asymptotic regime, one needs to go beyond $|z| \sim 1/\theta$ in which θ is the angle with the negative real line. In the case in which $z = x + iy$ with $x, y \in \mathbb{R}$ and $|y| \gg 1$, one has:

$$\Gamma(x+iy) = (1-i)\sqrt{\pi} e^{\frac{i\pi x}{2} - iy - \frac{\pi y}{2}} y^{iy + x - \frac{1}{2}} \ . \tag{A.2}$$

Barnes's lemma

The following identity [196, Theorem 2.4.3] is known as Barnes's second lemma:

$$\begin{aligned} \frac{1}{2\pi i} \int_{-i\infty}^{i\infty} ds\, \Gamma(-s) \frac{\Gamma(a+s)\Gamma(b+s)\Gamma(c+s)\Gamma(1-e-s)}{\Gamma(f+s)} & \\ = \frac{\Gamma(a)\Gamma(b)\Gamma(c)\Gamma(1-e+a)\Gamma(1-e+b)\Gamma(1-e+c)}{\Gamma(f-a)\Gamma(f-b)\Gamma(f-c)} & \end{aligned} \tag{A.3}$$

which holds when $e = a + b + c - d + 1$.

Gegenbauer

The Gegenbauer function is defined as [197, 8.932.1]

$$C_J^\alpha(z) = \frac{\Gamma(J+2\alpha)}{\Gamma(J+1)\Gamma(2\alpha)}\ {}_2F_1\left[\begin{matrix}-J, J+2\alpha \\ \alpha+\frac{1}{2}\end{matrix}\ \middle|\ \frac{1-z}{2}\right] \tag{A.4}$$

which matches with the Gegenbauer polynomials when J is a non-negative integer with the following orthogonality relations:

$$\int_{-1}^{1} dx\ (1-x^2)^{\alpha-\frac{1}{2}} C_n^\alpha(x) C_m^\alpha(x) = \frac{\pi 2^{1-2\alpha}\Gamma(n+2\alpha)}{\Gamma(n+1)\Gamma(n+\alpha)\Gamma(\alpha)^2}\ . \tag{A.5}$$

for n and m non-negative integer.

Hypergeometric function

In this thesis we may use two equivalent notation of hypergeometric functions:

$${}_pF_q(a_1, \cdots, a_p; b_1, \cdots, b_q; z) = {}_pF_q\left[\begin{matrix}a_1, \cdots, a_p \\ b_1, \cdots, b\end{matrix}\ \middle|\ z\right]\ . \tag{A.6}$$

Integrating a hypergeometric function against a monomial yields [197, 7.511]:

$$\int_0^\infty dt\ t^{\alpha-1}\ {}_2F_1(a, b; c; -t) = \frac{\Gamma(c)\Gamma(\alpha)\Gamma(a-\alpha)\Gamma(b-\alpha)}{\Gamma(a)\Gamma(b)\Gamma(c-\alpha)} \tag{A.7}$$

where we assume the $0 < \Re(\alpha) < \min\{\Re(a), \Re(b)\}$ for the integral to be convergent.

It is very useful to change the last argument of hypergeometric to its inverse. This can be done by the identity [198, sec 2.9]

$${}_2F_1(a, b; c; z) = \frac{\Gamma(b-a)\Gamma(c)}{\Gamma(b)\Gamma(c-a)}(-z)^{-a}{}_2F_1\left[\begin{matrix}a, a-c+1 \\ a-b+1\end{matrix}\ \middle|\ \frac{1}{z}\right]\ +\ a \leftrightarrow b\ . \tag{A.8}$$

There is also two other identities that happen to be helpful in some of the calculations in this thesis [198, sec 2.9]:

$${}_2F_1(a, b; c; z) = (1-z)^{c-a-b}\ {}_2F_1(c-a, c-b; c; z)\ , \tag{A.9}$$

and

$${}_2F_1(a, b; c; z) = \frac{\Gamma(b-a)\Gamma(c)}{\Gamma(b)\Gamma(c-a)}(1-z)^{-a}\ {}_2F_1\left[\begin{matrix}a, c-b \\ a-b+1\end{matrix}\middle|\frac{1}{1-z}\right]\ +\ a \leftrightarrow b\ . \tag{A.10}$$

Let us collect some results that involve the branch cut of the hypergeometric function ${}_2F_1(a, b, c; z)$ across the cut $z \in [1, \infty)$. In particular, we want to find the discontinuity

(Disc) and the average (Ave) along the cut, which are defined as

$$\text{Disc}\,[f(z)] := f(z+i\epsilon)-f(z-i\epsilon) \quad \text{and} \quad \text{Ave}\,[f(z)] := \frac{1}{2}\left(f(z+i\epsilon)+f(z-i\epsilon)\right)\ . \tag{A.11}$$

Using (A.8) and

$$\text{Disc}[z^a] = 2i\sin\pi a\,(-z)^a\ , \tag{A.12}$$

we find that

$$\begin{aligned} \text{Disc}\,[{}_2F_1(a,b;c;z)] &= \cos(\pi a)\frac{\Gamma(b-a)\Gamma(c)}{\Gamma(c-a)\Gamma(b)}z^{-a}{}_2F_1\left[\begin{matrix}a, a-c+1\\ a-b+1\end{matrix}\middle|\frac{1}{z}\right] + a\leftrightarrow b \qquad \text{(A.13)}\\ \text{Ave}\,[{}_2F_1(a,b;c;z)] &= 2i\sin(\pi a)\frac{\Gamma(b-a)\Gamma(c)}{\Gamma(c-a)\Gamma(b)}z^{-a}{}_2F_1\left[\begin{matrix}a, a-c+1\\ a-b+1\end{matrix}\middle|\frac{1}{z}\right] + a\leftrightarrow b\ . \end{aligned}$$

Another way to find the discontinuity is to consider the integral representation [199, 15.6.1]

$${}_2F_1(a,b;c;z) = \frac{\Gamma(c)}{\Gamma(b)\Gamma(c-b)}\int_0^1 x^{b-1}(1-x)^{c-b-1}(1-zx)^{-a}\,dx \qquad \Re(c)>\Re(b)>0. \tag{A.14}$$

together with A.12. This yields

$$\text{Disc}[{}_2F_1(a,b;c;z)] = \frac{2\pi i\Gamma(c)\;z^{1-c}\,(z-1)^{c-b-a}}{\Gamma(a)\Gamma(b)\Gamma(c-a-b+1)}\;{}_2F_1\left[\begin{matrix}1-b, 1-a\\ c-a-b+1\end{matrix}\middle|1-z\right] \tag{A.15}$$

which is in agreement with (A.1) using [199, 15.8.4].

Finally, the generalized hypergeometric function ${}_3F_2$ has the following integral representation:

$${}_3F_2(a_1,a_2,a_3;b_1,b_2;t) = \frac{\Gamma(b_2)}{\Gamma(a_3)\Gamma(b_2-a_3)}\int_0^1 z^{a_3-1}(1-z)^{-a_3+b_2-1}\,{}_2F_1(a_1,a_2;b_1;z)\ . \tag{A.16}$$

A.2 Estimates for $\tilde{F}$ at large Δ

In this section we will provide some estimates for the quantity $\tilde{F}$ defined in (5.46) appearing in the one-dimensional bootstrap equation (5.45). Since only expressions for $\ell=0$ are used in the present work, we will focus on that case, although the $\ell=1$ case can be studied similarly. The function $\tilde{F}$ consists of four terms:

$$\tilde{F}^{s-t}_{\Delta,\ell=0} = \mathcal{I}(\Delta,\gamma,\sigma) - \mathcal{I}(\Delta,\sigma,\gamma) + \mathcal{I}(1-\Delta,\gamma,\sigma) - \mathcal{I}(1-\Delta,\sigma,\gamma) \tag{A.17a}$$

with

$$\begin{aligned}\mathcal{I}(\Delta,\gamma,\sigma) = K^{\Delta_{re}+i\Delta_{im},\,\Delta_{re}-i\Delta_{im}}_{1-\Delta,0}\, &\frac{\Gamma(\Delta+\gamma+1)\Gamma(2\Delta_{re}+\sigma+1)}{\Gamma(\Delta+2\Delta_{re}+\gamma+\sigma+2)} \\ &\times {}_3F_2\left[\begin{matrix}\Delta+2i\Delta_{im},\ \Delta-2i\Delta_{im},\ \Delta+\gamma+1 \\ 2\Delta,\ \Delta+2\Delta_{re}+\gamma+\sigma+2\end{matrix}\,,1\right]\ .\end{aligned} \tag{A.17b}$$

Convergence of the hypergeometric functions requires that

$$1+2\Delta_{re}+\gamma>0 \quad \text{and} \quad 1+2\Delta_{re}+\sigma>0\ . \tag{A.18}$$

In order to study the convergence of the bootstrap problem, we need to consider the large-ν limit for $\Delta = 1/2+i\nu$ and the large-n limit of $\Delta = n \in \mathbb{N}$. Let's treat these cases separately.

Principal series

First of all, let's set $\Delta = 1/2+i\nu$ and analyze the limit $\nu \to \infty$. Notice that the four terms in $\tilde{F}$ are related to $\mathcal{I}(\Delta,\gamma,\sigma)$ via the permutations $\nu \mapsto -\nu$ and/or $\gamma \leftrightarrow \sigma$. Hence if we understand the large-ν asymptotics of $\mathcal{I}(\Delta,\gamma,\sigma)$, it is straightforward to understand the deduce the large-ν behavior of the full function $\tilde{F}$.

For the case at hand, it will prove convenient to rewrite the ${}_3F_2(1)$ using a hypergeometric transformation, which yields

$$\begin{aligned}\mathcal{I}(\Delta,\gamma,\sigma) =& K^{\Delta_{re}+i\Delta_{im},\,\Delta_{re}-i\Delta_{im}}_{1-\Delta,0}\, \frac{\Gamma(\Delta+\gamma+1)\Gamma(2\Delta_{re}+\sigma+1)^2}{\Gamma(\Delta+2\Delta_{re}+\gamma+\sigma+2)} \\ &\times\frac{\Gamma(2\Delta)}{\Gamma(\Delta-2i\Delta_{im})\Gamma(1+\Delta+2i\Delta_{im}+2\Delta_{re}+\sigma)} \\ &\times {}_3F_2\left[\begin{matrix}\Delta+2i\Delta_i,\ 1+2\Delta_{re}+\sigma,\ 2+\gamma+2i\Delta_{im}+2\Delta_{re}+\sigma \\ 2+\gamma+\Delta+2\Delta_{re}+\sigma,\ 1+\Delta+2i\Delta_{im}+2\Delta_{re}+\sigma\end{matrix}\,,1\right]\ .\end{aligned} \tag{A.19}$$

The new ${}_3F_2(1)$ converges when $\Re(\Delta)>0$, which holds in particular on the axis $\Re(\Delta) = 1/2$. To begin, let us analyze the different factors appearing in $\mathcal{I}$ from Eq. (A.19). The K-function goes as

$$K^{\Delta_{re}+i\Delta_{im},\,\Delta_{re}-i\Delta_{im}}_{\frac{d}{2}-i\nu,0} \underset{\nu\to\infty}{\sim} e^{-i\pi/4}\sqrt{\pi}\,\frac{4^{-i\nu}}{\sqrt{\nu}} \tag{A.20}$$

independently of Δ_{im} (and in fact $K_{1-\Delta}$ did not depend on Δ_{re} in the first place). Next, the gamma functions go as

$$\frac{\Gamma^4}{\Gamma^3} \underset{\nu\to\infty}{\sim} \frac{e^{i\pi\kappa}}{\sqrt{\pi}}\Gamma(1+2\Delta_{re}+\sigma)^2\,\frac{4^{i\nu}}{\nu^{3/2+4\Delta_{re}+2\sigma}}, \quad \kappa = \frac{5}{4}-2\Delta_{re}-\sigma\ . \tag{A.21}$$

It remains to find the $\nu \to \infty$ asymptotics of the ${}_3F_2(1)$ hypergeometric function. But it's easy to show that

$$ {}_3F_2\left[\begin{matrix} \Delta + 2i\Delta_i,\, 1 + 2\Delta_{re} + \sigma,\, 2 + \gamma + 2i\Delta_{im} + 2\Delta_{re} + \sigma \\ 2 + \gamma + \Delta + 2\Delta_{re} + \sigma,\, 1 + \Delta + 2i\Delta_{im} + 2\Delta_{re} + \sigma \end{matrix}, 1\right]\Bigg|_{\Delta=\frac{1}{2}+i\nu} \underset{\nu\to\infty}{\sim} 1 \ . \quad \text{(A.22)} $$

One way to show this is using the series representation of the ${}_3F_2(1)$, which converges for the case in question. Schematically it is of the form

$$ {}_3F_2(1) = 1 + \sum_{n=1}^{\infty} a_n(\Delta) \quad \text{with} \quad a_n(\Delta) \underset{\Delta\to\infty}{\sim} \frac{1}{\Delta^n} \quad \text{(A.23)} $$

so the terms with $n \geq 1$ are unimportant in the limit $|\Delta| \to \infty$. Bringing everything together, we conclude that

$$ \mathcal{I}(\tfrac{1}{2} + i\nu, \gamma, \sigma) \underset{\nu\to\infty}{\sim} \frac{\Gamma(1 + 2\Delta_{re} + \sigma)^2}{\nu^{2+4\Delta_{re}+2\sigma}} \quad \text{(A.24)} $$

up to some $O(1)$ numerical factor. Finally, we conclude that

$$ \tilde{F}^{s-t}_{\frac{1}{2}+i\nu,\ell=0} \underset{\nu\to\infty}{\sim} 1/\nu^{2+4\Delta_{re}+2\min(\gamma,\sigma)} \ . \quad \text{(A.25)} $$

Discrete series

The analysis for $\Delta = n \in \mathbb{N}$ is similar. First note that $\tilde{F}_n$ only consists of two terms:

$$ \tilde{F}^{s-t}_{n,\ell=0} = \mathcal{I}(n, \gamma, \sigma) - \mathcal{I}(n, \sigma, \gamma) \quad \text{(A.26)} $$

where $\mathcal{I}(n, \gamma, \sigma)$ is defined in (A.17b). For large n, the K-function behaves as:

$$ K^{\Delta_{re}+i\Delta_{im},\, \Delta_{re}-i\Delta_{im}}_{1-n,0} \underset{n\to\infty}{\sim} \sqrt{\pi}(1 + (-1)^n \cosh(2\pi\Delta_{im}))\frac{1}{2^{2n-1}\sqrt{n}} \ . \quad \text{(A.27)} $$

The large n limit of the rest of the terms in $I(n, \gamma, \sigma)$ are thus very similar to the above expression replacing $\nu \to n$. In the end, one finds:

$$ \mathcal{I}(n, \gamma, \sigma) \underset{n\to\infty}{\sim} (1 + (-1)^n \cosh(2\pi\Delta_i))\frac{\Gamma(1 + 2\Delta_{re} + \sigma)^2}{n^{2+4\Delta_{re}+2\sigma}} \ . \quad \text{(A.28)} $$

Including the second term with $\gamma \leftrightarrow \sigma$, we find that

$$ \tilde{F}^{s-t}_{n,\ell=0} \underset{n\to\infty}{\sim} 1/n^{2+4\Delta_{re}+2\min(\gamma,\sigma)} \ . \quad \text{(A.29)} $$

B Action of $SO(d+1,1)$ generators

In this appendix, we find the action of $SO(d+1,1)$ generators on scalar sates $|\Delta, k\rangle$ and $|\Delta, x\rangle$. For simplicity we focus on scalar states, but the generalization to traceless symmetric spinning states is straightforward.

Take the wavefunction defined in (3.11) or (2.61):

$$\Phi_x(x,\eta) = \langle\Omega|\phi(x,\eta)|\Delta,k\rangle = e^{-ik.x}(-\eta)^{\frac{d}{2}}h_{i\nu}(|k|\eta) \tag{B.1}$$

where $|\Omega\rangle$ is the Bunch-Davis vacuum. We again used $\Delta = \frac{d}{2} + i\nu$. The action of the conformal generators on the field can be also expressed as the differential operator

$$[Q, \phi(x)] = \hat{Q}\ \phi(x)\ , \tag{B.2}$$

in which Q is the corresponding Hilbert space charge operator of the Killing vector differential operator Q. We use notation $\hat{A}$ to a distinguish differential operator from a Hilbert space operator A. Acting on wavefunctions with $\hat{Q}$ and using the fact that the Bunch-Davis vacuum is invariant under our isometries i.e. $Q|0\rangle = 0$, one can find the action of the charges on the states $|\Delta, k\rangle$. For example, in the case of $Q = P_\mu$:

$$\begin{aligned}\hat{P}_\mu\ \Phi_k(x,\eta) &= \partial_\mu\Phi_k(x,\eta) = -ik_\mu\Phi_k(x,\eta) = -ik_\mu\langle 0|\phi(x)|\Delta,k\rangle \\ &= -\langle 0|\phi(x)P_\mu|\Delta,k\rangle\ .\end{aligned} \tag{B.3}$$

We find the familiar relation

$$P_\mu|\Delta,k\rangle = ik_\mu|\Delta,k\rangle\ . \tag{B.4}$$

With the same approach, one can find the action of the other generators on the chosen basis. The action of the dilatation operator is

$$\begin{aligned}
\hat{D}\langle 0|\phi(x)|\Delta, k\rangle &= (\eta\partial_\eta + x.\partial_x)\left[(-\eta)^{\frac{d}{2}} h_{i\nu}(|k|\eta) e^{ik.x}\right] && \text{(B.5)}\\
&= \left[(-ik.x + \frac{d}{2}) h_{i\nu}(|k|\eta)(-\eta)^{\frac{d}{2}} e^{ik.x} + k\partial_k h_{i\nu}(|k|\eta)(-\eta)^{\frac{d}{2}} e^{ik.x}\right] \\
&= (k.\partial_k + \frac{d}{2})\left[(-\eta)^{\frac{d}{2}} h_{i\nu}(|k|\eta) e^{ik.x}\right] \ , \\
\hat{D}\langle 0|\phi(x)|\Delta, k\rangle &= -\langle 0|\phi(x) D|\Delta, k\rangle \ , && \text{(B.6)}
\end{aligned}$$

in which we use the fact that $h_{i\nu}(|k|\eta)$ is symmetric under exchange of $k \leftrightarrow \eta$ and $k.\partial_k f(k) = k\partial_k f(k)$ to change the time derivative to momentum derivative. Hence the action of the Dilatation operator on this basis is

$$D|\Delta, k\rangle = -(k.\partial_k + \frac{d}{2})|\Delta, k\rangle \ . \tag{B.7}$$

Finally, for the case of $Q = K_\mu$ one finds

$$\begin{aligned}
\hat{K}_\mu\langle 0|\phi(x)|\Delta, k\rangle &= c_2((\eta^2 - x.x)\partial_{x^\mu} + 2x_\mu\eta\partial_\eta + 2x_\mu x.\partial_x)\left[(-\eta)^{\frac{d}{2}} H^{(2)}_{i\nu}(-k\eta)\ e^{ik.x}\right] \\
&= c_2\left[(-ik_\mu(\eta^2 - x.x) + 2x_\mu(-ik.x + \frac{d}{2}))H_{i\nu} + 2(-k\eta)H'_{i\nu}\right](-\eta)^{\frac{d}{2}} e^{ik.x} \ , \\
\hat{K}_\mu\langle 0|\phi(x)|\Delta, k\rangle &= -\langle 0|\phi(x) K_\mu|\Delta, k\rangle \ . && \text{(B.8)}
\end{aligned}$$

where $c_2 = \frac{\sqrt{\pi}}{2} e^{\frac{\pi\nu}{2}}$ and we dropped the Hankel function type index and dependence on $-\eta k$ to avoid clutter. We also write $\partial_{-\eta k} H_{i\nu}(-\eta k) = H'$. In parallel, we have

$$\begin{aligned}
\partial_{k^\mu}\Phi &= c_2(-ix_\mu H_{i\nu} + \frac{k_\mu}{k^2}(-\eta k)H'_{i\nu})(-\eta)^{\frac{d}{2}} e^{ik.x} \ , \\
\partial_{k^\alpha}\partial_{k^\mu}\Phi &= c_2[-x_\alpha x_\mu H_{i\nu} - ix_\mu\frac{k_\alpha}{k^2}(-\eta k)H'_{i\nu} - ix_\alpha\frac{k_\mu}{k^2}(-\eta k)H'_{i\nu} \\
&\quad + (\frac{\delta_{\mu\alpha}}{k^2} - \frac{k_\mu k_\alpha}{k^4})(-\eta k)H'_{i\nu} + (\frac{k_\mu k_\alpha}{k^4})(-\eta k)^2 H''_{i\nu}](-\eta)^{\frac{d}{2}} e^{ik.x}, \\
&= c_2[-x_\alpha x_\mu H_{i\nu} - ix_\mu\frac{k_\alpha}{k^2}(-\eta k)H'_{i\nu} - ix_\alpha\frac{k_\mu}{k^2}(-\eta k)H'_{i\nu} \\
&\quad + (\frac{\delta_{\mu\alpha}}{k^2} - 2\frac{k_\mu k_\alpha}{k^4})(-\eta k)H'_{i\nu} - (\frac{k_\mu k_\alpha}{k^4})(-\eta k)^2 H_{i\nu} - (\frac{k_\mu k_\alpha}{k^4})\nu^2 H_{i\nu}](-\eta)^{\frac{d}{2}} e^{ik.x} \ ,
\end{aligned}$$

in which we exchange second derivative of Hankel function with terms of the first derivative and zero derivatives using the its generating differential equation. This leads to

$$\begin{aligned}
k^{\alpha}\partial_{k^{\alpha}}\partial_{k^{\mu}}\Phi &= c_2(-\eta)^{\frac{d}{2}}e^{ik.x}\Big[-\frac{k_\mu}{k^2}(-\eta k)H'_{i\nu}-i(-\eta k)H'_{i\nu}(x_\mu+(k.x)\frac{k_\mu}{k^2})\\
&\quad -(k.x)x_\mu H_{i\nu}-\eta^2 k_\mu H_{i\nu}-\nu^2\frac{k_\mu}{k^2}H_{i\nu}\Big]\ ,\\
k_\mu\partial^{k^{\alpha}}\partial_{k^{\alpha}}\Phi &= c_2(-\eta)^{\frac{d}{2}}e^{ik.x}k_\mu\Big[\frac{d-2}{k^2}(-\eta k)H'_{i\nu}-i(-\eta k)\frac{2k.x}{k^2}H'_{i\nu}\\
&\quad -x.x\,H_{i\nu}-\eta^2 H_{i\nu}-\frac{\nu^2}{k^2}H_{i\nu}\Big]\ .
\end{aligned}$$

Then the particular linear combination of $(-2k^{\alpha}\partial_{k^{\alpha}}\partial_{k^{\mu}}+k_\mu\partial^{k^{\alpha}}\partial_{k^{\alpha}}-d\partial_{k^{\mu}})\Phi$ is equal to

$$c_2(-\eta)^{\frac{d}{2}}e^{ik.x}\left[2i(-\eta k)H'_{i\nu}x_\mu-2(k.x+i\frac{d}{2})x_\mu H_{i\nu}+(\eta^2-x.x)k_\mu H_{i\nu}+\frac{\nu^2}{k^2}k_\mu H_{i\nu}\right]\ .$$

Considering what we found in (B.8), we arrive at the following expression for K_μ acting on $|\Delta,k\rangle$:

$$xK_\mu|\Delta,k\rangle = i\left[k_\mu\partial^{k^{\alpha}}\partial_{k^{\alpha}}-2k^{\alpha}\partial_{k^{\alpha}}\partial_{k^{\mu}}-d\partial_{k^{\mu}}-\frac{\nu^2}{k^2}k_\mu\right]|\Delta,k\rangle\ . \tag{B.9}$$

The action of $M_{\mu\nu}$ is the trivial action of $SO(d)$ rotation group on scalars that we do not spell it out here. One can explicitly check the action of quadratic Casimir $C = D^2-\frac{1}{2}(K^\mu P_\mu+P^\mu K_\mu-M_{\mu\nu}M^{\mu\nu})$ will give the desired relation (2.64).

We may now derive the action of conformal generators on the position space states

$$|\Delta,x\rangle = \int d^dk\ e^{ik.x}k^{\Delta-\frac{d}{2}}\ |\Delta,k\rangle \tag{B.10}$$

mentioned in 2.114a and 2.114b.

One careful reader may ask why it is not simply the Fourier transformation and it has an extra factor of $k^{\Delta-\frac{d}{2}}$. This is due to the fact that we wanted this state to be like a primary state at point x with dimension Δ. In fact, one can put a general function instead and after imposing the right transformations under dilataion or special conformal isometries, will find the suggested factor. One can easily check the action of P_μ on these states:

$$\begin{aligned}
P_\mu|\Delta,x\rangle &= \int d^dk\ e^{ik.x}k^{\Delta-\frac{d}{2}}\ P_\mu|\Delta,k\rangle\\
&= i\int d^dk\ e^{ik.x}k^{\Delta-\frac{d}{2}}\ k_\mu|\Delta,k\rangle\\
&= \partial_\mu\int d^dk\ e^{ik.x}k^{\Delta-\frac{d}{2}}\ |\Delta,k\rangle\\
&\boxed{=\partial_\mu|\Delta,x\rangle}
\end{aligned} \tag{B.11}$$

We also may check the action of dilatation operator D:

$$\begin{aligned}
D|\Delta,x\rangle &= \int d^dk\ e^{ik.x}k^{\Delta-\frac{d}{2}}\ D|\Delta,k\rangle \\
&= -\int d^dk\ e^{ik.x}k^{\Delta-\frac{d}{2}}\ (k.\partial_k+\frac{d}{2})|\Delta,k\rangle \\
&= i\partial^\mu\int d^dk\ e^{ik.x}k^{\Delta-\frac{d}{2}}\partial_{k^\mu}|\Delta,k\rangle\ -\frac{d}{2}|\Delta,k\rangle \\
&= -i\partial^\mu\int d^dk\ \partial_{k^\mu}(e^{ik.x}k^{\Delta-\frac{d}{2}})|\Delta,k\rangle\ -\frac{d}{2}|\Delta,k\rangle \\
&= -i\partial^\mu\int d^dk\ \left[ix_\mu+(\Delta-\frac{d}{2})\frac{k_\mu}{k^2}\right](e^{ik.x}k^{\Delta-\frac{d}{2}})|\Delta,k\rangle\ -\frac{d}{2}|\Delta,k\rangle \\
&= (x.\partial_x+d+(\Delta-\frac{d}{2})-\frac{d}{2})|\Delta,x\rangle \\
&\boxed{=(x.\partial_x+\Delta)|\Delta,x\rangle}
\end{aligned} \tag{B.12}$$

where we performed integral by parts and dropped the boundary terms (at $k\to\infty$). The action of K_μ on (2.110) is

$$\begin{aligned}
K_\mu|\Delta,x\rangle &= \int d^dk\ e^{ik.x}k^{\Delta-\frac{d}{2}}\ K_\mu|\Delta,k\rangle \\
&= i\int d^dk\ e^{ik.x}k^{\Delta-\frac{d}{2}}\ (-2k^\alpha\partial_{k^\alpha}\partial_{k^\mu}+k_\mu\partial^{k^\alpha}\partial_{k^\alpha}-d\partial_{k^\mu}-\frac{\nu^2}{k^2}k_\mu)|\Delta,k\rangle
\end{aligned} \tag{B.13}$$

One might rewrite each of the four terms using integral by parts

$$\begin{aligned}
\text{1st term} &= -2\partial^\alpha\int d^dk\ e^{ik.x}k^{\Delta-\frac{d}{2}}\ \partial_{k^\alpha}\partial_{k^\mu}|\Delta,k\rangle \\
&= 2\partial^\alpha\int d^dk\ \left[ix_\alpha+(\Delta-\frac{d}{2})\frac{k_\alpha}{k^2}\right]e^{ik.x}k^{\Delta-\frac{d}{2}}\ \partial_{k^\mu}|\Delta,k\rangle \\
&= 2i(x.\partial_x+\Delta+\frac{d}{2})\int d^dk\ e^{ik.x}k^{\Delta-\frac{d}{2}}\ \partial_{k^\mu}|\Delta,k\rangle \\
&= -2i(x.\partial_x+\Delta+\frac{d}{2})\int d^dk\ e^{ik.x}k^{\Delta-\frac{d}{2}}\ \left[ix_\mu+(\Delta-\frac{d}{2})\frac{k_\mu}{k^2}\right]|\Delta,k\rangle \\
&= 2(x_\mu x.\partial_x+(\Delta+\frac{d}{2}+1)x_\mu)|\Delta,x\rangle-2i(x.\partial_x+\Delta+\frac{d}{2})(\Delta-\frac{d}{2})A_\mu \\
&= 2(x_\mu x.\partial_x+(\Delta+\frac{d}{2}+1)x_\mu)||\Delta,x\rangle-2i(\Delta+\frac{d}{2})(\Delta-\frac{d}{2})A_\mu-2i(\Delta-\frac{d}{2})x^\alpha\partial_\mu A_\alpha\ ,
\end{aligned} \tag{B.14}$$

$$\begin{aligned}
\text{2nd term} &= \partial_\mu \int d^dk\ e^{ik.x} k^{\Delta-\frac{d}{2}}\ \partial^{k^\alpha}\partial_{k^\alpha}|\Delta,k\rangle \\
&= -\partial_\mu \int d^dk\ e^{ik.x} k^{\Delta-\frac{d}{2}}\ \left[ix_\alpha + (\Delta-\frac{d}{2})\frac{k_\alpha}{k^2}\right]\partial_{k^\alpha}|\Delta,k\rangle \\
&= \partial_\mu \int d^dk\ e^{ik.x} k^{\Delta-\frac{d}{2}}\ \left[ix^\alpha + (\Delta-\frac{d}{2})\frac{k^\alpha}{k^2}\right]\left[ix_\alpha + (\Delta-\frac{d}{2})\frac{k_\alpha}{k^2}\right]|\Delta,k\rangle \\
&+ (d-2)(\Delta-\frac{d}{2})\partial_\mu \int d^dk\ e^{ik.x} k^{\Delta-\frac{d}{2}}\ \frac{1}{k^2}|\Delta,k\rangle \\
&= \partial_\mu \int d^dk\ e^{ik.x} k^{\Delta-\frac{d}{2}}\ [-x^2 + 2i(\Delta-\frac{d}{2})\frac{k.x}{k^2} + \frac{(\Delta-\frac{d}{2})^2}{k^2}]|\Delta,k\rangle \\
&\quad + (d-2)(\Delta-\frac{d}{2})\partial_\mu\psi \\
&= (-x^2\partial_\mu - 2x_\mu)|\Delta,x\rangle + 2i(\Delta-\frac{d}{2})\partial_\mu(x^\alpha A_\alpha) \\
&\quad + i[(\Delta-\frac{d}{2})^2 + (d-2)(\Delta-\frac{d}{2})]A_\mu\ ,
\end{aligned} \tag{B.15}$$

$$\begin{aligned}
\text{3rd term} &= id\int d^dk\ e^{ik.x} k^{\Delta-\frac{d}{2}}\ \left[ix_\mu + (\Delta-\frac{d}{2})\frac{k_\mu}{k^2}\right]|\Delta,k\rangle, \\
&= -dx_\mu|\Delta,x\rangle + id(\Delta-\frac{d}{2})A_\mu\ , \\
\text{4th term} &= -i\nu^2 A_\mu\ .
\end{aligned} \tag{B.16}$$

in which we defined $A_\mu \equiv \int d^dk\ e^{ik.x}k^{\Delta-\frac{d}{2}}\frac{k_\mu}{k^2}|\Delta,k\rangle$ and $\psi \equiv \int d^dk\ e^{ik.x}k^{\Delta-\frac{d}{2}}\frac{1}{k^2}|\Delta,k\rangle$. We also used the following identities: $\partial_\mu\psi = iA_\mu$ and $x^\alpha\partial_\alpha A_\mu = x^\alpha\partial_\mu A_\alpha$. Note that we assume the boundary terms coming from integrals by parts vanish. Putting all these together we find

$$\boxed{K_\mu|\Delta,x\rangle = \left(2x_\mu x.\partial_x - x^2\partial_\mu + 2\Delta\, x_\mu\right)|\Delta,x\rangle} \tag{B.17}$$

In conclusion, we showed that under the action of conformal generators D, K_μ, P_μ and $M_{\mu\nu}$, position space state $|\Delta,x\rangle$ defined in (2.110) behaves like a primary state in a conformal theory. Hence, anY correlation function made of n operators sandwiched between vacuum state $|\Omega\rangle$ and primary state $|\Delta,x\rangle$, behaves like $n+1$ point function with a insertion of primary operator $\mathcal{O}(x)$ with dimension Δ and spin ℓ:

$$\langle\Omega|\mathcal{O}_1(x_1)\cdots\mathcal{O}_n(x_n)\,|\Delta,x\rangle \sim \langle\Omega\mathcal{O}_1(x_1)\cdots\mathcal{O}_n(x_n)\mathcal{O}(x)\Omega\rangle\ . \tag{B.18}$$

C Spectral density inversion formula

In section 3.3, the analytic continuation of a two-point function on S^{d+1} to de Sitter was discussed. This appendix explains the proof of the inversion formula (3.38), which played an important role in that section. In passing, we discuss its convergence and large J limit.

C.1 Froissart-Gribov trick

The standard Gegenbauer inversion formula on S^{d+1} was shown in Eq. (3.36) in the main text. In what follows we will derive the inversion formula (3.38) for complex J through what is known as the Froissart-Gribov trick, which is a standard tool in S-matrix theory. We refer [200] and [201] for recent discussions.

Let us write $\alpha = d/2$ in what follows, and furthermore let

$$\omega(x) := (1-x^2)^{\alpha-1/2} \ .$$

Suppose that the function $G(x)$ appearing in (3.36) is analytic in a neighborhood of $[-1,1]$. Furthermore, suppose that we are given a function $Q_J^\alpha(z)$ that is analytic in a neighborhood of $[-1,1]$ but has the following discontinuity:

$$\mathrm{Disc}\left[(z^2-1)^{\alpha-1/2} Q_J^\alpha(z)\right] = -2\pi i\, \omega(x) C_J^\alpha(x) \quad \text{for} \quad z \in [-1,1] \ . \tag{C.1}$$

Given such a function, we have the following identity:

$$\int_{-1}^{1} dx\, \omega(x)\, C_J^\alpha(x) G(x) = \frac{1}{2\pi i} \oint_c dz\, (z^2-1)^{\alpha-1/2} Q_J^\alpha(z) G(z) \tag{C.2}$$

in which the contour c is a closed loop around the line segment $[-1,1]$, circled in the counterclockwise direction. It turns out that there exists a unique function satisfying (C.1), namely

$$Q_J^\alpha(z) := \int_{-1}^{1} dx' \left(\frac{1-x'^2}{z^2-1}\right)^{\alpha-1/2} \frac{C_J^\alpha(x')}{z-x'} \tag{C.3}$$

which by construction obeys (C.1); in fact, it can be shown that Q_J^α is the unique function obeying (C.1). In order to find an explicit representation of Q_J^α we first of all notice that Q_J^α obeys the same ODE as the Gegenbauer function $C_J^\alpha(x)$, namely

$$\left[(1-x^2)\frac{d^2}{dx^2} - (2\alpha+1)x\frac{d}{dx} + J(J+2\alpha)\right] f(x) = 0$$

which has a two-dimensional solution space. Either by computing the integral (C.3) explicitly, or by imposing (C.1), one concludes that $Q_J^\alpha(z)$ can be written as

$$Q_J^\alpha(z) = \frac{\mathcal{N}}{(z-1)^{J+2\alpha}}\, {}_2F_1\left[\begin{matrix} J+\alpha+\frac{1}{2}, J+2\alpha \\ 2J+2\alpha+1 \end{matrix} \middle| \frac{2}{1-z}\right] \tag{C.4a}$$

where

$$\mathcal{N} = \frac{\pi\Gamma(J+2\alpha)}{2^{J+2\alpha-1}\Gamma(\alpha)\Gamma(J+\alpha+1)}\ . \tag{C.4b}$$

An equivalent form is

$$Q_J^\alpha(z) = \frac{\mathcal{N}}{z^{J+2\alpha}}\, {}_2F_1\left[\begin{matrix} \frac{J}{2}+\alpha, \frac{J+1}{2}+\alpha \\ J+\alpha+1 \end{matrix} \middle| \frac{1}{z^2}\right] \tag{C.4c}$$

which agrees with [201], taking into account a different choice of normalization used there. Moreover we see that

$$Q_J^\alpha(z) \underset{z\to\infty}{\sim} 1/z^{J+2\alpha}$$

so for sufficiently large J the function decreases rapidly at infinity.

The formula (C.2) already provides a formula for a_J that is analytic in J:

$$a_J = \frac{2^{2\alpha-1}J!(J+\alpha)\Gamma(\alpha)^2}{\pi\Gamma(J+2\alpha)} \frac{1}{2\pi i} \oint_c dz\,(z^2-1)^{\alpha-1/2}\, Q_J^\alpha(z) G(z)\ . \tag{C.5}$$

However, we can further massage the RHS of (C.5) to obtain a form that is more convenient for computations. We already saw that the function $Q_J^\alpha(z)$ decreases faster than $1/z^J$ at large z, so at least for large J we can deform the contour and drop any arcs at infinity. Next, we expect that the function $G(z)$ has a branch cut on the real axis past the point $z=1$, say at $[1,\infty)$. Physically, this cut reflects the kinematics of the S^{d+1} correlator, since $z=1$ amounts to measuring the correlator at coincident points $X = X'$. The function $G(z)$ has to be finite on $(-1,1)$, since these points are physical. Finally $z=-1$ describes the correlator at antipodal points $X=-X'$, where it is completely regular. Consequently, we do not expect G to have a branch cut on the negative real axis

$(-\infty,-1]$. Blowing up the contour c, we can therefore write

$$a_J = \frac{J!\Gamma(\alpha)}{2^J\Gamma(J+\alpha)}\frac{1}{2\pi i}\int_1^\infty dx\,\frac{(x+1)^{\alpha-\frac{1}{2}}}{(x-1)^{J+\alpha+\frac{1}{2}}}\,{}_2F_1\left[\begin{matrix}J+2\alpha, J+\alpha+\frac{1}{2}\\ 2J+2\alpha+1\end{matrix}\,\middle|\,\frac{2}{1-x}\right]\mathrm{Disc}\,[G(x)]\ . \tag{C.6}$$

After setting $\alpha \to d/2$, this is precisely the inversion formula from Eq. (3.38). If $G(x)$ has any poles or other branch cuts beyond $[1,\infty)$, additional terms need to be added to formula (C.6).

The derivation presented here suffers from one minor issue. In writing (C.2) we had to assume that $G(x)$ extends to an analytic function in a small neighborhood around $[-1,1]$. Yet (C.6) allows for the possibility that $G(z)$ has a branch cut starting at $z=1$, and indeed typical S^{d+1} correlators have $z=1$ as a branch point. In practice, if $G(z)$ is not too singular near $z=1$ then the inversion formula still holds.

C.2 Example: a_J of the massive boson

We now check the proposed inversion formula in the case of the free field of mass $m^2R^2 = \Delta_\phi(d-\Delta_\phi)$. In the x-coordinate, the propagator reads

$$G_{\mathrm{f}}(x) = \frac{1}{R^{d-1}}\frac{1}{4\pi^{d/2+1}}\frac{\Gamma(\frac{d}{2})\Gamma(\Delta_\phi)\Gamma(d-\Delta_\phi)}{\Gamma(d)}\,{}_2F_1\left[\begin{matrix}\Delta_\phi, d-\Delta_\phi\\ \frac{d+1}{2}\end{matrix}\,\middle|\,\frac{1+x}{2}\right]\ . \tag{C.7}$$

The coefficients a_J are computed in [100], and the result is printed in (3.37). Here we will reproduce their result using the inversion formula. The discontinuity of the $G_{\mathrm{f}}(x)$ can be computed in various ways, for instance using (A.1). Finding discontinuity of two-point function reduces to calculating discontinuity of hyeprgeometric function in (C.7). Using (A.15), one finds

$$\mathrm{Disc}[G_{\mathrm{f}}(x)] = \frac{2^d\pi i\,R^{1-d}}{4\pi^{1+\frac{d}{2}}}\frac{\Gamma(\frac{d}{2})\Gamma(\frac{d+1}{2})}{\Gamma(d)\Gamma(\frac{3-d}{2})}\,(x^2-1)^{\frac{1}{2}-\frac{d}{2}}\,{}_2F_1\left[\begin{matrix}1+\Delta_\phi-d, 1-\Delta_\phi\\ \frac{3-d}{2}\end{matrix}\,\middle|\,\frac{1-x}{2}\right]\ . \tag{C.8}$$

Before calculating the inversion formula integral, let us comment on its convergence. By examining the limits $x\to 1^+$ and $x\to\infty$, we conclude that (C.6) converges iff

$$x\to 1^+:\quad \Re(J+\Delta_\phi)>0,\quad \Re(J+d-\Delta_\phi)>0\quad \text{as well as}\quad x\to\infty:\quad d<3\ .$$

Let us now calculate the integral (C.6). Inside the integrand, we replace the ${}_2F_1$ appearing in $\mathrm{Disc}\,G(x)$ with the help of the Barnes hypergeometric integral representation

$${}_2F_1(a,b,c,z) = \frac{\Gamma(c)}{2\pi i\Gamma(a)\Gamma(b)}\int_{\gamma-i\infty}^{\gamma+i\infty} ds\,\frac{\Gamma(s)\Gamma(a-s)\Gamma(b-s)}{\Gamma(c-s)}(-z)^{-s}\ , \tag{C.9}$$

where γ is chosen in such a way that the three families of poles in the s-plane that move to the left and right are separated. After the change of variable $x \to t = \frac{2}{x-1}$ and using the identity (A.7), we can compute the t-integral exactly. This yields

$$\begin{aligned} a_J = &\frac{\Gamma(\frac{3-d}{2})}{2^{J+d}\pi i\Gamma(1-\Delta_\phi)\Gamma(1+\Delta_\phi-d)} \frac{\Gamma(2J+d+1)}{\Gamma(J+d)\Gamma(J+\frac{d}{2}+\frac{1}{2})} \\ &\times \int_{\gamma-i\infty}^{\gamma+i\infty} ds\, \frac{-\Gamma(1-s)\Gamma(s)\Gamma(1+\Delta_\phi-d-s)\Gamma(1-\Delta_\phi-s)\Gamma(J+s+d-1)}{\Gamma(J-s+2)}\ . \end{aligned} \tag{C.10}$$

The remaining Mellin-Barnes integral can be done using (A.3), which yields

$$a_J = \frac{R^{1-d}}{4\pi^{1+\frac{d}{2}}2^{2J}} \frac{\Gamma^2(\frac{d}{2})\Gamma(\frac{d+1}{2})}{\Gamma(d)} \frac{\Gamma(2J+d+1)}{\Gamma(J+\frac{d}{2})\Gamma(J+\frac{d}{2}+\frac{1}{2})} \frac{1}{(J+d-\Delta_\phi)(J+\Delta_\phi)}\ . \tag{C.11}$$

Using some simplifications, we indeed recover the result (3.37).

C.3 Large J behavior

As discussed in section 3.3, we studied the analytic continuation of a_J using the inversion formula (3.38) to find the spectral density of the theory. As we change the contour in (3.42), we need to know the large J behavior of a_J and to be precise, we want to find the upper bound of a_J as we approach the limit $|J| \to \infty$. We will argue that the $J \to \infty$ behavior is related to the $x \to 1$ (or $\xi \to \infty$) limit of the correlator. We have already encountered this in one example: for the bulk CFT correlator (3.65), we computed that

$$G_\delta(x) = \frac{1}{(1-x)^\delta} \quad \Rightarrow \quad \rho_\delta(\tfrac{d}{2}+i\nu) \underset{\nu\to\infty}{\sim} \frac{2^{d+2}\pi^{(d+3)/2}}{\Gamma(\delta)\Gamma(\delta-\frac{d}{2}+\frac{1}{2})}\,\nu^{2\delta-d} \tag{C.12a}$$

or using (3.49) and setting $\nu \to J$, at least formally we obtain

$$a_J \underset{J\to\infty}{\sim} 1/J^{d-2\delta}\ . \tag{C.12b}$$

We want to put this relation (C.12b) on a more solid footing by means of Eq. (3.38).

Let us spell out the assumptions going in the derivation below. We assume that the discontinuity of $G(x)$ behaves as

$$x \geq 1: \quad \operatorname{Disc} G(x) = \left(\frac{x+1}{x-1}\right)^\delta \widehat{G}(x) \quad \text{for some} \quad \delta < 1\,. \tag{C.13}$$

Here $\widehat{G}(x)$ is a bounded and slowly varying function on $[1,\infty)$, having a finite limit as $x \to 1$. It turns out that the large-x behavior of $\widehat{G}(x)$ is not really important, provided that $\widehat{G}(x)$ does not grow faster than any power law. The restriction $\delta < 1$ is necessary to guarantuee convergence of the inversion formula at finite J, and the second assumption (which is stronger in $d < 2$ but weaker for $d \geq 2$) is needed to have a uniform $J \to \infty$ limit, as we will see. For values $\delta \geq 1$ the integrand needs to be regulated, and we will not discuss this case at present.

Given the above, we write the inversion formula for this case as

$$a_J \approx \frac{1}{4^J J^{d/2-1}} \int_1^\infty \frac{dx}{(x-1)^\delta} \left(\frac{2}{1+x}\right)^{J+1-\delta} \mathcal{F}_J(x)\, \widehat{G}(x) \tag{C.14}$$

where we defined

$$\mathcal{F}_J(x) := {}_2F_1\left[\begin{matrix} J+1, J+\frac{d}{2}+\frac{1}{2} \\ 2J+d+1 \end{matrix} \middle| \frac{2}{1+x}\right] . \tag{C.15}$$

We have dropped some J-independent factors in the prefactor, as they will not play a role later. Eq. (C.14) can be obtained from the inversion formula by a hypergeometric transformation. The function $\mathcal{F}_J(x)$ is a manifestly decreasing function of x that has a finite limit as $x \to 1$ (unless $d = 1$, in which case $\mathcal{F}_J(x)$ diverges logarithmically) and obeys $\mathcal{F}_J(x) \to 1$ as $x \to \infty$.

We now claim that in the $J \to \infty$ limit, a_J is dominated by the part of the integral near $x = 1$. To wit, fix some $c > 1$ and split the integral into two parts:

$$a_J = a_J^{(1)} + a_J^{(2)}, \quad a_J^{(1)} = \int_1^c [\ldots] \quad \text{and} \quad a_J^{(2)} = \int_c^\infty [\ldots] \ .$$

Using the above assumptions, it is easy to show that

$$J \gg 1: \qquad \left|a_J^{(2)}\right| \leq \frac{C}{2^J J^{d/2}} \tag{C.16}$$

for some constant $C > 0$. This contribution is exponentially small, whereas $a_J^{(1)}$ will scale as a power law. In order to estimate $a_J^{(1)}$, we first estimate $\mathcal{F}_J(x)$ using steepest descent. In order to do so we employ the integral representation

$$\mathcal{F}_J(1+y) = \frac{\Gamma(d+2J+1)}{\Gamma\big(J+\frac{d}{2}+\frac{1}{2}\big)^2} \int_0^1 dt\, \frac{(y+2)(t(1-t))^{\frac{d-1}{2}}}{2+y-2t} \left(\frac{t(1-t)(y+2)}{2+y-2t}\right)^J . \tag{C.17}$$

At large J, the integral is dominated by the contribution near

$$t = t_*(y) = \frac{2+y-\sqrt{y(2+y)}}{2}.$$

After evaluating the integral using steepest descent, at large J and fixed y we then obtain

$$\mathcal{F}_J(1+y) \underset{J\to\infty}{\sim} 4^J\, \widehat{F}(y)\, e^{-Jq(y)} \tag{C.18}$$

where $\widehat{F}(y)$ is a rather complicated function of y that does not depend on J and

$$q(y) = \ln 2 - \ln\Big[2 - (2+y)\sqrt{y(2+y)} + y(3+y)\Big] \approx \sqrt{2y} + O(y)\ . \tag{C.19}$$

Because of the exponential, values of $x = 1+y$ for which $q(y) \gtrsim 1/J$ are suppressed in the integral (C.14) (which is cut off at $x = c$). In terms of the variable

$$v := \sqrt{2y}J$$

this condition reads $v \lesssim 1$. The relevant limit is then

$$\mathcal{F}_J\left(1+\frac{v^2}{2J^2}\right) \underset{J\to\infty}{\sim} J^{1-\frac{d}{2}} 2^{d+2J} \frac{1}{\sqrt{\pi}} \int_0^\infty dr\, r^{\frac{d-3}{2}} e^{-r-\frac{v^2}{4r}} = J^{1-\frac{d}{2}} 2^{\frac{3+d+4J}{2}} \frac{1}{\sqrt{\pi}} v^{\frac{d-1}{2}} K_{\frac{d-1}{2}}(v) \tag{C.20}$$

where we used the integral representation (C.17) with $t = 1 - r/J$ because the integral is dominated by $1 - t \sim 1/J$. We can therefore remove the cutoff c, perform the indicated change of variable and take the limit $J \gg 1$. Keeping track of powers of J, this results in the following estimate:

$$a_J^{(1)} \underset{J\to\infty}{\sim} \frac{1}{J^{d-2\delta}} \frac{2^{\frac{3+d}{2}+\delta}\widehat{G}(0)}{\sqrt{\pi}} \int_0^\infty \frac{dv}{v^{2\delta-\frac{d+1}{2}}} K_{\frac{d-1}{2}}(v) = \frac{\widehat{G}(0)}{J^{d-2\delta}} \frac{2^{1+d-\delta}\Gamma(1-\delta)\Gamma(\frac{1+d-2\delta}{2})}{\sqrt{\pi}}\ . \tag{C.21}$$

This is the desired result, provided that the integral on the RHS converges. It does so precisely because of the assumption made in (C.13). This concludes the proof.

D From $SO(2,2)$ to $SO(2,1)$

A generic quantum field theory on dS have the symmetries dicatated by background metric of dS i.e. $SO(d+1,1)$. A conformal theory, on the other hand, has more symmetries. The fact that its energy-momentum tensor is traceless enhances it symmetry group to $SO(d+1,2)$. In this appendix, we study how the unitary irreducible representations of $SO(d+1,2)$ decompose into irreps of the subgroup $SO(d+1,1)$ in the case $d=1$.

Take the generators of $SO(d+1,2)$ to be the Lorentz generators J_{AB} in embedding space $\mathbb{R}^{d+1,2}$, with the metric $\eta = \text{diag}(-1,-1,+1,\dots,+1)$ in which $A,B \in \{-1,0,1,\dots,d+1\}$. These satisfy these commutation relations (2.31) and are anti-hermitian $J_{AB}^\dagger = -J_{AB}$.

The generators of the $SO(d+1,2)$ conformal group can be written as

$$\tilde{D} = -iJ_{-10} \tag{D.1}$$

$$\tilde{P}_a = -iJ_{-1a} + J_{0a} \tag{D.2}$$

$$\tilde{K}_a = -iJ_{-1a} - J_{0a} \tag{D.3}$$

$$\tilde{M}_{ab} = -iJ_{ab}\,. \tag{D.4}$$

where $a,b \in 1,2,\dots,d+1$ and we used tildes to distinguish from the $SO(d+1,1)$ generators defined by (2.32). The hermiticity properties are then

$$\tilde{D}^\dagger = \tilde{D}\,, \qquad (\tilde{P}_a)^\dagger = \tilde{K}_a\,, \qquad (\tilde{M}_{ab})^\dagger = M_{ab}\,. \tag{D.5}$$

Notice that the conventions here differ from those in the main text, namely (2.32), which led to anti-hermitian generators.

Let us now focus in the case $d=1$ which corresponds to $SO(2,1) \cong SL(2,\mathbb{R})$ (at the level of the algebra). In this case, it is convenient to use the following basis for the algebra

$$\begin{aligned} S^z &= -iJ_{12} = \tilde{M}_{12} \ , \\ S^+ &= -iJ_{01} - J_{02} = \frac{\tilde{K}_2 - \tilde{P}_2}{2} + i\frac{\tilde{K}_1 - \tilde{P}_1}{2} \ , \\ S^- &= -iJ_{01} + J_{02} = -\frac{\tilde{K}_2 - \tilde{P}_2}{2} + i\frac{\tilde{K}_1 - \tilde{P}_1}{2} \ . \end{aligned} \tag{D.6}$$

This leads to the usual $SL(2,\mathbb{R})$ commutation relations

$$[S^z, S^\pm] = \pm S^\pm \, , \qquad\qquad [S^+, S^-] = -2S^z \, , \tag{D.7}$$

and Casimir

$$C = (S^z)^2 - \frac{1}{2}(S^+S^- + S^-S^+) \, . \tag{D.8}$$

The hermiticity properties are

$$(S^z)^\dagger = S^z \, , \qquad\qquad (S^+)^\dagger = S^- \, . \tag{D.9}$$

Principal series representations have Casimir eigenvalue $C = -\frac{1}{4} - \nu^2 \leq -\frac{1}{4}$. Complementary series have $-\frac{1}{4} \leq C \leq 0$. Discrete series have $C = k(k-1)$ with $k = 1, 2, \ldots$.

A highest weight representation of $SO(2,2)$ is the vector space generated by the states

$$|n, \bar{n}\rangle = (\tilde{P}_1 - i\tilde{P}_2)^n (\tilde{P}_1 + i\tilde{P}_2)^{\bar{n}} |\Delta, \ell\rangle \, , \qquad n, \bar{n} \in \{0, 1, 2, \ldots\} \, , \tag{D.10}$$

with $|\Delta, \ell\rangle$ a primary state,[1]

$$\tilde{K}_1|\Delta,\ell\rangle = \tilde{K}_2|\Delta,\ell\rangle = 0 \, , \qquad \tilde{M}_{12}|\Delta,\ell\rangle = \ell|\Delta,\ell\rangle \, , \qquad \tilde{D}|\Delta,\ell\rangle = \Delta|\Delta,\ell\rangle \, . \tag{D.11}$$

We would like to diagonalize the Casimir C in this vector space. First notice that S^z is already diagonal

$$S^z|n,\bar{n}\rangle = (n - \bar{n} + \ell)|n,\bar{n}\rangle \equiv s|n,\bar{n}\rangle \ . \tag{D.12}$$

The action of the Casimir takes the form

$$C|n,\bar{n}\rangle = q(n)|n,\bar{n}\rangle + w(n)|n-1,\bar{n}-1\rangle + \frac{1}{4}|n+1,\bar{n}+1\rangle \ , \tag{D.13}$$

where

$$\begin{aligned} q(n) &= -n(\Delta - \ell + 2\bar{n}) - \bar{n}(\Delta + \ell) + \left(\ell^2 - \Delta\right) \\ &= \Delta(-\ell - 2n + s - 1) + \ell(s - 2n) + 2n(s - n) \ . \end{aligned} \tag{D.14}$$

---

[1] Notice that here we use Δ to denote the eigenvalue of the $SO(2,2)$ dilatation generator $\tilde{D}$. The notation $\tilde{\Delta}$, used in the main text, would be appropriate but we shall use simply Δ to avoid cluttering the equations in this appendix.

and

$$\begin{aligned} w(n) &= 4\sum_{k=1}^{n}(\Delta+\ell+2k-2)\sum_{q=1}^{\bar{n}}(\Delta-\ell+2q-2) \\ &= 4n(\Delta+\ell+n-1)(\ell+n-s)(\Delta+n-s-1)\ . \end{aligned} \tag{D.15}$$

These functions were computed using the commutators

$$\begin{aligned} [C,P] &= K(\tilde{D}+S^z)-P(\tilde{D}-S^z)\ , \\ [C,\bar{P}] &= \bar{K}(\tilde{D}-S^z)-\bar{P}(\tilde{D}+S^z)\ , \\ [K,\bar{P}] &= 4(\tilde{D}-S^z)\ , \\ [\bar{K},P] &= 4(\tilde{D}+S^z)\ , \\ [K,P] &= 0\ , \\ [\bar{K},\bar{P}] &= 0\ . \end{aligned} \tag{D.16}$$

where $P \equiv \tilde{P}_1 - i\tilde{P}_2$, $\bar{P} \equiv \tilde{P}_1 + i\tilde{P}_2$, $K \equiv \tilde{K}_1 - i\tilde{K}_2$ and $\bar{K} \equiv \tilde{K}_1 + i\tilde{K}_2$. In practice, we used

$$C|n,\bar{n}\rangle = \sum_{k=1}^{n} P^{n-k}[C,P]P^{k-1}\bar{P}^{\bar{n}}|\Delta,\ell\rangle + \sum_{k=1}^{\bar{n}} P^{n}\bar{P}^{\bar{n}-k}[C,\bar{P}]\bar{P}^{k-1}|\Delta,\ell\rangle + P^n\bar{P}^{\bar{n}}C|\Delta,\ell\rangle$$

together with

$$\begin{aligned} K\bar{P}^{\bar{n}}|\Delta,\ell\rangle &= \sum_{q=1}^{\bar{n}}\bar{P}^{\bar{n}-q}[K,\bar{P}]\bar{P}^{q-1}|\Delta,\ell\rangle = 4\sum_{q=1}^{\bar{n}}(\Delta+q-1-\ell+q-1)\bar{P}^{\bar{n}-1}|\Delta,\ell\rangle \\ C|\Delta,\ell\rangle &= \left(\ell^2-\Delta\right)|\Delta,\ell\rangle + \frac{1}{4}P\bar{P}|\Delta,\ell\rangle\ . \end{aligned} \tag{D.17}$$

Simultaneous eigenstates of S^z (with eigenvalue $s \le \ell$) and the Casimir C can be written as

$$|\psi\rangle = \sum_{n=0}^{\infty} a_n|n,\ell-s+n\rangle\ . \tag{D.18}$$

Then, $C|\psi\rangle = \lambda|\psi\rangle$ leads to the recursion equation

$$\lambda a_n = q(n)a_n + w(n+1)a_{n+1} + \frac{1}{4}a_{n-1}\ . \tag{D.19}$$

The eigenvalues λ will be fixed by requiring that the solution to this equation has finite norm

$$\begin{aligned} \langle\psi|\psi\rangle &= \sum_{n=0}^{\infty}|a_n|^2\langle n,\ell-s+n|n,\ell-s+n\rangle \\ &= \sum_{n=0}^{\infty}|a_n|^2 4^{\ell-s+2n}n!(\ell-s+n)!(\Delta+\ell)_n(\Delta-\ell)_{n+\ell-s} \end{aligned} \tag{D.20}$$

where we used

$$\langle n,\bar{n}|n,\bar{n}\rangle = 4^{n+\bar{n}} n!\bar{n}!(\Delta+\ell)_n(\Delta-\ell)_{\bar{n}} \ . \tag{D.21}$$

This expression for the norm follows from (using (D.17))

$$\begin{aligned}\langle n,\bar{n}|n,\bar{n}\rangle &= \langle\Delta,\ell|K^{\bar{n}}\bar{K}^n P^n\bar{P}^{\bar{n}}|\Delta,\ell\rangle \\ &= 4\bar{n}(\Delta-\ell+\bar{n}-1)\langle\Delta,\ell|K^{\bar{n}-1}\bar{K}^n P^n\bar{P}^{\bar{n}-1}|\Delta,\ell\rangle \\ &= 4\bar{n}(\Delta-\ell+\bar{n}-1)\langle n,\bar{n}-1|n,\bar{n}-1\rangle \ .\end{aligned} \tag{D.22}$$

It is convenient to define

$$c_n = a_n\sqrt{4^{\ell-s+2n} n!(\ell-s+n)!(\Delta+\ell)_n(\Delta-\ell)_{n+\ell-s}} \tag{D.23}$$

so that the inner product becomes

$$\langle\psi|\psi'\rangle = \sum_{n=0}^{\infty} c_n^* c_n' \, . \tag{D.24}$$

The recursion relation then becomes

$$\begin{aligned}&\frac{\big(\Delta+\lambda+\ell(\Delta+2n-s)+2n^2+2n(\Delta-s)-\Delta s\big)}{\sqrt{n(\Delta+\ell+n-1)(\ell+n-s)(\Delta+n-s-1)}}c_n \\ &\qquad\qquad -\sqrt{\frac{(n+1)(\Delta+\ell+n)(\ell+n-s+1)(\Delta+n-s)}{n(\Delta+\ell+n-1)(\ell+n-s)(\Delta+n-s-1)}}c_{n+1} = c_{n-1} \ .\end{aligned}$$

This implies the following asymptotic behavior

$$c_n = \frac{R}{n^{\frac{1-i\nu}{2}}}\left[1+O(1/n)\right] + \text{c.c} \ . \tag{D.25}$$

where $4\lambda+1=-\nu^2$. The complex parameter R cannot be determined from an asymptotic analysis of the recursion relation. Here we assumed that the parameter ν is real as required for principal series representations. In this case, the state $|\psi\rangle$ is delta-function normalizable. Let us see how this works

$$\begin{aligned}\langle\psi|\psi'\rangle &\sim 2|RR'|\sum_n^{\infty}\frac{1}{n}\left[\cos\left(\frac{\nu-\nu'}{2}\log n+\phi-\phi'\right)+\cos\left(\frac{\nu+\nu'}{2}\log n+\phi+\phi'\right)\right] \\ &\sim 2|RR'|\int^{\infty}dy\left[\cos\left(\frac{\nu-\nu'}{2}y+\phi-\phi'\right)+\cos\left(\frac{\nu+\nu'}{2}y+\phi+\phi'\right)\right] \\ &\sim 4\pi|RR'|\left[\delta(\nu-\nu')+\delta(\nu+\nu')\right]\end{aligned} \tag{D.26}$$

where we used $R=|R|e^{i\phi}$ and $R'=|R'|e^{i\phi'}$. Notice that the appearance of the $\delta-$functions follows solely from the asymptotic behavior of the coefficients c_n. On the other hand, orthogonality between eigenstates of different Casimir eigenvalue is guaranteed. We conclude that the $SO(2,2)$ highest weight unitary irreducible representations contains $SO(2,1)$ principal series representations for all values of $\nu \in \mathbb{R}$ (with ν and $-\nu$ identified).

For complementary and discrete series representations, we have $4\lambda + 1 = v^2$ with $v > 0$. This leads to

$$c_n = \frac{R_+}{n^{\frac{1+v}{2}}}\left[1 + O(1/n)\right] + \frac{R_-}{n^{\frac{1-v}{2}}}\left[1 + O(1/n)\right] \ . \tag{D.27}$$

Generically, this leads to non-normalizable states

$$\langle\psi|\psi'\rangle \sim \sum_n^{\infty} n^{-1+\frac{v+v'}{2}} \to \infty \, . \tag{D.28}$$

Of course, if $R_- = 0$ then we obtain a normalizable state. In fact, we will now construct some exact solutions with $R_- = 0$. We suspect these exhaust the solutions with $R_- = 0$ but have no proof of this fact.

Discrete series irreps are highest/lowest weight for S^z and therefore, they must contain a state that is annihilated by S^+/S^-. This condition leads to a first order recursion relation. Firstly, notice that

$$-2iS^+|n,\bar{n}\rangle = (K-P)\,P^n\bar{P}^{\bar{n}}|\Delta,\ell\rangle = 4\bar{n}(\Delta-\ell+\bar{n}-1)|n,\bar{n}-1\rangle - |n+1,\bar{n}\rangle \tag{D.29}$$

where we used (D.17). Therefore, $S^+|\psi\rangle = 0$ leads to

$$4(\ell - s + n)(\Delta - s + n - 1)a_n - a_{n-1} = 0 \ . \tag{D.30}$$

In particular, the equation with $n = 0$ can only be satisfied if $s = \ell$ or $a_0 = 0$.[2] If $a_0 \neq 0$ then we find

$$a_n = \frac{a_0}{4^n n! (\Delta - \ell)_n} \tag{D.31}$$

with associated norm

$$\langle\psi|\psi\rangle = |a_0|^2 \sum_{n=0}^{\infty} \frac{(\Delta+\ell)_n}{(\Delta-\ell)_n} \sim \sum_n^{\infty} n^{2\ell} \tag{D.32}$$

which converges for (half-integer) $\ell \leq -1$. Indeed, this solves the recursion relation (D.19) with $\lambda = \ell(\ell+1)$. This matches exactly the expectation from the discrete series. In fact there are more solutions of the form $a_n = 0$ for $n < s - \ell$ and

$$a_{s-\ell+\bar{n}} = \frac{a_{s-\ell}}{4^{\bar{n}}\bar{n}!(\Delta-\ell)_{\bar{n}}} \, , \qquad \bar{n} \geq 0. \tag{D.33}$$

---

[2] There is another formal solution with $\ell > s = \Delta - 1$. The unitarity bound $\Delta \geq |\ell|$ then implies that the second possibility only works for $\Delta = \ell$ and $s = \ell - 1$. But then the states with non-zero $\bar{n}$ have zero norm (they are descendants of the state associated to the divergence of the conserved current).

The norm of this state is (here $n = \bar{n} + s - \ell$)

$$\langle \psi | \psi \rangle = |a_{s-\ell}|^2 \sum_{\bar{n}=0}^{\infty} 4^{n-\bar{n}} \frac{n!}{\bar{n}!} \frac{(\Delta + \ell)_n}{(\Delta - \ell)_{\bar{n}}} \sim \sum_{\bar{n}}^{\infty} \bar{n}^{2s} \,. \tag{D.34}$$

We conclude that there is a normalizable highest weight state for every $s = -1, -2, \ldots, -|\ell|$.

Similarly, looking for lowest weight states obeying $S^- |\psi\rangle = 0$ we find states with $s = 1, 2, \ldots, |\ell|$. We conclude that for each $SO(2,2)$ conformal family based on a primary of non-zero spin ℓ, there are $|\ell|$ discrete series irreps of $SO(2,1)$ with Casimir eigenvalue $\lambda = s(s-1)$ with $s \in \{1, 2, \ldots, |\ell|\}$. This seems to be confirmed by numerical experiments where we diagonalize matrix truncations of the Casimir operator.

There is also a complementary series irrep with Casimir eigenvalue $\lambda = \Delta(\Delta - 1)$ for conformal families with $\Delta < \frac{1}{2}$. In this case, there is an exact solution

$$a_n = \frac{(\ell - s)!}{4^n \, n!(n + \ell - s)!} a_0 \ . \tag{D.35}$$

which matches the expansion (D.27) with $R_- = 0$. This gives a normalizable state in the complementary series. Notice that this state is really normalizable as opposed to delta-function normalizable like the principal series states. Finally, notice that the unitarity bound $\Delta > |\ell|$ implies that this complementary series irrep only exists for $\ell = 0$ conformal families. The presence of this state matches the comments after equation (3.67) about the Källén-Lehmann decomposition of the two-point function of a CFT primary operator with scaling dimension smaller than $\frac{d}{2}$.

E Semidefinite Programming for Conformal Bootstrap

Semidefinite Programming (SDP) [202, 118, 124] has been proven to be a powerful tool for the bootstrap program. The fact that, unlike linear programming, one is not required to discretize the space of dimension of exchange operators, makes this method incredibly faster especially for our case which involves numerically expensive functions ${}_3F_2$. Therefore, it is convenient to set up SDP for the crossing symmetry equation of $\tilde{F}$ found in chapter 5 to bootstrap correlators. This section is based on [203].

Let us review the main idea of translating the conformal bootstrap crossing equation to an SDP problem where the unitarity condition implies that the dimension of the exchange operator to be non-negative. Later, we will go back to the dS crossing equation where instead of a sum, we deal with an integral over principal series and we already traded the z-dependence with parameters γ and σ. For simplicity, we focus on one-dimensional CFTs while the generalization to higher dimensions is straightforward.

E.1 Expanding the blocks in polynomials of Δ

The $s-t$ channel of conformal crossing equation for the four-point function of all identical operators ϕ, takes the form of [60]

$$\sum_{\mathcal{O}\in\phi\times\phi} c^2_{\phi\phi\mathcal{O}} F_\Delta(z) = 0 \ . \tag{E.1}$$

where

$$F_\Delta(z) = z^{-2\Delta_\phi} G_\Delta(z) - (1-z)^{-2\Delta_\phi} G_\Delta(1-z) \ , \tag{E.2}$$

and the sum is over the operators that appear in OPE of $\phi\times\phi$ with real OPE coefficient $c_{\phi\phi\mathcal{O}}$ and z and $G(z)$ are the cross ratio and conformal block respectively, defined in (5.6).

Note that since we deal with all identical operators, we only have parity even $\ell = 0$ contribution with discrete series on even integers. One can expand the conformal block as a sum over its poles. To see this, imagine a function $f(z)$ that asymptote to $f_\infty(z)$ at large z which is analytical on the complex plane except on a series of poles. Then we have

$$f(z) = \frac{1}{2\pi i}\int_{\mathcal{C}} \frac{f(z')}{z'-z} = f_\infty(z) + \sum_{\text{poles}} \frac{\text{Res}(f, z_i)}{z - z_i}\ . \tag{E.3}$$

Using this, we are able to expand the conformal blocks in its poles.

$G_\Delta(z) \propto {}_2F_1(\Delta, \Delta, 2\Delta, z)$ has poles on non-positive half integers: $\Delta_k = -\frac{k}{2}$ $(k \in \mathbb{Z}, k \geq 0)$. Following the logic above, after factoring out $(4\rho)^\Delta$, the blocks in ρ coordinates look like:

$$G_{\Delta,\ell}(z) = (-1)^\ell (4\rho)^\Delta h_\infty(z) + (-1)^\ell \sum_{k=0}^{\infty} (4\rho)^{\Delta_k} \frac{\text{Res}(h, \Delta_k)}{\Delta - \Delta_k} \tag{E.4}$$

where

$$h_\Delta(z) = (-1)^\ell (4\rho)^{-\Delta} G_\Delta(z), \quad h_\infty = \frac{1}{\sqrt{1-\rho^2}}, \quad \rho = \frac{z}{(1+\sqrt{1-z})^2}\ .$$

The residues in the sum above decay exponentially which result in fast convergence. So, it would be a good approximation even if we truncate the sum above at an upper limit k_{max}. If one combines terms in the sum above over a common denominator, the n-th derivative of the block will be of the form

$$\partial_z^n G_\Delta(z)\bigg|_{z=z_0} = (-1)^\ell (4\rho_0)^\Delta \frac{P'_n(\Delta)}{\prod_{k=0}^{k_{\text{max}}}(\Delta - \Delta_k)} \equiv \Theta'(\Delta, \Delta_i) P'_n(\Delta)\ , \tag{E.5}$$

in which $P'_n(\Delta)$ is a polynomial of some degree n. Notice that since all of Δ_is are negative and ρ is a positive number, $\Theta'(\Delta, \Delta_i) > 0$. $F_\Delta(z)$ also has the same form at $z = \frac{1}{2}$

$$\partial_z^n F_\Delta(z)\bigg|_{z=\frac{1}{2}} = (4\rho_0)^\Delta \frac{P_n(\Delta)}{\prod_{k=0}^{k_{\text{max}}}(\Delta - \Delta_k)} \equiv \Theta(\Delta, \Delta_i) P_n(\Delta) \tag{E.6}$$

with positive $\Theta(\Delta, \Delta_i)$ and Polynomial $P_n(\Delta)$.

E.2 SDP set up

Let us go back to the crossing equation. If we find a functional α e.g a linear combination of derivatives of z evaluated at some point $z = z_0$

$$\alpha[f] = \sum_n \alpha_n \partial_z^n f\bigg|_{z=z_0}.$$

such that

$$\alpha[F_0] = 1 \ , \tag{E.7}$$

$$\alpha[F_{\Delta_i}] > 0, \quad \forall\Delta \geq \Delta^* \ , \tag{E.8}$$

then we rule out any theory that does not have any operator in OPE with $\Delta < \Delta^*$. Since $\Theta(D, \Delta_i) > 0$ the condition above is equivalent to:

$$\sum_n \alpha_n P_0(\Delta) = 1 \ , \tag{E.9}$$

$$\sum_n \alpha_n P_n(\Delta) > 0, \quad \forall\Delta \geq \Delta^* \ . \tag{E.10}$$

With the help of the following elementary theorem, this set of conditions become a Semidefinite Programming problem:

Theorem. *Let $P(x)$ be a polynomial in x. It satisfies*

$$P_n(x) \geq 0, \qquad \forall x \geq 0 \tag{E.11}$$

if and only if it can be written in the form of $P(x) = v^T(x)M_1v(x) + xv^T(x)M_2v(x)$ for some semidefinite matrices M_1 and M_2 and $v = (1, x, x^2, ..., x^{\lceil \frac{n}{2} \rceil})^T$.

We can find a bound for OPE coefficients too. Imagine we isolate a term in the sum of eq. (E.1) corresponding to the operator $\mathcal{O}_0$. Then acting with a functional α we may rewrite eq. (E.1) as

$$c^2_{\phi\phi\mathcal{O}_0}\alpha[F_{\Delta_0}] = -\alpha[F_0] - \sum_{\mathcal{O}_i \neq \mathcal{O}_0} c^2_{\phi\phi\mathcal{O}_i}\alpha[F_{\Delta_i}] \ . \tag{E.12}$$

Requiring the constraints

$$\alpha[F_{\Delta_0}] = 1 \ , \tag{E.13}$$

$$\alpha[F_{\Delta_i}] \geq 0, \quad \forall\Delta \geq \Delta^* \ , \tag{E.14}$$

leads to the bound $c^2_{\phi\phi\mathcal{O}_0} \leq -\alpha[F_0]$. If we ask the SDP question to minimize $-\alpha[F_0]$ with the constraints above, we would find a bound on $c^2_{\phi\phi\mathcal{O}_0}$ coefficients. For a more pedological review of this see e.g. [27, 204, 203, 124]

E.3 SDP for $\tilde{F}$

For the crossing equation of $\tilde{F}^{s-t}$ which has been integrated over z, we essentially follow the logic presented above. We would like to expand $\tilde{F}^{s-t}$ in terms of its poles and rewrite it as a polynomial times a positive function like the right-hand side of eq. (E.6).

The first step is to find the poles and residues of $\tilde{F}^{\text{s-t}}$. For later convenience let us split $\tilde{F}^{\text{s-t}}$ to four parts

$$\tilde{F}^{\text{s-t}}_{\Delta,\ell} = \tilde{f}^s_{\Delta,\ell} + \tilde{f}^s_{1-\Delta,\ell} + \tilde{f}^t_{\Delta,\ell} + \tilde{f}^t_{1-\Delta,\ell} \ , \tag{E.15}$$

where

$$\tilde{f}^t_{\Delta,\ell} = -\tilde{f}^s_{\Delta,\ell}(\gamma \leftrightarrow \sigma) \ , \tag{E.16}$$

$$\begin{aligned}\tilde{f}^s_{\Delta,\ell} = \frac{(-1)^\ell K^s_{1-\Delta,\ell}}{\Gamma(\Delta+2\Delta_r+\gamma+\sigma+2)}&\Gamma(\Delta+\gamma+1)\Gamma(2\Delta_r+\sigma+1)\times \\ &\times {}_3F_2\left[\begin{matrix}\Delta+2i\Delta_i, \Delta-2i\Delta_i, \Delta+\gamma+1 \\ 2\Delta, \Delta+2\Delta_r+\gamma+\sigma+2\end{matrix}\middle| 1\right] \ .\end{aligned} \tag{E.17}$$

corresponding to the contribution of different channels and their shadow counterpart. We use Δ_i and Δ_r as a shorter notation of Δ_{im} and Δ_{re}. For the moment, we focus on $\tilde{f}_{\Delta,\ell}$ and later we come back to $\tilde{F}_{\Delta,\ell}$.

The poles of $\tilde{f}_{\Delta,\ell}$ have there different origins. One set of poles is coming from $K_{1-\Delta,\ell}$ and the rest is coming the $\Gamma(\Delta+\gamma+1)$ and ${}_3F_2$:

$$\text{poles from } {}_3F_2: \ \Delta = -\frac{k}{2} \qquad ; \qquad \text{poles from } \Gamma(\Delta+\gamma+1): \ \Delta = -(1+\gamma)-k$$

$$\text{poles from } K_{1-\Delta,\ell}: \ \begin{cases}\Delta = & \frac{1}{2}+k \\ \Delta = & -2k-\ell\pm 2i\Delta_i\end{cases}$$

where k is a non negative integer number.

Finding the residue of the poles coming from $K_{1-\Delta,\ell}$ and $\Gamma(\Delta+\gamma+1)$ are straightforward considering that the residue of Gamma functions are: $\text{Res}(\Gamma,-k) = \frac{(-1)^k}{k!}$. For the poles of ${}_3F_2$ term, we use the power series expansion of ${}_3F_2$. After re-summing, we end up with another ${}_3F_2$. In summary, we find $\text{Res}(\tilde{f}^s_{\Delta,\ell}) =$

$$\begin{cases} \frac{(-1)^{k+\ell}\sqrt{\pi}\Gamma(2k+2\ell\mp 2i\Delta_i)\Gamma(2k+\ell\mp 2i\Delta_i+\frac{1}{2})\Gamma(-k\pm 2i\Delta_i)}{k!\,\Gamma(k+\ell+\frac{1}{2})\Gamma(k+\ell\mp 2i\Delta_i+\frac{1}{2})\Gamma(2k+\ell\mp 2i\Delta_i)\Gamma(-2k\pm 2i\Delta_i)}\frac{\Gamma(2\Delta_r+\sigma+1)\Gamma(\Delta+\gamma+1)}{\Gamma(\Delta+2\Delta_r+\gamma+\sigma+2)} & \\ \qquad\times{}_3F_2\left[\begin{matrix}\Delta+2i\Delta_i,\Delta-2i\Delta_i,\Delta+\gamma+1\\ 2\Delta,\Delta+2\Delta_r+\gamma+\sigma+2\end{matrix}\middle|1\right]\ , & \Delta=-2k-\ell\pm 2i\Delta_i \\[2ex] \frac{\pi(-1)^{k+\ell+1}\Gamma(\ell-k-\frac{1}{2})\Gamma(\frac{1}{2}(k+\ell+2i\Delta_i+\frac{1}{2}))\Gamma(\frac{1}{2}(k+\ell-2i\Delta_i+\frac{1}{2}))}{k!\Gamma(k+\ell+\frac{1}{2})\Gamma(-k-\frac{1}{2})\Gamma(\frac{1}{2}(\ell-k+2i\Delta_i+\frac{1}{2}))\Gamma(\frac{1}{2}(\ell-k-2i\Delta_i+\frac{1}{2}))}\frac{\Gamma(\Delta+\gamma+1)\Gamma(2\Delta_r+\sigma+1)}{\Gamma(\Delta+2\Delta_r+\gamma+\sigma+2)} & \\ \qquad\times{}_3F_2\left[\begin{matrix}\Delta+2i\Delta_i,\Delta-2i\Delta_i,\Delta+\gamma+1\\ 2\Delta,\Delta+2\Delta_r+\gamma+\sigma+2\end{matrix}\middle|1\right]\ , & \Delta=\frac{1}{2}+k \\[2ex] \frac{(-1)^k}{k!}\frac{\Gamma(2\Delta_r+\sigma+1)K_{1-\Delta,\ell}}{\Gamma(\Delta+2\Delta_r+\gamma+\sigma+2)} & \\ \qquad\times{}_3F_2\left[\begin{matrix}\Delta+2i\Delta_i,\Delta-2i\Delta_i,\Delta+\gamma+1\\ 2\Delta,\Delta+2\Delta_r+\gamma+\sigma+2\end{matrix}\middle|1\right]\ , & \Delta=-(1+\gamma)-k \\[2ex] -\frac{\Gamma(2\Delta_r+\sigma+1)K_{1-\Delta,\ell}}{2\Gamma(\Delta+2\Delta_r+\gamma+\sigma+2)}\frac{(-1)^k(1+\gamma-\frac{k}{2})_{k+1}(-\frac{k}{2}+2i\Delta_i)_{k+1}(-\frac{k}{2}-2i\Delta_i)_{k+1}}{k!(k+1)!(-\frac{k}{2}+2\Delta_r+\gamma+\sigma+2)_{k+1}} & \\ \qquad\times{}_3F_2\left[\begin{matrix}-\Delta+1+2i\Delta_i,-\Delta+1-2i\Delta_i,-\Delta+\gamma+2\\ -2\Delta+2,-\Delta+2\Delta_r+\gamma+\sigma+3\end{matrix}\middle|1\right]\ , & \Delta=-\frac{k}{2}\ . \end{cases}$$

Having the residues' explicit expressions in hands, the natural thing to do is to put the residues back into the sum in eq. (E.3) and truncate the sum at some upper limit $k_{\max}$ considering the fact that $\tilde{f}_\infty = 0$. However, the residues above will grow and the sum is not convergent. One may try to group the poles and sum the poles inside a circle of radius R in Δ plane but the sum would not be convergent.

Empirically, we know that the residues grow like

$$\text{Res}(\tilde{f}^s_\Delta) \propto k^{2\beta}\ ,$$

where $\beta = 2\Delta_\phi + \gamma + \sigma + 1$. We get around this problem by factorizing $\Delta^\delta + 1$ where δ is an integer $\delta \geq \lceil 2\beta \rceil + 1$, so the sum over residues converges. We pick δ to be an integer to avoid any branch cut. Defining $\tilde{g}$ as

$$\tilde{g}^s_\Delta = \frac{1}{\Delta^\delta + 1}\tilde{f}^s_\Delta\ , \tag{E.18}$$

we find the pole expansion of $\tilde{g}$ which is a convergent sum at a cost of introducing new poles because of factor $\frac{1}{\Delta^\delta+1}$. In the end, one finds

$$\tilde{f}^s_\Delta = (\Delta^\delta + 1)\sum_i \frac{\text{Res}(\tilde{g})}{\Delta - \Delta_i}\ . \tag{E.19}$$

Indeed, one can check this numerically and find the convergence to the exact value in eq. (E.17).

Let us simplify the s-channel part of $\tilde{F}$ on principal series where by adding the shadow part we find a function of ν^2 for $\Delta = \frac{d}{2} + i\nu$:

$$\begin{aligned}
\tilde{F}^s_{\frac{d}{2}+i\nu} &= ((\frac{1}{2} + i\nu)^\delta + 1)\sum_j \frac{\mathrm{Res}(\tilde{g})_j}{i\nu - \underbrace{(\Delta_j - \frac{1}{2})}_{\bar{\Delta}_i}} + ((\frac{1}{2} - i\nu)^\delta + 1)\sum_j \frac{\mathrm{Res}(\tilde{g})_j}{-i\nu - \underbrace{(\Delta_j - \frac{1}{2})}_{\bar{\Delta}_i}} \\
&= \sum_j \frac{i((1/2+i\nu)^\delta) - (1/2-i\nu)^\delta)\nu + ((1/2+i\nu)^\delta) + (1/2-i\nu)^\delta)\bar{\Delta}_j + 2\bar{\Delta}_j}{\nu^2 + \bar{\Delta}_j^2} \mathrm{Res}(\tilde{g})_j \\
&= \sum_j \frac{p(\nu^2)}{\nu^2 + \bar{\Delta}_j^2} = \frac{P_n(\nu^2)}{\prod_j (\nu^2 + \bar{\Delta}_j^2)}
\end{aligned}$$

where $p(\nu^2)$ and $P_n(\nu^2)$ are polynomials. As you can see, we end up with a similar form as the theorem above where $\nu^2 > 0$ can be treated as $x \geq 0$ which allows us to use the powerful machinery of SDPB [124] to cosmological correlators.

F Symmetry constraints on matrix elements

In this appendix, we consider constraints coming from AdS isometries (or boundary conformal symmetry) on matrix elements of the operator

$$V := R^{\Delta_\mathcal{V}} \int_{-\pi/2}^{\pi/2} \frac{dr}{(\cos r)^2}\, \mathcal{V}(\tau = 0, r) \tag{F.1}$$

where $\mathcal{V}$ is any local bulk operator. To this end, we fix two boundary primary states $|\psi_i\rangle$ and $|\psi_j\rangle$ of dimension Δ_i and Δ_j. We will use $SL(2,\mathbb{R})$ symmetry to derive relations between different matrix elements between descendants, that is to say between the matrix elements

$$\mathbf{V}^{j,m}{}_{i,n} := \langle \psi_j, m | V | \psi_i, n\rangle. \tag{F.2}$$

The argument will make use of a second operator W, defined as follows:

$$W := R^{\Delta_\mathcal{V}} \int_{-\pi/2}^{\pi/2} \frac{dr}{(\cos r)^2}\, \sin r\, \mathcal{V}(0, r) \tag{F.3}$$

along with its matrix elements which we denote as $\mathbf{W}^{j,m}{}_{i,n}$ as in eq. (F.2). Parts of our discussion will be similar in spirit to section 2.1 of reference [45], where relations between matrix elements in AdS$_3$ were derived using $SO(2,2)$ group theory.

F.1 Relations between matrix elements of descendants

Let us proceed with the derivation of the promised relations. We derive them simply by evaluating Ward identities. If G is a generator of $SL(2,\mathbb{R})$, then $G\,|\psi_i, n\rangle$ can be computed using eq. (7.10). To wit

$$H\,|\psi_i,n\rangle = (\Delta_i+n)\,|\psi_i,n\rangle\,, \tag{F.4a}$$

$$K\,|\psi_i,n\rangle = \gamma(\Delta_i,n)\,|\psi_i,n-1\rangle\,, \tag{F.4b}$$

$$P\,|\psi_i,n\rangle = \gamma(\Delta_i,n+1)\,|\psi_i,n+1\rangle \tag{F.4c}$$

where $\gamma(\Delta,n)=\sqrt{n(2\Delta+n-1)}$. At the same time, G acts on the local operators $\mathcal{V}$ as a differential operator $\mathcal{D}_G$, as specified in Eq. (7.6). For general G, we then have the identity

$$\langle\psi_j,m|[G,\mathcal{V}(\tau,r)]|\psi_i,n\rangle = \mathcal{D}_G\cdot\langle\psi_j,m|\mathcal{V}(\tau,r)|\psi_i,n\rangle \tag{F.5a}$$

$$= (\langle\psi_j,m|\,G)\mathcal{V}(\tau,r)\,|\psi_i,n\rangle - \langle\psi_j,m|\,\mathcal{V}(\tau,r)(G\,|\psi_i,n\rangle). \tag{F.5b}$$

For $G=H$, this implies that

$$\left(\frac{\partial}{\partial\tau}+\Delta_{ij}+n-m\right)\langle\psi_j,m|\mathcal{V}(\tau,r)|\psi_i,n\rangle = 0 \tag{F.6}$$

where $\Delta_{ij}:=\Delta_i-\Delta_j$. This completely fixes the τ-dependence of $\langle\psi_j,m|\mathcal{V}(\tau,r)|\psi_i,n\rangle$. Likewise, for P we get

$$\mathcal{D}_P\cdot\langle\psi_j,m|\mathcal{V}(\tau,r)|\psi_i,n\rangle = \gamma(\Delta_j,m)\langle\psi_j,m-1|\mathcal{V}(\tau,r)|\psi_i,n\rangle - \gamma(\Delta_i,n+1)\langle\psi_j,m|\mathcal{V}(\tau,r)|\psi_i,n+1\rangle \tag{F.7}$$

and finally for K we have

$$\mathcal{D}_K\cdot\langle\psi_j,m|\mathcal{V}(\tau,r)|\psi_i,n\rangle = \gamma(\Delta_j,m+1)\langle\psi_j,m+1|\mathcal{V}(\tau,r)|\psi_i,n\rangle - \gamma(\Delta_i,n)\langle\psi_j,m|\mathcal{V}(\tau,r)|\psi_i,n-1\rangle. \tag{F.8}$$

To proceed, we explicitly apply the operators $\mathcal{D}_P$ and $\mathcal{D}_K$, which are first order both in ∂_τ and ∂_r. The τ-derivatives can be computed by means of (F.6). The LHS of (F.7) then becomes

$$(\ldots) = \left[(-\Delta_{ij}+m-n)\sin r+\cos r\,\frac{\partial}{\partial r}\right]\langle\psi_j,m|\mathcal{V}(0,r)|\psi_i,n\rangle \tag{F.9}$$

setting $\tau=0$ from now on. The $\sin r$ term can be integrated over r yielding something proportional to the matrix element $\mathbf{W}^{j;m}{}_{i;n}$. The second term can be computed similarly after employing integration by parts:

$$\int_{-\pi/2}^{\pi/2}\frac{dr}{(\cos r)^2}\cos r\,\frac{\partial}{\partial r}\langle\psi_j,m|\mathcal{V}(0,r)|\psi_i,n\rangle = -\int_{-\pi/2}^{\pi/2}\frac{dr}{(\cos r)^2}\sin r\,\langle\psi_j,m|\mathcal{V}(0,r)|\psi_i,n\rangle \tag{F.10a}$$

$$= -\mathbf{W}^{j;m}{}_{i;n} \tag{F.10b}$$

discarding a boundary term that vanishes. Integrating the RHS of (F.7) at $\tau = 0$ as well, we obtain the relation

$$(-\Delta_{ij} + m - n - 1){\mathbf{W}^{j;m}}_{i;n} = \gamma(\Delta_j, m){\mathbf{V}^{j;m-1}}_{i;n} - \gamma(\Delta_i, n+1){\mathbf{V}^{j;m}}_{i;n+1}. \tag{F.11a}$$

If we repeat this for K, we get in addition

$$(-\Delta_{ij} + m - n + 1){\mathbf{W}^{j;m}}_{i;n} = \gamma(\Delta_j, m+1){\mathbf{V}^{j;m+1}}_{i;n} - \gamma(\Delta_i, n){\mathbf{V}^{j;m}}_{i;n-1}. \tag{F.11b}$$

Moreover, matrix elements with either $n = 0$ or $m = 0$ can be computed as definite integrals over

$$f_{ji}(r) := \langle \psi_j | \mathcal{V}(0, r) | \psi_i \rangle \tag{F.12}$$

which only involves the primary states $|\psi_{i,j}\rangle$. To wit:

$$\begin{aligned} {\mathbf{V}^{j;m}}_{i;0} &= (-1)^m \sqrt{\frac{m!}{(2\Delta_j)_m}} \int_{-\pi/2}^{\pi/2} \frac{dr}{(\cos r)^2}\, C_m^{-\frac{1}{2}(m-\Delta_{ij})}(\sin r) f_{ji}(r), && \text{(F.13a)} \\ {\mathbf{W}^{j;m}}_{i;0} &= (-1)^{m+1}(m+1) \sqrt{\frac{m!}{(2\Delta_j)_m}} \int_{-\pi/2}^{\pi/2} \frac{dr}{(\cos r)^2}\, \frac{C_{m+1}^{-\frac{1}{2}(m-\Delta_{ij}+1)}(\sin r)}{m - \Delta_{ij} + 1}\, f_{ji}(r). && \text{(F.13b)} \end{aligned}$$

Here $C_n^{(\nu)}(\cdot)$ denotes a Gegenbauer polynomial. Matrix elements with $m = 0$ but $n \neq 0$ can be computed similarly, exchanging $\Delta_i \leftrightarrow \Delta_j$ in the above formulas. In order to derive (F.13), let

$$\mathcal{F}_m(r) := \langle \psi_j, m | \mathcal{V}(0, r) | \psi_i \rangle \tag{F.14}$$

omitting labels for the external states $|\psi_{i,j}\rangle$, and in particular $\mathcal{F}_0(r) = f_{ji}(r)$. Setting $n = 0$ in (F.8), we get the recurrence relation

$$\mathcal{F}_{m+1}(r) = \frac{1}{\gamma(\Delta_j, m+1)} \left[(-\Delta_{ij} + m) \sin r - \cos r \frac{\partial}{\partial r} \right] \mathcal{F}_m(r). \tag{F.15}$$

After repeatedly integrating by parts and discarding (vanishing) boundary terms, the formulas (F.13) are recovered.

The interpretation of the above results depends on the precise value of $\Delta_{ij} = \Delta_i - \Delta_j$. We will discuss the cases where Δ_{ij} is fractional and integer separately:

- If Δ_{ij} is non-integer, the relations (F.11) together with the "initial conditions" (F.13) are sufficient to compute *any* matrix element of $\mathbf{V}$. This can be done simply by eliminating $\mathbf{W}$ from the equations (F.11).

- On the other hand, if Δ_{ij} is an integer, it is not always possible to eliminate $\mathbf{W}$ from the above equations. Instead, we find *new* relations between specific matrix elements:

$$\gamma(\Delta_j, m+1)\mathbf{W}^{j;m+1}{}_{i;m-\Delta_{ij}} = \gamma(\Delta_i, m-\Delta_{ij})\mathbf{W}^{j;m}{}_{i;m-\Delta_{ij}-1} + \mathbf{V}^{j;m}{}_{i;m-\Delta_{ij}}, \tag{F.16a}$$

$$\gamma(\Delta_i, m+1)\mathbf{W}^{j;m+\Delta_{ij}}{}_{i;m+1} = \gamma(\Delta_j, m+\delta_{ij})\mathbf{W}^{j;m+\Delta_{ij}-1}{}_{i;m} + \mathbf{V}^{j;m+\Delta_{ij}}{}_{i;m} \tag{F.16b}$$

which are once more derived by a judicious application of integration by parts. It turns out that these identities are again sufficient to reduce the computation of the matrix $\mathbf{V}$ to its boundary.

If Δ_{ij} is integer, certain selection rules apply. For concreteness, consider the case $\Delta_i = \Delta_j$. Then by setting $m = n+1$ in the first relation of (F.11), we obtain the identity

$$0 = \gamma(\Delta_i, n+1)\mathbf{V}^{j;n}{}_{i;n} - \gamma(\Delta_i, n+1)\mathbf{V}^{i;n+1}{}_{i;n+1} \tag{F.17}$$

which implies that all matrix elements $\mathbf{V}^{j;n}{}_{i;n}$ with $n = 0, 1, 2, \ldots$ are identical. This result has a simple physical meaning. Indeed, if $\psi_j = \psi_i$, the diagonal of the matrix $\mathbf{V}^{i;n}{}_{i;n}$ is proportional to the tree-level energy shift of the states $|\psi_i, n\rangle$. But by conformal symmetry, all such energy shifts (or anomalous dimensions) must be identical. Consequently, it is necessary that for $\Delta_i = \Delta_j$, the diagonal of the matrix $\mathbf{V}$ is constant.

Next, consider the case where Δ_{ij} is a non-zero integer, say $\Delta_{ij} =: s$ with $s \in \{1, 2, 3, \ldots\}$. Then from (F.13a) it follows that $\mathbf{V}^{j;s}{}_{i;0}$ vanishes — this is simply a property of the Gegenbauer polynomials. But from Eq. (F.11) it follows that

$$\gamma(\Delta_j, n+s+1)\mathbf{V}^{j;n+s+1}{}_{i;n+1} = \gamma(\Delta_i, n+1)\mathbf{V}^{j;n+s}{}_{i;n} \tag{F.18}$$

for any n. Consequently, *all* matrix elements of the form $\mathbf{V}^{j;n+s}{}_{i;n}$ vanish! If Δ_{ij} is a negative integer, a similar argument can be made.

Let us finally comment on parity. If $|\psi_{i,j}\rangle$ have the same parity and $\mathcal{V}$ respects parity, then $f_{ji}(r)$ is even under $r \mapsto -r$. But then using (F.13) and (F.11), it can be shown that matrix elements of $\mathbf{V}$ (resp. $\mathbf{W}$) vanish if $m+n$ is odd (resp. even). The same result could have been derived directly since

$$\langle\psi_i, m|\mathtt{P}V\mathtt{P}^{-1}|\psi_j, n\rangle = (-1)^{m+n}\langle\psi_i, m|V|\psi_j, n\rangle = +\langle\psi_i, m|V|\psi_j, n\rangle \tag{F.19}$$

(using the fact that $\mathtt{P}V\mathtt{P}^{-1} = +V$) which for odd $m+n$ is only possible if $\mathbf{V}^{j;m}{}_{i;n} = 0$. A similar argument can be applied to the case where $|\psi_{i,j}\rangle$ have opposite parity.

F.2 Example: vacuum amplitudes

As an application of the above formalism, let's consider the case where the in-state is the vacuum $|\Omega\rangle$. By $SL(2,\mathbb{R})$ symmetry, the wavefunction $f_{i,\Omega}$ is completely fixed, up to an overall constant:

$$f_{i,\Omega}(r) = \langle\psi_i|\mathcal{V}(r)|\Omega\rangle = \alpha_i(\cos r)^{\Delta_i}. \tag{F.20}$$

The coefficient α_i can be interpreted as the bulk-boundary OPE coefficient of $\mathcal{V} \to \mathcal{O}_i$ (up to a convention-dependent constant), see (7.13). A short computation shows that

$$\mathbf{V}^{i;2n+1}{}_{\Omega} = 0, \quad \mathbf{V}^{i;2n}{}_{\Omega} = \alpha_i(\Delta_i + 2n)B(\tfrac{1}{2}\Delta_i - \tfrac{1}{2}, \tfrac{3}{2})\sqrt{\frac{(\frac{1}{2})_n(\Delta_i)_n}{n!(\Delta_i+\frac{1}{2})_n}} \tag{F.21}$$

where B is the beta function. As an application of this result, we note that

$$\lim_{n\to\infty} \frac{\mathbf{V}^{i;2n}{}_{\Omega}}{\sqrt{n}\,\mathbf{V}^{i;0}{}_{\Omega}} = \frac{2}{\Delta\sqrt{B(\frac{1}{2},\Delta)}} \tag{F.22}$$

that is to say that the matrix elements $\mathbf{V}^{i;2n}{}_{\Omega}$ grow as $\sqrt{n}$ at large n. In particular, this result implies that the Casimir energy diverges at least linearly at second order in perturbation theory.

F.3 Universality of matrix elements if $\Delta_i - \Delta_j$ is an even integer

If Δ_{ij} is an even integer, that is to say $|\Delta_i - \Delta_j| = 2s$ for some integer s, and the in- and out-states $|\psi_{i,j}\rangle$ have the same parity, the matrix $\mathbf{V}^{j;m}{}_{i;n}$ is severely constrained. In fact, we will prove that it is fixed in terms of $s+1$ constants.

Theorem: let $|\psi_{i,j}\rangle$ be two primaries with $\pi_i = \pi_j$ that satisfy $\Delta_j = \Delta_i \pm 2s$ with $s \in \{0,1,2,\ldots\}$, and let V be a parity-preserving bulk perturbation. Then the matrix $\mathbf{V}^{j;m}{}_{i;n}$ is completely fixed by $SL(2,\mathbb{R})$ symmetry in terms of the $s+1$ constants

$$c_a(\psi_j,\psi_i) := \int_{-\pi/2}^{\pi/2} \frac{dr}{(\cos r)^2}\,(\sin r)^{2a} f_{ji}(r), \quad a = 0,1,\ldots,s. \tag{F.23}$$

Proof: by parity, only matrix elements with even $m+n$ can be non-zero. Thus all non-vanishing matrix elements with $n=0$ are proportional to the following integral:

$$\mathbf{V}^{j;2m}{}_{i;0} \propto \int_{-\pi/2}^{\pi/2} \frac{dr}{(\cos r)^2}\, C_{2m}^{-m\pm s}(\sin r) f_{ji}(r), \quad m = 0,1,2,\ldots$$

as an immediate consequence of (F.13). But it's easy to show that any such Gegenbauer polynomial is a polynomial of degree $\leq s$ in the variable $z = (\sin r)^2$. Indeed, we have

$$C_{2m}^{-m+s}(\sin r) = \frac{(1-s)_m}{m!}\,{}_2F_1(-m, s, \tfrac{1}{2}, z), \quad C_{2m}^{-m-s}(\sin r) = \frac{(1+s)_m}{m!}\,{}_2F_1(-s, -m, \tfrac{1}{2}, z). \tag{F.24}$$

The first of these functions vanishes if $m \geq s$, due to the prefactor $(1-s)_m$; for $m < s$ it's indeed a polynomial of degree m in the variable z. Likewise, the second function in (F.24) is a polynomial in z of degree $\min(m, s)$. Consequently, any matrix element with $n = 0$ can be expressed in terms of the parameters $c_a(\psi_j, \psi_i)$.

Now, the same argument can be applied to matrix elements with $m = 0$. Finally, all other matrix elements, having $m, n \neq 0$ can be computed in terms of the previous ones using the relations described in section F.1. ☐

In particular, for $s = 0$ (i.e. whenever $\Delta_i = \Delta_j$) the matrix $\mathbf{V}^{j;m}{}_{i;n}$ is completely universal, meaning that it is fixed by symmetry up to an overall normalization. To be precise, we have the following corollary:

Corollary: let $|\psi_{i,j}\rangle$ be two primaries with $\Delta_i = \Delta_j$ and $\pi_i = \pi_j$. Then for any parity-preserving bulk perturbation V, we have

$$\langle \psi_j, m | V | \psi_i, n \rangle = \mathscr{V}_{mn}(\Delta_i)\, \langle \psi_j | V | \psi_i \rangle \tag{F.25}$$

where $\mathscr{V}_{mn}(\Delta_i)$ is a matrix that only depends on Δ_i, to wit:

$$\mathscr{V}_{mn}(\Delta) = \begin{cases} 0 & \text{if } m+n \text{ is odd;} \\ \sqrt{(m+1)_{n-m}/(2\Delta+m)_{n-m}} & m \leq n,\ m+n \text{ even;} \\ \mathscr{V}_{nm}(\Delta) & m > n. \end{cases} \tag{F.26}$$

Note: setting $m = n$, we see that the diagonal matrix elements are constant (since $\mathscr{V}_{nn}(\Delta) = 1$). This is consistent with the discussion from the end of section F.1.

Proof. Since any possible solution to the Ward identities is unique in this case, it suffices to check that $\mathscr{V}_{mn}(\Delta_i)$ solves (F.11). Indeed (F.26) is a valid solution, if we also have

$$\langle \psi_j, m | W | \psi_i, n \rangle = \mathscr{W}_{mn}(\Delta_i)\, \langle \psi_j | V | \psi_i \rangle \tag{F.27a}$$

for

$$\mathscr{W}_{mn}(\Delta) = \begin{cases} 0 & \text{if } m+n \text{ is even;} \\ \sqrt{(m+1)_{n-m}/(2\Delta+m)_{n-m}} & m < n,\ m+n \text{ odd;} \\ \mathscr{W}_{nm}(\Delta) & m > n. \end{cases} \tag{F.27b}$$

This can be checked easily. ☐

G Rayleigh-Schrödinger perturbation theory revisited

G.1 Rayleigh-Schrödinger coefficients and connected correlators

In this appendix, we prove a relation between coefficients in Rayleigh-Schrödinger perturbation theory and correlation functions. To be precise, we have in mind a Hamiltonian of the form $H = H_0 + \lambda V$, where H_0 has a non-degenerate discrete spectrum

$$0 = e_0 < e_1 < e_2 < \dots$$

associated to normalized eigenstates $|i\rangle$, such that $|0\rangle$ is the H_0 vacuum state. In perturbation theory, the interacting energies can be expanded as

$$\mathcal{E}_i = e_i + \sum_{n=1}^{\infty} (-1)^{n+1} c_{i,n} \lambda^n \tag{G.1}$$

for some constants $c_{i,n}$ to be determined. Moreover, we can expand the eigenstates $|\Omega_j\rangle$ of H in terms of the eigenstates of H_0 with certain coefficients:

$$|\langle i|\Omega_j\rangle|^2 = \delta_{ij} + \sum_{n=2}^{\infty} (-1)^n a_n(j \to i)\, \lambda^n. \tag{G.2}$$

Normalization of the states $|\Omega_i\rangle$ and $|i\rangle$ means that

$$a_n(i \to i) = -\sum_{j \neq i} a_n(i \to j) = -\sum_{j \neq i} a_n(j \to i). \tag{G.3}$$

From now on, we will use rule (G.3) to only consider coefficients with $j \neq i$.

It's the goal of Rayleigh-Schrödinger perturbation theory to provide formulas for $c_{i,n}$ and

$a_n(j \to i)$. Some simple formulas are

$$c_{i,1} = \langle i|V|i\rangle, \quad c_{i,2} = \sum_{j \neq i} \frac{|\langle i|V|j\rangle|^2}{e_j - e_i} \quad \text{and} \quad a_2(j \to i) = \frac{|\langle i|V|j\rangle|^2}{(e_j - e_i)^2}. \tag{G.4}$$

At higher orders in perturbation theory, similar formulas quickly become cumbersome.

We claim that, roughly speaking, the coefficients $c_{i,n}$ can be expressed as an integral over the n-point correlation function of the operator V inside the state $|i\rangle$. Considering the vacuum state at second order in perturbation theory, it is for instance well-known that

$$c_{0,2} = \int_0^\infty d\tau\, \langle 0|V(\tau)V(0)|0\rangle_{\text{conn}} \tag{G.5}$$

where the subscript $\langle i|\mathcal{O}_n \cdots \mathcal{O}_1|i\rangle_{\text{conn}}$ means that contractions between the operators $\mathcal{O}_j$ must be subtracted in the state $|i\rangle$, e.g.

$$\langle i|V(\tau)V(0)|i\rangle_{\text{conn}} = \langle i|V(\tau)V(0)|i\rangle - \langle i|V|i\rangle^2 =: \mathfrak{g}_i(\tau) \tag{G.6a}$$

$$\begin{aligned}\langle i|V(\tau_1+\tau_2)V(\tau_1)V(0)|i\rangle_{\text{conn}} &= \langle i|V(\tau_1+\tau_2)V(\tau_1)V(0)|i\rangle - \langle i|V|i\rangle^3 \\ &\quad - \langle i|V|i\rangle \Big[\mathfrak{g}_i(\tau_1) + \mathfrak{g}_i(\tau_2) + \mathfrak{g}_i(\tau_1+\tau_2)\Big]\end{aligned} \tag{G.6b}$$

and so forth. However, it's not possible to simply replace the in- and out-states in (G.5) by $|i\rangle$ and $\langle i|$ to reproduce the expression from Eq. (G.4) — in fact, the resulting integral would diverge for a generic state $|i\rangle$. To proceed, we therefore define a spectral density $\rho_{i,n}$ as follows:

$$\boxed{\langle i|V(\tau_1+\ldots+\tau_{n-1})\cdots V(\tau_1)V(0)|i\rangle_{\text{conn}} = \prod_{\ell=1}^{n-1} \int_0^\infty d\alpha_\ell\, e^{-(\alpha_\ell - e_i)\tau_\ell}\, \rho_{i,n}(\alpha_1,\ldots,\alpha_{n-1})} \tag{G.7}$$

which has the following inverse:

$$\rho_{i,n}(\vec{\alpha}) = \prod_{\ell=1}^{n-1} \int_{\gamma-i\infty}^{\gamma+i\infty} \frac{d\tau_\ell}{2\pi i}\, e^{(\alpha_\ell - e_i)\tau_\ell}\, \langle i|V(\tau_1+\ldots\tau_{n-1})\cdots V(\tau_1+\tau_2)V(\tau_1)V(0)|i\rangle_{\text{conn}}$$

for $\gamma > 0$.[1] For $n = 1,2,3$ we have for instance

$$\rho_{i,1} = \langle i|V|i\rangle \tag{G.8a}$$

$$\rho_{i,2}(\alpha_1) = \sum_{k\neq i} \delta(\alpha_1 - e_k)\, |\langle i|V|k\rangle|^2 \tag{G.8b}$$

$$\rho_{i,3}(\alpha_1,\alpha_2) = \sum_{k,\ell\neq i} \delta(\alpha_1 - e_k)\delta(\alpha_2 - e_\ell)\, \langle i|V|\ell\rangle \Big(\langle \ell|V|k\rangle - \delta_{k\ell}\langle i|V|i\rangle\Big)\langle k|V|i\rangle\,. \tag{G.8c}$$

---

[1] We use that on the right half plane $\Re(\tau_j) > 0$ the correlator is analytic.

We will see that the Rayleigh-Schrödinger coefficients can be compactly expressed in terms of the densities $\rho_{i,n}$, to wit:

$$\boxed{c_{i,n} = \prod_{\ell=1}^{n-1} \int_0^\infty \frac{d\alpha_\ell}{\alpha_\ell - e_i}\, \rho_{i,n}(\alpha_1, \ldots, \alpha_{n-1}).} \tag{G.9}$$

For $n = 1, 2$, it is easy to check that (G.9) agrees with (G.4). In the rest of this section, the proof of formula (G.9) will be explained.

First, let us comment on some general features of the $\rho_{i,n}(\vec{\alpha})$.[2] This object is generally a complex-valued distribution, in fact a sum (generally infinite) of delta functions. Also notice that ρ only has support on $\alpha_\ell \geq 0$ since there are no states with energy $e < 0$, and the distribution vanishes at $\alpha_\ell = e_i$ since ρ describes *connected* correlation functions. In fact, it will be useful in the proof of (G.9) to write ρ as follows

$$\rho_{i,n}(\alpha_1, \ldots, \alpha_{n-1}) = \sum_{j_1 \neq i} \cdots \sum_{j_{n-1} \neq i} \delta(\alpha_1 - e_{j_1}) \ldots \delta(\alpha_{n-1} - e_{j_{n-1}}) U_{j_1, \ldots, j_{n-1}}\,. \tag{G.10}$$

Moreover, since V is a Hermitian operator it can be shown that

$$\overline{\rho_{i,n}(\alpha_1, \ldots, \alpha_k, \ldots, \alpha_{n-1})} = \rho_{i,n}(\alpha_{n-1}, \ldots, \alpha_{n-k}, \ldots, \alpha_1) \tag{G.11}$$

reflecting a peculiarity from the configuration of the τ_j in the correlator (G.7). For $n = 2$ the above identity means that $\rho_{i,2}(\alpha) \in \mathbb{R}$. We also remark that the behavior of the $\rho_{i,n}$ at infinity depends on the high-energy behavior of the quantum theory in question. For instance, if $\kappa \geq 1$ then

$$\mathfrak{g}_i(\tau) \underset{\tau \to 0}{\sim} \frac{c}{\tau^\kappa} \quad \leftrightarrow \quad \rho_{i,2}(\alpha) \underset{\alpha \to \infty}{\sim} \frac{c}{\Gamma(\kappa)}\, \alpha^{\kappa - 1} \tag{G.12}$$

appealing to a Tauberian theorem. In AdS$_2$, this Tauberian formula applies with $\kappa = 2$, but in UV-finite quantum mechanics all correlators are integrable (having in particular $\kappa < 1$). In what follows it will be assumed that the integrals (G.9) are well-defined, without requiring any additional subtractions.

The reader may worry about the seemingly divergent denominator $\prod_{\ell=1}^{n-1} 1/(\alpha_\ell - e_i)$ in (G.9). However, recall that $\rho_{i,n}$ vanishes on some domain $|\alpha_\ell - e_j| \leq \epsilon$ due to the connectedness of the correlator it describes, and consequently the integral (G.9) is well-defined. If necessary, one can therefore replace all of the integrals by their principal value

$$\prod_{\ell=1}^{n-1} \int_{\mathbb{R}} \frac{d\alpha_\ell}{\alpha_\ell - e_i}\, \rho_{i,n}(\vec{\alpha}) \to \lim_{\epsilon \to 0^+} \prod_{\ell=1}^{n-1} \int_{\mathbb{R} \setminus [e_i - \epsilon, e_i + \epsilon]} \frac{d\alpha_\ell}{\alpha_\ell - e_i}\, \rho_{i,n}(\vec{\alpha}) \tag{G.13}$$

without changing the result.

---

[2] Here, we use the shorthand notation $\vec{\alpha} = (\alpha_1, \ldots, \alpha_{n-1})$.

Proof of (G.9)

Let us now describe a proof of the identity (G.9). The proof will rely on a systematic evaluation of the Dyson operator

$$U(b,a) := \mathrm{T}\exp\left[-\lambda \int_a^b d\tau\, V(\tau)\right]. \tag{G.14}$$

inside matrix elements. The operator U has the defining property

$$e^{-H(b-a)} = e^{-H_0 b} U(b,a) e^{H_0 a} \tag{G.15}$$

which can easily be shown (the identity (G.15) is a tautology for $b=a$, and the two sides obey the same differential equation with respect to b).

For concreteness, let us first consider the vacuum state $|0\rangle = |\mathrm{vac}\rangle$, for which the proof of (G.9) is easiest. There we have for any $T > 0$ the exact identity

$$\langle \mathrm{vac}|U(T,0)|\mathrm{vac}\rangle = \sum_j \langle \mathrm{vac}|e^{H_0 T} e^{-HT}|\Omega_j\rangle\langle\Omega_j|\mathrm{vac}\rangle = \sum_{i=0}^{\infty} \exp(-\mathcal{E}_i T)|\langle \mathrm{vac}|\Omega_j\rangle|^2 \tag{G.16}$$

where we have inserted a complete basis of states $|\Omega_j\rangle$ and used Eq. (G.15) to rewrite U. Taking the limit $T \to \infty$, we have[3]

$$\mathcal{E}_0(\lambda) = -\lim_{T\to\infty} \frac{1}{T} \ln \langle \mathrm{vac}|U(T,0)|\mathrm{vac}\rangle. \tag{G.17}$$

The object on the RHS is precisely the generator of connected correlation functions inside the vacuum state. At n-th order in perturbation theory, we read off that

$$c_{\mathrm{vac},n} = \prod_{\ell=1}^{n-1} \int_0^\infty d\tau_\ell \, \langle \mathrm{vac}|V(\tau_1 + \ldots \tau_{n-1}) \cdots V(\tau_1+\tau_2)V(\tau_1)V(0)|\mathrm{vac}\rangle_{\mathrm{conn}} \tag{G.18a}$$

$$= \prod_{\ell=1}^{n-1} \int_0^\infty \frac{d\alpha_\ell}{\alpha_\ell}\, \rho_{\mathrm{vac},n}(\alpha_1,\ldots,\alpha_{n-1}) \tag{G.18b}$$

as claimed. Formula (G.18a) for the vacuum energy is not new — see a disussion below equation (8.16) — and a formal version of (G.9) appeared previously without proof in [161].[4]

For excited states the proof of (G.9) goes along the same lines, but it is more complicated. To proceed, we insert the operator $\exp(\mathcal{E}_i T)\exp(-HT)$ inside the unperturbed state $|i\rangle$.

---

[3] Notice that $\langle \mathrm{vac}|U(T,0)|\mathrm{vac}\rangle > 0$ so the logarithm is well-defined.

[4] The formula in question involves connected correlators that are integrated over all of spacetime. Beyond short-distance divergences, such correlators are also IR-divergent due to intermediate states of energy *below* the energy e_i of the external state $|i\rangle$. Our formula (G.9) takes such divergences into account and does not need any additional renormalization.

This yields

$$
\begin{aligned}
e^{\delta\mathcal{E}_i T}\langle i|U(T,0)|i\rangle &= \sum_{j=0}^{\infty} |\langle i|\Omega_j\rangle|^2 \, e^{-(\mathcal{E}_j-\mathcal{E}_i)T} \\
&= 1 - \sum_{j\neq i}^{\infty} |\langle i|\Omega_j\rangle|^2 \left[1 - e^{-(\delta\mathcal{E}_j-\delta\mathcal{E}_i)T} e^{-(e_j-e_i)T}\right] \qquad \text{(G.19)}
\end{aligned}
$$

writing $\delta\mathcal{E}_i = \mathcal{E}_i - e_i = \mathrm{O}(\lambda)$. We have used the identity

$$
|\langle i|\Omega_i\rangle|^2 + \sum_{j\neq i} |\langle i|\Omega_j\rangle|^2 = 1 \qquad \text{(G.20)}
$$

to obtain the above expression. We will show that formula (G.9) follows from matching the terms linear in T on both sides of (G.19).

The **LHS** of (G.19) can be recast as

$$
\ln(\mathsf{LHS}) = \delta\mathcal{E}_i(\lambda)T + \sum_{n=1}^{\infty}(-1)^n\lambda^n\mathcal{X}_{i,n}(T), \qquad \text{(G.21)}
$$

$$
\mathcal{X}_{i,n}(T) := \int_0^T d\tau_1 \cdots \int_{\tau_{n-1}}^T d\tau_n \, \langle i|V(\tau_n)\cdots V(\tau_1)|i\rangle_{\text{conn}}. \qquad \text{(G.22)}
$$

Using the spectral representation (G.7) we can write (G.22) as follows

$$
\mathcal{X}_{i,n}(T) = \int_0^{\infty} d\alpha_1 \dots d\alpha_{n-1} \, \mathcal{W}_n(\alpha_1 - e_i, \dots, \alpha_{n-1} - e_i|T) \, \rho_{i,n}(\vec{\alpha}) \qquad \text{(G.23)}
$$

where [5]

$$
\mathcal{W}_n(\vec{\alpha}|T) = \int_0^T dt_0 \int_0^{T-t_0} dt_1 \, e^{-\alpha_1 t_1} \cdots \int_0^{T-t_0\cdots-t_{n-2}} dt_{n-1} \, e^{-\alpha_{n-1}t_{n-1}} \,. \qquad \text{(G.24)}
$$

Equivalently, we can define $\mathcal{W}$ by

$$
\mathcal{W}_n(\vec{\alpha}|T) = \int_0^T dt_0 \mathcal{Q}_{n-1}(\alpha_1, \dots, \alpha_{n-1}|T - t_0) \qquad \text{(G.25)}
$$

with $\mathcal{Q}$ defined recursively

$$
\mathcal{Q}_i(\alpha_1, \dots, \alpha_i|T) = \int_0^T dt \, e^{-\alpha_1 t} \mathcal{Q}_{i-1}(\alpha_2, \dots, \alpha_i|T - t) \,, \qquad \mathcal{Q}_0 = 1 \,. \qquad \text{(G.26)}
$$

---

[5] This follows from (G.22) changing integration variables to $t_i = \tau_{i+1} - \tau_i$ with $i = 0, 1, \dots, n-1$ and $\tau_0 = 0$.

It is not hard to see that this recursion relation leads to

$$\mathcal{Q}_i(\alpha_1, \dots, \alpha_i|T) = \frac{1}{\alpha_1\alpha_2 \dots \alpha_i} - \sum_{\ell=1}^{i} \frac{e^{-\alpha_\ell T}}{\alpha_\ell} \prod_{\substack{j=1 \\ j\neq\ell}}^{i} \frac{1}{\alpha_j - \alpha_\ell} \,. \tag{G.27}$$

This can be easily checked by plugging (G.27) in (G.26) and using the identity

$$0 = \frac{1}{\alpha_1\alpha_2 \dots \alpha_i} - \sum_{\ell=1}^{i} \frac{1}{\alpha_\ell} \prod_{\substack{j=1 \\ j\neq\ell}}^{i} \frac{1}{\alpha_j - \alpha_\ell} \,, \tag{G.28}$$

which follows from the fact this rational function of α_1 vanishes as $\alpha_1 \to \infty$ and does not have any poles (the reader may easily check that the apparent poles have vanishing residue).

We can now use (G.27) in (G.24) to obtain

$$\mathcal{W}_n(\vec{\alpha}|T) = \frac{T}{\alpha_1\alpha_2 \dots \alpha_i} - \mathcal{K}_n(\vec{\alpha}|T) \tag{G.29}$$

where

$$\mathcal{K}_n(\vec{\alpha}|T) := \sum_{\ell=1}^{n-1} \frac{1 - e^{-\alpha_\ell T}}{\alpha_\ell^2} \prod_{\substack{j=1 \\ j\neq\ell}}^{n-1} \frac{1}{\alpha_j - \alpha_\ell}. \tag{G.30}$$

This allows us to write (G.23), for $n \geq 2$, as follows:

$$\mathcal{X}_{i,n}(T) = T \int_0^\infty \frac{d\vec{\alpha}}{\vec{\alpha} - e_i}\, \rho_{i,n}(\vec{\alpha}) - \int_0^\infty d\vec{\alpha}\, \mathcal{K}_n(\vec{\alpha} - e_i|T)\rho_{i,n}(\vec{\alpha})\,. \tag{G.31}$$

Here and in what follows we use a vector notation for spectral integrals, for instance

$$\int_0^\infty \frac{d\vec{\alpha}}{\vec{\alpha} - e_i} f(\vec{\alpha}) = \prod_{\ell=1}^{n-1} \int_0^\infty \frac{d\alpha_\ell}{\alpha_\ell - e_i} f(\alpha_1, \dots, \alpha_{n-1}). \tag{G.32}$$

We will now show that the only term that grows linearly with T in (G.31) is the first term. More precisely, we will show that the second term in (G.31) evaluates to something of the form

$$\text{const.} + \sum_{\beta\neq 0} P_\beta(T) e^{-\beta T}\,, \tag{G.33}$$

for some values of $\beta \neq 0$ and $P_\beta(T)$ some polynomial of T. For $n = 1$ we simply have

$$\mathcal{X}_{i,1}(T) = T\rho_{i,1} = T\langle i|V|i\rangle. \tag{G.34}$$

For $n = 2$ the second integral is straightforward to do:

$$\int_0^\infty d\alpha \, \mathcal{K}_2(\alpha - e_i; T)\rho_{i,2}(\alpha) = \sum_{j \neq i} |\langle i|V|j\rangle|^2 \mathcal{K}_2(e_j - e_i|T). \tag{G.35}$$

However, for $n \geq 3$ we have to worry about the denominators $\alpha_j - \alpha_\ell$. It is clear from the definition (G.24) that $\mathcal{W}_n(\alpha_1, \ldots, \alpha_{n-1}|T)$ is completely regular when some of its arguments α_ℓ coincide. Therefore, from (G.29) we conclude the same must be true of $\mathcal{K}_n$ although this is not obvious from the explicit formula (G.30).

For instance for $n = 3$ we have

$$\lim_{\alpha' \to \alpha} \mathcal{K}_3(\alpha, \alpha'|T) = \frac{2}{\alpha^3} - \frac{2 + \alpha T}{\alpha^3} \exp(-\alpha T) =: \mathcal{K}_3^\sharp(\alpha|T). \tag{G.36}$$

Therefore, for $n = 3$ the second term in (G.31) evaluates to

$$\begin{aligned} \int_0^\infty d\vec{\alpha} \, \mathcal{K}_3(\vec{\alpha} - e_i|T)\rho_{i,3}(\vec{\alpha}) = &\sum_{j,k \neq i \,\wedge\, j \neq k} \langle i|V|k\rangle\langle k|V|j\rangle\langle j|V|i\rangle \, \mathcal{K}_3(e_j - e_i, e_k - e_i|T) \\ &+ \sum_{j \neq i} (\langle j|V|j\rangle - \langle i|V|i\rangle)|\langle i|V|j\rangle|^2 \, \mathcal{K}_3^\sharp(e_j - e_i|T), \end{aligned} \tag{G.37}$$

which is of the general form (G.33).

For general n, we can use (G.10) to write the second term in (G.31) as follows

$$\int_0^\infty d\vec{\alpha} \, \mathcal{K}_n(\vec{\alpha} - e_i|T)\rho_{i,n}(\vec{\alpha}) = \sum_{j_1 \neq i} \cdots \sum_{j_{n-1} \neq i} U_{j_1, \ldots, j_{n-1}} \mathcal{K}_n(e_{j_1} - e_i, \ldots, e_{j_{n-1}} - e_i|T) \, . \tag{G.38}$$

Clearly the arguments of $\mathcal{K}_n$ are always different from zero. Therefore, from (G.30) we conclude that this is of the general form (G.33). The only subtlety is that for some terms in the sum (G.38) the arguments of $\mathcal{K}_n$ are exactly equal. In this case, one cannot use (G.30) due to the presence of vanishing denominators. However, as explained above $\mathcal{K}_n$ always has a finite limit when several of its arguments coincide. Moreover, we can write

$$\mathcal{K}_n(\vec{\alpha}|T) = g_0(\vec{\alpha}) - \sum_{\ell=1}^{n-1} e^{-\alpha_\ell T} g_\ell(\vec{\alpha}) \, , \tag{G.39}$$

with $g_\ell(\vec{\alpha})$ some rational functions that can be read off from (G.30). If α_1 and α_2 coincide then

$$\mathcal{K}_n(\alpha_1, \alpha_1, \alpha_3, \ldots |T) = g_0(\vec{\alpha}) - \sum_{\ell=3}^{n-1} e^{-\alpha_\ell T} g_\ell(\vec{\alpha}) - e^{-\alpha_1 T} \tilde{g}_1(\vec{\alpha}|T) \, , \tag{G.40}$$

where g_0 and $g_{\ell\geq 3}$ have finite limits when $\alpha_2 \to \alpha_1$ and

$$\tilde{g}_1(\vec{\alpha}|T) = \lim_{\epsilon\to 0}\left[g_1(\alpha_1, \alpha_1+\epsilon, \alpha_3, \dots) + e^{-\epsilon T} g_2(\alpha_1, \alpha_1+\epsilon, \alpha_3, \dots)\right] \tag{G.41}$$

$$= T\frac{1}{\alpha_1^2}\prod_{j=3}^{n-1}\frac{1}{\alpha_j-\alpha_1} - \frac{\partial}{\partial\alpha_1}\left[\frac{1}{\alpha_1^2}\prod_{j=3}^{n-1}\frac{1}{\alpha_j-\alpha_1}\right]. \tag{G.42}$$

Due to the collision $\alpha_2 \to \alpha_1$ the coefficient of the exponential $e^{-\alpha_1 T}$ became a linear function of T. This is a general phenomena. When several α's coincide the coefficient of the associated exponential $e^{-\alpha_\ell T}$ becomes a polynomial in T.[6] However, as long as every $\alpha_\ell \neq 0$ the exponential never disappears and therefore (G.38) is indeed of the form (G.33).

The **RHS** of (G.19) can also be expanded to

$$\ln(\mathsf{RHS}) = \sum_{n=2}^{\infty}(-1)^n\lambda^n\mathcal{Y}_{i,n}(T) \tag{G.44}$$

for some functions $\mathcal{Y}_{i,n}(T)$:

$$\mathcal{Y}_{i,2}(T) = -\sum_{j\neq i} a_2(j\to i)\left[1-e^{-(e_j-e_i)T}\right] \tag{G.45a}$$

$$\mathcal{Y}_{i,3}(T) = -\sum_{j\neq i} a_3(j\to i)\left[1-e^{-(e_j-e_i)T}\right] - T\sum_{j\neq i}(c_{j,1}-c_{i,1})a_2(j\to i)e^{-(e_j-e_i)T} \tag{G.45b}$$

and likewise for higher n. The coefficients a_n were defined in (G.2).

We can now directly compare (G.22) and (G.44) to obtain the desired formula, Eq. (G.9). For $n=2$, we obtain the relation

$$T\left[c_{i,2} - \int_0^\infty \frac{d\alpha}{\alpha-e_i}\rho_{i,2}(\alpha)\right] = \int_0^\infty d\alpha\,\frac{1-e^{-(\alpha-e_i)T}}{(\alpha-e_i)^2}\rho_{i,2}(\alpha) - \sum_{j\neq i}a_2(j\to i)\left[1-e^{-(e_j-e_i)T}\right]. \tag{G.46}$$

Since this equation must hold for *any* $T>0$, we recover the $n=2$ case of (G.9) along with the standard result

$$a_2(j\to i) = \frac{|\langle i|V|j\rangle|^2}{(e_i-e_j)^2}. \tag{G.47}$$

---

[6] For example,

$$\lim_{\alpha',\alpha''\to\alpha}\mathcal{K}_4(\alpha,\alpha',\alpha''|T) = \frac{3}{\alpha^4} + \frac{6+4\alpha T+\alpha^2T^2}{2\alpha^4}\exp(-\alpha T). \tag{G.43}$$

The same strategy can be used to prove (G.9) for higher n. The logic is always the same, namely to match all terms of order λ^n appearing in Eqs. (G.22) and (G.44). The LHS has two purely linear pieces in T, namely

$$(-1)^{n+1} c_{i,n} T + (-1)^n T \int_0^\infty \frac{d\vec{\alpha}}{\vec{\alpha} - e_i} \rho_{i,n}(\vec{\alpha}) + \ldots . \tag{G.48}$$

which perfectly cancel, provided that (G.9) holds. The remaining term on the LHS comes from the kernel $\mathcal{K}_n$, and crucially it never contains a term growing linearly with T at large T: at most it contains a constant and polynomials in T multiplied by (growing or decaying) exponentials. This remainder term can be matched against the RHS — which does not contain any term growing linearly with T — and this procedure gives expressions for the coefficients $a_n(j \to i)$.

As mentioned at the beginning, the spectrum of the unperturbed Hamiltonian was taken to be non-degenerate. Let us briefly discuss how the proof breaks down in case H_0 is degenerate. Suppose for instance that there are two vacua, that is to say $g \geq 2$ states $|\mathrm{vac}_\alpha\rangle$ with $e_\alpha = 0$. Equation (G.16) still holds when $|\mathrm{vac}\rangle$ is replaced by any of the $|\mathrm{vac}_\alpha\rangle$, or in fact by any linear combination $|v\rangle = c^\alpha\, |\mathrm{vac}_\alpha\rangle$. Equation (G.17) also holds, provided that the true vacuum $|\Omega\rangle$ at finite coupling has non-zero overlap with the starting state $|v\rangle$. However, it is no longer true that the coefficients $c_{\mathrm{vac},n}$ are described by equation (G.18a), and indeed such integrated correlators generically diverge. In other words, the $T \to \infty$ limit and the perturbative expansion do not commute.

G.2 Feynman diagrams

This section is dedicated to a detailed explanation of the diagrammatic representation of RS perturbation theory, introduced in section 8.1. The reader may refer to figure G.1 to fix ideas, although similar pictures can be drawn for a generic interaction term. The diagram is to be read from bottom to top, with time flowing upwards. The horizontal axis corresponds to the mode numbers, *e.g.* the state $|1,2,2,4\rangle$ would be represented by single lines at $n = 1, 4$ and a double line at $n = 2$. Polynomial vertices can either lower or raise occupation numbers. The diagram in figure G.1 would occur at second order in perturbation theory for a theory with potential $V_3 = \int :\phi^3:$. In the time domain it can be read as

$$\langle 0,1|V_3(\tau_2)|1,1,3\rangle\langle 1,1,3|V_3(\tau_1)|0,1\rangle \tag{G.49}$$

or when computing energies it would contribute an amount

$$\delta\mathcal{E}_{0,1} \supset \bar{\lambda}^2 \frac{|\langle 1,1,3|V_3|0,1\rangle|^2}{E_{0,1} - E_{1,1,3}} = -\frac{72\bar{\lambda}^2}{\Delta + 4} \left| \int_{-\pi/2}^{\pi/2} \frac{dr}{(\cos r)^2} f_0(r) f_1(r) f_3(r) \right|^2 \tag{G.50}$$

to the energy of the state $|0,1\rangle$. The functions $f_n(r)$ are defined in eq. (9.4). Vice versa, by "cutting open" diagrams like figure G.1 horizontally, one easily recovers the intermediate state and its energy.

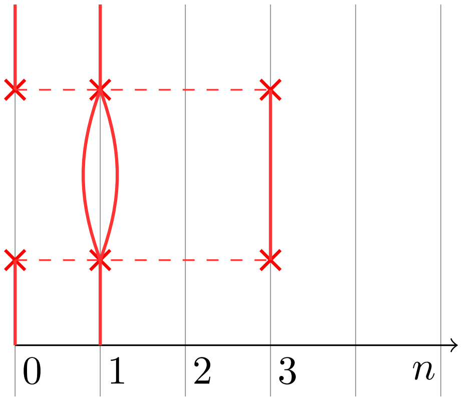

Figure G.1: An example Feynman diagram arising at second order in ϕ^3 perturbation theory. This diagram involves $|0,1\rangle$ resp. $\langle 0,1|$ as in- and out-states and $|1,1,3\rangle$ as an intermediate state.

G.3 Explicit calculations at second order in perturbation theory

This section is a complement to section 8.1. There, after writing the potential V in terms of ladder operators and introducing a truncation cutoff Λ, we expand the energy of the vacuum $|\Omega\rangle$ and of the excited state $|\chi\rangle \equiv a_0^\dagger |\Omega\rangle$ up to second order in $\bar\lambda$ using Rayleigh-Schrödinger perturbation theory:

$$\mathcal{E}_\Omega = e_\Omega + \bar\lambda \langle\Omega|V|\Omega\rangle - \bar\lambda^2 \sum_{i=2\text{ p.s.}} \frac{|\langle\Omega|V|i\rangle|^2}{e_i - e_\Omega} + \mathrm{O}(\bar\lambda^3) \ , \tag{G.51a}$$

$$\mathcal{E}_\chi = e_\chi + \bar\lambda \langle\chi|V|\chi\rangle - \bar\lambda^2 \sum_{\substack{i=1\text{ p.s.},\\ 3\text{ p.s.}}} \frac{|\langle\chi|V|i\rangle|^2}{e_i - e_\chi} + \mathrm{O}(\bar\lambda^3) \ . \tag{G.51b}$$

in which "n p.s." stands for n-particle states and we used the fact that $:\phi^2:$ acting on an n-particle state produces $n-2, n$ and $(n+2)$-particle states. Substituting the operator V in the sums above in terms of A_{mn} using eq. 9.15 and summing the states up to cutoff Λ gives

$$
\begin{aligned}
\mathscr{E}_\Omega(\Lambda) &= -4\bar{\lambda}^2 \sum_{m,n=0}^{m+n+2\Delta\leq\Lambda} \frac{1}{N(m,n)} \frac{A_{mn}^2(\Delta)}{2\Delta+m+n} \ , \\
\mathscr{E}_\chi(\Lambda) &= \Delta + 2\bar{\lambda}A_{00} - 4\bar{\lambda}^2 \sum_{m=1}^{m+\Delta\leq\Lambda} \frac{A_{0m}^2(\Delta)}{m} \\
&\quad - 4\bar{\lambda}^2 \sum_{m,n=0}^{m+n+3\Delta\leq\Lambda} \frac{1}{N(m,n,0)} \frac{(A_{mn}(\Delta)+\delta_{0m}A_{0n}+\delta_{0n}A_{0m})^2}{2\Delta+m+n} \ .
\end{aligned}
$$

where $N(\ell,m,\ldots,n)$ is the norm of the state $a_\ell^\dagger a_m^\dagger \cdots a_n^\dagger \left|\Omega\right\rangle$. In particular,

$$
\begin{aligned}
N(m,n) &= 1+\delta_{m,n} \ , && && \text{(G.53a)}\\
N(m,n,0) &= 1+\delta_{m,n} \ , && m,n\neq 0 \ , && \text{(G.53b)}\\
N(m,0,0) &= 2 \ , && m\neq 0 \ , && \text{(G.53c)}\\
N(0,0,0) &= 6 \ . && && \text{(G.53d)}
\end{aligned}
$$

In the large Λ limit, the two double sums in eq. (G.52) have the same linear asymptotic behaviour. To see this, let us define

$$
\sigma_N(\Delta) := \sum_{m+n=2N} \frac{|\langle\Omega|V_2|m,n\rangle|^2}{2\Delta+m+n} \ . \tag{G.54}
$$

such that

$$
\mathscr{E}_\Omega(\Lambda) \underset{\Lambda\to\infty}{\sim} -\bar{\lambda}^2 \sum_{N=0}^{\frac{1}{2}\Lambda} \sigma_N(\Delta) + \mathrm{O}(\lambda^3) \ . \tag{G.55}
$$

Eq. G.54 is a sum of $\mathrm{O}(N)$ terms that can be expressed in terms of the explicit coefficients $\mathscr{V}_{mn}(\Delta)$ from eq. 9.16 . At large N we can replace this sum by an integral

$$
\lim_{N\to\infty} \sigma_N(\Delta) = \sigma_\infty(\Delta) = \frac{1}{(2\Delta-1)^2} \int_0^1 dx \left(\frac{x}{2-x}\right)^{2\Delta-1} \ , \tag{G.56}
$$

which can be expressed in terms of special functions if desired. We then have

$$
\begin{aligned}
\mathscr{E}_\Omega(\Lambda) &\underset{\Lambda\to\infty}{\sim} -\bar{\lambda}^2\sigma_\infty(\Delta)\Lambda + \mathrm{O}(\lambda^3,\Lambda^0) \ , && \text{(G.57a)}\\
\mathscr{E}_\chi(\Lambda) &\underset{\Lambda\to\infty}{\sim} -\bar{\lambda}^2\sigma_\infty(\Delta)\Lambda + \mathrm{O}(\lambda^3,\Lambda^0) \ . && \text{(G.57b)}
\end{aligned}
$$

As emphasized in section 8, the naive difference $\mathscr{E}_\chi(\Lambda) - \mathscr{E}_\Omega(\Lambda)$ does not reproduce the exact result (8.6). Let us show instead that the prescription (8.1) does the job. We begin by computing

$$\mathcal{E}_\chi(\Lambda) - \mathcal{E}_\Omega(\Lambda - \Delta) = \Delta + 2\bar{\lambda} A_{00} - 4\bar{\lambda}^2 \sum_{m=1}^{m+\Delta \leq \Lambda} \frac{A_{0m}^2(\Delta)}{m} - 4\bar{\lambda}^2 \sum_{m=0}^{m+3\Delta \leq \Lambda} \frac{A_{0m}^2(\Delta)}{m+2\Delta} \,. \tag{G.58}$$

In the limit $\Lambda \to \infty$, the above sums can be written in terms of hypergeometric functions:

$$\sum_{m=1}^{\infty} \frac{A_{0m}^2(\Delta)}{m} = \frac{2}{\Delta(2\Delta-1)^2}\; {}_3F_2\left(\begin{matrix} \frac{1}{2}, 1, 1 \\ \frac{1}{2}+\Delta, 1+\Delta \end{matrix} \middle| \, 1 \right) \,, \tag{G.59}$$

$$\sum_{m=0}^{\infty} \frac{A_{0m}^2(\Delta)}{m+2\Delta} = \frac{2}{\Delta(2\Delta+1)(2\Delta-1)^2}\; {}_3F_2\left(\begin{matrix} \frac{3}{2}, 1, 1 \\ \frac{3}{2}+\Delta, 1+\Delta \end{matrix} \middle| \, 1 \right) \,. \tag{G.60}$$

These formulas furnish a completely explicit expression for the energy shift (G.58) in the limit $\Lambda \to \infty$, which agrees with the expected result (9.18).[7]

Similarly, we have checked that the second-order energy shift of the states $a_n^\dagger \left|\Omega\right\rangle$ for small values of n is correctly reproduced with our prescription. In addition, we also checked that the *third*-order energy shift of the state $\left|\chi\right\rangle$ is correctly reproduced.

Alternatively, we can reproduce the second-order energy shift of the state $\left|\chi\right\rangle$ by computing the two-point connected correlator of $V_2(\tau)$ inside the state $\left|i\right\rangle$. Computing such correlators is an efficient way to extract spectral densities more generally, that is to say for other states or for energy shifts at higher orders in perturbation theory. Let us therefore briefly spell out this computation. The correlator we need to compute is given by

$$g_\chi(\tau) := \langle\chi|V_2(\tau)V_2(0)|\chi\rangle_{\text{conn}} - \langle\Omega|V_2(\tau)V_2(0)|\Omega\rangle_{\text{conn}}. \tag{G.61}$$

We will see that g_χ can be expressed in terms of the special function

$$\mathfrak{g}_\Delta(z) := \sum_{n=0}^{\infty} \mathscr{V}_{0,2n}(\Delta)^2 z^n = {}_3F_2\left[\begin{matrix} \frac{1}{2},\, 1,\, 1 \\ \Delta,\, \Delta+\frac{1}{2} \end{matrix} \middle| \, z \right] . \tag{G.62}$$

To derive this result, we recall that $\left|\chi\right\rangle = a_0^\dagger \left|\Omega\right\rangle$ and use the identities

$$\begin{aligned} [a_k,\, {:}\phi^n(\tau,r){:}] &= n \cdot e^{(\Delta+k)\tau}\, f_k(r)\; {:}\phi^{n-1}(\tau,r){:}\,, \\ [{:}\phi^n(\tau,r){:}, a_k^\dagger] &= n \cdot e^{-(\Delta+k)\tau}\, f_k(r)\; {:}\phi^{n-1}(\tau,r){:} \end{aligned}$$

---

[7] This check requires verifying an identity involving a sum of two hypergeometric ${}_3F_2(1)$ functions. We have checked this identity numerically for many values of Δ, but we do not have an analytical proof for any Δ.

for $k = 0$ and $n = 2$. Now, equation (G.61) can be restated as

$$g_\chi(\tau) = \langle\Omega|[a_0, V_2(\tau)][V_2(0), a_0^\dagger]|\Omega\rangle + \langle\Omega|[V_2(\tau), a_0^\dagger][a_0, V_2(0)]|\Omega\rangle - \langle\chi|V_2|\chi\rangle^2 \tag{G.63}$$

using the fact that $\langle\Omega|V_2|\Omega\rangle$ vanishes. The first term in (G.63) works out to

$$\begin{aligned} 4e^{\Delta\tau}\int [dr][dr']\, f_0(r)f_0(r')G(\tau, r|0, r') &= 4\sum_{n=0}^{\infty} e^{-2n\tau} A_{0,2n}(\Delta)^2 \\ &= \frac{4}{(2\Delta-1)^2}\, \mathfrak{g}_\Delta(e^{-2\tau}) \end{aligned} \tag{G.64}$$

where $G = \langle\phi\phi\rangle$ is the scalar propagator and using the shorthand notation

$$\int [dr] := \int_{-\pi/2}^{\pi/2} \frac{dr}{(\cos r)^2}. \tag{G.65}$$

Here we have used that all *odd* matrix elements $A_{0,2n+1}$ vanish, and that $A_{m,n}$ is proportional to $\mathscr{V}_{m,n}$. The second term in (G.63) works out to

$$4e^{-\Delta\tau}\int [dr][dr']\, f_0(r)f_0(r')G(\tau, r|0, r') = \frac{4}{(2\Delta-1)^2}\, e^{-2\Delta\tau}\, \mathfrak{g}_\Delta(e^{-2\tau}). \tag{G.66}$$

Finally,

$$\langle\chi|V_2|\chi\rangle^2 = \frac{4}{(2\Delta-1)^2} \tag{G.67}$$

and thus

$$g_\chi(\tau) = \frac{4}{(2\Delta-1)^2}\left[(1 + e^{-2\Delta\tau})\, \mathfrak{g}_\Delta(e^{-2\tau}) - 1\right]. \tag{G.68}$$

Indeed we recover (by testing for various values of Δ) that

$$\int_0^\infty d\tau\, g_\chi(\tau) = \frac{4}{(2\Delta-1)^3}. \tag{G.69}$$

H Short time singularities in the correlators of V

In this appendix, we study the singularities of the following class of correlators,

$$\langle i|V_\epsilon(\tau_1+\dots\tau_{n-1})\cdots V_\epsilon(\tau_1+\tau_2)V_\epsilon(\tau_1)V_\epsilon(0)|i\rangle_{\text{conn}}\ , \tag{H.1}$$

when a subset of the τ_i goes to zero. The subscript ϵ denotes the regularized interaction, as defined in eq. (8.13).

In this appendix, it will be convenient to redefine the spatial coordinate as

$$\theta = r+\frac{\pi}{2}\ , \tag{H.2}$$

so that $\theta\in[0,\pi]$. Hence,

$$V_\epsilon(\tau) = R^{\Delta_{\mathcal{V}}}\int_\epsilon^{\pi-\epsilon}\frac{d\theta}{(\sin\theta)^2}\,\mathcal{V}(\tau,\theta). \tag{H.3}$$

Furthermore, we set $R=1$ from now on.

H.1 The vacuum two-point function

Let us begin with the vacuum two-point function of the potential:

$$\langle\Omega|V_\epsilon(\tau)V_\epsilon(0)|\Omega\rangle = \int_\epsilon^{\pi-\epsilon}\frac{d\theta_1 d\theta_2}{\sin^2\theta_1\sin^2\theta_2}\langle\Omega|\mathcal{V}(\tau,\theta_1)\mathcal{V}(0,\theta_2)|\Omega\rangle\ . \tag{H.4}$$

The matrix elements in eq. (H.4) are computed by a Euclidean correlator as long as $\tau>0$, which we assume throughout this section. Notice that, since the vacuum expectation value of V_ϵ vanishes by definition, the full correlator coincides with its connected part. It will be convenient to keep in mind that the two-point function of $\mathcal{V}$ depends on the position of the insertions only through their geodesic distance, or equivalently through the cross ratio ξ defined in eq. (7.8), which in the notation of this section reads

$$\xi = \frac{\cosh\tau - \cos(\theta_1 - \theta_2)}{2\sin\theta_1 \sin\theta_2} \ . \tag{H.5}$$

Hence, we also denote

$$\langle\Omega|\mathcal{V}(\tau,\theta_1)\mathcal{V}(0,\theta_2)|\Omega\rangle = f_\Omega(\xi) \ . \tag{H.6}$$

As discussed in section 8.3, the large energy limit of the Laplace transform of this correlator controls the cutoff dependence of the vacuum energy at second order in perturbation theory.

We start by discussing the $\epsilon = 0$ case. There are two possible sources of non-analyticities as $\tau \to 0$. First, the two-point function of the perturbing operator $\mathcal{V}$ has a short distance singularity fixed by the OPE at the UV fixed point:[1]

$$f_\Omega(\xi) \sim (4\xi)^{-\Delta_\mathcal{V}} \ , \qquad \xi \to 0 \ . \tag{H.7}$$

In order to isolate the contribution of this short distance limit to eq. (H.4), we approximate f_Ω as in eq. (H.7) and we rescale the difference $(\theta_1 - \theta_2) \to \tau(\theta_1 - \theta_2)$, keeping $\theta_1 + \theta_2$ fixed. After sending $\tau \to 0$ and integrating, we obtain

$$\langle\Omega|V(\tau)V(0)|\Omega\rangle \sim \frac{\pi\,\Gamma\left(\Delta_\mathcal{V} - \frac{3}{2}\right)\Gamma\left(\Delta_\mathcal{V} - \frac{1}{2}\right)}{\Gamma(\Delta_\mathcal{V})\Gamma(\Delta_\mathcal{V} - 1)}\,\tau^{-2\Delta_\mathcal{V}+1} + \dots \qquad \tau \to 0 \ . \tag{H.8}$$

It is interesting to notice that the exponent is a property of the short distance physics, and accordingly the integral over $(\theta_1 - \theta_2)$ reduces to an integral over a flat space two-point function. It converges as long as $\Delta_\mathcal{V} > 1/2$, otherwise an IR divergence makes the approximation (H.7) inadequate. On the other hand, the integral over $(\theta_1 + \theta_2)$ is sensitive to the AdS geometry, and requires the stronger condition $\Delta_\mathcal{V} > 3/2$. As we shall see momentarily, precisely when this condition is not satisfied the leading small τ singularity is *not* given by eq. (H.8).

Indeed, a second source of non-analyticity arises from the region where both insertions of $\mathcal{V}$ reach the same point on the boundary. In this case, the important contribution comes from the region where $\theta_1 \sim \theta_2 \sim \tau$, and from its image under parity $(\pi-\theta_1) \sim (\pi-\theta_2) \sim \tau$. It is simple to guess that this is the case by considering the cross ratio ξ in eq. (H.5). When θ_i and τ all vanish at the same rate, ξ attains a finite limit. After performing the change of variables $\theta_i = z_i\tau$ in eq. (H.4) – still at $\epsilon = 0$ – and multiplying by 2 to keep into account the contribution from the other AdS boundary, the leading contribution as $\tau \to 0$ is

$$\langle\Omega|V(\tau)V(0)|\Omega\rangle \sim \frac{2}{\tau^2}\int_0^\infty \frac{dz_1 dz_2}{z_1^2 z_2^2} f_\Omega\left(\frac{1 - z_{12}^2}{4z_1z_2}\right) + \dots \tag{H.9}$$

---

[1] Logarithms arise when the UV fixed point is a free theory, like in chapter 9. Also, notice that the subtraction of the vacuum expectation value of $\mathcal{V}$ has no effect on the leading singularity.

Let us briefly discuss the convergence of this integral. As at least one of the z_i's goes to zero, the boundary OPE can be used to factorize the double integral into a product. We conclude that the integral converges at small z_i if the boundary OPE of $\mathcal{V}$ does not contain operators with scaling dimension $\Delta \leq 1$. This is precisely the condition (7.17) which ensures finiteness of the matrix elements of V, and is therefore satisfied by assumption. At the other end of the integration region the integrand is suppressed, unless z_{12} stays finite. In the latter case, f_Ω is dominated by the bulk OPE limit as in eq. (H.7). Hence, the integral in (H.9) converges as long as $\Delta_{\mathcal{V}} < 3/2$. In the opposite case, the leading small τ singularity comes instead from the bulk OPE limit considered above, see eq. (H.8).

Notice that, contrary to eq. (H.8), the theory dependence of the singularity in eq. (H.9) is through the full two-point function f_Ω. Although we could still perform one of the two integrals to simplify the coefficient, we shall later obtain precisely this result as a by-product of a more general analysis – see eqs. (H.10,H.17).

Although the previous analysis is sufficient to isolate the leading small τ singularities, for completeness we now develop a more systematic formalism, which yields the matrix element in eq. (H.4), with $\epsilon = 0$, as a single integral over the correlator (H.6). Since f_Ω only depends on the coordinates through the cross ratio ξ, it is convenient to separate the kinematical from the theory dependent data as follows:

$$\langle \Omega | V(\tau) V(0) | \Omega \rangle = \int_{\xi_{\min}(\tau)}^{\infty} d\xi \, K(\xi|\tau) f_\Omega(\xi) \ , \qquad \xi_{\min}(\tau) = \tfrac{1}{2}(\cosh\tau - 1) \ . \tag{H.10}$$

The kernel K is defined as

$$K(\xi|\tau) := \int_0^\pi \frac{d\theta_1 \, d\theta_2}{\sin^2\theta_1 \sin^2\theta_2} \, \delta(\xi(\tau,\theta_1,\theta_2) - \xi), \qquad \xi(\tau,\theta_1,\theta_2) = \frac{\cosh\tau - \cos(\theta_1 - \theta_2)}{2\sin\theta_1 \sin\theta_2} \ . \tag{H.11}$$

The kernel (H.11) can be expressed in terms of an elliptic integral for generic $\tau > 0$. We will first integrate in θ_2. In Poincaré coordinates, the curve of constant geodesic distance from a point $x_1 = (z, \bar{z})$, $z = \exp(\tau + \mathrm{i}\theta)$, is a circle:

$$\xi = \frac{(z - z')(\bar{z} - \bar{z}')}{4 \operatorname{Im} z \operatorname{Im} z'} \ , \qquad \Longleftrightarrow \qquad (\Re z' - \Re z)^2 + (\operatorname{Im} z' - c)^2 = r^2,$$
$$c = \operatorname{Im} z (1 + 2\xi) \ , \quad r = 2 \operatorname{Im} z \sqrt{\xi(\xi+1)} \ . \tag{H.12}$$

Therefore, the δ-function in eq. (H.11) has support at most in two points, at fixed θ_1, see fig. H.1. We can then evaluate the integral in $d\theta_2$ by changing variables, being careful about the sign of the Jacobian $\partial\xi(\tau,\theta_1,\theta_2)/\partial\theta_2$. Referring again to fig. H.1, the geodesic distance of the marked point at angle θ_2 from the point at angle θ_1 is decreasing while the former enters the solid circle, and increasing while it exits it. This fixes the sign of

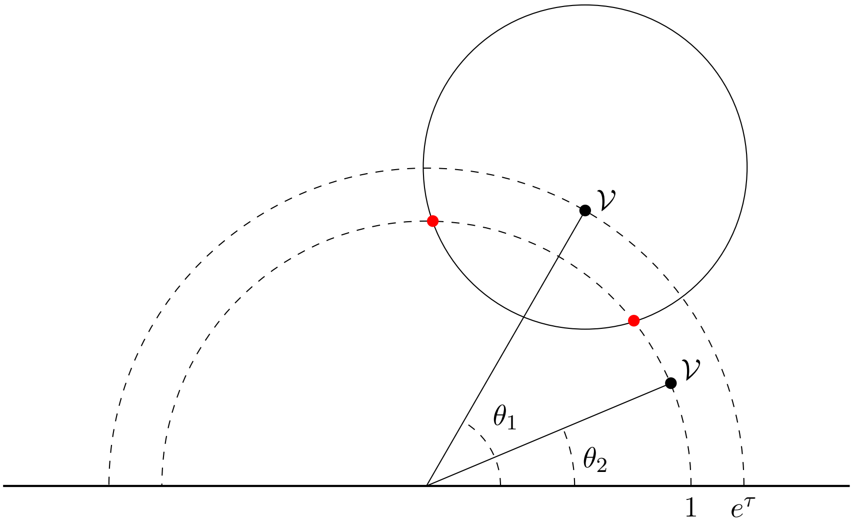

Figure H.1: The dashed semi-circles are constant global time surfaces. The solid circle is a surface of fixed geodesic distance from the $\mathcal{V}$ insertion at angle θ_1. The $\mathcal{V}$ insertion at angle θ_2 is generic. The δ function in eq. (H.11) has support at the location of the two red points.

the Jacobian. We obtain the following expression for the kernel:

$$K(\xi|\tau) = \frac{4(1+2\xi)\cosh\tau}{\sqrt{\xi(\xi+1)}} \int_{\theta_{\min}(\tau)}^{\pi/2} d\theta_1 \frac{1}{\left(\sin^2\theta_1 + 4\xi(1+\xi)\sin^2\theta_{\min}(\tau)\right)\sqrt{\sin^2\theta_1 - \sin^2\theta_{\min}(\tau)}}\ , \tag{H.13}$$

where

$$\theta_{\min}(\tau) = \arcsin\frac{\sinh\tau}{2\sqrt{\xi(1+\xi)}}\ , \tag{H.14}$$

We used the reflection symmetry $\theta \to \pi - \theta$ to restrict the integration region to $\theta_1 < \pi/2$. At the minimal angle $\theta_{\min}$ the solid circle of fig. H.1 becomes tangent to the semi-circle of radius 1. As promised, eq. (H.13) expresses the kernel in terms of the incomplete elliptic integral of the third kind:

$$K(\xi|\tau) = \frac{4(1+2\xi)}{\sqrt{\xi(\xi+1)}\cosh\tau}\frac{1}{\sqrt{1-\sin^2\theta_{\min}(\tau)}}\,\Pi\left(\frac{1}{\cosh^2\tau}, \frac{\pi}{2} - \theta_{\min}(\tau), \frac{1}{1-\sin^2\theta_{\min}(\tau)}\right)\ . \tag{H.15}$$

The full matrix element at fixed τ may now be obtained by integrating the kernel as in eq. (H.10). Alternatively, one can recover the small τ limits in eqs. (H.8,H.9) as limits of the kernel itself.

In particular, the bulk channel singularity is obtained by rescaling $\xi \to \tau^2\xi$. In the $\tau \to 0$

limit, this reduces the kernel to a complete elliptic integral of the second kind:

$$K(\tau^2\xi|\tau) \sim \frac{16}{\tau}\sqrt{\xi}\, E\left(1-\frac{1}{4\xi}\right) , \qquad \tau \to 0. \tag{H.16}$$

This approximation to the kernel can then be used in eq. (H.10) together with eq. (H.7), to recover eq. (H.8).

The kernel $K(\xi|\tau)$ is more useful in deriving the coefficient of the boundary channel small τ singularity, eq. (H.9). Indeed, in this case the cross ratio is held fixed, and the rescaling $\theta \to \tau\,\theta$ in the integral form (H.13) yields a simple algebraic result:

$$K(\xi|\tau) \sim \frac{8}{\tau^2}\,\mathrm{arcsinh}\left(2\sqrt{\xi(\xi+1)}\right) , \qquad \tau \to 0 \ . \tag{H.17}$$

Replacing eq. (H.17) in eq. (H.10), we obtain the coefficient of the small τ singularity in eq. (H.9) as a single integral over the cross ratio, as promised.

To conclude this section, let us describe how the introduction of a non vanishing ϵ cutoff changes the kernel (H.11). Referring to fig. H.1, now the integration region of the potential only extends on the wedge defined by $\theta \in [\epsilon, \pi-\epsilon]$. Depending on the values of ξ, τ and ϵ, one of three cases happens: none, one or both of the intersections marked in red lie inside this wedge. Hence, the kernel is a piecewise continuous function. We shall focus on the limit ϵ, $\tau \to 0$, while keeping ϵ/τ fixed. It is useful to define the following constants:

$$\alpha = \frac{\tau^2}{\epsilon^2} \ , \qquad \alpha_* = 4\xi(\xi+1) \ , \qquad \xi_* = \frac{1}{2}\left(\sqrt{\alpha+1}-1\right) \ . \tag{H.18}$$

If we perform the change of variable $\theta \to \epsilon\theta$, it is not difficult to find the following result:

$$K(\xi|\tau,\epsilon) \sim \frac{1}{\tau^2}\begin{cases} 8\,\mathrm{arcsinh}\sqrt{\alpha_*} \ , \quad \xi < \xi_* \ , \\ -4\log\left[\frac{\sqrt{\alpha_*+1}-\sqrt{\alpha_*}}{\sqrt{\alpha_*+1}+\sqrt{\alpha_*}}\left(\frac{\sqrt{\alpha_*+1}+\sqrt{\alpha_*-\alpha}}{\sqrt{\alpha_*+1}-\sqrt{\alpha_*-\alpha}}\right)^2\right] \ , \quad \xi_* < \xi < \alpha/4 \ , \\ -2\log\left[(\alpha+1)\left(\frac{(\sqrt{\alpha_*+1}-\sqrt{\alpha_*})(\sqrt{\alpha_*+1}+\sqrt{\alpha_*-\alpha})}{\sqrt{\alpha_*+1}+\sqrt{\alpha_*}}\right)^2\frac{\sqrt{\alpha_*+1}+\sqrt{\alpha_*-\alpha}}{\sqrt{\alpha_*+1}-\sqrt{\alpha_*-\alpha}}\right] \ , \quad \xi > \alpha/4 \ . \end{cases} \tag{H.19}$$

We plot this function in fig H.2. As expected, the contribution to the two-point function (H.4) of points whose cross ratio is larger than the value ξ_* is suppressed.

H.2 The two-point function in a generic state

The aim of this section is to prove eq. (8.33). As discussed in section 8.4, this result is instrumental in deriving a bound on the UV behavior of the spectral density $\boldsymbol{\Delta}\rho^{\epsilon}_{i,2}(\alpha)$. The object of interest is the following difference of correlation functions:

$$g_\epsilon(\tau) = \langle i|V_\epsilon(\tau)V_\epsilon(0)|i\rangle_{\mathrm{conn}} - \langle\Omega|V_\epsilon(\tau)V_\epsilon(0)|\Omega\rangle_{\mathrm{conn}} \ . \tag{H.20}$$

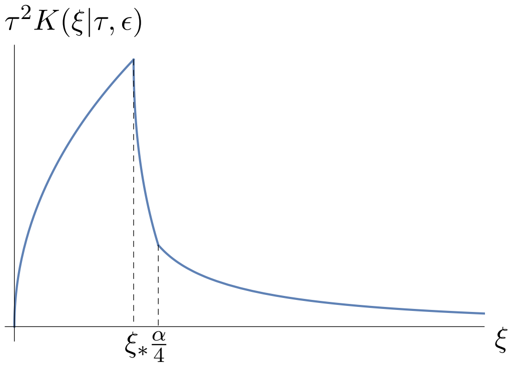

Figure H.2: Plot of eq. (H.19) for a choice of α.

The operators in the expectation values are ordered as written. Hence, only for $\tau > 0$ is $g_\epsilon(\tau)$ computed by a Euclidean correlator. The left hand side of eq. (H.20) is defined by analytic continuation everywhere else. We shall make the simplifying assumption that the leading non-analytic behavior in $g_\epsilon(\tau)$ as $\tau \to 0$ can be detected by approaching the limit from real and positive τ. This is true in particular if $\tau = 0$ is not an essential singularity.[2]

As discussed in the previous section, there are two sources of non analyticities at small τ: the bulk $\mathcal{V} \times \mathcal{V}$ OPE, and the simultaneous fusion of the same operators with the boundary of AdS. Let us first focus on the latter, more complicated scenario. Clearly, as long as ϵ is finite, this singularity cannot arise. In other words, assuming for a moment that the bulk OPE is sufficiently soft, $g_\epsilon(\tau)$ is bounded by a constant as $\tau \to 0$. However, the bound is lost as we also take $\epsilon \to 0$. What we need is a different bound, which persist as the spatial cutoff is removed.

Let us begin by recalling that the connected two-point function with respect to any state $|i\rangle$ can be written as

$$\langle i|\mathcal{V}(\tau,\theta_1)\mathcal{V}(0,\theta_2)|i\rangle_{\text{conn}} = \langle i|\mathcal{V}(\tau,\theta_1)\mathcal{V}(0,\theta_2)|i\rangle - \langle i|\mathcal{V}(\tau,\theta_1)|i\rangle\langle i|\mathcal{V}(0,\theta_2)|i\rangle \ . \tag{H.21}$$

Although the connected correlator is invariant under a shift of $\mathcal{V}$ by any c-number, recall that our definition of $\mathcal{V}$ includes the subtraction of the cosmological constant, when needed to make the matrix elements of the potential well defined. In this way, the second addend on the right hand side of eq. (H.21) is τ independent and, upon integration, gives a finite contribution to g_ϵ also in the $\epsilon \to 0$ limit. Since we are interested in the non-analytic part, we shall drop it from now on. Hence, we replace eq. (H.20) by the following:

$$G_\epsilon(\tau) = \int_\epsilon^{\pi-\epsilon} \frac{d\theta_1 d\theta_2}{\sin^2\theta_1 \sin^2\theta_2} f(\tau,\theta_1,\theta_2) \ , \\ f(\tau,\theta_1,\theta_2) = \langle i|\mathcal{V}(\tau,\theta_1)\mathcal{V}(0,\theta_2)|i\rangle - \langle \Omega|\mathcal{V}(\tau,\theta_1)\mathcal{V}(0,\theta_2)|\Omega\rangle \ . \tag{H.22}$$

---

[2] For instance, logarithmic singularities are allowed as well.

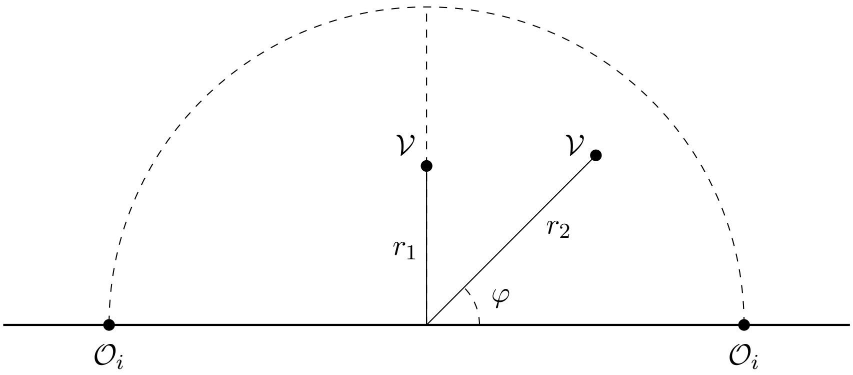

Figure H.3: The configuration which defines the ρ-coordinates. The largest dashed semicircle has unit radius. Notice that an isometry can be used to place one of the bulk operators perpendicularly above the middle point between the boundary operators, without displacing the latter. Furthermore, using an inversion one can set $r_1 < 1$.

We immediately obtain an ϵ-independent bound as follows:

$$|G_\epsilon(\tau)| \leq \int_0^\pi \frac{d\theta_1 d\theta_2}{\sin^2\theta_1 \sin^2\theta_2} |f(\tau,\theta_1,\theta_2)| \ . \tag{H.23}$$

Our aim will be now to bound the right hand side as $\tau \to 0$. Let us make some simplifying assumptions, which will be reconsidered at the end:

1 the state $|i\rangle$ is created by a primary operator $\mathcal{O}_i$,

2 the boundary spectrum contains at least one operator with $\Delta \leq 2$, and the three-point function $\langle O_\Delta \mathcal{V}\mathcal{V}\rangle$ is non zero,

3 the bulk OPE $\mathcal{V} \times \mathcal{V}$ does not contain operators of dimension smaller than $2\Delta_{\mathcal{V}}$, apart from the identity.

Since we are interested in the limit where both $\mathcal{V}$'s go to the boundary simultaneously, it is convenient to introduce the ρ-coordinates depicted in fig. H.3. These are related to the (τ,θ) coordinates as follows:

$$r_1 = \tan\frac{\theta_1}{2} \ , \quad r_2 = \left(\frac{1+e^{2\tau}-2e^{\tau}\cos\theta_2}{1+e^{2\tau}+2e^{\tau}\cos\theta_2}\right)^{1/2} \ , \quad \cos\varphi = \frac{1-e^{-2\tau}}{\sqrt{1+e^{-4\tau}-2e^{-2\tau}\cos 2\theta_2}} \ . \tag{H.24}$$

Notice that the inversion symmetry $(r_1, r_2, \cos\varphi) \to (1/r_1, 1/r_2, \cos\varphi)$ is mapped to the symmetry $(\theta_1,\theta_2) \to (\pi-\theta_1, \pi-\theta_2)$. We used it to restrict θ_1 to lie in the interval $[0,\pi/2]$, and correspondingly $r_1 \in [0,1]$. On the other hand, the symmetry under swapping

$x_1 \leftrightarrow x_2$ is not explicit in eq. (H.24). The inverse map is

$$\theta_1 = 2\arctan r_1 \ , \quad \cos\theta_2 = \frac{1-r_2^2}{\sqrt{1+(2-4\cos^2\varphi)r_2^2+r_2^4}} \ , \quad \tau = -\frac{1}{2}\log\frac{1-2r_2\cos\varphi+r_2^2}{1+2r_2\cos\varphi+r_2^2} \ . \tag{H.25}$$

Although the integration domain in eq. (H.23) covers a region where $r_2 > 1$, the singularity at small τ arise from the limits θ_1, $\theta_2 \to 0$ or π. Up to the inversion symmetry, both of the limits are mapped to r_1, $r_2 \to 0$. Hence, we can focus on the region where r_1, $r_2 < r_0 < 1$. It is convenient to trade (θ_1, θ_2) for r_1 and r_2 in the integral (H.23), while keeping the τ dependence explicit. Therefore, we use

$$\theta_1 = 2\arctan r_1 \ , \quad \theta_2 = \arccos\left(\frac{1-r_2^2}{1+r_2^2}\cosh\tau\right) \ , \quad \cos\varphi = \frac{1+r_2^2}{2r_2}\tanh\tau \ , \tag{H.26}$$

to obtain

$$|G_\epsilon(\tau)| \leq \frac{\cosh\tau}{2\cosh^6\frac{\tau}{2}}\int_0^{r_0} dr_1 \int_{\tanh(\tau/2)}^{r_0} dr_2 \, \frac{1+r_1^2}{r_1^2}\, \frac{r_2(1+r_2^2)|f(r_1,r_2,\varphi(r_2,\tau))|}{\left[\left(r_2^2-\tanh^2\frac{\tau}{2}\right)\left(1-r_2^2\tanh^2\frac{\tau}{2}\right)\right]^{3/2}} + \text{terms finite at } \tau = 0 \ , \tag{H.27}$$

In eq. (H.27), we slightly abused notation in the argument of f. Notice also that we inserted a factor 2 accounting for the inversion symmetry. We can further simplify the integrand by bounding with constants all the parts which are regular, at $\tau = 0$, throughout the region of integration. We thus obtain

$$|G_\epsilon(\tau)| \leq A(r_0,\tau)G(t) \ , \quad t = \tanh\frac{\tau}{2} \ , \tag{H.28}$$

$$G(t) = \int_0^{r_0} dr_1 \int_t^{r_0} dr_2 \, \frac{r_2}{r_1^2\left(r_2^2-t^2\right)^{3/2}}|f(r_1,r_2,\varphi(r_2,t))| \ , \qquad \cos\varphi = \frac{(1+r_2^2)t}{(1+t^2)r_2} \ . \tag{H.29}$$

The function A in eq. (H.28) has a finite value at $\tau = 0$, and since $G(t)$ turns out to diverge at small t, A can be chosen large enough to also account for the dropped finite terms in eq. (H.27).

Let us discuss the dangerous limits in the region of integration of eq. (H.29). Due to assumption 3 and the subtraction of the vacuum correlator in eq. (H.22), the bulk OPE is non singular, hence the limit $r_1 \to r_2$ as $t \to 0$ will not be discussed. The singularities at the lower end of the integration range for r_1 and r_2 are associated to the infinite volume of AdS. At finite t, the condition (7.17) guarantees the integrability of the function in the region where either r_1 or $(r_2 - t)$ are small: notice in particular that both limits are boundary OPE limits, since $\varphi = 0$ when $r_2 = t$. On the other hand, the singularity of the integrand is enhanced at $t = 0$, and the boundary OPE of each of the $\mathcal{V}$'s does not fix the behavior of f when $r_1 \sim r_2 \to 0$. The usefulness of the ρ-coordinates is precisely that they allow to write a power expansion for the correlator centered around r_1, $r_2 = 0$ with a finite radius of convergence. Indeed, the quantization on the unit half-circle dashed in fig. H.3 yields an expansion in term of boundary operators. Dubbing $r_M = \max(r_1, r_2)$, $r_m = \min(r_1, r_2)$, we find[3]

$$f(r_1, r_2, \varphi) = \sum_{\Delta>0} r_M^{\Delta} \, \langle\Omega|\mathcal{O}_i(-1)\mathcal{O}_i(1)|\Delta\rangle\langle\Delta|\mathcal{V}(1, \varphi_M)\mathcal{V}(r_m/r_M, \varphi_m)|\Omega\rangle \ , \tag{H.30}$$

where

$$(\varphi_M, \varphi_m) \leftrightarrow \left(\varphi, \frac{\pi}{2}\right) \ . \tag{H.31}$$

Again, we are abusing notation with respect to, *e.g.*, eq. (H.22): the arguments of $\mathcal{V}$ are (r, φ) from now on. The assignment of (φ_M, φ_m) depends on r_M. Here, the states $|\Delta\rangle$ form a complete set of eigenstates of the unperturbed Hamiltonian, but notice that the identity is excluded from the sum, due to the subtraction of the vacuum correlator in eq. (H.22). This subtraction differentiates the energy gaps from the eigenvalues of the Hamiltonian themselves, and is ultimately what makes the former finite.

We first focus on the finitely many terms in eq. (H.31) with $\Delta \leq 2$, which are present by the assumption 2 above. To this end, we separate them using the triangular inequality:

$$|f(r_1, r_2, \varphi)| = \left|\sum_{\Delta\leq 2} c_{i,\Delta}\text{block}_\Delta + f_R(r_1, r_2, \varphi)\right| \leq \sum_{\Delta\leq 2} |c_{i,\Delta}\text{block}_\Delta| + |f_R(r_1, r_2, \varphi)| \ , \tag{H.32}$$

with

$$c_{i,\Delta} = \langle\Omega|O_i(-1)O_i(1)|\Delta\rangle \ ,$$

where block_Δ is a shorthand notation for each addend in eq. (H.31) and f_R is defined by the equation itself. We dub G_Δ the contribution of each block with $\Delta \leq 2$ to eq. (H.29). It is convenient to extract the singularity as $r_1 \sim r_2 \sim t \to 0$ via the change of variables $r_i = z_i t$, which yields

$$G_\Delta(t) = t^{\Delta-2} \int_0^{\frac{r_0}{t}} dz_1 \int_1^{\frac{r_0}{t}} dz_2 \frac{z_2}{z_1^2\left(z_2^2 - 1\right)^{3/2}} z_M^{\Delta} \langle\Delta|\mathcal{V}(1, \varphi_M)\mathcal{V}(z_m/z_M, \varphi_m)|\Omega\rangle \ ,$$
$$(\varphi_M, \varphi_m) \leftrightarrow \left(\arccos\left(\frac{1 + (z_2 t)^2}{z_2(1 + t^2)}\right), \frac{\pi}{2}\right) \ . \tag{H.33}$$

Let us now discuss the behavior of the double integral as $t \to 0$. In this limit, when $1 < z_2 < r_0/t$, $\cos\varphi \to 1/z_2$ uniformly. Hence, the only t dependence is left in the upper limits of integration. But firstly, there are the infinite volume singularities of the measure, at $z_1 = 0$ and $z_2 = 1$. Close to this point, $z_M = z_2 \sim 1$ and we can study the following simpler integral:

---

[3] The operators $\mathcal{O}_i$ are normalized so that $\langle\Omega|\mathcal{O}_i(-1)\mathcal{O}_i(1)|\Omega\rangle = 1$.

$$\int_0 \frac{dz_1}{z_1^2}\int_1 \frac{dz_2}{(z_2^2-1)^{3/2}}|\langle\Delta|\mathcal{V}(1,\varphi(z_2))\mathcal{V}(z_1,\pi/2)|\Omega\rangle|\ , \qquad \sin\varphi(z_2)\sim\sqrt{2}(z_2-1)^{1/2}\ . \tag{H.34}$$

The z_1, $(z_2-1)\to 0$ limits are controlled by the boundary OPEs of the two insertions respectively. Hence, the integrals factorize and we get

$$\int_0 \frac{dz_1}{z_1^2}z_1^{\Delta_0}\int_1 \frac{dz_2}{(z_2^2-1)^{3/2}}(z_2-1)^{\Delta_0/2}\ . \tag{H.35}$$

Here, Δ_0 is the lightest operator in the boundary OPE of $\mathcal{V}$. As advertised, well-definiteness of the matrix elements of the potential $V(\tau)$ – *i.e.* eq. (7.17) – requires $\Delta_0>1$. Therefore the integrals converge in this region. We also need to show convergence in the region $z_i\sim r_0/t\to\infty$. Here, we can use a different approximation to the full integral. Defining $z_1=\nu\cos\omega$ and $z_2=\nu\sin\omega$, the relevant integral is

$$\int^{\frac{1}{t}} d\nu\nu^{\Delta-3}\int_0^{\frac{\pi}{2}} d\omega\frac{1}{\sin^2\omega\cos^2\omega}\max(\sin\omega,\cos\omega)^{\Delta} \\ \times|\langle\Delta|\mathcal{V}\left(1,\frac{\pi}{2}\right)\mathcal{V}\left(\min(\tan\omega,\cot\omega),\frac{\pi}{2}\right)|\Omega\rangle|\ . \tag{H.36}$$

The limits $\omega\to 0,\pi/2$ are identical and are again OPE limits for the correlator. For instance, at small ω the integrand behaves as ω^{Δ_0-2}, and so it converges. The integral over ν converges as $t\to 0$ if $\Delta<2$. On the contrary, if $\Delta=2$ this region gives the dominating logarithmic contribution to the bound of the correlator at small τ.[4]

We now need to go back and estimate the contribution to $G(t)$ of all the states with $\Delta>2$ in the decomposition (H.31). Using eq. (H.32), this amounts in replacing $f\to f_R$ in eq. (H.29). In this case, we can simply set $t=0$ in the right hand side of the equation,[5] and study the following integral:

$$\int_0^{r_0}\frac{dr_1dr_2}{r_1^2r_2^2}\,|f_R(r_1,r_2,\pi/2)|\ . \tag{H.37}$$

Now, f_R is a finite linear combination of two-point functions of $\mathcal{V}$ in the presence of various boundary operators, and as such, it has the same OPE bounds already discussed as $r_1\to 0$ at fixed r_2 or vice versa. Hence, the integral converges there. On the other hand, when $r_1 \sim r_2 \sim \nu \to 0$, the subtractions make the behavior of the integrand softer: $f_R \sim \nu^\Delta$ with $\Delta > 2$. To show rigorously that this suffices for the integral to converge, let us go to polar coordinates in the (r_1, r_2) plane:

---

[4] We would like to remark that this bound does not need to be saturated: there is no fundamental reason why the correlator on the right hand side of eq. (H.36) cannot vanish in this specific configuration. This happens for instance in the Ising model with a thermal deformation – see section 10.4 – as it is easy to check directly. While this implies the absence of a $\log\tau$ for any external state at second order in perturbation theory, the connected correlator (H.20) can be computed exactly at $\epsilon=0$ at least for $|i\rangle=L_{-2}\,|\Omega\rangle$: $g_0(\tau)=8\pi^2\cosh 2\tau$ in this case. Not only there is no $\log\tau$, g_0 is in fact analytic at $\tau=0$. The corresponding spectral density has a finite number of states, whose contribution to the energy gap cancels exactly, as expected for the theory of a free fermion.

[5] One might object that $\cos\varphi(r_2,t)$ has a non uniform limit as $t\to 0$. However, f_R depends on φ only through the positions $(r_2\cos\varphi,r_2\sin\varphi)$, which approaches $(0,r_2)$ uniformly.

$$\int_0^{r_0} \frac{d\nu}{\nu^3} \int_0^{\frac{\pi}{2}} d\omega \frac{1}{\cos^2\omega \sin^2\omega} |f_R(\nu,\omega)| \ . \tag{H.38}$$

At any fixed value of ν, the angular integral converges. Since f_R can be expressed as an absolutely convergent series there, using eq. (H.31), the series can be integrated term by term, and we obtain

$$\int_0^{r_0} \frac{d\nu}{\nu^3} \sum_{\Delta>3} \kappa_\Delta \nu^\Delta \ . \tag{H.39}$$

While the κ_Δ are theory dependent, the previous equation shows that the small ν behavior of the integrand is not enhanced by the integration over ω. This is sufficient to show that the integral converges. This concludes the proof that eq. (H.33) provides the leading singularity as $\tau \to 0$. As we stated at the beginning of the section, we work under the assumption that the strength of the singularity is independent of the phase of τ. Hence, although our manipulations are only valid for $\tau > 0$, we extend the conclusion to a neighborhood of the origin:

$$|G_\epsilon(\tau)| < C(\tau_0) \begin{cases} |\tau|^{\Delta_*-2} \ , & \Delta_* < 2 \\ \log|\tau| \ , & \Delta_* = 2 \ , \end{cases} \qquad |\tau| < \tau_0 \ . \tag{H.40}$$

Here, Δ_* is the lowest dimensional operator in the OPE (H.31).

We would like now to comment on the assumptions 1 - 3 above, in reversed order. If the bulk OPE contains singularities above the identity, they can be added to the analysis. In this thesis, the bulk OPE is relevant only for the ϕ^4 deformation of a massive theory considered in section 9.2, so we analyze this case separately in section 9.2. Here, we limit ourselves to the simple scenario where the unperturbed Hamiltonian is a CFT, and furthermore we assume the gap in the boundary spectrum is large enough to avoid any enhancement of the bulk OPE singularity by boundary effects. As we will see in a moment, a sufficient condition for this to happen is that the lowest boundary operator has dimension $\Delta > 3$. The limit where the two operators collide is controlled by the OPE in the UV theory, schematically:

$$\mathcal{V} \times \mathcal{V} = 1 + \tilde{\mathcal{V}} \ . \tag{H.41}$$

The contribution of the identity cancels in the difference in eq. (H.22), so we concentrate on the first non-trivial operator. Its contribution to eq. (H.23) can be computed by rescaling $(\theta_1 - \theta_2) \to \tau(\theta_1 - \theta_2)$, as we did in section H.1. In the small τ limit, we obtain

$$G_\epsilon(\tau) \sim \tau^{1+\Delta_{\tilde{\mathcal{V}}}-2\Delta_{\mathcal{V}}} \int_\epsilon^{\pi-\epsilon} \frac{d\theta}{\sin^4\theta} \langle i|\tilde{\mathcal{V}}(0,\theta)|i\rangle \int_{-\infty}^{\infty} d\theta_-(1+\theta_-^2)^{\Delta_{\tilde{\mathcal{V}}}/2-\Delta_{\mathcal{V}}} \ . \tag{H.42}$$

The integral over $\theta_- = (\theta_1 - \theta_2)/\tau$ is dominated by the UV and is the same as in flat space. The integral over $\theta = (\theta_1 + \theta_2)/2$ is sensitive to the AdS geometry. The former converges only when $\Delta_{\tilde{\mathcal{V}}}/2 - \Delta_{\mathcal{V}}$ is large enough. However, this IR feature is spurious: one can for instance take derivatives of $G_\epsilon(\tau)$, improving convergence without modifying the non analytic parts of the result. On the other hand, the integral over θ converges when the leading boundary operator coupling to $\tilde{\mathcal{V}}$ has dimension $\Delta > 3$. If this is not the case, the crude approximations in eqs. (H.41,H.42) are inadequate: both bulk and boundary effects must be taken into account to compute the small τ singularity. We shall not treat this more general case here.

The remaining assumptions are easier to relax. The role of assumption 2 is to make the $\tau \to 0$ limit singular, so that any finite contribution to $G_\epsilon(\tau)$ can be disregarded. When this is not the case, one may consider derivatives of $G_\epsilon(\tau)$ instead. Clearly, the leading non analytic behavior can be made singular in this way. What needs to be proven, is that said non analytic behavior can also be traced to the region covered by eq. (H.33), and so still leads to an equation analogous to (H.40). Technically, this should come about because of the dependence of r_2 from τ in eq. (H.24), which turns derivatives wrt τ into derivatives wrt r_M in eq. (H.31), in the region where $r_M = r_2$. We have not done this analysis in detail, but these considerations prompt us to claim that eq. (H.40) can be extended to $\Delta_* > 2$, simply by taking enough derivatives of both sides so that the right hand side becomes singular. This is confirmed, for instance, in the case of the ϕ^2 deformation in section 9.1.

Finally, the purpose of assumption 1 is to make the transformation properties of the matrix elements involved under AdS isometries simple. This is used in eq. (H.31) to write $f(r_1, r_2, \varphi)$ in terms of the scaling operator O_i evaluated at special positions. Had the state $|i\rangle$ been created by a descendant in the origin, a more complicated linear combination of descendants would have appeared in eq. (H.31). However, this only contributes a numerical prefactor to the final result, and does not affect the τ dependence. Hence, the result (H.40) immediately extends to generic states in the Hilbert space. This concludes our analysis.

H.3 Free scalar example

In this example, we consider the potential

$$V(\tau) = \int_{-\pi/2}^{\pi/2} \frac{dr}{\cos^2 r} :\phi^2(\tau, r): \,. \tag{H.43}$$

Let us concentrate to the the second-order contribution to the energy of the state $|\chi\rangle = a_0^\dagger\,|\text{vac}\rangle$. The relevant object is

$$g_\chi(\tau) = \langle \chi | V(\tau) V(0) | \chi \rangle_{\text{conn}} - \langle \Omega | V(\tau) V(0) | \Omega \rangle_{\text{conn}} \,. \tag{H.44}$$

This difference was computed exactly in appendix G.3, with the result

$$g_\chi(\tau) = \frac{4}{(2\Delta-1)^2}\left[(1+e^{-2\Delta\tau})\mathfrak{g}_\Delta(e^{-2\tau}) - 1\right] \ , \tag{H.45}$$

where

$$\mathfrak{g}_\Delta(z) := \sum_{n=0}^{\infty} \mathscr{V}_{0,2n}(\Delta)^2 z^n = {}_3F_2\left[\begin{array}{c} \frac{1}{2},\, 1,\, 1 \\ \Delta,\, \Delta+\frac{1}{2} \end{array}\middle|\, z\right] . \tag{H.46}$$

We can use the result to explore in particular the behavior of $g_\chi(\tau)$ for *imaginary* τ, which escapes the analysis of the previous sections. But first of all, at small τ we have

$$g_\chi(\tau) \underset{\tau\to 0}{\sim} \text{analytic} - \frac{4\pi}{(2\Delta-1)\sin(2\pi\Delta)}\,\tau^{2\Delta-2} + \dots \tag{H.47}$$

which is consistent with eq. (H.40), since the leading operator in the boundary OPE of ϕ^2 has dimension $\Delta_* = 2\Delta$.

On the other hand, the behavior of $g_\chi(\tau)$ for imaginary τ depends on Δ. The function $\mathfrak{g}_\Delta(e^{-2\tau})$ is invariant under $\tau \to \tau + \pi i$. Now if Δ is *rational*, say of the form $\Delta = p/q$, the exponential $e^{2\Delta\tau} = e^{2p/q\cdot\tau}$ appearing in $g_\chi(\tau)$ is invariant under $\tau \to \tau + q\cdot\pi i$. Consequently, on the imaginary axis g_χ is exactly periodic, with period $q\cdot\pi$. The same behavior occurs in the case of minimal models in the identity module: there, all correlators are exactly invariant under $\tau \to \tau + \pi i$. In contrast, if Δ is irrational, the function $g_\chi(\tau)$ cannot be exactly periodic. In Fig. H.4 we plot $|G(\tau = \mathrm{i}t)|$ for a range of t, both for rational and irrational Δ (namely $\Delta = 2$ and $\Delta = \sqrt{7}$). Nevertheless, in both cases we can check that there are no non-analyticities stronger than the one in eq. (H.47) for imaginary τ. This fact simply follows from eqs. (H.45) and (H.46). Indeed, the only source of singularities in $g_\chi(\mathrm{i}t)$ is the hypergeometric function, and, as stated above, $\mathfrak{g}_\Delta(e^{-2\mathrm{i}t})$ is periodic in t with period π. Then, the only non-analyticity along the path is the branch point at $t = \pi n$, $n \in \mathbb{Z}$. We conclude that the analytic structure of $g_\chi(\tau)$ is of the form presented in figure 8.6, with power law monodromies along the imaginary axis, all with the same exponent.

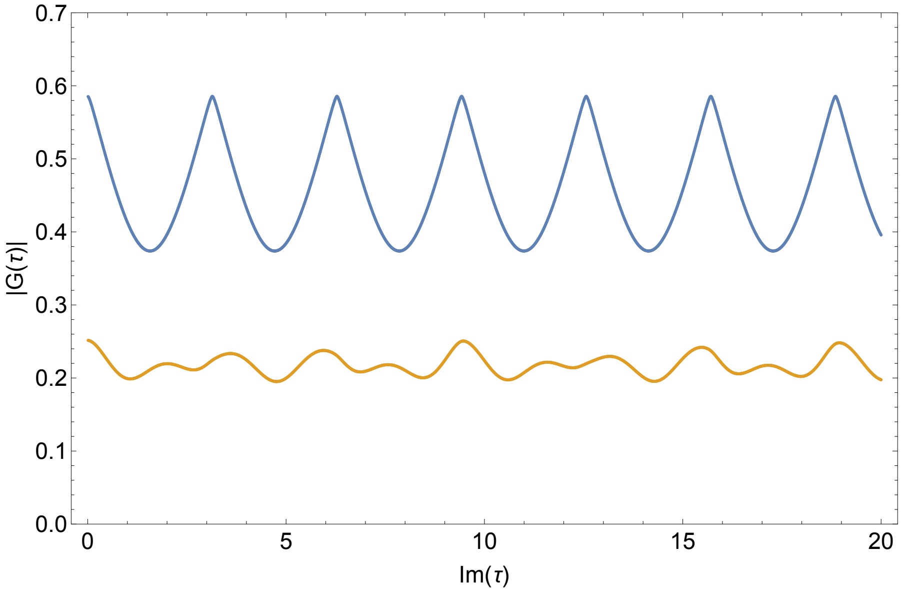

Figure H.4: Plot of the correlator $g_\chi(\tau)$ for imaginary τ, for both $\Delta = 2$ (blue) and $\Delta = \sqrt{7}$ (orange). Notice the periodicity of the blue curve (rational Δ), whereas the orange curve (irrational Δ) does not have any obvious features.

I Algorithms

In this chapter, we present some of the algorithms we used in the numerics. The calculations consist of three parts:

- finding the basis of states,
- constructing the Hamiltonian,
- diagonalizing the Hamiltonian.

Depending on the theory we study and the algorithm we use, each of the above can be the bottleneck in runtime or memory.

I.1 Scalar field

As discussed in chapter 9, we construct the Hamiltonian in the truncated Fock space of the free theory. The basis at cutoff Λ is made of states[1]

$$|\psi\rangle = |n_0, n_1, n_2, ..., n_{i_{\max}}\rangle \equiv \frac{1}{\mathcal{N}_{|\psi\rangle}} (a^\dagger_{i_{\max}})^{n_{i_{\max}}} ... (a^\dagger_2)^{n_2} (a^\dagger_1)^{n_1} (a^\dagger_0)^{n_0} |\Omega\rangle \ , \tag{I.1}$$

with energies $E_{|\psi\rangle} = \sum_{i=0}^{i=i_{\max}} n_i(\Delta + i) \leq \Lambda$. In particular, $i_{\max} = \lfloor \Lambda - \Delta \rfloor$ is the highest mode possible for a one-particle state. The factor $\mathcal{N}_{|\psi\rangle} > 0$ makes the state unit-normalized. Finding the set of states in the free scalar theory is very fast and requires little memory, compared to the other parts of the code. In table I.1, we present the number of states for a few different cutoffs.

---

[1] The labelling of the states introduced here differs from the one used in the rest of the thesis: see *e.g.* eq. (8.8a).

Table I.1: Number of states at cutoff Λ for $\Delta = 1.62$ in scalar theory

Λ	10	15	20	25	30	35	40
#states	52	237	886	2904	8613	23620	60783

To build the Hamiltonian, we construct the V matrix once for each desired Δ and then save it. The Hamiltonian can then quickly be calculated using $H = H_0 + \bar{\lambda} V$.

One method to build the V matrix is to directly compute $\langle\psi_j| V |\psi_i\rangle$ by commuting the ladder operators.[2] A generic matrix element V_{ij} is given by

$$\begin{aligned}
(V_2)_{ij} &= \langle\psi_j| \sum_{m,n=0}^{\infty} A_{mn}(\Delta)(a_m^\dagger a_n^\dagger + 2a_m^\dagger a_n + a_m a_n) |\psi_i\rangle \ , \\
(V_4)_{ij} &= \langle\psi_j| \sum_{m,n,p,q=0}^{\infty} A_{mnpq}(\Delta)(a_m^\dagger a_n^\dagger a_p^\dagger a_q^\dagger + \\
&\qquad + 4a_m^\dagger a_n^\dagger a_p^\dagger a_q + 6a_m^\dagger a_n^\dagger a_p a_q + 4a_m^\dagger a_n a_p a_q + a_m a_n a_p a_q) |\psi_i\rangle \ ,
\end{aligned}$$

where the states ψ_i are defined as in eq. (I.1). Here A_{mn} can be expressed in closed form in eq. (9.15), and if desired the A_{mnpq} can be computed analytically via a recursion relation [205]. However, we calculated each of the A_{mnpq} numerically and independently, since the runtime of this operation is negligible compared to other parts of the code. Let us emphasize a few points regarding the calculation of V:

- Both the ϕ^2 and ϕ^4 deformations preserve parity and $\mathbb{Z}_2$ symmetry. Therefore, we divide the Fock space into four sectors according to the eigenvalue under these symmetries.
- The matrix A_{mn} is symmetric. So, the sum above can be reduced to $m \geq n$. This decreases the runtime by almost a factor of 2. Similarly, the runtime for the ϕ^4 deformation decreases with a factor of $\sim 4!$, as we can reduce the sum $\sum_{m,n,p,q=0}$ to $\sum_{m\geq n\geq p\geq q\geq 0}$.
- The potential is symmetric: $V_{ji} = V_{ij}$. So, it is sufficient to calculate the upper triangular part.
- Most of the elements of the potential V_{ij} vanish: V is a *sparse matrix*. This is because $:\phi^2:$, acting on a state with p particles, only produces states with p and $p \pm 2$ particles. Of course, taking this into account drastically reduces the number of matrix elements which it is necessary to compute and store.

---

[2] Another way is to act with the V operator on the state $|\psi_i\rangle$ and expand it in our basis: $V|\psi_i\rangle = \sum_j V_i^j |\psi_j\rangle$. Typically, the method we used takes up more memory, whereas this method requires longer runtimes.

The last step is the diagonalization of the Hamiltonian. As we mentioned, we diagonalize the four sectors with different parity and $\mathbb{Z}_2$ symmetry separately. In this work, we used *Spectra*, a *C++* library, which uses the Arnoldi/Lanczos method to find the smallest eigenvalues of a sparse matrix.

Let us give the reader an idea of the runtime of a typical code. In the case of the ϕ^2 deformation, for $\Delta = 1.62$ and $\Lambda = 34.13$ (which corresponds to 19939 states), it takes ~ 44 CPU-seconds to compute the matrix V and ~ 5 CPU-seconds to diagonalize the full Hamiltonian, for a single coupling $\bar{\lambda}$.

I.2 Minimal models

In the case of a minimal model, as discussed in chapter 10, the Hilbert space is composed by states of the form:

$$|\psi\rangle = L_{-n_p} \cdots L_{-n_1} |\Omega\rangle \ , \tag{I.2}$$

where $n_1, \ldots, n_p \geq 1$. In fact, it is sufficient to choose, say, $1 \leq n_1 \leq \ldots \leq n_p$ in order to span the whole Hilbert space. We dub this the *ascending* basis. We also define the *level* of the state (I.2) as the sum $\sum_i n_i$. The level is the eigenvalue of the state (I.2) under the application of the unperturbed Hamiltonian L_0.

The states (I.2) form in general a reducible representation of the Virasoro algebra. Indeed, the identity module of a minimal model $\mathcal{M}(p,q)$ has two null primary states at level 1 and $(p-1)(q-1)$. The set of physical states is obtained by quotienting out the submodules composed of all the Virasoro descendants of these two states. The null state at level 1 is $L_{-1}|\Omega\rangle$, for every minimal model. The other primary null state, for the Lee-Yang model and the Ising model respectively, is

$$|\text{null}\rangle_{\text{LY}} = \left(L_{-4} - \frac{5}{3}L_{-2}^2\right)|\Omega\rangle \ , \tag{I.3a}$$

$$|\text{null}\rangle_{\text{Ising}} = \left(L_{-6} + \frac{22}{9}L_{-4}L_{-2} - \frac{31}{36}L_{-3}^2 - \frac{16}{27}L_{-2}^3\right)|\Omega\rangle \ . \tag{I.3b}$$

Let us emphasize that null states constitute the large majority of the states (I.2): for instance, in the Lee-Yang model, at level 30 there are 5604 states of the kind (I.2), and only 568 physical states. Quotienting out the submodule generated by $L_{-1}|\Omega\rangle$ is trivial in the ascending basis: we just take $n_1 > 1$. On the contrary, in order to quotient out the descendants of (I.3) we need to write them in the ascending basis, which requires performing a large number of commutators. Rather than performing the commutators directly, we employed a more efficient method, which we briefly describe with an example. Consider the state

$$L_{-3}L_{-2}^2L_{-4}|\Omega\rangle \ . \tag{I.4}$$

It is not hard to understand which states of the ascending basis are required to decompose it. We first consider all distinct subsets of the indices of the Virasoro generators which appear in eq. (I.4) already in ascending order, *i.e.* excluding -4:[3]

$$\Big\{(-3),(-2),(-3,-2),(-2,-2),(-3,-2,-2)\Big\}\ . \tag{I.5}$$

Then, we sum the elements of each subset to -4, and we apply the resulting Virasoro generator on the vacuum, together with the complement of the generators in the same subset. Finally, we add the obvious $L_{-4}L_{-3}L_{-2}^2 |\Omega\rangle$ to the basis which is an element of:

$$\text{Span}\left\{L_{-7}L_{-2}^2|\Omega\rangle\,, L_{-6}L_{-3}L_{-2}|\Omega\rangle\,, L_{-9}L_{-2}|\Omega\rangle\,, L_{-8}L_{-3}|\Omega\rangle\,, L_{-11}|\Omega\rangle\,, L_{-4}L_{-3}L_{-2}^2|\Omega\rangle\right\}$$

The coefficient of each state in the decomposition can be easily computed knowing the multiplicities of the subsets (I.5) and the Virasoro algebra (10.1). The reason why this method is faster than the blind application of the Virasoro algebra follows precisely from the multiplicities of the subsets. When considering a descendant built by applying the same generator many times, the distinct subsets are far less than the total number. Correspondingly, when applying the commutation relations, a large number of identical sub-operations are performed. The method just described allows to avoid this redundancy.

Since L_0 is the unperturbed Hamiltonian, truncating the spectrum at cutoff Λ translates into keeping physical states of level $p \leq \Lambda$. We collect in the table below the dimension of the truncated Hilbert space for a few values of the cutoff:

Λ	5	10	15	20	25	30	35	40
#states of Lee-Yang	5	19	52	126	276	568	1103	2059
#states of Ising	7	30	95	260	632	1426	3019	6099

Contrary to the case of free theory, the basis of states obtained with the procedure above is not orthogonal. Hence, before proceeding to the computation of the potential V, we need to evaluate the Gram matrix G, *i.e.* the matrix of scalar products in the basis of physical states. This essentially reduces to the computation of overlaps of the kind

$$\langle\psi_j|\psi_i\rangle = \langle\Omega|\, L_{j_1}\cdots L_{j_q}L_{-i_p}\cdots L_{-i_1}\,|\Omega\rangle\ , \tag{I.6}$$

where the indices obey $i_p \geq \ldots \geq i_1 > 1$ and $j_p \geq \ldots \geq j_1 > 1$. Since L_0 is Hermitian, and the states (I.2) are eigenvectors of L_0 with eigenvalues equal to their level, the matrix element (I.6) vanishes unless $\sum_m j_m - \sum_n i_n = 0$. Then, the overlap is simply computed by using the Virasoro algebra to commute the generator with a larger index towards the right, and recalling that the vacuum is annihilated by all the modes L_n, $n > -2$.

The potential V involves the integral over the local operator $\mathcal{V}$, see *e.g.* eq. (10.18).

---

[3] When decomposing more complicated states, in general not all the subsets contribute to the result. The condition for a subset to be relevant is immediate and easy to implement in the code.

Therefore, to compute its matrix elements we need the overlaps

$$\langle\psi_j|\mathcal{V}|\psi_i\rangle = \langle\Omega|\, L_{j_1}\cdots L_{j_q}\,\mathcal{V}\, L_{-i_p}\cdots L_{-i_1}\,|\Omega\rangle \ . \tag{I.7}$$

Notice that this vanishes unless $|\psi_i\rangle$ and $|\psi_j\rangle$ share the same parity. These overlaps can be computed by applying the Virasoro algebra, together with the action of the generators on $\mathcal{V}$, eq. (10.11),

$$[L_n,\mathcal{V}] = \left[z^{n+1}\partial_z + \bar{z}^{n+1}\partial_{\bar{z}} + \frac{\Delta_{\mathcal{V}}}{2}\left((n+1)(z^n+\bar{z}^n) - 2\,\frac{z^{n+1}-\bar{z}^{n+1}}{z-\bar{z}}\right)\right]\mathcal{V} \ , \tag{I.8}$$

that we define as $\hat{\mathcal{D}}_n(z,\bar{z})\mathcal{V}$. Finally, using the fact that the expectation value of $\mathcal{V}$ in the vacuum is a constant. More specifically, the strategy goes as follows. We first commute $\mathcal{V}$ all the way to the left vacuum in eq. (I.7), and we reorder the result, such that in

$$\langle\Omega|\,\mathcal{V}\, L_{-i_{p'}}\cdots L_{-i_1}\,|\Omega\rangle \tag{I.9}$$

there are only negative Virasoro modes. Then we commute the generators again to the left of $\mathcal{V}$. In the end, we find a sum over a set of differential operators acting on a constant $a_{\mathcal{V}}$:

$$\langle\psi_j|\mathcal{V}|\psi_i\rangle = \sum_l c_l \prod_{m_l}\hat{\mathcal{D}}_{m_l}(z,\bar{z})\ a_{\mathcal{V}} = \sum_l c_l \mathfrak{D}_l(z,\bar{z})\ a_{\mathcal{V}} \ . \tag{I.10}$$

In order to compute the integral of eq. (I.7) over AdS, it is useful to describe the objects $\mathfrak{D}_l(z,\bar{z})$ in some detail. Since, albeit not explicitly, the operators (I.8) are polynomials in z and $\bar{z}$, it follows that $\mathfrak{D}_l(z,\bar{z})$ are polynomials as well. Furthermore, they are homogeneous, and their degree d equals the sum of the indices m_l in eq. (I.10). This sum is independent of l, since it equals the difference of the levels of the states $|\psi_j\rangle$ and $|\psi_i\rangle$:

$$d = \sum m_l = (j_1+j_2+\ldots+j_q) - (i_1+i_2+\ldots+i_p) \ . \tag{I.11}$$

Finally, $\mathfrak{D}_l(z,\bar{z})$ is symmetric under $z \leftrightarrow \bar{z}$. Now, $\mathfrak{D}_l(z,\bar{z})$ can be easily evaluated on the $\tau=0$ slice in global coordinates, which corresponds to $z = 1/\bar{z} = \mathrm{i}\,e^{\mathrm{i}r}$. The previous constraints then translate in the following equality:

$$\mathfrak{D}_l = \sum_{k=0}^{d/2}\alpha_{l,k}\left(z^{2k}+z^{-2k}\right) = \sum_{k=0}^{d/2}\alpha_{l,k}\left(e^{\mathrm{i}k(2r+\pi)}+e^{-\mathrm{i}k(2r+\pi)}\right) = \sum_{k=0}^{d/2}2\alpha_{l,k}\cos(2kr+k\pi) \ . \tag{I.12}$$

To find V, we now need to integrate these trigonometric functions against the AdS measure. It is simple to do this analytically, keeping in mind that we know that all the matrix elements are finite. Hence, the constant terms $\alpha_{l,0}$ in eq. (I.12) must all combine to yield integrals of the following form:

$$\int_{-\frac{\pi}{2}}^{\frac{\pi}{2}}\frac{\cos(2kr+k\pi)-1}{\cos^2(r)}dr = -2k\pi \ , \tag{I.13}$$

where $k \in \mathbb{N}$. Hence, the matrix elements of the potential are rational factors times π. Of course, computing V once for the highest interesting cutoff yields the Hamiltonian for any value of the coupling λ. Like in the free scalar case, both V and the Gram matrix are symmetric, so we only compute their upper triangular part. Furthermore, V is parity preserving, so H is block diagonal.

The last step is to diagonalize the Hamiltonian. Due to the presence of a non-trivial Gram matrix G, we need to solve the following generalized eigenvalue problem:

$$H.v = E\, G.v \ , \tag{I.14}$$

Empirically, we find that a higher precision in numerics is required to diagonalize the Hamiltonian with respect to the scalar case. In fact, this step is the bottleneck in the code runtime. Notice that, since the potential couples states with arbitrarily different unperturbed energy, when $\bar{\lambda}$ is order one the off-diagonal matrix elements of the Hamiltonian are large, contrary to the example discussed in section I.1.

We wrote the code for the minimal models in Mathematica. To give the reader an idea of the runtime, it takes ~ 100 core-hours to find V at cutoff $\Lambda = 40$ (with 2059 states) in the Lee-Yang model, whereas it takes ~ 400 core-hours to find V at cutoff $\Lambda = 35$ (with 3019 states) in the Ising model with thermal deformation. The diagonalization also typically takes a core-hour for a single matrix. In order to produce a plot like the one in figure 10.9, we need to diagonalize several Hamiltonians, corresponding to different couplings $\bar{\lambda}$ and truncation cutoffs Λ.

In appendix F, relations between matrix elements of the operator V were derived. As a matter of principle, these recursion relations make it possible to compute many matrix elements indirectly — once a small number of matrix elements is computed using the algorithm discussed above, the rest of the matrix can be "filled in" using equations (F.11). In our setup, we have instead chosen to compute all matrix elements directly. Indeed, computing matrix elements indirectly requires organizing the Hilbert space of the theory in terms of $SL(2,\mathbb{R})$ primaries and descendants, which is doable but adds additional complexity to the algorithm. Moreover, for moderate values of the cutoff Λ, a sizeable fraction of the Hilbert space consists of $SL(2,\mathbb{R})$ primaries, which in turns means that many matrix elements of V still need to be computed explicitly.

J Spontaneous symmetry breaking in AdS

This appendix contain computations that have to do with symmetry breaking in AdS and different boundary conditions.

J.1 All or nothing

Consider the following Euclidean action for a scalar field in AdS

$$S = \int d^{d+1}x\sqrt{g}\left[\frac{1}{2}(\partial\phi)^2 + V(\phi)\right] \tag{J.1}$$

where $V(0) = V'(0) = 0$. The global minimum of $V(\phi)$ is attained at $\phi = \phi_t \neq 0$. We use the AdS metric

$$ds^2 = R^2\left[d\rho^2 + \sinh^2\rho\, d\Omega_d^2\right] \tag{J.2}$$

and impose boundary conditions

$$\lim_{\rho\to\infty}\phi(\rho)e^{\frac{d}{2}\rho} = 0\ , \tag{J.3}$$

so that the action gets a finite contribution from $\rho \to \infty$. We claim that there are only two possibilities:

1. Within field configurations satisfying the boundary condition (J.3), the global minimum of the action is zero and it is attained by the constant solution $\phi = 0$.
2. The action is not bounded from below and its value can always be decreased by setting $\phi = \phi_t$ in a bigger region of AdS.

In J.1 we will use the thin wall approximation to get some intuition for the claim above. Then, we will present a more general argument in J.1.

Thin wall approximation

In the thin wall approximation [206], the action is given in terms of the volume of the region in the true vacuum and the area of the walls separating it from the false vacuum $\phi = 0$,

$$S = V(\phi_t)\,\text{volume} + T\,\text{area}\ , \tag{J.4}$$

where T is the tension of the walls. To minimize the action, it is preferable to use spherical bubbles because these have the minimal area for a given volume. For this reason we consider a single spherical bubble of geodesic radius ρ, centred at $\rho = 0$ in the coordinates (J.2). This gives

$$S(\rho) = TR^d\,\text{Vol}(\Omega_d)\left[\sinh^d\rho - b\int_0^\rho dt\,\sinh^d t\right]\ , \qquad b \equiv \frac{|V(\phi_t)|R}{T}\ . \tag{J.5}$$

Case **1.** above corresponds to $b \leq d$ and the action is positive for bubbles of any size. This follows from the fact that $S(\rho)$ is positive for very small ρ and that its derivative, $\frac{dS}{d\rho} \propto d\cosh\rho - b\sinh\rho$, is always positive if $b \leq d$. Case **2.** corresponds to $b > d$ and very large bubbles decrease the action without bound. Indeed, in this case $S(\rho) \sim e^{d\rho}\left(1 - \frac{b}{d}\right) < 0$ for large bubbles.

General spherical bubbles

Let us now consider the case of a general potential $V(\phi)$ and drop the thin wall approximation. We will analyse a single spherical bubble because breaking of spherical symmetry should increase the action (from the kinetic term).

It is convenient to trade the boundary condition (J.3) for $\phi(\rho_\star) = 0$ for some fixed $\rho_\star$. The action for the finite region $\rho < \rho_\star$ is clearly bounded from below if $V(\phi)$ is bounded from below. We will determine its absolute minimum and then study its dependence with $\rho_\star$. This class of field configurations is sufficient to show that the action can be unbounded from below in the limit $\rho_\star \to \infty$.

We are interested in the field profile $\phi(\rho)$ that obeys the boundary condition $\phi(\rho_\star) = 0$ and minimizes the action

$$S = R^{d+1}\,\text{Vol}(\Omega_d)\int_0^{\rho_\star} d\rho\,\sinh^d\rho\left[\frac{1}{2}\phi'(\rho)^2 + V(\phi(\rho))\right]\ . \tag{J.6}$$

The corresponding Euler-Lagrange equations,

$$\phi''(\rho) = V'(\phi(\rho)) - \frac{d}{\tanh\rho}\phi'(\rho)\ , \tag{J.7}$$

describe a particle with position ϕ moving in the potential $-V(\phi)$ with a friction force depending on the time ρ (see figure J.1). This equation of motion allows for the following behaviour when $\rho \to 0$: either $\phi'(\rho) \sim \rho$ or ϕ diverges. We exclude the second possibility because it would give an infinite contribution to the action (J.6).[1] Therefore we can use the boundary condition $\phi'(0) = 0$, which means we are interested in trajectories that start from rest. It is clear that $\phi(\rho) = 0$ is a solution but it may not be the only one. The particle motion interpretation of (J.7), depicted in figure J.1, makes it clear that if there is a non-trivial solution that arrives at $\phi = 0$ for some finite time $\rho_\star$ then a similar solution will also exist for an arbitrary large $\rho_\star$. Recall that we are interested in the limit of large $\rho_\star$ that allows for arbitrary large bubbles of true vacuum in AdS. Using standard methods, we can compute[2]

$$\frac{1}{R^{d+1}\,\mathrm{Vol}(\Omega_d)\sinh^d \rho_\star}\frac{d}{d\rho_\star}S_{\min} = -\frac{1}{2}\phi'(\rho_\star)^2 \ . \tag{J.8}$$

Moreover, if a non-trivial solution exist then $\phi'(\rho_\star)^2$ tends to a positive constant as $\rho_\star \to \infty$, which implies that $S_{\min} \to -\infty$ in this limit.[3] This corresponds to case **2.** above. If the potential is such that for any $\rho_\star$ the minimum of (J.6) is zero, then we fall in case **1.**

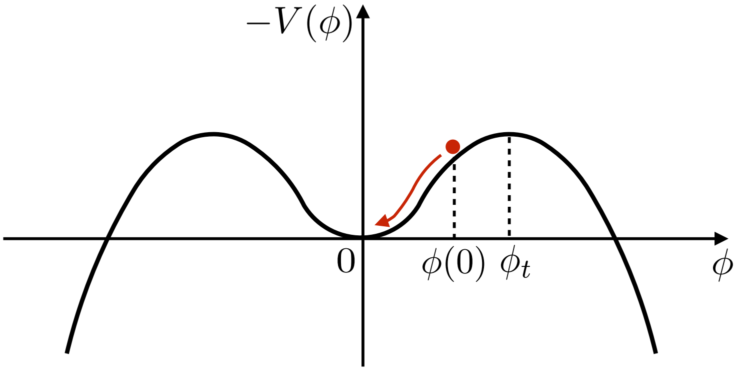

Figure J.1: The equation of motion (J.7) can be interpreted as a particle moving in the potential $-V(\phi)$ with time-dependent friction. We are interested in trajectories that start from rest at $\rho = 0$ and reach $\phi = 0$ at the time $\rho = \rho_\star$. Apart from the trivial trajectory $\phi(\rho) = 0$, there may be other classical trajectories with lower action. This depends on the potential. However, if such a trajectory exist for some $\rho_\star$ then it will also exist for larger $\rho_\star$. Indeed, it is sufficient to start with a larger $\phi(0)$, and $\phi(0) \to \phi_t$ when $\rho_\star \to \infty$. If $V''(0) < -\frac{d^2}{4}$ then there is always another trajectory because the late time motion around $\phi = 0$ is oscillatory. This corresponds to the Breitenlohner-Freedman criteria for the instability of the trivial vacuum around $\phi = 0$.

---

[1] If the potential goes like $V \sim \phi^n$ for large ϕ then the divergent solution has $\phi'(\rho) \sim \rho^{-\gamma}$ when $\rho \to 0$ with $\gamma = \min\left(d, \frac{n}{n-2}\right)$. One can check that this leads to a divergent integral in (J.6).

[2] Recall the classical result $\frac{\partial}{\partial t_f}S(q_i, t_i; q_f, t_f) = -E$, relating the action S of the classical path from $q(t_i) = q_i$ to $q(t_f) = q_f$ to its energy E.

[3] Indeed, suppose that a solution exists which starts at rest at $\phi(0) = \phi_0 < \phi_t$ and arrives at $\phi(\rho_*) = 0$. Then the solution with $\phi(0) \to \phi_t$ passes by ϕ_0 with a non-vanishing velocity, and so arrives at $\phi = 0$ with a larger velocity than the original solution.

It is convenient to analyse the asymptotic behaviour of the equation of motion (J.7) for large ρ and around $\phi = 0$, where it reduces to a linear ODE:

$$\phi''(\rho) + d\,\phi'(\rho) - V''(0)\phi(\rho) = 0 \ . \tag{J.9}$$

The general solution is $\phi(\rho) = c_+ e^{-\alpha_+\rho} + c_- e^{-\alpha_-\rho}$ with

$$\alpha_\pm = \frac{d}{2} \pm \sqrt{\frac{d^2}{4} + V''(0)} \ . \tag{J.10}$$

We conclude that for $V''(0) < -\frac{d^2}{4}$ the late-time motion is oscillatory and therefore the particle reaches $\phi = 0$ in finite time. This means that the vacuum $\phi = 0$ is unstable if $V''(0)$ is below the Breitenlohner-Freedman bound [155]. If $V''(0) > -\frac{d^2}{4}$ then the late-time motion is repulsive or over-damped and we cannot decide if we fall in case **1.** or **2.** with an asymptotic analysis. A purely quadratic potential with $V''(0) > -\frac{d^2}{4}$ corresponds to case **1.**, as it can be checked explicitly.

J.2 Inverted harmonic oscillator

In this appendix we will consider the fact of the harmonic oscillator with a *negative* mass, and in particular how such a system would be analyzed using Hamiltonian truncation methods. To be precise, we consider the following Hamiltonian:

$$H = a^\dagger a + g\left[(a^\dagger)^2 + a^2 + 2a^\dagger a\right] \tag{J.11}$$

where $[a, a^\dagger] = 1$. Physically, this is nothing but a harmonic oscillator with unit frequency, perturbed by the normal-ordered operator X^2 with an (at least for now) arbitrary real coupling g. The spectrum of H can easily be obtained using a Bogoliubov transformation, using the Ansatz

$$b = \cosh(\theta)a + \sinh(\theta)a^\dagger \tag{J.12}$$

for some $\theta \in \mathbb{R}$ to be determined. By construction, the annihilation operator b from (J.12) and its partner $b^\dagger$ obey the canonical commutation relation $[b, b^\dagger] = 1$ for any θ. Setting

$$\theta = \frac{1}{4}\ln(1 + 4g) \tag{J.13}$$

we find that

$$H = \sqrt{1+4g}\, b^\dagger b + \mathcal{E}_\Omega, \quad \mathcal{E}_\Omega = \frac{1}{2}\sqrt{1+4g} - \frac{1}{2} - g \leq 0. \tag{J.14}$$

In other words, H is a harmonic oscillator with frequency $\omega = \sqrt{1+4g}$ in disguise, up to a finite shift in the ground state energy.

The above reasoning applies to positive g, and in fact it's easy to see that the same formulas apply to slightly negative values of the coupling constant. By inspection of (J.13) and (J.14) we see that the Bogoliubov transformation (J.12) works for any $g \geq g_\star := -1/4$. However, the theory ceases to exist for $g < g_\star$ — for instance, the energy $\sqrt{1+4g}$ has a branch cut starting at $g = g_\star$.

At the same time, we can analyze H using truncation methods. To do so we work in Fock space, in a basis of the first N eigenstates of the $g = 0$ Hamiltonian, to wit

$$|k\rangle := \frac{1}{\sqrt{k!}} (a^\dagger)^k |\text{vac}\rangle \quad \text{for} \quad k = 0, \ldots, N. \tag{J.15}$$

The Hamiltonian then becomes a Hermitian matrix $H_N(g)$ of size $(N+1) \times (N+1)$, which is diagonalizable for *any* real value of g. Note that $H_N(g)$ does not mix states with even and odd mode number k, since the theory is invariant under the $\mathbb{Z}_2$ symmetry $(a, a^\dagger) \mapsto (-a, -a^\dagger)$. In figure J.2 we plot the first 10 energy levels of $H_N(g)$ for a range of negative g, working at cutoff $N = 50$. For $g \geq g_\star$ Hamiltonian truncation is in excellent agreement with the analytic formula (J.14). Yet for $g < g_\star$, we observe that states with even and odd $\mathbb{Z}_2$ parity become near-degenerate, emulating spontaneous symmetry breaking in quantum field theory.

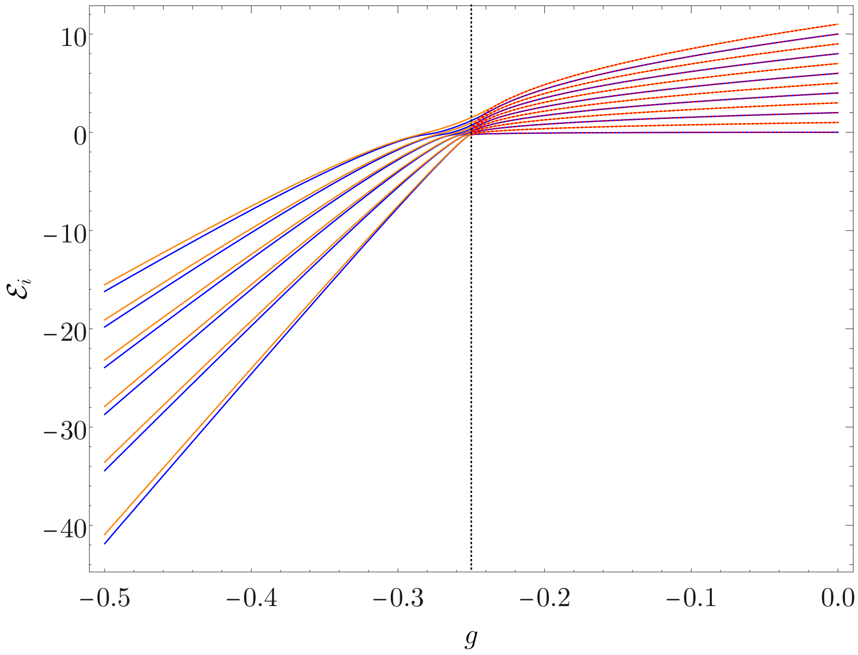

Figure J.2: Spectrum of the cutoff Hamiltonian $H_N(g)$ for $N = 50$ for $g \in [-1/2, 0]$. The blue (resp. orange) curves have even (odd) $\mathbb{Z}_2$ parity. The dotted red lines for $g \geq g_\star$ show the exact spectrum of the theory; the vertical black dotted line indicates $g_\star$.

Although the theory is unphysical for $g < g_\star$, we can nevertheless study the eigenstates and eigenvalues of $H_N(g)$ numerically. When Hamiltonian truncation converges, the ground state $|\Omega\rangle$ should not be sensitive to the cutoff, N in this case. This means that the overlap of $|\Omega\rangle$ with Fock space states $|k\rangle$ having $k \sim N$ ought to be negligeable when N is large. To make this quantitative, we can introduce the integrated probability density

$$\mathbb{P}_k^{(N)} = \sum_{j=0}^{k} |\langle \Omega | j \rangle|^2 \tag{J.16}$$

which grows with k and obeys $\mathbb{P}_N^{(N)} = 1$ (since $|\Omega\rangle$ is normalized). Below in figure J.3 we display $\mathbb{P}_k^{(N)}$ for various values of g, setting $N = 200$. For $g > g_\star$ we see that $|\Omega\rangle$ has little overlap with states close to the cutoff, as expected (because Hamiltonian truncation converges very rapidly in quantum mechanics). However, this behavior changes dramatically as we lower g to $g_\star$. Already for $g = g_\star - 10^{-3}$, the ground state $|\Omega\rangle$ consists mostly of high-energy states, and as we lower g this effect becomes even more important. Plots of $\mathbb{P}_k^{(N)}$ are shown in figure J.3. It is clear that for $g < g_\star$, at least some states in

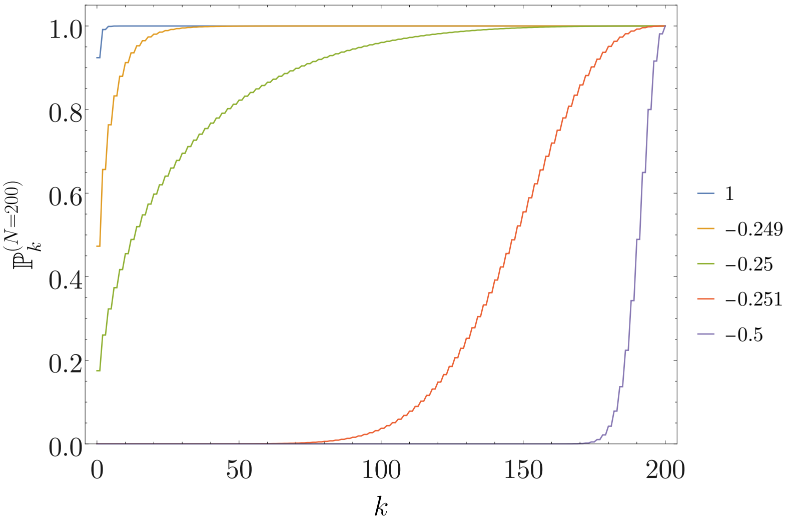

Figure J.3: Probability $\mathbb{P}_k^{(N)}$ to find the truncation ground state $|\Omega\rangle$ in the first k Fock space states, working at cutoff $N = 200$. For $g = 1$ the ground state has almost no overlap with high-energy states. As $g \searrow g_\star$, the overlap with states close to the cutoff grows dramatically, and for values of g below $g_\star$, the ground state is very UV-sensitive.

the spectrum of H_N are extremely UV-sensitive; indeed, the spectrum $\mathcal{E}_\Omega, \mathcal{E}_1, \ldots$ for such values of g depends strongly on the cutoff N, as shown in figure J.4.[4] Surprisingly, the parity of the k-th excited state goes as $(-1)^{k+N}$, that is to say that it alternates with N.

---

[4] From the plot, it appears that $\mathcal{E}_1 - \mathcal{E}_\Omega$ has a finite limit as $N \to \infty$, but $\mathcal{E}_2 - \mathcal{E}_\Omega$ does not converge as the cutoff is removed.

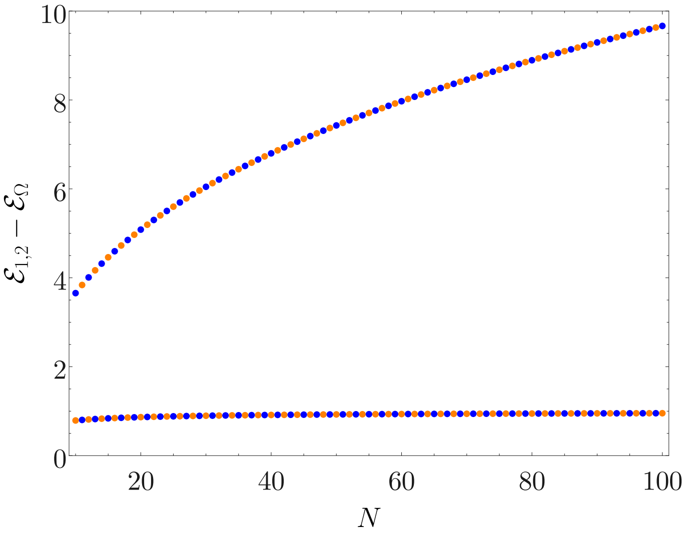

Figure J.4: The first two energies $\mathcal{E}_1$ and $\mathcal{E}_2$ (after subtracting the Casimir energy $\mathcal{E}_\Omega$) of the Hamiltonian $H_N(g)$ for $g = -1/2$, scanning over a range of cutoffs N. Blue (resp. orange) points label $\mathbb{Z}_2$ even (odd) states. In particular, it is clear that $\mathcal{E}_2 - \mathcal{E}_\Omega$ does not have a finite limit as $N \to \infty$, and that the parity of the k-th eigenstate of H depends on the sign $(-1)^N$.

Bibliography

[1] S. Weinberg, *The Quantum theory of fields. Vol. 1: Foundations.* Cambridge University Press, 6, 2005.

[2] M. E. Peskin and D. V. Schroeder, *An Introduction to quantum field theory.* Addison-Wesley, Reading, USA, 1995.

[3] A. H. Guth, "The Inflationary Universe: A Possible Solution to the Horizon and Flatness Problems," *Phys. Rev. D* **23** (1981) 347–356.

[4] A. D. Linde, "A New Inflationary Universe Scenario: A Possible Solution of the Horizon, Flatness, Homogeneity, Isotropy and Primordial Monopole Problems," *Phys. Lett. B* **108** (1982) 389–393.

[5] D. Baumann, "Inflation," in *Theoretical Advanced Study Institute in Elementary Particle Physics: Physics of the Large and the Small.* 7, 2009. `arXiv:0907.5424 [hep-th]`.

[6] J. M. Maldacena, "The Large N limit of superconformal field theories and supergravity," *Adv. Theor. Math. Phys.* **2** (1998) 231–252, `arXiv:hep-th/9711200`.

[7] C. Vafa, "The String landscape and the swampland," `arXiv:hep-th/0509212`.

[8] H. Ooguri and C. Vafa, "On the Geometry of the String Landscape and the Swampland," *Nucl. Phys. B* **766** (2007) 21–33, `arXiv:hep-th/0605264`.

[9] G. Obied, H. Ooguri, L. Spodyneiko, and C. Vafa, "De Sitter Space and the Swampland," `arXiv:1806.08362 [hep-th]`.

[10] A. Bedroya, R. Brandenberger, M. Loverde, and C. Vafa, "Trans-Planckian Censorship and Inflationary Cosmology," *Phys. Rev. D* **101** no. 10, (2020) 103502, `arXiv:1909.11106 [hep-th]`.

[11] A. Bedroya and C. Vafa, "Trans-Planckian Censorship and the Swampland," *JHEP* **09** (2020) 123, `arXiv:1909.11063 [hep-th]`.

[12] A. Bedroya, "de Sitter Complementarity, TCC, and the Swampland," `arXiv:2010.09760 [hep-th]`.

[13] J. Maldacena, "Vacuum decay into Anti de Sitter space," `arXiv:1012.0274 [hep-th]`.

[14] T. Hertog and G. T. Horowitz, "Towards a big crunch dual," *JHEP* **07** (2004) 073, `arXiv:hep-th/0406134`.

[15] T. Hertog and G. T. Horowitz, "Holographic description of AdS cosmologies," *JHEP* **04** (2005) 005, `arXiv:hep-th/0503071`.

[16] N. Turok, B. Craps, and T. Hertog, “From big crunch to big bang with AdS/CFT,” `arXiv:0711.1824 [hep-th]`.

[17] B. Craps, T. Hertog, and N. Turok, “On the Quantum Resolution of Cosmological Singularities using AdS/CFT,” *Phys. Rev. D* **86** (2012) 043513, `arXiv:0712.4180 [hep-th]`.

[18] J. L. F. Barbon and E. Rabinovici, “AdS Crunches, CFT Falls And Cosmological Complementarity,” *JHEP* **04** (2011) 044, `arXiv:1102.3015 [hep-th]`.

[19] N. Arkani-Hamed and J. Maldacena, “Cosmological Collider Physics,” `arXiv:1503.08043 [hep-th]`.

[20] H. Goodhew, S. Jazayeri, and E. Pajer, “The Cosmological Optical Theorem,” *JCAP* **04** (2021) 021, `arXiv:2009.02898 [hep-th]`.

[21] L. Di Pietro, V. Gorbenko, and S. Komatsu, “Analyticity and unitarity for cosmological correlators,” *JHEP* **03** (2022) 023, `arXiv:2108.01695 [hep-th]`.

[22] C. Sleight and M. Taronna, “From dS to AdS and back,” *JHEP* **12** (2021) 074, `arXiv:2109.02725 [hep-th]`.

[23] N. Arkani-Hamed, D. Baumann, H. Lee, and G. L. Pimentel, “The Cosmological Bootstrap: Inflationary Correlators from Symmetries and Singularities,” *JHEP* **04** (2020) 105, `arXiv:1811.00024 [hep-th]`.

[24] D. Baumann, C. Duaso Pueyo, A. Joyce, H. Lee, and G. L. Pimentel, “The cosmological bootstrap: weight-shifting operators and scalar seeds,” *JHEP* **12** (2020) 204, `arXiv:1910.14051 [hep-th]`.

[25] D. Baumann, C. Duaso Pueyo, A. Joyce, H. Lee, and G. L. Pimentel, “The Cosmological Bootstrap: Spinning Correlators from Symmetries and Factorization,” `arXiv:2005.04234 [hep-th]`.

[26] V. Gorbenko and L. Senatore, “$\lambda\phi^4$ in dS,” `arXiv:1911.00022 [hep-th]`.

[27] R. Rattazzi, V. S. Rychkov, E. Tonni, and A. Vichi, “Bounding scalar operator dimensions in 4D CFT,” *JHEP* **12** (2008) 031, `arXiv:0807.0004 [hep-th]`.

[28] D. Poland, S. Rychkov, and A. Vichi, “The Conformal Bootstrap: Theory, Numerical Techniques, and Applications,” *Rev. Mod. Phys.* **91** (2019) 015002, `arXiv:1805.04405 [hep-th]`.

[29] J. Polchinski, “Scale and Conformal Invariance in Quantum Field Theory,” *Nucl. Phys. B* **303** (1988) 226–236.

[30] D. Dorigoni and V. S. Rychkov, “Scale Invariance + Unitarity => Conformal Invariance?,” `arXiv:0910.1087 [hep-th]`.

[31] V. Riva and J. L. Cardy, “Scale and conformal invariance in field theory: A Physical counterexample,” *Phys. Lett. B* **622** (2005) 339–342, `arXiv:hep-th/0504197`.

[32] Y. Nakayama, “Scale invariance vs conformal invariance,” *Phys. Rept.* **569** (2015) 1–93, `arXiv:1302.0884 [hep-th]`.

[33] M. A. Luty, J. Polchinski, and R. Rattazzi, “The a-theorem and the Asymptotics of 4D Quantum Field Theory,” *JHEP* **01** (2013) 152, `arXiv:1204.5221 [hep-th]`.

[34] A. Dymarsky, Z. Komargodski, A. Schwimmer, and S. Theisen, “On Scale and Conformal Invariance in Four Dimensions,” *JHEP* **10** (2015) 171, `arXiv:1309.2921 [hep-th]`.

[35] S. Ferrara, A. F. Grillo, and R. Gatto, "Tensor representations of conformal algebra and conformally covariant operator product expansion," *Annals Phys.* **76** (1973) 161–188.

[36] A. M. Polyakov, "Nonhamiltonian approach to conformal quantum field theory," *Zh. Eksp. Teor. Fiz.* **66** (1974) 23–42.

[37] F. Kos, D. Poland, D. Simmons-Duffin, and A. Vichi, "Precision Islands in the Ising and $O(N)$ Models," *JHEP* **08** (2016) 036, `arXiv:1603.04436 [hep-th]`.

[38] M. F. Paulos, J. Penedones, J. Toledo, B. C. van Rees, and P. Vieira, "The S-matrix bootstrap. Part I: QFT in AdS," *JHEP* **11** (2017) 133, `arXiv:1607.06109 [hep-th]`.

[39] V. Yurov and A. Zamolodchikov, "Truncated Conformal Space Approach to scaling Lee-Yang model," *Int. J. Mod. Phys. A* **5** (1990) 3221–3246.

[40] M. Hogervorst, S. Rychkov, and B. C. van Rees, "Truncated conformal space approach in d dimensions: A cheap alternative to lattice field theory?," *Phys. Rev. D* **91** (2015) 025005, `arXiv:1409.1581 [hep-th]`.

[41] S. Rychkov and L. G. Vitale, "Hamiltonian truncation study of the ϕ^4 theory in two dimensions," *Phys. Rev. D* **91** (2015) 085011, `arXiv:1412.3460 [hep-th]`.

[42] M. Hogervorst, "RG flows on S^d and Hamiltonian truncation," `arXiv:1811.00528 [hep-th]`.

[43] E. Katz, Z. U. Khandker, and M. T. Walters, "A Conformal Truncation Framework for Infinite-Volume Dynamics," *JHEP* **07** (2016) 140, `arXiv:1604.01766 [hep-th]`.

[44] N. Anand, A. L. Fitzpatrick, E. Katz, Z. U. Khandker, M. T. Walters, and Y. Xin, "Introduction to Lightcone Conformal Truncation: QFT Dynamics from CFT Data," `arXiv:2005.13544 [hep-th]`.

[45] A. L. Fitzpatrick, E. Katz, D. Poland, and D. Simmons-Duffin, "Effective Conformal Theory and the Flat-Space Limit of AdS," *JHEP* **07** (2011) 023, `arXiv:1007.2412 [hep-th]`.

[46] R. C. Brower, C. V. Cogburn, A. L. Fitzpatrick, D. Howarth, and C.-I. Tan, "Lattice Setup for Quantum Field Theory in AdS$_2$," `arXiv:1912.07606 [hep-th]`.

[47] N. Anand, E. Katz, Z. U. Khandker, and M. T. Walters, "Nonperturbative dynamics of (2+1)d ϕ^4-theory from Hamiltonian truncation," `arXiv:2010.09730 [hep-th]`.

[48] P. Di Francesco, P. Mathieu, and D. Senechal, *Conformal Field Theory*. Graduate Texts in Contemporary Physics. Springer-Verlag, New York, 1997.

[49] S. Rychkov, *EPFL Lectures on Conformal Field Theory in D>= 3 Dimensions*. SpringerBriefs in Physics. 1, 2016. `arXiv:1601.05000 [hep-th]`.

[50] J. Penedones, "TASI lectures on AdS/CFT," in *Proceedings, Theoretical Advanced Study Institute in Elementary Particle Physics: New Frontiers in Fields and Strings (TASI 2015): Boulder, CO, USA, June 1-26, 2015*, pp. 75–136. 2017. `arXiv:1608.04948 [hep-th]`.

[51] D. Simmons-Duffin, "The Conformal Bootstrap," in *Theoretical Advanced Study Institute in Elementary Particle Physics: New Frontiers in Fields and Strings*, pp. 1–74. 2017. `arXiv:1602.07982 [hep-th]`.

[52] M. S. Costa, J. Penedones, D. Poland, and S. Rychkov, "Spinning Conformal Correlators," *JHEP* **11** (2011) 071, `arXiv:1107.3554 [hep-th]`.

[53] D. Pappadopulo, S. Rychkov, J. Espin, and R. Rattazzi, "OPE Convergence in Conformal Field Theory," *Phys. Rev. D* **86** (2012) 105043, `arXiv:1208.6449 [hep-th]`.

[54] M. Gillioz, M. Meineri, and J. Penedones, "A scattering amplitude in Conformal Field Theory," *JHEP* **11** (2020) 139, `arXiv:2003.07361 [hep-th]`.

[55] A. M. Polyakov, "Conformal symmetry of critical fluctuations," *JETP Lett.* **12** (1970) 381–383.

[56] F. A. Dolan and H. Osborn, "Conformal four point functions and the operator product expansion," *Nucl. Phys. B* **599** (2001) 459–496, `arXiv:hep-th/0011040`.

[57] F. A. Dolan and H. Osborn, "Conformal Partial Waves: Further Mathematical Results," `arXiv:1108.6194 [hep-th]`.

[58] J. a. Penedones, E. Trevisani, and M. Yamazaki, "Recursion Relations for Conformal Blocks," *JHEP* **09** (2016) 070, `arXiv:1509.00428 [hep-th]`.

[59] M. S. Costa, J. Penedones, D. Poland, and S. Rychkov, "Spinning Conformal Blocks," *JHEP* **11** (2011) 154, `arXiv:1109.6321 [hep-th]`.

[60] D. Mazac and M. F. Paulos, "The analytic functional bootstrap. Part I: 1D CFTs and 2D S-matrices," *JHEP* **02** (2019) 162, `arXiv:1803.10233 [hep-th]`.

[61] D. Mazac and M. F. Paulos, "The analytic functional bootstrap. Part II. Natural bases for the crossing equation," *JHEP* **02** (2019) 163, `arXiv:1811.10646 [hep-th]`.

[62] S. El-Showk, M. F. Paulos, D. Poland, S. Rychkov, D. Simmons-Duffin, and A. Vichi, "Solving the 3D Ising Model with the Conformal Bootstrap," *Phys. Rev. D* **86** (2012) 025022, `arXiv:1203.6064 [hep-th]`.

[63] J. A. Wolf, "Spaces of constant curvature," *New York: McGraw-Hill* (1967) .

[64] V. K. Dobrev, G. Mack, I. T. Todorov, V. B. Petkova, and S. G. Petrova, "On the Clebsch-Gordan Expansion for the Lorentz Group in n Dimensions," *Rept. Math. Phys.* **9** (1976) 219–246.

[65] V. Dobrev, G. Mack, V. Petkova, S. Petrova, and I. Todorov, *Harmonic Analysis On the n-Dimensional Lorentz Group and Its Application to Conformal Quantum Field Theory*. Springer, 1977.

[66] T. Basile, X. Bekaert, and N. Boulanger, "Mixed-symmetry fields in de Sitter space: a group theoretical glance," *JHEP* **05** (2017) 081, `arXiv:1612.08166 [hep-th]`.

[67] D. Karateev, P. Kravchuk, and D. Simmons-Duffin, "Harmonic Analysis and Mean Field Theory," *JHEP* **10** (2019) 217, `arXiv:1809.05111 [hep-th]`.

[68] G. Sengör and C. Skordis, "Unitarity at the Late time Boundary of de Sitter," *JHEP* **06** (2020) 041, `arXiv:1912.09885 [hep-th]`.

[69] Z. Sun, *A group theoretical approach to quantum gravity in (A)dS*. PhD thesis, Columbia U., 2021.

[70] Z. Sun, "A note on the representations of $\mathrm{SO}(1,d+1)$," `arXiv:2111.04591 [hep-th]`.

[71] N. J. Vilenkin and A. U. Klimyk, *Representation of Lie Groups and Special Functions, Vols. 1-3*. Springer, 1991.

[72] A. W. Knapp, *Representation Theory of Semisimple Groups*. Princeton University Press, 1986.

[73] R. E. Howe and E. C. Tan, *Non-Abelian Harmonic Analysis*. Springer, 1992.

[74] A. Kitaev, "Notes on $\widetilde{\mathrm{SL}}(2, \mathbb{R})$ representations," arXiv:1711.08169 [hep-th].

[75] T. Anous and J. Skulte, "An invitation to the principal series," *SciPost Phys.* **9** no. 3, (2020) 028, arXiv:2007.04975 [hep-th].

[76] D. Anninos, D. M. Hofman, and J. Kruthoff, "Charged Quantum Fields in AdS_2," *SciPost Phys.* **7** no. 4, (2019) 054, arXiv:1906.00924 [hep-th].

[77] M. A. Naimark, "Decomposition of a tensor product of irreducible representations of the proper Lorentz group into irreducible representations. I. The case of a tensor product of representations of the fundamental series," *Tr. Mosk. Mat. Obs., 8, GIFML, Moscow* (1959) 121–153.

[78] R. P. Martin, "Tensor Products of Principal Series for the DeSitter Group," *Transactions of the American Mathematical Society* **265** no. 1, (1981) 121–135.

[79] J. Repka, "Tensor Products of Unitary Representations of $\mathrm{SL}_2(\mathbb{R})$," *American Journal of Mathematics, vol. 100, no. 4* (1978) 747–774.

[80] D. Simmons-Duffin, D. Stanford, and E. Witten, "A spacetime derivation of the Lorentzian OPE inversion formula," *JHEP* **07** (2018) 085, arXiv:1711.03816 [hep-th].

[81] J. Penedones, K. Salehi Vaziri, and Z. Sun, "Tensor products of irreducible representations of $SO(d+1,1)$, *To appear*,".

[82] D. M. McAvity and H. Osborn, "Conformal field theories near a boundary in general dimensions," *Nucl. Phys. B* **455** (1995) 522–576, arXiv:cond-mat/9505127.

[83] E. Lauria, M. Meineri, and E. Trevisani, "Radial coordinates for defect CFTs," *JHEP* **11** (2018) 148, arXiv:1712.07668 [hep-th].

[84] H. Epstein, "Remarks on quantum field theory on de Sitter and anti-de Sitter space-times," *Pramana* **78** (2012) 853–864.

[85] V. Mukhanov and S. Winitzki, *Introduction to quantum effects in gravity*. Cambridge University Press, 6, 2007.

[86] S. Weinberg, "Quantum contributions to cosmological correlations," *Phys. Rev. D* **72** (2005) 043514, arXiv:hep-th/0506236.

[87] C. Sleight and M. Taronna, "Bootstrapping Inflationary Correlators in Mellin Space," *JHEP* **02** (2020) 098, arXiv:1907.01143 [hep-th].

[88] C. Sleight, "A Mellin Space Approach to Cosmological Correlators," *JHEP* **01** (2020) 090, arXiv:1906.12302 [hep-th].

[89] B. Allen and T. Jacobson, "Vector Two Point Functions in Maximally Symmetric Spaces," *Commun. Math. Phys.* **103** (1986) 669.

[90] M. Spradlin, A. Strominger, and A. Volovich, "Les Houches lectures on de Sitter space," in *Les Houches Summer School: Session 76: Euro Summer School on Unity of Fundamental Physics: Gravity, Gauge Theory and Strings*. 10, 2001. arXiv:hep-th/0110007.

[91] J. de Boer, V. Jejjala, and D. Minic, "Alpha-states in de Sitter space," *Phys. Rev. D* **71** (2005) 044013, arXiv:hep-th/0406217.

[92] K. Goldstein and D. A. Lowe, "A Note on alpha vacua and interacting field theory in de Sitter space," *Nucl. Phys. B* **669** (2003) 325–340, arXiv:hep-th/0302050.

[93] H. Collins, R. Holman, and M. R. Martin, "The Fate of the alpha vacuum," *Phys. Rev. D* **68** (2003) 124012, `arXiv:hep-th/0306028`.

[94] D. Anninos, T. Anous, D. Z. Freedman, and G. Konstantinidis, "Late-time Structure of the Bunch-Davies De Sitter Wavefunction," *JCAP* **11** (2015) 048, `arXiv:1406.5490 [hep-th]`.

[95] J. Bros, "Complexified de Sitter space: Analytic causal kernels and Kallen-Lehmann type representation," *Nucl. Phys. B Proc. Suppl.* **18** (1991) 22–28.

[96] J. Bros and U. Moschella, "Two point functions and quantum fields in de Sitter universe," *Rev. Math. Phys.* **8** (1996) 327–392, `arXiv:gr-qc/9511019`.

[97] J. Bros, H. Epstein, and U. Moschella, "Analyticity properties and thermal effects for general quantum field theory on de Sitter space-time," *Commun. Math. Phys.* **196** (1998) 535–570, `arXiv:gr-qc/9801099`.

[98] J. Bros, H. Epstein, and U. Moschella, "Particle decays and stability on the de Sitter universe," *Annales Henri Poincare* **11** (2010) 611–658, `arXiv:0812.3513 [hep-th]`.

[99] J. Bros, H. Epstein, M. Gaudin, U. Moschella, and V. Pasquier, "Triangular invariants, three-point functions and particle stability on the de Sitter universe," *Commun. Math. Phys.* **295** (2010) 261–288, `arXiv:0901.4223 [hep-th]`.

[100] D. Marolf and I. A. Morrison, "The IR stability of de Sitter: Loop corrections to scalar propagators," *Phys. Rev. D* **82** (2010) 105032, `arXiv:1006.0035 [gr-qc]`.

[101] D. Marolf and I. A. Morrison, "The IR stability of de Sitter QFT: results at all orders," *Phys. Rev. D* **84** (2011) 044040, `arXiv:1010.5327 [gr-qc]`.

[102] S. Hollands, "Correlators, Feynman diagrams, and quantum no-hair in deSitter spacetime," *Commun. Math. Phys.* **319** (2013) 1–68, `arXiv:1010.5367 [gr-qc]`.

[103] S. Hollands, "Massless interacting quantum fields in deSitter spacetime," *Annales Henri Poincare* **13** (2012) 1039–1081, `arXiv:1105.1996 [gr-qc]`.

[104] D. Marolf, I. A. Morrison, and M. Srednicki, "Perturbative S-matrix for massive scalar fields in global de Sitter space," *Class. Quant. Grav.* **30** (2013) 155023, `arXiv:1209.6039 [hep-th]`.

[105] M. Hogervorst, "Crossing Kernels for Boundary and Crosscap CFTs," `arXiv:1703.08159 [hep-th]`.

[106] G. Mack, "D-independent representation of Conformal Field Theories in D dimensions via transformation to auxiliary Dual Resonance Models. Scalar amplitudes," `arXiv:0907.2407 [hep-th]`.

[107] M. S. Costa, V. Gonçalves, and J. Penedones, "Spinning AdS Propagators," *JHEP* **09** (2014) 064, `arXiv:1404.5625 [hep-th]`.

[108] D. Simmons-Duffin, "Projectors, Shadows, and Conformal Blocks," *JHEP* **04** (2014) 146, `arXiv:1204.3894 [hep-th]`.

[109] L. J. Boya, E. C. G. Sudarshan, and T. Tilma, "Volumes of compact manifolds," *Reports on Mathematical Physics* **52** no. 3, (Dec., 2003) 401–422, `arXiv:math-ph/0210033 [math-ph]`.

[110] M. S. Costa, V. Goncalves, and J. Penedones, "Conformal Regge theory," *JHEP* **12** (2012) 091, `arXiv:1209.4355 [hep-th]`.

[111] M. Delladio and V. Gorbenko, "To appear.".

[112] H. Liu and A. A. Tseytlin, "On four point functions in the CFT / AdS correspondence," *Phys. Rev. D* **59** (1999) 086002, `arXiv:hep-th/9807097`.

[113] D. Z. Freedman, S. D. Mathur, A. Matusis, and L. Rastelli, "Comments on 4 point functions in the CFT / AdS correspondence," *Phys. Lett. B* **452** (1999) 61–68, `arXiv:hep-th/9808006`.

[114] C. Sleight and M. Taronna, "From AdS to dS Exchanges: Spectral Representation, Mellin Amplitudes and Crossing," `arXiv:2007.09993 [hep-th]`.

[115] L. Di Pietro, V. Gorbenko, and S. Komatsu, "Analyticity and Unitarity for Cosmological Correlators," *to appear* .

[116] X. Zhou, "Recursion Relations in Witten Diagrams and Conformal Partial Waves," *JHEP* **05** (2019) 006, `arXiv:1812.01006 [hep-th]`.

[117] D. Poland and D. Simmons-Duffin, "The conformal bootstrap," *Nature Phys.* **12** no. 6, (2016) 535–539.

[118] F. Kos, D. Poland, and D. Simmons-Duffin, "Bootstrapping Mixed Correlators in the 3D Ising Model," *JHEP* **11** (2014) 109, `arXiv:1406.4858 [hep-th]`.

[119] J. Maldacena and D. Stanford, "Remarks on the Sachdev-Ye-Kitaev model," *Phys. Rev. D* **94** no. 10, (2016) 106002, `arXiv:1604.07818 [hep-th]`.

[120] D. Mazáč, "A Crossing-Symmetric OPE Inversion Formula," *JHEP* **06** (2019) 082, `arXiv:1812.02254 [hep-th]`.

[121] M. Hogervorst and S. Rychkov, "Radial Coordinates for Conformal Blocks," *Phys. Rev. D* **87** (2013) 106004, `arXiv:1303.1111 [hep-th]`.

[122] A. L. Fitzpatrick, J. Kaplan, D. Poland, and D. Simmons-Duffin, "The Analytic Bootstrap and AdS Superhorizon Locality," *JHEP* **12** (2013) 004, `arXiv:1212.3616 [hep-th]`.

[123] Z. Komargodski and A. Zhiboedov, "Convexity and Liberation at Large Spin," *JHEP* **11** (2013) 140, `arXiv:1212.4103 [hep-th]`.

[124] D. Simmons-Duffin, "A Semidefinite Program Solver for the Conformal Bootstrap," *JHEP* **06** (2015) 174, `arXiv:1502.02033 [hep-th]`.

[125] J. Liu, E. Perlmutter, V. Rosenhaus, and D. Simmons-Duffin, "d-dimensional SYK, AdS Loops, and $6j$ Symbols," *JHEP* **03** (2019) 052, `arXiv:1808.00612 [hep-th]`.

[126] J. M. Maldacena and G. L. Pimentel, "On graviton non-Gaussianities during inflation," *JHEP* **09** (2011) 045, `arXiv:1104.2846 [hep-th]`.

[127] J. Polchinski, "S matrices from AdS space-time," `arXiv:hep-th/9901076`.

[128] M. Gary, S. B. Giddings, and J. Penedones, "Local bulk S-matrix elements and CFT singularities," *Phys. Rev. D* **80** (2009) 085005, `arXiv:0903.4437 [hep-th]`.

[129] T. Okuda and J. Penedones, "String scattering in flat space and a scaling limit of Yang-Mills correlators," *Phys. Rev. D* **83** (2011) 086001, `arXiv:1002.2641 [hep-th]`.

[130] J. Penedones, "Writing CFT correlation functions as AdS scattering amplitudes," *JHEP* **03** (2011) 025, `arXiv:1011.1485 [hep-th]`.

[131] S. Raju, "New Recursion Relations and a Flat Space Limit for AdS/CFT Correlators," *Phys. Rev. D* **85** (2012) 126009, `arXiv:1201.6449 [hep-th]`.

[132] E. Hijano, "Flat space physics from AdS/CFT," *JHEP* **07** (2019) 132, `arXiv:1905.02729 [hep-th]`.

[133] S. Komatsu, M. F. Paulos, B. C. Van Rees, and X. Zhao, "Landau diagrams in AdS and S-matrices from conformal correlators," *JHEP* **11** (2020) 046, `arXiv:2007.13745 [hep-th]`.

[134] E. Pajer, D. Stefanyszyn, and J. Supel, "The Boostless Bootstrap: Amplitudes without Lorentz boosts," *JHEP* **12** (2020) 198, `arXiv:2007.00027 [hep-th]`.

[135] D. Meltzer, E. Perlmutter, and A. Sivaramakrishnan, "Unitarity Methods in AdS/CFT," *JHEP* **03** (2020) 061, `arXiv:1912.09521 [hep-th]`.

[136] D. Meltzer and A. Sivaramakrishnan, "CFT unitarity and the AdS Cutkosky rules," *JHEP* **11** (2020) 073, `arXiv:2008.11730 [hep-th]`.

[137] D. Meltzer, "The Inflationary Wavefunction from Analyticity and Factorization," `arXiv:2107.10266 [hep-th]`.

[138] A. M. Polyakov, "Infrared instability of the de Sitter space," `arXiv:1209.4135 [hep-th]`.

[139] D. Krotov and A. M. Polyakov, "Infrared Sensitivity of Unstable Vacua," *Nucl. Phys. B* **849** (2011) 410–432, `arXiv:1012.2107 [hep-th]`.

[140] E. T. Akhmedov, U. Moschella, K. E. Pavlenko, and F. K. Popov, "Infrared dynamics of massive scalars from the complementary series in de Sitter space," *Phys. Rev. D* **96** no. 2, (2017) 025002, `arXiv:1701.07226 [hep-th]`.

[141] E. T. Akhmedov, F. K. Popov, and V. M. Slepukhin, "Infrared dynamics of the massive $\phi 4$ theory on de Sitter space," *Phys. Rev. D* **88** (2013) 024021, `arXiv:1303.1068 [hep-th]`.

[142] A. Strominger, "The dS / CFT correspondence," *JHEP* **10** (2001) 034, `arXiv:hep-th/0106113`.

[143] E. Witten, "Quantum gravity in de Sitter space," `arXiv:hep-th/0106109`.

[144] D. Anninos, T. Hartman, and A. Strominger, "Higher Spin Realization of the dS/CFT Correspondence," *Class. Quant. Grav.* **34** no. 1, (2017) 015009, `arXiv:1108.5735 [hep-th]`.

[145] C. G. Callan, Jr. and F. Wilczek, "Infrared Behavior at Negative Curvature," *Nucl. Phys. B* **340** (1990) 366–386.

[146] S. Giombi and H. Khanchandani, "CFT in AdS and boundary RG flows," *JHEP* **11** (2020) 118, `arXiv:2007.04955 [hep-th]`.

[147] D. Carmi, L. Di Pietro, and S. Komatsu, "A Study of Quantum Field Theories in AdS at Finite Coupling," *JHEP* **01** (2019) 200, `arXiv:1810.04185 [hep-th]`.

[148] O. Aharony, M. Berkooz, D. Tong, and S. Yankielowicz, "Confinement in Anti-de Sitter Space," *JHEP* **02** (2013) 076, `arXiv:1210.5195 [hep-th]`.

[149] O. Aharony, D. Marolf, and M. Rangamani, "Conformal field theories in anti-de Sitter space," *JHEP* **02** (2011) 041, `arXiv:1011.6144 [hep-th]`.

[150] B. Doyon and P. Fonseca, "Ising field theory on a Pseudosphere," *J. Stat. Mech.* **0407** (2004) P07002, `arXiv:hep-th/0404136 [hep-th]`.

[151] M. Beccaria and A. A. Tseytlin, "On boundary correlators in Liouville theory on AdS_2," *JHEP* **07** (2019) 008, `arXiv:1904.12753 [hep-th]`.

[152] C. P. Herzog and I. Shamir, "On Marginal Operators in Boundary Conformal Field Theory," *JHEP* **10** (2019) 088, `arXiv:1906.11281 [hep-th]`.

[153] J. Kaplan, "Lectures on AdS/CFT from the Bottom Up," 2016. https://sites.krieger.jhu.edu/jared-kaplan/files/2016/05/AdSCFTCourseNotesCurrentPublic.pdf.

[154] P. Dorey, A. Pocklington, R. Tateo, and G. Watts, "TBA and TCSA with boundaries and excited states," *Nucl. Phys. B* **525** (1998) 641–663, `arXiv:hep-th/9712197`.

[155] P. Breitenlohner and D. Z. Freedman, "Stability in Gauged Extended Supergravity," *Annals Phys.* **144** (1982) 249.

[156] J. Elias-Miró and E. Hardy, "Exploring Hamiltonian Truncation in $\mathbf{d = 2 + 1}$," *Phys. Rev. D* **102** no. 6, (2020) 065001, `arXiv:2003.08405 [hep-th]`.

[157] S. de Haro, S. N. Solodukhin, and K. Skenderis, "Holographic reconstruction of space-time and renormalization in the AdS / CFT correspondence," *Commun. Math. Phys.* **217** (2001) 595–622, `arXiv:hep-th/0002230 [hep-th]`.

[158] C. M. Bender and T. T. Wu, "Analytic structure of energy levels in a field theory model," *Phys. Rev. Lett.* **21** (1968) 406–409.

[159] C. M. Bender and T. T. Wu, "Anharmonic oscillator," *Phys. Rev.* **184** (1969) 1231–1260.

[160] T. R. Klassen and E. Melzer, "The thermodynamics of purely elastic scattering theories and conformal perturbation theory," *Nucl. Phys. B* **350** (1991) 635–689.

[161] T. R. Klassen and E. Melzer, "Spectral flow between conformal field theories in (1+1)-dimensions," *Nucl. Phys. B* **370** (1992) 511–550.

[162] S. Pal, "Bound on asymptotics of magnitude of three point coefficients in 2D CFT," *JHEP* **01** (2020) 023, `arXiv:1906.11223 [hep-th]`.

[163] M. Billò, V. Gonçalves, E. Lauria, and M. Meineri, "Defects in conformal field theory," *JHEP* **04** (2016) 091, `arXiv:1601.02883 [hep-th]`.

[164] P. Giokas and G. Watts, "The renormalisation group for the truncated conformal space approach on the cylinder," `arXiv:1106.2448 [hep-th]`.

[165] G. M. T. Watts, "On the renormalisation group for the boundary Truncated Conformal Space Approach," *Nucl. Phys. B* **859** (2012) 177–206, `arXiv:1104.0225 [hep-th]`.

[166] S. Rychkov and L. G. Vitale, "Hamiltonian truncation study of the ϕ^4 theory in two dimensions. II. The $\mathbb{Z}_2$ -broken phase and the Chang duality," *Phys. Rev. D* **93** no. 6, (2016) 065014, `arXiv:1512.00493 [hep-th]`.

[167] J. Elias-Miro, M. Montull, and M. Riembau, "The renormalized Hamiltonian truncation method in the large E_T expansion," *JHEP* **04** (2016) 144, `arXiv:1512.05746 [hep-th]`.

[168] J. Elias-Miro, S. Rychkov, and L. G. Vitale, "NLO Renormalization in the Hamiltonian Truncation," *Phys. Rev. D* **96** no. 6, (2017) 065024, `arXiv:1706.09929 [hep-th]`.

[169] J. Elias-Miro, S. Rychkov, and L. G. Vitale, "High-Precision Calculations in Strongly Coupled Quantum Field Theory with Next-to-Leading-Order Renormalized Hamiltonian Truncation," *JHEP* **10** (2017) 213, `arXiv:1706.06121 [hep-th]`.

[170] J. L. Cardy, “Conformal Invariance and Surface Critical Behavior,” *Nucl. Phys. B* **240** (1984) 514–532.

[171] A. A. Belavin, A. M. Polyakov, and A. B. Zamolodchikov, “Infinite Conformal Symmetry in Two-Dimensional Quantum Field Theory,” *Nucl. Phys. B* **241** (1984) 333–380.

[172] J. L. Cardy, “Effect of Boundary Conditions on the Operator Content of Two-Dimensional Conformally Invariant Theories,” *Nucl.Phys.* **B275** (1986) 200–218.

[173] J. L. Cardy, “Boundary Conditions, Fusion Rules and the Verlinde Formula,” *Nucl.Phys.* **B324** (1989) 581.

[174] J. L. Cardy and D. C. Lewellen, “Bulk and boundary operators in conformal field theory,” *Phys.Lett.* **B259** (1991) 274–278.

[175] R. E. Behrend, P. A. Pearce, V. B. Petkova, and J.-B. Zuber, “Boundary conditions in rational conformal field theories,” *Nucl. Phys.* **B570** (2000) 525–589, `arXiv:hep-th/9908036 [hep-th]`. [Nucl. Phys.B579,707(2000)].

[176] A. Recknagel and V. Schomerus, *Boundary Conformal Field Theory and the Worldsheet Approach to D-Branes*. Cambridge Monographs on Mathematical Physics. Cambridge University Press, 11, 2013.

[177] N. Ishibashi, “The Boundary and Crosscap States in Conformal Field Theories,” *Mod. Phys. Lett. A* **4** (1989) 251.

[178] P. Dorey, I. Runkel, R. Tateo, and G. Watts, “g function flow in perturbed boundary conformal field theories,” *Nucl. Phys. B* **578** (2000) 85–122, `arXiv:hep-th/9909216`.

[179] J. L. Cardy and G. Mussardo, “S Matrix of the Yang-Lee Edge Singularity in Two-Dimensions,” *Phys. Lett. B* **225** (1989) 275–278.

[180] A. B. Zamolodchikov, “Mass scale in the sine-Gordon model and its reductions,” *Int. J. Mod. Phys. A* **10** (1995) 1125–1150.

[181] H. A. Kramers and G. H. Wannier, “Statistics of the two-dimensional ferromagnet. Part 1.,” *Phys. Rev.* **60** (1941) 252–262.

[182] A. B. Zamolodchikov, “Integrals of Motion and S Matrix of the (Scaled) $T = T_c$ Ising Model with Magnetic Field,” *Int. J. Mod. Phys. A* **4** (1989) 4235.

[183] A. B. Zamolodchikov, “Integrable field theory from conformal field theory,” *Adv. Stud. Pure Math.* **19** (1989) 641–674.

[184] P. Fonseca and A. Zamolodchikov, “Ising field theory in a magnetic field: Analytic properties of the free energy,” `arXiv:hep-th/0112167`.

[185] P. Fonseca and A. Zamolodchikov, “Ising spectroscopy. I. Mesons at $T < T_c$,” `arXiv:hep-th/0612304`.

[186] A. Zamolodchikov and I. Ziyatdinov, “Inelastic scattering and elastic amplitude in Ising field theory in a weak magnetic field at $T > T_c$: Perturbative analysis,” *Nucl. Phys. B* **849** (2011) 654–674, `arXiv:1102.0767 [hep-th]`.

[187] A. Zamolodchikov, “Ising Spectroscopy II: Particles and poles at $T > T_c$,” `arXiv:1310.4821 [hep-th]`.

[188] B. Gabai and X. Yin, "On The S-Matrix of Ising Field Theory in Two Dimensions," `arXiv:1905.00710 [hep-th]`.

[189] J. Frohlich, J. Fuchs, I. Runkel, and C. Schweigert, "Kramers-Wannier duality from conformal defects," *Phys. Rev. Lett.* **93** (2004) 070601, `arXiv:cond-mat/0404051`.

[190] C. Bachas, I. Brunner, and D. Roggenkamp, "A worldsheet extension of O(d,d:Z)," *JHEP* **10** (2012) 039, `arXiv:1205.4647 [hep-th]`.

[191] D. B. Kaplan, J.-W. Lee, D. T. Son, and M. A. Stephanov, "Conformality Lost," *Phys. Rev. D* **80** (2009) 125005, `arXiv:0905.4752 [hep-th]`.

[192] V. Gorbenko, S. Rychkov, and B. Zan, "Walking, Weak first-order transitions, and Complex CFTs," *JHEP* **10** (2018) 108, `arXiv:1807.11512 [hep-th]`.

[193] D. Rutter and B. C. van Rees, "Counterterms in Truncated Conformal Perturbation Theory," `arXiv:1803.05798 [hep-th]`.

[194] M. Luscher, "Volume Dependence of the Energy Spectrum in Massive Quantum Field Theories. 2. Scattering States," *Commun. Math. Phys.* **105** (1986) 153–188.

[195] S. Dubovsky, V. Gorbenko, and M. Mirbabayi, "Asymptotic fragility, near AdS$_2$ holography and $T\overline{T}$," *JHEP* **09** (2017) 136, `arXiv:1706.06604 [hep-th]`.

[196] G. Andrews, R. Askey, and R. Roy, *Special Functions*. Cambridge University Press, Cambridge, 1999.

[197] I. Gradshteyn and I. Ryzhik, *Table of Integrals, Series, and Products*. Academic Press, 2007.

[198] H. Bateman, *Higher transcendental functions Vol.1*. McGraw-Hill, 1953.

[199] "NIST Digital Library of Mathematical Functions." http://dlmf.nist.gov/.

[200] S. Caron-Huot, "Analyticity in Spin in Conformal Theories," *JHEP* **09** (2017) 078, `arXiv:1703.00278 [hep-th]`.

[201] M. Correia, A. Sever, and A. Zhiboedov, "An Analytical Toolkit for the S-matrix Bootstrap," `arXiv:2006.08221 [hep-th]`.

[202] F. Kos, D. Poland, and D. Simmons-Duffin, "Bootstrapping the $O(N)$ vector models," *JHEP* **06** (2014) 091, `arXiv:1307.6856 [hep-th]`.

[203] P. Kravchuk, "Lectures on conformal blocks and linear programming," *Bootstrap 2020, Held Online* .

[204] D. Poland, D. Simmons-Duffin, and A. Vichi, "Carving Out the Space of 4D CFTs," *JHEP* **05** (2012) 110, `arXiv:1109.5176 [hep-th]`.

[205] T. H. Koornwinder, "Dual addition formulas associated with dual product formulas," *Frontiers in Orthogonal Polynomials and q-Series* (2018) 373–392, `arXiv:1607.06053 [math]`.

[206] S. R. Coleman, "The Fate of the False Vacuum. 1. Semiclassical Theory," *Phys. Rev. D* **15** (1977) 2929–2936. [Erratum: Phys.Rev.D 16, 1248 (1977)].

KAMRAN SALEHI VAZIRI

E-mail: kamran.salehivaziri@epfl.ch
Phone Number: +41 (0)78 731 95 38
Address: Avenue du Silo 5, Renens, Vaud, Switzerland
Researcher ID: INSPIRE-HEP: `K.Salehi.Vaziri.1`
ORCID: `0000-0002-1494-311X`
arXiv: `salehivaziri_k_1`

EDUCATION:

- **École Polytechnique Fédérale de Lausanne (EPFL)**
  Lausanne, Switzerland. *October 2017 - Expected: July 2022*
  Ph.D. in Theoretical Physics, Advisor: Joao Penedones.

- **University of California, Riverside**
  Riverside, California, USA. *September 2016 - September 2017*
  Master of science in physics.

- **Sharif University of Technology**
  Tehran, Iran. *September 2011 - June 2016*
  Bachelor of science in physics.

HONORS AND AWARDS:

- Awarded **Dean's fellowship**, University of California, Riverside. *September 2016*
- **Ranked** 4^{th}, Master of physics national entrance exam, Iran. *May 2016*
- **Silver medal**, National Physics Olympiad, Iran. *August 2010*
- Member of **Iran's National Elites Foundation**. *September 2010- July 2015*

PUBLICATIONS:

- **Towards the non-perturbative cosmological bootstrap**
  Introducing an inversion formula for de Sitter Källén-Lehmann spectral representation. Uncovering positivity conditions for partial wave expansion of boundary correlators dictated by bulk unitarity and fining bounds using conformal bootstrap.
  M. Hogervorst, J. a. Penedones, and K. S. Vaziri, "Towards the non-perturbative cosmological bootstrap," arXiv:2107.13871 [hep-th].

- **Hamiltonian truncation in Anti-de Sitter**
  Applying Hamiltonian truncation method to study theories such as scalar field theory and deformations of minimal models in AdS_2. Studying spontaneous symmetry breaking in AdS and deriving a compact formula for perturbation theory in quantum mechanics at arbitrary order.
  M. Hogervorst, M. Meineri, J. a. Penedones, and K. Salehi Vaziri, "Hamiltonian truncation in Anti-de Sitter spacetime," arXiv:2104.10689 [hep-th].
- **Anomaly induced quantum correction to charged black holes; geometry and thermodynamics**
  Corrections to uncharged and charged black hole horizons, gravitational collapse, entropy and Hawking radiation due to trace anomaly.
  J. Abedi, H. Arfaei, A. Bedroya, A. Mehin-Rasuliani, M. Noorikuhani, and K. Salehi-Vaziri, "Anomaly induced quantum correction to charged black holes; geometry and thermodynamics," arXiv:1707.02545 [hep-th].

SUPERVISION OF JUNIOR RESEARCHERS:

- Co-mentoring of Antoine Gravina, Master student of Joao Penedones.
  Title of the thesis: *"Perturbative QFT in AdS", 2019*
- Co-mentoring of Jan-Joris Stauffer, Master student of Joao Penedones.
  Title of the thesis: *"Hamiltonian truncation study of scalar field theory in 2d Anti-de Sitter spacetime", 2018*

PRESENTATIONS:

- **Nonperturbative cosmological bootstrap**
  - King's College London, United Kingdom. *March 2, 2022*
  - Crete Center for Theoretical Physics (CCTP), Greece. *December 9, 2021*
  - Ludwig Maximilian University, Munich, Germany. *November 16, 2021*
  - International Conference on Strings, Fields and Holograms, Ascona, Switzerland. *October 14, 2021*
- **Hamiltonian truncation in AdS_2**
  - Simons Bootstrap Collaboration Seminar Series. *May 5, 2021*
  - Sharif University of Technology. *April 27, 2021*
  - University of Porto. *February 12, 2021*
- **An introduction to nonperturbative methods in QFT**. A crash course at Sharif University of Technology in Persian. *February 7, 2021*

TEACHING ACTIVITIES:

- **École Polytechnique Fédérale de Lausanne (EPFL)**
  - Path Integral approach to Quantum Mechanics: *spring 2020, spring 2021*
  - Electrodynamics: *fall 2018, fall 2019, fall 2020, fall 2021*
  - General Physics: *spring 2018, spring 2019*

- **University of California, Riverside**
  - General Physics Lab: *fall 2016, winter 2017, spring 2017*
- **Sharif University of Technology**
  - Special Relativity: *fall 2015*
  - Cosmology: *spring 2014*
  - Modern Physics: *fall 2014*
  - Acoustic Lab: *spring 2016*
  - Thermodynamics and Statistical Mechanics 1: fall 2015

WORKSHOP AND CONFERENCES:

- International Conference on Strings, Fields and Holograms,
  Monte Verità Conference Center, Ascona, Switzerland: *October 11-15, 2021*
- Bootstrap Workshop and School,
  held virtually, USA: *June 1-26, 2020*
- Bootstrap Workshop and School,
  California Institute of Technology, Pasadena, California, USA: *July 2-27, 2018*
- Workshop on S-matrix Bootstrap,
  ICTP-SAIFR, São Paulo, Brazil: *September 9-13, 2019*
- Hamiltonian methods in strongly coupled Quantum Field Theory Workshop,
  Institut des Hautes Etudes Scientifiques (IHES), Paris, France: *January 8-12, 2018*
- Simons Summer Workshop on non-supersymmetric QFTs and String Theory,
  Simons Center for Geometry and Physics, Stony Brook University, Long Island, New York, USA: *July 17 - August 11, 2017*
- Herbig Observational Astronomy Workshop,
  Lick Observatory, San Jose, California, USA: *October 2016*

SKILLS:

- **Languages:** Persian (native), English (fluent), French (basic)
- **Programming skills:** C, C++, Mathematica
- **Typesetting**: LaTeX